ECHINOID EVOLUTION

ACROSS THE

CRETACEOUS-TERTIARY BOUNDARY

Submitted to the University of London

as a thesis for the degree of

Doctor of Philosophy

by

Charlotte Hannah Jeffery

Imperial College of Science, Technology & Medicine and

The Natural History Museum, London

ABSTRACT

Previous estimates of the global generic diversity loss for echinoids at the Cretaceous-Tertiary boundary have been as high as 70%. However, these estimates are based on compilations of occurrence data from the existing literature and are plagued by problems of inconsistent taxonomic usage. To overcome this problem, a revision of Maastrichtian and Palaeocene atelostomate echinoids (holasteroids and spatangoids) has been undertaken to create a taxonomically standardized data set. This demonstrates that the generic extinction rate for atelostomate echinoids was 35%, and that holasteroids and spatangoids suffered markedly different fates. Whereas holasteroids lost 56% of their generic diversity at the end of the Cretaceous, only 21% of spatangoid genera became extinct.

Generic and specific level cladistic analyses have been used to resolve phylogenetic relationships between taxa and to clarify patterns of survivorship selectivity amongst holasteroids and spatangoids. Correlation of extinction with a range of geographical, environmental and biological factors has been explored using chi-squared tests of independence. Survivorship is significantly correlated only with feeding strategy, implying that atelostomate extinctions were nutrient driven. In addition, feeding strategy is correlated with atelostomate higher taxonomy, explaining the differential fates of holasteroids and spatangoids at the end of the Cretaceous.

The study of life-history strategies and their effect on echinoid survivorship at the Cretaceous-Tertiary boundary shows that non-feeding development first evolved, and was independently adopted, in nine clade in the last ten million years of the Cretaceous. These near-synchronous shifts in developmental mode, which occurred over a broad taxonomic and latitudinal range, point to increasing seasonality as a forcing factor and provide the first clear evidence that environmental change on a global scale can drive synchronised shifts in life-history strategy.

CONTENTS

ABSTRACT 2

CONTENTS 3

LIST OF TABLES 8

LIST OF FIGURES 10

LIST OF PLATES 15

ACKNOWLEDGEMENTS 16

CHAPTER 1: INTRODUCTION:

THE CRETACEOUS-TERTIARY BOUNDARY DEBATE 18

Previous work on the K-T boundary 19

Sedimentological and geochemical evidence 19

Palaeontological evidence 20

Local patterns of extinction 21

Regional and global patterns of extinction 22

Survivorship selectivity 23

CHAPTER 2: ECHINOIDS AND THE CRETACEOUS-TERTIARY BOUNDARY 25

Why study echinoids? 25

Previous work on echinoids at the K-T boundary 26

Local patterns of extinction 26

Global patterns of extinction 27

CHAPTER 3: A TAXONOMIC REVISION OF MAASTRICHTIAN AND PALAEOCENE ATELOSTOMATE ECHINOIDS 29

SYSTEMATIC PALAEONTOLOGY 30

Series ATELOSTOMATA Zittel 30

Order HOLASTEROIDA Durham & Melville 30
Superfamily ORTHOSTERNATA nov. 36
Family CORISTIDAE Foster & Philip 36
non-corystid ORTHOSTERNATA 37
Family STEGASTERIDAE Lambert 50
Family ECHINOCORIDAE Lambert 75
Family CARDIASTERIDAE Lambert 88
Family LABROTAXIDAE nov. 100
Indeterminate holasteroids 115
Order SPATANGOIDA Claus 130
Family MICRASTERIDAE Lambert 136
Family BRISSIDAE Gray 190
Family HEMIASTERIDAE Clark 196
Family SCHIZASTERIDAE Lambert 225
Family PERICOSMIDAE Lambert 254
Family CORASTERIDAE Lambert 283
Family AEROPSIDAE Lambert 291
Family SOMALIASTERIDAE Wagner & Durham 304
Indeterminate spatangoids 321

CHAPTER 4: **PHYLOGENETIC ANALYSES OF MAASTRICHTIAN AND PALAEOCENE ATELOSTOMATE ECHINOIDS** 342
Methods 342
Holasteroid generic level analysis 345
Stegasterid species level analysis 349
Spatangoid generic level analysis 353
Micrasterid species level analysis 361
Cyclaster *and* Isaster *species level analysis* 365
Taxonomic position of the somaliasterids 369

CHAPTER 5: **ATELOSTOMATE EXTINCTION AT THE CRETACEOUS-TERTIARY BOUNDARY** 373

Atelostomate extinction in the Maastrichtian and Danian 373

Atelostomate extinction and taxonomy 381

Atelostomate extinction and higher taxonomy 382

CHAPTER 6: **ATELOSTOMATE EXTINCTION AND GEOGRAPHICAL AND ENVIRONMENTAL CORRELATES** 387

Methods 387

Geographic range 388

Determining geographic ranges 388

Atelostomate survivorship and geographic range 389

Absolute geographic distribution 398

Determining absolute geographic distribution 398

Atelostomate extinction and absolute geographic distribution 399

Water depth 406

Inferring water depth 406

Atelostomate extinction and water depth 406

Sedimentary environment 412

Inferring echinoid substrate preferences 412

Atelostomate extinction and sedimentary environment 413

CHAPTER 7: **ATELOSTOMATE EXTINCTION AND BIOLOGICAL CORRELATES** 418

Life-position in sediment 418

Methods of inferring burrowing habit in atelostomes 418

Atelostomate extinction and life-position in the sediment 419

Larval strategy 422

Methods of inferring non-planktotrophy in echinoids 423

Atelostomate extinction and larval strategy 426

Why are there so few Maastrichtian lecithotrophs? 426

First occurrences of non-planktotrophy in echinoids 427

Global environmental change and the shift to non-planktotrophy in echinoids 428

Feeding strategy 437

Inferring feeding strategy in atelostomate echinoids 437

Atelostomate extinction and feeding strategy 438

CHAPTER 8: **CAN WE TELL WHAT HAPPENED AT THE CRETACEOUS-TERTIARY BOUNDARY** 447

Size of the extinction event 447

Selectivity of the extinction event 447

What happened at the K-T boundary? 449

When the dust settles..... 450

REFERENCES 452

APPENDIX 1: **MAASTRICHTIAN AND PALAEOCENE ECHINOID LOCALITIES** 482

APPENDIX 2: **DETAILS OF MAASTRICHTIAN AND PALAEOCENE STRATIGRAPHIC UNITS YIELDING ATELOSTOMATE ECHINOIDS** 489

APPENDIX 3: **INFERRING ECHINOID LARVAL TYPE FROM APICAL DISC CRYSTALLOGRAPHY** 505

APPENDIX 4: **EXTINCTION DATA AND POSSIBLE TAXONOMIC AND GEOGRAPHIC CORRELATES** 508

APPENDIX 5: EXTINCTION DATA AND POSSIBLE ENVIRONMENTAL AND BIOLOGICAL CORRELATES

513

LIST OF TABLES

Table 3.1.	Institutions housing Maastrichtian and Palaeocene echinoids	29
Table 3.2.	Indeterminate holasteroid taxa	117
Table 3.3.	Indeterminate spatangoid taxa	323
Table 4.1.	Characters used in the generic level cladistic analysis of holasteroids	345
Table 4.2.	Character matrix for taxa included in the generic level cladistic analysis of holasteroids	346
Table 4.3.	Characters used in the species level cladistic analysis of stegasterids	349
Table 4.4.	Character matrix for taxa included in the species level cladistic analysis of stegasterids	350
Table 4.5.	Characters used in the generic level cladistic analysis of spatangoids	354
Table 4.6.	Character matrix for taxa included in the generic level cladistic analysis of the Micrasterina	353
Table 4.7.	Character matrix for taxa included in the generic level cladistic analysis of the Hemiasterina	355
Table 4.8.	Characters used in the species level cladistic analysis of four-gonopored, petaloid micrasterids	361
Table 4.9.	Character matrix for taxa included in the species level cladistic analysis of four-gonopored, petaloid micrasterids	362
Table 4.10.	Characters used in the cladistic analysis of species of *Cyclaster* and *Isaster*	365
Table 4.11.	Character matrix for taxa included in the species level cladistic analysis of *Cyclaster* and *Isaster*	366
Table 4.12.	Characters used in the cladistic analysis of somaliasterids with holasteroid and spatangoid representatives	370

Table 4.13. Character matrix for taxa included in the cladistic analysis of somaliasterids with holasteroid and spatangoid representatives 370
Table 5.1. Summary statistics of contingency tables testing the independence of extinction with regard to taxonomy 381
Table 5.2. Possible correlates to atelostomate survivorship at the end of the Cretaceous 382
Table 6.1. Summary statistics of contingency tables testing the independence of extinction with regard to possible geographic correlates 389
Table 6.2. Summary statistics of contingency tables testing the independence of higher taxonomy with regard to possible geographical correlates 398
Table 6.3. Summary statistics of contingency tables testing the independence of extinction with regard to possible environmental correlates 407
Table 6.4. Summary statistics of contingency tables testing the independence of higher taxonomy with regard to possible environmental correlates 407
Table 7.1. Summary statistics of contingency tables testing the independence of extinction with regard to possible biological correlates 419
Table 7.2. Summary statistics of contingency tables testing the independence of higher taxonomy with regard to possible biological correlates 422
Table 7.3. First occurrences of lecithotrophy and brooding in echinoids during the late Campanian and Maastrichtian 428
Table A3.1. Larval development in Maastrichtian and Palaeocene echinoids 507

LIST OF FIGURES

Figure 3.1.	Camera lucida drawings of holasteroid plastron types	33
Figure 3.2.	Range chart for Maastrichtian and Palaeocene holasteroid genera	35
Figure 3.3.	Camera lucida drawings of *Galeaster bertrandi*	43
Figure 3.4.	Camera lucida drawings of *Basseaster rostratus*	45
Figure 3.5.	Camera lucida drawings of *Garumnaster michaleti*	47
Figure 3.6.	Range chart for Maastrichtian and Palaeocene species of Orthosternata	49
Figure 3.7.	Camera lucida drawings of *Stegaster bouillei*	62
Figure 3.8.	Camera lucida drawings of *Stegaster cotteaui*	64
Figure 3.9.	Camera lucida drawings of *Tholaster munieri*	66
Figure 3.10.	Camera lucida drawings of *Pseudoffaster caucasicus*	68
Figure 3.11.	Camera lucida drawings of *Rispolia subtrigonata*	70
Figure 3.12.	Camera lucida drawings of *Guettaria rocardi*	72
Figure 3.13.	Range chart for Maastrichtian and Palaeocene stegasterid species	74
Figure 3.14.	Camera lucida drawings of *Echinocorys scutata*	81
Figure 3.15.	Camera lucida drawings of *Jeronia pyrenaica*	83
Figure 3.16.	Camera lucida drawings of *Offaster pilula*	85
Figure 3.17.	Range chart for Maastrichtian and Palaeocene echinocorid species	87
Figure 3.18.	Camera lucida drawings of *Cardiaster granulosus*	95
Figure 3.19.	Camera lucida drawings of *Cardiotaxis heberti*	97
Figure 3.20.	Range chart for Maastrichtian and Palaeocene cardiasterid species	99
Figure 3.21.	Camera lucida drawings of *Labrotaxis faxensis*	110
Figure 3.22.	Camera lucida drawings of *Hemipneustes pyrenaicus*	112

Figure 3.23. Range chart for Maastrichtian and Palaeocene labrotaxid species 114
Figure 3.24. Range chart for Maastrichtian and Palaeocene genera of Micrasterina 133
Figure 3.25. Range chart for Maastrichtian and Palaeocene genera of Hemiasterina 135
Figure 3.26. Camera lucida drawings of *Micraster schroederi* 163
Figure 3.27. Camera lucida drawings of *Micraster aturicus* 165
Figure 3.28. Camera lucida drawings of *Micraster grimmensis* 167
Figure 3.29. Camera lucida drawings of *Mokotibaster nobilis* 169
Figure 3.30. Camera lucida drawings of *Pseudogibbaster akkajensis* 171
Figure 3.31. Camera lucida drawings of *Diplodetus duponti* 173
Figure 3.32. Camera lucida drawings of *Diplodetus coloniae* 175
Figure 3.33. Camera lucida drawings of *Ovulaster auberti* 177
Figure 3.34. Range chart for Maastrichtian and Palaeocene four-gonopored micrasterid species 179
Figure 3.35. Camera lucida drawings of *Cyclaster aturicus* 181
Figure 3.36. Camera lucida drawings of *Cyclaster pfenderae* 183
Figure 3.37. Camera lucida drawings of *Cyclaster galei* 185
Figure 3.38. Camera lucida drawings of *Isaster aquitanicus* 187
Figure 3.39. Range chart for Maastrichtian and Palaeocene three-gonopored micrasterid species 189
Figure 3.40. Camera lucida drawings of *Eupatagus mortenseni* 193
Figure 3.41. Range chart for Maastrichtian and Palaeocene brissid species 195
Figure 3.42. Camera lucida drawings of *Hemiaster prunella* 214
Figure 3.43. Camera lucida drawings of *Hemiaster paronai* 216
Figure 3.44. Camera lucida drawings of *Leiostomaster gentili* 218
Figure 3.45. Camera lucida drawings of *Leymeriaster maestrichtensis* 220
Figure 3.46. Camera lucida drawings of *Mecaster fourneli* 222

Figure 3.47. Range chart for Maastrichtian and Palaeocene hemiasterid species 224
Figure 3.48. Camera lucida drawings of *Linthia sudanensis* 256
Figure 3.49. Camera lucida drawings of *Paraster indicus* 258
Figure 3.50. Camera lucida drawings of *Tessieria senegalensis* 260
Figure 3.51. Camera lucida drawings of *Proraster geayi* 262
Figure 3.52. Camera lucida drawings of *Trachyaster oldhami* 264
Figure 3.53. Camera lucida drawings of *Holcopneustes cristatus* 266
Figure 3.54. Camera lucida drawings of *Prenaster oviformis* 268
Figure 3.55. Camera lucida drawings of *Mauritanaster gentili* 270
Figure 3.56. Camera lucida drawings of *Brisaster micropetalus* 272
Figure 3.57. Camera lucida drawings of *Pseudolinthia triporata* 274
Figure 3.58. Camera lucida drawings of *Opissaster elongatus* 276
Figure 3.59. Camera lucida drawings of *Kertaster termiri* 278
Figure 3.60. Range chart for Maastrichtian and Palaeocene species of *Linthia*, *Paraster* and *Tessieria* 280
Figure 3.61. Range chart for Maastrichtian and Palaeocene pericosmid and schizasterid species, excluding species of *Linthia*, *Paraster* and *Tessieria* 282
Figure 3.62. Camera lucida drawings of *Coraster vilanovae* 295
Figure 3.63. Camera lucida drawings of *Orthaster dagestanensis* 297
Figure 3.64. Camera lucida drawings of *Homoeaster tunetanus* 299
Figure 3.65. Camera lucida drawings of *Sphenaster larumbensis* 301
Figure 3.66. Range chart for Maastrichtian and Palaeocene corasterid and aeropsid species 303
Figure 3.67. Camera lucida drawings of *Iraniaster morgani* 310
Figure 3.68. Camera lucida drawings of *Iraniaster douvillei* 312
Figure 3.69. Camera lucida drawings of *Pseudiraniaster omanensis* 314
Figure 3.70. Camera lucida drawings of *Leviechinus gregoryi* 316
Figure 3.71. Camera lucida drawings of *Brightonia macfadyeni* 318

Figure 3.72. Range chart for Maastrichtian and Palaeocene somaliasterid species 320
Figure 4.1. Cladogram for Maastrichtian and Palaeocene holasteroid genera plus *Infulaster* 348
Figure 4.2. Cladogram for Maastrichtian and Palaeocene stegasterid species plus *Sanchezaster habanensis* 352
Figure 4.3. Cladogram for Maastrichtian and Palaeocene genera of Micrasterina plus *Habanaster* 358
Figure 4.4. Cladogram for Maastrichtian and Palaeocene genera of Hemiasterina 360
Figure 4.5. Cladogram for Maastrichtian and Palaeocene species of four-gonopored, petaloid micrasterid 364
Figure 4.6. Cladogram for Maastrichtian and Palaeocene species of *Cyclaster* plus *Isaster aquitanicus* 368
Figure 4.7. Cladogram for Maastrichtian and Palaeocene species of somaliasterid plus representatives of the Holasteroida and Spatangoida 372
Figure 5.1. Stratigraphic distribution of Maastrichtian and Palaeocene holasteroid genera and inferred phylogenetic tree 376
Figure 5.2. Stratigraphic distribution of Maastrichtian and Palaeocene genera of the Micrasterina and inferred phylogenetic tree 378
Figure 5.3. Stratigraphic distribution of Maastrichtian and Palaeocene genera of the Hemiasterina and inferred phylogenetic tree 380
Figure 5.4. Atelostomate survivorship plotted against number of species in each clade 384
Figure 5.5. Generic extinction levels at the end of the Cretaceous in holasteroids and spatangoids 386
Figure 6.1. Atelostomate survivorship plotted against total longitudinal range 391
Figure 6.2. Atelostomate survivorship plotted against total latitudinal range 393
Figure 6.3. Atelostomate survivorship plotted against number of regions 395

Figure 6.4.	Atelostomate survivorship plotted against number of localities	397
Figure 6.5.	Atelostomate survivorship plotted against absolute longitude	401
Figure 6.6.	Atelostomate survivorship plotted against absolute latitude	403
Figure 6.7.	Atelostomate survivorship plotted against latitudinal tolerance	405
Figure 6.8.	Atelostomate survivorship plotted against sediment type	409
Figure 6.9.	Atelostomate survivorship plotted against sedimentary tolerance	411
Figure 6.10.	Atelostomate survivorship plotted against water depth	415
Figure 6.11	Atelostomate survivorship plotted against number of depth zones occupied	417
Figure 7.1.	Atelostomate survivorship plotted against burrowing habit	421
Figure 7.2.	Stereographic projections of c-axis orientations of apical disc plates in fossil echinoids	425
Figure 7.3.	Atelostomate survivorship plotted against larval strategy	432
Figure 7.4.	Stratigraphic range chart for major post-Jurassic echinoid clades with first occurrences of nonplanktotrophic development	434
Figure 7.5.	First occurrences of lecithotrophy and brooding in late Campanian and Maastrichtian echinoids plotted onto Maastrichtian geography	436
Figure 7.6.	Atelostomate survivorship plotted against feeding strategy	441
Figure 7.7	Histogram of Danian maximum size as a percentage of Maastrichtian maximum size for surviving clades	443
Figure A1.1.	Localities yielding Maastrichtian atelostomate echinoids plotted onto Maastrichtian geography	486
Figure A1.2.	Localities yielding Palaeocene atelostomate echinoids plotted onto Maastrichtian geography	488

LIST OF PLATES

Plate 1.	*Galeaster bertrandi*; *Stegaster altus*	119
Plate 2.	*Stegaster cotteaui*; *Pseudoffaster caucasicus*; *Guettaria rocardi*	121
Plate 3.	*Tholaster munieri*; *Rispolia subtrigonata*	123
Plate 4.	*Echinocorys scutata*; *Jeronia pyrenaica*	125
Plate 5.	*Offaster pilula*; *Cardiaster granulosus*; *Cardiotaxis heberti*; *Hagenowia elongata*	127
Plate 6.	*Labrotaxis faxensis*; *Hemipneustes striatoradiatus*	129
Plate 7.	*Micraster schroederi*; *Mokotibaster hourcqi*	325
Plate 8.	*Pseudogibbaster tercensis*; *Diplodetus americanus*; *Cyclaster integer*	327
Plate 9.	*Cyclaster aturicus*; *Isaster aquitanicus*	329
Plate 10.	*Hemiaster prunella*; *Hemiaster hattaensis*; *Leiostomaster gentili*	331
Plate 11.	*Leymeriaster leymerieĭ*; *Mecaster fourneli*; *Mauritanaster mirabilis*	333
Plate 12.	*Linthia sudanensis*; *Paraster indicus*; *Proraster geayi*	335
Plate 13.	*Holcopneustes cristatus*; *Opissaster somaliensis*; *Prenaster* sp.	337
Plate 14.	*Coraster vilanovae*; *Homoeaster tunetanus*; *Sphenaster larumbensis*	339
Plate 15.	*Iraniaster morgani*; *Pseudiraniaster omanensis*; *Leviechinus gregoryi*	341

ACKNOWLEDGEMENTS

First of all, thanks to Sue Rigby whose doughnuts and gin & tonics first encouraged me to study palaeontology as an undergraduate. You're glad I'm not a librarian anymore. So am I.

Many thanks to Andrew Smith for encouragement and boundless enthusiasm in all things echinoderm. Thanks to Harry Shaw for smoothing my path at Imperial College.

Thanks to everyone who has helped with access to museum specimens at the Dansk Geologisk Forening Mineralogisk Museum, Copenhagen; Ernst-Moritz-Arndt-Universität, Greifswald; Geological Survey of India, Calcutta; Museu de Geologia, Barcelona; Muséum National d'Histoire Naturelle, Paris; Natuurhistorisch Museum, Maastricht; Palaeontological Institute, Academy of Science, Moscow; Colecciones de Paleontologia, Universitat Autonoma de Barcelona; University of Cambridge, Sedgwick Museum; University of Glasgow, Hunterian Museum; University of Rome, Geological Museum; United States National Museum; University of Washington, Burke Museum. Special thanks to Jaume Gallemi and John Jagt for help in the field. Thanks also to Richard Emlet for help with apical disc crystallography; I look forward to starting my post-doc in Oregon.

To everyone in the Department of Palaeontology at the Natural History Museum who has offered helpful advice, thoughtful discussion and friendship over the past three years. There are too many of you to mention - thanks for my watch and discman!

Mum, Dad, Kath - you didn't laugh, when as a six year old, I said I wanted to live in the Natural History Museum. I know you're proud of me. As I am of you. Thanks for all your love, support and encouragement.

To the man I met in Norfolk, bumped into again in Anglesea and who turned out to be the brightest star of them all. David Jones, you deserve awards for your patience.

For my Uncle Alan, who has a space for my graduation photo on his living room wall, and most especially for my Grandad, Joe Templeton, who always looked out for fossils on BBC2. Thank you.

Many thanks to you all.

Along the way, it is true that a lot of species have fallen off the ark.

Michael Bean
United States Senator
1978

CHAPTER 1

INTRODUCTION:

THE CRETACEOUS-TERTIARY BOUNDARY DEBATE

Today's biota accounts for only a tiny proportion of the number of species that have existed over the course of earth history. Indeed, it is estimated that as many as four billion plant and animal species have lived at some time. With somewhere in the order of a few million species alive today (Raup 1986), it is clear that extinction must play a major role in the biological history of the planet.

Studies exploring patterns of taxonomic diversity through time (e.g. Sepkoski 1993) have identified periods when there was significant and rapid loss of biological diversity on a global scale. These periods stand out as peaks against the more usual background extinction levels, and where biological loss was of sufficient taxonomic and geographic proportions, these peaks in extinction intensity are termed "mass extinction events". The sheer magnitude and apparently indiscriminate nature of these events have long been considered indicative of the involvement of external factors. Altogether, five mass extinction events are recognized. All five (along with a larger number of less pervasive events) have generated a great deal of research interest, both individually and collectively, with a number of workers suggesting periodicity in extinction (e.g. Raup & Sepkoski 1984) or a common cause for a number of the events (e.g. Rampino & Haggerty 1996; Courtillot *et al.* 1996).

However, the famous demise of the dinosaurs and other taxa at the Cretaceous-Tertiary (or K-T) boundary, has made it possibly the most comprehensively studied, and hotly debated, time period in earth history. Research has been particularly intensive over the past two decades, since the debate was stimulated by the claim that iridium anomalies encountered at the Cretaceous-Tertiary boundary were the product of an extraterrestrial bolide impact (Alvarez *et al.* 1980).

Previous work on the K-T boundary.

Recent research on the Cretaceous-Tertiary boundary has followed two main avenues: (i) assessing the evidence for an impact and (ii) determining the palaeontological patterns of the extinctions.

Sedimentological and geochemical evidence.

The first approach has concentrated on the sedimentological and geochemical evidence for an impact and its location. Possible impact sites so far discovered include the Chicxulub crater off the coast of Mexico (Hildebrand *et al.* 1991) and another smaller site off the Indian coast (Negi *et al.* 1993). Further evidence of extraterrestrial bolide bombardment comes from the presence of shocked quartz (Officer 1990), tektites (Smit 1990) and a minimum in the $^{187}Os/^{186}Os$ osmium isotope ratio (Peucker-Ehrenbrink *et al.* 1994) in boundary sections.

There has also been a great deal of speculation over the way in which a bolide impact and the end-Cretaceous extinctions are linked and many differing, but not necessarily exclusive, "killing mechanisms" have been proposed. Hypotheses have included global darkness due to debris thrown up by the impact and an associated breakdown of the food chain (Alvarez *et al.* 1980) as well as global cooling due to dust in the atmosphere (Pollack *et al.* 1983). Soot in boundary sections world-wide has been interpreted as evidence of widespread forest fires caused by the combustion of impact ejecta on atmospheric reentry (Wolbach *et al.* 1985, 1990; Hildebrand 1993). The chemical composition of rocks at the impact site would have been significant since volatization of carbon dioxide from carbonate target rocks could have led to greenhouse warming (O'Keefe & Ahrens 1989) whilst sulphate originating from an impact in evaporitic deposits may have caused acid rain (Weil 1994; Robinson 1995) and surface water acidification (D'Hondt *et al.* 1994). It has also been postulated that nitric acid rain was produced by the oxidation of atmospheric nitrogen during reentry of impact debris (Crutzen 1987; Zahnle 1990). Impact-induced volcanism has also been proposed as a cause of the extinctions (Negi *et al.* 1993; Sutherland 1994).

Sedimentological and geochemical evidence for an impact at the end of the Cretaceous is overwhelming (Glen 1994; MacLeod 1996a) and it is now generally accepted that there was a bolide impact at or near the stratigraphic K-T boundary. However, there is growing evidence from biological (e.g. Barrera & Keller 1994; MacLeod *et al.* 1996; see also Chapter 7) and physical (e.g. Haq 1991 (sea level changes); Barrera 1994; Huber *et al.* 1995 (climate); Courtillot *et al.* 1996 (volcanism); MacLeod *et al.* 1997) datasets that the latest Cretaceous was a time of increasing (wholly terrestrial) environmental instability. In addition, the incidence of several large impact craters, such as the Campanian Manson Crater (Izett *et al.* 1993) and the Upper Miocene Reis Crater (Pohl *et al.* 1977), without associated extinctions in the fossil record throws doubt onto the causative correlation of the Chicxulub impact structure and the end-Cretaceous extinctions (MacLeod 1996a; Gale in press). Thus, the extent to which the impact (rather than the environmental perturbations) influenced, or was responsible for, the extinctions at the Cretaceous-Tertiary boundary is still the subject of controversy (Flessa 1990; Glen 1994; MacLeod *et al.* 1997).

Palaeontological evidence.

Palaeontological analysis of the Cretaceous-Tertiary boundary has focused on calculating the magnitude and duration of the mass extinction event and speculating on how the observed patterns relate to proposed extinction scenarios. To date, documentation of biological change has employed data from two main sources:

- detailed cm- or mm-scale investigations of sections spanning the boundary to assess the rapidity and duration of the extinction event (concentrating on the analysis of microfossil data) (e.g. Hansen *et al.* 1993; Keller *et al.* 1993).
- analysis of regional or global taxonomic compilations to gauge the biological extent of the mass extinction (e.g. Roman 1984; Jablonski & Raup 1995).

Local patterns of extinction. A huge amount of research time has been invested in looking at so called "complete" sections across the boundary and documenting the pattern and tempo of taxonomic change, with the aim of determining the rapidity and duration of the extinction event. However, there are a number of problems inherent in this approach and "the pitfalls to taking local or even regional data at face value are still little appreciated, resulting in massive overinterpretation of palaeontological patterns" (Jablonski 1996, p. 1; see also Jeffery 1997[b]).

Only a small number of continuous boundary sections exist, many of which are barren of macrofossils. If research was limited to the study of these sections alone, knowledge of taxonomic change across the K-T boundary would be severely restricted. Major sea-level fluctuations and subsequent facies changes in the latest Cretaceous (Haq 1991; Keller *et al.* 1993; Gale, in press) offer one explanation for this paucity of boundary sections, as well as for the small total number of Palaeocene outcrops with preserved macrofauna, especially in shallow water settings (Jeffery & Smith, in press). The most complete sections spanning the K-T boundary tend to contain deeper water facies, preserving a sparser benthic fauna. In the more affected shallow water settings, facies-dependent taxa migrate away from the studied section giving a false extinction signal, and the survival of these taxa can be confirmed only by looking elsewhere in more recent deposits of similar facies type. In addition, even if biodiversity remained constant across the Cretaceous-Tertiary boundary, the lack of suitable Palaeocene outcrops could lead to a perceived drop in the number of species (Jeffery & Smith, in press).

Even if a section appears complete and free from facies change, there may still be hiatuses "hidden" within the section with no lithological expression (MacLeod & Keller 1991). Depositional breaks, causing the truncation of stratigraphic ranges of taxa, give the impression of many simultaneous extinctions. This issue is particularly relevant to study of the end-Cretaceous biotic turnover since the absence of intervals close to the boundary has been demonstrated for many of the classic "continuous" sections (MacLeod & Keller 1991; Kennedy 1993). Techniques such as the application of confidence intervals to stratigraphic ranges of fossils have been developed, and are being

increasingly used (e.g. Marshall & Ward 1996), in an attempt to overcome such sampling biases.

A further drawback encountered when working at the cm- or mm-scale is that of reworking. This is particularly pertinent in microfossil studies where arguments continue as to whether fossils collected are still in their original depositional settings (MacLeod & Keller 1992; Huber 1996; MacLeod 1996b; Pospichal 1996).

Regional and global patterns of extinction. The second line of palaeontological investigation seeks to assess the extent of diversity change regionally or globally but with far lower temporal resolution, often drawing on data in the form of compendia of occurrences. However, compilations of this type commonly suffer from problems of inconsistent taxonomic usage (Wingard 1993). Artefacts of nomenclature, such as the naming of species solely on the basis of their occurrence in a particular geographic locality or stratigraphic horizon, as well as the idiosyncrasies of each individual taxonomist, can lead to taxonomic disappearances (or pseudoextinctions) and a subsequent inflation of extinction estimates. A thorough taxonomic revision should therefore form the basis of every study of biological turnover. Yet, although the "non-trivial problem of integrating local and synoptic databases" (Jablonski 1996, p. 3) is recognized, the amount of error that taxonomic inconsistencies can contribute to any regional or global analysis is still grossly underestimated.

The presence of large numbers of non-monophyletic taxa in the literature demonstrates that traditional taxonomy does not always reflect genuine biological groupings and processes, and can conceal lineage continuity. The last appearance of a non-monophyletic taxon may correspond to a true biological extinction but equally may just reflect a change in nomenclature. By taking a phylogenetic, rather than a taxic approach, and therefore knowing the historical relationships of the taxa involved, it is possible to distinguish between real evolutionary patterns in the fossil record and spurious patterns due to preservation or collection bias. It is now widely recognized that the construction of robust phylogenies will allow the more reliable calculation of extinction

rates in the fossil record (MacLeod 1996a; Jablonski 1997; MacLeod *et al.* 1997; Jeffery & Smith, in press).

Survivorship selectivity. It has been suggested that the factors which influence survivorship during periods of "background" extinction are ineffective during mass extinctions (Jablonski 1986a). For example, although lineages containing small numbers of species are prone to higher extinction levels during normal times, it seems that species richness does not act as a significant buffer during mass extinction events (Jablonski 1986a, 1989, 1995). So are mass extinctions indiscriminate with respect to taxonomic position, or do some taxa possess biological or ecological traits that increase their chances of survival? To date, the detailed study of survivorship selectivity has only been attempted with molluscan faunas, as well as some microfossil groups, and as yet there is little consensus about survival selectivity patterns recognized at the Cretaceous-Tertiary boundary.

A number of studies have recorded differences in extinction intensity correlated with feeding type (Sheehan & Hansen 1986; Ward *et al.* 1991; Jablonski & Raup 1995; Sheehan *et al.* 1996) and linked to the hypothesized collapse in primary productivity (Paul & Mitchell 1994). In all these studies, detritivores show significantly lower extinction rates than those taxa which rely on primary productivity. However, among deposit feeding bivalves the low overall rate is due to extremely low extinction levels in just two groups, the Nuculoida and the Lucinoidea (Jablonski & Raup 1995). Thus the preferential survivorship exhibited by these groups is attributable to factors other than, or in addition to, feeding strategy (Levinton 1996).

Some studies have recorded higher rates of extinction among infaunal and semi-infaunal organisms (Kauffman 1978; Stanley 1986). This result is not corroborated by Jablonski & Raup (1995) but it should be noted that rudists were excluded from their analysis.

It has also been suggested that taxa with a planktotrophic mode of larval development fared badly over the K-T boundary (Kennedy 1989, 1993; Gallagher 1991) associated with the collapse in primary productivity. In contrast, Jablonski (1986b)

recorded similar levels of extinction in gastropods across the K-T boundary regardless of developmental strategy.

Geographic patterns of selectivity have also been explored and it is generally accepted that geographically widespread taxa were less effected over this time period than those with narrow geographic ranges (Jablonski 1989; Jablonski & Raup 1995). However, this could be an artefact since widespread taxa are likely to be more common and thus better sampled. It has also been claimed that extinction levels were highest in the tropics during the K-T crisis and indeed, a correlation between high latitudes and lower extinction intensities has been demonstrated in a number of fossil groups (e.g. Rosen & Turnsek 1989; Keller *et al.* 1993; Elliot *et al.* 1994). Calcareous nannoplankton extinctions, on the other hand, show no latitudinal bias (Pospichal 1996). It has been argued that the preponderance of endemic taxa in the tropics could in itself explain the latitudinal patterns. The exclusion of rudists from the bivalve analysis produces fairly uniform extinction intensities at all palaeolatitudes (Raup & Jablonski 1993).

These examples clearly illustrate the lack of consensus so far recorded in patterns of survivorship selectivity at the Cretaceous-Tertiary boundary. Research into other groups, where taxonomy has been revised and standardized, is necessary if patterns of selectivity are to be clarified. That is the primary goal of this thesis.

CHAPTER 2

ECHINOIDS AND THE CRETACEOUS-TERTIARY BOUNDARY

From a biological perspective there are three principal questions that need to be considered.

- What was the magnitude of the event? How many taxa became extinct?
- What was the duration of the event? Was it long-term or instantaneous?
- Was extinction selective? Are there biological or environmental correlates to survivorship?

Echinoids (and macrofossils in general) have little to contribute to the temporal debate, since the fine stratigraphic resolution that is possible for microfossils within a single section is clearly lacking for echinoids. However, by sacrificing temporal resolution for geographic coverage, it will be possible to determine the size of the extinction event and to ascertain whether or not extinction was selective.

Despite the volume of work that has been published on the end-Cretaceous mass extinction, relatively little is known in detail about how the marine benthic macrofauna was affected, both in terms of geographical and biological selectivity patterns. Work to date has concentrated on molluscan faunas with varying degrees of extinction selectivity recognised by different workers. Research into major marine invertebrate groups is necessary if patterns of selectivity are to be clarified.

Why study echinoids?

Holasteroids and spatangoids, known collectively as atelostomate echinoids, provide an ideal model organism on which to focus. They form an important and diverse component of the marine benthos both before and after the Cretaceous-Tertiary boundary, and since the preservation potential of echinoids is comparatively high,

especially amongst the irregulars (Kier 1977), fossil echinoids are abundant in differing facies types from the poles to the equator in late Cretaceous and early Tertiary strata.

In addition, atelostomate echinoids are morphologically complex making them relatively simple to classify taxonomically and phylogenetically. Correlation between morphology and palaeobiology is also good (e.g. Kanazawa 1992), allowing the association of survivorship with key biological traits to be investigated. For example, mucus string feeding can be inferred from spatangoids with a deeply sunken frontal groove and modified spines and tubercles (Bromley *et al.* 1995).

Perhaps most significantly, the Atelostomata encompasses some clades that survived and others that became extinct at the end of the Cretaceous. In the extinction debate, the limelight has often been given to taxa, such as ammonites and dinosaurs, that were totally annihilated. Yet there is little that can be deduced about extinction processes if there are no surviving lineages, and the factors that are important in survival can only be deduced by looking at a group where only some clades became extinct.

Despite this, the atelostomes (and echinoids generally) have been surprisingly neglected in studies of the K-T biotic transition.

Previous work on echinoids at the K-T boundary.

Local patterns of extinction.

Changes in the echinoid fauna across the Cretaceous-Tertiary boundary of Denmark were documented by Asgaard (1979) and Gravesen (1979). For the regular echinoids, Gravesen found that faunal changes were restricted to species level, with most genera passing across the boundary. Asgaard attributed the change in the irregular echinoid fauna to an alteration in facies in the Danian and the preferential survival of ploughing (compared to deeper burrowing) holasteroids.

Van der Ham *et al.* (1987) described the echinoids from Late Campanian to Danian strata of the Maastricht area. The study showed that although Maastrichtian and Danian faunas were of equal diversity (33 species in the uppermost Maastrichtian Meerssen Chalk; 32 species in the Danian Geulhem Chalk), there were only 7 species in common, indicating that there was a major biotic turnover in this region.

Most recently, Jeffery (1997b) produced an account of echinoid faunal changes in continuous Maastrichtian to Danian sections of the Mangyshlak Peninsula, Kazakhstan. She found that although extinction levels within the sections were extremely high (100% at species level and 82% at generic level), the inclusion of occurrence data for the same species outside of Kazakhstan reduced species level extinction to 60% and generic extinction to 25%, highlighting the difficulties associated with the extrapolation of local extinction patterns. Furthermore, she found that the same pattern of local extinction and replacement was repeated in other K-T sections outside of Kazakhstan, and that if occurrences away from the studied sections were considered, extinction rates were again significantly reduced. In Denmark a 56% extinction across the Cretaceous-Tertiary boundary at the genus level was reduced to 25%, and in the Maastricht area, a loss of 68% of Maastrichtian genera dropped to 39%. Thus migration, rather than extinction, accounts for at least some of the perceived local loss of taxa at the Cretaceous-Tertiary boundary.

Global patterns of extinction.

Only a few studies have focused on global patterns of biological turnover in echinoids at the end of the Cretaceous, perhaps because the available species compilations are old (Lambert & Thiéry 1909-1925), unsuitable for this type of study (Kier & Lawson 1978) or in Russian (Moskvin *et al.* 1980). Where these datasets have been used, none have been taxonomically standardized for the subsequent analyses.

Kier (1974) used Lambert & Thiéry's (1909-1925) compilation to assess diversity changes in echinoids throughout the post-Palaeozoic. For the interval spanning the K-T boundary, he tallied only 108 species recorded from Palaeocene strata compared to 1137 from the Senonian.

Using data from Lambert & Thiéry (1909-1925), Moskvin & Poslavskaya (1959), Poslavskaya & Moskvin (1960) and Kier & Lawson (1978), Stokes (1979) studied spatangoids across the K-T boundary and concluded that they were hardly affected by the crisis at the end of the Cretaceous. He also concluded that the major faunal changes in atelostomate echinoids at the Cretaceous-Tertiary boundary, noted by Poslavskaya &

Moskvin (1960), were due primarily to disappearances of holasteroid taxa.

Moskvin *et al.* (1980) produced a compendium of Campanian to Palaeocene occurrences for echinoid species from the former Soviet Union and echinoid genera world-wide. They found significant generic diversity losses at the end of the Maastrichtian for all orders, except in the cidaroids and spatangoids.

The data were subsequently analyzed by Shimanskii & Solovjev (1982) who asserted that extinctions over this time period were progressive, starting in the Upper Senonian.

Roman (1984) employed the same dataset for his analysis of echinoids at the Cretaceous-Tertiary boundary and demonstrated that the K-T boundary coincided with the single most important event in post-Palaeozoic echinoid history, with 2 out of 14 orders, 9 out of 38 families and 83 out of 127 genera present for the last time during the Maastrichtian. Irregulars were more severely affected than regulars, with species turnover rates of 83% and 57% respectively. Within the irregulars, holasteroids and spatangoids suffered disparate fates. Whilst the species turnover was 80% in the holasteroids, it reached only 61% in the spatangoids. Roman attributed the preferential survivorship of spatangoids to their better adaptation for infaunal living.

Kier & Lawson's (1978) compilation of echinoid species only covers taxa described between 1925 and 1970, and does not take account of the many abundant species which had been previously described. However, the resulting unsuitability of the dataset did not deter McKinney (1995) from using it to gauge patterns of diversity change within echinoids from the Cenomanian to the Late Miocene. From this data, McKinney estimated that 57% of Maastrichtian echinoid genera did not survive into the Tertiary. Previous authors agree that holasteroids suffered more substantial losses than spatangoids at the end of the Cretaceous. However, estimates of extinction intensity vary widely among these studies of echinoids at the K-T boundary, from the low local extinction rates recognized within the Danish sections (Asgaard 1979; Gravesen 1979) to the high levels calculated from global compilations (e.g. Roman 1984). More work is needed within a rigorously revised taxonomic framework to determine the true pattern of the end-Cretaceous extinction within the atelostomate echinoids.

CHAPTER 3

A TAXONOMIC REVISION OF MAASTRICHTIAN AND PALAEOCENE ATELOSTOMATE ECHINOIDS

Previous investigations into the extent of regional or global diversity change at major geological boundaries have often drawn on data in the form of compendia of occurrences. However, since compilations of this type have rarely been subjected to taxonomic standardization, they very often suffer from problems of inconsistent taxonomic usage (Wingard 1993).

To overcome these problems and produce a global database with a uniform taxonomy for this study, it is necessary to ensure that all morphologically identical taxa are synonymised, and to verify that taxa assigned the same name by different workers are morphologically consistent. To this end, a taxonomic revision of all the atelostomate echinoid species recorded in the literature from Maastrichtian and Palaeocene strata world-wide has been undertaken, based largely on museum holdings. Where specimens from these collections have been studied by me, the museum abbreviation (see Table 3.1) appears in parentheses in the occurrence list of the taxon.

Table 3.1. Institutions housing Maastrichtian and Palaeocene echinoid specimens, with abbreviations.

BMNH	The Natural History Museum, London.
DGFMM	Dansk Geologisk Forening Mineralogisk Museum, Copenhagen.
EMAUG	Ernst-Moritz-Arndt-Universität Greifswald.
GSI	Geological Survey of India, Calcutta.
MGB	Museu de Geologia, Barcelona.
MNHN	Muséum National d'Histoire Naturelle, Paris.
NMM	Natuurhistorisch Museum, Maastricht.
PI	Palaeontological Institute, Academy of Science, Moscow.
PUAB	Colecciones de Paleontologia, Universitat Autonoma de Barcelona.
UCSM	University of Cambridge, Sedgwick Museum.
UGHM	University of Glasgow, Hunterian Museum.
URGM	University of Rome, Geological Museum.
USNM	United States National Museum.
UWBM	University of Washington, Burke Museum.

Some 300 nominal species from over 100 stratigraphic formations have been revised, including newly collected material from the type Danian (Stevn Klint, Denmark) and the type Maastrichtian. Field work at several important Maastrichtian and Palaeocene localities in Spain has added a number of new species to the dataset.

Since apical disc and plastron plating are of classificatory importance (Lambert 1893) within the atelostomate echinoids, producing plating diagrams of poorly known taxa has been given a high priority. Diagrams and species stratigraphic range charts follow each family.

Classification follows Wagner & Durham (1966) and Fischer (1966) except where indicated.

SYSTEMATIC PALAEONTOLOGY

Series ATELOSTOMATA Zittel, 1879

Diagnosis. Heart-shaped or ovate sea urchins with ambulacrum III and paired ambulacra commonly differentiated. Interambulacrum 5 differentiated adorally to form plastron. Apical system without fifth genital plate.

Order HOLASTEROIDA Durham & Melville, 1957

Diagnosis. Apical system elongate or disjunct. Plastron weakly differentiated or meridosternous, including orthosternous, metasternous and almost protosternous types (Figure 3.1). Paired ambulacra flush.

Remarks. As originally conceived (Durham & Melville 1957), the Holasteroida contained seven families. A number of attempts have been made to revise holasteroid taxonomy concentrating on the most easily characterized groupings. Two families, the Collyritidae and Disasteridae, were removed to a separate (paraphyletic) order, the Disasteroida by Mintz (1968). Foster and Philip (1978) added a new family, the Corystidae.

Only Pomel (1883) and Lambert (1893, 1917) have attempted to subdivide the large and diverse Holasteridae. More recent classifications (Mortensen 1950; Durham & Melville 1957; Wagner & Durham 1966) have restricted the number of subfamilies, referring the majority of genera to a single undivided Holasteridae. Lambert's classification uses the differentiation and degree of sunkeness of the unpaired ambulacrum, the arrangement of fascioles and the position of the periproct to subdivide the holasterids. However, the scheme produces poorly characterized groupings containing taxa with diverse suites of characters and disparate test architecture.

Nevertheless, the Holasteroida constitutes a large and diverse group that does merit subdivision based on structural differences in test architecture (see David 1988 and Mooi & David 1996 for a discussion of suitable characters). Cladistic analysis using such characters produces a phylogeny that can be used in a revised classification of taxa formerly referred to the holasterids. A complete revision will be published elsewhere.

KEY TO MAASTRICHTIAN & PALAEOCENE FAMILIES

1 Plastron orthosternous.....2

Plastron not orthosternous.....4

2 Subanal fasciole.....3

No subanal fasciole; mouth in parallel sided groove.....Stegasteridae

3 Rostral plate.....Corystidae

No rostral plate.....non-corystid Orthosternata

4 Test with no/indistinct frontal groove; flat base; paired ambulacra non-petaloid.....Echinocoridae

Test with distinct frontal groove; paired ambulacra petaloid.....5

5 Hexagonal labral plate followed by series of single plates.....Cardiasteridae

Triangular labral plate touches first post-sternal plate at right margin of plastron.....Labrotaxidae

Figure 3.1. Camera lucida drawings of holasteroid plastron types. a, orthosternous with rostral plate - *Corystus dysasteroides* (Duncan) (after Foster & Philip 1978, text fig. 1a). b, orthosternous without rostral plate - *Pseudoffaster caucasicus* (Dru), BMNH EE5573. c, standard meridosternous - *Offaster pilula* (Lamarck), BMNH E31845. d, metastemous - *Cardiotaxis heberti* (Cotteau), BMNH EE5627. e, protosternous - *Labrotaxis faxensis*, BMNH E2877. Scale bars = 2mm.

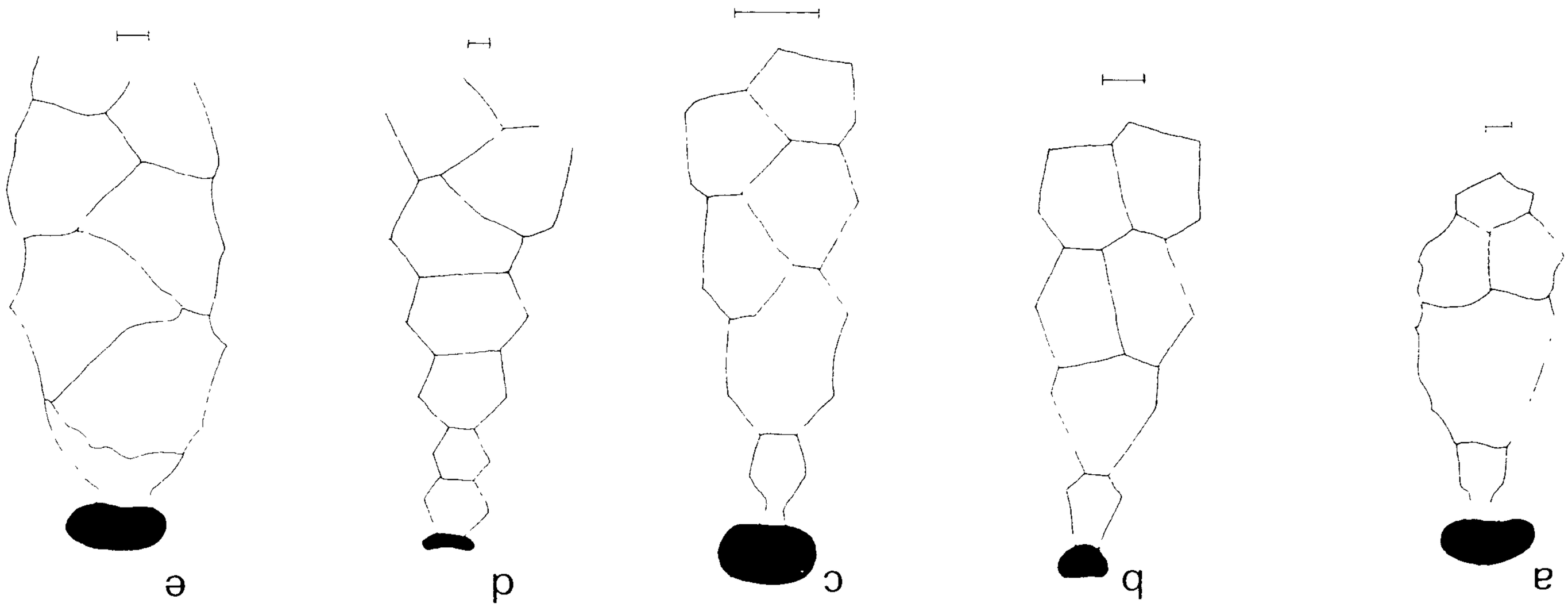
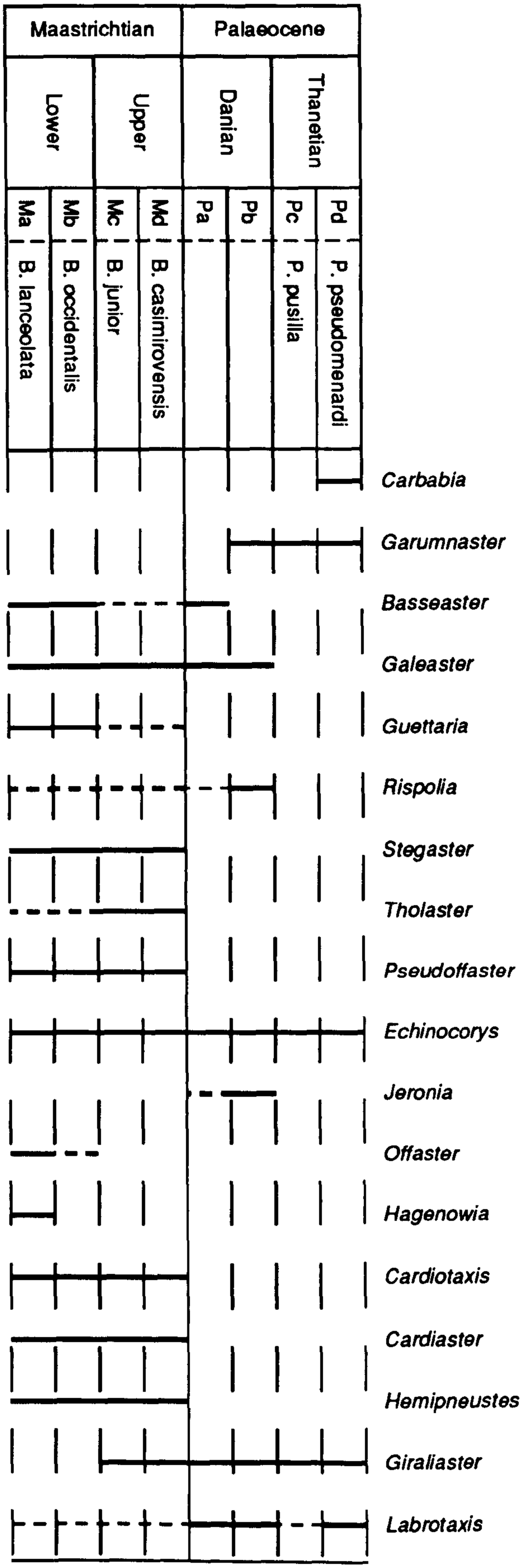

a
b
c
d
e

Figure 3.2. Range chart for Maastrichtian and Palaeocene holasteroid genera. As in all the following range charts, stratigraphically constrained occurrences are shown as solid lines; occurrences in stage (e.g. "Maastrichtian") or substage (e.g. "Lower Maastrichtian") are shown as thick dashed lines; thin dashed lines represent inferred range between definite occurrences. Pa = nannoplankton zones NP1-2; Pb = nannoplankton zones NP3-4; Pc = planktic foraminifera zone P3; Pd = planktic foraminifera zones P4-6 (Haq *et al.* 1987).


Maastrichtian
Palaeocene
Lower
Upper
Danian
Thanetian
Ma
Mb
Mc
Md
Pa
Pb
Pc
Pd
B. lanceolata
B. occidentalis
B. junior
B. casimirovensis
P. pusilla
P. pseudomenardi
Carbabia
Garumnaster
Basseaster
Galeaster
Guettaria
Rispolia
Stegaster
Tholaster
Pseudoffaster
Echinocorys
Jeronia
Offaster
Hagenowia
Cardiotaxis
Cardiaster
Hemipneustes
Giraliaster
Labrotaxis

Superfamily ORTHOSTERNATA nov.

Diagnosis. All ambulacra non-petaloid. Orthosternous plastron with or without rostral plate (Figure 3.1). Labral and sternal plates may or may not be in contact. Apical system with three or four gonopores. May be disjunct. Subanal fasciole.

Remarks. Phylogenetic analysis including extant taxa (e.g. Pourtalesiids, Urechinids) is necessary to place Maastrichtian and Palaeocene genera in their correct phylogenetic, and hence classificatory, positions within this group. At present it is possible to diagnose just one family, the Corystidae, characterized by the presence of a rostral plate. Further division of the Orthosternata must await a phylogenetic analysis of the whole group.

Family CORYSTIDAE Foster & Phillip, 1978

Diagnosis. All ambulacra non-petaloid. Orthosternous plastron with rostral plate. Apical system with three or four gonopores. Subanal fasciole.

Genus CARDABIA Foster & Phillip, 1978

[Type species *Cardabia bullarensis* Foster & Philip, 1978, by OD]

Diagnosis. Test ovate with no frontal groove. All ambulacra non-petaloid with small, round pores. Plastron orthosternous with rostral plate behind first pair of episternal plates. Apical system elongate with three gonopores (madreporite not perforated). Subanal fasciole encircles rostral plate. Dense tuberculation on upper surface.

Remarks. Easily distinguished from all other Maastrichtian and Palaeocene genera in having three gonopores in the apical system and above all in having a rostral plate on the oral surface.

Cardabia bullarensis Foster & Phillip, 1978

1978 *Cardabia bullarensis* Foster & Philip, p. 798, pl. 90, figs 3-4, pl. 91, figs 1-3.

Occurrence. Thanetian Wadera, Pirie and Cashin Calcarenites (Cardabia Group) of the Carnarvon Basin, Western Australia.

Diagnosis. As generic diagnosis.

non-corystid ORTHOSTERNATA

Diagnosis. Non-petaloid paired ambulacra. Orthosternous plastron; may be disjunct. No rostral plate. Apical system may be disjunct; genital plates may be fused. Subanal fasciole.

KEY TO MAASTRICHTIAN & PALAEOCENE GENERA

1 4 gonopores.....2

3 gonopores.....*Garumnaster*

2 Distinct frontal groove; globular test; genital plates 2 and 3 fused.....*Galeaster*

Shallow indistinct frontal groove; flat-based test; genital plates 2 and 3 not fused.....*Basseaster*

Genus GALEASTER Seunes, 1889

[Type species *Galeaster bertrandi* Seunes, 1889, by OD]

Diagnosis. Heart-shaped outline with sunken frontal ambulacrum persisting to mouth. Test globular with inflated upper and keeled lower surface. All ambulacra non-petaloid with small round pores. Plates high in paired ambulacra. Plastron orthosternous to disjunct without rostral plate. Apical system elongate with four gonopores. Genital plates 2 and 3 fused. Posterior ocular plates often disjunct from remainder of apical system. Subanal fasciole.

Remarks. Distinguished from *Basseaster* and *Garumnaster* by having a heart shaped outline with deep frontal groove, a gibbous lateral profile and fused genital plates 2 and 3. Differs additionally from *Garumnaster* in having four not three gonopores.

Galeaster bertrandi Seunes, 1889

(Plate 1, figures 1-4; Figure 3.3)

1889 *Galeaster bertrandi* Seunes, p. 822, pl. 27, figs 2-3.
1927 *Galeaster carinatus* Ravn, p. 342, pl. 2, fig. 9.
1959 *Galeaster minor* Poslavskaya; Moskvin & Poslavskaya, p. 273, pl. 17, figs 9-10, text fig. 83.
1959 *Galeaster sumbaricus* Poslavskaya; Moskvin & Poslavskaya, p. 273, pl. 17, figs 7-8, text fig. 82.
1960 *Galeaster carinatus* Ravn; Poslavskaya & Moskvin, p. 58, pl. 2, fig. 5, text fig. 8.
1960 *Galeaster minor* Poslavskaya; Poslavskaya & Moskvin, p. 58, pl. 2, figs 3-4, text fig. 7.
1960 *Galeaster sumbaricus* Poslavskaya; Poslavskaya & Moskvin, p. 57, pl. 2, figs 1-2, text fig. 6.
1960 *Galeaster dagestanensis* Poslavskaya & Moskvin, p. 59, pl. 2, fig. 6, text fig. 9.
1964 *Galeaster carinatus* Ravn; Poslavskaya & Solovjev, p. 181, pl. 34, fig. 6, text fig. 217.
1979 *Galeaster* cf. *bertrandi* Seunes; Gongadze, p. 107, pl. 25, fig. 2.
1979 *Galeaster* cf. *minor* Poslavskaya & Moskvin; Gongadze, p. 108, pl. 25, fig. 3, text figs 23-24.
1979 *"Galeaster" carinatus* Ravn; Asgaard, table 2.
1997b *Galeaster bertrandi* Seunes; Jeffery, p. 693, pl. 7, figs 1-8, text figs 14-15.

Occurrence. Danian of the French Pyrenees (Seunes 1889). Lower Danian Bryozoan Limestone of Denmark (Ravn 1927; Asgaard 1979) (DGFMM). Upper Maastrichtian to Upper Danian of Georgia (Gongadze 1979). Lower Danian of Mangyshlak, Kazakhstan (Jeffery 1997b) (BMNH). Lower to Upper Danian of the Crimea (Poslavskaya & Moskvin 1960) (PI). Lower to Lower Upper Maastrichtian (Moskvin & Poslavskaya 1959) and Lower to Upper Danian (Moskvin & Poslavskaya 1959; Poslavskaya & Moskvin 1960) of the Northern Caucasus (PI). Upper Lower to Lower Upper Maastrichtian and Lower to Mid Danian of the Transcaspian Region (Poslavskaya & Moskvin 1960) (PI). Maastrichtian to Danian of Kopet Dag, Mangyshlak, Dagestan, Crimea and the Northern Caucasus (Poslavskaya & Solovjev 1964) (PI).

Diagnosis. As generic diagnosis.

Remarks. The taxonomic confusion surrounding this genus is due in part to the absence of reliable plating information for the named species. Poslavskaya & Moskvin (1960) provide the same text figures with their descriptions of both *G. minor* and *G. sumbaricus.* All species recognized to date are distinguished either on the degree of disjunctness of the plastron or on subtleties of test shape with no other discernible structural differences. However, it has been suggested (David 1988, p. 336) that slight breaks between the labrum and sternum may represent intraspecific variation. In modern taxa such variation in the degree of separation has been shown to occur with growth (David 1987). Study of material in the collections of the Palaeontological Institute, Moscow demonstrates that specimens with separated labrum and sternum tend to be larger and it seems likely that this pattern of increasing disjunction is a function of increased size and that all nominal species form part of a single growth series.

Genus BASSEASTER Lambert, 1936

[Type species *Basseaster rostratus* Lambert, 1936, by OD]

Diagnosis. Test thin with ovate outline and shallow frontal groove. All ambulacra non-petaloid with small, round pores. Pores smaller and ambulacral plates lower in anterior ambulacrum. Plastron orthosternous; no rostral plate. Apical system elongate with four gonopores and posterior ocular plates disjunct. Circular mouth centrally positioned. Subanal fasciole.

Remarks. Most similar to *Garumnaster* from which it differs in having four gonopores in the apical system and a shallow frontal groove. *Galeaster* differs in having a deeply sunken frontal sulcus and a gibbous lateral profile.

Basseaster rostratus Lambert, 1936

(Figure 3.4)

1936 *Basseaster rostratus* Lambert, p. 25, pl. 3, figs 8-12, pl. 4, fig. 10.

1959 *Basseaster rostratus* Lambert; Moskvin & Poslavskaya, p. 272, pl. 17, fig. 6.

1960 *Basseaster rostratus* Lambert; Poslavskaya & Moskvin, p. 54, pl. 1, fig. 5, text fig. 3.

1964 *Basseaster rostratus* Lambert; Poslavskaya & Solovjev, p. 181, pl. 34, pl. 4, text figs 215b, 216b.

Occurrence. Lower Maastrichtian of southwestern Madagascar (Lambert 1936; Besairie 1971) and Maastrichtian of eastern Madagascar (Besairie 1971). Lower Danian of Dagestan (Moskvin & Poslavskaya 1959; Poslavskaya & Moskvin 1960; Poslavskaya & Solovjev 1964) (Pl).

Diagnosis. As generic diagnosis.

Remarks. Neither the type specimen nor topotype material could not be found in the Lambert Collection (MNHN).

Genus GARUMNASTER Lambert, 1907a

[Type species *Garumnaster michaleti* Lambert, 1907a, by OD]

Synonym. *Duncaniaster* Poslavskaya & Solovjev, 1964. *non Duncaniaster* Lambert, 1896 (= *Corystus* Pomel, 1883).

Diagnosis. Ovate test with no frontal groove. All ambulacra non-petaloid with small, round pores. Plastron orthosternous; no rostral plate. Apical system elongate with three gonopores (madreporite not perforated). Indistinct subanal fasciole.

Remarks. *Garumnaster* closely resembles *Cardabia*. It differs only in the lack of a rostral plate.

Garumnaster michaleti Lambert, 1907a

(Figure 3.5)

1907a *Garumnaster michaleti* Lambert, p. 718, pl. 25, figs 21-24.

1934 *Pomaster parvus* Bajarunas (ms).

1960 *Garumnaster michaleti* Lambert; Poslavskaya & Moskvin, p. 55, text fig. 4.

1960 *Garumnaster parvus* (Bajarunas); Poslavskaya & Moskvin, p. 56, text fig. 5.

1964 *Garumnaster parvus* (Bajarunas); Poslavskaya & Solovjev, p. 181, pl. 5, text figs 215c, 216c.

?1979 *Garumnaster michaleti* Lambert; Gongadze, tables 1 & 2.

Occurrence. Lower to Mid Thanetian of the French Pyrenees (Lambert 1907a) (MNHN). Upper Danian of Georgia (Poslavskaya & Moskvin 1960; Gongadze 1979) (PI). Upper Palaeocene of Mangyshlak (Poslavskaya & Moskvin 1960), Dagestan, the Crimea and the Transcaspian Region (Poslavskaya & Solovjev 1964) (PI).

Diagnosis. Widest point anteriorly. Mouth at one quarter test length from anterior margin. Slight subanal heel.

Remarks. Lambert's original description of this species (and genus) was based on a single specimen. Re-examination of this specimen reveals that it has only three gonopores in the apical system and not four as originally characterized. No topotype material is known.

Garumnaster luppovi (Poslavskaya & Solovjev, 1964)

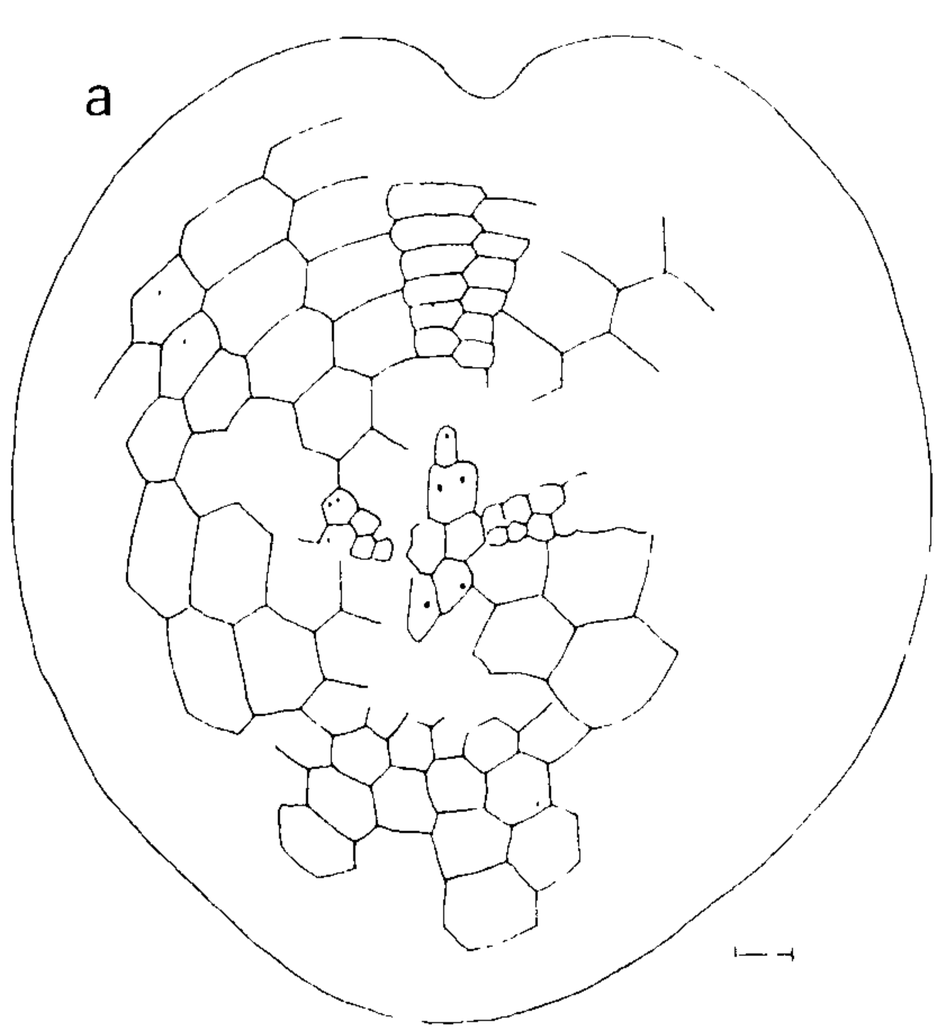
1934 *Pomaster luppovi* Bajarunas (ms).

1964 *Duncaniaster luppovi* (Bajarunas); Poslavskaya & Solovjev, p. 181, pl. 5, fig. 3, text figs 215a, 216a.

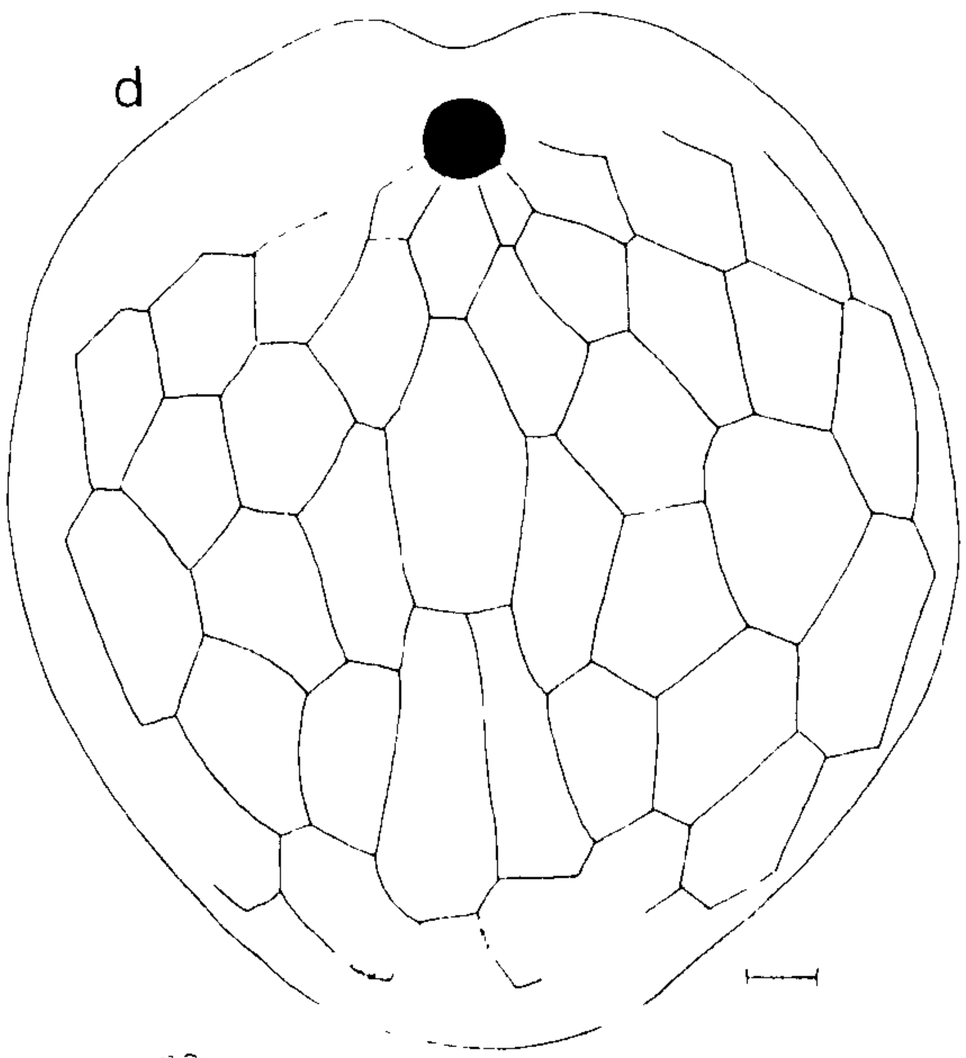
Occurrence. Upper Palaeocene of Mangyshlak, Kazakhstan (Poslavskaya & Solovjev 1964) (PI).

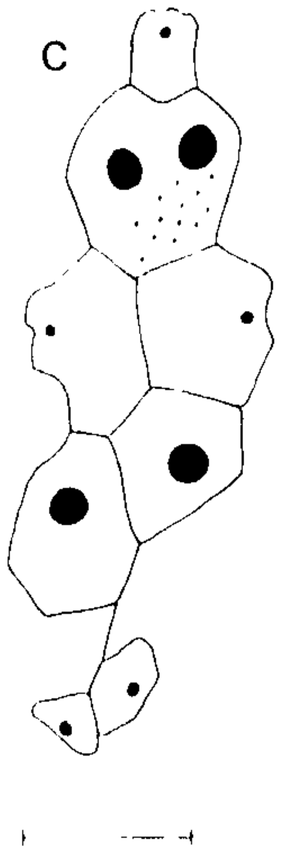
Diagnosis. Widest point at mid-length. Mouth at one third test length from anterior margin. Truncate posterior.

Figure 3.3. Camera lucida drawings of *Galeaster bertrandi* Seunes. a-c, Maastrichtian of Kopet Dag. a & b, PI 93/42 12; a, apical view; b, lateral view. c, PI 93/42 2, disjunct apical disc plating. d & e, Danian of Mangyshlak, Kazakhstan. d, PI 15493, oral view. e, PI 15443, non-disjunct apical disc plating. a, b & d, scale bars = 2 mm. c & e, scale bars = 1 mm.


a

b


d


c

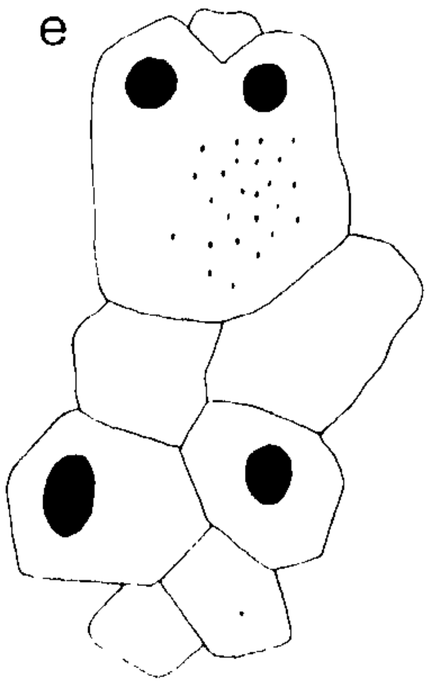

e

Figure 3.4. Camera lucida drawings of *Basseaster rostratus* Lambert, Pl 229, Danian of Dagestan; a, oral view; b, apical disc plating; c, posterior view; d, lateral view. a, c & d, scale bars = 2 mm. b, scale bar = 1 mm.

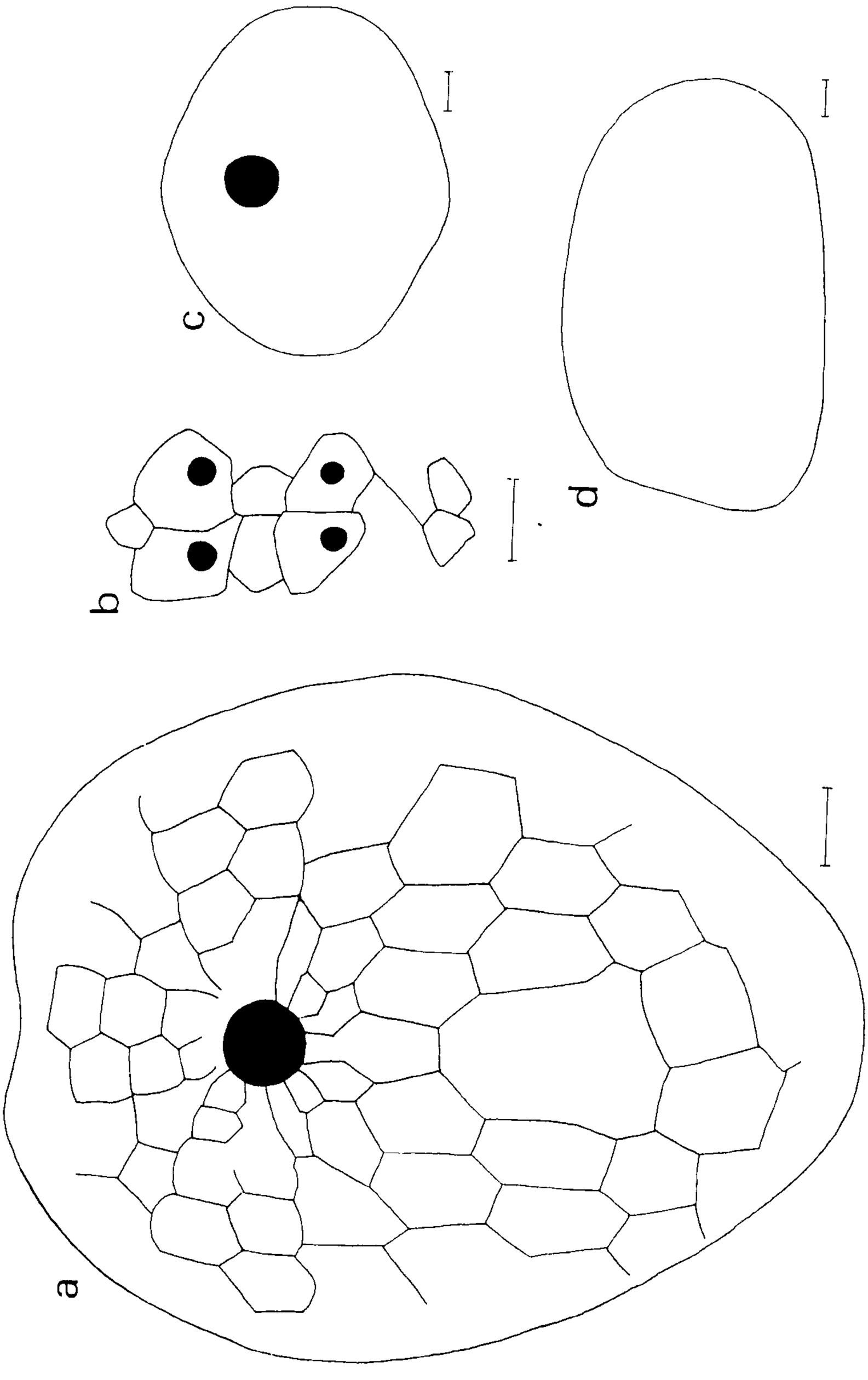
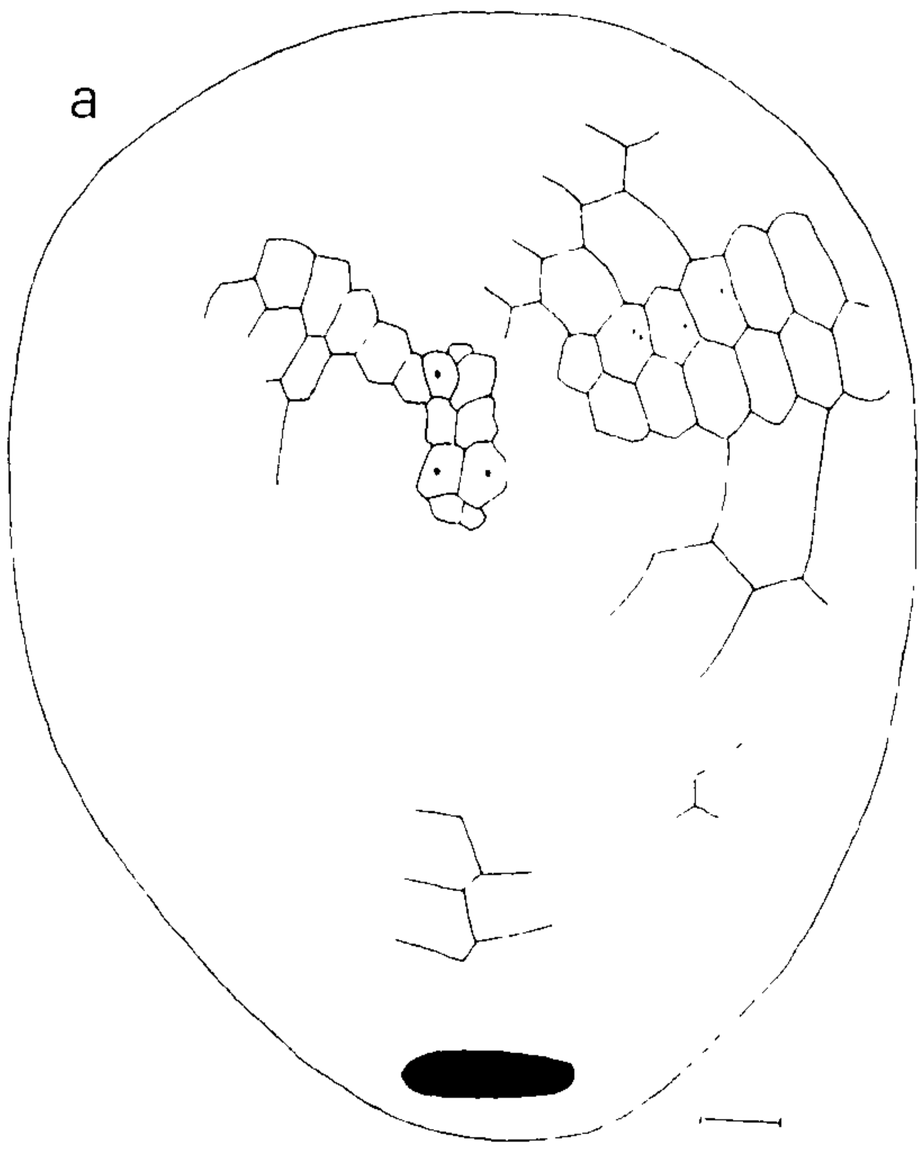
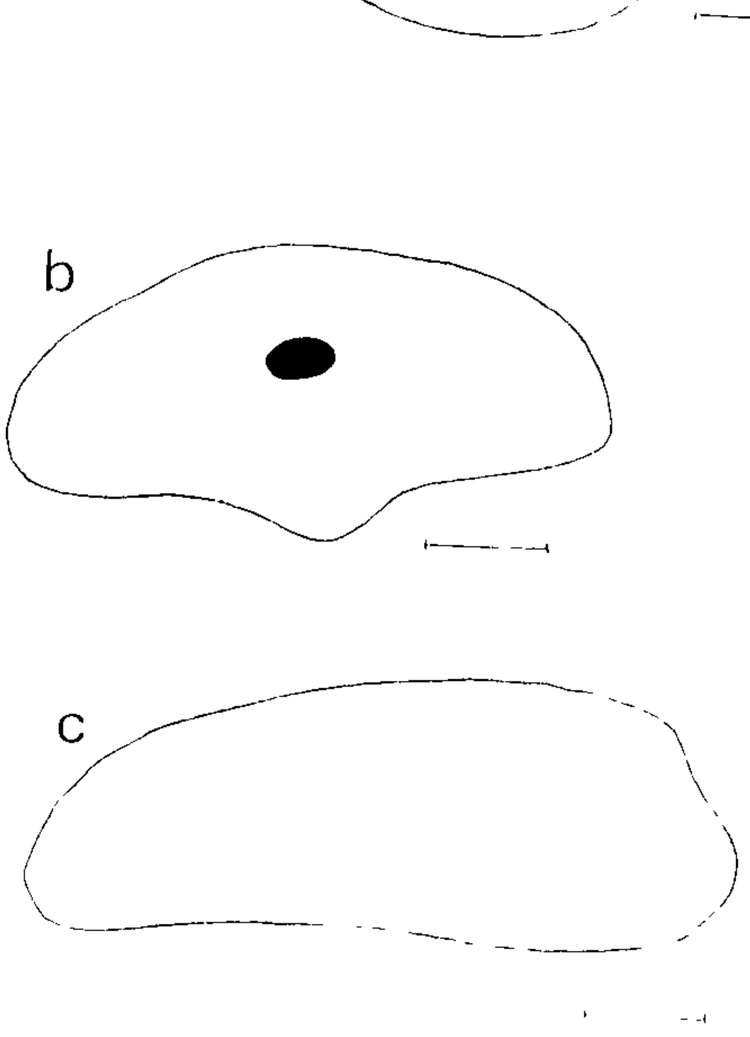
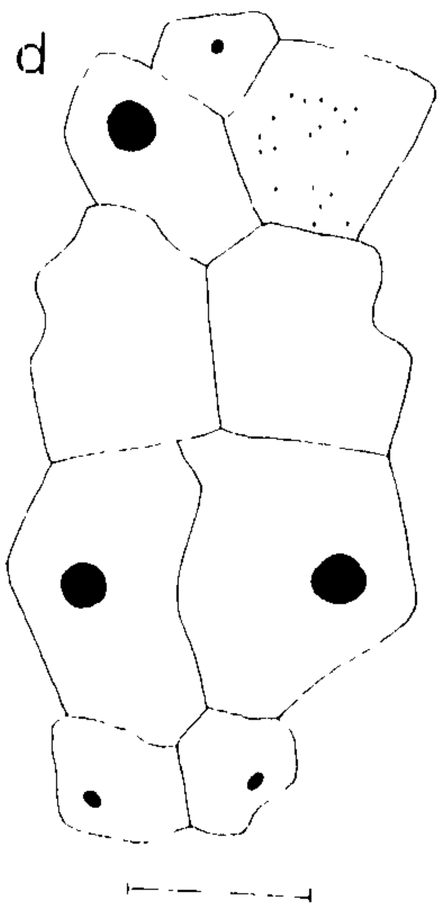

a
b
c
d

Figure 3.5. Camera lucida drawings of *Garumnaster michaleti* Lambert. a-d, MNHN no specimen number (HOLOTYPE), Danian of the French Pyrenees; a, apical view; b, posterior view; c, lateral view; d, apical disc plating. e, PI no specimen number, oral view. a & e, scale bars = 2 mm. b & c, scale bars = 5 mm. d, scale bar = 1 mm.


a

b


c


d

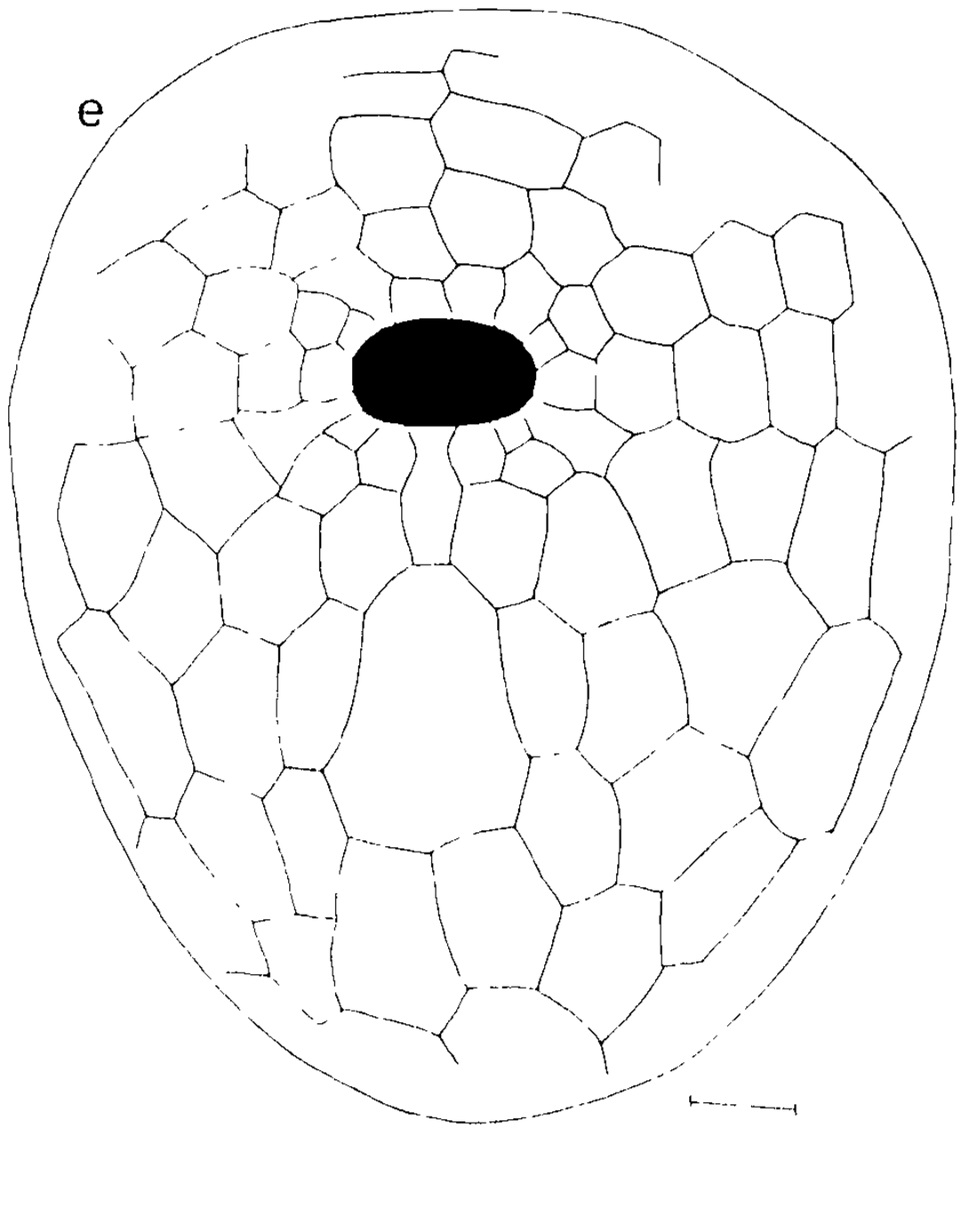
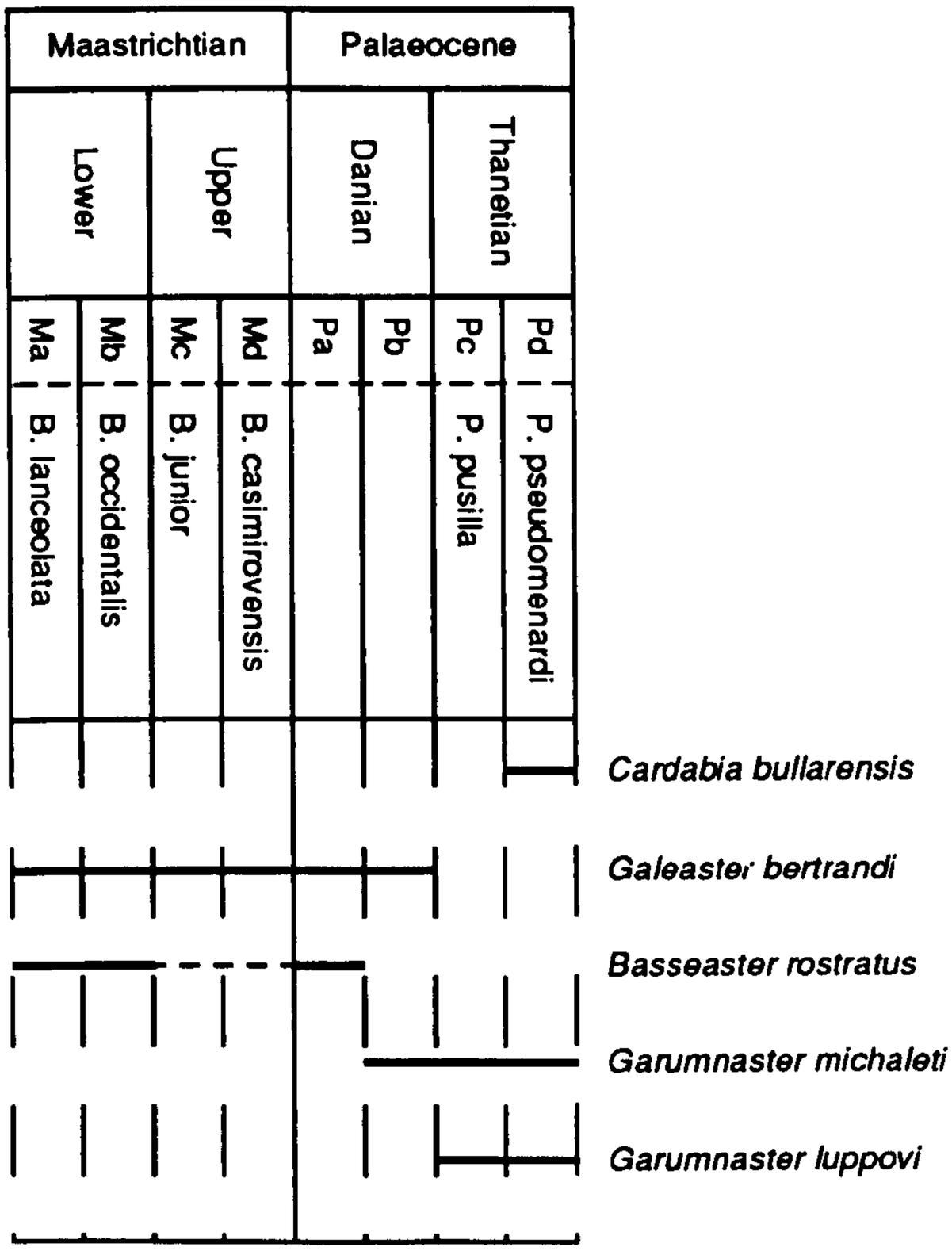

e

Figure 3.6. Range chart for Maastrichtian and Palaeocene species of Orthosternata. See Figure 3.2 for explanation of symbols.


Maastrichtian
Palaeocene
Lower
Upper
Danian
Thanetian
Ma
Mb
Mc
Md
Pa
Pb
Pc
Pd
B. lanceolata
B. occidentalis
B. junior
B. casimirovensis
P. pusilla
P. pseudomenardi
Cardabia bullarensis
Galeaster bertrandi
Basseaster rostratus
Garumnaster michaleti
Garumnaster luppovi

Family STEGASTERIDAE Lambert, 1917

Emended diagnosis. Deep frontal notch extending as parallel-sided groove to mouth. Orthosternous plastron without rostral plate. Paired ambulacra non- to sub-petaloid. May have marginal fasciole. No other fascioles.

KEY TO MAASTRICHTIAN GENERA

1	Marginal fasciole	2
	No fascioles	4
2	Supplementary gonopores in ocular plates	*Guettaria*
	No supplementary gonopores	3
3	Globular shape; paired ambulacra non-petaloid	*Pseudoffaster*
	Flat based test; paired ambulacra petaloid; distinct heel	*Rispolia*
4	Large scrobiculate tubercles on apical surface	*Tholaster*
	No large tubercles on apical surface	*Stegaster*

Genus STEGASTER Pomel, 1883

[Type species *Cardiaster gillieroni* de Loriol, 1873, by OD]

Synonyms. *Seunaster* Lambert *in* Blayac, 1912 (type species *Holaster bouillei* Cotteau *in* de Bouillé, 1873); *Synochitis* Lambert, 1917 (type species *Holaster bouillei* Cotteau).

Diagnosis. Thick test. Heart-shaped with sharply defined frontal notch reaching mouth. Ambulacral plates may be high. Pores in paired ambulacra small and round to somewhat elongate. Plastron orthosternous to disjunct. Apical system elongate with four gonopores. No fascioles.

Remarks. *Stegaster* and *Seunaster* are distinguished on the structure of the paired ambulacra. In *Stegaster*, ambulacral plates are high and pores are small and round. By contrast, *Seunaster* was erected for forms with lower ambulacral plates and more elongate pores in the paired ambulacra. However, specimens with intermediate morphologies exist

and form a gradational series between those with round pores and high ambulacral plates and those with elongate pores and lower ambulacral plates. Hence, the two genera are synonymized.

Stegaster is most similar to *Tholaster* from which it differs in having no enlarged tubercles on the apical surface and in having the highest point central or towards the anterior of the test. *Stegaster* differs from the remaining stegasterids, *Guettaria*, *Rispolia* and *Pseudoffaster* in lacking a marginal fasciole.

KEY TO MAASTRICHTIAN SPECIES

1	labrum and sternum separated by ambulacra	*S. cotteaui*
	labral and sternal plates in contact	2
2	elongate outline with highest point anterior	*S. bouillei*
	broad, cordate outline	3
3	domed or conical forms (height >50% TL); 1-2 ambulacral plates to each interambulacral plate	*S. altus*
	low forms (height <50% TL); more than 2 ambulacral plates to each interambulacral plate	*S. heberti*

Stegaster altus Seunes, 1889

(Plate 1, figures 5-9)

1889 *Stegaster altus* Seunes, p. 815, pl. 26, fig. 1.
1891 *Stegaster chalmasi* Seunes, p. 23, pl. 1, fig. 1, text figs 1-2.
1892 *Stegaster chalmasi* Seunes; Nicklès, p. 110.
1892 *Stegaster altus* Seunes; Nicklès, p. 111.
1931 *Stegaster novoi* Lambert, p. M6, pl. 1, figs 1-4.
1931 *Stegaster charlesi* Lambert, p. M7, pl. 1, figs 8-9.
1932 *Stegaster altus* Seunes; Lambert, p. 97.
1932 *Stegaster chalmasi* Seunes; Lambert, p. 98.
1934 *Lampadaster lamberti* Tzankov (*pars*), p. 211, pl. 4, fig. 2.
1934 *Stegaster* cfr. n. sp. Tzankov, p. 211, pl. 4, fig. 4.
1937 *Stegaster novoi* Lambert; Charles *in* Lambert & Charles, p. 381, text fig. 2.

1940 *Seunaster georgicus* Rouchadze, p. 95, 143, 164, pl. 1, fig. 3, text fig. 4.

1940 *Seunaster lazicus* Rouchadze, p. 97, 144, 165, pl. 1, fig. 4 , text fig 5.

1959 *Stegaster chalmasi* Seunes; Moskvin & Poslavskaya, p. 267, pl. 15, fig. 5, text fig. 74.

1964 *Stegaster chalmasi* Seunes; Poslavskaya & Solovjev, p. 179, pl. 33, fig. 2, text figs 213a, 214a.

1979 *Stegaster chalmasi* Seunes; Gongadze, p. 96, pl. 22, fig. 1.

1979 *Stegaster georgicus* (Rouchadze); Gongadze, p. 98, pl. 22, fig. 2, text fig. 21.

1995 *Stegaster novoi* Lambert; Gallemí *et al.*, table 1.

Occurrence. Maastrichtian of the French Pyrenees (Seunes 1889, 1891) and Bidart, France (BMNH). Maastrichtian of Navarra (BMNH) and Maastrichtian Quipar-Jorquera Formation of Alicante, Spain (Nicklès 1892; Lambert 1931; Gallemí *et al.* 1995) (BMNH, MGB, MNHN). Maastrichtian white chalk and Marnes de Bartine of northwest Turkey (Lambert 1931; Lambert & Charles 1937) (MNHN). Maastrichtian white limestone of Tunisia (Lambert 1932). Lower Maastrichtian Upper Chalk of Bulgaria (Tzankov 1934). Lower to Upper Maastrichtian of Georgia (Rouchadze 1940; Gongadze 1979). Lower Maastrichtian of the Northern Caucasus (Moskvin & Poslavskaya 1959; Poslavskaya & Solovjev 1964) (Pl).

Diagnosis. Circular outline. Flat lower surface. Upper surface domed to conical. Posterior truncate. Frontal groove very deep at ambitus and on oral surface. Ambulacral plates high with small round pores.

Remarks. Specimens referred to *S. chalmasi* and *S. georgicus* have a conical rather than domed upper surface. However, within populations, specimens with all intermediate morphologies exist and hence all three species are treated as synonymous. *S. charlesi* represents small, slightly elongate specimens of this species.

Stegaster bouillei (Cotteau *in* de Bouillé, 1873)

(Figure 3.7)

1873 *Holaster bouillei* Cotteau *in* de Bouillé, p. 450.

1889 *Stegaster bouillei* Cotteau; Seunes, p. 816, pl. 26, fig. 2.

1892 *Stegaster bouillei* Seunes; Nicklès, p. 111.

1932 *Stegaster bouillei* Seunes; Lambert, p. 98.

1934 *Lampadaster lamberti* Tzankov (*pars*), p. 211, pl. 1 , fig. 1.

1937 *Seunaster lamberti* Charles *in* Lambert & Charles, p. 383, pl. 8, figs 6-8.

1940 *Seunaster* cf. *bouihei* Cotteau; Rouchadze, p. 164.

1940 *Cardiotaxis heberti* Cotteau; Rouchadze, p. 89, 141, 162, text fig. 2.

1940 *Cardiotaxis* sp. indet. Rouchadze, p. 90, 141, 163, pl. 1, fig. 1, text fig. 3.

1959 *Seunaster altus* (Seunes); Moskvin & Poslavskaya, p. 268, pl. 15, fig. 7, text fig. 76.

1959 *Seunaster lamberti* Charles; Moskvin & Poslavskaya, p. 268, pl. 16, fig. 1, text fig. 77.

1964 *Seunaster lamberti* Charles; Poslavskaya & Solovjev, p. 12, pl. 34, fig. 1, text figs 213d, 214d.

1979 *Seunaster lamberti* Charles; Gongadze, p. 100, pl. 23, fig. 1.

1995 *Stegaster* sp. Gallemí *et al.*, table 1.

Occurrence. Maastrichtian of the French Pyrenees (Seunes 1889) (BMNH). Maastrichtian of Navarra (BMNH) and Maastrichtian Quipar-Jorquera Formation of Alicante, Spain (Nicklès 1892; Gallemí *et al.* 1995) (BMNH, MGB). Lower to Upper Maastrichtian of Zumaya, Spain (UWBM). Maastrichtian white chalk of northwestern Turkey (Lambert & Charles 1937) (MNHN) and Maastrichtian white limestone of Tunisia (Lambert 1932). Lower Maastrichtian Upper Chalk of Bulgaria (Tzankov 1934). Lower to Upper Maastrichtian of Georgia (Rouchadze 1940; Gongadze 1979), Kopet Dag (Poslavskaya & Solovjev 1964), the Crimea and the Northern Caucasus (Moskvin & Poslavskaya 1959) (PI).

Diagnosis. Elongate outline tapering to posterior. Highest anteriorly. Truncate posterior. Ambulacral plates low with elongate pores placed *en chevron*.

***Stegaster cotteaui* Seunes, 1889**

(Plate 2, figures 1-4; Figure 3.8)

1889 *Stegaster cotteaui* Seunes, p. 813, pl. 25, fig. 3.

?1931 *Stegaster mairei* Lambert, p. M8, pl. 1, figs 12-13.

Occurrence. Maastrichtian of the French Pyrenees (Seunes 1889) (MNHN) and Biarritz, France (BMNH). Lower to Upper Maastrichtian of Zumaya, Spain (UWBM). ?Maastrichtian of Senegal (Lambert 1931) (MNHN).

Diagnosis. Low forms with disjunct orthosternous plastron. Ambulacral plates high with small, round pores.

Remarks. Specimens referred to *S. cotteaui* are commonly crushed. *S. mairiei* is identical in all respects other than the fact that the test is somewhat globular. It appears to represent an uncrushed specimen of *S. cotteaui*. *S. cotteaui* resembles *S. heberti* from which it is distinguished by having higher ambulacral plates and a disjunct plastron.

However, *S. cotteaui* is most similar to *Sanchezaster habanensis* from the Eocene of Cuba. Both have very high, hexagonal ambulacral plates, a disjunct plastron and a circular mouth at the end of a deep frontal groove. *S. habanensis* differs in having single pores placed centrally on the ambulacral plates and in the presence of a distinct marginal fasciole.

Stegaster heberti Seunes, 1889

1889 *Stegaster heberti* Seunes, p. 812, pl. 25, figs 1-2.

?1931 *Stegaster* cf. *zonarius* Lambert, p. M7, pl. 1, fig. 7.

Occurrence. Maastrichtian of the French Pyrenees (Seunes 1889) (MNHN) and ?white chalk of northwestern Turkey (Lambert 1931) (MNHN).

Diagnosis. Low forms with labral and sternal plates in broad contact. Ambulacral plates somewhat lower than in *S. cotteaui*.

Stegaster sp. indet.

1979 *Seunaster* sp. Gongadze, p. 101, pl. 23, fig. 2.

Occurrence. Upper Maastrichtian of Georgia.

Remarks. Poorly preserved material. Specific identification impossible.

Genus THOLASTER Seunes, 1891

[Type species *Gibbaster munieri* Seunes, 1889, by OD]

Synonym. *Gibbaster* Seunes, 1889. *non Gibbaster* Gauthier, 1887.

Diagnosis. Ovate outline with deep frontal groove. Highest point towards posterior. Anterior portion of upper surface concave. All ambulacra non-petaloid with small, round pores. Ambulacral plates high. Apical system ethmophract with four gonopores. Plastron orthosternous. No fascioles. Very large tubercles around apex and along edges of frontal groove.

Remarks. Distinguished from all other stegasterids by its posterior apical system and very large tubercles on the apical surface.

Tholaster munieri (Seunes, 1889)

(Plate 3, figures 1-3; Figure 3.9)

1889 *Gibbaster munieri* Seunes, p. 819, pl. 27, fig. 1.

1891 *Tholaster munieri* (Seunes); Seunes, p. 23.

Occurrence. Maastrichtian of the French Pyrenees (Seunes 1889, 1891) (BMNH, MNHN) and Upper Maastrichtian of Zumaya, Spain (UWBM).

Diagnosis. As generic diagnosis.

Genus PSEUDOFFASTER Lambert *In* Lambert & Thiéry, 1924

[Type species *Offaster caucasicus* Dru, 1884, by OD]

Diagnosis. Gibbous profile with highly inflated upper surface and convex lower surface. Unpaired ambulacrum deeply sunken on oral surface, reaching mouth. All ambulacra non-petaloid with small, round pores. Ambulacral plates high. Plastron orthosternous. Apical system elongate with four gonopores. Marginal fasciole. Large tubercles at apex, along edges of frontal groove and in interambulacra 1 and 4 on oral surface.

Remarks. Like *Rispolia* and *Guettaria*, *Pseudoffaster* has a marginal fasciole. However, it differs from both *Rispolia* and *Guettaria* in its gibbous profile with inflated lower surface. It differs additionally from *Guettaria* in lacking supplementary gonopores in the apical system.

Pseudoffaster caucasicus (Dru, 1884)

(Plate 2, figures 5-8; Figure 3.10)

1884 *Offaster caucasicus* Dru, p. 514, pl. 26, figs 5-10.

1899 *Stegaster caucasicus* (Dru); Anthula, p. 63, pl. 2, figs 7-8.

1927 *Pseudoffaster caucasicus* (Dru); Lambert, p. 42.

1938 *Pseudoffaster caucasicus* (Dru); Schmidt, p. 78, pl. 25, figs 6-9, pl. 26, figs 4-7.

1938 *Pseudoffaster renngarteni* Schmidt, p. 80, pl. 25, figs 1-5, pl. 26, figs 1-3.

1940 *Pseudooffaster caucasicus* (Dru); Rouchadze, p. 93, 142, 163.

1959 *Pseudoffaster renngarteni* Schmidt; Moskvin & Poslavskaya, p. 271, pl. 17, fig. 3, text fig. 81.

1964 *Pseudoffaster caucasicus* (Dru); Poslavskaya & Solovjev, p. 179, pl. 33, fig. 5, text figs 213c, 214c.

1979 *Pseudoffaster renngarteni* Schmidt; Gongadze, p. 105, pl. 24, fig. 3.

1979 *Pseudoffaster* sp. Gongadze, p. 106, pl. 25, fig. 1.

1997b *Pseudoffaster caucasicus* (Dru); Jeffery, p. 698, pl. 8, figs 4-7, text fig. 14.

Occurrence. Upper Maastrichtian of the northern Caucasus (Dru 1884; Anthula 1899; Schmidt 1938; Moskvin & Poslavskaya 1959) (Pl) and Kazakhstan (Jeffery 1997b) (BMNH). Maastrichtian of Kopet Dag, the Northern Caucasus and Kazakhstan (Poslavskaya & Solovjev 1964). Lower to Upper Maastrichtian of Georgia (Rouchadze 1940; Gongadze 1979). Lower Maastrichtian Cabo de Late Formation of Santander (BMNH) and Areny Sandstone of Tremp (Lambert 1927), Spain.

Diagnosis. As generic diagnosis.

Remarks. *P. caucasicus* and *P. schmidti* are both recorded from the Campanian of the former Soviet Union, whilst *P. renngarteni* has been collected exclusively from Maastrichtian strata. However, all three species are distinguished merely on subtleties of shape and size and form a gradational series. There appear to be no structural differences on which to differentiate them and they are consequently synonymized.

Genus RISPOLIA Lambert, 1917

[Type species *Nucleolites subtrigonatus* Catullo, 1827, by OD]

Diagnosis. Test with high vaulted upper surface and flat oral surface, sharp frontal notch reaching mouth and bi-lobed subanal heel. Paired ambulacra form open petals with

somewhat elongate pores. Plastron orthosternous. Apical system elongate with four gonopores. Marginal fasciole.

Remarks. Most similar to *Guettaria*, from which it differs in lacking supplementary gonopores in the ocular plates of the apical system.

Rispolia subtrigonata (Catullo, 1827)

(Plate 3, figures 4-6; Figure 3.11)

1827 *Nucleolites subtrigonatus* Catullo, p. 226, pl. 2, fig. Dd.
1892 *Cardiaster subtrigonatus* (Catullo); Gauthier, p. 34, pl. 1, figs 10-13, pl. 2, figs 1-2.
1909 *Cardiaster subtrigonatus* (Catullo); Cottreau *in* Blayac & Cottreau, p. 426.
1924 *Rispolia subtrigonata* (Catullo); Dalloni, p. 117.
1932 *Rispolia subtrigonata* (Catullo); Lambert, p. 75.
1987 *Rispolia subtrigonata* (Catullo); Zagbib-Turki, p. 293, text figs 100-101.

Occurrence. Maastrichtian of Constantine (Blayac & Cottreau 1909; Lambert 1932) and Oran, Algeria (Dalloni 1924; Lambert 1932). Also known from the Coniacian / Santonian of Tunisia (Gauthier 1892; Zagbib-Turki 1987) (MNHN) and originally described from the Coniacian of Scaglia, Italy (Catullo 1827) (BMNH).

Diagnosis. Broad frontal groove with anterior interambulacra forming rounded keels. Pores in paired petals only slightly elongate.

Rispolia douvillei Lambert *in* Lambert & Thiéry, 1924

1924 *Rispolia* nov. sp. Dalloni, p. 117.
1924 *Rispolia douvillei* Lambert *in* Lambert & Thiéry, p. 413, pl. 11, figs 4-6.
1932 *Rispolia douvillei* Lambert, p. 75.
1937 *Rispolia douvillei* Lambert, p. 79.
1959 *Rispolia douvillei* Lambert; Petitot, p. 161.

Occurrence. Maastrichtian of Oran, Algeria (Dalloni 1924; Lambert & Thiéry 1924; Lambert 1932) (MNHN) and Morocco (Lambert 1937; Petitot 1959).

Diagnosis. Differs from *R. subtrigonata* in having a more pronounced frontal groove starting closer to apex with more carinate adjoining interambulacra. *R. douvillei* also has more elongate pores in the paired ambulacra.

Rispolia sp. indet.

Occurrence. Early Maastrichtian reworked nodules of the Kangilia Formation of East Greenland (DGFMM).

Remarks. Differs from *R. subtrigonata* in having widest point at mid-length, a more truncate posterior and a lower periproct. However, material is not well enough preserved to allow specific identification.

Rispolia? sp. indet.

Occurrence. Upper Danian of Aristregui, Navarra, Spain (MGB).

Remarks. The two available specimens resemble *Rispolia* in the sharp keels adjoining the anterior sulcus and the deep non-parallel sided groove on the oral surface. However, no marginal fasciole is visible although this could be due to poor preservation. This is the first record of an unequivocable post-Maastrichtian stegasterid.

Genus GUETTARIA Gauthier, 1887

[Type species *Guettaria angladei* Gauthier, 1887, by OD]

Diagnosis. Thick test with flat base and bi-lobed subanal heel. Deep, sharp frontal groove reaches mouth. Paired ambulacra form open petals. Apical system elongate with two supplementary genital pores in each of ocular plates II and IV. Plastron orthosternous. Marginal fasciole immediately above ambitus. Very large tubercles scattered on apical surface.

Remarks. Easily distinguished from all other stegasterids by its supplementary gonopores in the ocular plates of the apical system.

Guettaria rocardi Cotteau, 1889

(Plate 2, figures 9-12; Figure 3.12)

1889 *Guettaria rocardi* Cotteau, p. 87.

1896 *Guettaria rocardi* Cotteau; Lambert, p. 314, pl. 10, figs 1-3, text figs 1-2.

1897 *Guettaria danglesi* Gauthier, p. 831, pl. 24, figs 1-8.

1930 *Guettaria rocardi* Cotteau; Besairie, p. 232, pl. 24, fig. 3.

1931 *Tholaster fourmarieri* Lambert, p. M8, pl. 1, figs 5-6.

1959 *Guettaria rocardi* Cotteau; Moskvin & Poslavskaya, p. 269, pl. 16, figs 2-3, text fig. 78.

1964 *Guettaria rocardi* Cotteau; Poslavskaya & Solovjev, p. 179, pl. 33, figs 1-3, text figs 213b, 214b.

1979 *Guettaria* cf. *rocardi* Cotteau; Gongadze, p. 102, pl. 24, fig. 1, text fig. 22.

1987 *Guettaria fourmarieri* (Lambert); Zagbib-Turki, p. 287, pl. 14, figs 12-21, text. fig. 99.

Occurrence. Lower Maastrichtian of northeastern Madagascar (Cotteau 1889; Lambert 1896; Besairie 1930; Collignon 1968) (BMNH, MNHN). Maastrichtian Marnes de Bartine of northwestern Turkey (Lambert 1931) (MNHN). Lower Maastrichtian of Georgia (Gongadze 1979) and the northern Caucasus (Moskvin & Poslavskaya 1959) (PI). Maastrichtian of Kopet Dag, Georgia and the northern Caucasus (Poslavskaya & Solovjev 1964). Maastrichtian of Oran, Algeria (Gauthier 1897) (MNHN). Uppermost Campanian of northern Tunisia (Zagbib-Turki 1987).

Diagnosis. Large tubercles on upper surface encircle test just above ambitus.

Remarks. Of the three specimens studied by Zagbib-Turki (1987), two were found in Uppermost Campanian deposits. The third specimen came from the collections of the Faculté des Sciences, Tunis and was labelled "Maastrichtian" but it is likely that this is also from older deposits.

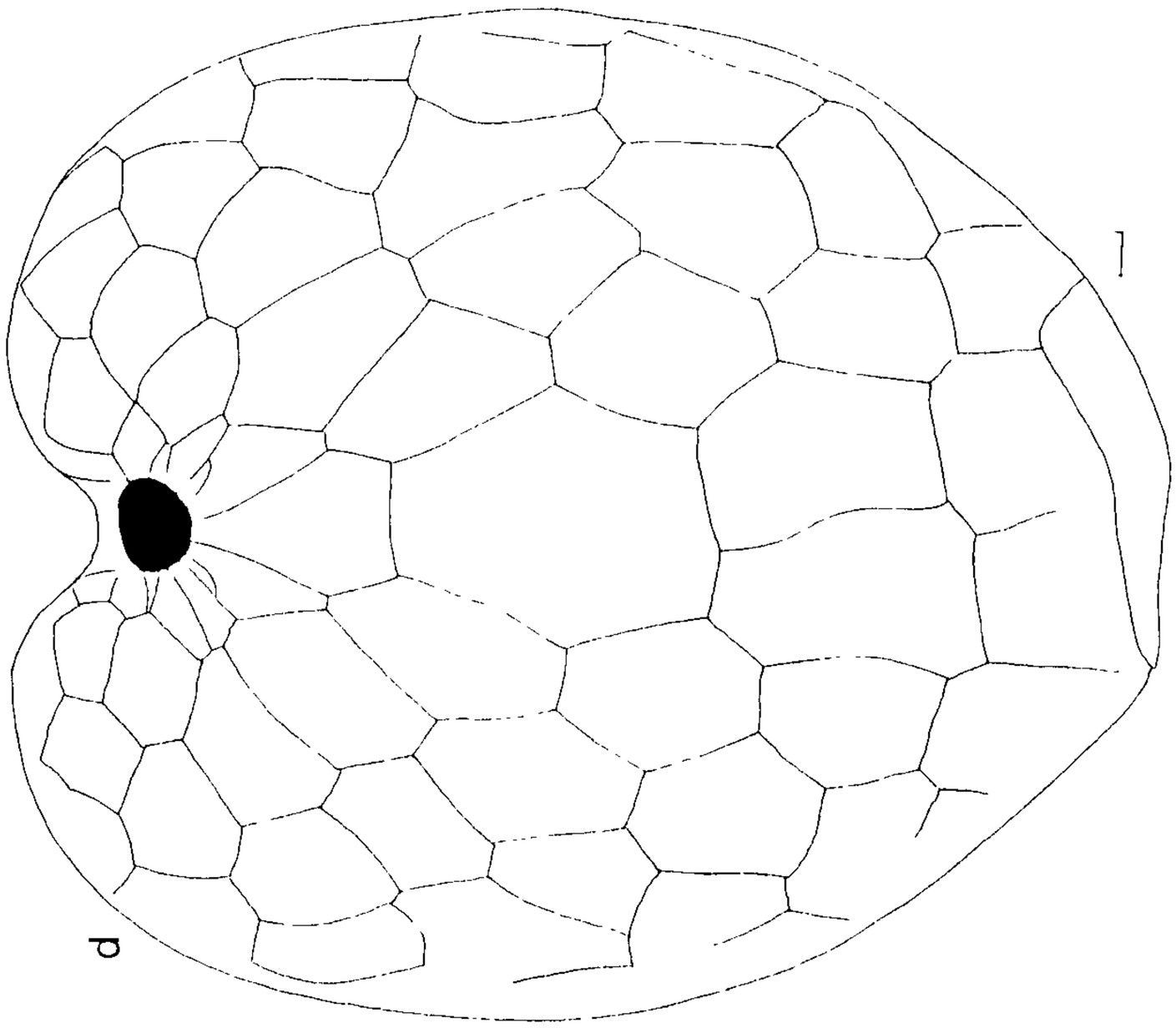
Guettaria fecunda Schulz, 1983

1983 *Guettaria fecunda* Schulz, p. 718, pl. 1, figs 2-3, text fig. 2d.

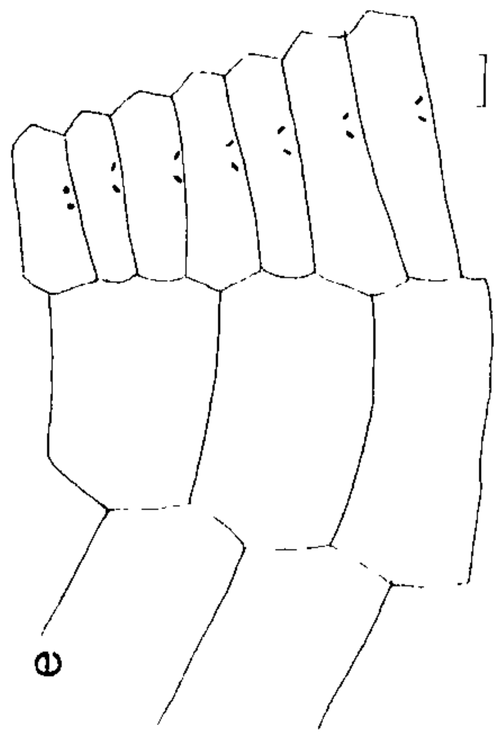
Occurrence. Lower Maastrichtian *Inoceramus* Marls of Bavaria.

Diagnosis. Large tubercles on upper surface positioned close to apex and low down in anterior interambulacra. Supplementary gonopore on ocular plate III. Less distinct subanal keel than *G. rocardi*.

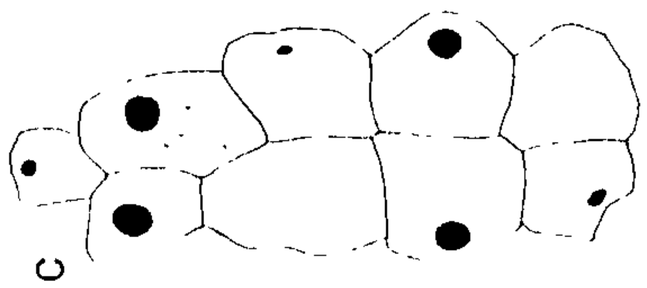
Figure 3.7. Camera lucida drawings of *Stegaster bouillei* (Cotteau). a & b, BMNH EE6066, Maastrichtian Quipar-Jorquera Formation of Alicante, Spain; a, apical view; b, lateral view. c & d, PI 1584, Maastrichtian of the Northern Caucasus; c, apical disc plating; d, oral view. e, UWBM 94994, Maastrichtian of Zumaya, Spain, detail of ambulacrum V. a & b, scale bars = 5 mm. c, scale bar = 1 mm. d & e, scale bars = 2 mm.



d



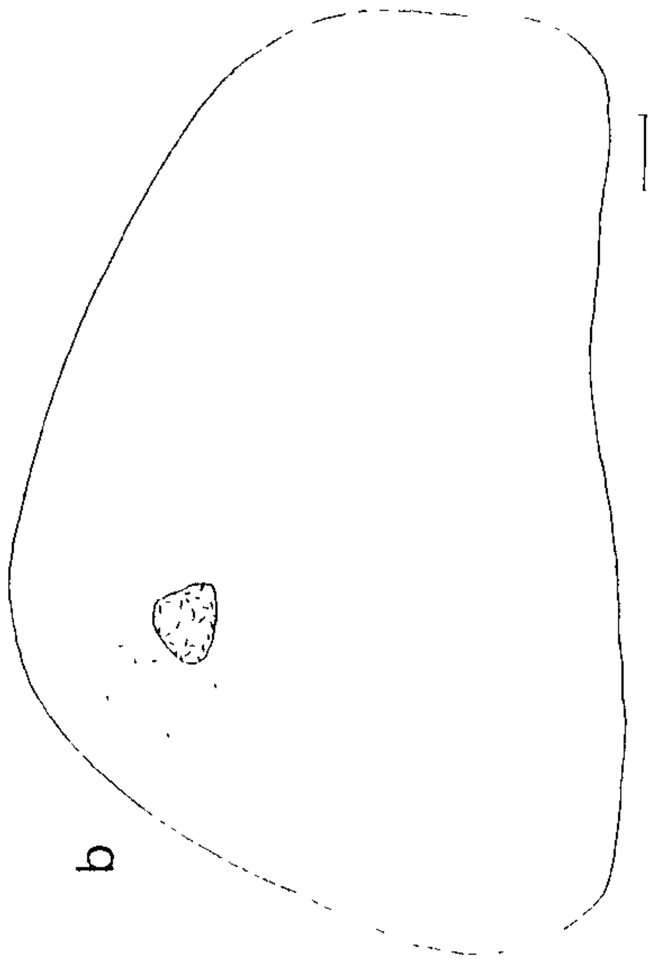
e



c



a



b

Figure 3.8. Camera lucida drawings of *Stegaster cotteaui* Seunes, BMNH E2916, Maastrichtian of Biarritz, France; a, apical view; b, oral view; c, detail of ambulacral structure showing ambulacra V and I. a, scale bar = 5 mm. b & c, scale bars = 2 mm.

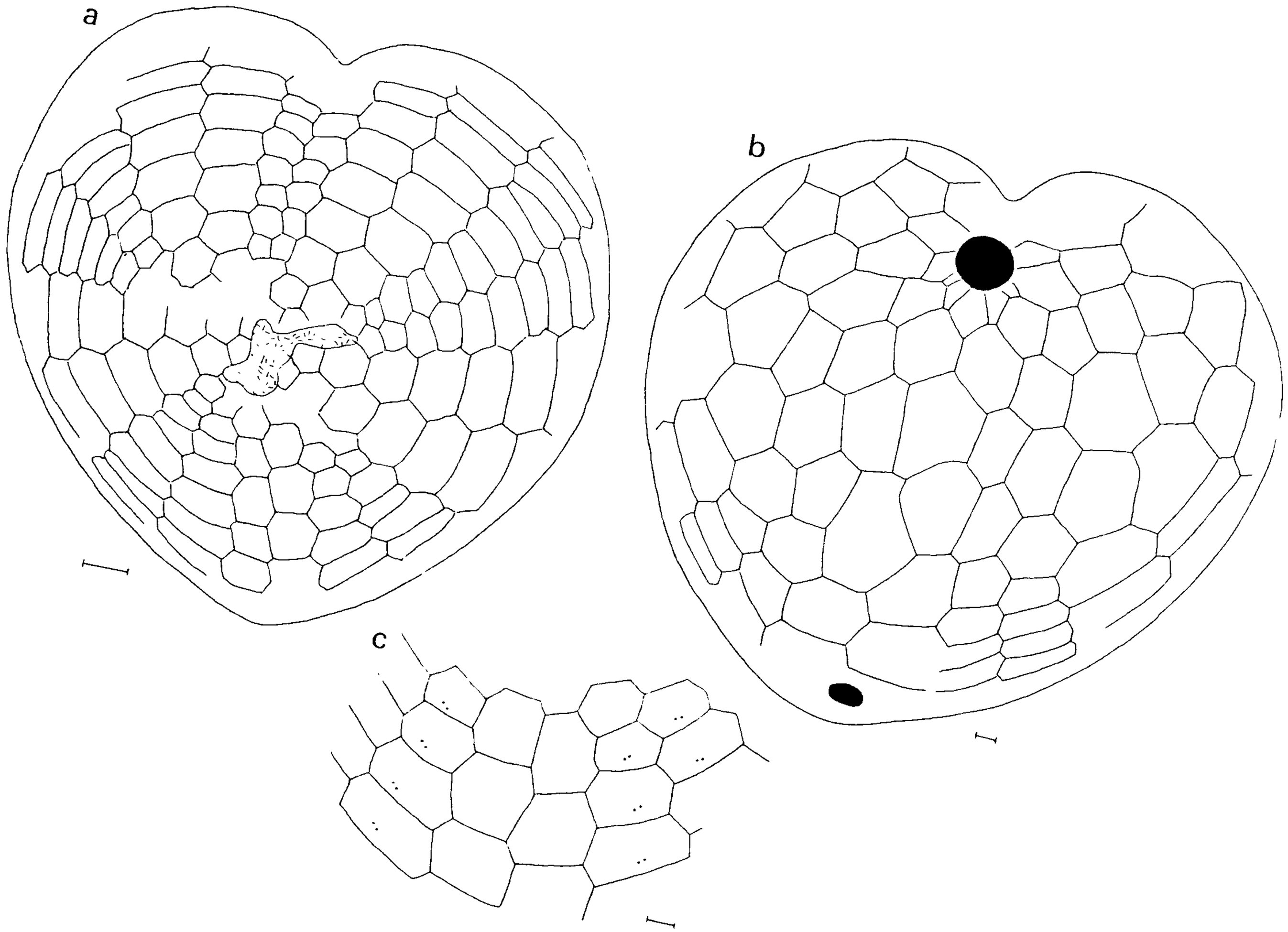

a
1
b
1
c
1

Figure 3.9. Camera lucida drawings of *Tholaster munieri* (Seunes). a-c, UWBM 94993, Maastrichtian of Zumaya, Spain; a, apical view; b, oral view; c, lateral view. d, Museum d'Histoire Naturelle, Paris 1260, Maastrichtian of Gan, Pyrenees, apical disc plating. a-c, scale bars = 5 mm. d, scale bar = 1 mm.

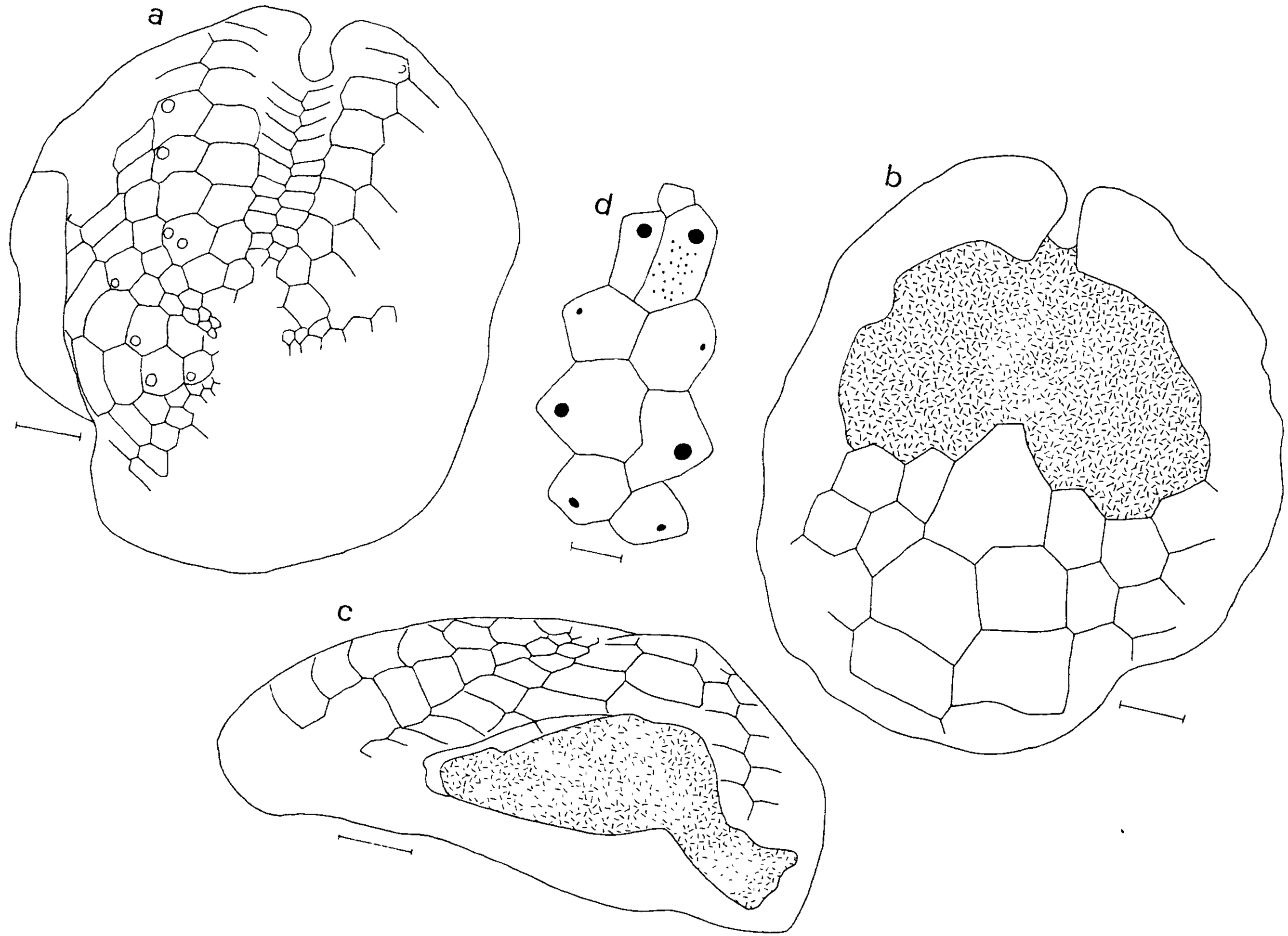
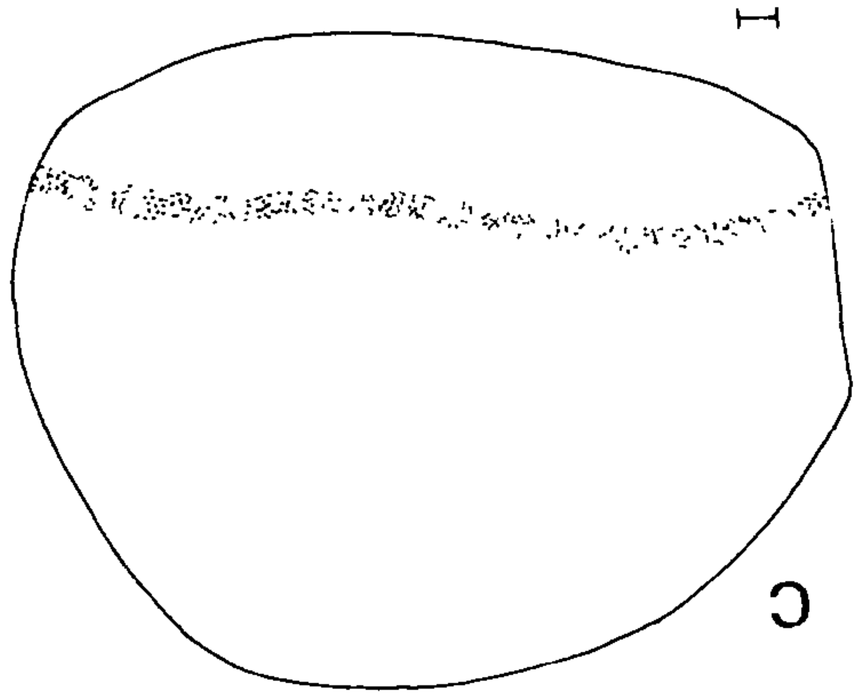
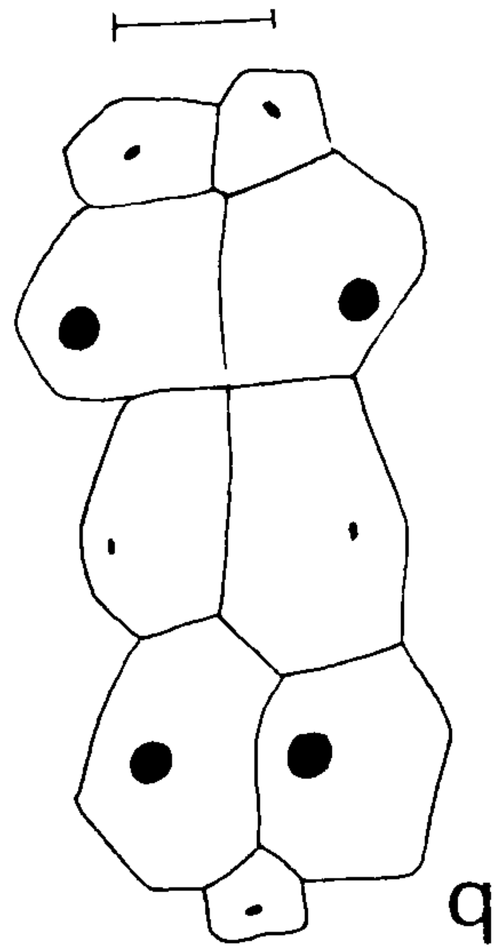

a
d
b
c

Figure 3.10. Camera lucida drawings of *Pseudoffaster caucasicus* (Dru), BMNH EE5573, Upper Maastrichtian of Mangyshlak, Kazakhstan; a, oral view; b, apical disc plating; c, lateral view. Scale bars = 1 mm.


c


b

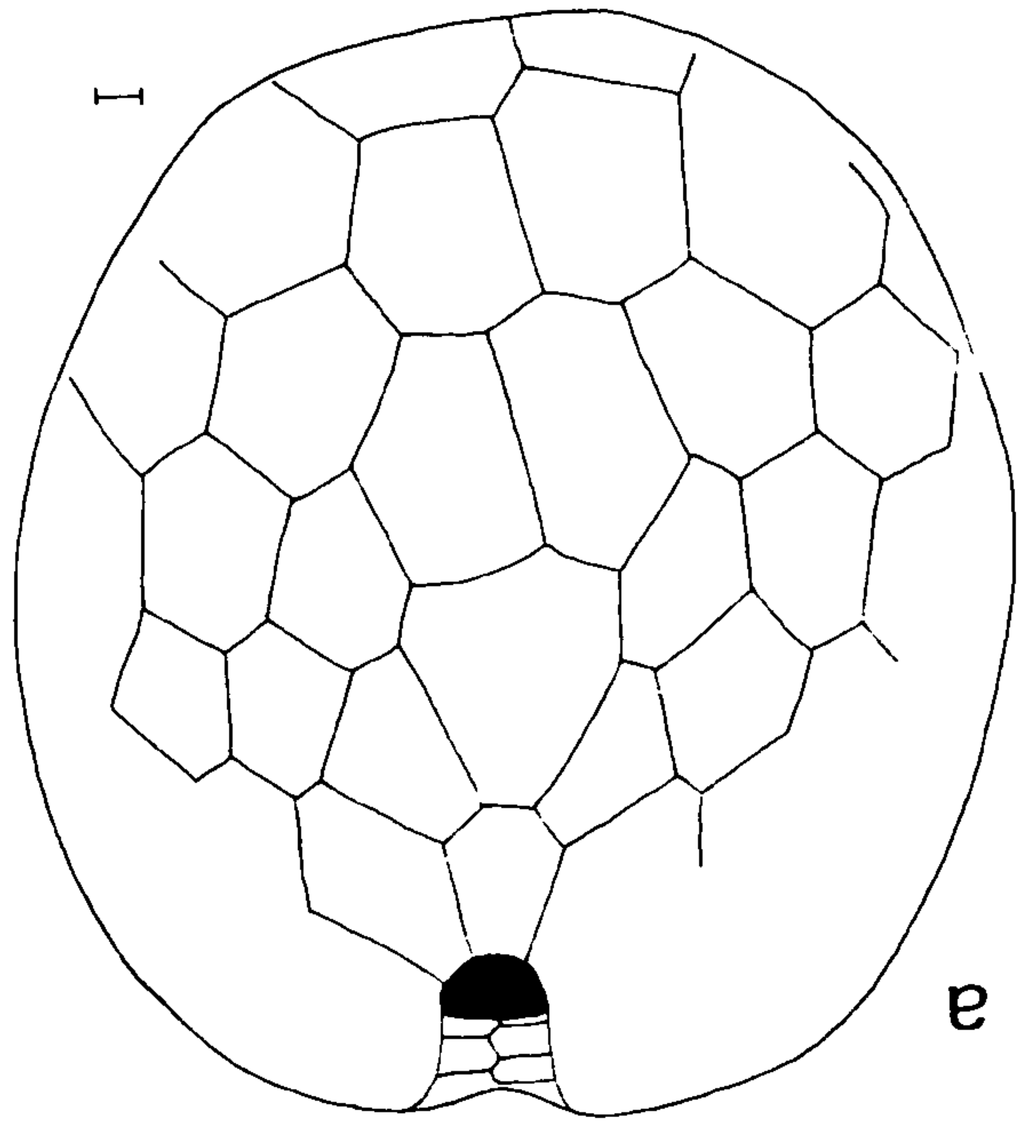
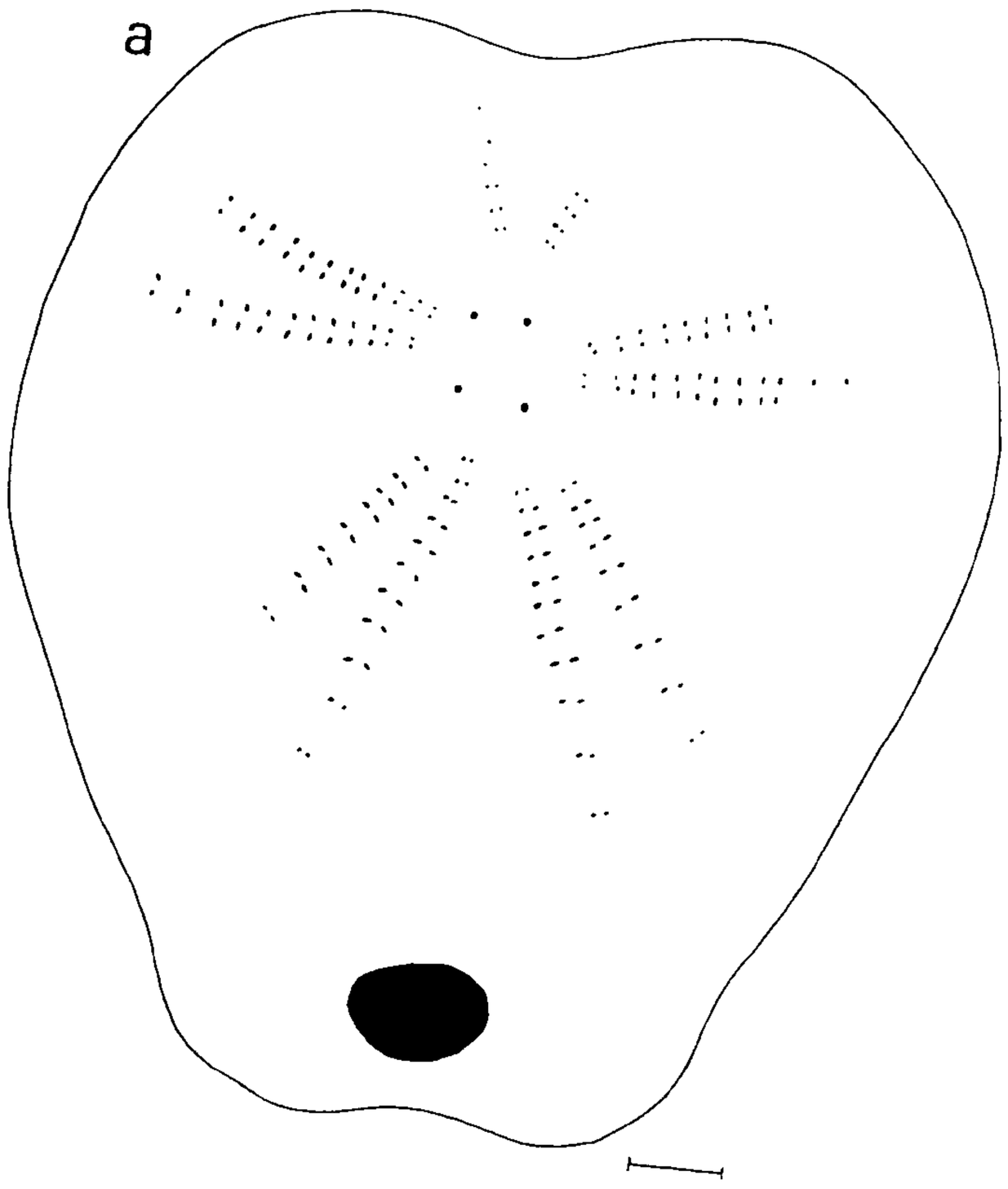
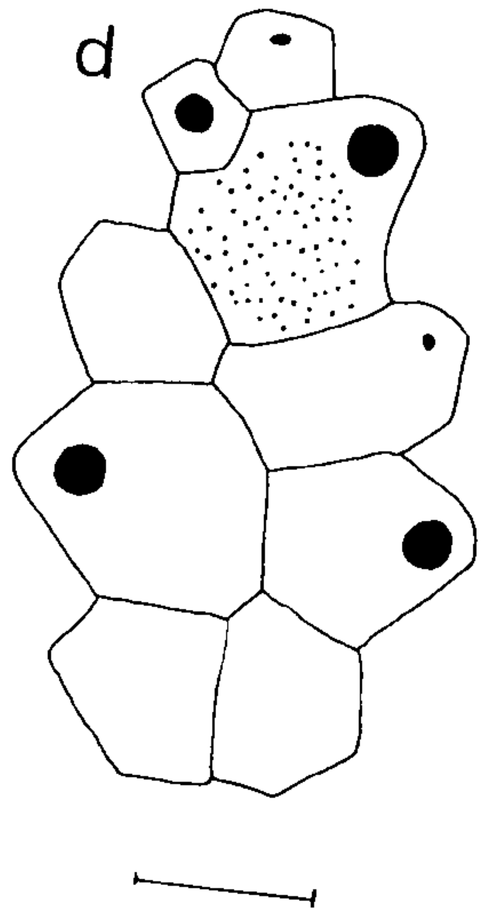
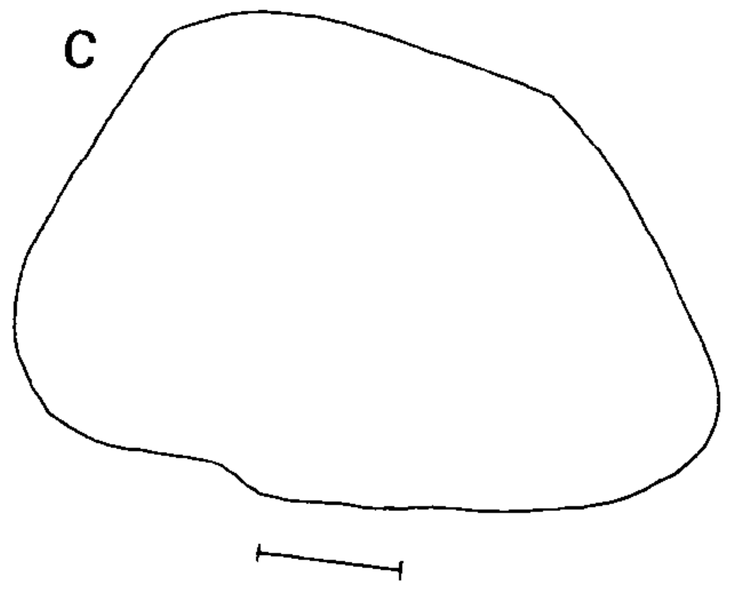

a

Figure 3.11. Camera lucida drawings of *Rispolia subtrigonata* (Catullo), MNHN (Lambert Collection) no specimen number, Maastrichtian of Constantine, Algeria; a, apical view; b, oral view; c, lateral view; d, apical disc plating. a & b, scale bars = 2 mm. c, scale bar = 5 mm. d, scale bar = 1 mm.


a


d


c

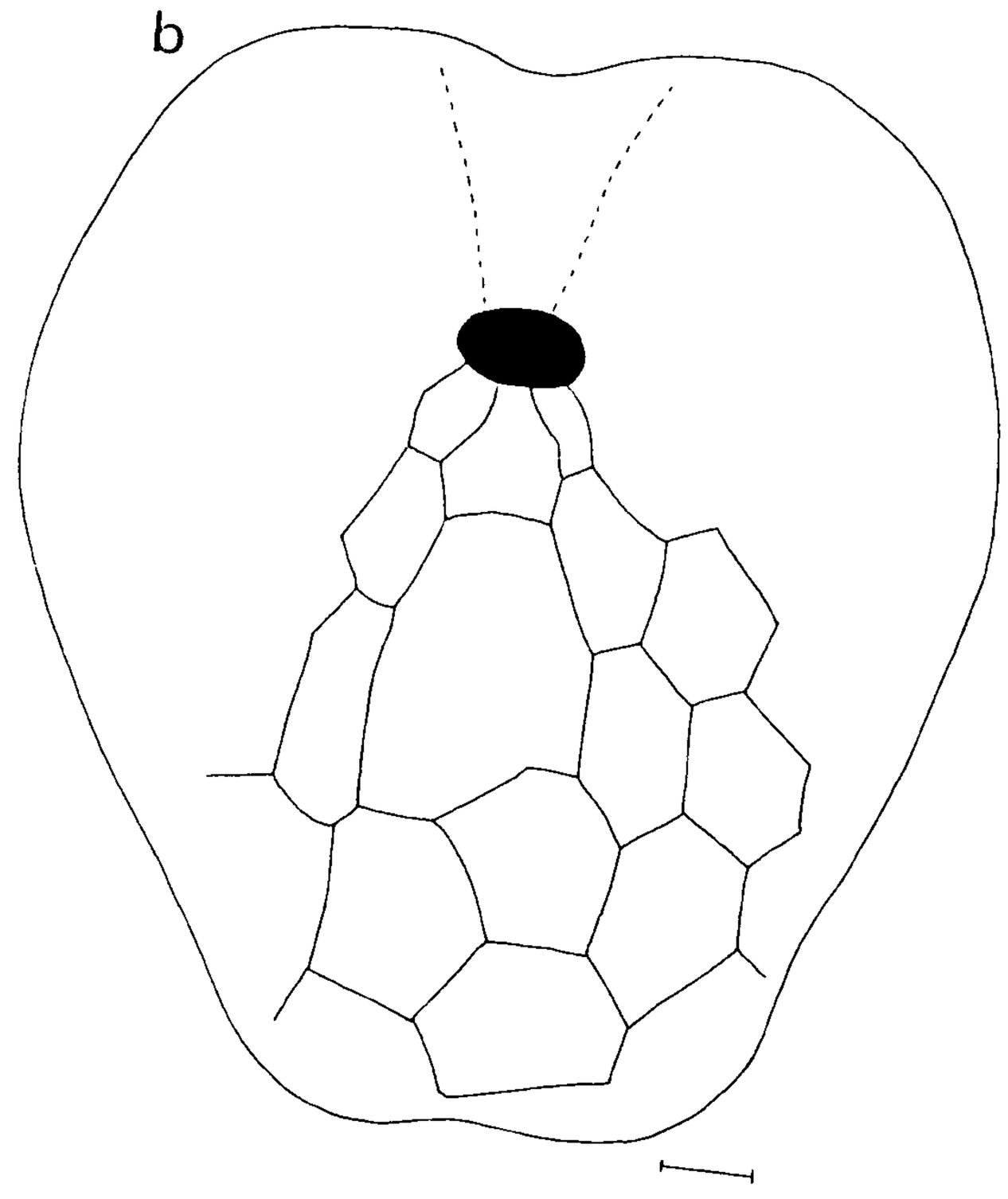
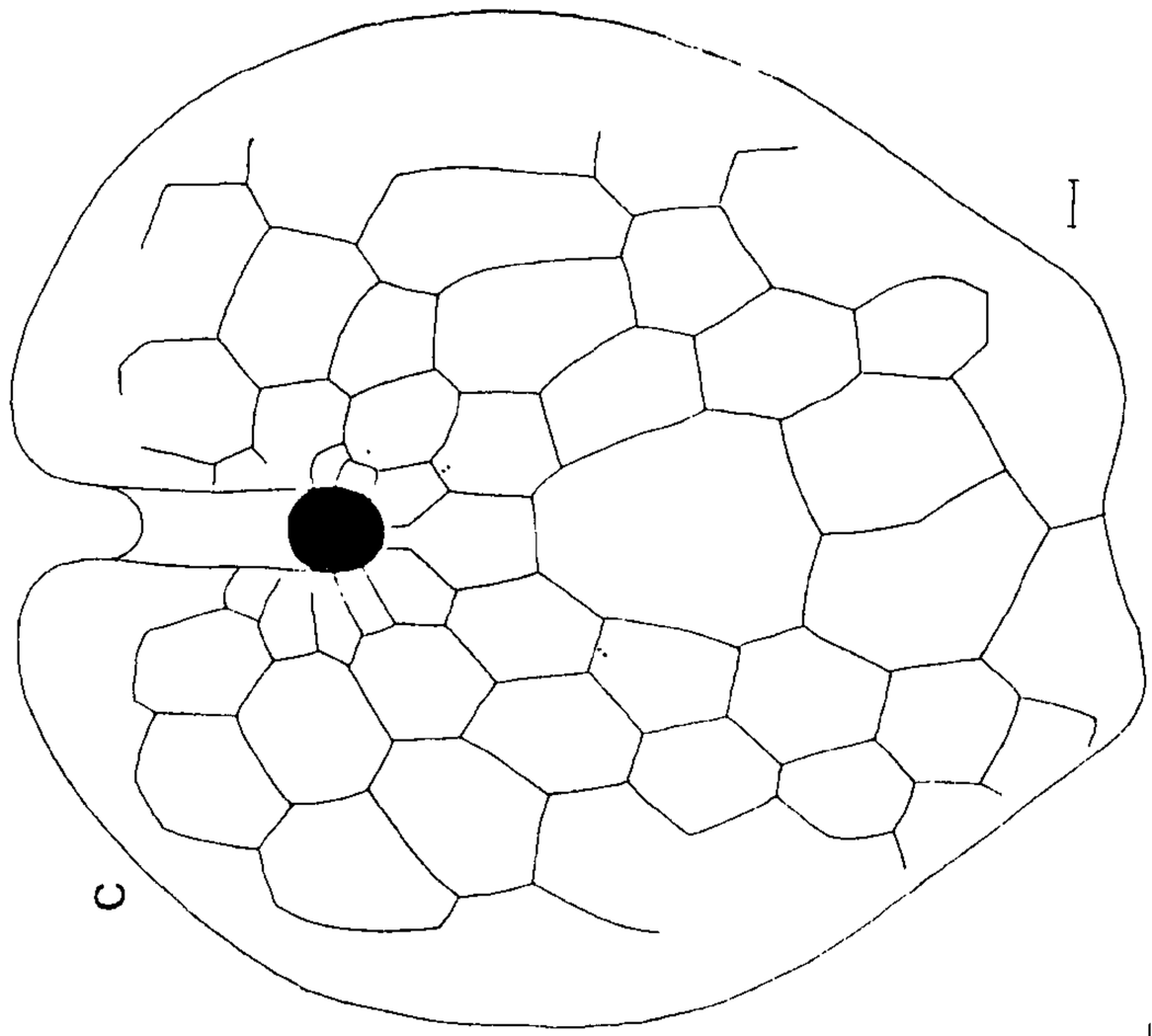
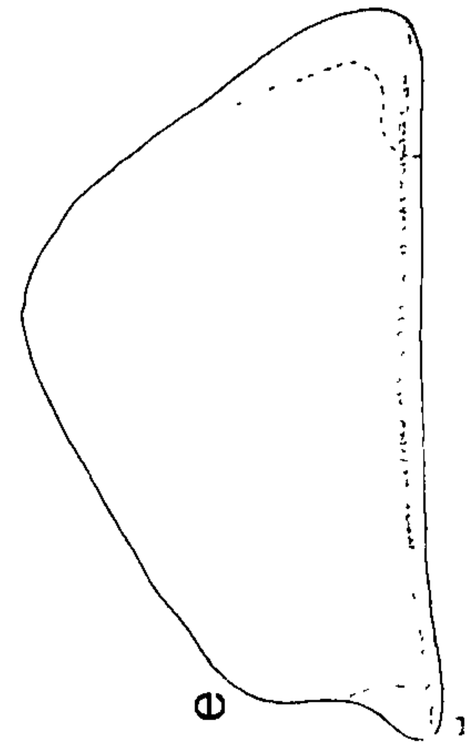

b

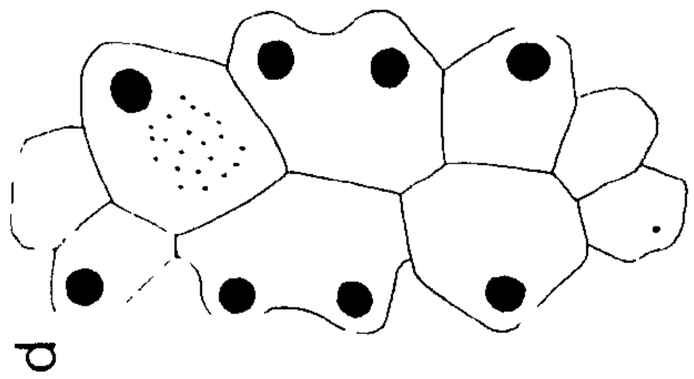
Figure 3.12. Camera lucida drawings of *Guettaria rocardi* Cotteau. a-d, Lower Maastrichtian of northern Madagascar. a & b, BMNH E18706; a, apical view; b, detail of ambulacrum IV. c & d, MNHN no specimen number (HOLOTYPE); c, oral view; d, apical disc plating. e, PI 722, Maastrichtian of the northern Caucasus; lateral view. a, scale bar = 5 mm. c & e, scale bars = 2 mm. b & d, scale bars = 1 mm.



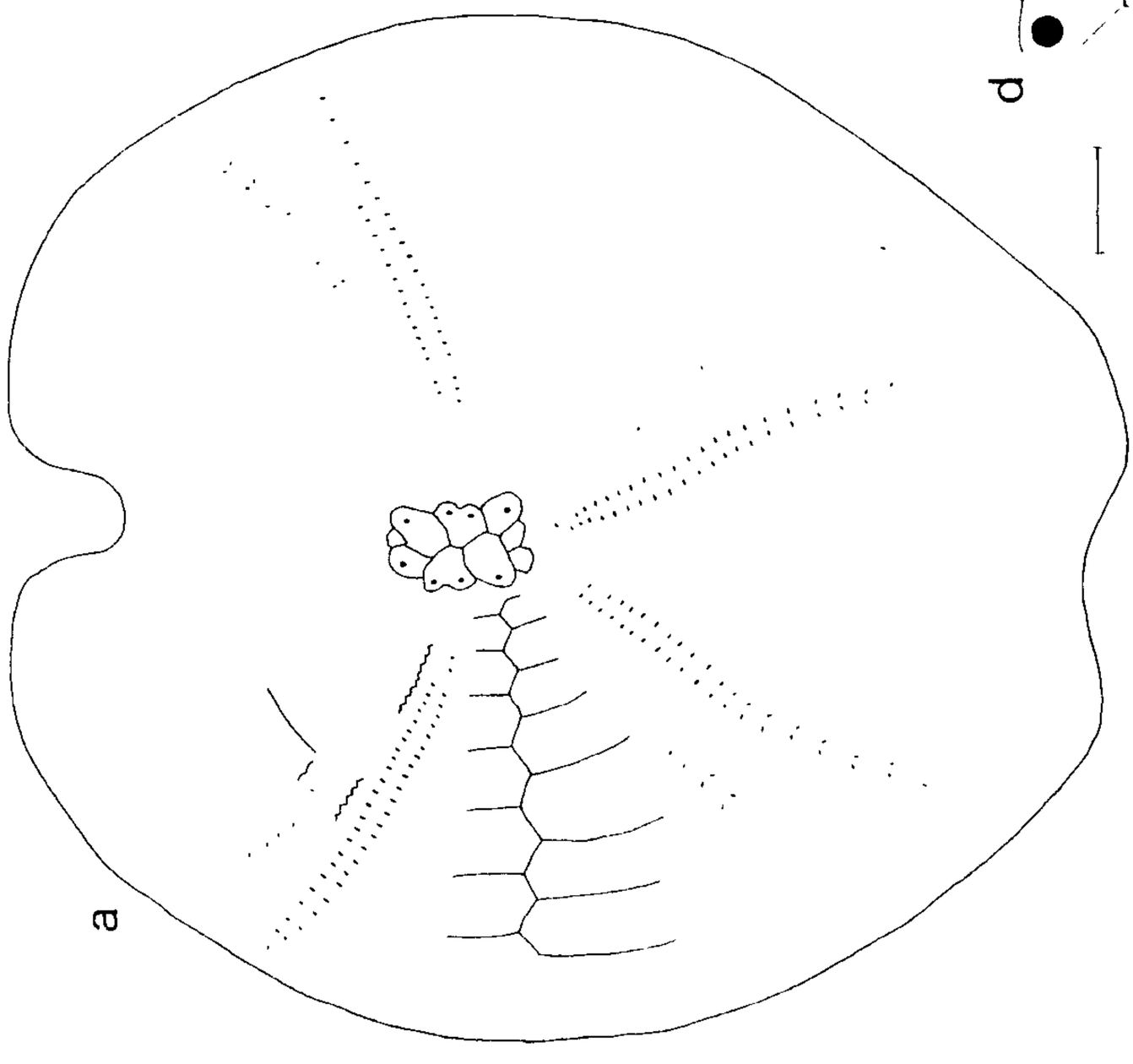
c



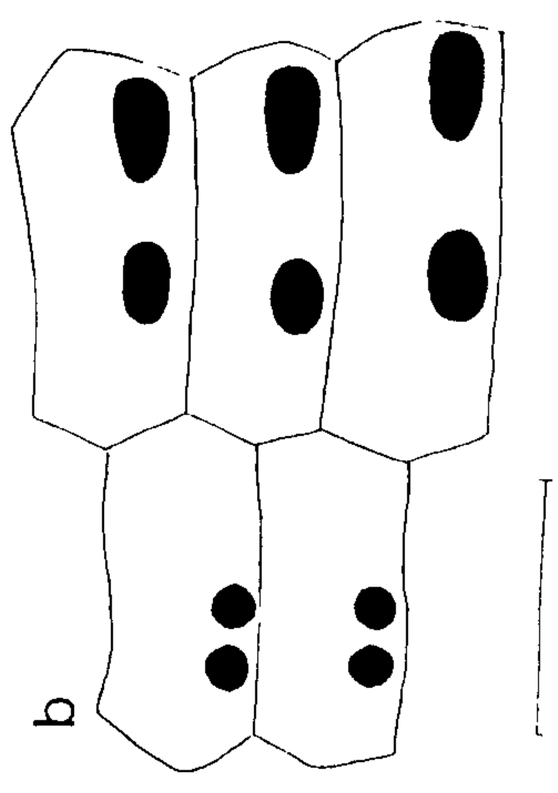
e



d

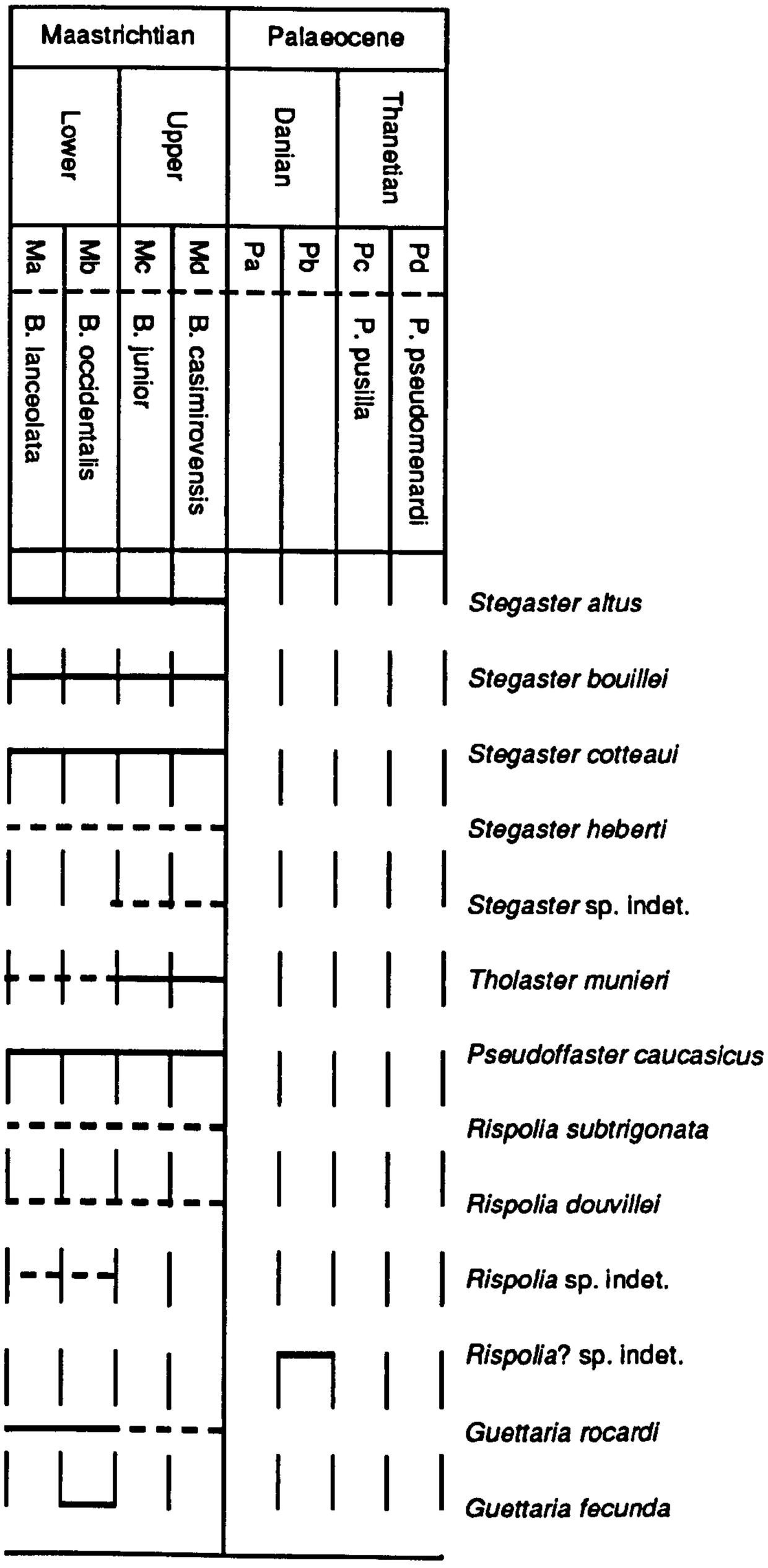


a



b

Figure 3.13. Range chart for Maastrichtian and Palaeocene stegasterid species. See Figure 3.2 for explanation of symbols.


Maastrichtian
Palaeocene
Lower
Upper
Danian
Thanetian
Ma
Mb
Mc
Md
Pa
Pb
Pc
Pd
B. lanceolata
B. occidentalis
B. junior
B. casimirovensis
P. pusilla
P. pseudomenardi
Stegaster altus
Stegaster bouillei
Stegaster cotteaui
Stegaster heberti
Stegaster sp. indet.
Tholaster munieri
Pseudoffaster caucasicus
Rispolia subtrigonata
Rispolia douvillei
Rispolia sp. indet.
Rispolia? sp. indet.
Guettaria rocardi
Guettaria fecunda

Family ECHINOCORIDAE Lambert, 1917

Emended diagnosis. No or very slight frontal groove. Flat base with mouth facing downwards. Plastron meridosternous approaching orthosternous - sternal plate pentagonal. No fascioles or marginal fasciole only.

KEY TO MAASTRICHTIAN & PALAEOCENE GENERA

1	Marginal fasciole; periproct supramarginal	*Offaster*
	no fascioles; periproct inframarginal	2
2	3 gonopores; large tubercles around ambitus	*Jeronia*
	4 gonopores; no large tubercles	*Echinocorys*

Genus ECHINOCORYS Leske, 1778

[Type species *Echinocorys scutata* Leske, 1778, by SD of Lambert, 1898]

Diagnosis. Flat base and inflated apical surface. Ovate outline. All ambulacra alike - non-petaloid with round pores. Plastron meridosternous. Apical system ethmophract with four gonopores. Periproct inframarginal. No fascioles.

Echinocorys scutata Leske, 1778

(Plate 4, figures 1-4; Figure 3.14)

Occurrence. Known from chalk and calcarenite facies worldwide ranging throughout the Maastrichtian and Palaeocene.

Lower Maastrichtian Ciply Phosphatic Chalk of Belgium (Lambert 1898; Lambert 1911) (BMNH). Lower Maastrichtian Vijlen and Lixhe Chalks of the Maastricht area (Smiser 1935a, b; van der Ham *et al.* 1987; van der Ham & van Birgelen 1988) (BMNH, NMM). Upper Maastrichtian White Chalk, Lower Danian Bryozoan and Cerithium Limestones and Upper Danian calcarenite of Denmark (Ødum 1926; Ravn 1927; Asgaard

1979) (DGFMM). Upper Danian Saltholm Limestone of Denmark (Brünnich Nielsen 1926) (DGFMM). Lower to Upper Maastrichtian of the Don Basin (Savchinskaya 1974). Lower Maastrichtian to Upper Danian of Georgia (Rouchadze 1940; Gongadze 1979), the Crimea and northern Caucasus (Moskvin & Poslavskaya 1959) (PI). Upper Maastrichtian to Lower Danian of Kazakhstan (Jeffery 1997b) (BMNH). Lower Maastrichtian Rügener Schreibkreide of the Isle of Rügen (Nietsch 1921; Nestler 1982) (BMNH). Lower to Upper Maastrichtian (Maczynska 1989) and Lower to Mid Danian Siwak (Kongiel 1935; Kongiel 1949) of southeastern Poland. Lower Maastrichtian Upper Chalk of Bulgaria (Tzankov 1934; Mileva-Ilieva 1995). Palaeocene of Austria (Traub 1938). Upper Maastrichtian Calcaire à *Baculites* of Normandy (Lambert 1909). Maastrichtian (Seunes 1891; Lambert 1907a), Danian (Cotteau 1877; Seunes 1888, 1891; Cotteau 1891; Lambert 1907a; Plaziat *et al.* 1975) and Lower to Mid Thanetian (Plaziat *et al.* 1975) of the Pyrenees. Lower Maastrichtian Cabo de Lata Formation of Santander (Lambert 1920a; Wilmsen *et al.* 1996) (BMNH) and Lower Maastrichtian Areny Sandstone of Tremp, Spain (Lambert 1927; Gallemí 1992) (PUAB). Upper Danian and Upper Thanetian of Navarra, Spain (BMNH). Maastrichtian Quipar-Jorquera Formation (Nicklès 1892; Lambert 1935; Gallemí *et al.* 1995) (BMNH, MGB). Upper Thanetian Tarwan Chalk (Hassan 1969) of the Western Desert, Egypt. Lower Maastrichtian Ulupinar Formation of Central Turkey (Akkus 1971). Danian of northwest Turkey (Böhm 1927) (BMNH). Lower Maastrichtian (Besairie 1930) and Danian (Besairie 1971) of northwest Madagascar (MNHN). Upper Maastrichtian Miria Marl (McNamara 1987) and Upper Thanetian Wadera Calcarenite (Foster & Philip 1978) of the Carnarvon Basin, Western Australia. Upper Thanetian Vincentown Sand of New Jersey, USA (Clark 1893, 1915; Cooke 1959).

Remarks. Specimens of *Echinocorys* are often very variable in shape, from flat based and conical to exceptionally globular. Previous papers have erected large numbers of species names to accommodate such differently shaped varieties, but the boundaries between species are commonly gradational and ambiguous with species differentiated on subtleties of size and shape, and not on structural differences. Many of the named varieties are recognizable regionally and are useful for stratigraphic correlation. However,

they only form end members of a gradational series and so, for the purposes of this thesis, are treated as a single species complex.

Genus JERONIA Seunes, 1888

[Type species, *Jeronia pyrenaica* Seunes, 1888, by OD]

Diagnosis. Overall test morphology very similar to *Echinocorys* - flat base and domed upper surface, but distinctly pointed posteriorly. All ambulacra flush and non-petaloid. Ambulacral plates fairly high. Plastron meridosternous. Apical system remarkably variable - complementary plate may be present or anterior genital plates may be fused. Always with three gonopores - madreporite without genital pore. Periproct inframarginal. No fascioles. Large tubercles encircle test at ambitus.

Remarks. *Jeronia* most closely resembles *Echinocorys*. It differs in having a more pointed posterior in horizontal outline, three gonopores in the apical system and large tubercles forming a ring around the ambitus.

Jeronia pyrenaica Seunes, 1888

(Plate 4, figures 5-7; Figure 3.15)

1888 *Jeronia pyrenaica* Seunes, p. 810, pl. 30, fig. 1, text figs 1-3.
1891 *Jeronia pyrenaica* Seunes, p. 29, pl. 2, figs 1-2, text figs 4-5.
1975 *Jeronia pyrenaica* Seunes; Plaziat *et al.*, p. 634, 643.

Occurrence. Danian of the Pyrenees (Seunes 1888, 1891; Plaziat *et al.* 1975) (MNHN), Bidart, France (BMNH) and Navarra, Spain (MGB).

Diagnosis. As generic diagnosis.

Genus OFFASTER Desor, 1858

[Type species *Ananchytes pilula* Lamarck, 1816 by SD of Quenstedt, 1874]

Diagnosis. Ovate test with indistinct or no frontal groove. Upper surface vaulted, lower

surface flat. Plastron meridosternous (but approaching orthosternous structure). Apical system elongate with four gonopores. Periproct on posterior. Marginal fasciole.

Remarks. Differs from *Echinocorys* and *Jeronia* in possessing a marginal fasciole and in having the periproct positioned on the truncate posterior of the test.

Offaster pilula (Lamarck, 1816)

(Plate 5, figures 1-4; Figure 3.16)

1854	*Cardiaster pilula* (Lamarck); d'Orbigny, p. 126, pl. 824.
1854	*Holaster senonensis* d'Orbigny, p. 118, pl. 822.
1978a	*Offaster granulosus* Kutscher, p. 630, pl. 3, figs 1-4.
1992	*Offaster* aff. *senonensis* (d'Orbigny); Gallemí, p. 261, photo 15.

Occurrence. Lower Maastrichtian of Tremp, Spain (Gallemí 1992) (PUAB). Lower Maastrichtian Rügener Schreibkreide of the Isle of Rügen (Kutscher 1978a) (EMAUG).

Diagnosis. Convex or flat across anterior margin. Convex to almost flat base (small specimens are more globular) and inflated upper surface (height >50% TL). Vertical or slightly undercut truncate posterior. Ambulacral plates fairly high - two ambulacral plates to each interambulacral plate at the ambitus. Mouth small (15% TW) and approximately circular.

Remarks. Specimens assigned to *O. senoniensis* have a more undercut posterior and a lower periproct. Specimens referred to *O. granulosus* have somewhat pustular tuberculation on the apical surface but resemble *O. pilula* in all other respects. They may represent a variety of *O. pilula*.

Cotteau (1877) recorded *O. pilula* from the Danian of the Pyrenees. However, Lambert (1907a) considers these deposits to be Campanian and Cotteau's taxonomic identification to be erroneous. Thus, the species is known only from Campanian and Lower Maastrichtian strata.

Offaster dallonii Lambert, 1927

1927 *Offaster dallonii* Lambert, p. 43, pl. 3, figs 12-15.

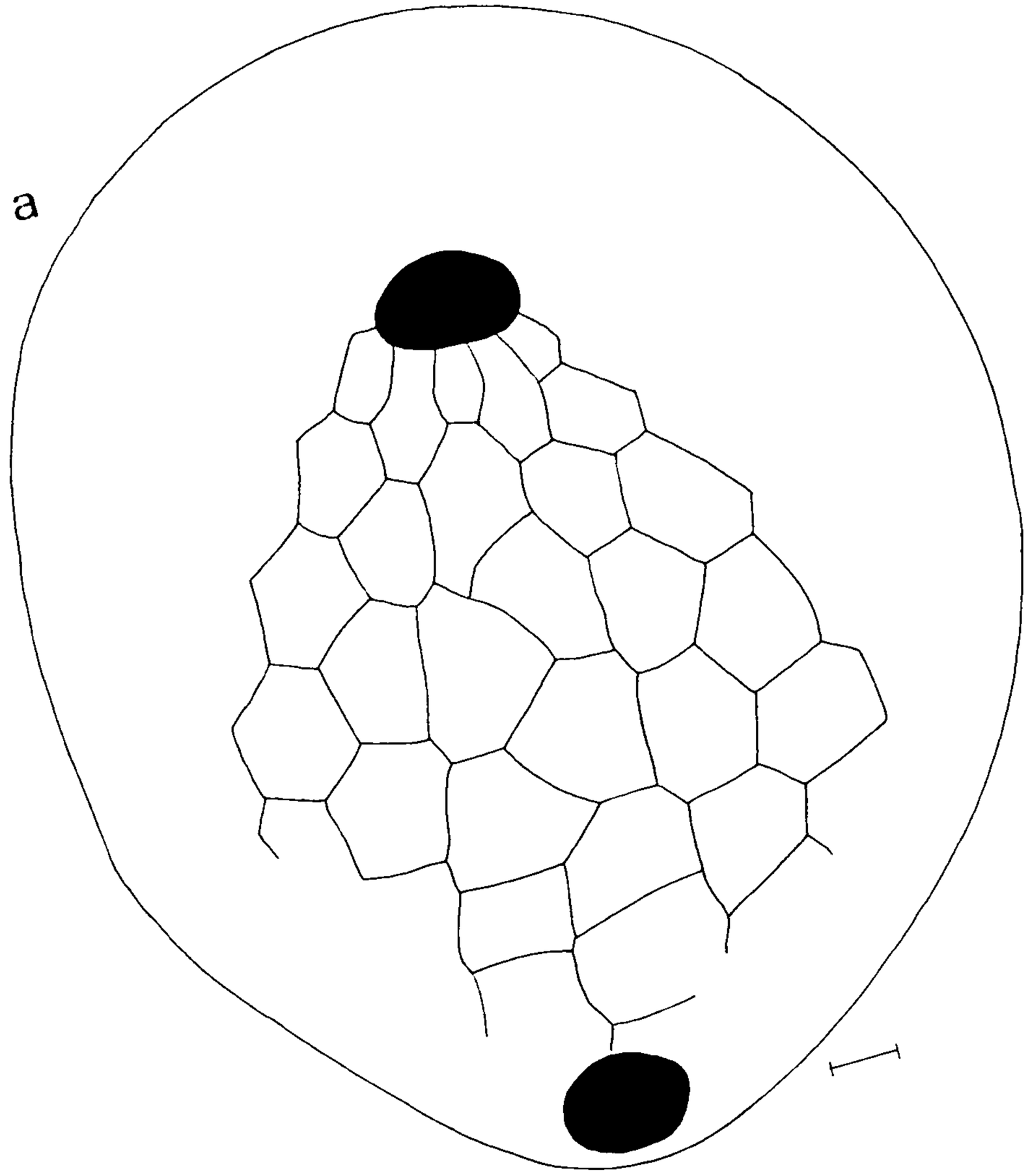
1992 *Offaster dallonii* Lambert; Gallemí, p. 257, photo 14.

1996 *Offaster dallonii* Lambert, Wilmsen *et al.*, fig. 7.

Occurrence. Lower Maastrichtian of the Tremp Basin (Lambert 1927; Gallemí 1992) (PUAB) and Cabo de Lata Formation of Santander (Wilmsen *et al.* 1996) (BMNH, MGB), Spain.

Diagnosis. Differs from *O. pilula* in its lower profile (<50% TL) and in having a larger (>18% TW), renate peristome.

Figure 3.14. Camera lucida drawings of *Echinocorys scutata* Leske, Lower Danian Cerithium Limestone of Denmark. a, DGFMM 1983.833, oral view. b, DGFMM 1984.11, apical disc plating. a, scale bar = 2 mm. b, scale bar = 1 mm.


a

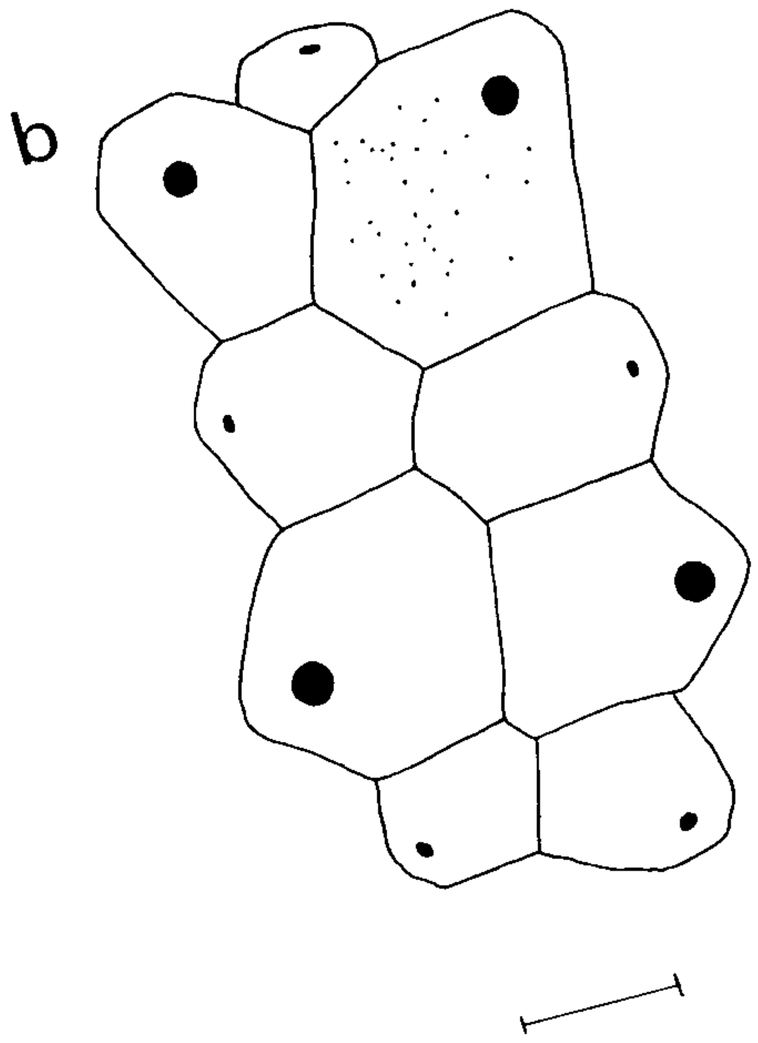
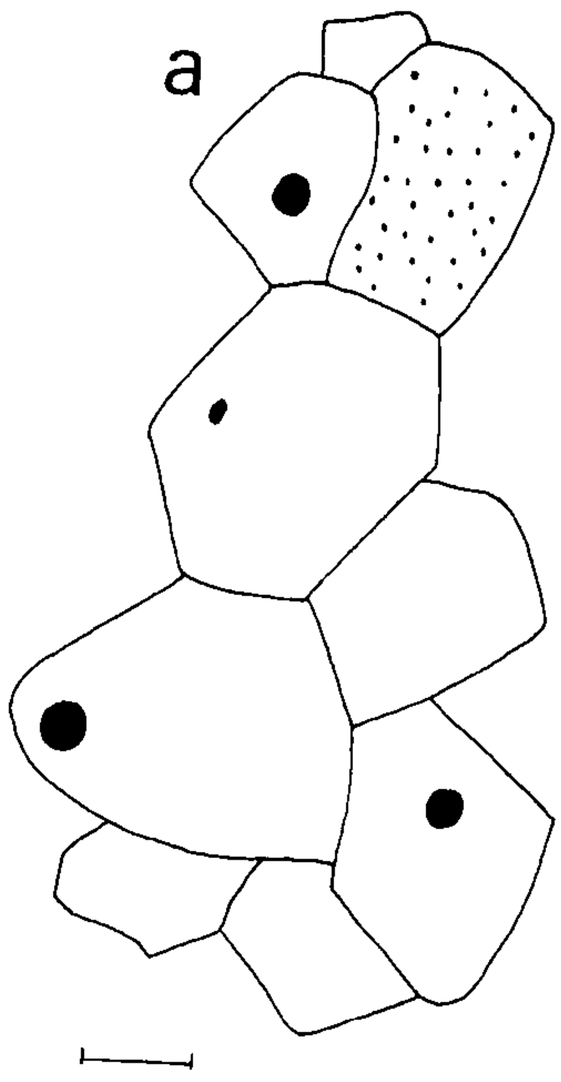

b

Figure 3.15. Camera lucida drawings of *Jeronia pyrenaica* Seunes, MNHN (Lambert Collection) no specimen number, Danian of Gan, Pyrenees; a, apical disc plating; b, detail of ambulacrum. a, scale bar = 1 mm. b, scale bar = 2 mm.


a

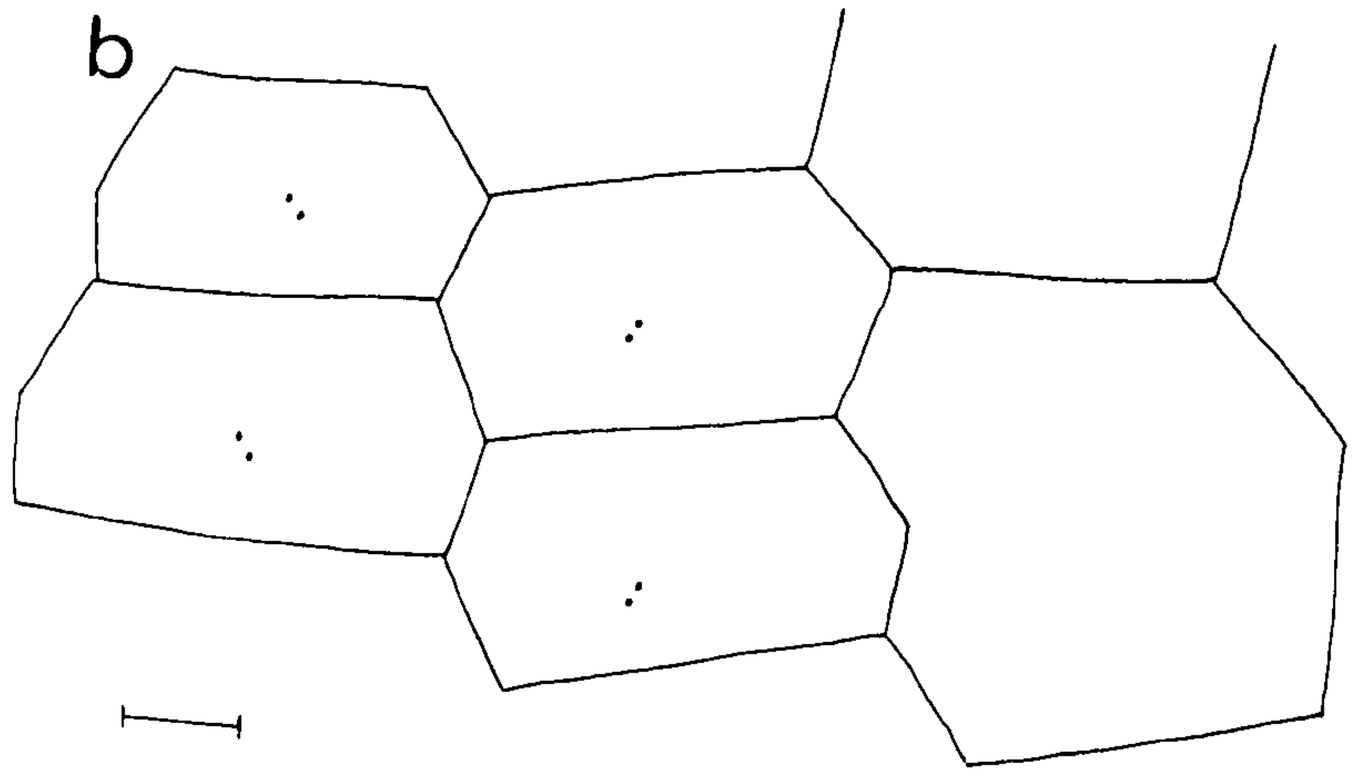
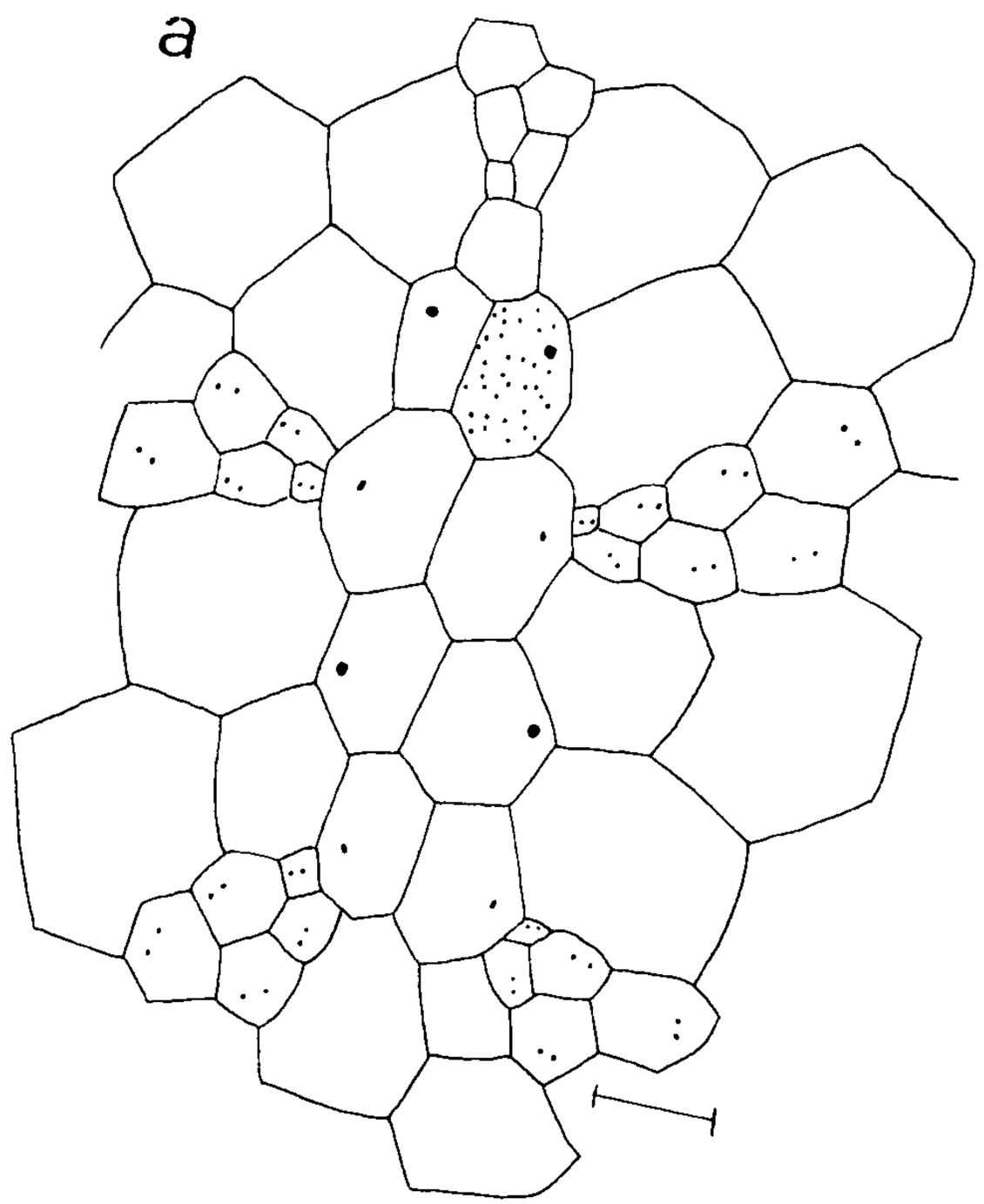

b

Figure 3.16. Camera lucida drawings of *Offaster pilula* (Lamarck), BMNH E31845, Campanian of Salisbury, UK; a, apical disc plating; b, oral view. a, scale bar = 1 mm. b, scale bar = 2 mm.


a

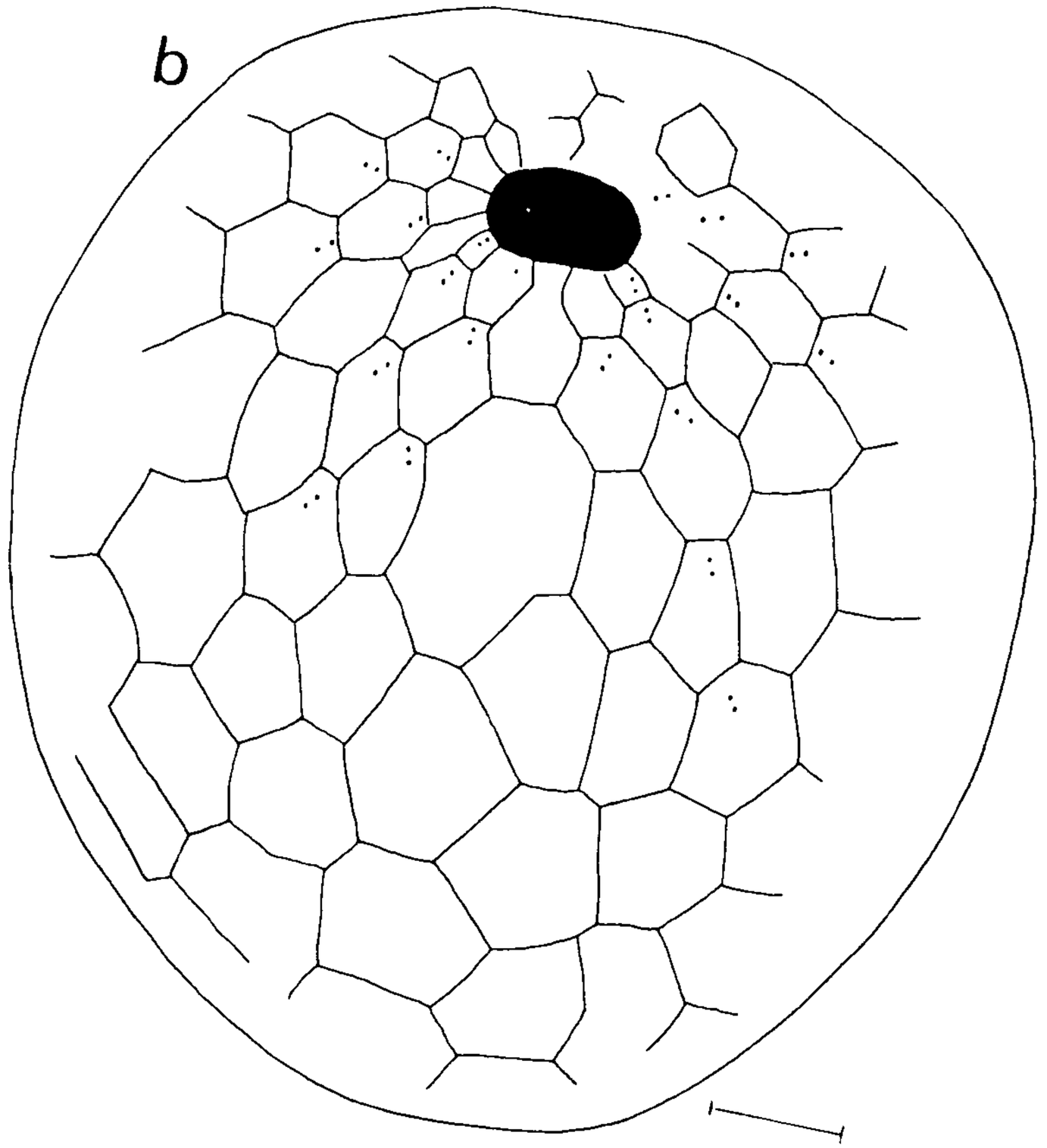
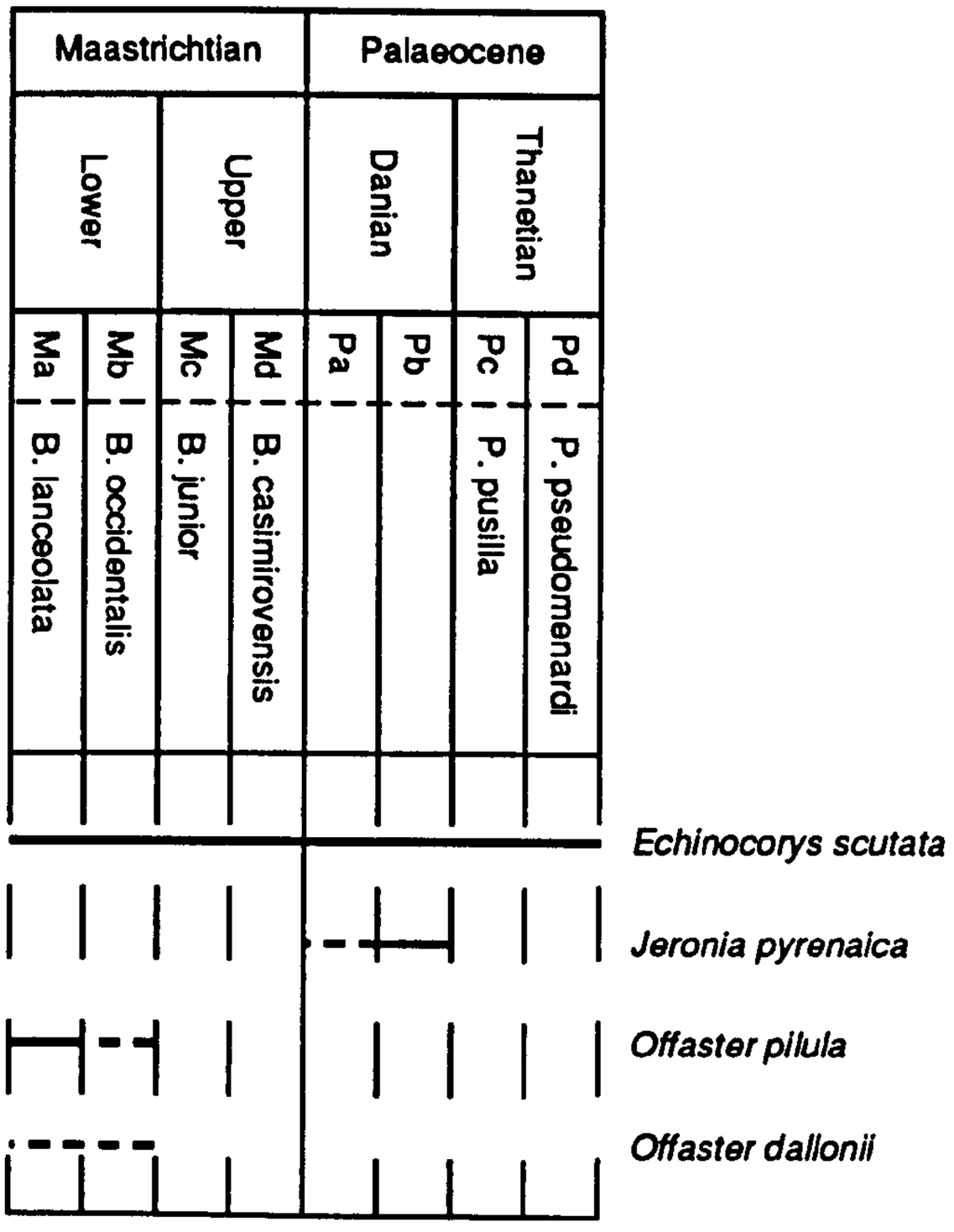

b

Figure 3.17. Range chart for Maastrichtian and Palaeocene echinocorid species. See Figure 3.2 for explanation of symbols.


Maastrichtian
Palaeocene
Lower
Upper
Danian
Thanetian
Ma
Mb
Mc
Md
Pa
Pb
Pc
Pd
B. lanceolata
B. occidentalis
B. junior
B. casimirovensis
P. pusilla
P. pseudomenardi
Echinocorys scutata
Jeronia pyrenaica
Offaster pilula
Offaster dallonii

Family CARDIASTERIDAE Lambert, 1917

Emended diagnosis. Deep frontal notch reaching forward-facing mouth. Plastron metasternous or approaching metasternous with two or more plates in single column. Labral and sternal plates hexagonal. Marginal fasciole.

KEY TO MAASTRICHTIAN GENERA

1	Plastron metasternous	2
	Plastron not metasternous	*Cardiaster*
2	Paired ambulacra non-petaloid; long slender anterior rostrum; fused plates in disjunct apical system	*Hagenowia*
	Paired ambulacra petaloid; no anterior rostrum; apical system elongate but not disjunct	*Cardiotaxis*

Genus CARDIASTER Forbes, 1850

[Type species *Spatangus granulosus* Goldfuss, 1829, by OD]

Diagnosis. Heart-shaped test with deep frontal groove. Anterior interambulacra form sharp keels. Flush paired ambulacra made up of comma shaped pores; columns unequally developed. Plastron meridosternous with series of alternating plates. Apical system elongate with four gonopores. Peristome somewhat labiate. Marginal fasciole.

KEY TO MAASTRICHTIAN SPECIES

1	Distinct frontal notch	2
	Indistinct frontal notch	*C. palmeri*
2	Periproct postitioned high on truncate posterior	3
	Periproct inframarginal	*C.* sp. nov.

3 Columns in paired ambulacra strongly differentiated.....*C. leonensis*

Columns in paired ambulacra only slightly differentiated.....*C. granulosus*

***Cardiaster granulosus* (Goldfuss, 1829)**

(Plate 5, figures 5-8; Figure 3.18)

1874 *Cardiaster ananchytis* d'Orbigny; Cotteau, p. 655.

1898 *Cardiaster granulosus* (Goldfuss); Lambert, p. 173, pl. 3, figs 9-10, text fig. 6.

1909 *Cardiaster granulosus* (Goldfuss); Lambert, p. 24.

1911 *Cardiaster granulosus* (Goldfuss); Lambert, p. 45, 55.

1921 *Cardiaster granulosus* (Goldfuss); Nietsch, p. 11, pl. 11, figs 3-10.

1927 *Cardiaster granulosus* (Goldfuss); Ravn, p. 340, pl. 4, fig. 3.

1935b *Cardiaster granulosus* (Goldfuss); Smiser, p. 68.

1935b *Cardiotaxis ananchytes* (Leske); Smiser, p. 68, pl. 7, fig. 5.

1953 *Cardiaster deciper* Cooke, p. 27, pl. 10, figs 3-6.

1959 *Cardiaster granulosus* (Goldfuss); Moskvin & Poslavskaya, p. 255, pl. 5, figs 3-4, text fig. 54.

1964 *Cardiaster granulosus* (Goldfuss); Poslavskaya & Solovjev, p. 178, pl. 31, figs 3-4, text figs 210c, 211c.

1974 *Cardiaster granulosus* (Goldfuss); Savchinskaya, p. 319, pl. 101, figs 1-7.

1979 *Cardiaster granulosus* (Goldfuss); Asgaard, table 2.

1982 *Cardiaster granulosus* (Goldfuss); Nestler, p. 81, text fig. 140.

1987 *Cardiaster granulosus* (Goldfuss); van der Ham *et al.*, p. 31, pl. 12, fig. 1.

1987 *Cardiaster rutoti* (Lambert); van der Ham *et al.*, p. 31, pl. 13.

1992 *Cardiaster granulosus* (Goldfuss); Gallemí, p. 195, fig. 57.

1992 *Cardiaster granulosus* (Goldfuss); van der Ham & van Birgelen, p. 150, pl. 4, fig. 5.

Occurrence. Lower Maastrichtian Ciply Phosphatic Chalk of Belgium (Cotteau 1874; Lambert 1898; Lambert 1911; Smiser 1935b) (BMNH). Lower Maastrichtian Vijlen, Lixhe and Lanaye Chalks and Upper Maastrichtian Kunrade, Nekum and Meerssen Chalks of the Maastricht area (van der Ham *et al.* 1987; van der Ham & van Birgelen 1992) (NMM). Upper Maastrichtian Calcaire à *Baculites* of Normandy, France (Lambert 1909). Lower Maastrichtian of Tremp, Spain (Gallemí 1992) (PUAB). Lower Maastrichtian Rügener Schreibkreide of the Isle of Rügen (Nietsch 1921; Nestler 1982) and Upper Maastrichtian Pommerschen Kreide of northern Germany (Nietsch 1921). Lower to Upper Maastrichtian white chalk of Denmark (Ravn 1927; Asgaard 1979) (DGFMM). Lower Maastrichtian of

the Don Basin (Savchinskaya 1974) and Lower to Upper Maastrichtian of the Crimea (Moskvin & Poslavskaya 1959; Poslavskaya & Solovjev 1964) (PI). Early Maastrichtian Saratoga Chalk of Arkansas, USA (Cooke 1953).

Diagnosis. Well defined anterior sulcus with sharply keeled adjoining interambulacra. Large tubercles adapically and along edges of frontal groove. Pores in paired ambulacra only slightly differentiated.

Cardiaster leonensis Stephenson, 1941

1941 *Cardiaster leonensis* Stephenson, p. 62, pl. 5, figs 4-7, pl. 6, figs 5-6.
1953 *Cardiaster leonensis* Stephenson; Cooke, p. 28, pl. 11, figs 1-7.

Occurrence. Mid to Late Maastrichtian Corsicana Marl of Texas, USA (Cooke 1953).

Diagnosis. Small test with broad, shallow frontal groove. Pores in paired ambulacra somewhat asymmetric - anterior series small and round, posterior series elongate.

Cardiaster palmeri Sanchez Roig, 1949

1949 *Cardiaster palmeri* Sanchez Roig, p. 172, pl. 5, figs 3-5.
1984 *Cardiaster palmeri* Sanchez Roig; Kier, p. 11, pl. 1, figs 1-3, text fig. 1.

Occurrence. Upper Cretaceous of Cuba - precise age uncertain.

Diagnosis. Unpaired ambulacrum flush at apical system; very slightly sunken at apex. Pore columns in paired ambulacra very asymmetric. Pores of anterior column small and round; in posterior column, anterior pores circular, posterior pores very elongate.

Remarks. Easily distinguished by its almost complete lack of frontal groove and very asymmetric paired ambulacra.

Cardiaster sp. nov.

Occurrence. Maastrichtian upper Tercis Formation of Tercis, French Pyrenees (UWBM).

Diagnosis. Broad heart-shaped test with low lateral profile. Periproct very low, inframarginal.

Remarks. Most similar to *C. leonensis* but easily distinguished by its inframarginal periproct.

Cardiaster sp. Indet.

1968 *Cardiaster perorientalis* Nisiyama, p. 151, pl. 18, figs 6-7.

Occurrence. Maastrichtian Miyakura (Furushiroyama) Formation of Ehime Prefecture, Japan.

Remarks. According to Nisiyama (1968), this species is most similar to *C. orientalis*. However, preservation is too poor to allow specific identification.

Genus CARDIOTAXIS Lambert, 1917

[Type species *Cardiaster peroni* Lambert *in* Peron, 1887, by OD]

Diagnosis. As *Cardiaster* but plastron metasternous - made up of series of single plates. Anterior interambulacra form rounded keels along frontal groove. No enlarged pore-pairs around mouth.

Cardiotaxis heberti (Cotteau *In* Cotteau & Triger, 1860)

(Plate 5, figures 9-11; Figure 3.19)

1860 *Cardiaster heberti* Cotteau *in* Cotteau & Triger, p. 240.
1874 *Cardiaster heberti* Cotteau, p. 655.
1898 *Cardiaster heberti* Cotteau; Lambert, p. 176, pl. 2, figs 11-12.
1900 *Cardiaster maximus* Schlüter, p. 273, pl. 17, figs 1-2, pl. 18, figs 1-2.
1911 *Cardiaster heberti* Cotteau; Lambert, p. 19, 45, pl. 1, figs 7-9.
1927 *Cardiaster heberti* Cotteau; Ravn, p. 341.
1978a *Cardiotaxis heberti* (Cotteau); Kutscher, p. 627, pl. 1.
1979 *Cardiotaxis heberti* (Cotteau); Asgaard, table 2.
1997b *Cardiotaxis heberti* (Cotteau); Jeffery, p. 688, pl. 7, figs 9-11, text fig. 11.

Occurrence. Lower Maastrichtian Ciply Phosphatic Chalk of Belgium (Cotteau 1874; Lambert 1898; Lambert 1911). Lower Maastrichtian Craie de Meudon of the Paris region (Cotteau & Triger 1960; Schlüter 1900). Lower Maastrichtian Rügener Schreibkreide of the Isle of Rügen (Kutscher 1978a). Lower to Upper Maastrichtian white chalk of Denmark (Ravn 1927; Asgaard 1979) (DGFMM). Uppermost Maastrichtian of Kazakhstan (Jeffery 1997b) (BMNH).

Diagnosis. Very thin, large test with distinct frontal groove. Mouth very anterior - almost marginal. Tuberculation fine and sparse.

Genus HAGENOWIA Duncan, 1889

[Type species *Cardiaster rostratus* Forbes, 1852, by OD]

(Plate 5, figures 12-14)

Synonym. *Martinosigra* Brünnich Nielsen, 1942 (type species *Martinosigra elongata* Brünnich Nielsen, 1942).

Diagnosis. Apical part of test elongated forming tapered rostrum. Distinct sulcus from apex to mouth. Apical system disjunct with 2 or 4 gonopores. Posterior ocular plates at base of rostrum, remainder on rostral apex. Plastron metasternous. Marginal fasciole.

Remarks. Distinguished from all other cardiasterids by its elongated anterior rostrum.

Hagenowia elongata (Brünnich Nielsen, 1942)

1942	*Martinosigra elongata* Brünnich Nielsen, p. 163, pl. 2, fig. 2.
1949	*Hagenowia rostrata* (Forbes); Wright & Wright, p. 462.
1972	*Hagenowia elongata* (Nielsen); Schmid, p. 179, pls 1-4, text figs 1, 2.
1978a	*Hagenowia elongata* (Brünnich Nielsen); Kutscher, p. 629, pl. 2.
1982	*Hagenowia elongata* (Nielsen); Gale & Smith, p. 22, pl. 4, figs 4, 7-9, pl. 5, figs 7, 9, pl. 6, figs 1, 3, 10.

Occurrence. Lower Maastrichtian white chalk of Denmark (Brünnich Nielsen 1942) and northwest Germany (Schmid 1972). Lower Maastrichtian Rügener Schreibkreide of the Isle of Rügen (Kutscher 1978a).

Diagnosis. Rostrum very long and narrow with shallow, flat sulcus. Genital plates 2 and 3 separated from ocular plates II and IV by interambulacra meeting at the midline. Madreporite with two vertically positioned pores.

Figure 3.18. Camera lucida drawings of *Cardiaster granulosus* (Goldfuss), *Belemnitella mucronata* zone of Norfolk, UK. a-b, BMNH E35600; a, apical view; b, apical disc plating. c, BMNH E41284, oral view. a & c, scale bars = 5 mm. b, scale bar = 1 mm.

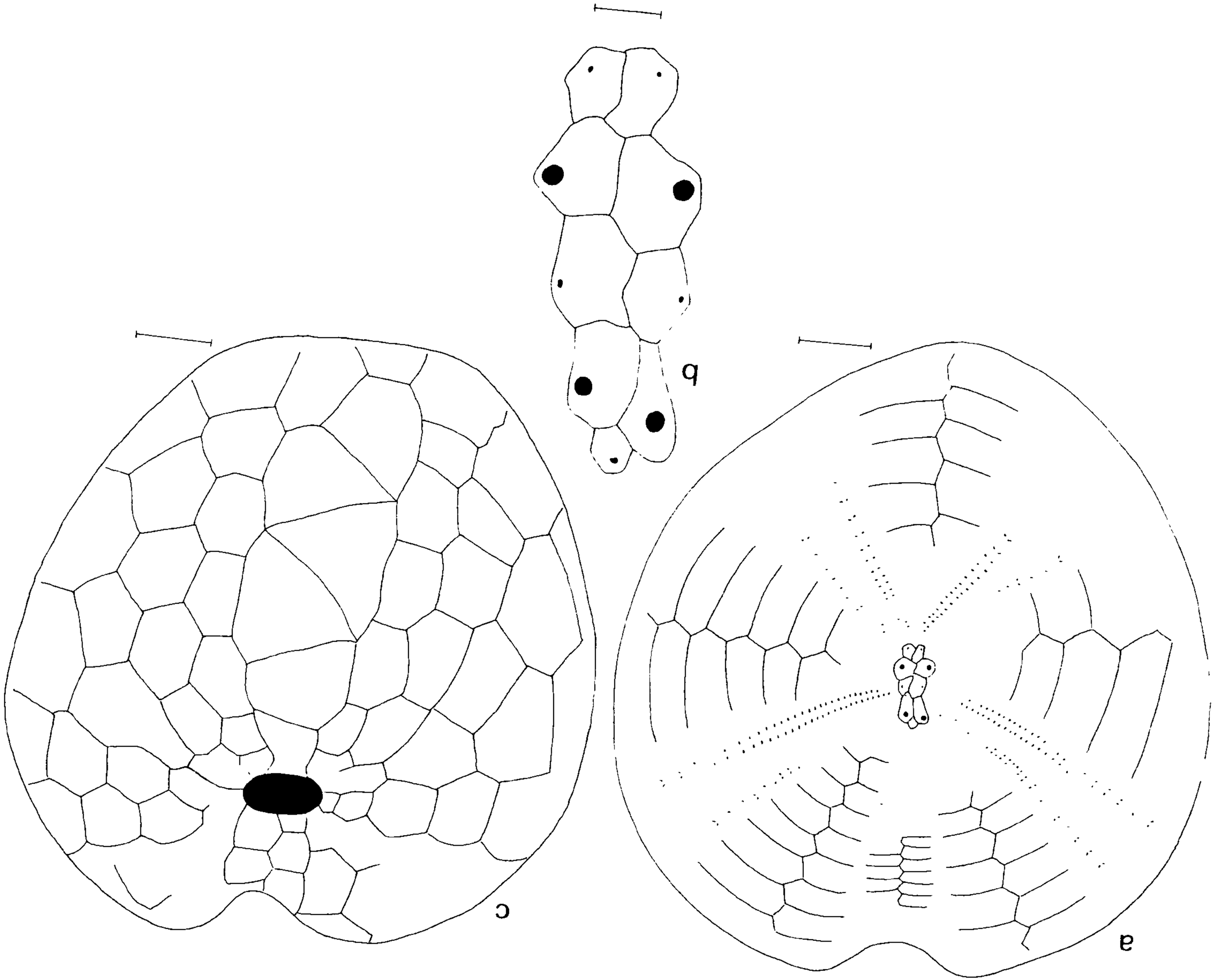

q
c
a

Figure 3.19. Camera lucida drawings of *Cardiotaxis heberti* (Cotteau), BMNH EE5627, Upper Maastrichtian of Mangyshlak, Kazakhstan; a, apical disc plating; b, oral view. a, scale bar = 1 mm. b, scale bar = 2 mm.

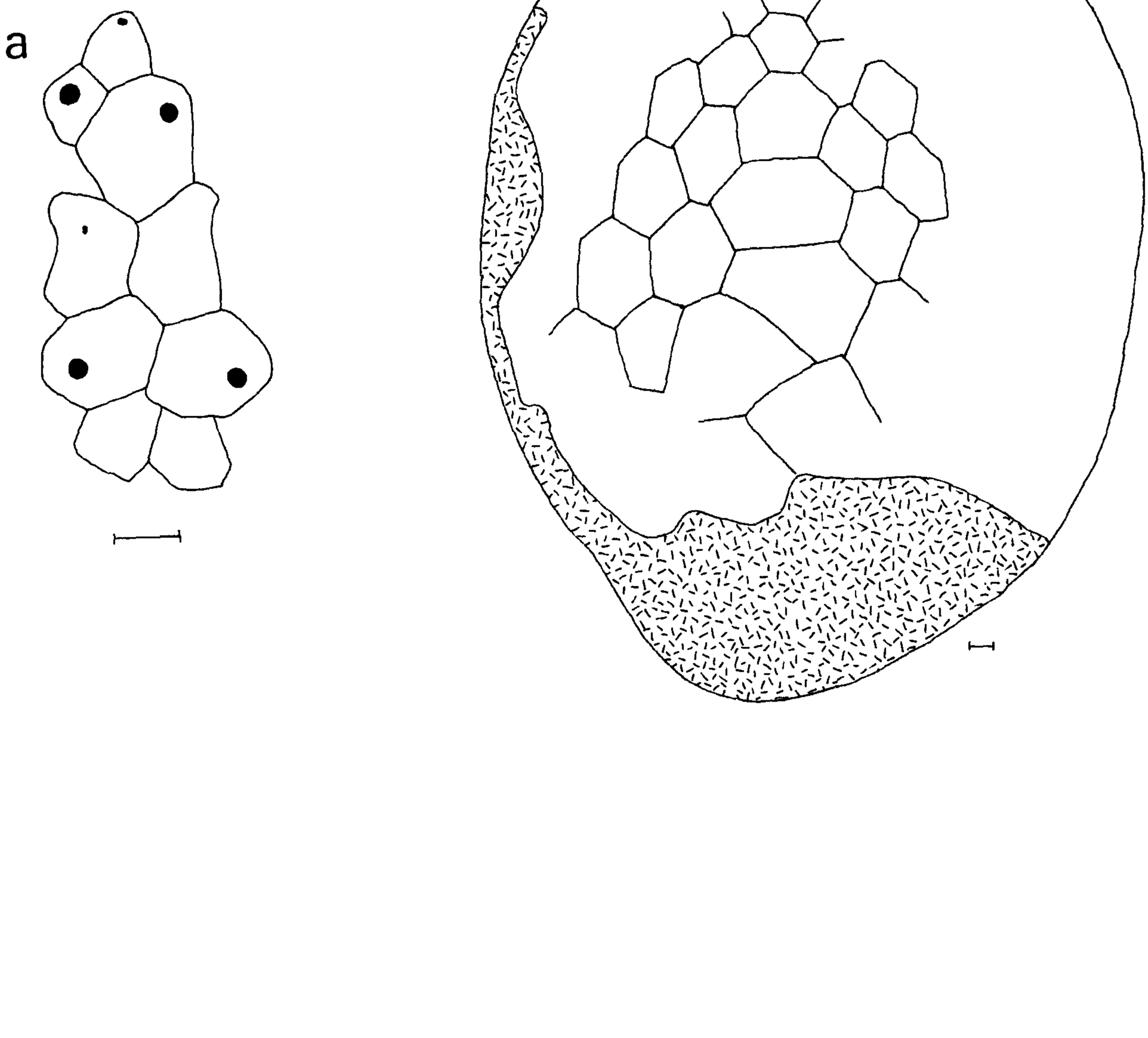
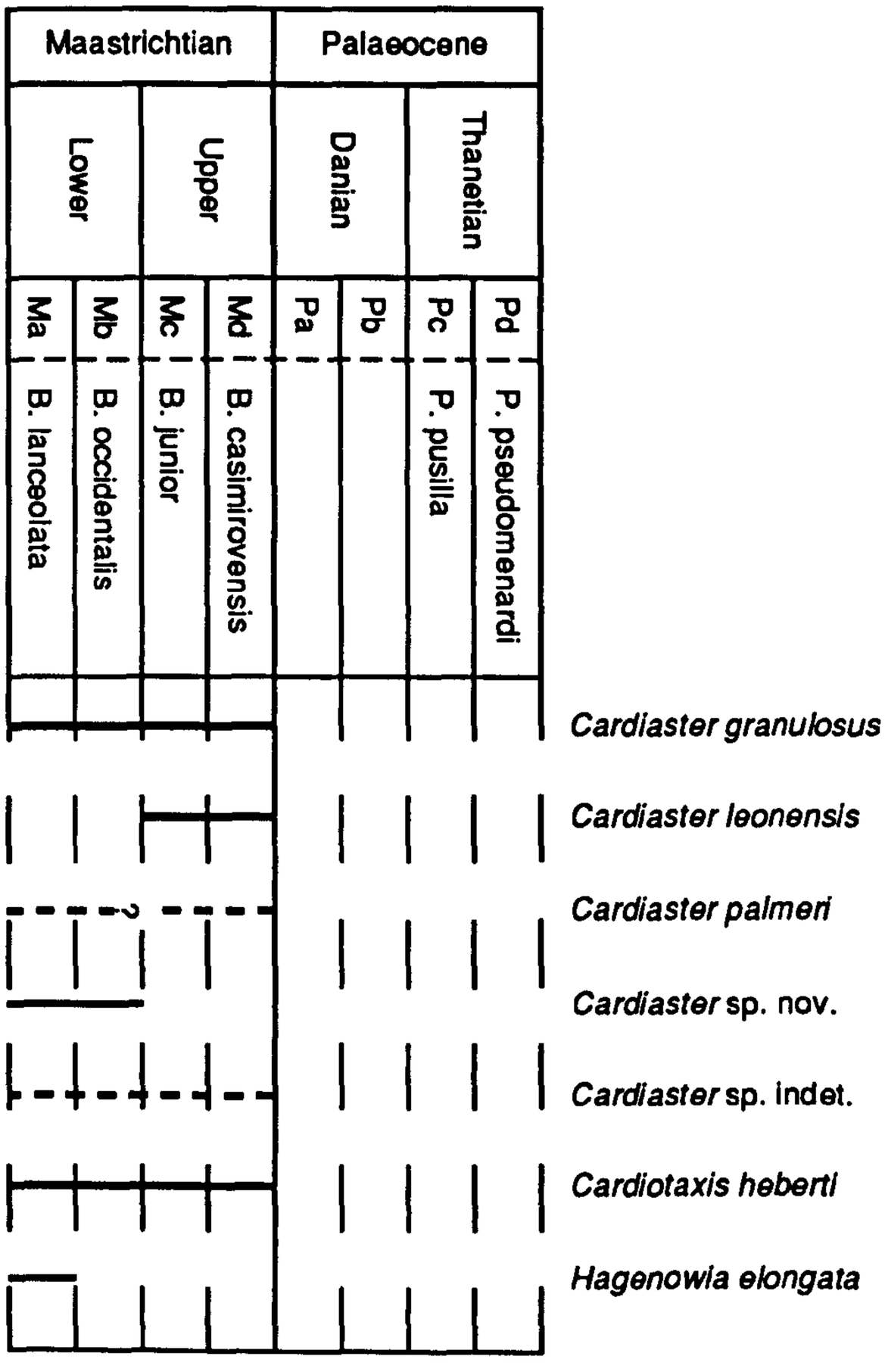

a
b

Figure 3.20. Range chart for Maastrichtian and Palaeocene cardiasterid species. See Figure 3.2 for explanation of symbols.


Maastrichtian
Palaeocene
Lower
Upper
Danian
Thanetian
Ma
Mb
Mc
Md
Pa
Pb
Pc
Pd
B. lanceolata
B. occidentalis
B. junior
B. casimirovensis
P. pusilla
P. pseudomenardi
Cardiaster granulosus
Cardiaster leonensis
Cardiaster palmeri
Cardiaster sp. nov.
Cardiaster sp. indet.
Cardiotaxis heberti
Hagenowia elongata

Family LABROTAXIDAE nov.

Type genus. *Labrotaxis* Casey, 1960.

Diagnosis. Distinct frontal groove. Paired ambulacra sub-petaloid. Plastron is or approaches protosternous structure with triangular sternal plate touching first post-sternal plate at right margin of plastron.

KEY TO MAASTRICHTIAN & PALAEOCENE GENERA

1 Plastron with large alternating triangular plates; strongly asymmetric pore columns in paired ambulacra.....*Hemipneustes*

Plastron protosternous; paired ambulacra with pore columns equally developed.....2

2 No fascioles.....*Labrotaxis*

Subanal fasciole; pores in ambulacra single on oral surface.....*Giraliaster*

Genus LABROTAXIS Casey, 1960

[Type species *Holaster (Labrotaxis) cantianus* Casey, 1960, by OD]

Diagnosis. Heart-shaped test. Paired ambulacra form open petals with elongate pores. Plastron almost protosternous. Apical system elongate with four gonopores. Mouth semicircular, generally not labiate. No fascioles.

Remarks. *Labrotaxis* is most similar to *Holaster*. It differs principally in having a plastron of almost protosternous structure with the labral plate in contact with the first post-sternal plate.

Labrotaxis faxensis (Hennig, 1898)

(Plate 6, figures 1-3; Figure 3.21)

?1830 *Ananchytes cinctus* Morton, p. 246, pl. 3, fig. 7.

?1834 *Ananchytes cinctus* Moron, p. 78, pl. 3, fig. 19.

?1893 *Cardiaster cinctus* (Morton); Clark, p. 75, pl. 37, fig. 1.

1898 *Holaster faxensis* Hennig, p. 6, pl. 1, figs 1-5.

?1915 *Cardiaster cinctus* (Morton); Clark, p. 83, pl. 36, fig. 2.

1926 *Holaster faxensis* Hennig; Brünnich Nielsen, p. 13.

1926 *Holaster faxensis* Hennig; Ødum, p. 162.

1927 *Holaster faxensis* Hennig; Ravn, p. 339, pl. 5, figs 3-4.

?1959 *Holaster cinctus* (Morton); Cooke, p. 65, pl. 27, figs 1-5.

1979 *"Holaster" faxensis* Hennig; Asgaard, table 2.

Occurrence. Lower Danian Bryozoan Limestone (Ødum 1926; Ravn 1927; Asgaard 1979) (DGFMM), Mid Danian Faxe Limestone (Hennig 1898) (BMNH, DGFMM) and Mid to Upper Danian Saltholm Limestone (Brünnich Nielsen 1926; Ravn 1927) (DGFMM) of Denmark. ?Upper Thanetian Vincentown Sand (Morton 1830, 1834; Clark 1893, 1915; Cooke 1959) of New Jersey, USA.

Diagnosis. Plastron raised orally to form keel. Mouth large and somewhat labiate.

Remarks. *Holaster cinctus* of New Jersey is similar in all respects to *Labrotaxis faxensis* except that the mouth appears to be somewhat smaller. Not enough material is available to determine whether this character is gradational or whether *Holaster cinctus* should be maintained as a separate species. In light of this, the two species are only tentatively synonymized.

Labrotaxis sp. Indet.

Occurrence. Late Thanetian of Casas di Oreyon, Navarra, Spain (BMNH).

Remarks. The only available specimen lacks the entire upper surface and specific identification is not possible. However, plastron plating confirms that this specimen is a *Labrotaxis.*

Genus GIRALIASTER Foster & Philip, 1978

[Type species *Giraliaster jubileensis* Foster & Philip, 1978]

Diagnosis. Heart-shaped test with frontal groove traceable to mouth. Paired ambulacra

sub-petaloid. Posterior pore zones made up of elongate pores. Anterior pore zone made up of small, round pores. Posterior paired ambulacra have single pores adorally. Apical system elongate with four gonopores. Plastron meridosternous forming keel. Subanal fasciole.

Remarks. *Giraliaster* is superficially similar in appearance to *Cardiaster*. It differs in possessing a subanal rather than marginal fasciole and in having an almost protosternous plastron with the labral plate almost touching the first post-sternal plate.

Giraliaster jubileensis Foster & Philip, 1978

1978 *Giraliaster jubileensis* Foster & Philip, p. 804, pl. 89, figs 1-6, text figs 3, 4a.

Occurrence. Maastrichtian Miria Marl to Late Thanetian Cardabia Group (Wadera, Pirie and Cashin Calcarenites) of the Carnarvon Basin, Western Australia.

Diagnosis. Steep anterior slope and abrupt posterior truncation. Pores in anterior series of paired ambulacra small and round. Posterior pore zones of paired ambulacra contain only slightly elongate pores.

Genus HEMIPNEUSTES Agassiz, 1836

[Type species *Spatangus striatoradiatus* Leske, 1778, by OD]

Diagnosis. Ovate outline with sharply defined frontal notch. Paired ambulacra sub-petaloid and flexuous with strongly dissimilar development of pore-pairs in anterior and posterior columns. Anterior pore series of small round pores. Posterior pore series contains elongate pores. Plastron made up of cuneiform, alternating plates. Apical system elongate with four gonopores. Hydropores extend over genital plates 2 and 3 and ocular plates II, III and IV.

Remarks. Most similar in appearance to *Opisopneustes*. Both genera have asymmetric sub-petaloid paired ambulacra and a plastron made up of alternating wedge-shaped plates. *Opisopneustes* differs in its low, flattened lateral profile, its marginal fasciole and

in having large, scrobiculate tubercles on the apical surface.

KEY TO MAASTRICHTIAN SPECIES

1	frontal groove narrow and parallel sided	2
	frontal groove broadens away from apex	*H. africanus*
2	low profile; apical system at mid-length	3
	more inflated quadrate profile; apical system anterior	6
3	very large forms with pinched keels adjoining frontal groove	*H. oculatus*
	smaller forms without pinched keels	4
4	almost as broad as long; flat apical surface	*H.* sp.
	more elongate forms with rounded upper surface	5
5	deep, sharp frontal groove	*H. arabicus*
	shallow groove, flush at apex	*H. persicus*
6	anterior ambulacrum depressed at apex	*H. striatoradiatus*
	anterior ambulacrum flush at apex	*H. pyrenaicus*

Hemipneustes striatoradiatus (Leske, 1778)

(Plate 6, figures 4-7)

1778	*Spatangus striatoradiatus* Leske, p. 234.
1874	*Hemipneustes striatoradiatus* d'Orbigny; Cotteau, p. 654.
1875	*Hemipneustes leymeriei* Hébert, p. 594, pl. 20.
1892	*Hemipneustes leymeriei* Hébert; Nicklès, p. 110.
1907a	*Hemipneustes leymeriei* Hébert; Lambert, p. 709.
1934	*Hemipneustes striatoradiatus* d'Orbigny; Tzankov, p. 213.
1935b	*Spatagoides striatoradiatus elevatus* Smiser, p. 71, pl. 8, fig. 1e.
1935b	*Spatagoides striatoradiatus conicus* Smiser, p. 71, pl. 8, fig. 1g.
1935b	*Spatagoides striatoradiatus depressus* Smiser, p. 71, pl. 8, fig. 1h.
1935b	*Toxopatagus rutoti* (Lambert); Smiser, p. 73, pl. 9, fig. 1.
1940	*Spatagoides striato-radiatus* (Leske); Rouchadze, p. 163.
1959	*Spatagoides striatoradiatus* (Leske); Moskvin & Poslavskaya, p. 264, pl. 12, fig. 1, pl. 13, fig. 1, text fig. 72.
1964	*Hemipneustes striatoradiatus* (Leske); Poslavskaya & Solovjev, p. 178, pl. 33, fig. 1, text figs 210h, 211h.

1969 *Hemipneustes striatoradiatus* (Leske); Dzhalilov & Egorov, p. 111, fig. 1.

1969 *Hemipneustes striatoradiatus elevatus* Smiser; Dzhalilov & Egorov, p. 113, fig. 2.

1973 *Hemipneustes leymeriei* Hébert; Radig, p. 58, pl. 9, figs 5-8.

1979 *Hemipneustes* cf. *striatoradiatus* Leske; Gongadze, p. 94, pl. 21, fig. 1, text fig. 18.

1987 *Hemipneustes striatoradiatus* (Leske); van der Ham *et al.*, p. 32, pl. 18, fig. 2.

1992 *Hemipneustes striatoradiatus* (Leske); van der Ham & van Birgelen, p, 150.

1994 *Hemipneustes striatoradiatus* (Leske); Mileva-Ilieva, p. 65, pl. 3, figs 1-2.

1995 *Hemipneustes striatoradiatus* (Leske); Gallemí *et al.*, table 1.

Occurrence. Lower Maastrichtian Lanaye Chalk and Upper Maastrichtian Kunrade, Nekum and Meerssen Chalks of the Maastricht area (Cotteau 1874; Smiser 1935b; van der Ham *et al.* 1987; van der Ham & van Birgelen 1992) (BMNH, NMM). Lower Maastrichtian Upper Chalk of Bulgaria (Tzankov 1934; Mileva-Ilieva 1994). Lower to Upper Maastrichtian of Georgia (Rouchadze 1940; Gongadze 1979), Kazakhstan (Poslavskaya & Solovjev 1964) and the northern Caucasus (Moskvin & Poslavskaya 1959) (PI). Maastrichtian of Tadzhikistan (Dzhalilov & Egorov 1969). Maastrichtian of the French Pyrenees (Hébert 1875; Lambert 1907a) (MNHN) and Lower Maastrichtian Olazaguthia Formation of Navarra, Spain (Radig 1973) (BMNH, MGB). Maastrichtian Quipar-Jorquera Formation of Alicante, Spain (Nicklès 1892; Gallemí *et al.* 1995) (MGB).

Diagnosis. Sides vertical. Upper surface may be flat topped or highest anteriorly. Apical system somewhat anterior. Approximately rectangular in lateral profile. Narrow, shallow frontal sulcus.

Hemipneustes pyrenaicus Hébert, 1875

(Figure 3.22)

1875 *Hemipneustes pyrenaicus* Hébert, p. 593, pl. 19.

1892b *Hemipneustes arnaudi* Cotteau, p. 165, pl. 21, figs 3-4.

1892 *Hemipneustes pyrenaicus* Hébert; Nicklès, p. 110.

1897 *Hemipneustes pyrenaicus* Hébert; Noetling, p. 29, pl. 6, figs 2-4, pl. 7, fig. 1.

1897 *Hemipneustes compressus* Noetling, p. 34, pl. 7, figs 3-4, pl. 8, figs 1-2.

1897 *Hemipneustes leymeriei* Hébert; Noetling, p. 32, pl. 7, fig. 2.

1907a *Hemipneustes pyrenaicus* Hébert; Lambert, p. 709.

1920a *Hemipneustes pyrenaicus* Hébert; Lambert, p. 25.

1921 *Hemipneustes zuffardii* Checchia-Rispoli, p. 30, pl. 9, figs 8-11.

1927 *Spatagoides pyrenaicus* (Hébert); Lambert, p. 41.

1931 *Spatagoides aichinoi* Checchia-Rispoli, p. 3, figs 4-6, text fig. 1.

1931 *Spatagoides martellii* Checchia-Rispoli, p. 7, figs 1-3, text fig. 2.

1931 *Spatagoides tripolitanus* Checchia-Rispoli, p. 11, figs 7-8, text fig. 3.

1935 *Spatagoides pyrenaicus* (Hébert); Lambert, p. 362.

1935 *Hemipneustes perrieri* Cottreau, p. 261, fig. 4.

1967 *Hemipneustes compressus* Noetling; Devriès, p. 188, pl. 6, figs 31-33.

1973 *Hemipneustes pyrenaicus* Hébert; Radig, p. 57, pl. 8, figs 6-9, pl. 9, figs 1-4.

1976 *Hemipneustes compressus* Noetling, Wu & Mu, p. 370, pl. 9. figs 6-7.

1976 *Hemipneustes striatoradiatus* (Leske); Wu & Mu, p. 370, pl. 9, figs 1-5.

1976 *Cardiaster* sp. A Wu & Mu, p. 369, pl. 8, figs 1-10.

1976 *Holaster* sp. Wu & Mu, p. 370, pl. 8, figs 14-17.

1990 *Hemipneustes indicus* Aziz & Badve, p. 326, fig. 2.

1992 *Hemipneustes pyrenaicus* Hébert; Gallemí, p. 244, photo 13.

1995 *Hemipneustes compressus* Noetling; Smith, p. 223, pl. 31, figs 8-11, text figs 76-78.

1996 *Hemipneustes pyrenaicus* Hébert; Wilmsen *et al.*, fig. 7.

Occurrence. Maastrichtian of the French Pyrenees (Hébert 1875; Cotteau 1892b; Lambert 1907a) (MNHN) and Lower Maastrichtian Olazaguthia Formation of Navarra, Spain (Radig 1973) (BMNH, MGB). Lower Maastrichtian of Tremp (Lambert 1927; Gallemí 1992) (PUAB) and Lower Maastrichtian Cabo de Lata Formation of Santander, Spain (Lambert 1920a; Wilmsen *et al.* 1996). Maastrichtian Quipar-Jorquera Formation of Alicante, Spain (Nicklès 1892; Lambert 1935). Mid to Upper Maastrichtian Al Gharbiyah Formation (Lower Tar Member) of Tripolitania, Libya (Checchia-Rispoli 1921, 1931) (URGM Checchia-Rispoli Collection). Early Upper Maastrichtian Simsima Formation of UAE / Oman (Smith 1995) (BMNH). Maastrichtian Besni Formation of Cortinek, Central Turkey (Devriès 1967). Maastrichtian of southwestern Madagascar (Cottreau 1935; Besairie 1971). Lower Maastrichtian Kallankurichchi Formation, Ariyalur Group of southern India (Aziz & Badve 1990). Maastrichtian of Baluchistan (Noetling 1897) (GSI). Mid to Late Maastrichtian of the foothills of Mount Everest, China (Wu & Mu 1976).

Diagnosis. Subquadrate lateral profile. Anterior sulcus deepens towards ambitus. Apical system somewhat anterior.

Remarks. Specimens previously referred to *H. compressus* have a more sharply defined anterior groove with somewhat pinched edges. However, Noetling's type material and specimens from the same locality referred by him to *H. pyrenaicus* exhibit a gradational

range of morphologies. The two species are treated as synonymous.

Hemipneustes persicus Cotteau & Gauthier, 1895

1895 *Hemipneustes persicus* Cotteau & Gauthier, p. 15, pl. 2, figs 1-6.
1895 *Hemipneustes minor* Cotteau & Gauthier, p. 17, pl. 2, figs 7-9
1941 *Hemipneustes persicus* Cotteau & Gauthier; Furon, p. 305.
1941 *Hemipneustes minor* Cotteau & Gauthier; Furon, p. 305.
1995 *Hemipneustes persicus* Cotteau & Gauthier; Smith, p. 227, pl. 31, figs 1-7, pl. 32, figs 1-4, text figs 76, 78, 79.

Occurrence. Maastrichtian of Persia and the Iranian Plateau (Cotteau & Gauthier 1895; Furon 1941) (BMNH). Early Upper Maastrichtian Simsima Formation of UAE / Oman (Smith 1995) (BMNH).

Diagnosis. Low, rounded profile. Broad, shallow frontal groove, flush at apex. Apical disc at mid-length.

Hemipneustes arabicus Ali, 1989

1989 *Hemipneustes arabicus* Ali, p. 408, figs 6 (1-3), 7.
1989 *Hemipneustes persicus* Cotteau & Gauthier; Ali, p. 408, fig. 6(4).
1995 *Hemipneustes arabicus* Ali; Smith, p. 230, pl. 30, figs 1-4, text figs 76, 78, 80.

Occurrence. Lower to Lower Upper Maastrichtian Simsima Formation of UAE / Oman (Ali 1989; Smith 1995) (BMNH).

Diagnosis. Elongate outline with deep, sharp, narrow frontal groove. Low profile. Apical disc at mid-length.

Hemipneustes africanus Deshayes *in* Agassiz & Desor, 1847

1847 *Hemipneustes africanus* Deshayes *in* Agassiz & Desor, p. 137.
1862 *Hemipneustes deletttrei* Coquand, p. 239, pl. 24, figs 1-3.
1862 *Hemipneustes africanus* Deshayes; Coquand, p. 238, pl. 23, figs 9-11.
1881 *Hemipneustes africanus* Deshayes; Cotteau *et al.*, p. 119, pl. 9, figs 1-4.

1881 *Hemipneustes delettrei* Coquand; Cotteau *et al.*, p. 122, pl. 10, figs 1-4.

1892 *Hemipneustes africanus* Deshayes; Nicklès, p. 110.

1892 *Hemipneustes delettrei* Coquand, Nicklès, p. 110.

Occurrence. Maastrichtian of Alicante, Spain (Nicklès 1892). Late Campanian of Algeria (Coquand 1862; Cotteau *et al.* 1881) (BMNH, MNHN).

Diagnosis. Distinguished by very broad, non-parallel sided anterior sulcus.

Remarks. Specimens referred to *H. africanus* are higher but otherwise identical to *H. delettrei*.

Hemipneustes oculatus Cotteau, 1892a

1892a *Hemipneustes oculatus* Cotteau, p. 4, pl. 1, figs 1-3.

1935b *Spatagoides oculatus* (Cotteau); Smiser, p. 72.

1987 *Hemipneustes oculatus* Cotteau; van der Ham *et al.*, p. 32, pl. 19, figs 1-2.

Occurrence. Upper Maastrichtian Nekum Chalk of the Maastricht area (Cotteau 1892a; Smiser 1935b, van der Ham *et al.* 1987) (BMNH, NMM).

Diagnosis. Large, low forms with a very deep frontal groove. Adjoining interambulacra sharply keeled. Paired ambulacra strongly flexuous.

Hemipneustes sp.

1992 *Hemipneustes leymeriei* Hébert; Gallemí, p. 240, photo 12.

Occurrence. Lower Maastrichtian Areny Sandstone of Tremp (Gallemí 1992) and Cabo de Lata Formation of Santander, Spain (BMNH).

Diagnosis. Characterized by its very low lateral profile with a broad flat apical surface and almost circular horizontal outline.

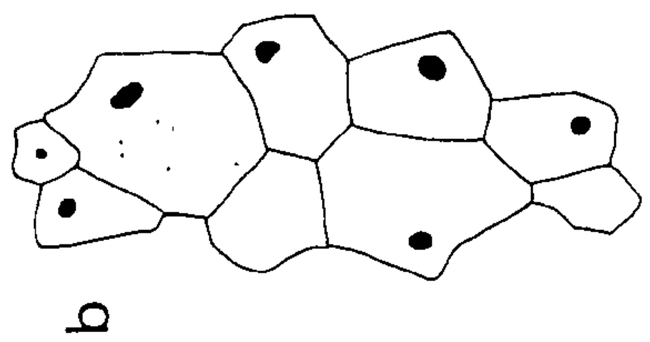
Hemipneustes sp. Indet.

1976 *Cardiaster* sp. B Wu & Mu, p. 370, pl. 8, figs 11-13.

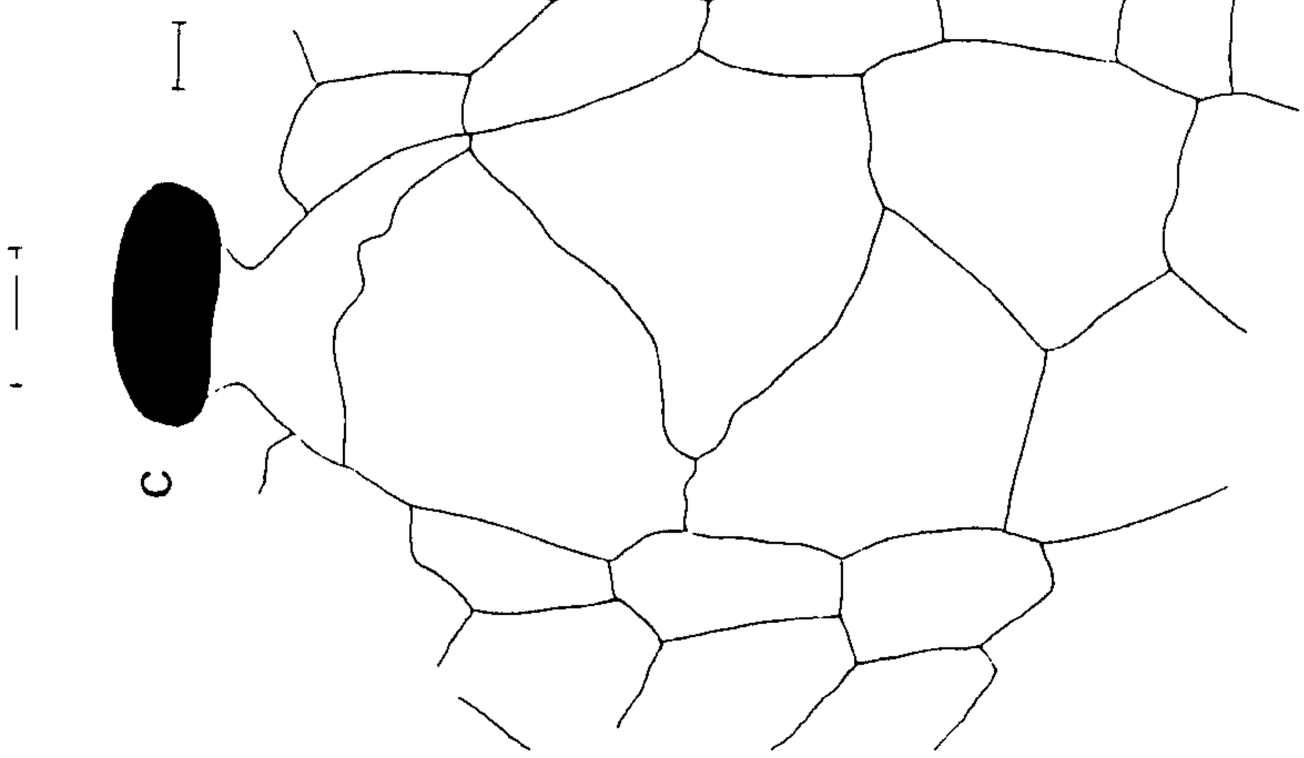
Occurrence. Mid Maastrichtian of the foothills of Mount Everest, China.

Remarks. Figures and description inadequate to allow specific identification.

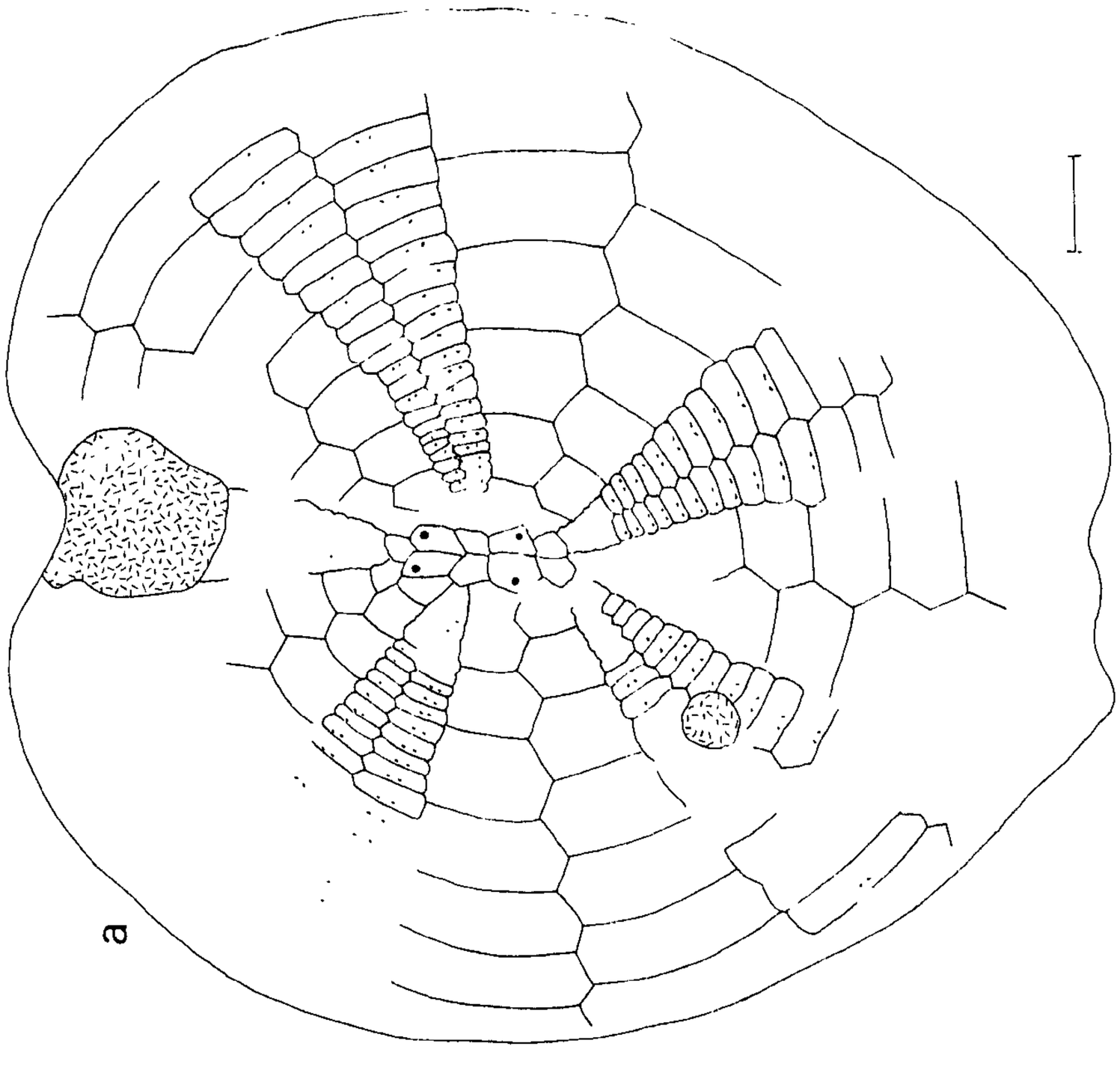
Figure 3.21. Camera lucida drawings of *Labrotaxis faxensis* (Hennig), mid Danian Faxe Limestone of Denmark. a-b, BMNH E12173; a, apical view; b, apical disc plating. c, BMNH E2877, part of oral surface. a, scale bar = 5 mm. b-c, scale bars = 2 mm.



b



c



a

Figure 3.22. Camera lucida drawings of *Hemipneustes pyrenaicus* Hebert, Maastrichtian of Baluchistan. a, GSI 2997, oral view. b & c, GSI 2995; b, apical view; c, apical disc plating. a & b, scale bars = 5 mm. c, scale bar = 1 mm.

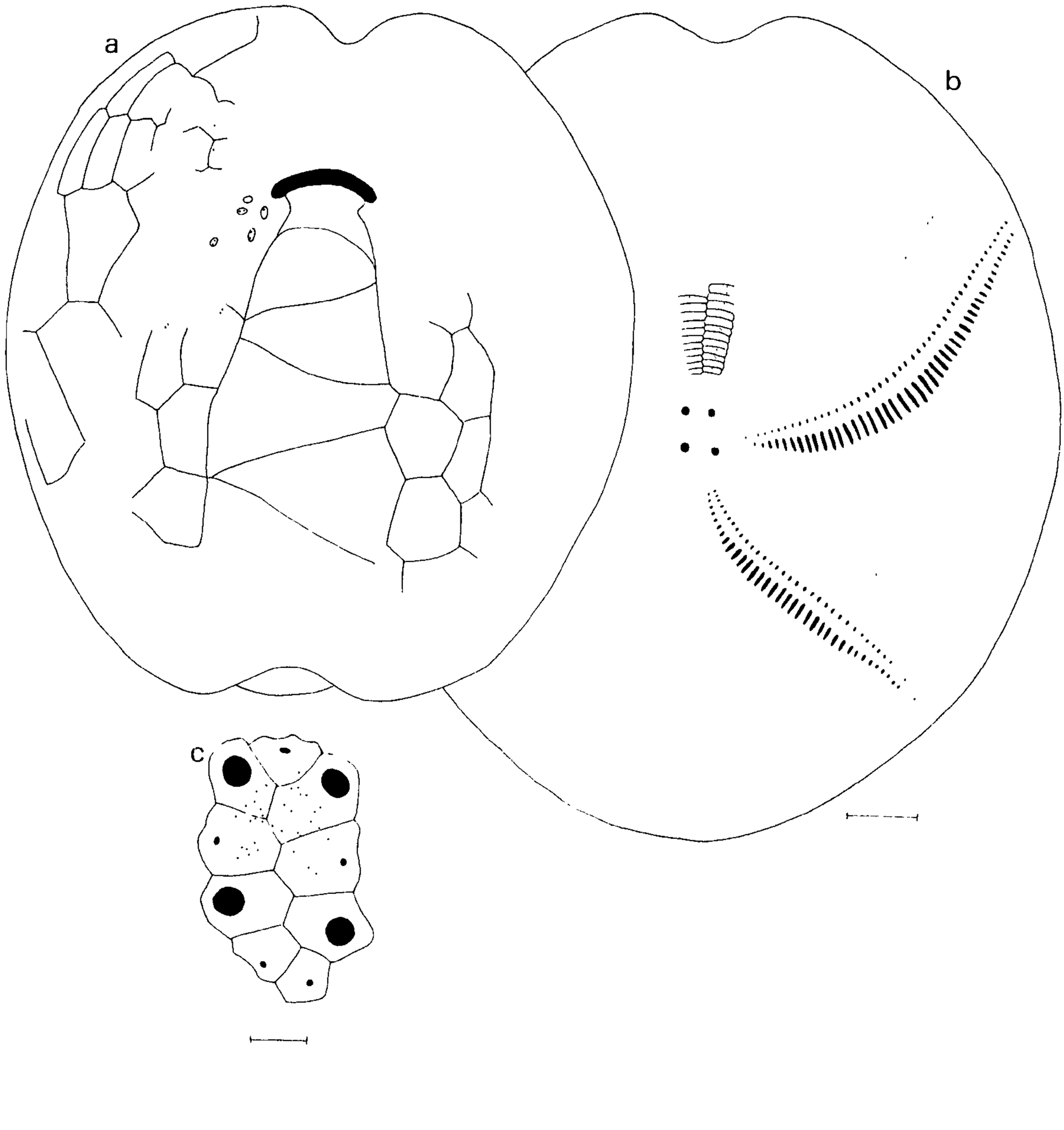
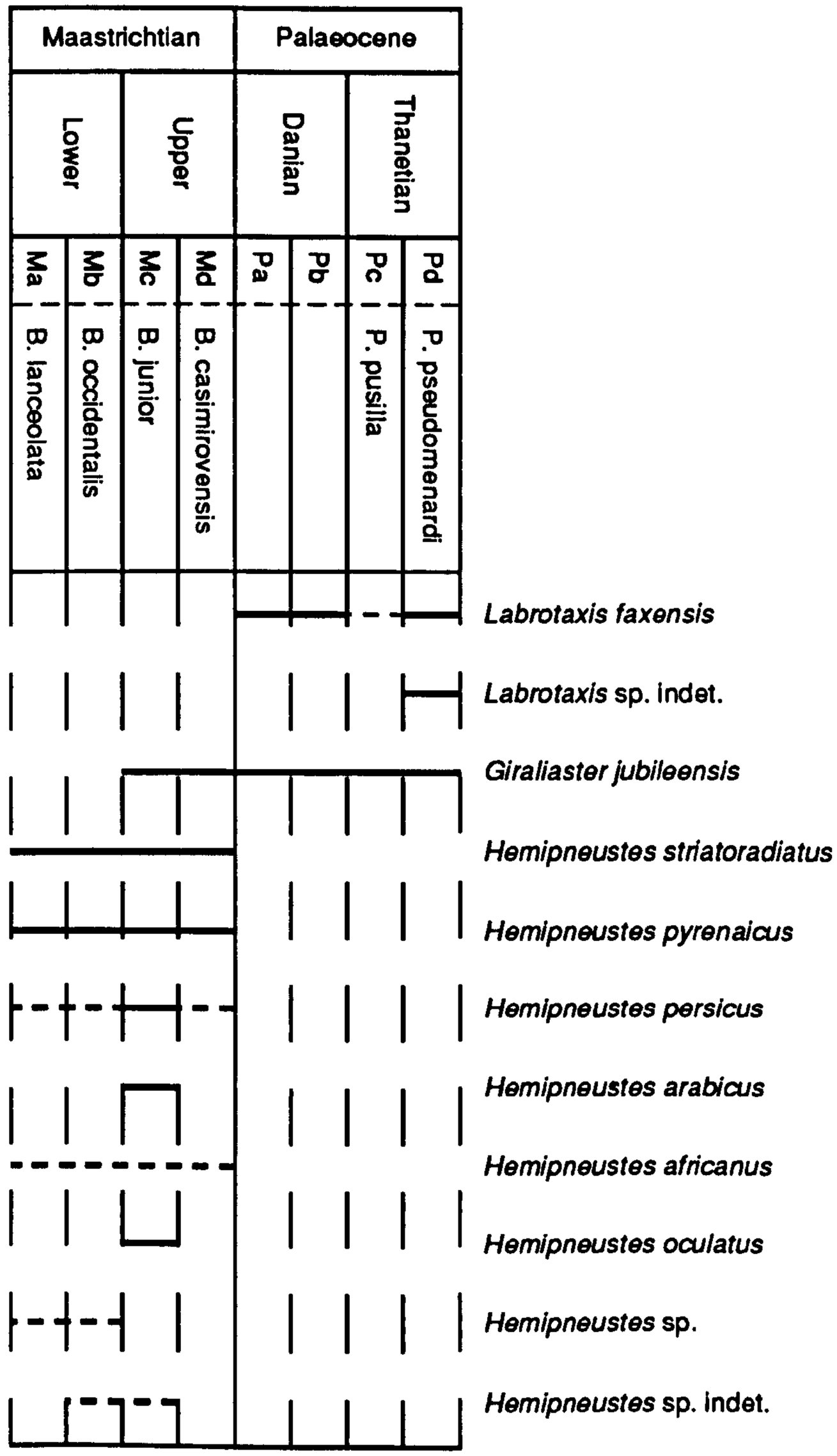

a
b
c

Figure 3.23. Range chart for Maastrichtian and Palaeocene labrotaxid species. See Figure 3.2 for explanation of symbols.


Maastrichtian
Palaeocene
Lower
Upper
Danian
Thanetian
Ma
Mb
Mc
Md
Pa
Pb
Pc
Pd
B. lanceolata
B. occidentalis
B. junior
B. casimirovensis
P. pusilla
P. pseudomenardi
Labrotaxis faxensis
Labrotaxis sp. indet.
Giraliaster jubileensis
Hemipneustes striatoradiatus
Hemipneustes pyrenaicus
Hemipneustes persicus
Hemipneustes arabicus
Hemipneustes africanus
Hemipneustes oculatus
Hemipneustes sp.
Hemipneustes sp. indet.

Indeterminate holasterolds.

i) Material too poorly preserved to allow identification:

1848 *Holaster indicus* Forbes, p. 159, pl. 19, fig. 4.

1873 *Cardiaster regularis* Stoliczka, p. 23, pl. 4, figs 3-4.

Occurrence. Late Campanian to Maastrichtian Ariyalur Group of Southern India (Forbes 1848; Stoliczka 1873) (BMNH, GSI).

Remarks. Plastron plating, fascioles and tuberculation is not preserved in any specimens. However, the sharp carinae running along the edges of the anterior ambulacrum are suggestive of *Cardiaster*.

1873 *Cardiaster orientalis* Stoliczka, p. 22, pl. 4, figs 1-2.

Occurrence. Maastrichtian Ariyalur Group of southern India (Stoliczka 1873) (GSI).

Diagnosis. Broad, shallow frontal groove. Pores in paired ambulacra somewhat asymmetric - anterior series small and round, posterior series elongate. Plastron not preserved. No fascioles preserved.

ii) The following two genera were both erected on the basis of poorly preserved single specimens. Complete diagnoses are lacking and affinities are uncertain.

Genus CORECHINUS Kongiel, 1936

[Type species *Corechinus pulaviensis* Kongiel, 1936, by OD]

Corechinus pulaviensis Kongiel, 1936

1935 *genus novus* Kongiel, pl. 1, fig. 4, pl. 2, fig. 6.

1936 *Corechinus pulaviensis* Kongiel, p. 3 & 8.

Occurrence. Middle Danian Siwak of Central Poland (Kongiel 1935, 1936).

Remarks. The affinities of this poorly known genus are uncertain. Nothing is known of the plastron structure or presence of fascioles making comparison with other genera impossible. Kongiel compares *Corechinus pulaviensis* to the stegasterids, and more particularly to *Galeaster*. Affinities to either seem unlikely as the frontal groove does not extend onto the oral surface to form a distinct sulcus as is the case in the stegasterids, and *Galeaster* has high ambulacral plates unlike those in *Corechinus*.

Genus GANBIRRETIA Gauthier, 1903

[Type species *Ganbirretia douvillei* Gauthier, 1903, by OD]

Ganbirretia douvillei Gauthier, 1903

1903 *Ganbirretia douvillei* Gauthier, p. 20, pl. 1, figs 1-6.

Occurrence. Maastrichtian of the French Pyrenees.

Diagnosis (as far as can be determined). Test ovate - no anterior groove. Ambulacral plates high - pores small and round. Apical system elongate with four gonopores. Details of plastron structure unknown.

Remarks. Only one poorly preserved specimen has been referred to this genus. Affinities are thus somewhat uncertain. *Ganbirretia* has been compared to low forms of *Stegaster* but the absence of a frontal groove makes the synonymy of the two genera unlikely. *Ganbirretia* has also been compared to *Garumnaster*. Without details of fascioles or plastron structure, however, further comparison is impossible.

Table 3.2. Indeterminate holasteroid taxa recorded from Maastrichtian and Palaeocene deposits. Material unavailable for study. Descriptions and / or illustrations of these taxa are inadequate to allow even generic identification.

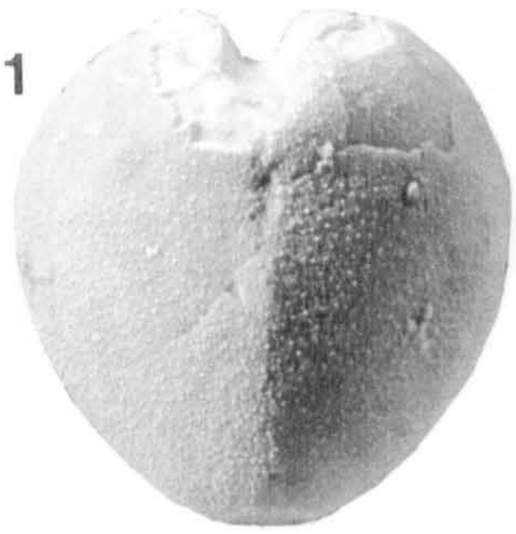
Taxon	Reference	Age	Locality
Tholaster sp.	Asgaard 1979	Upper Maas. white chalk	Denmark
Cardiaster sp.	Ødum 1926	Maas. white chalk	Denmark
Cardiaster sp.	Nicklès 1892	Maas.	Alicante
Cardiaster marylandica Clark	Clark 1916	Mid Maas. Monmouth Fm.	Maryland, USA
Cardiaster marylandicus Clark	Cooke 1953	"	"
Toxopatagus rutoti (Lambert)	Savchinskaya 1974	Upper Lower-Lower Upper Maas.	Don Basin

PLATE 1

Figs 1-4. *Galeaster bertrandi* Seunes, Danian of the Mangyshlak Peninsula, Kazakhstan. 1-2, BMNH EE5596; 1, apical view; 2, oral view. 3-4, BMNH EE5595; 3, anterior view; 4, lateral view. All x2.

Figs 5-9. *Stegaster altus* Seunes, BMNH EE4396, Maastrichtian of Navarra, Spain. 5, apical view; 6, oral view; 7, lateral view; 8, anterior view; 9, posterior view. All x1 1/2.

1



2



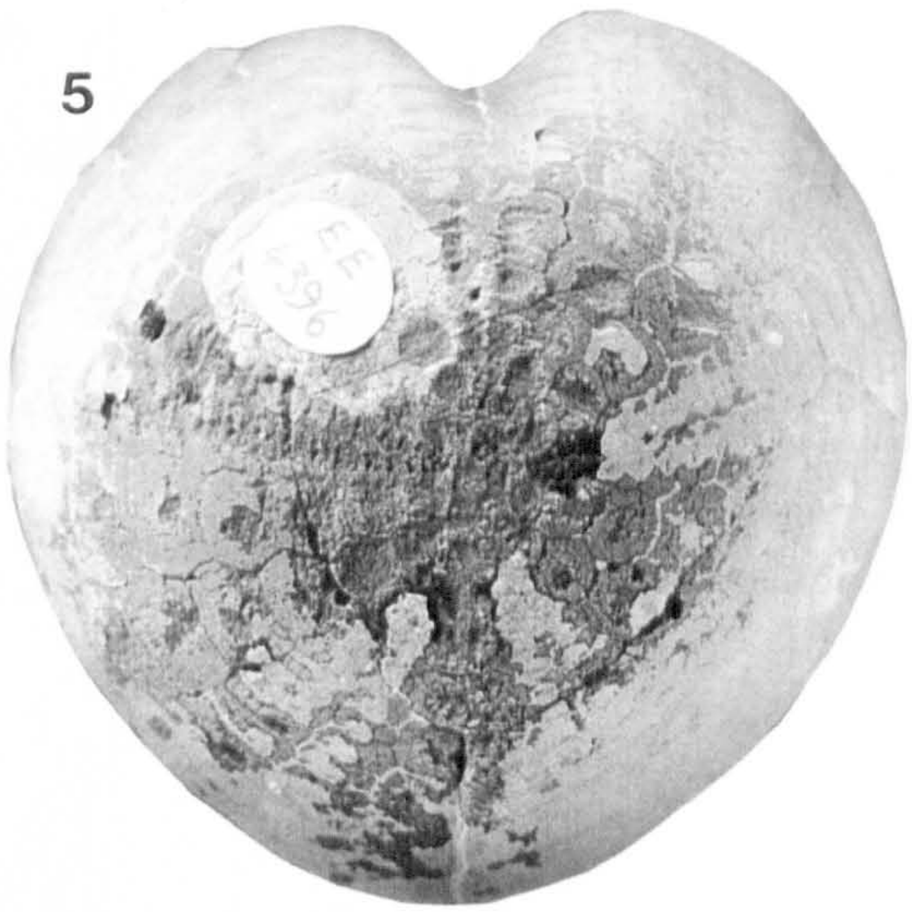
3



4



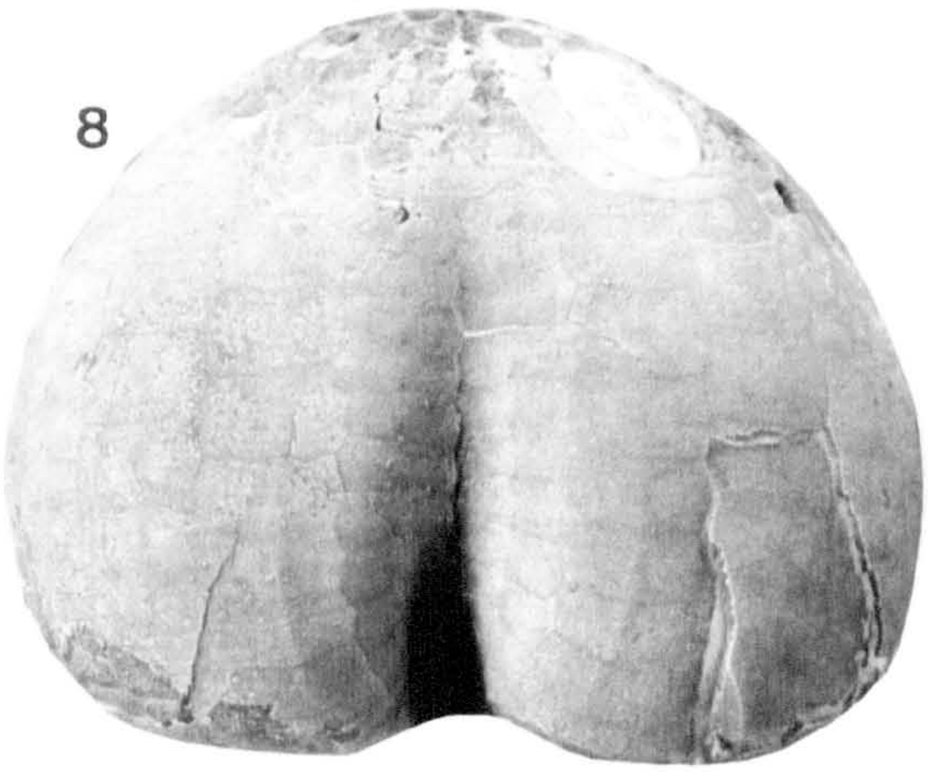
5



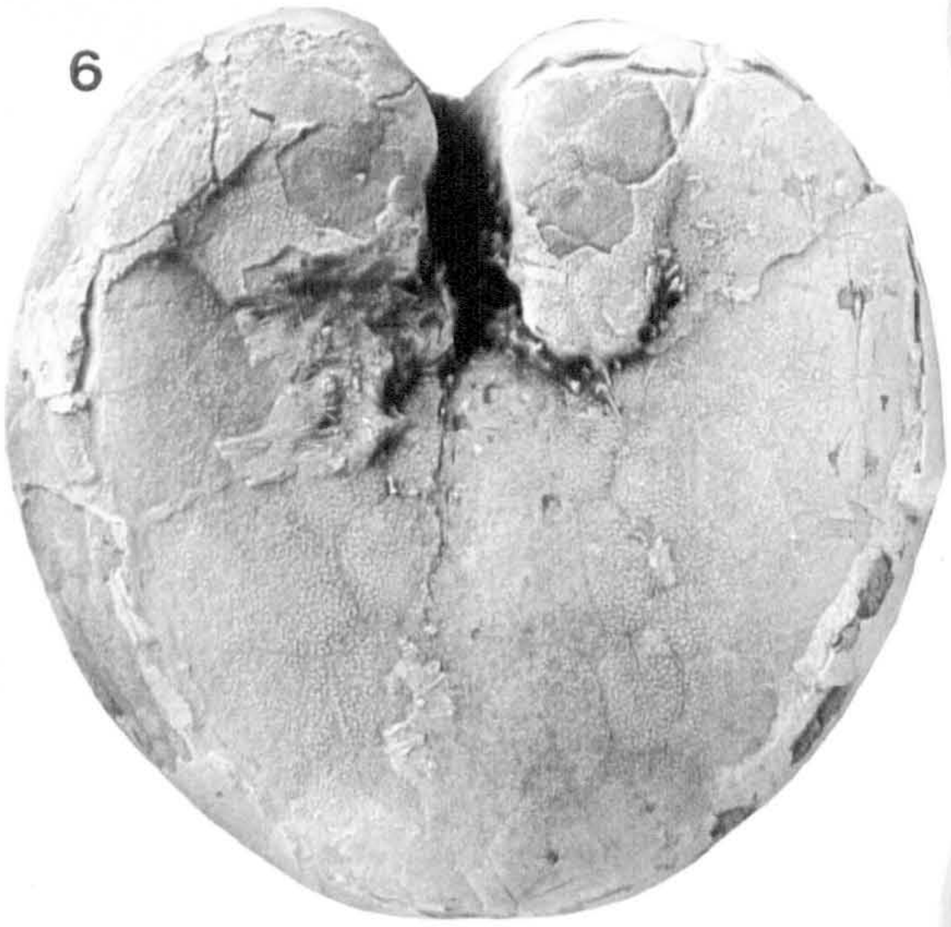
7



8



6



9

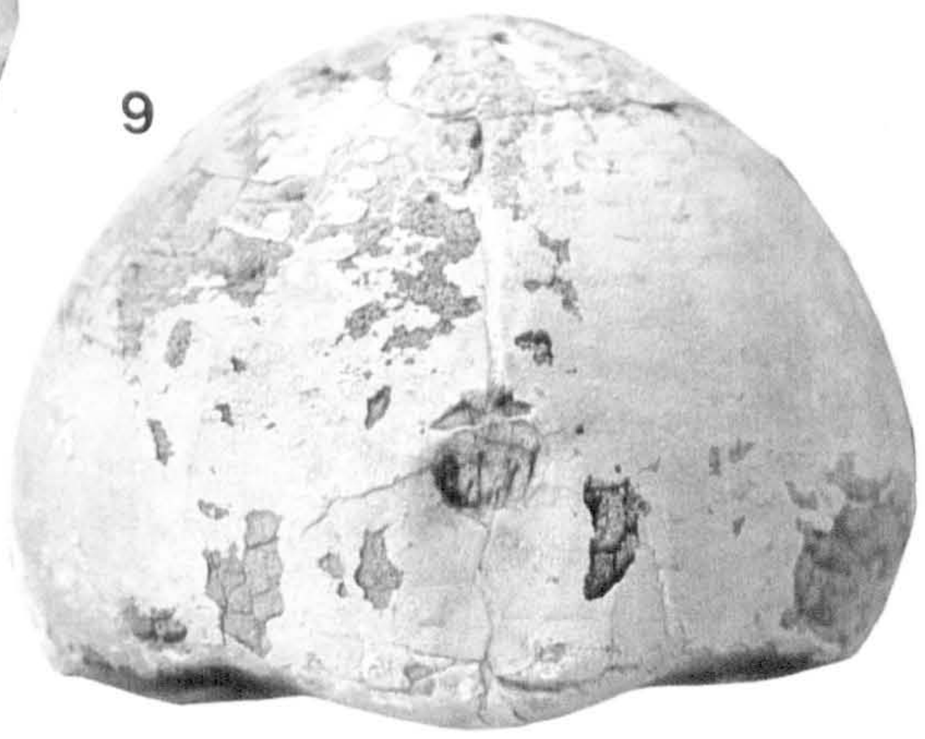


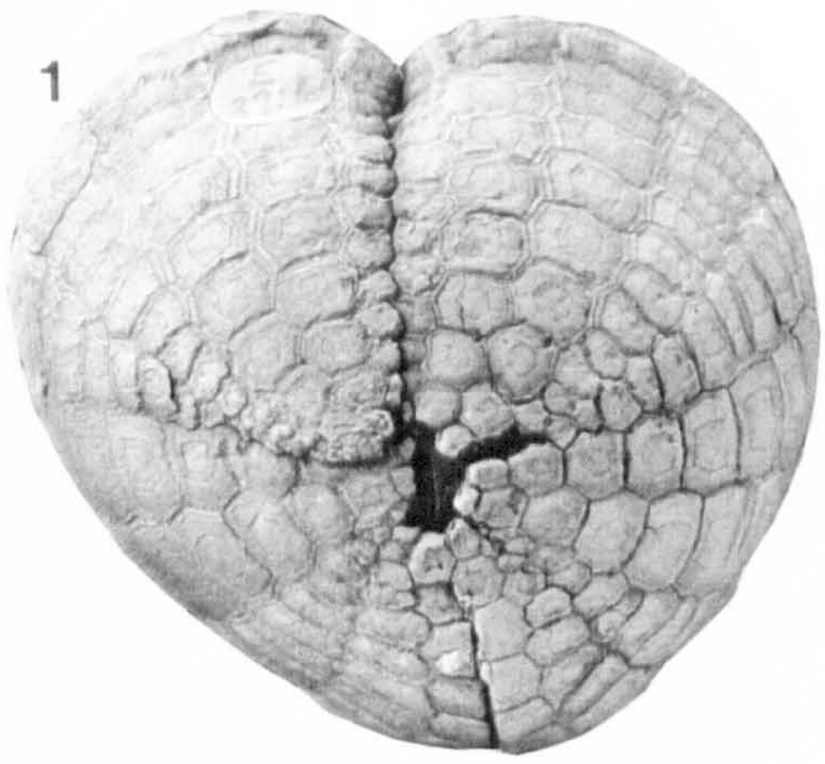
PLATE 2

Figs 1-4. *Stegaster cotteaui* Seunes, BMNH E2916, Maastrichtian of Biarritz, France. 1, apical view; 2, oral view; 3, lateral view; 4, posterior view. All x1.

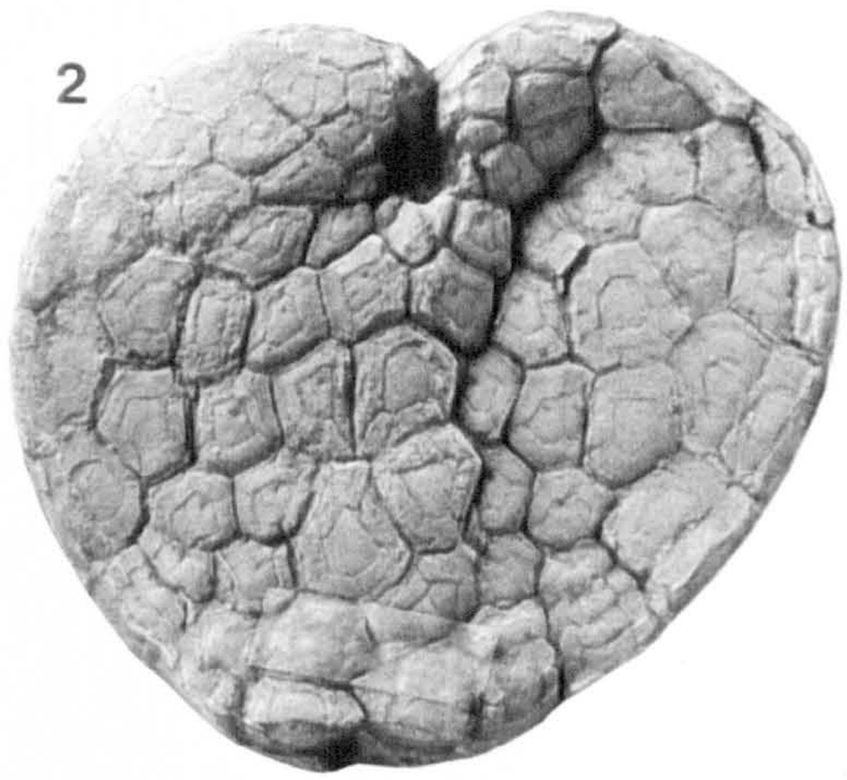
Figs 5-8. *Pseudoffaster caucasicus* (Dru), BMNH EE5573, Uppermost Maastrichtian of the Mangyshlak Peninsula, Kazakhstan. 5, apical view; 6, oral view; 7, lateral view; 8, posterior view. All x2.

Figs 9-12. *Guettaria rocardi* Cotteau. 9-10, BMNH E18706 (TOPOTYPE), Lower Maastrichtian of northernmost Madagascar. 9, apical view; 10, oral view. 11-12, EE4797, Upper Campanian or Lower Maastrichtian of northern Turkey. 11, posterior view; 12, lateral view. All x1.

1



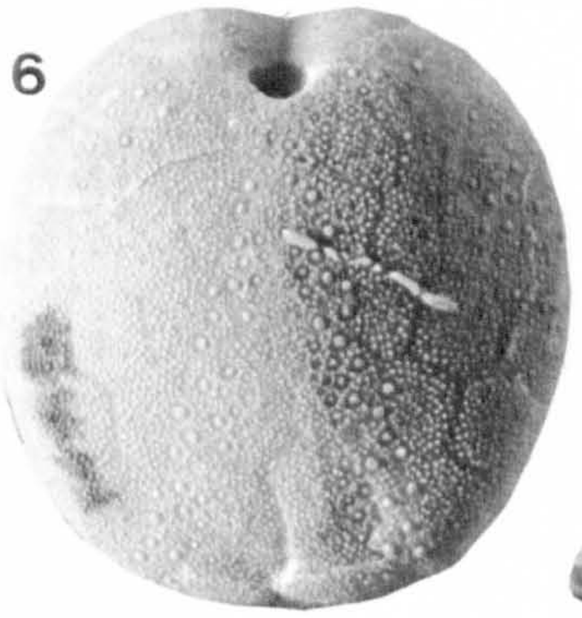
2



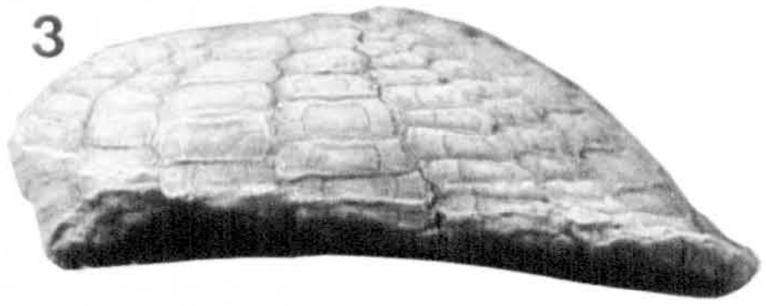
5



6



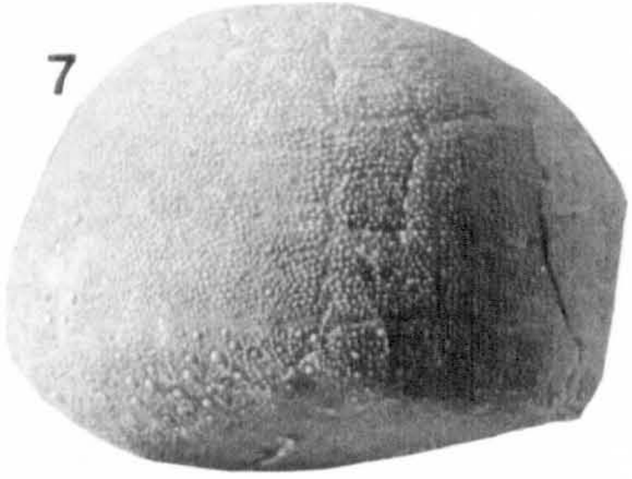
3



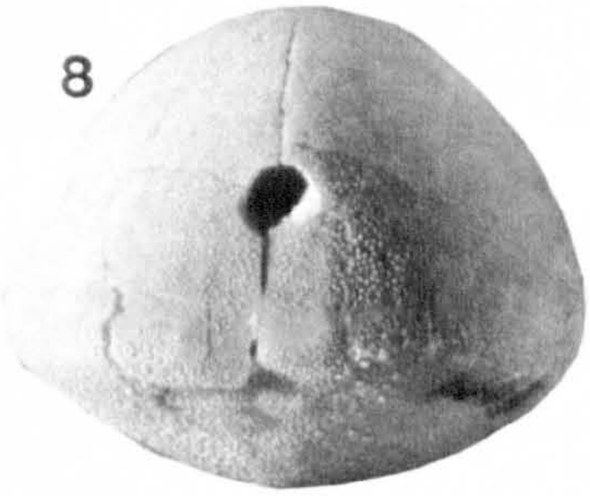
4



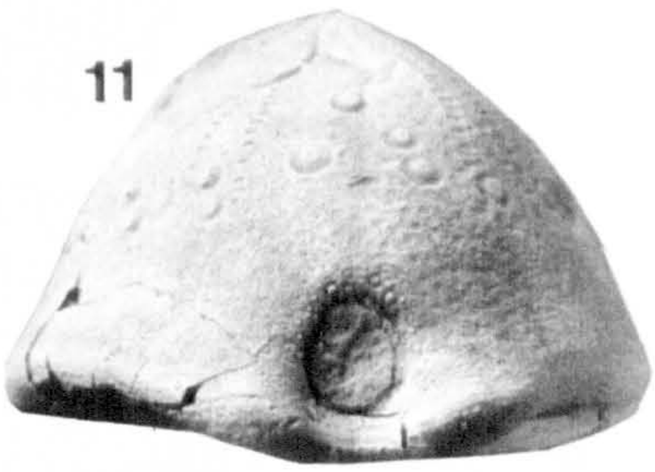
7



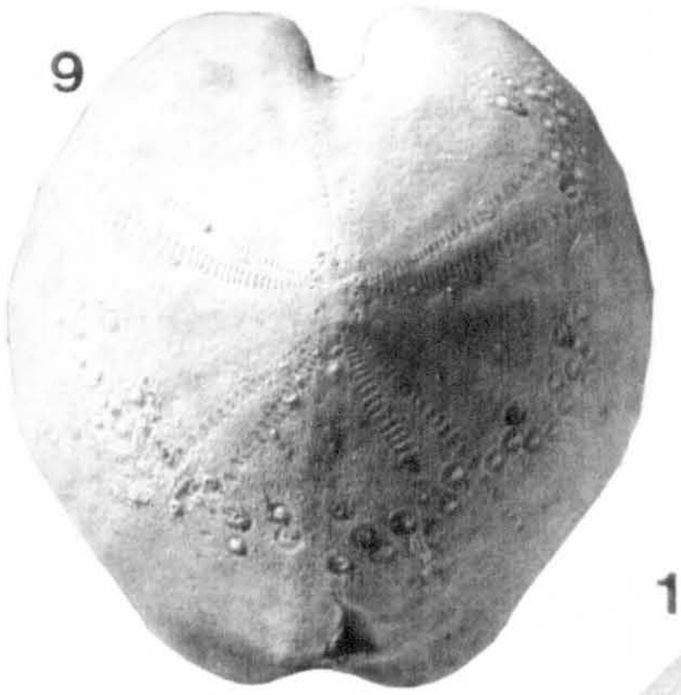
8



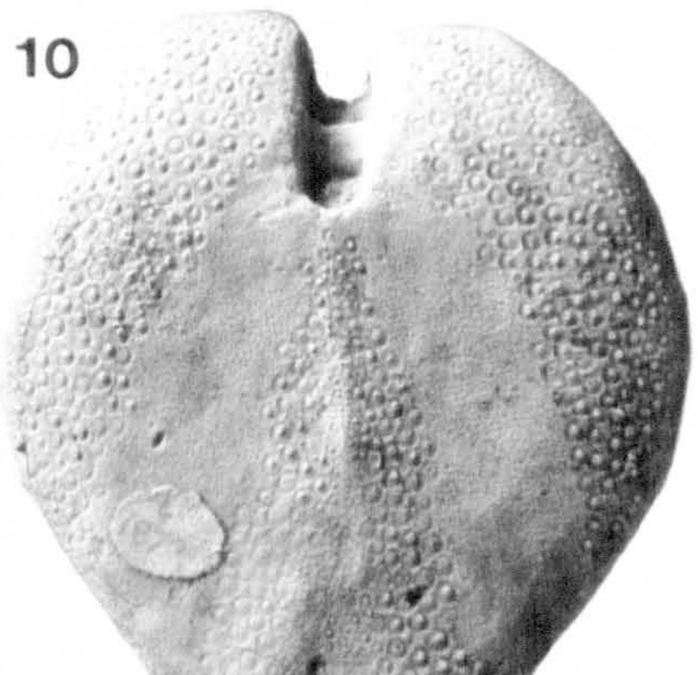
11



9



10



12

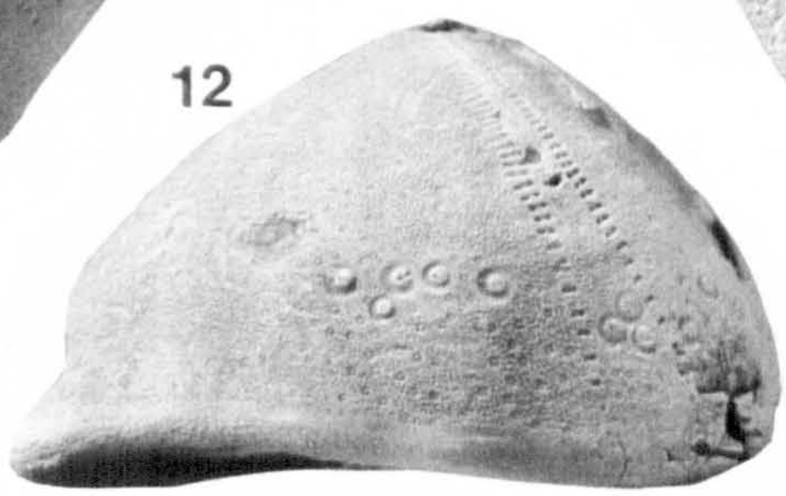
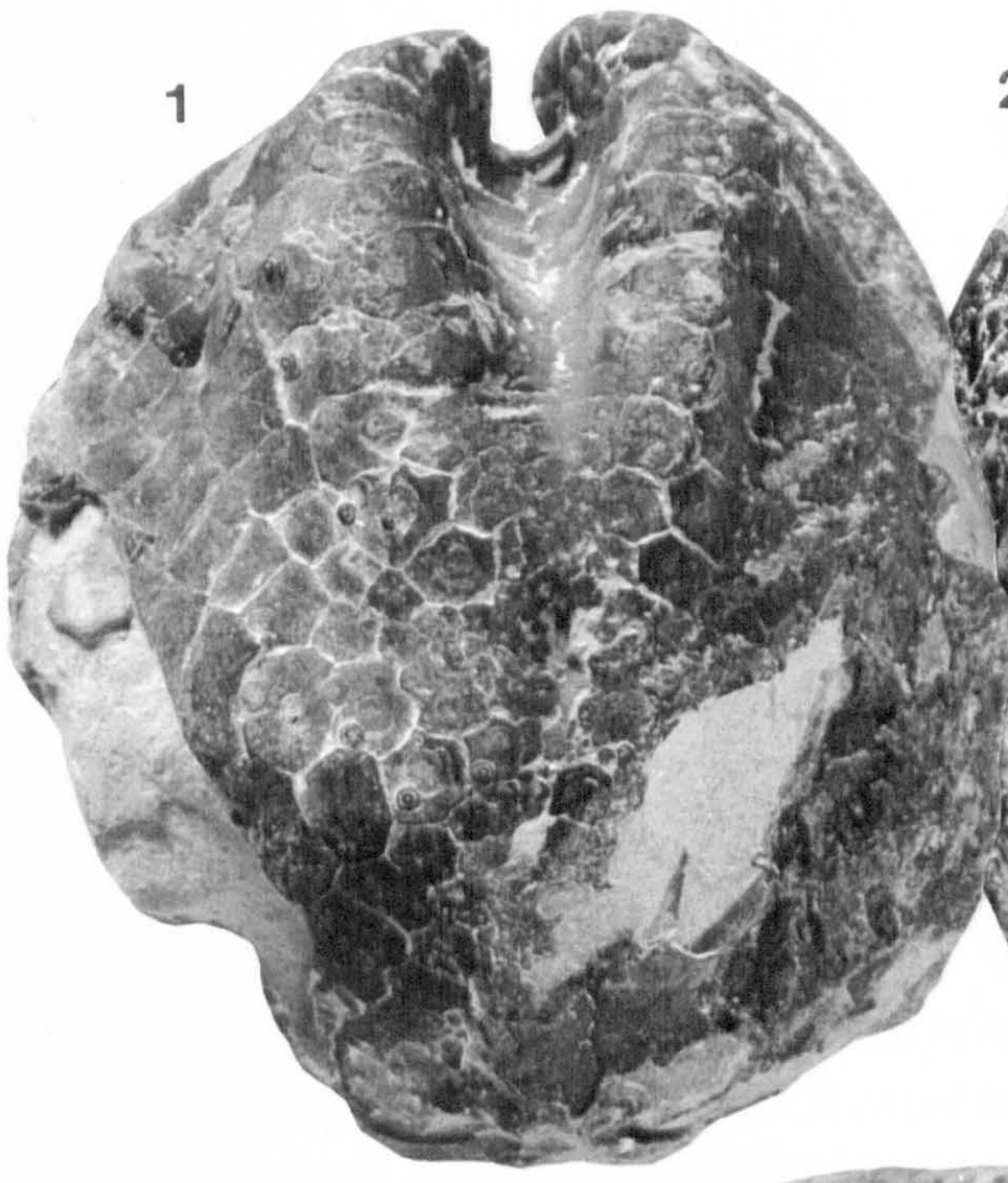


PLATE 3

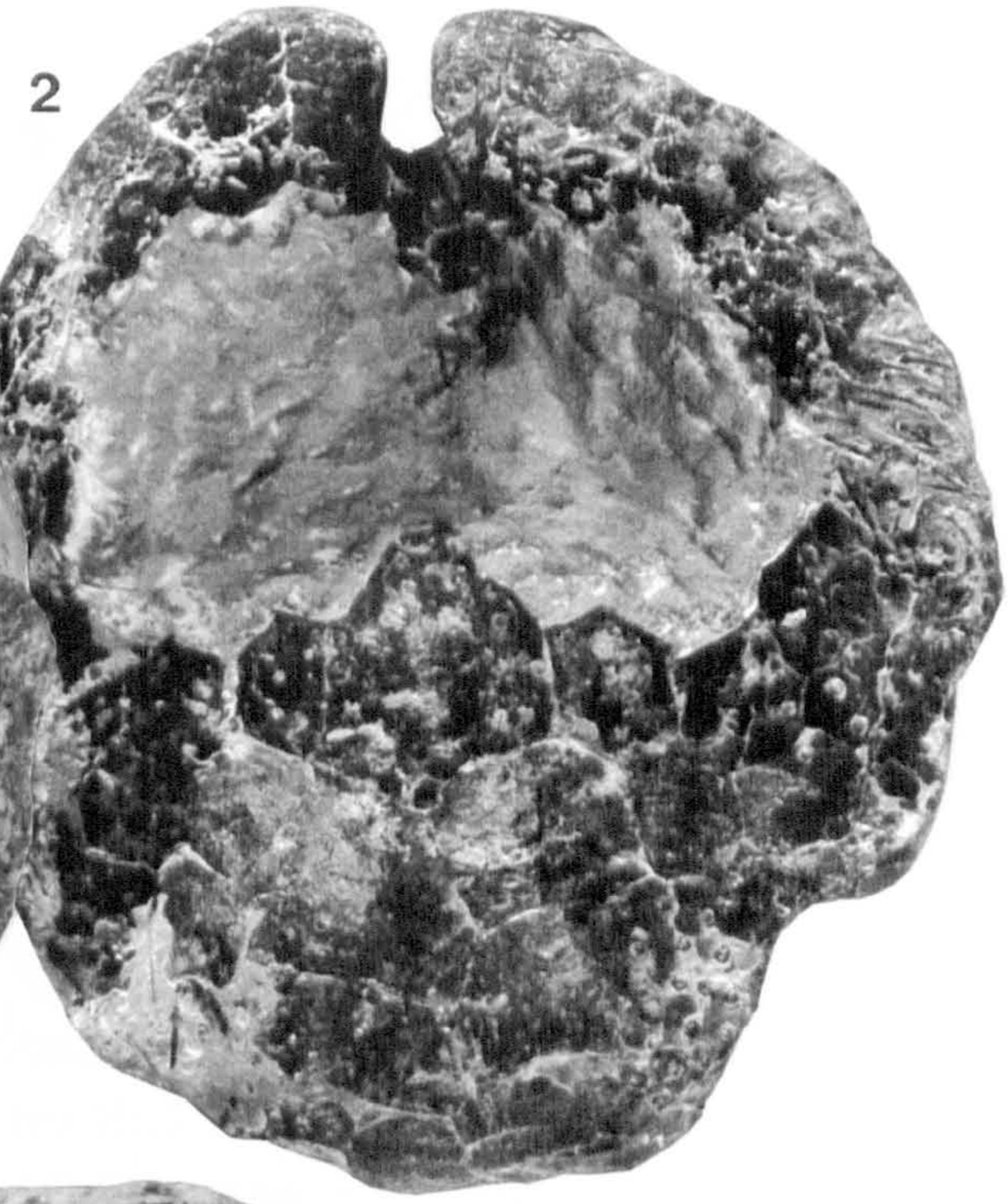
Figs 1-3. *Tholaster munieri* (Seunes), UWBM 94993, Maastrichtian of Zumaya, Spain. 1, apical view; 2, oral view; 3, lateral view. All x2.

Figs 4-6. *Rispolia subtrigonata* (Catullo), BMNH E4587, Coniacian of Scagglio, Italy. 4, apical view; 5, oral view; 6, lateral view. All x1$^1/_2$.

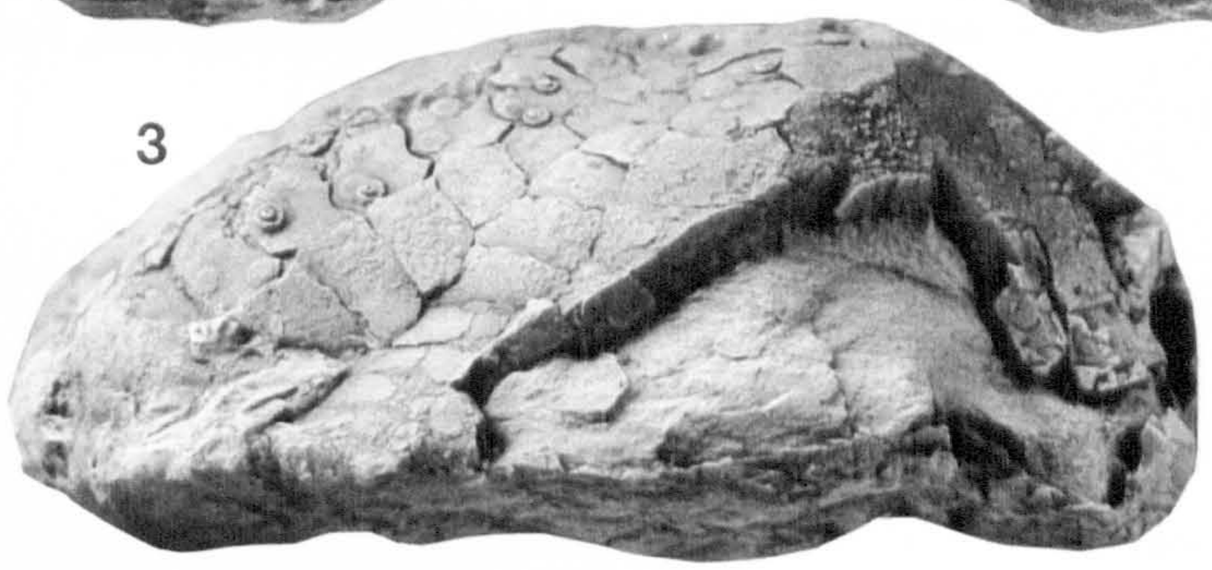
1



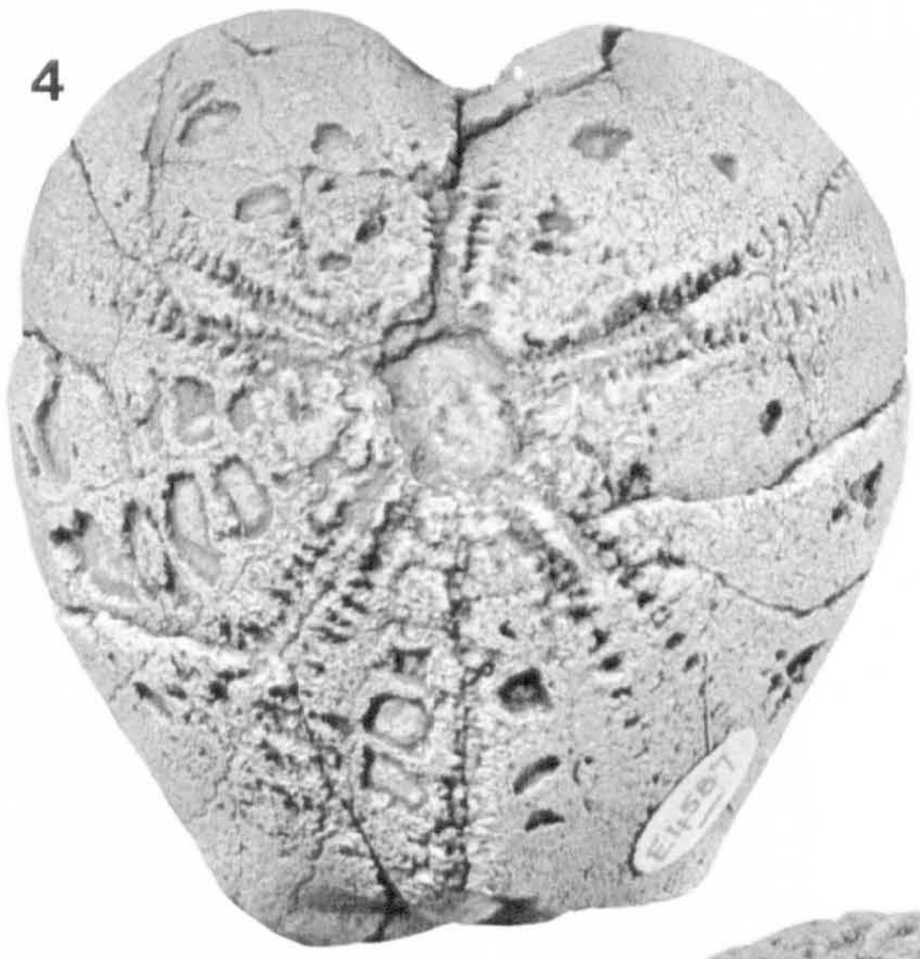
2



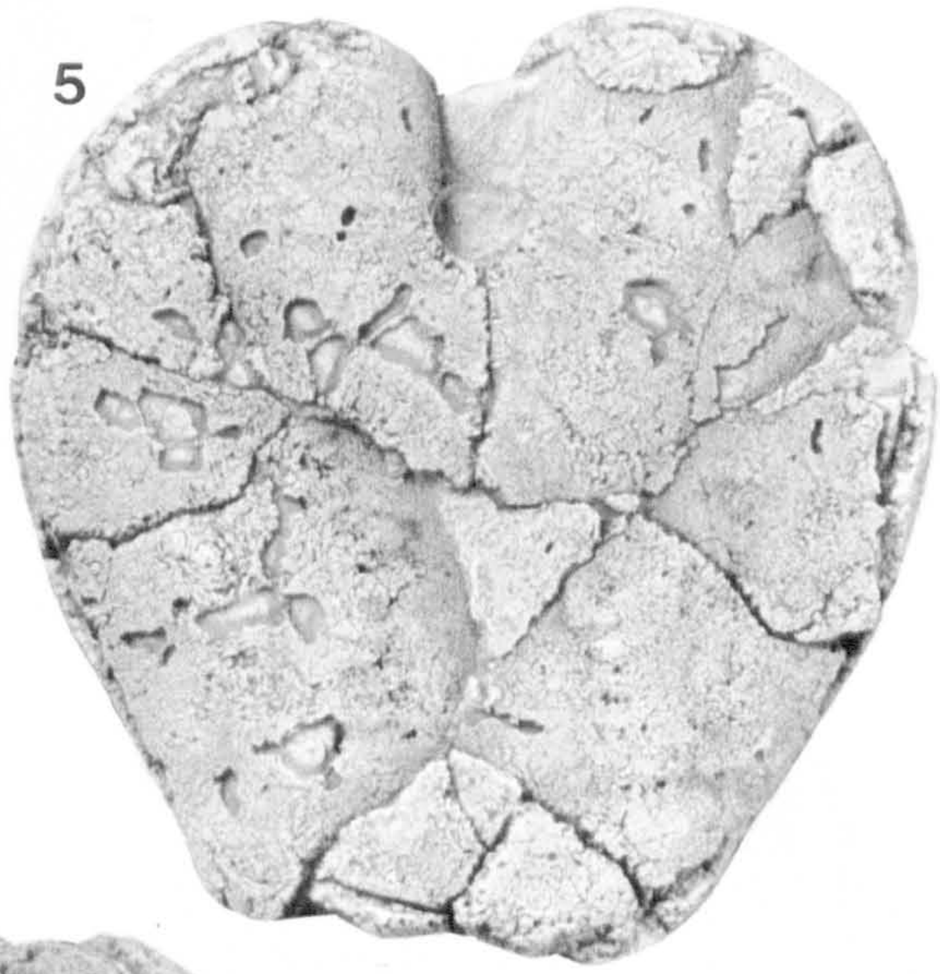
3



4



5



6

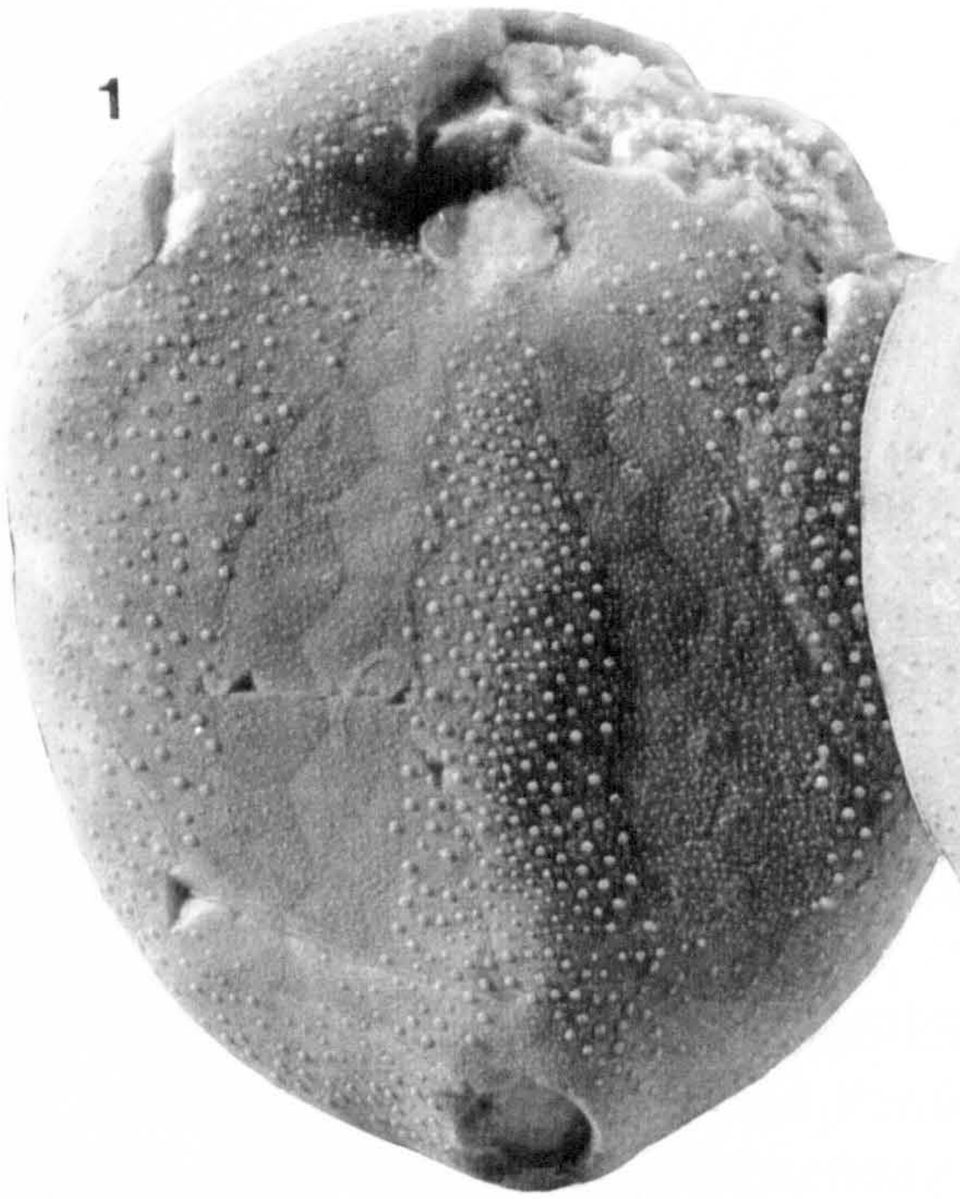


PLATE 4

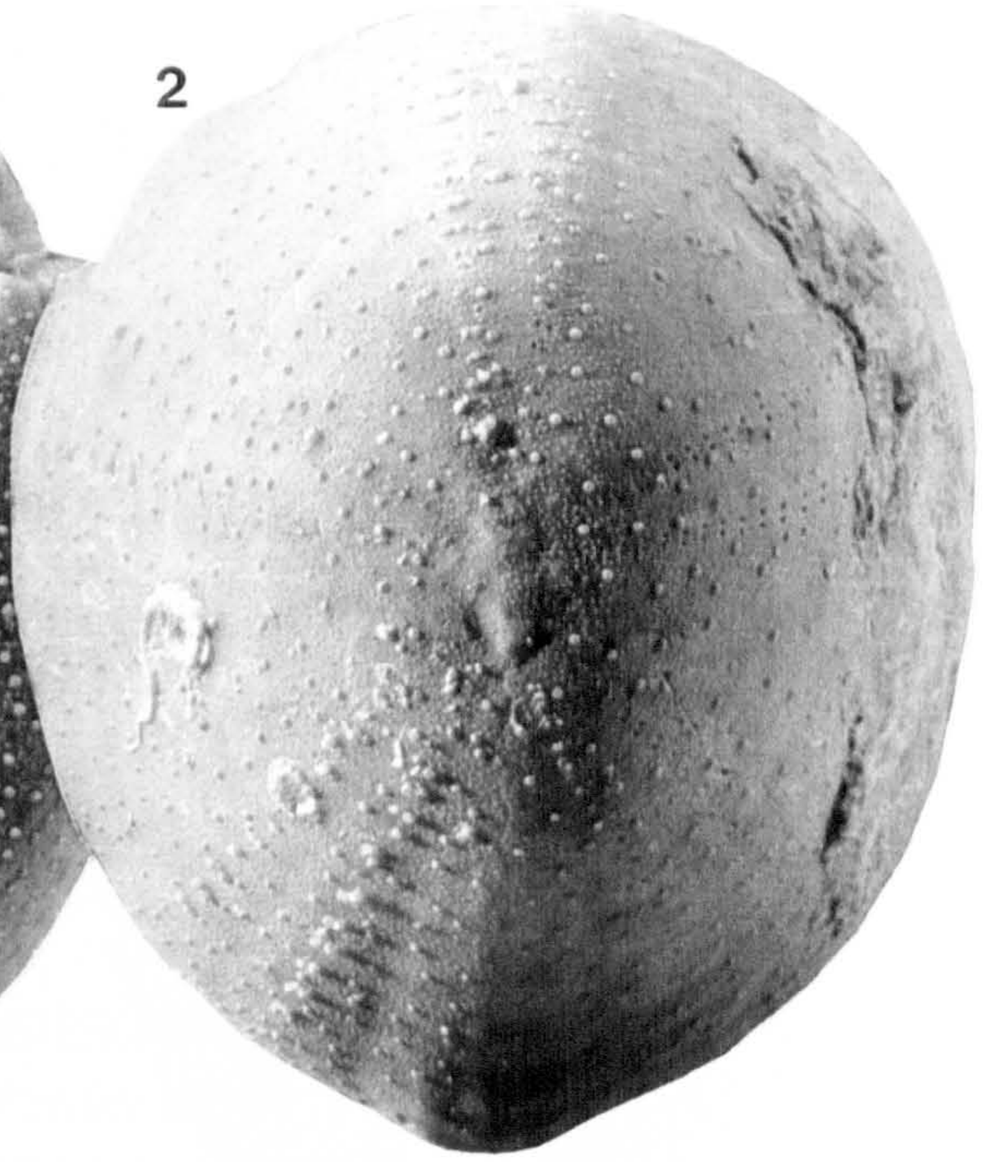
Figs 1-4. *Echinocorys scutata* Leske, BMNH EE5609, Danian of the Mangyshlak Peninsula, Kazakhstan. 1, oral view; 2, apical view; 3, lateral view; 4, posterior view. All x2.

Figs 5-7. *Jeronia pyrenaica* Seunes, BMNH E10643, Danian of Bidart, France. 5, oral view; 6, lateral view; 7, posterior view. All x2.

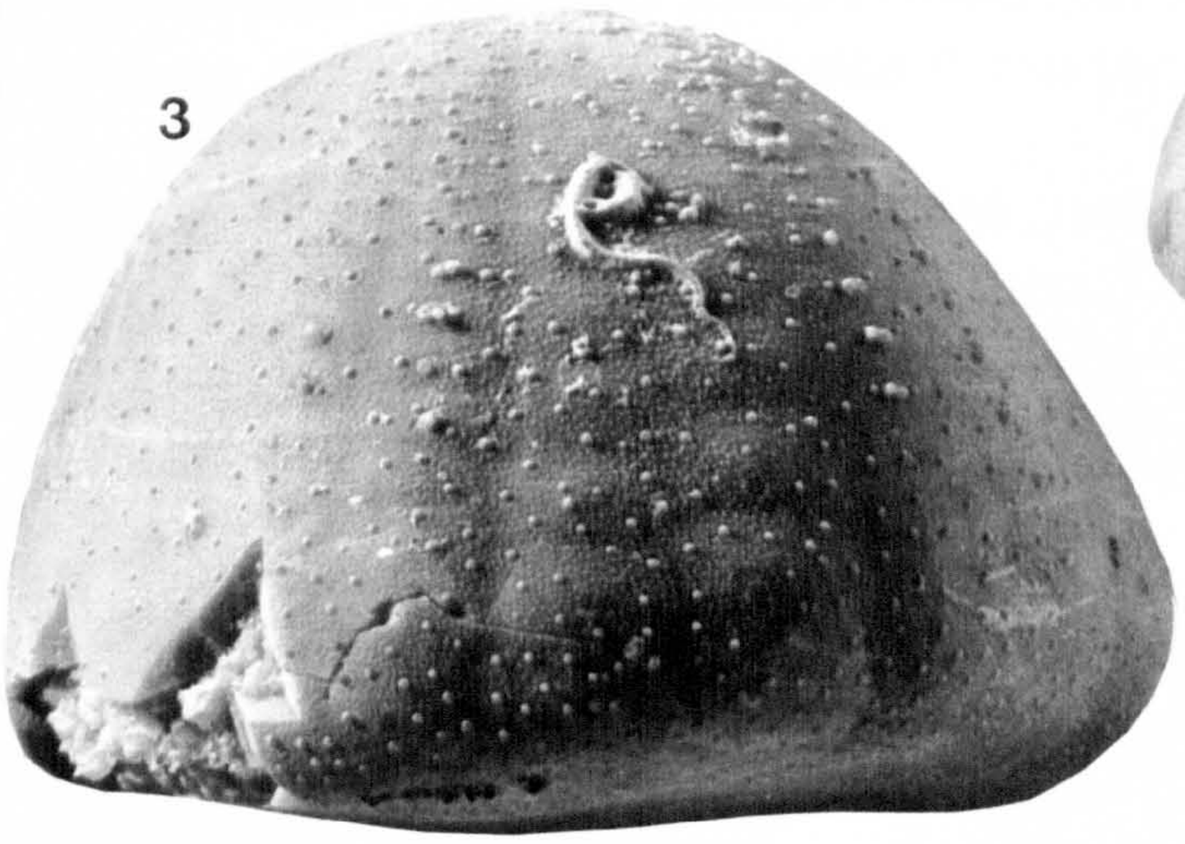
1



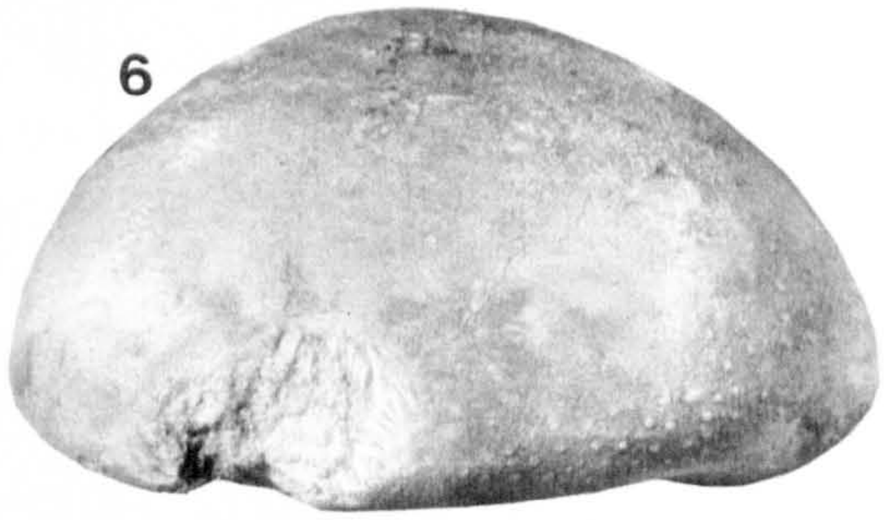
2



3



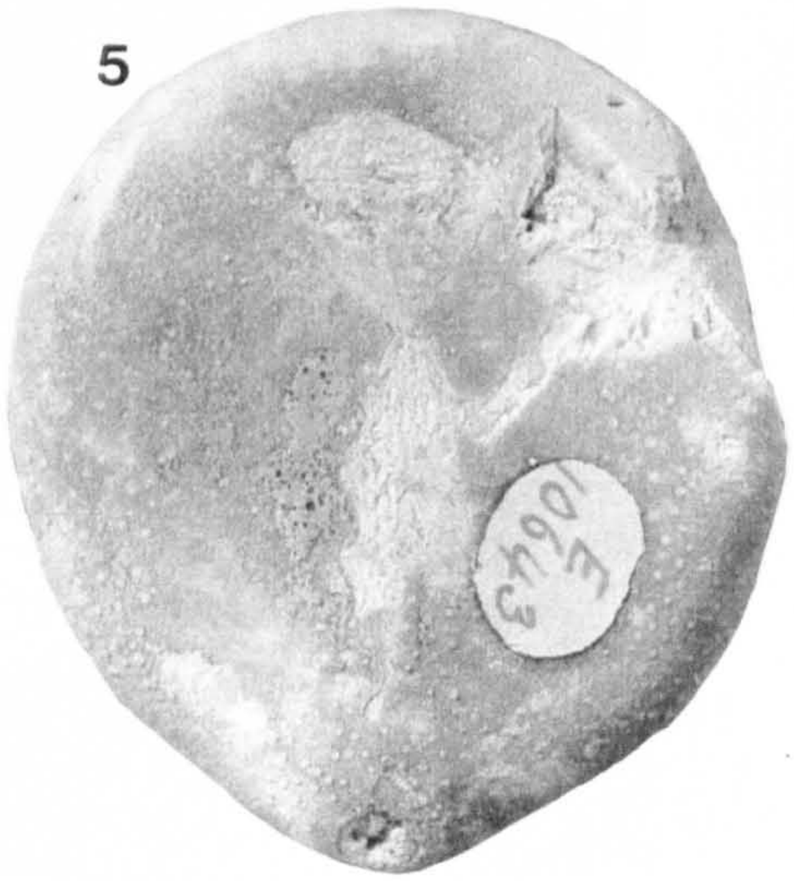
6



7



5



4

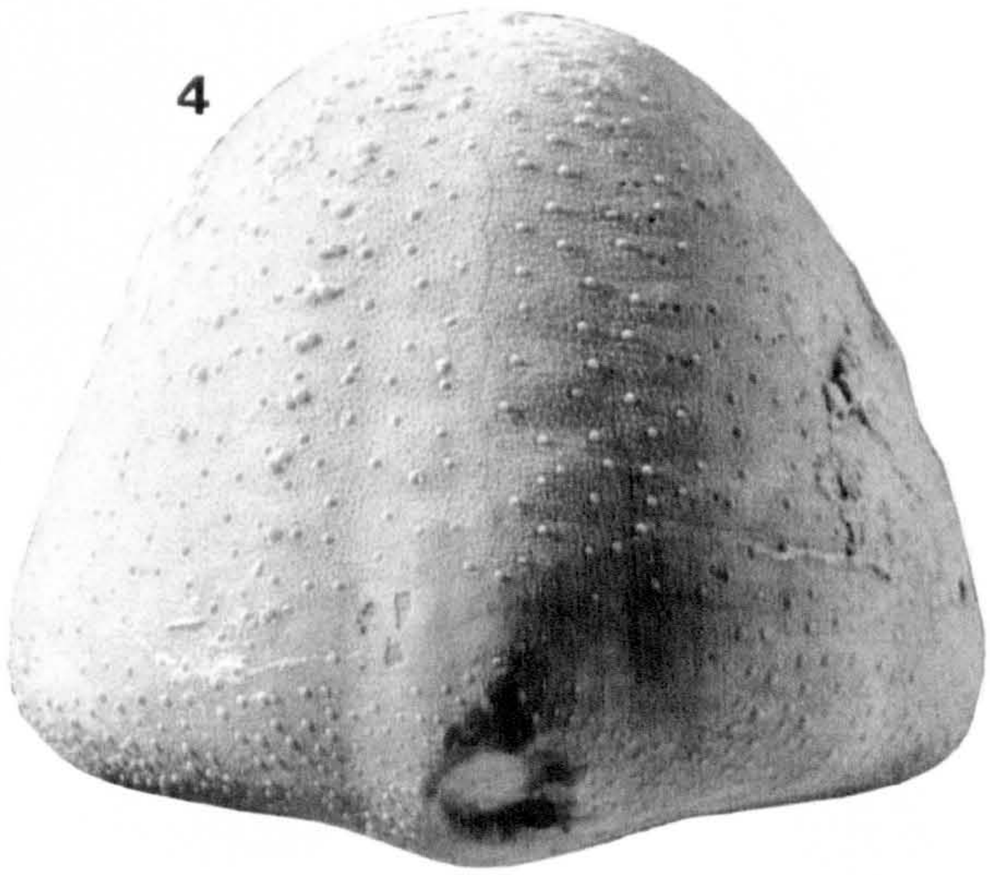


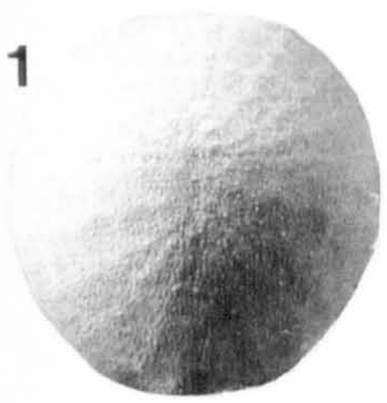
PLATE 5

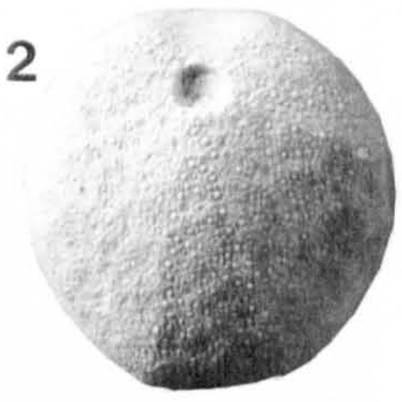
Figs 1-4. *Offaster pilula* (Lamarck), BMNH E31845, Senonian of Salisbury, UK. 1, apical view; 2, oral view; 3, lateral view; 4, posterior view. All x2.

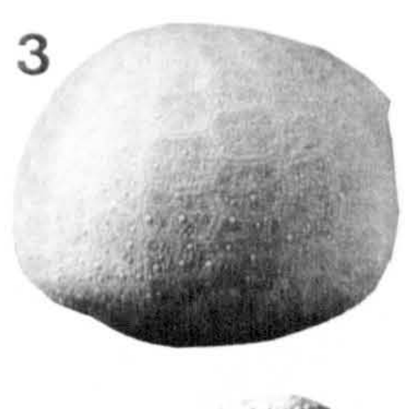
Figs 5-8. *Cardiaster granulosus* (Goldfuss), BMNH E32798, *Belemnitella mucronata* zone of Norfolk, UK. 5, apical view; 6, oral view; 7, posterior view; 8, lateral view. All x1.

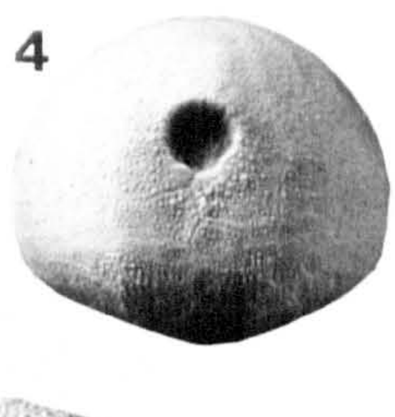
Figs 9-11. *Cardiotaxis heberti* (Cotteau), BMNH EE5627, Uppermost Maastrichtian of the Mangyshlak Peninsula, Kazakhstan. 9, apical view; 10, oral view; 11, lateral view. All x1.

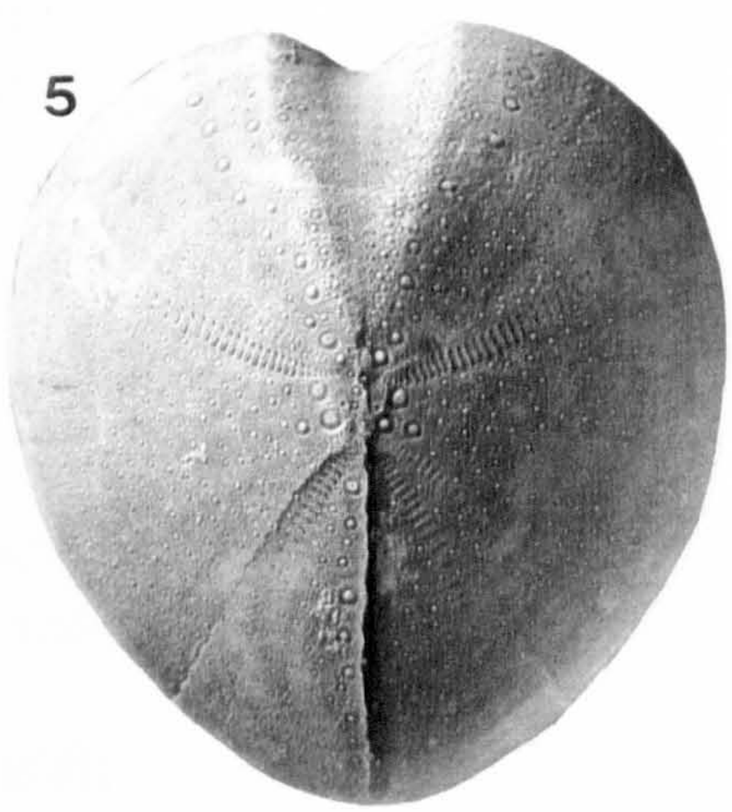
Figs 12-14. *Hagenowia rostrata* (Forbes), BMNH 76849, *Micraster coranguinum* zone of Kent, UK. 12, lateral view; 13, apical view; 14, oral view. All x2.

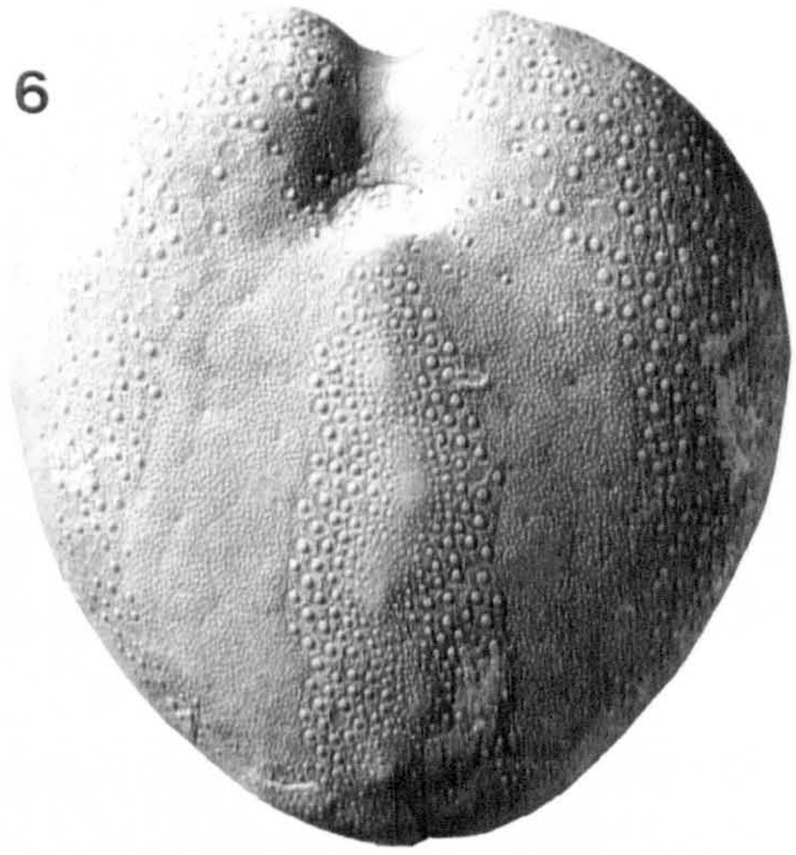

1

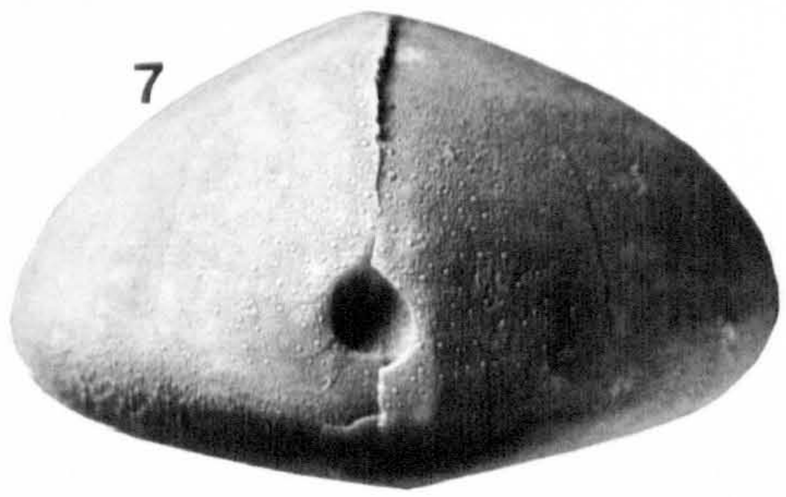

2

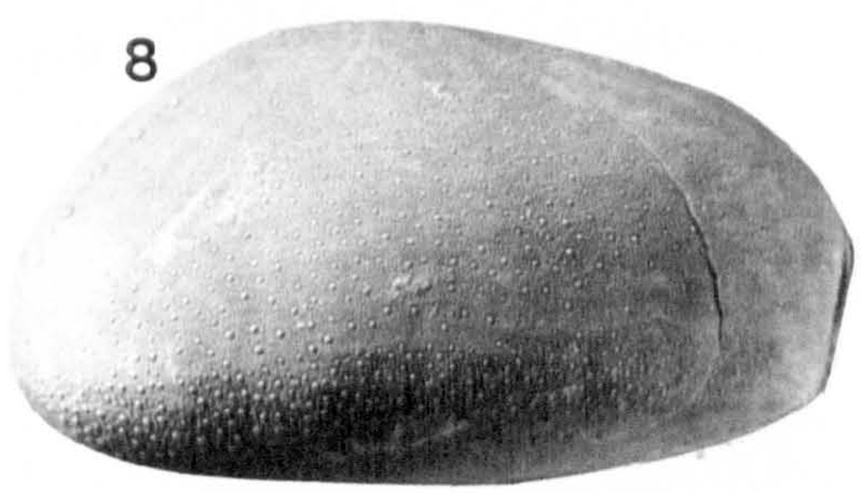

3

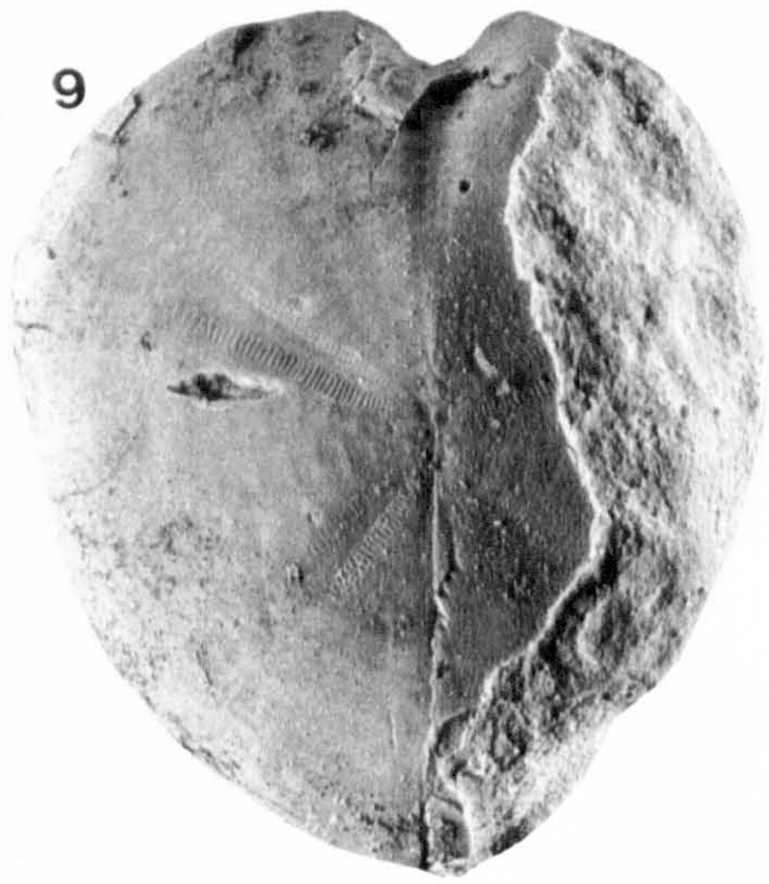

4

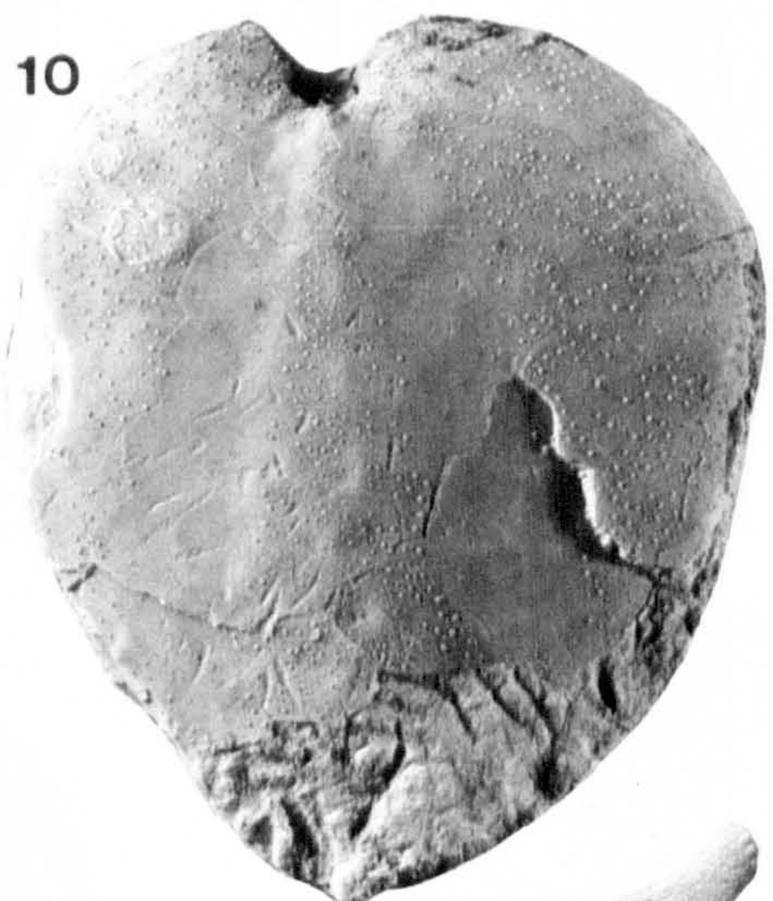

5

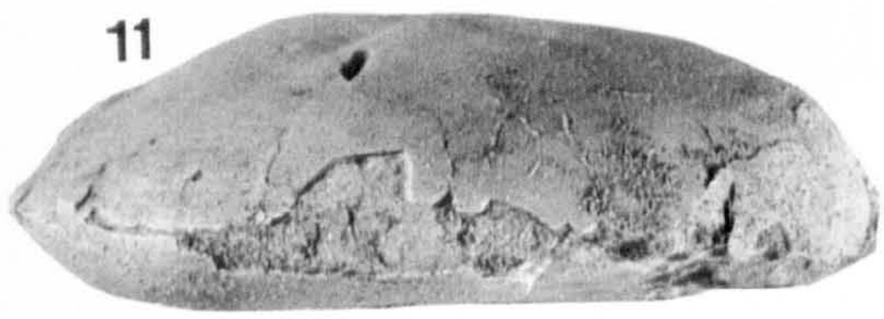

6


7


8


9


10


11


12


13

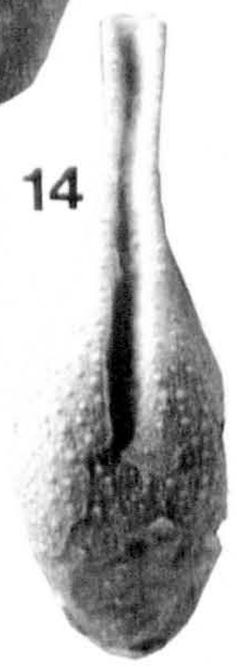
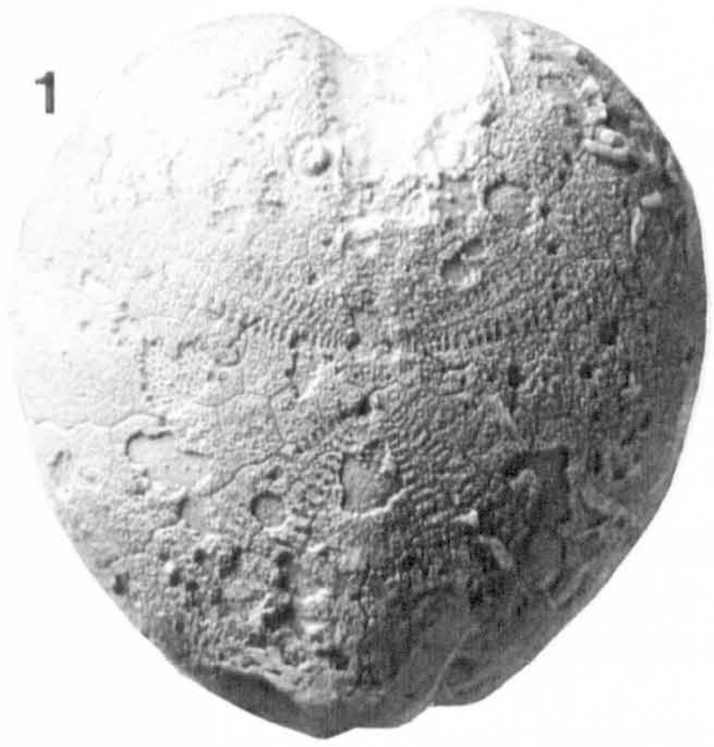

14

PLATE 6

Figs 1-3. *Labrotaxis faxensis* (Hennig), Mid Danian Faxe Limestone of Faxe, Denmark. 1-2, BMNH E12173; 1, apical view; 2, lateral view. 3, BMNH E2877, oral view. All x1.

Figs 4-7. *Hemipneustes striatoradiatus* (Leske), BMNH E75822, Upper Maastrichtian Meerssen Chalk of the Maastricht, Netherlands. 4, apical view; 5, oral view; 6, lateral view; 7, posterior view. All $x^{2}/_{3}$.

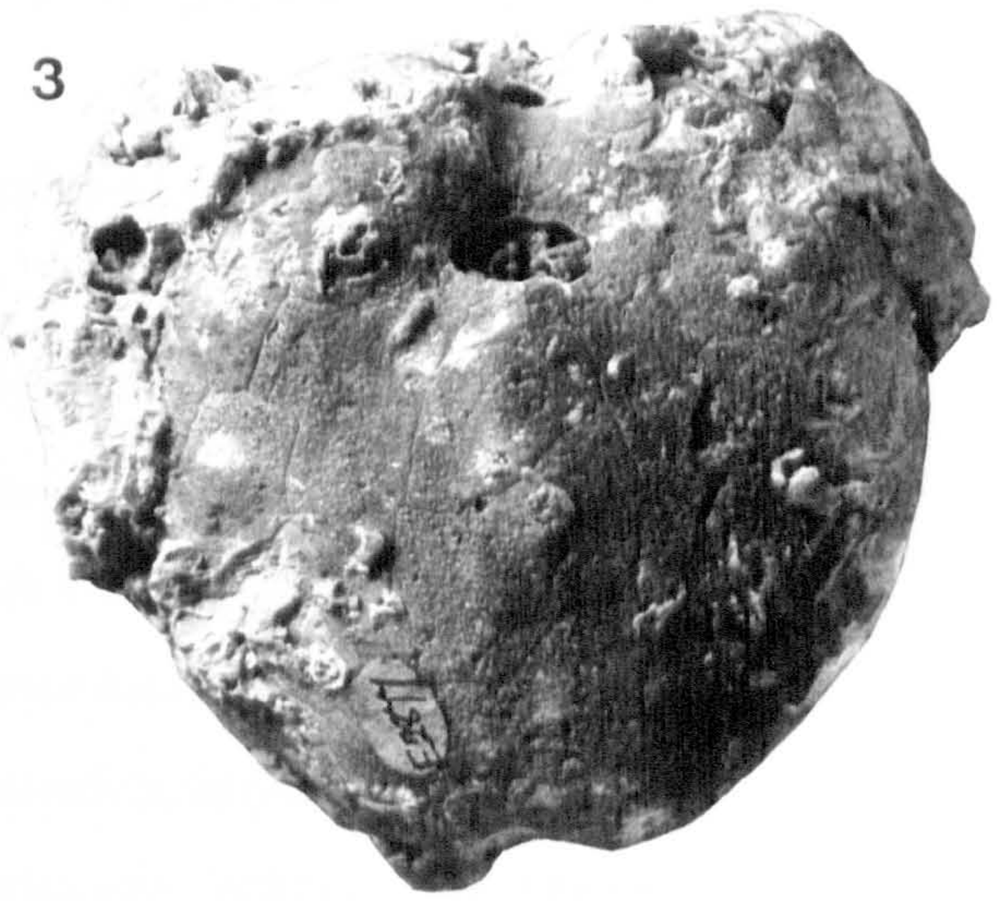
1



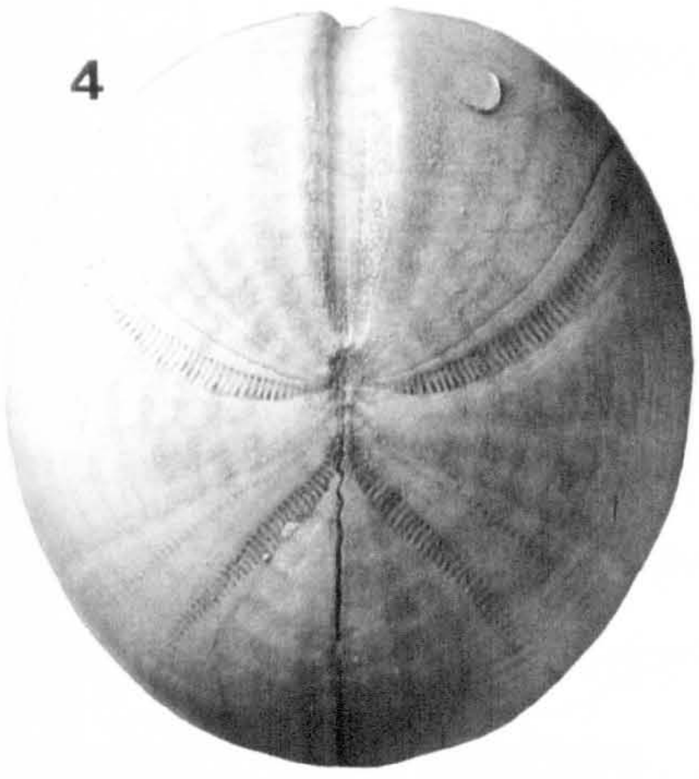
2



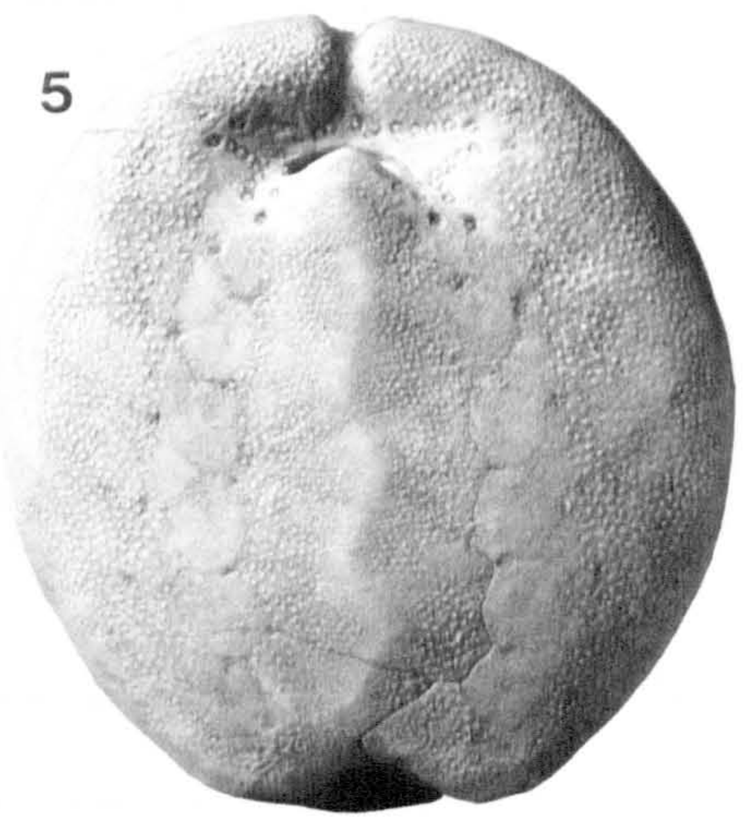
3



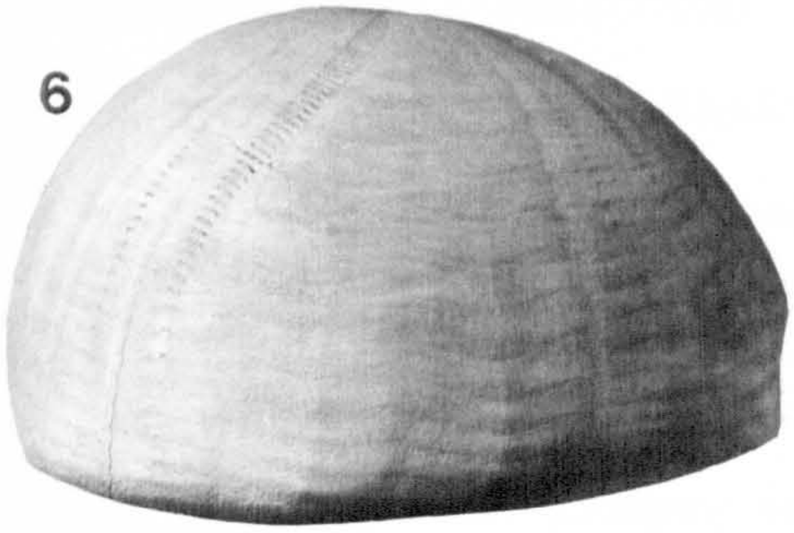
4



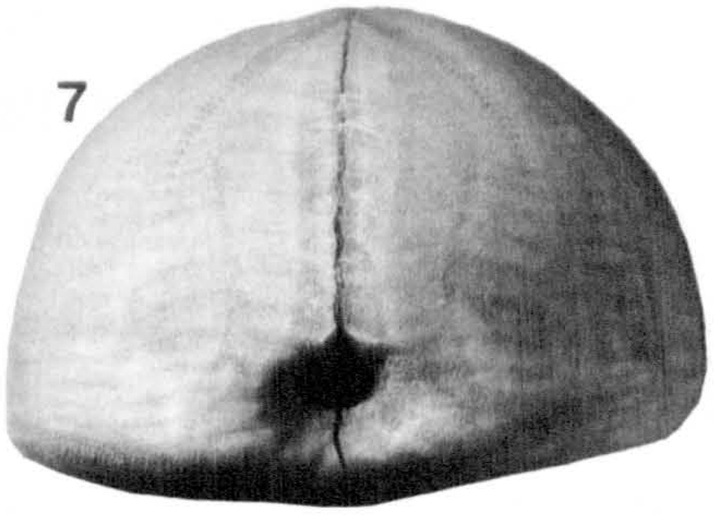
5



6



7



Order SPATANGOIDA Claus, 1876

Diagnosis. Compact apical system with four or less gonopores. Amphisternous or, very rarely, meridosternous plastron.

Remarks. Many spatangoids also have differentiated paired ambulacra forming sunken petals.

High level taxonomy among spatangoids has conventionally relied almost exclusively on the presence or absence of fascioles. However, fascioles "may appear and disappear in closely-related forms" (Nichols 1959) or during ontogeny (McNamara & Philip 1980; McNamara 1985) and, in an extreme example, this could lead to juveniles and adults of the same species being classified in separate families. Without a thorough overhaul of the taxonomic framework of all spatangoids (which is outside the scope of this thesis), I have based my taxonomy on a cladistic analysis of Maastrichtian and Palaeocene spatangoids with emphasis on test architecture. Taxa have been fitted into the existing taxonomic framework, although in many cases family diagnoses have been emended to reflect the inclusion of additional taxa.

KEY TO MAASTRICHTIAN & PALAEOCENE FAMILIES

1	Aboral tuberculation without dense granulation.....2	
	Aboral tuberculation with uniform covering of fine tubercles and very dense granulation.....	Micrasteridae
2	Non-petaloid paired ambulacra.....3	
	Petaloid paired ambulacra.....4	
3	All ambulacra non- to sub-petaloid.....	Corasteridae
	Unpaired ambulacrum enlarged and somewhat petaloid.....	Aeropsidae
4	Apical disc ethmophract to transitional.....5	
	Apical disc ethmolytic.....6	
5	Plastron regularly amphisternous.....	Hemiasteridae
	Plastron approaches meridosternous structure.....	Somaliasteridae

6 Peripetalous and subanal fascioles.....Brissidae

No subanal fasciole.....7

7 Peripetalous and marginal fascioles.....Pericosmidae

No separate marginal fasciole.....Schizasteridae

Figure 3.24. Range chart for Maastrichtian and Palaeocene genera of Micrasterina. See Figure 3.2 for explanation of symbols.

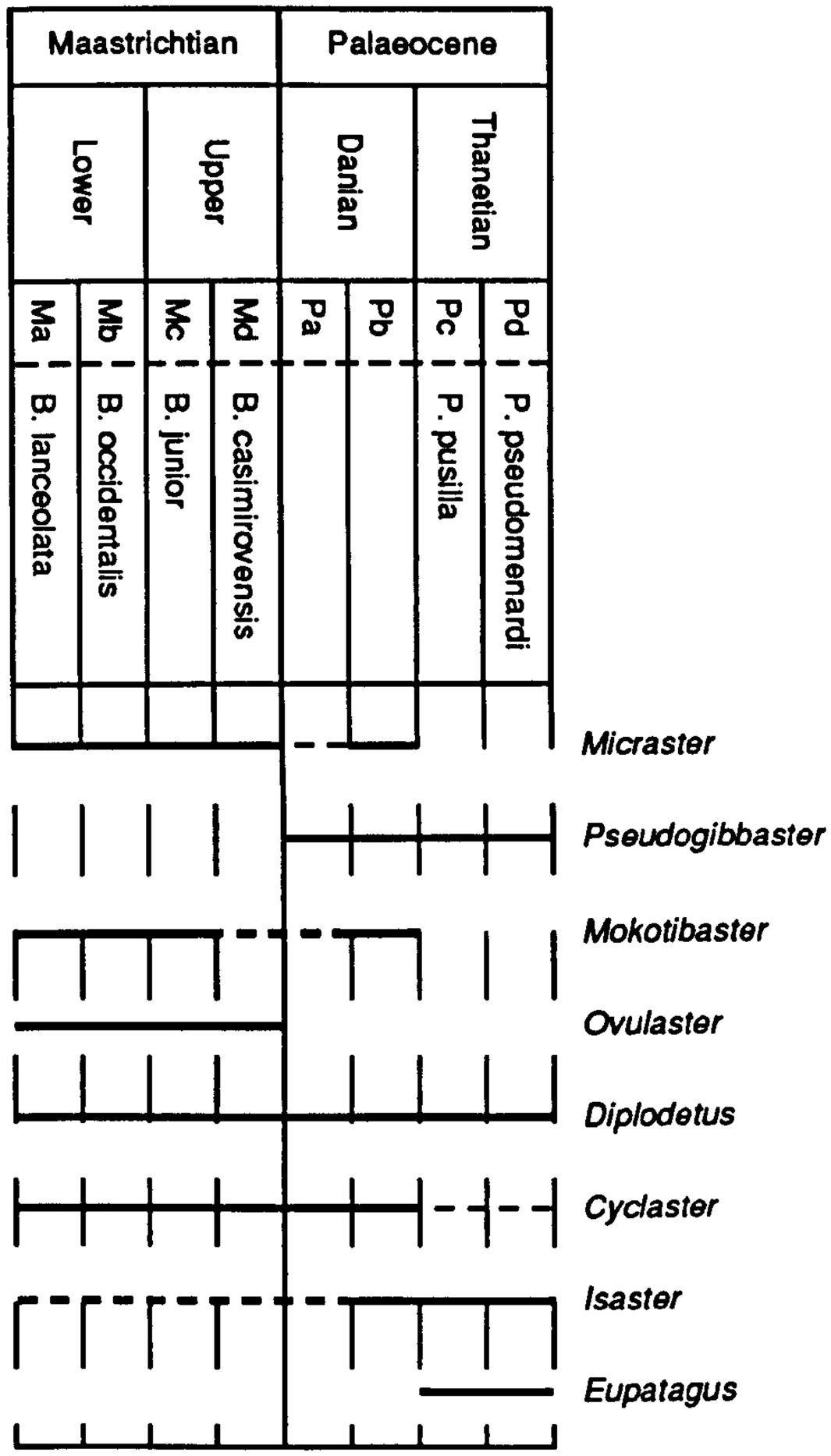
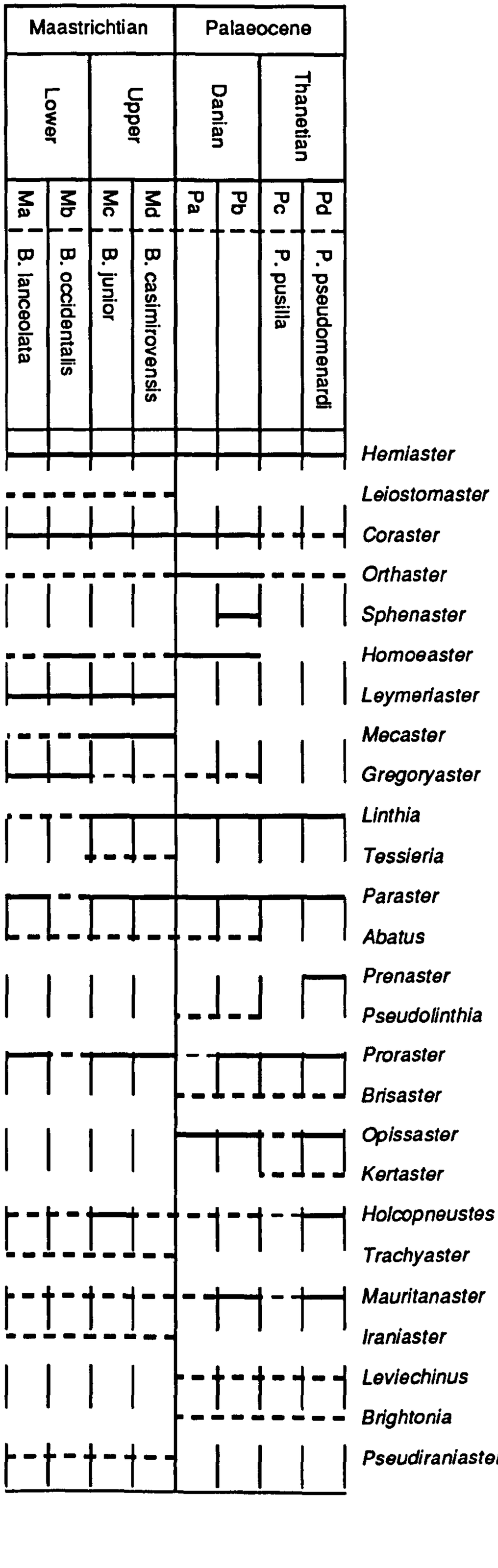

Maastrichtian
Palaeocene
Upper
Lower
Danian
Thanetian
Ma
Mb
Mc
Md
Pa
Pb
Pc
Pd
B. lanceolata
B. occidentalis
B. junior
B. casimirovensis
P. pusilla
P. pseudomenardi
Micraster
Pseudogibbaster
Mokotibaster
Ovulaster
Diplodetus
Cyclaster
Isaster
Eupatagus

Figure 3.25. Range chart for Maastrichtian and Palaeocene genera of Hemiasterina. See Figure 3.2 for explanation of symbols.


Maastrichtian
Palaeocene
Lower
Upper
Danian
Thanetian
Ma
Mb
Mc
Md
Pa
Pb
Pc
Pd
B. lanceolata
B. occidentalis
B. junior
B. casimirovensis
P. pusilla
P. pseudomenardi
Hemiaster
Leiostomaster
Coraster
Orthaster
Sphenaster
Homoeaster
Leymeriaster
Mecaster
Gregoryaster
Linthia
Tessieria
Paraster
Abatus
Prenaster
Pseudolinthia
Proraster
Brisaster
Opissaster
Kertaster
Holcopneustes
Trachyaster
Mauritanaster
Iraniaster
Leviechinus
Brightonia
Pseudiraniaster

Suborder MICRASTERINA Fischer, 1966

Family MICRASTERIDAE Lambert, 1920b

Emended diagnosis. Plastron mesamphisternous. Apical system ethmophract to transitional with four (or less commonly three) gonopores. Distinctive tuberculation with uniform covering of fine tubercles and very dense granulation on aboral surface.

Remarks. The possession of a subanal fasciole has commonly been used as a diagnostic characteristic of the micrasterids. However, a number of taxa conforming to the family diagnosis in all other respects lack a subanal fasciole. Thus in my emended diagnosis, the presence or absence of a subanal fasciole is ignored and the style of aboral tuberculation is used as the primary characteristic for family placement.

KEY TO MAASTRICHTIAN & PALAEOCENE GENERA

1	Apical system with 3 gonopores	2
	Apical system with 4 gonopores	3
2	Subanal fasciole	*Cyclaster*
	No fascioles	*Isaster*
3	Petaloid paired ambulacra	4
	Non-petaloid paired ambulacra	*Ovulaster*
4	Mouth <15% TL from anterior margin; strongly labiate; posterior undercut with submarginal periproct	*Micraster*
	Mouth >15% TL from anterior margin; vertically truncate or outward sloping posterior	5
5	Test highest posteriorly	*Diplodetus*
	Test highest centrally	6
6	Gibbous test; deeply sunken narrow petals	*Pseudogibbaster*
	Test flat based; petals flush to shallow	*Mokotibaster*

Genus MICRASTER Agassiz, 1836

[Type species *Spatangus coranguinum* Leske, 1778, by OD]

Emended diagnosis. Heart-shaped test with distinct frontal groove. Test highest centrally with undercut truncate posterior. Posterior paired petals diverge at an angle greater than 65 degrees. Apical system ethmophract with four gonopores. Peristome anterior with strong labral projection. Periproct submarginal. May or may not have subanal fasciole. No other fascioles.

KEY TO MAASTRICHTIAN & PALAEOCENE SPECIES

1	Anterior part of test convex in lateral view	2
	Anterior part of test concave in lateral view	*M. aturicus*
2	Labral and sternal plates disjunct	*M. grimmensis*
	Labral and sternal plates in contact	3
3	Short petals reaching <40% distance to ambitus	*M.* sp.
	Long petals reaching 50-60% distance to ambitus	*M. schroederi*

Micraster schroederi Stolley, 1892

(Plate 7, figures 1-4; Figure 3.26)

1892	*Micraster schröderi* Stolley, p. 259, pl. 8, fig. 5, pl. 9, fig. 1.
1897	*Micraster(?) ciplyensis* Schlüter, p. 19, pl. 2, figs 1-2.
1898	*Micraster ciplyensis* Schlüter; Lambert, p. 185, pl. 2, figs 1-2.
1911	*Micraster schroderi* Stolley; Lambert, p. 52, pl. 1, fig. 6.
1935b	*Isomicraster ciplyensis* (Schlüter); Smiser, p. 83.
1959	"*Isomicraster*" *ciplyensis* Schlüter; Moskvin & Poslavskaya, p. 289, pl. 25, fig. 5.
1987	*Micraster schroederi* Stolley; van der Ham *et al.*, p. 33, pl. 22.
1995	*Micraster* gr. *stolleyi* Lambert; Gallemí *et al.*, table 1.

Occurrence. Lower Maastrichtian Beutenaken Chalk of the Maastricht area (Lambert 1911; van der Ham *et al.* 1987) (NMM). Lower Maastrichtian Ciply Phosphatic Chalk

(Smiser 1935b) and "Poudingue de la Malogne" (Lambert 1898) of Belgium. Lower Maastrichtian of the northern Caucasus (Moskvin & Poslavskaya 1959) (PI). Maastrichtian Quipar-Jorquera Formation of Alicante, Spain (Gallemí *et al.* 1995) (MGB). Also found in Campanian strata of northern Germany (Stolley 1892) (BMNH).

Diagnosis. Sunken paired petals reaching 50-60% distance to ambitus. Anterior petals 1.5 times longer than posterior. Pores in paired petals round in inner series, elongate in outer series. Long narrow labral plate. Mouth very anteriorly situated, obscured from below by projecting labral plate. Broad subanal fasciole.

Remarks. The name *Isomicraster ciplyensis* has been used for Campanian specimens without a subanal fasciole. However, Schlüter's original drawings show that *Micraster ciplyensis* has a clear subanal fasciole and is identical to *M. schroederi* in all other respects. The two species are treated as synonyms.

Micraster aturicus Seunes, 1891

(Figure 3.27)

1891 *Micraster aturicus* Seunes, p. 30, pl. 4, fig. 1, pl. 5, fig. 1.
1892 *Micraster aturicus* Seunes; Nicklès, p. 110.
1979 *Micraster aturicus* Seunes; Gongadze, tables 1 & 2.

Occurrence. Campanian of the French Pyrenees (Seunes 1891) (MNHN). Maastrichtian Quipar-Jorquera Formation of Alicante, Spain (Nicklès 1892) and Lower to Upper Maastrichtian of the Georgian Republic (Gongadze 1979).

Diagnosis. Differs from *M. schroederi* only in lateral profile of anterior part of test. *M. aturicus* is concave in this region whilst *M. schroederi* is convex.

Micraster grimmensis Nietsch, 1921

(Figure 3.28)

1921 *Micraster grimmensis* Nietsch, p. 20, pl. 10, figs 8-9.
1959 *Micraster grimmensis* Nietsch; Moskvin & Poslavskaya, p. 284, pl. 22, fig. 4, text fig. 99.

Occurrence. Late Maastrichtian Pommerschen Kreide of northern Germany (Nietsch 1921). Campanian of Kopet Dag and the northern Caucasus (Moskvin & Poslavskaya 1959) (Pl).

Diagnosis. Differs from *M. schroederi* in having labral and sternal plates separated by adjoining ambulacra and in having plastronal suture offset to right.

Micraster sp.

?1926 *Micraster desori* Ødum, p.162 & 257, pl. 2, figs 1b and 1c [not 1a = *Proraster oedumi* Stokes].

Occurrence. ?Upper Danian Coccolith Limestone of Denmark (Ødum 1926). Upper Danian "Danian 5" of Denmark (BMNH).

Diagnosis. Upper surface of test highly inflated. Petals short (reaching up to 40% distance to ambitus) with elongate pores. Anterior petals 1.7 times longer than posterior. Plastronal suture offset to right. Mouth very anteriorly placed. Distinct subanal fasciole.

Remarks. Most similar to *M. schroederi* from which it differs in having shorter petals and the plastronal suture offset to the right.

This is the only record of a post-Cretaceous *Micraster*. Nannofossils confirm the Upper Danian age.

Genus MOKOTIBASTER Lambert, 1933a

[Type species *Mokotibaster hourcqi* Lambert, 1933a]

Diagnosis. Test with highest point central and shallow to non-existent frontal groove. Paired ambulacra form long straight flush to slightly depressed petals, with elongate pores. Mouth non-labiate without distinct rim.

Remarks. *Mokotibaster* may additionally have elongate pores in the unpaired ambulacrum and a subanal fasciole. *Mokotibaster* is most similar to *Micraster* and in fact the two genera were synonymized by Stokes (1975). *Mokotibaster* represents more southerly species and may be distinguished from Maastrichtian and Palaeocene species

of *Micraster* by its longer, broader, less sunken petals and its non-labiate, less anteriorly positioned mouth.

KEY TO MAASTRICHTIAN & PALAEOCENE SPECIES

1 Pores in anterior ambulacrum elongate.....2

Pores in anterior ambulacrum small and round.....3

2 Mouth <20% test length from anterior margin;

anterior and posterior petals reach >80% distance to ambitus.....*M. hourcqi*

Mouth >20% test length from anterior margin;

posterior petals reach <80% distance to ambitus.....*M. nobilis*

3 Apical system at one third of test length from anterior;

petal width >40% petal length.....*M. nicklesi*

Apical system at mid-length;

petal width <40% petal length.....4

4 Plastronal suture central.....*M. trangahyensis*

Plastronal suture offset to right.....*M. amnicus*

Mokotibaster hourcqi Lambert, 1933a

(Plate 7, figures 5-8)

1933a *Mokotibaster hourcqi* Lambert, p. 18, pl. 3, figs 1-3.

1936 *Mokotibaster hourcqi* Lambert, p. 26, pl. 2, figs 1-5.

Occurrence. Lower Maastrichtian of northwestern Madagascar (Lambert 1933a, 1936; Besairie 1971) (BMNH).

Diagnosis. Very variable lateral profile, with broad flat base and smoothly rounded to vertically truncate posterior. Horizontal outline heart-shaped with very slight frontal notch. Pores of anterior ambulacrum elongate. Paired ambulacra are about equal in length and form broad, flush petals reaching over 80% of distance to ambitus; anterior diverging at 125 to 130 degrees. Mouth less than 20% of test length from anterior. Periproct very low,

from about 30% of test height from base to inframarginal. No fascioles.

Remarks. Most similar to *M. nobilis*. Those specimens of *M. hourcqi* with a vertically truncate posterior are most alike. However, *M. hourcqi* may be distinguished on the basis of its flatter base, longer flush petals and more anterior mouth.

Mokotlbaster nobilis (Stollczka, 1873)

(Figure 3.29)

1873	*Epiaster nobilis* Stoliczka, p. 20, pl. 3, figs 7-8.
1908a	*Micraster* cf. *turoniensis* Cottreau, p. 168, pl. 3, fig. 6.
1930	*Epiaster nobilis* Stolickza; Besairie, p. 231, pl. 25, fig. 3, pl. 24, fig. 8.

Occurrence. Maastrichtian Ariyalur Group of southern India (Stoliczka 1873) (GSI). Lower Maastrichtian of northwestern Madagascar (Cottreau 1908a; Besairie 1930, 1971) (BMNH).

Diagnosis. Subcordate horizontal outline with shallow anterior groove. Pores of anterior ambulacrum elongate. Paired ambulacra form long, broad, slightly sunken petals. Anterior petals 1.1 to 1.2 times longer than posterior; diverge at 120 to 125 degrees. Posterior petals reach approximately two thirds of distance to ambitus. Peristome more than 20% test length from anterior. Periproct at about one third of test height from base. No distinct fascioles.

Mokotlbaster trangahyensis (Lambert, 1936)

?1908a	*Epiaster* cf. *henrici* Peron & Gauthier; Cottreau, p. 163, pl. 3, fig. 9, text fig. 10.
1936	*Micraster trangahyensis* Lambert, p. 27, pl. 2, figs 9-10.

Occurrence. Lower Maastrichtian of southwestern Madagascar (Cottreau 1908a; Lambert 1936; Besairie 1971) (MNHN).

Diagnosis. Test with shallow but distinct frontal groove. Pores of anterior ambulacrum round. Paired ambulacra form broad, sunken petals. Anterior pair diverge at 120 to 130 degrees and are 1.2 to 1.3 times longer than posterior. Anterior petals reach 67-68%

distance to ambitus. Plastronal suture central. Apical system at mid-length; shows sexual dimorphism. Periproct high on truncate posterior. Subanal fasciole.

Remarks. *M. trangahyensis* is most similar to *M. amnicus*. The two may be differentiated on the position of the plastronal suture; central in *M. trangahyensis* and offset to the right in *M. amnicus*. In addition, the petals of *M. amnicus* are broader and the anterior pair reach further towards the ambitus.

Mokotibaster amnicus (Greyling, 1996)

1990 *Hemiaster jacobi* Besairie & Lambert; Cooper & Greyling, p. 412, figs 2-6 (pars).

1996 *Micraster amnicus* Greyling, p. 25, figs 2-7.

Occurrence. Lower Maastrichtian St. Lucia Formation of Zululand (Cooper & Greyling 1990; Greyling 1996). Upper Maastrichtian of Tunisia (BMNH).

Diagnosis. Test with shallow but distinct frontal groove. Pores of anterior ambulacrum round. Paired ambulacra form broad, sunken petals. Anterior pair diverge at 125 to 130 degrees. Anterior petals are 1.1 to 1.2 times longer than posterior and reach 76-82% of distance to ambitus. Plastronal suture offset to right. Apical system at mid-length. Periproct high on truncate posterior. Subanal fasciole.

Mokotibaster nicklesi (Collignon & Lambert, 1928)

1928 *Plesiaster nicklesi* Collignon & Lambert, p. 271, pl. 21, figs 8-10.

Occurrence. Danian *Coraster* beds of Alicante, Spain.

Diagnosis. Test has very shallow frontal groove. Well developed anterior ambulacrum with enlarged pore-pairs for much of distance from apex to anterior. Paired ambulacra form very broad, shallow petals. Anterior and posterior petals of equal lengths. Anterior pair diverge at 140 degrees and reach 78% distance to ambitus. Apical system anteriorly placed. Periproct high on truncate posterior. Subanal fasciole.

Remarks. *M. nicklesi* is easily distinguished from all other species of *Mokotibaster* by its

anterior apical system and extremely broad petals.

Mokotibaster? gregalis (Böhm, 1927)

1927 *Isomicraster gregalis* Böhm, p. 198, pl. 12, fig. 2.

Occurrence. Danian of Turkey (BMNH).

Diagnosis. High domed test. Broad heart-shaped horizontal outline with distinct frontal notch. Unpaired ambulacrum with slightly elongate pores. Paired ambulacra form long, straight, narrow petals. Petals are flush and subequal. Ethmophract apical system with four gonopores. Periproct 15-20% of test height from base. No fascioles.

Remarks. Distinctive tuberculation and an ethmophract apical disc allow this species to be placed in the micrasterids. Its long straight petals and unpaired ambulacrum with somewhat elongate pores make it possible to tentatively assign this species to *Mokotibaster.* Its highly domed test and narrow petals make it easily distinguishable from all other species of *Mokotibaster.*

Genus PSEUDOGIBBASTER Moskvin, 1983

[Type species *Protobrissus akkajensis* Moskvin & Poslavskaya, 1959, by OD]

Synonym. *Protobrissus* Poslavskaya & Moskvin, 1960; Gongadze, 1979. *non* *Protobrissus* Lambert, 1907a (= *Eupatagus* Agassiz *in* Agassiz & Desor, 1847).

Diagnosis. Inflated, gibbous test with highest point centrally and a vertically truncate posterior. Deeply sunken paired ambulacra containing elongate pores. Subanal fasciole. Clusters of miliary tubercles at ends of petals give impression of diffuse peripetalous fasciole.

Remarks. Most similar to *Micraster*, from which it differs in having a more inflated shape and a vertically truncate posterior. Differs additionally from Maastrichtian and Palaeocene species of *Micraster* in having a less anterior, far less labiate mouth and the trace of a peripetalous fasciole. The petals of *Pseudogibbaster* are shorter, narrower and more

deeply sunken than those of *Mokotibaster*. *Diplodetus* has an elongate test with the highest point posterior, a shallower frontal notch and enlarged pores for a greater proportion of the unpaired ambulacrum.

KEY TO PALAEOCENE SPECIES

1 anterior petals <1.4 times longer than posterior.....2
anterior petals >1.4 times longer than posterior.....*P. depressus*
2 small forms; petal width >30% of petal length.....*P. akkajensis*
large forms; petal width <30% of petal length.....*P. tercensis*

Pseudogibbaster akkajensis **(Moskvin & Poslavskaya, 1959)**

(Figure 3.30)

1959 *Protobrissus ak-kajensis* (Weber); Moskvin & Poslavskaya, p. 290, pl. 26, fig. 1.
1960 *Protobrissus canaliculatus* (Cotteau); Poslavskaya & Moskvin, p. 75, pl. 7, fig. 1, text fig. 26.
1979 *Protobrissus akkajensis* (Weber); Gongadze, p. 128, pl. 32, fig. 1.
1983 *Pseudogibbaster akkajensis* (Moskvin & Poslavskaya); Moskvin, p. 111, fig. 2.

Occurrence. Lower Danian of the Crimea, northern Caucasus and the Transcaspian Region (Moskvin & Poslavskaya 1959; Poslavskaya & Moskvin 1960; Moskvin 1983) (PI). Lower Danian of Georgia (Poslavskaya & Moskvin 1960; Gongadze 1979). Danian of Alicante, Spain (PUAB).

Diagnosis. Test small. Flat base curves up at edges. Width of paired ambulacra is 33-39% of petal length. Anterior petals are 1.0 to 1.3 longer than posterior. Periproct situated high on truncate posterior.

Pseudogibbaster tercensis **(Cotteau, 1877)**

(Plate 8, figures 1-4)

1877 *Micraster tercensis* Cotteau, p. 69, pl. 7, figs 29-32.
1907a *Micraster tercensis* Cotteau; Lambert, p. 719.

1960 *Protobrissus tercensis* (Cotteau); Poslavskaya & Moskvin, p. 77, pl. 7, fig. 3, pl. 8, fig. 1, text fig. 28.

1975 *Micraster tercensis* Cotteau; Plaziat *et al.*, p. 643, fig. 10.

1979 *Protobrissus tercensis* (Cotteau); Gongadze, tables 1 & 2.

1983 *Pseudogibbaster tercensis* (Cotteau); Moskvin, p. 111, fig. 2.

Occurrence. Palaeocene (Cotteau 1877; Lambert 1907a) and Lower to Mid Thanetian (Plaziat *et al.* 1975) of the French Pyrenees (BMNH). Upper Thanetian Casas di Oreyon, Navarra, Spain (BMNH). Upper Danian of Georgia (Gongadze 1979), Crimea and the northern Caucasus (Poslavskaya & Moskvin 1960; Moskvin 1983) (Pl).

Diagnosis. Large gibbous test with inflated upper and lower surfaces. Petal width is 25-27% of petal length. Anterior petals are 1.1 to 1.3 times longer than posterior. Periproct is positioned high on the truncate posterior.

Remarks. Differs from *P. akkajensis* in its larger size, more inflated lower surface and narrower petals.

Pseudogibbaster depressus (Kongiel *In* Kongiel & Matwiejewowna, 1937)

1937 *Micraster depressus* Kongiel *in* Kongiel & Matwiejewowna, p. 116 and 139, pl. 1, figs 6-9.

1959 *Protobrissus depressus* (Kongiel); Moskvin & Poslavskaya, p. 290, pl. 26, figs 2-3, text fig. 106.

1960 *Protobrissus depressus* (Kongiel); Poslavskaya & Moskvin, p. 76, pl. 7, fig. 2, text fig. 27.

1960 *Protobrissus indolensis* Poslavskaya & Moskvin, p. 78, pl. 8, fig. 2, text fig. 29.

1979 *Protobrissus depressus* (Kongiel); Gongadze, p. 130, pl. 32, fig. 2.

1983 *Pseudogibbaster depressus* (Kongiel); Moskvin, p. 111, fig. 2.

1983 *Pseudogibbaster indolensis* (Poslavskaya & Moskvin); Moskvin, p. 111, fig. 2.

Occurrence. Lower to Mid Danian Siwak of southeast Poland (Kongiel & Matwiejewowna 1937). Mid to Upper Danian of Georgia (Gongadze 1979). Lower to Mid Danian (Moskvin & Poslavskaya 1959; Poslavskaya & Moskvin 1960; Moskvin 1983) and Lower Thanetian (Poslavskaya & Moskvin 1960; Moskvin 1983) of Crimea and the northern Caucasus (Pl).

Diagnosis. Large test with flat base curving at edges. Anterior petals are 1.4 to 1.5 times longer than posterior. Petal width is 27% of length. Labral plate narrow. Periproct

positioned fairly low on truncate posterior.

Remarks. Differs from *P. akkajensis* and *P. tercensis* in having a longer, narrower labral plate, proportionally longer anterior petals and a lower periproct. In addition, *P. depressus* differs from *P. akkajensis* in having narrower petals.

Genus DIPLODETUS Schlüter, 1900

[Type species *Diplodetus brevistella* Schlüter, 1900, by OD]

Diagnosis. Test longer than wide, with highest point posteriorly. Frontal notch shallow or absent. Paired ambulacra petaloid with elongate pores, sunken to deeply sunken. Subanal fasciole. May also be trace of peripetalous fasciole.

Remarks. Differs from other four-gonopored micrasterids in having a more elongate test with the highest point posteriorly. In addition, *Diplodetus* differs from *Mokotibaster* in having shorter, more deeply sunken, narrower petals.

KEY TO MAASTRICHTIAN & PALAEOCENE SPECIES

1 Deeply sunken paired ambulacra; shallow frontal groove; pustular tuberculation.....2

Shallow paired ambulacra; no frontal groove; even tuberculation.....4

2 Peristome one quarter of test length from anterior margin.....3

Peristome one third of test length from anterior margin.....*D. nutrix*

3 Anterior petals diverge at 105-110 degrees.....*D. americanus*

Anterior petals diverge at 125-130 degrees.....*D. duponti*

4 Paired petals of approximately equal lengths.....5

Anterior petals 1.4-1.6 times longer than posterior.....*D. parvistella*

5 Anterior petals diverge at 140-150 degrees.....*D. coloniae*

Anterior petals diverge at 115 degrees.....*D. gauthieri*

Diplodetus americanus (Stephenson, 1941)

(Plate 8, figures 5-7)

1941	*Micraster (Plesiaster) americanus* Stephenson, p. 69, pl. 7, figs 1-4.
1953	*Micraster americanus* Stephenson; Cooke, p. 38, pl. 15, figs 10-13.

Occurrence. Early Maastrichtian Saratoga Chalk, Early to Mid Maastrichtian Ripley Formation, Mid to Late Maastrichtian Corsicana Marl and Prairie Bluff Chalk of Texas, Arkansas and Mississippi, USA (USNM).

Diagnosis. Test has shallow frontal notch and a vertically truncate posterior. Paired ambulacra deeply sunken. Anterior pair diverge at 105 to 100 degrees and are 1.2 to 1.3 times longer than posterior. Labrum 2.3 times longer than wide. Peristome positioned a quarter of test length from anterior margin. Distinct subanal fasciole and partial peripetalous fasciole clearest towards posterior. Large tubercles adapically and along the edges of the unpaired and anterior paired ambulacra.

Remarks. Most similar to *D. duponti* and *D. nutrix* from which it differs in having less divergent anterior petals and a longer, narrower labral plate. Differs additionally from *D. nutrix* in having a more anterior mouth.

Diplodetus duponti (Lambert, 1911)

(Figure 3.31)

?1902	*Micraster maestrichtensis* Lambert, p. 122, pl. 6, figs 1-4, text fig. 1 [*nomen dubium*].
1911	*Micraster duponti* Lambert, p. 50, pl. 2, fig. 21, pl. 3, figs 1-2.
?1911	*Micraster maestrichtensis* Lambert, p. 52.
1935b	*Micraster duponti* Lambert; Smiser, p. 81.
1987	*Diplodetus duponti* (Lambert); van der Ham *et al.*, p. 34, pl. 24, fig. 1.
1987	*Diplodetus bucardium* (Goldfuss); van der Ham *et al.*, p. 34, pl. 23, fig. 2.
1992	*Diplodetus duponti* (Lambert); van der Ham & van Birgelen, p. 150, pl. 4, figs 7-8.

Occurrence. Upper Lower Maastrichtian Vijlen Chalk and Upper Maastrichtian lowermost Maastricht Formation and Kunrade Chalk of the Maastricht area (Lambert 1902, 1911; Smiser 1935b; van der Ham *et al.* 1987; van der Ham & van Birgelen 1992) (NMM).

Diagnosis. Test has shallow frontal notch and an undercut truncate posterior. Paired ambulacra form deeply sunken petals. Anterior petals diverge at 125 to 130 degrees and are 1.3 to 1.5 times longer than posterior. Labrum 1.5 times longer than wide. Peristome positioned a quarter of test length from anterior margin; strongly labiate with prominent rim. Broad subanal fasciole. Slight crowding of miliary tubercles at distal ends of posterior paired petals may or may not make up part of a very faint peripetalous fasciole. Some larger tubercles near to apex.

Remarks. Only one specimen of *Micraster (Brissopneustes) maestrichtensis* has ever been reported. All similar spatangoids since recorded from this area have four gonopores and it is possible that this specimen is a misidentified *Diplodetus duponti.*

Differs from *D. americanus* in having proportionally longer, more divergent anterior petals and from *D. nutrix* in having a more anterior mouth with a thickened rim.

Diplodetus nutrix (Lambert *in* Boule, 1899)

1899 *Epiaster nutrix* Lambert *in* Boule, p. 132.
1903 *Epiaster nutrix* Lambert, p. 86, pl. 3, figs 3-5.
1906 *Epiaster nutrix* Lambert *in* Boule & Thevenin, p. 52, pl. 2, fig. 5.
1908a *Micraster nutrix* (Lambert); Cottreau, p. 169, pl. 4, fig. 4.
1922 *Micraster nutrix* (Lambert); Cottreau, p. 117.
?1930 *Hemiaster* sp. Besairie, p. 230, pl. 24, fig. 6.

Occurrence. Maastrichtian of the east coast of Madagascar (Boule 1899; Lambert 1903; Boule & Thevenin 1906; Cottreau 1908a, 1922; Besairie 1971) (MNHN) ?Lower Maastrichtian Craie d'Andrkaraka of northwestern Madagascar (Besairie 1930).

Diagnosis. Test has very shallow frontal notch and an outwardly truncate posterior. Paired ambulacra petaloid and deeply sunken. Anterior pair diverge at 125 degrees and are 1.3 to 1.5 times longer than posterior. Labrum 1.8 times longer than wide. Apical system shows sexual dimorphism in gonopore size. Peristome positioned about one third of test length from anterior. Tuberculation pustular towards anterior on lower surface.

Remarks. *D. nutrix* is most similar in appearance to *D. americanus* and *D. duponti.* It is easily distinguished by its less anterior peristome.

Diplodetus gauthieri Cottreau, 1908a

1908a *Diplodetus gauthieri* Cottreau, p. 174, pl. 3, fig. 7.
1979 *Diplodetus (Protobrissus)* cf. *gauthieri* Cottreau; Tanaka *et al.*, p. 45, pl. 3, fig. 5.

Occurrence. Danian of northwest Madagascar (Cottreau 1908a; Collignon 1968; Besairie 1971; Tanaka *et al.* 1979). Maastrichtian of southwest Madagascar (Besairie 1971).

Diagnosis. Ovate horizontal outline and outwardly projecting posterior. Paired ambulacra form sunken petals. Anterior petals are 1.1 times longer than posterior and diverge at 115 degrees. Apical system at mid-length. Mouth at approximately one third of test length from anterior margin. Subanal fasciole and diffuse peripetalous fasciole. Few scattered large tubercles near to apex.

Remarks. *D. gauthieri* is most similar to *D. parvistella* from which it differs in having a more inflated test and paired petals of approximately equal lengths. *D. gauthieri* differs from *D. coloniae* in its less divergent anterior petals and its centrally positioned apical system.

Diplodetus parvistella (Schlüter, 1899)

1899 *Plesiaster (?) parvistella* Schlüter, 1899, p. 121, pl. 9, fig. 5.
1987 *Diplodetus parvistella* (Schlüter); van der Ham *et al.*, p. 34, pl. 24, fig. 2.

Occurrence. Lower Maastrichtian Vijlen and Lanaye Chalks and Upper Maastrichtian Kunrade Chalk of the Maastricht area (Schlüter 1899; van der Ham *et al.* 1987) (NMM).

Diagnosis. Low test with ovate horizontal outline. Outwardly projecting truncate posterior. Paired ambulacra shallow. Anterior petals diverge at 105 to 110 degrees and are 1.4 to 1.6 times longer than posterior. Apical system at mid-length. Peristome positioned one quarter to one third of test length from anterior margin. Distinct subanal fasciole and very diffuse peripetalous fasciole.

Remarks. *D. parvistella* is distinguished from *D. gauthieri* and *D. coloniae* by its very low

test and proportionally longer anterior petals.

Diplodetus coloniae (Cotteau, 1877)

(Figure 3.32)

1877 *Cyclaster coloniae* Cotteau, p. 70, pl. 7, figs 33-34.
1892 *Cyclaster coloniae* Cotteau; Nicklès, p. 110.
1907a *Cyclaster coloniae* Cotteau; Lambert, p. 719.
1935b *Isopneustes eysdenensis* Smiser, p. 84, pl. 7, fig. 7.
1935b *Isopneustes montensis* Smiser, p. 84, pl. 7, fig. 8.
1960 *Isopneustes coloniae* (Cotteau); Poslavskaya & Moskvin, p. 74, pl. 6, fig. 4, text fig. 25.
1975 *Diplodetus coloniae* (Cotteau); Plaziat *et al.*, p. 643, fig. 10.

Occurrence. Palaeocene (Cotteau 1877; Lambert 1907a) and Lower to Mid Thanetian (Plaziat *et al.* 1975) of the French Pyrenees (MNHN). Maastrichtian of Alicante, Spain (Nicklès 1892). Montian Calcaire Grossier de Mons of Belgium (Smiser 1935b). Mid to Upper Danian of the Crimea (Poslavskaya & Moskvin 1960) (PI).

Diagnosis. Ovate outline; may have very slight anterior depression. Vertically truncate posterior. Paired ambulacra approximately equal length. Anterior petals diverge at 140-150 degrees. Apical system at one third test length from anterior. Mouth at one quarter test length from anterior. Distinct subanal fasciole. Presence of peripetalous fasciole uncertain.

Remarks. Differs from *D. gauthieri* and *D. parvistella* in having very divergent anterior petals and a more anteriorly positioned apical system.

Diplodetus? sp. indet.

1959 *Hemiaster moscovensis* Cooke, p. 68, pl. 28, figs 5-9.

Occurrence. Palaeocene Porters Creek Clay of Alabama, USA.

Remarks. A damaged and somewhat worn single specimen, most similar in overall appearance to *Diplodetus parvistella*. This specimen is only tentatively assigned to

Diplodetus since the subanal area is missing and the presence of a subanal fasciole cannot therefore be confirmed. There is a peripetalous fasciole and an ethmophract apical system with four gonopores.

Genus OVULASTER Cotteau, 1884

[Type species *Ovulaster gauthieri* Cotteau, 1884, by OD]

Diagnosis. Test small and globular. Paired ambulacra sub-petaloid and flush. Plastron amphisternous with long narrow labrum and sternal plates. Distinct subanal fasciole.

Remarks. Easily distinguished from all other Micrasterids by its sub-petaloid paired ambulacra and non-labiate mouth.

Habanaster from the Eocene of Cuba is sister group to *Ovulaster*. *Habanaster* differs in having non-petaloid paired ambulacra and only three gonopores in the apical system.

Ovulaster zignoanus (d'Orbigny, 1854)

1854 *Cardiaster zignoanus* d'Orbigny, p. 145, pl. 832, figs 8-13.
1884 *Ovulaster gauthieri* Cotteau, p. 38, pl. 5, figs 1-5.
1892 *Ovulaster zignoanus* (d'Orbigny); Gauthier, p. 40.
1909 *Ovulaster obtusus* Cottreau *in* Blayac & Cottreau, p. 427, pl. 14, figs 20-28, text fig. 1.
1924 *Ovulaster zignoi* (d'Orbigny); Dalloni, p. 118.
1924 *Ovulaster* n. sp. Dalloni, p. 118.
1932 *Ovulaster obtusus* Cottreau; Lambert, p. 77.
1940 *Ovulaster zignoi* (d'Orbigny); Rouchadze, p. 170.
1971 *Ovulaster* aff. *obtusus* Cottreau & Blayac; Akkus, p. 16.
1979 *Ovulaster zignoanus* (d'Orbigny); Gongadze, p. 121, pl. 27, fig. 3.

Occurrence. Maastrichtian of Constantine (Blayac & Cottreau 1909; Lambert 1932) and Oran, Algeria (Dalloni 1924; Lambert 1932) (MNHN). Maastrichtian of North Africa (Cotteau 1884). Lower to Upper Maastrichtian of Georgia (Rouchadze 1940; Gongadze 1979). Lower Maastrichtian Ulupinar Formation of Central Turkey (Akkus 1971).

Diagnosis. Test ovoid with very slight frontal groove. Anterior paired ambulacra widely

divergent. Mouth somewhat sunken.

Remarks. Gauthier (1892) records this from the Maastrichtian of northern Tunisia. However, on the basis of the microfossil content, Zagbib-Turki (1987) considers these deposits to be Coniacian.

Smaller forms previously known as *Ovulaster obtusus* have greater width relative to length than *Ovulaster zignoanus*, shorter, broader labral and sternal plates and in some specimens a higher periproct. All these features are a function of size and the two species are synonymized.

Ovulaster auberti Gauthier, 1892

(Figure 3.33)

1892 *Ovulaster auberti* Gauthier, p. 42, pl. 1, figs 3-9.

1909 *Ovulaster auberti* Gauthier; Cottreau *in* Blayac & Cottreau, p. 426, pl. 14, figs 1-3.

1909 *Ovulaster auberti* var. *sabathensis* Cottreau *in* Blayac & Cottreau, p. 427, pl. 14, figs 4-6.

1932 *Ovulaster auberti* Gauthier; Lambert, p. 76.

1971 *Ovulaster* aff. *auberti* Gauthier; Akkus, p. 16.

Occurrence. Maastrichtian of Constantine (Blayac & Cottreau 1909; Lambert 1932) and Oran, Algeria (Lambert 1932) (MNHN). Lower Maastrichtian Ulupinar Formation of Central Turkey (Akkus 1971).

Diagnosis. Differs from *O. zignoanus* in having no frontal groove and a flush peristome.

Remarks. The Tunisian specimens previously recorded as Maastrichtian (Gauthier 1892) (MNHN) are now considered to be Coniacian (Zagbib-Turki 1987).

micrasterid gen. & sp. indet.

1927 *Micraster piriformis* Böhm, p. 197, pl. 12, fig. 7.

Occurrence. Danian of Turkey (BMNH).

Remarks. The type specimen is worn and somewhat damaged. No fascioles are visible although where tuberculation is preserved it appears to be of micrasterid type. The apical

system is damaged and plating details are impossible to determine.

Genus CYCLASTER Cotteau *in* Leymerie & Cotteau, 1856

[Type species *Cyclaster declivus* Cotteau *in* Leymerie & Cotteau, 1856, by OD]

Synonyms. *Brissopneustes* Cotteau, 1886 (type species *Brissopneustes vilanovae* Cotteau, 1886); *Isopneustes* Seunes, 1888. *non Isopneustes* Pomel, 1883.

Emended diagnosis. Paired ambulacra petaloid - short and virtually flush to slightly sunken. Pores round to transversely elongate. Apical system ethmophract with three large gonopores, madreporite without gonopore. Peristome anterior, labiate. Subanal fasciole. May or may not have peripetalous fasciole.

Remarks. Despite being placed in separate families (*Cyclaster* in the Brissidae and *Brissopneustes* in the Micrasteridae), *Cyclaster* and *Brissopneustes* differ in their original definitions only in the presence or absence of a peripetalous fasciole. However, several of the species studied have either a partial peripetalous fasciole, which is distinct posteriorly and completely absent anteriorly, or an indistinct peripetalous fasciole most obvious at the ends of the petals and elsewhere made up of miliary tubercles crowded together to varying degrees. There is a complete gradation between those forms with a fully developed peripetalous fasciole and those without. The presence of a peripetalous fasciole is therefore not a reliable diagnostic feature and consequently *Cyclaster* and *Brissopneustes* are synonymized.

The presence of subanal and peripetalous fascioles has been used as a diagnostic character for the Brissidae. As the presence of a peripetalous fasciole has been demonstrated to be an impersistent character this practise is no longer sufficient by itself for family placement. Other differences between the Micrasteridae and Brissidae include an ethmophract apical system and mesamphisternous plastron structure in the micrasterids compared to an ethmolytic arrangement and an ultramphisternous plastron in the brissids. Since plastron plating is consistently mesamphisternous and the apical system always ethmophract within the *Cyclaster* species studied, *Cyclaster* is here assigned to the Micrasteridae. A further difference between the two families is in the style

of adapical tuberculation. Micrasterids show dense granulation interspersed with fine uniform tuberculation. This is the arrangement seen in *Cyclaster*. In contrast, the tuberculation in brissids usually includes a number of large tubercles and a far sparser cover of granulation.

The genus *Isopneustes* Pomel, with the type species *Cyclaster bourgeoisi* Cotteau, has four gonopores and a petaloid unpaired ambulacrum. However, Seunes (1888) assigned three gonopored Cretaceous spatangoids to *Isopneustes*, claiming that the name *Cyclaster* was only applicable to post-Cretaceous species. *Isopneustes* Seunes is thus synonymized with *Cyclaster*.

Isaster is the only other spatangoid genus to have an ethmophract apical system with the madreporite unperforated. *Isaster* differs from *Cyclaster* in having no fascioles and long petaloid paired ambulacra. The remaining micrasterids all have ethmophract apical systems with four gonopores.

KEY TO MAASTRICHTIAN & PALAEOCENE SPECIES

1 Distinct frontal groove at ambitus.....2
Indistinct or no frontal groove at ambitus.....3

2 Short paired petals; globular test.....*C. gindrei*
Long paired petals with large number of
closely spaced pores.....*C. aturicus*

3 Ovate horizontal outline; well developed petals;
pustulous tuberculation on adapical surface.....4
Rectangular or coffin-shaped horizontal outline;
aboral tuberculation fine.....5

4 Distinctly pustular tuberculation on upper surface.....*C. pfenderae*
Somewhat pustular tuberculation on upper surface;
large sparse tuberculation on oral surface.....*C. platornatus*

5 Coffin-shaped tapered horizontal outline.....6
Rectangular horizontal outline.....8

6 Paired petals with small, round pores in

anterior series, slightly elongate in posterior.....*C. integer*

Broad paired petals with distinctly elongate pores.....7

7 Low profile with broad apical and oral surfaces;

Large number of pore-pairs per petal.....*C. heberti*

Inflated profile; smaller number of pores in each petal.....*C. vilanovae*

8 Broad rectangular shape, width > 85% of test length.....9

Narrow rectangular shape, width < 85% of

test length; anterior petals diverge at 90 degrees.....*C. galei*

9 High, inflated test; anterior petals diverge at 130

degrees or more.....*C. suecicus*

Large low test; anterior petals diverge at 110 degrees.....*C. ruegensis*

Cyclaster aturicus **(Seunes, 1888)**

(Plate 9, figures 1-3; Figure 3.35)

1888 *Isopneustes aturicus* Seunes, p. 797, pl. 28, fig. 3.

1960 *Brissopneustes aturicus* (Seunes) Poslavskaya & Moskvin, p. 72, pl. 6, fig. 1, text fig. 23.

1960 *Brissopneustes schwetzovi* Poslavskaya & Moskvin, p. 73, pl. 6, figs 2-3, text fig. 24.

1979 *Brissopneustes aturicus* (Seunes) Gongadze, tables 1 & 2.

Occurrence. Danian of the French Pyrenees (Seunes 1888) (MNHN) and Spanish Pyrenees (BMNH). Mid to Upper Danian of Western Georgia, Northern Caucasus and the Transcaspian Region (Poslavskaya & Moskvin 1960) (PI). Lower to Upper Danian of Georgia (Gongadze 1979).

Diagnosis. Coffin-shaped horizontal outline with distinct frontal groove. Highly inflated, carinate upper surface. Long sunken paired petals with large number of closely spaced, elongate pores. Petals of equal length. Anterior petals diverge at 125-130 degrees. Long, narrow labrum. Apical system anterior. No peripetalous fasciole.

Cyclaster gindrei (Seunes, 1888)

1888 *Isopneustes gindrei* Seunes, p. 795, pl. 28, fig. 2.
1940 *Cyclaster pyriformis* Cotteau; Rouchadze, p. 127, 154, 174, pl. 3 fig. 6.
1959 *Cyclaster gindrei* (Seunes); Moskvin & Poslavskaya, p. 292, pl. 26, fig. 7, text fig. 109.
1960 *Cyclaster gindrei* (Seunes); Poslavskaya & Moskvin, p. 71, pl. 5, fig. 7, text fig. 22.
1979 *Cyclaster gindrei* (Seunes); Gongadze, p. 132, pl. 32, fig. 3.
?1996 *Isopneustes* sp. Wilmsen *et al.*, fig. 7.

Occurrence. Danian of the French Pyrenees (Seunes 1888) (MNHN) (UWBM). Mid Danian of Georgia (Gongadze 1979), the northern Caucasus and the Transcaspian region (Moskvin & Poslavskaya 1959; Poslavskaya & Moskvin 1960) (PI). Maastrichtian to Danian of Georgia (Rouchadze 1940). Lower Maastrichtian Cabo de Lata Formation of Santander, Spain (Wilmsen *et al.* 1996) (BMNH, MNHN) and Areny Sandstone of Tremp, Spain (PUAB).

Diagnosis. Rectangular to coffin-shaped with shallow frontal groove. Highly inflated upper surface with strongly carinate posterior. Short, slightly sunken petals with well developed, elongate pores. Anterior petals longer than posterior, diverge at 125-130 degrees. Long, narrow labrum. Apical system anterior. Extent of peripetalous fasciole unknown.

Cyclaster vilanovae (Cotteau, 1886)

1886 *Brissopneustes vilanovae* Cotteau, p. 74, pl. 9, figs 9-12.
1892 *Brissopneustes vilanovae* Cotteau; Nicklès, p. 115.
1927 *Cyclaster vilanovae* (Cotteau); Böhm, p. 196.
1995 *Brissopneustes vilanovae* Cotteau; Gallemí *et al.*, table 1.

Occurrence. Danian of Alicante, Spain (Cotteau 1886; Nicklès 1892; Gallemí *et al.* 1995) (BMNH, MGB) and northwest Turkey (Böhm 1927) (BMNH).

Diagnosis. Coffin-shaped outline with no or very slight frontal notch. Inflated in lateral profile with carinate upper surface. Paired ambulacra of equal length, slightly sunken with very well developed elongate pores. Narrow labrum. Indistinct peripetalous fasciole -

crowding of granular tubercles at ends of petals.

Cyclaster heberti (Nicklès, 1892)

1892 *Isopneustes heberti* Nicklès, p. 111, p. 202, pl. 9, figs 12-13.
1973 *Isopneustes heberti* Nicklès; Radig, p. 62, pl. 10, fig. 8, pl. 11, figs 1-2.
1995 *Isopneustes heberti* Nicklès; Gallemí *et al.*, table 1.
1995 *Isopneustes heberti?* Nicklès; Gallemí *et al.*, table 1.
1995 *Isopneustes* sp. Gallemí *et al.*, table 1.

Occurrence. Maastrichtian Quipar-Jorquera Formation of Alicante (Nicklès 1892; Gallemí *et al.* 1995) (BMNH, MGB) and Campanian of Navarra (Radig 1973), Spain.

Diagnosis. Coffin-shaped with slight frontal groove. Low profile. Paired ambulacra slightly sunken with elongate, well developed pores. Each petal with a large number of pores. Labrum long and narrow. Mouth with prominent rim. Complete peripetalous fasciole.

Cyclaster integer (Seunes, 1888)

(Plate 8, figures 8-11)

1888 *Isopneustes integer* Seunes, p. 798, pl. 28, fig. 1.
1888 *Isopneustes munieri* Seunes, p. 798, pl. 28, fig. 4.
1897 *Brissopneustes danicus* Schlüter, p. 18, pl. 1, figs 1-4.
1926 *Brissopneustes danicus* Schlüter; Ødum, p. 163.
1926 *Cyclaster brünnichi* Ravn; Ødum, p. 163.
1926 *Cyclaster brünnichi* Ravn; Ødum, p. 163.
1927 *Cyclaster brünnichi* Ravn, p 345, pl. 5, fig. 5.
1927 *Brissopneustes danicus* Schlüter; Ravn, p. 349, pl. 4, figs 5-6
1933a *Brissopneustes decaryi* Lambert, p. 19, pl. 3, figs 9-10.
1940 *Cyclaster pygmeus* Rouchadze, p. 129, 155, 174, pl. 3, fig. 7.
1959 *Cyclaster integer* (Seunes); Moskvin & Poslavskaya, p. 291, pl. 26, figs 4-5, text fig. 107.
1959 *Cyclaster danicus* (Schlüter); Moskvin & Poslavskaya, p. 291, pl. 26, fig 6, text fig. 108.
1960 *Cyclaster integer* (Seunes); Poslavskaya & Moskvin, p. 69, pl. 5, figs 4-5, text fig. 20.
1960 *Cyclaster danicus* (Schlüter); Poslavskaya & Moskvin, p. 70, pl. 5, fig. 6, text fig. 21.
1979 *Cyclaster danicus* (Schlüter); Gongadze, p. 131, pl. 33, figs 1-2.
1979 *Cyclaster bruennichi* Ravn; Asgaard, tables 1 & 2 .

1979 *Cyclaster danicus* (Schlüter); Asgaard, tables 1 & 2.

1979 *Brissopneustes decaryi* Lambert; Tanaka *et al.*, p. 44, pl. 3, fig. 8.

1997b *Cyclaster integer* (Seunes); Jeffery, p. 699, pl. 10, figs 1-4, text figs 16-17.

Occurrence. Maastrichtian to Danian of the French Pyrenees (Seunes 1888) (MNHN). Maastrichtian of Azerbaijan (Rouchadze 1940). Upper Maastrichtian to Lower Danian of the northern Caucasus and the Transcaspian Region (Moskvin & Poslavskaya 1959; Poslavskaya & Moskvin 1960) (PI). Lower Danian of Georgia (Gongadze 1979) and the Mangyshlak Peninsula, Kazakhstan (Jeffery 1997b) (BMNH, PI). Danian of northwest Madagascar (Lambert 1933a; Besairie 1971; Tanaka *et al.* 1979) and Lower to Upper Danian chalk and Lower Danian Bryozoan and Cerithium Limestones of Denmark (Schlüter 1897; Ødum 1926; Ravn 1927; Asgaard 1979) (BMNH, DGFMM).

Diagnosis. Rectangular to coffin-shaped horizontal outline with broad, shallow frontal groove. Inflated, somewhat carinate upper surface. Short, slightly sunken petals of approximately equal length. Anterior petals diverge at 115 degrees. Pores round in inner series, elongate in outer series. Labrum long and narrow. Sexual dimorphism in gonopore size. Complete peripetalous fasciole.

Remarks. Topotype material of *C. danicus* is more elongate and rectangular in shape with smaller pores in the paired petals than specimens traditionally referred to *C. integer*. In the former Soviet Union, the name *C. integer* has been used for specimens found below the K-T boundary and *C. danicus* for those specimens from above the boundary. However, within populations of each age housed in the Palaeontological Institute, Moscow, there are rectangular and coffin-shaped specimens as well as all intermediate forms. Since a gradational series exists between the two named forms, the two species are treated as synonymous.

Cyclaster pfenderae Lambert, 1936

(Figure 3.36)

1936 *Cyclaster pfenderae* Lambert, p. 27, pl. 4, figs 17-19.

Occurrence. Lower Maastrichtian (Lambert 1936; Collignon 1968) to Danian of northwest Madagascar (Besairie 1971) (MNHN).

Diagnosis. Ovate horizontal outline. Low profile. Depressed sutures between plates. Sunken, well developed petals. Anterior petals slightly longer than posterior. Anterior pair diverge at 105-110 degrees. Mouth has distinct rim. Broad labral plate does not taper posteriorly. Complete peripetalous fasciole. Dense pustular tuberculation on apical surface.

Cyclaster platornatus Kutscher, 1978b

1978b	*Cyclaster platornatus* Kutscher, p. 1028, pl. 3, figs 1-5.
1982	*Cyclaster platornatus* Kutscher; Nestler, p. 82.
1987	*Cyclaster platornatus* Kutscher; Jagt & Michels, p. 58, figs 1-6.
1987	*Cyclaster platornatus* Kutscher; van der Ham *et al.*, p. 34.
1990	*Cyclaster platornatus* Kutscher; Jagt & Michels, p. 181, figs 1-6.

Occurrence. Lower Maastrichtian Rügener Schreibkreide of the Isle of Rügen (Kutscher 1978b; Nestler 1982) (EMAUG). Upper Lower Maastrichtian Vijlen Chalk of the Maastricht area (Jagt & Michels 1987, 1990; van der Ham *et al.* 1987) (NMM).

Diagnosis. Rounded oval outline. Sunken paired ambulacra. Anterior pair longer than posterior. Anterior petals diverge at 90 degrees. Broad labrum does not taper posteriorly. Peristome large and renate with prominent rim. Sexual dimorphism in gonopore size. Complete peripetalous fasciole well developed but not sharply defined. Some prominent pustulous tubercles on upper surface. Scattered large tubercles on oral surface.

Cyclaster suecicus (Schlüter, 1897)

1897	*Brissopneustes suecicus* Schlüter, p. 34, pl. 1, figs 5-8.
1926	*Brissopneustes suecicus* Schlüter; Ødum, p. 164.
1926	*Brissopneustes suecicus* Schlüter; Brünnich Nielsen, p. 13.
1927	*Brissopneustes suecicus* Schlüter; Ravn, p. 351, pl. 4, fig. 4.
1979	*Cyclaster suecicus* (Schlüter); Asgaard, tables 1 & 2.

Occurrence. Mid Danian Faxe Limestone of Sweden (Schlüter 1897) and Mid to Upper Danian Saltholm Limestone of Denmark (Brünnich Nielsen 1926; Ødum 1926; Ravn 1927). Lower Danian Bryozoan (Asgaard 1979) and Cerithium Limestones of Denmark (Ravn 1927) (DGFMM).

Diagnosis. Broad rectangular horizontal outline. Inflated upper surface with no posterior carina. Petals short and of equal length, open distally, virtually flush. Anterior petals widely divergent. Pores round in anterior series and elongate in posterior series. Long, narrow labrum. No peripetalous fasciole.

Cyclaster ruegensis (Kutscher, 1978b)

1978b *Brissopneustes rügensis* Kutscher, p. 1027, pl. 2.

Occurrence. Lower Maastrichtian Rügener Schreibkreide of the Isle of Rügen (Kutscher 1978b) (EMAUG).

Diagnosis. Large specimens with broad rectangular horizontal outline. Short petals of equal length, hardly sunken. Anterior pair diverge at 110 degrees. Pores small and round. No peripetalous fasciole.

Cyclaster galei Jeffery, 1997b

(Figure 3.37)

1997b *Cyclaster galei* Jeffery, p. 704, pl. 10, figs 5-8, text figs 16, 18.

Occurrence. Uppermost Maastrichtian (*B. casimirovensis* Zone) of the Mangyshlak Peninsula, Kazakhstan (BMNH).

Diagnosis. Elongate rectangular horizontal outline. Flat upper and lower surfaces. Very short, virtually flush petals of approximately equal length. Anterior pair diverge at 90 degrees. Pores small and round. Mouth large and strongly labiate with thickened rim. Peripetalous fasciole only visible posteriorly.

Genus ISASTER Desor, 1858

[Type species *Spatangus aquitanicus* Grateloup, 1836, by OD]

Synonym. *Ismidaster* Böhm, 1927 (type species *Ismidaster toulai* Böhm, 1927).

Diagnosis. Ovate *Echinocorys*-type shape with domed upper surface. Ambulacra alike - flush to slightly depressed, petaloid with slightly elongate pores. Apical system ethmophract with three gonopores - madreporite lacking gonopore. Anterior mouth and inframarginal periproct. No fascioles.

Isaster aquitanicus (Grateloup, 1836)

(Plate 9, figures 4-7; Figure 3.38)

1836 *Spatangus aquitanicus* Grateloup, p. 176 , pl. 2, fig. 17.

1927 *Ismidaster toulai* Böhm, p. 194, pl. 11, fig. 3.

1960 *Isaster aquitanicus* d'Orbigny; Poslavskaya & Moskvin, p. 67, pl. 4, figs 4-6, text fig. 18.

1960 *Isaster abkhasicus* (Schwetzov); Poslavskaya & Moskvin, p. 68, pl. 5, figs 1-3, text fig. 19.

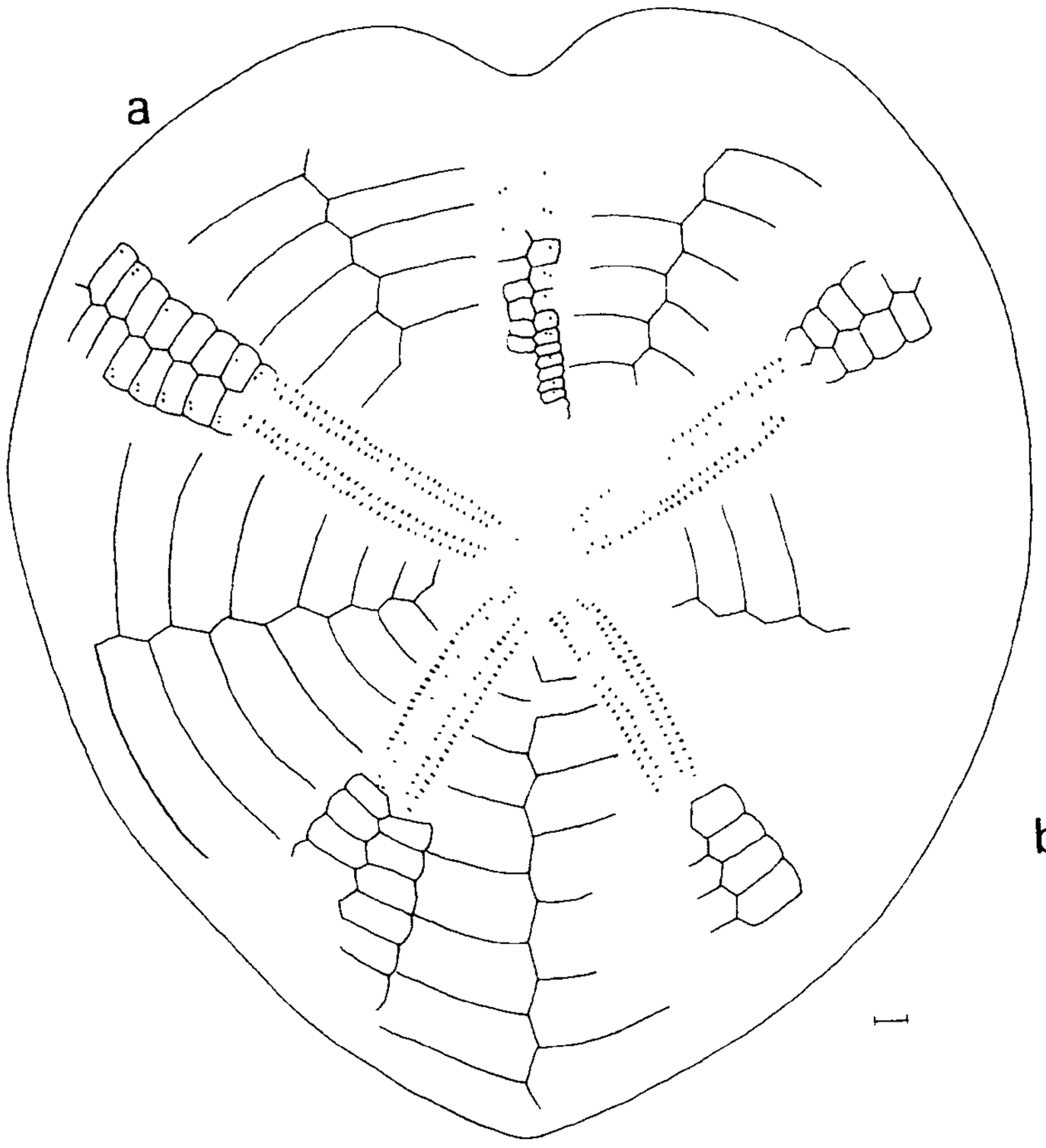
1986 *Isaster toulai* (Böhm); Stokes, p. 171, text figs 1-2.

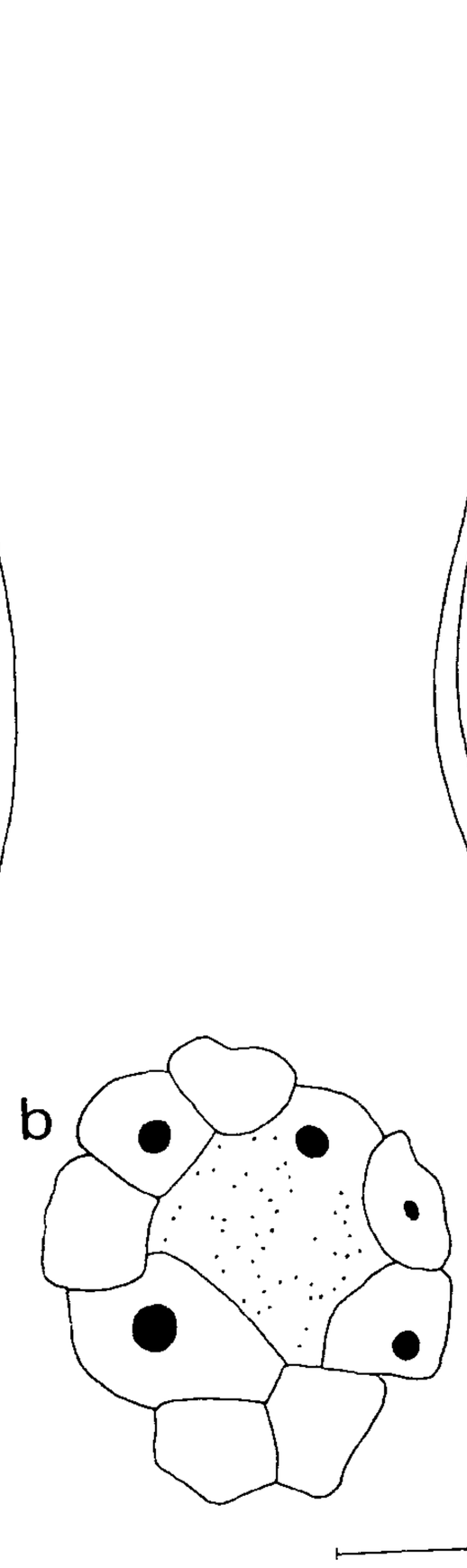
1996 *Isaster* sp. Wilmsen *et al.*, fig. 7.

Occurrence. Upper Danian to Thanetian of the Crimea and the Mangyshlak Peninsula of Kazakhstan (Poslavskaya & Moskvin 1960) (PI). Danian of northwest Turkey (Böhm 1927) (BMNH). Upper Thanetian of of Casas di Oreyon, Navarra, Spain (BMNH). Lower Maastrichtian Cabo de Lata Formation of Santander, Spain (Wilmsen *et al.* 1996) and Maastrichtian of Alicante, Spain (BMNH).

Diagnosis. As generic description.

Figure 3.26. Camera lucida drawings of *Micraster schroederi* Stolley, Campanian of Hanover, Germany. a & b, BMNH EE4808; a, apical view; b, apical disc plating. c, BMNH E75824, oral view. a & c, scale bars = 2 mm. b, scale bar = 1 mm.


a


b

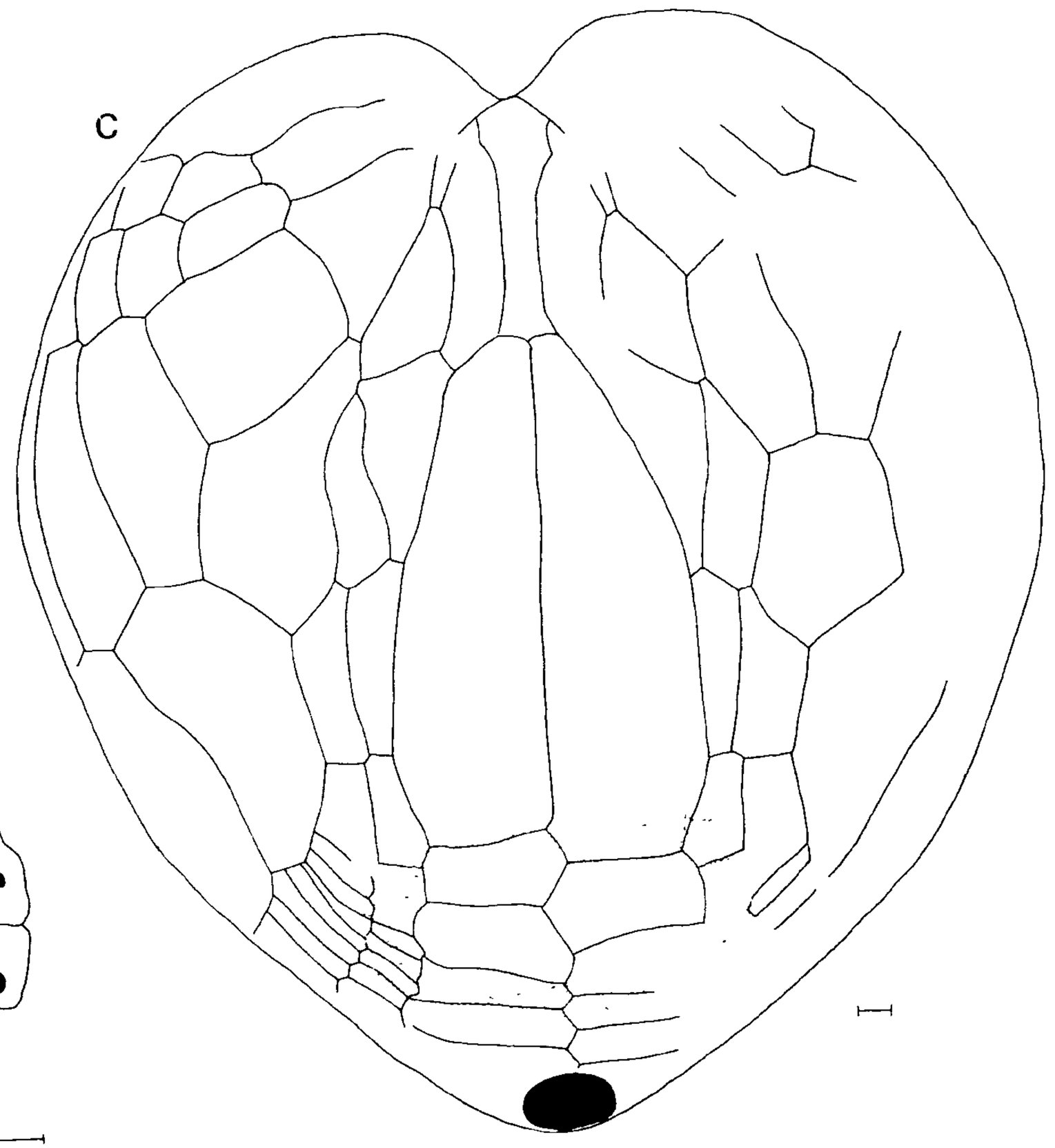

c

Figure 3.27. Camera lucida drawings of *Micraster aturicus* Seunes, MNHN no specimen number, Maastrichtian of Tercis, France; a, apical disc plating; b, lateral view. a, scale bar = 1 mm. b, scale bar = 5 mm.

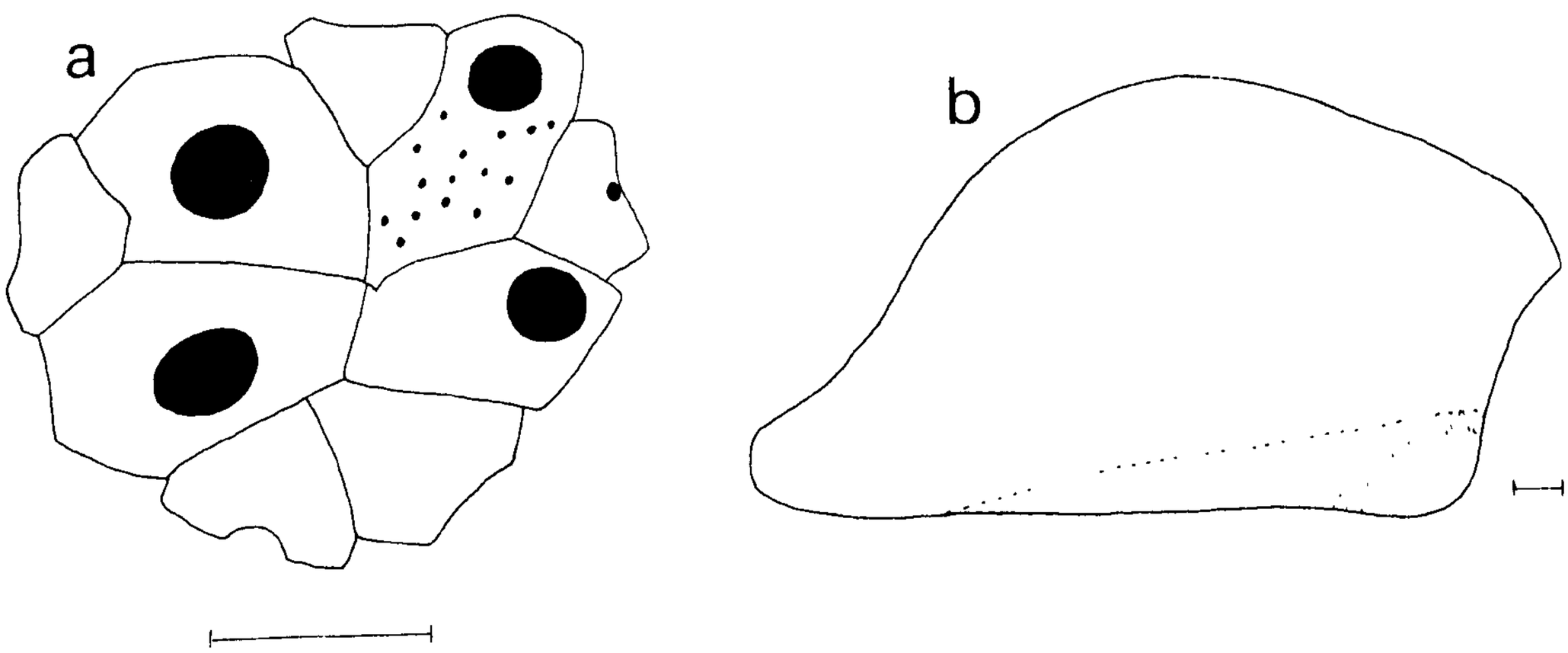
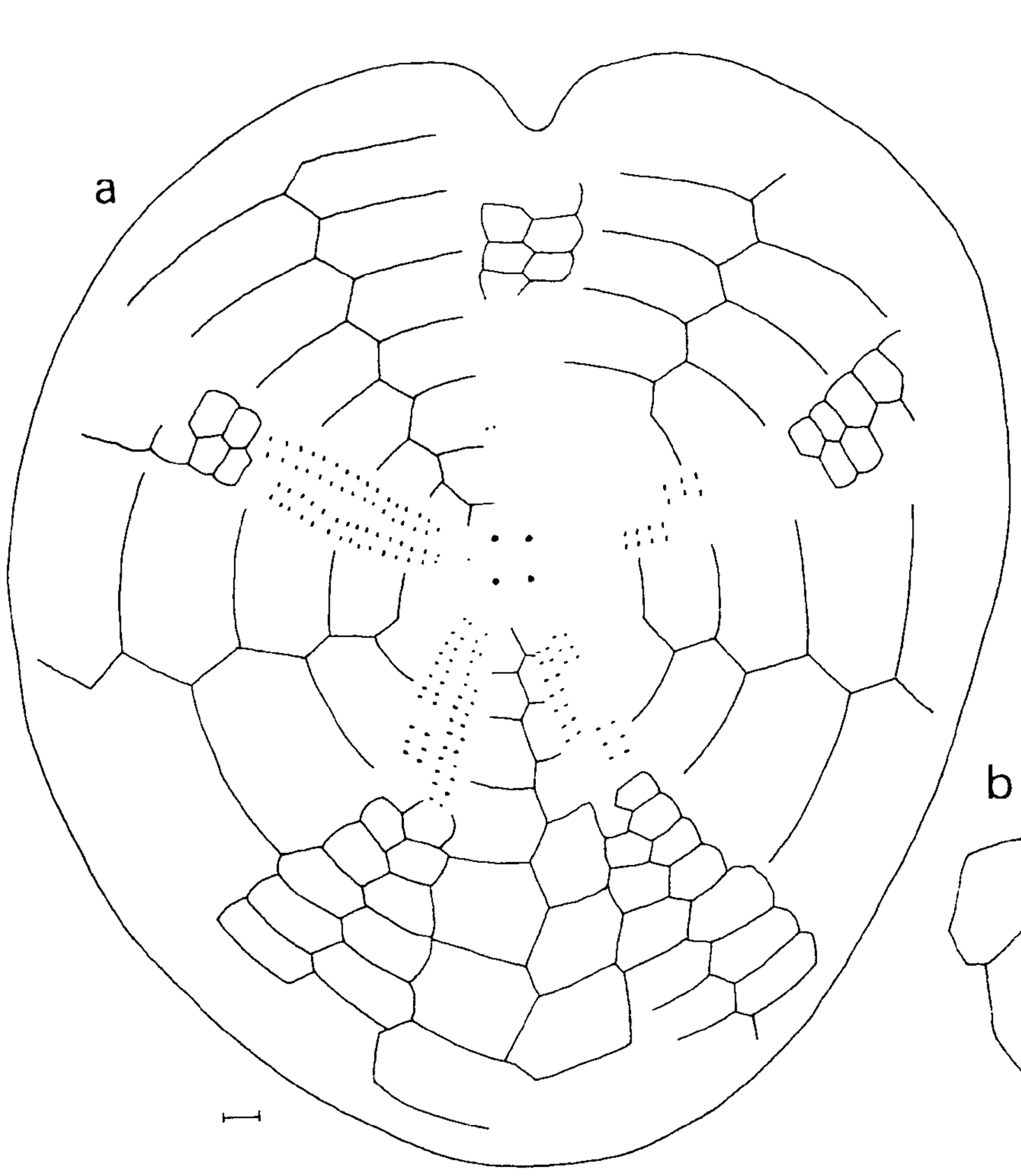
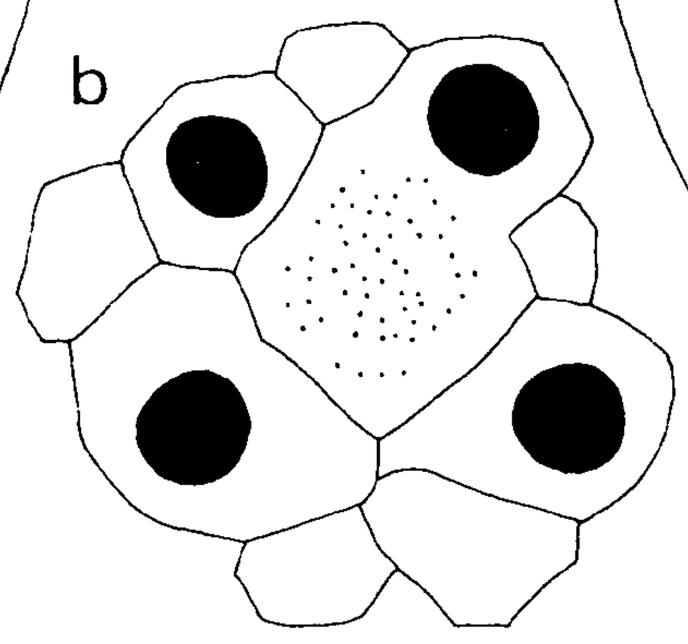

a
b

Figure 3.28. Camera lucida drawings of *Micraster grimmensis* Nietsch, Campanian of Kopet Dag. a, PI 35/36 5, apical view. b & c, PI 35/36 2; b, apical disc plating; c, oral view. Scale bars = 1 mm.


a
1


b

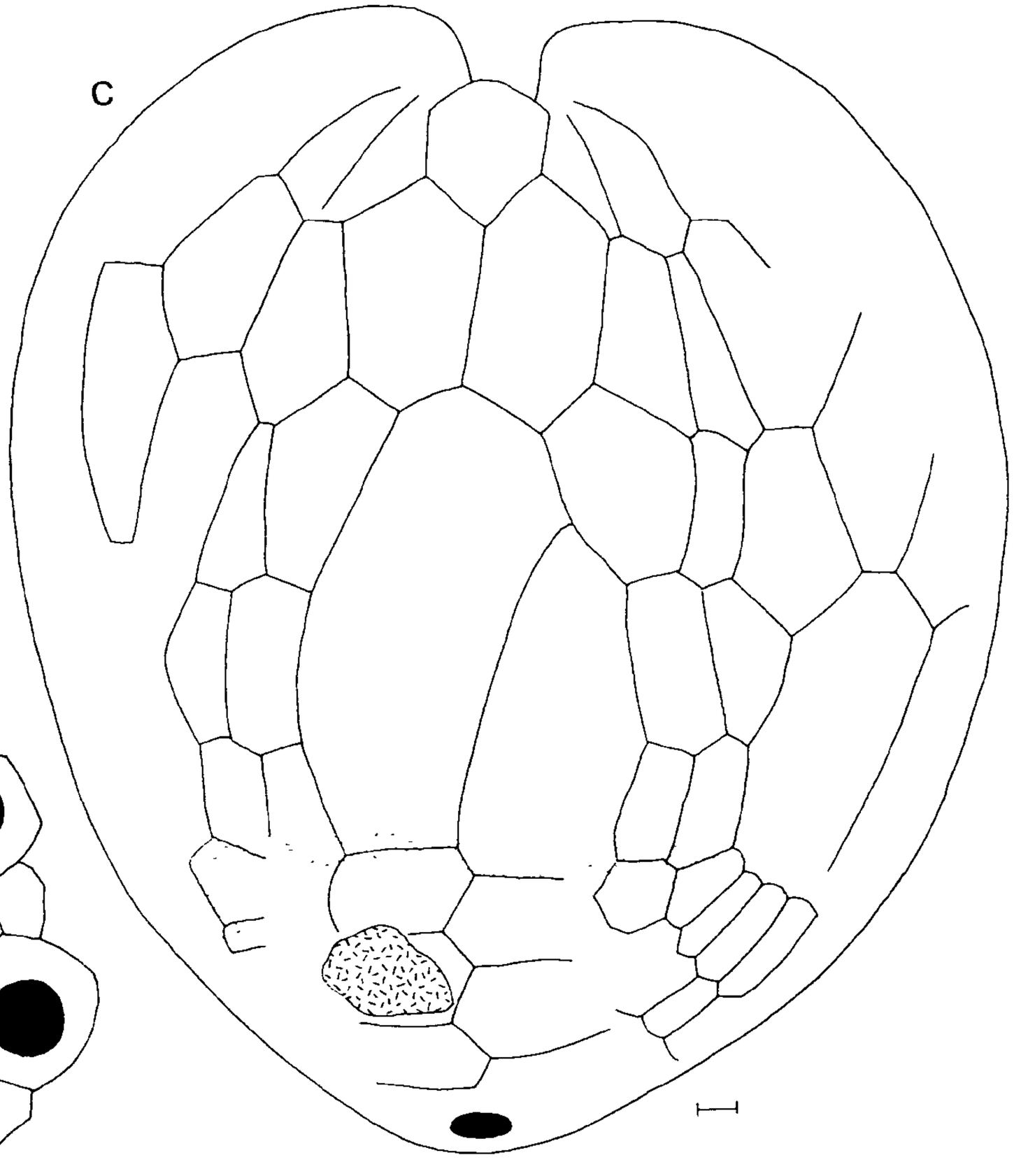

c
1

Figure 3.29. Camera lucida drawings of *Mokotibaster nobilis* (Stoliczka). a & b, BMNH E18704, Campanian of northwestern Madagascar; a, apical view; b, apical disc plating. c, GSI 1655 (PARATYPE), Maastrichtian Ariyalur Group of southern India, oral view. a, scale bar = 5 mm. b, scale bar = 1 mm. c, scale bar = 2 mm.

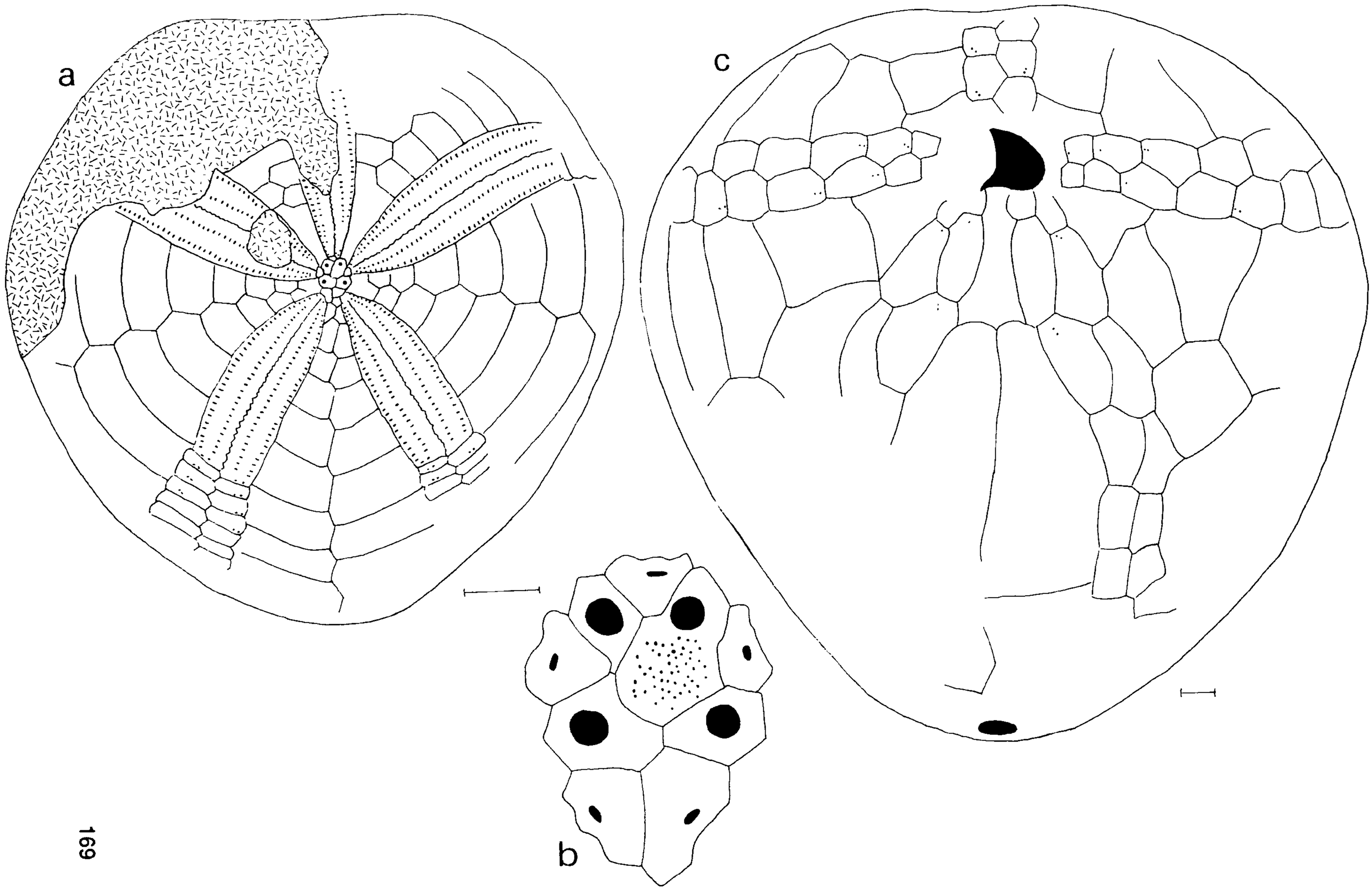
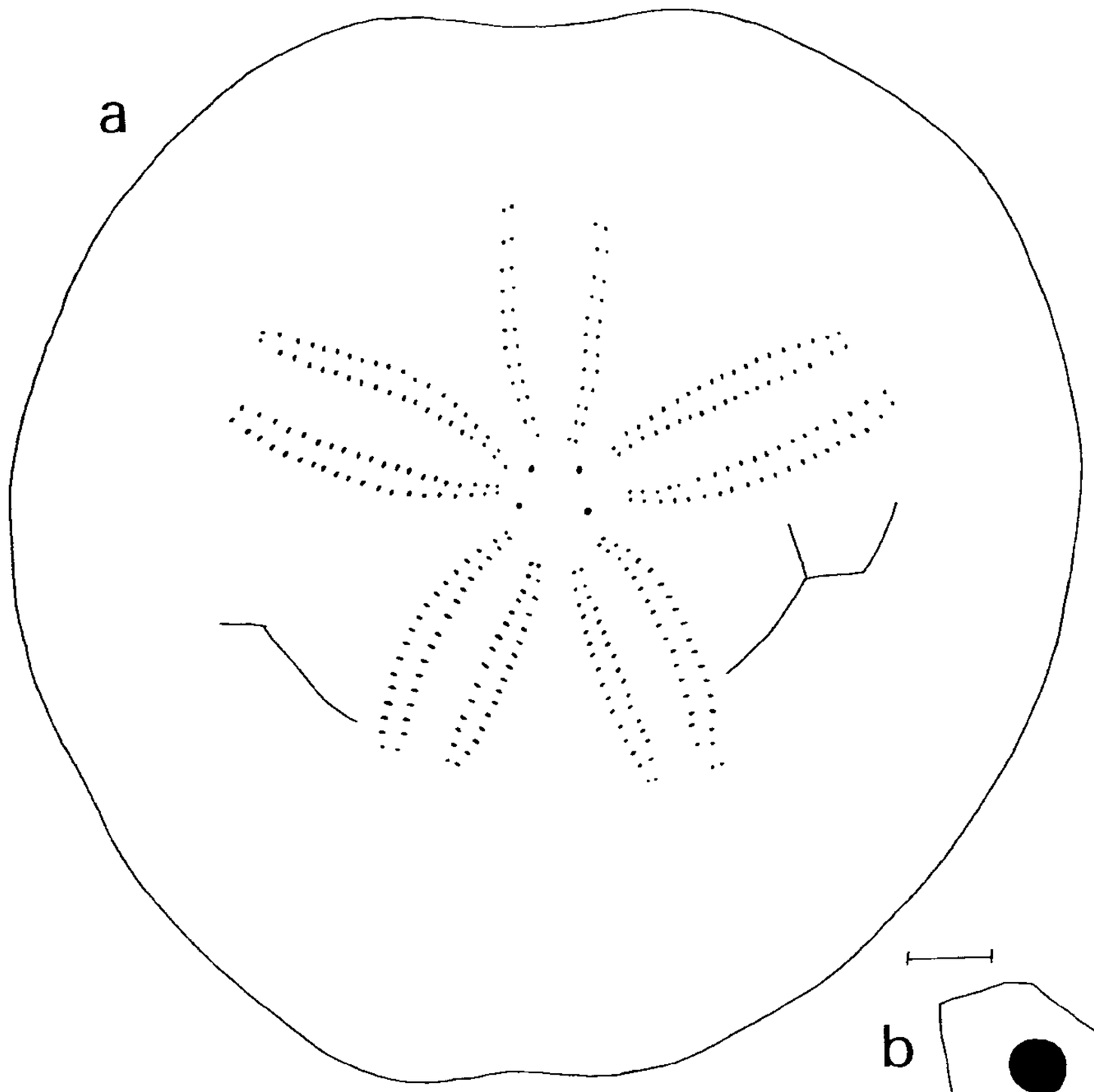
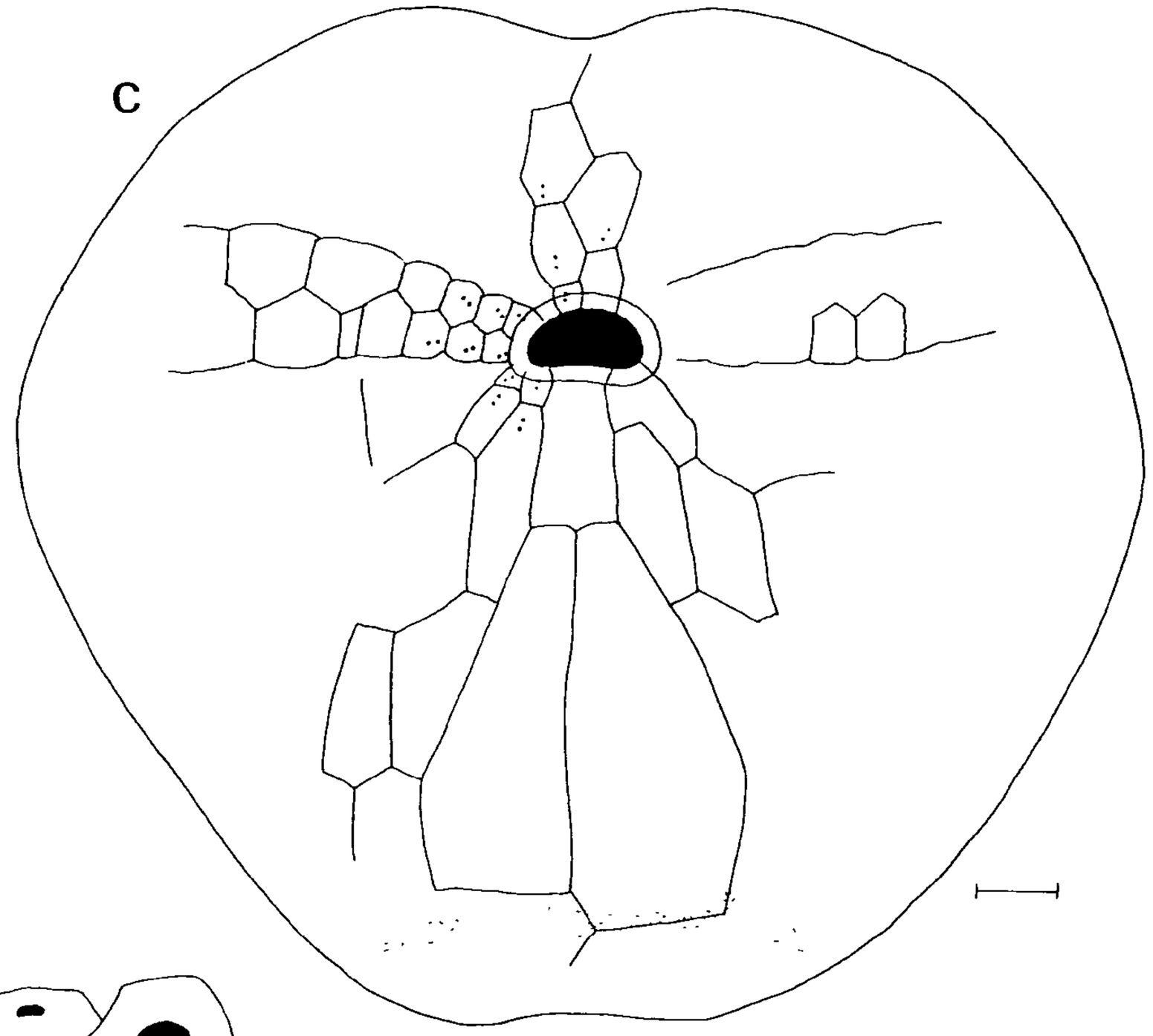

a
c
b

Figure 3.30. Camera lucida drawings of *Pseudogibbaster akkajensis* (Weber), Danian of Crimea. a, PI 335/56, apical view. b, PI 586, apical disc plating. c, PI 583/3, oral view. a & c, scale bars = 2 mm. b, scale bar = 1 mm.


a


c

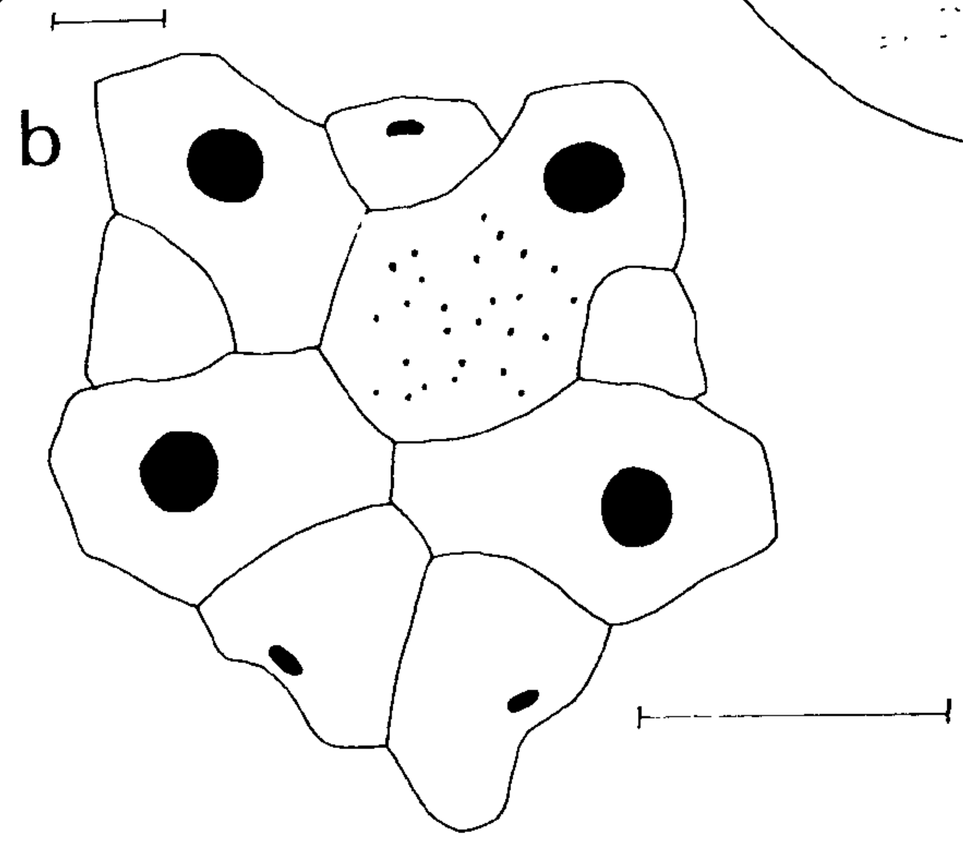
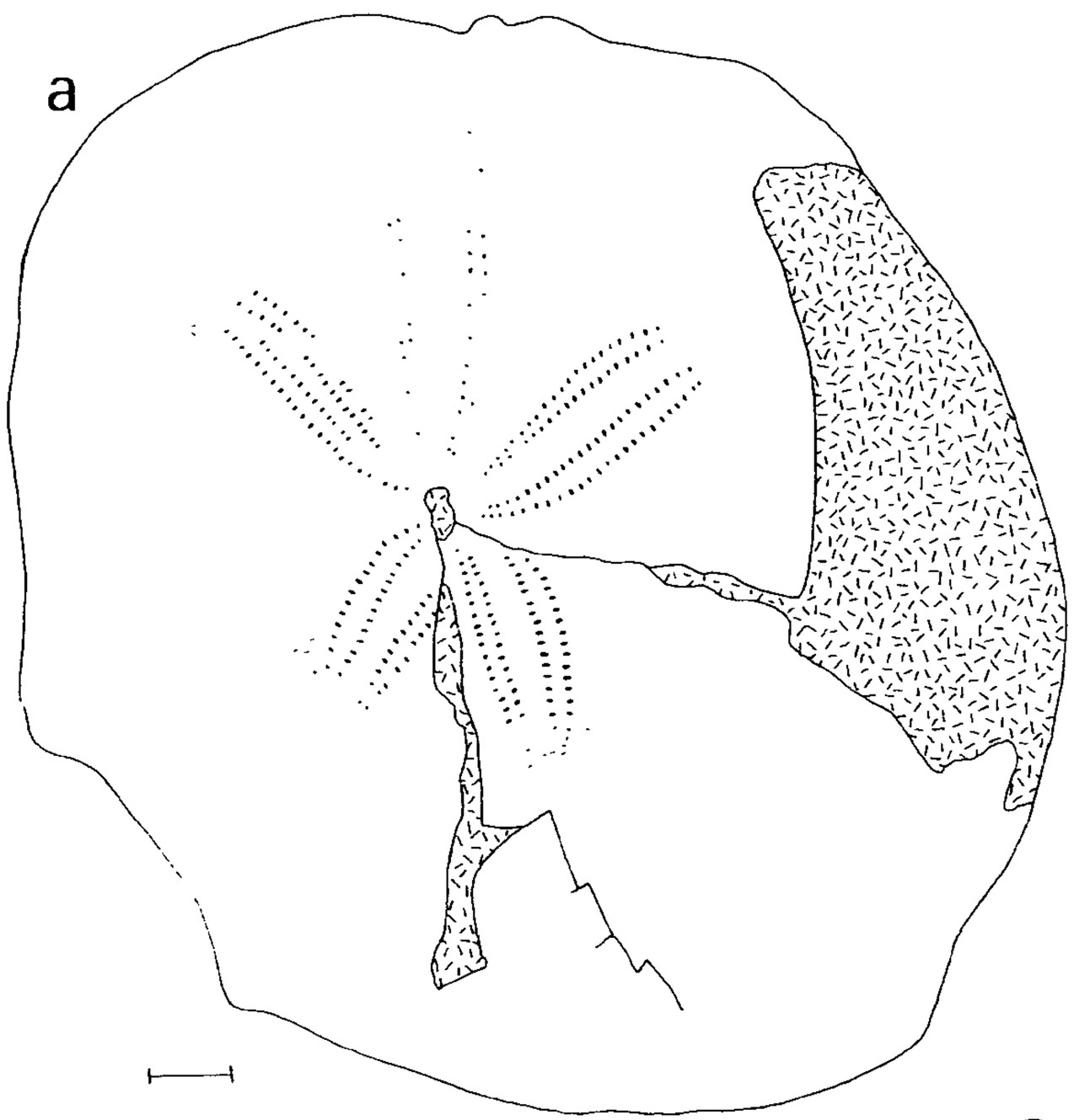
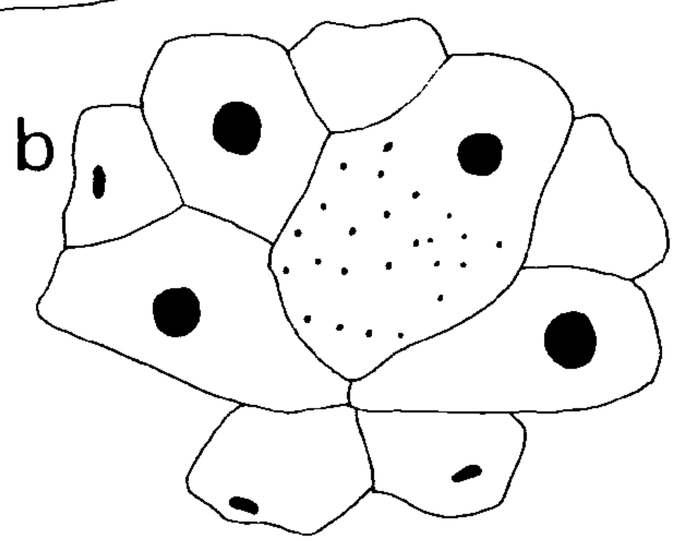

b

Figure 3.31. Camera lucida drawings of *Diplodetus duponti* (Lambert), Lower Maastrichtian Vijlen Chalk of the Maastricht region. a, NMM MM811, apical view. b, Indeherberge Collection (private) no specimen number, apical disc plating. c., NMM (Jagt Collection) 3425, part of oral surface. a & c, scale bars = 2 mm. b, scale bar = 1 mm.


a


b

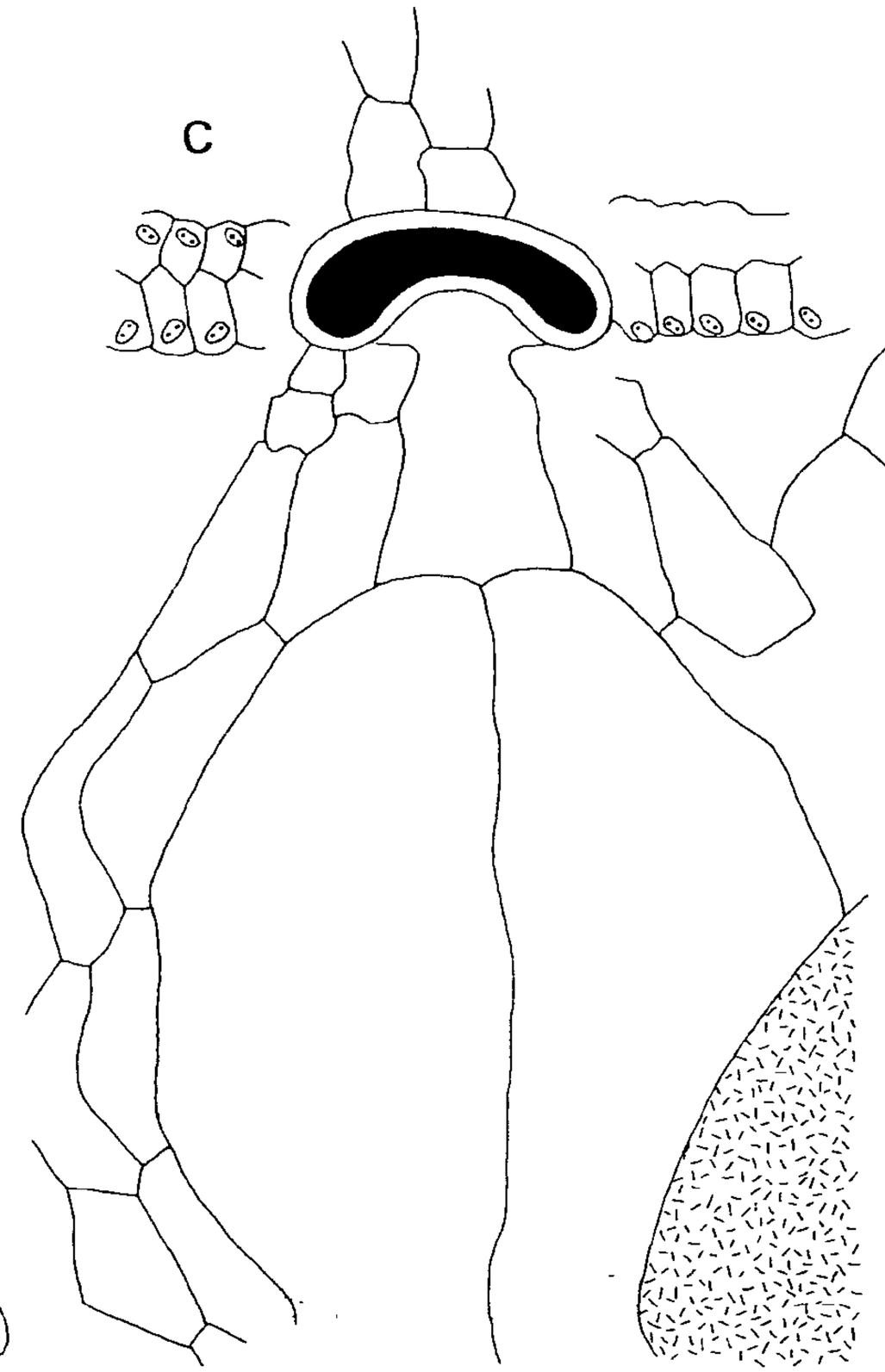
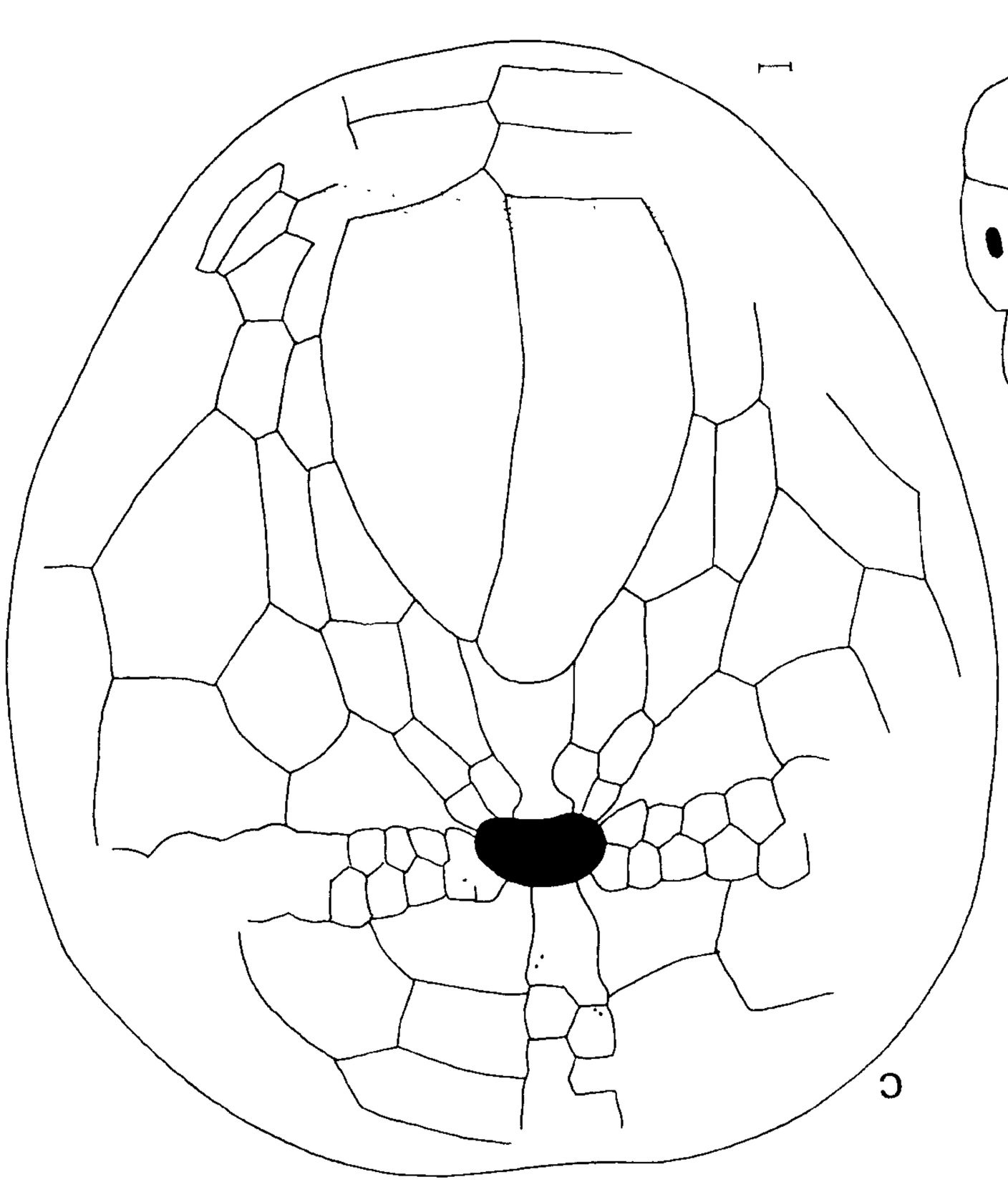
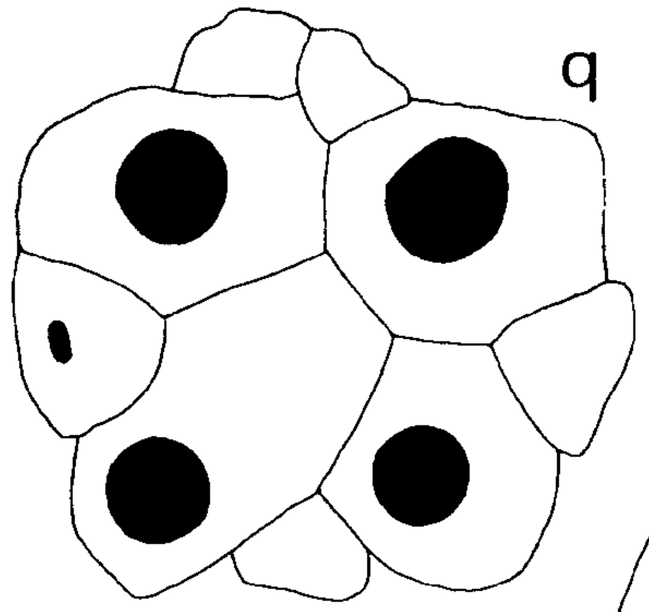

c

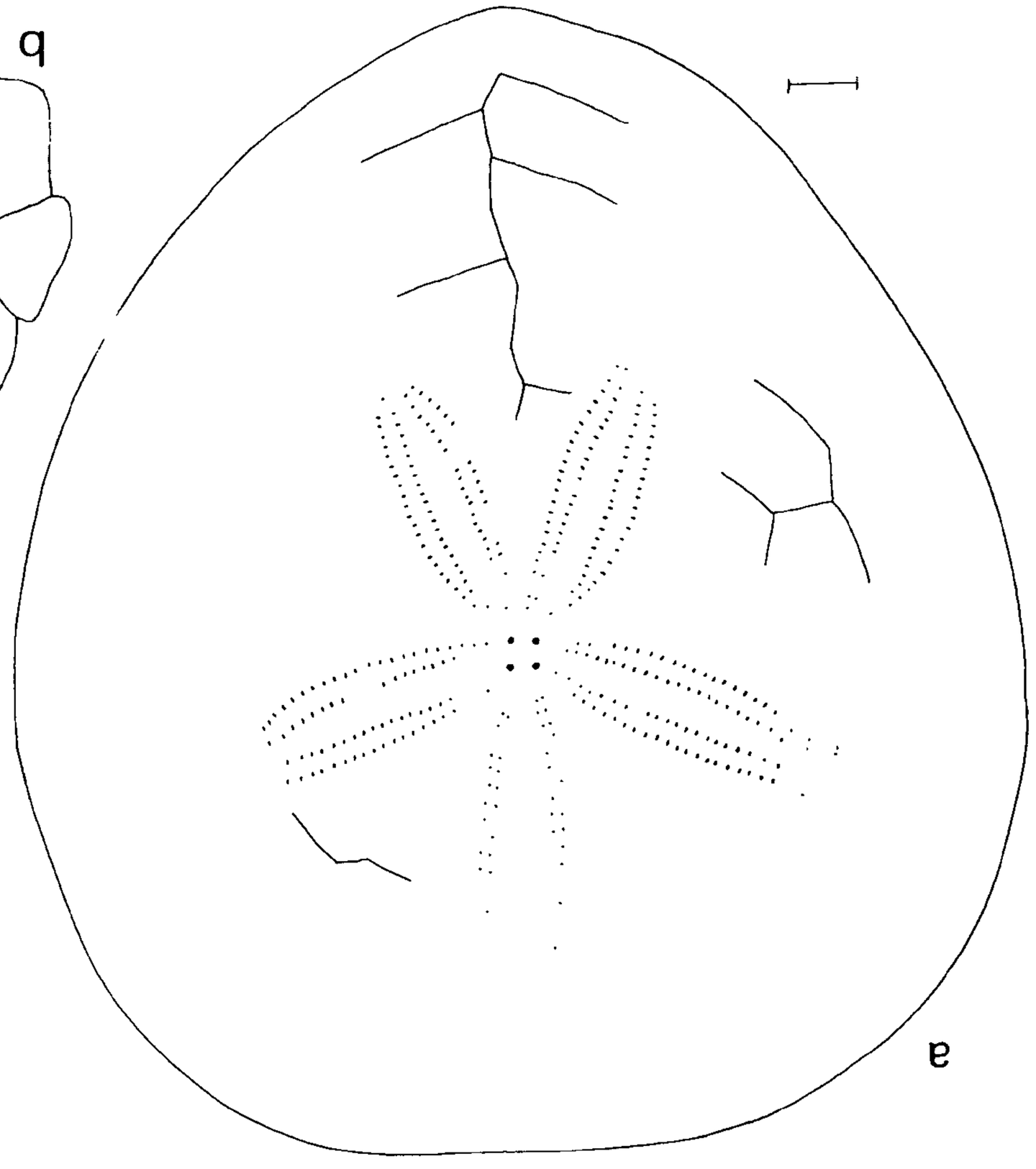
Figure 3.32. Camera lucida drawings of *Diplodetus coloniae* (Cotteau), PI no specimen number, Danian of Crimea; a, apical view; b, apical disc plating; c, oral view. a, scale bar = 2 mm. b & c, scale bars = 1 mm.



c

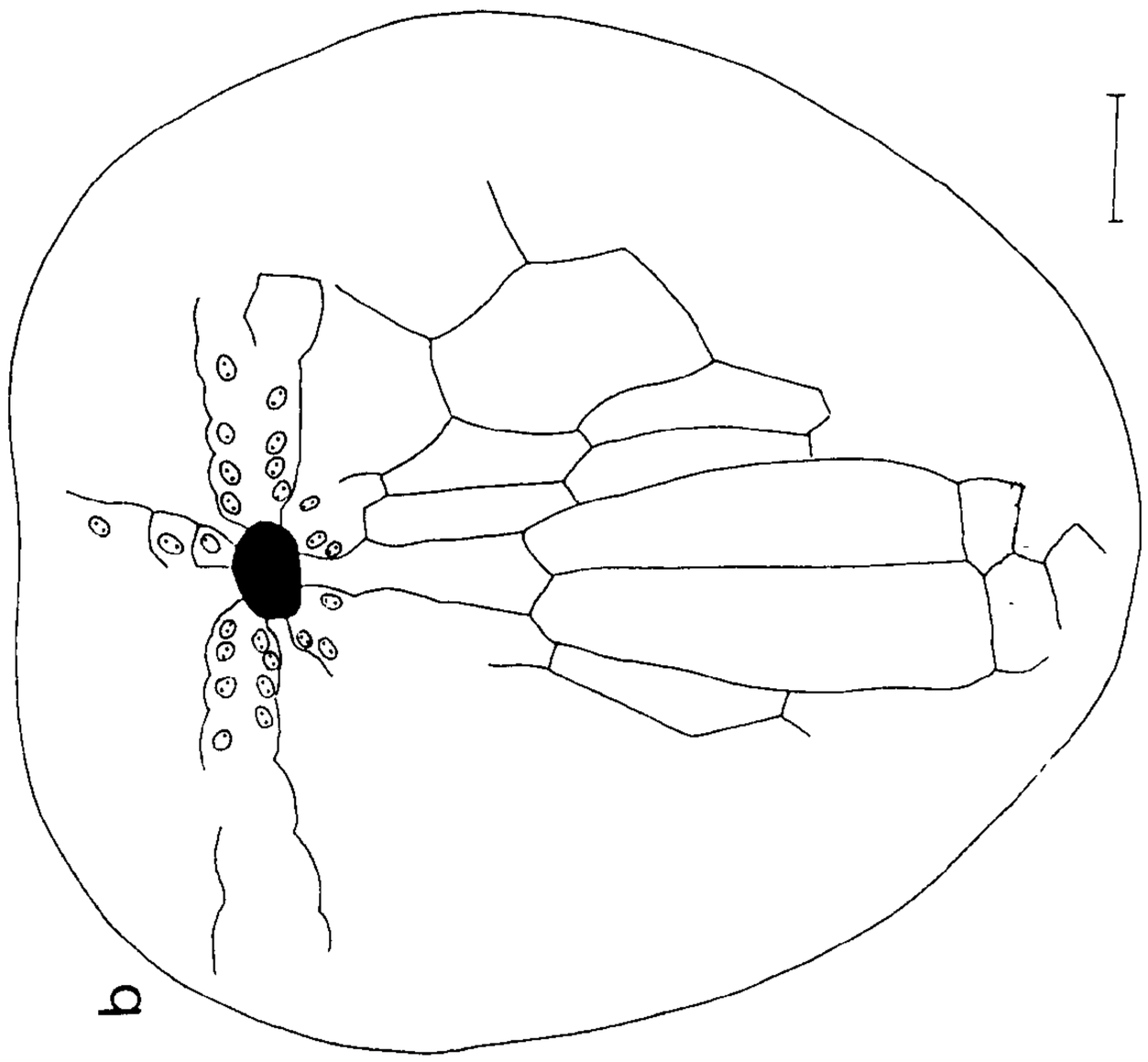


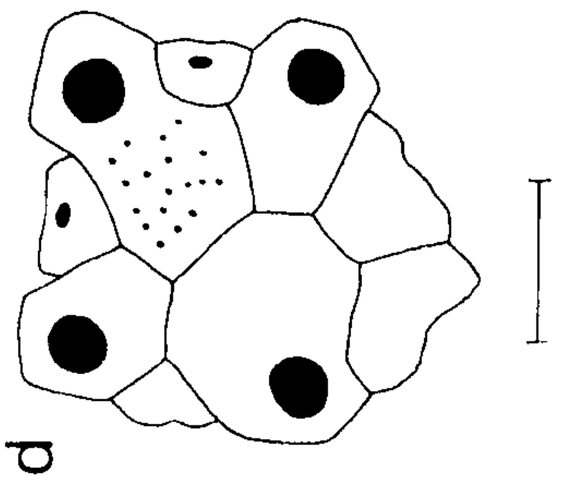
q



a

Figure 3.33. Camera lucida drawings of *Ovulaster auberti* Gauthier, MNHN (Lambert Collection) 1391 (HOLOTYPE), Coniacian? of Tunisia; a, apical view; b, oral view; c, lateral view; d, apical disc plating. a-c, scale bars = 3 mm. d, scale bar = 1 mm.


b


d

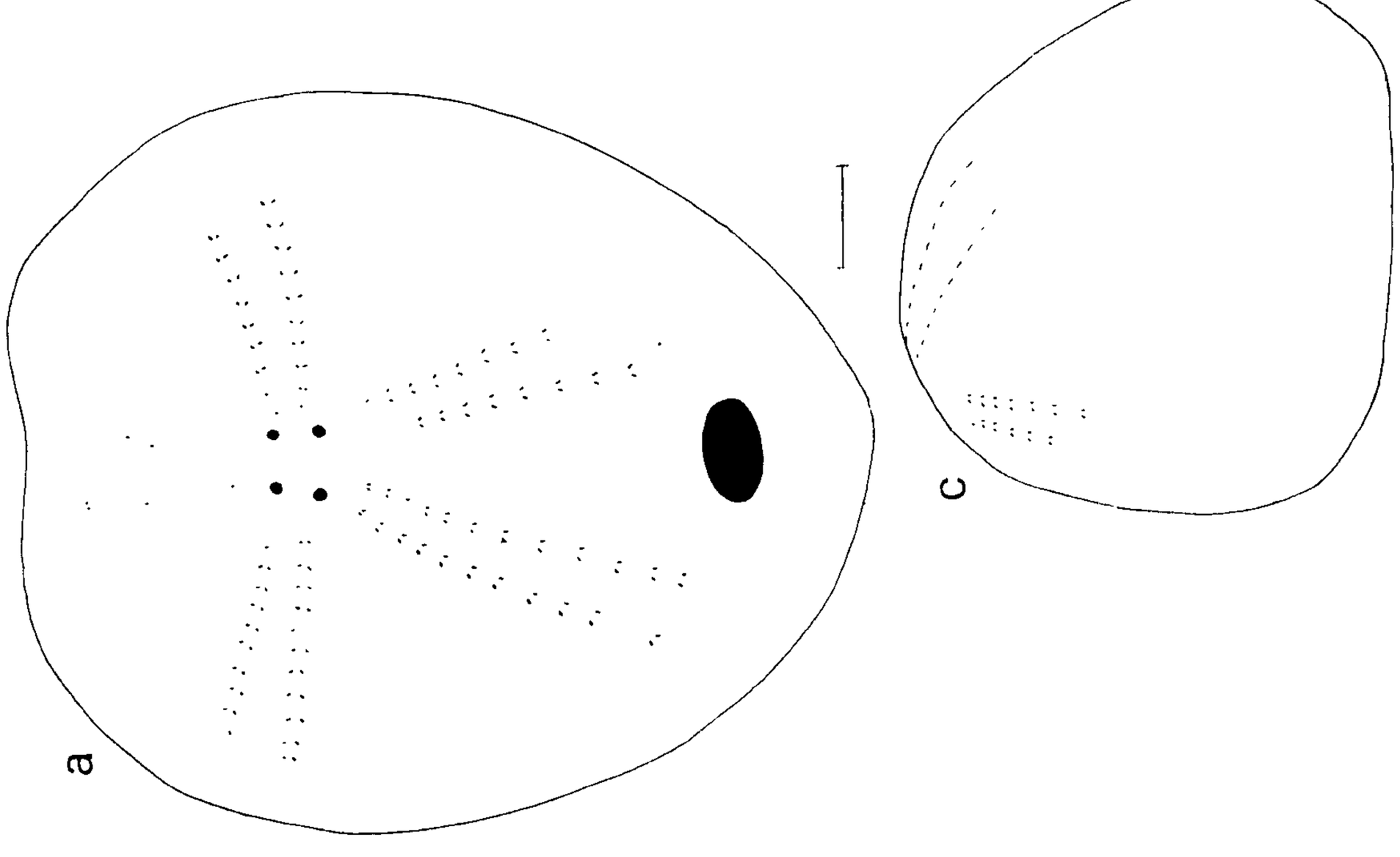

a
c

Figure 3.34. Range chart for Maastrichtian and Palaeocene four-gonopored micrasterid species. See Figure 3.2 for explanation of symbols.

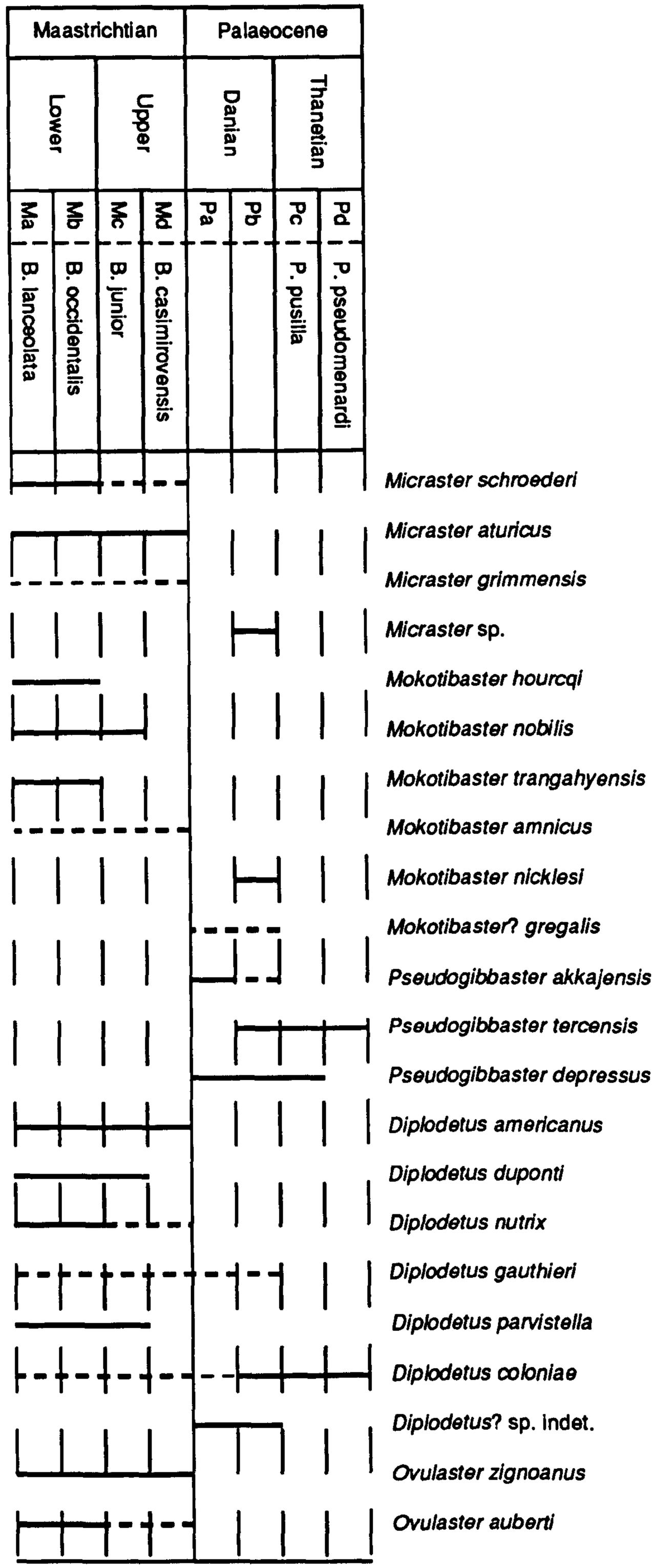
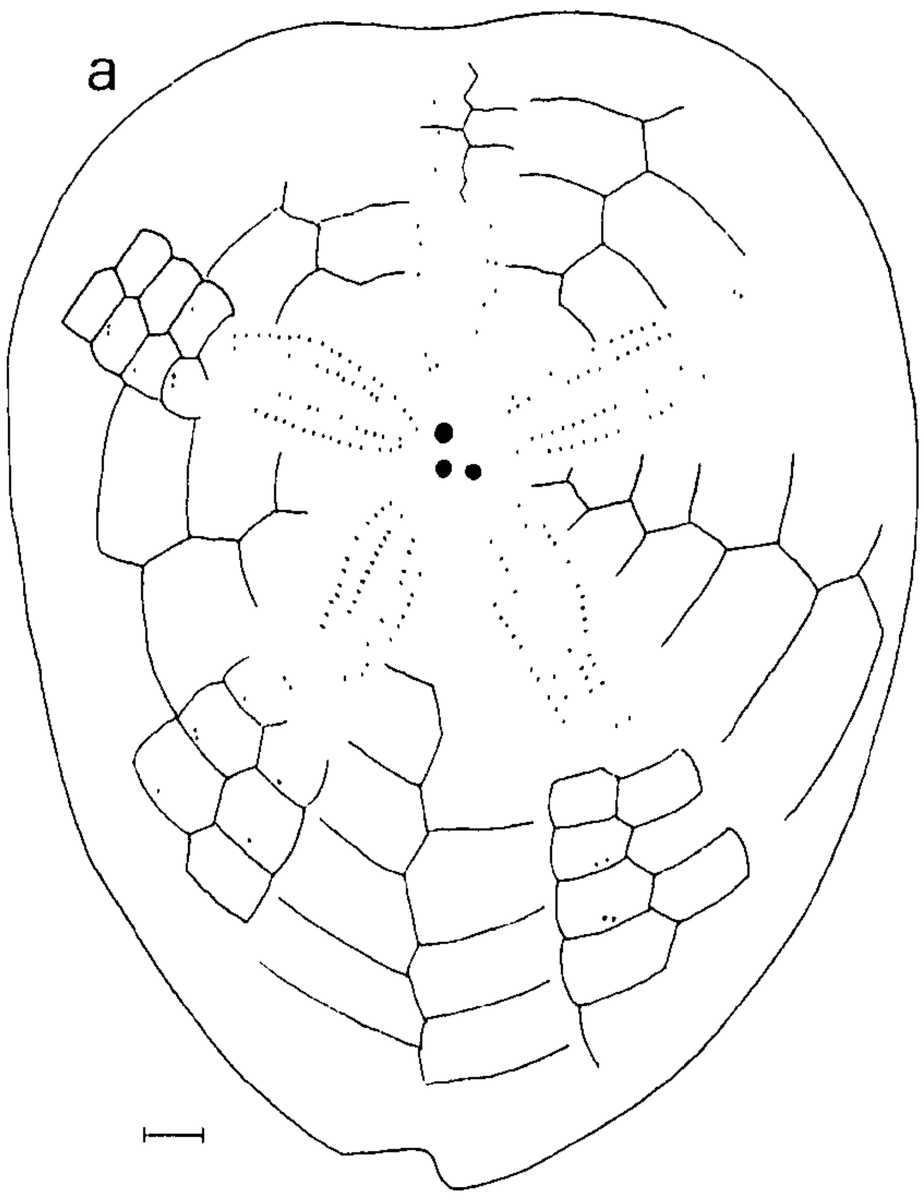
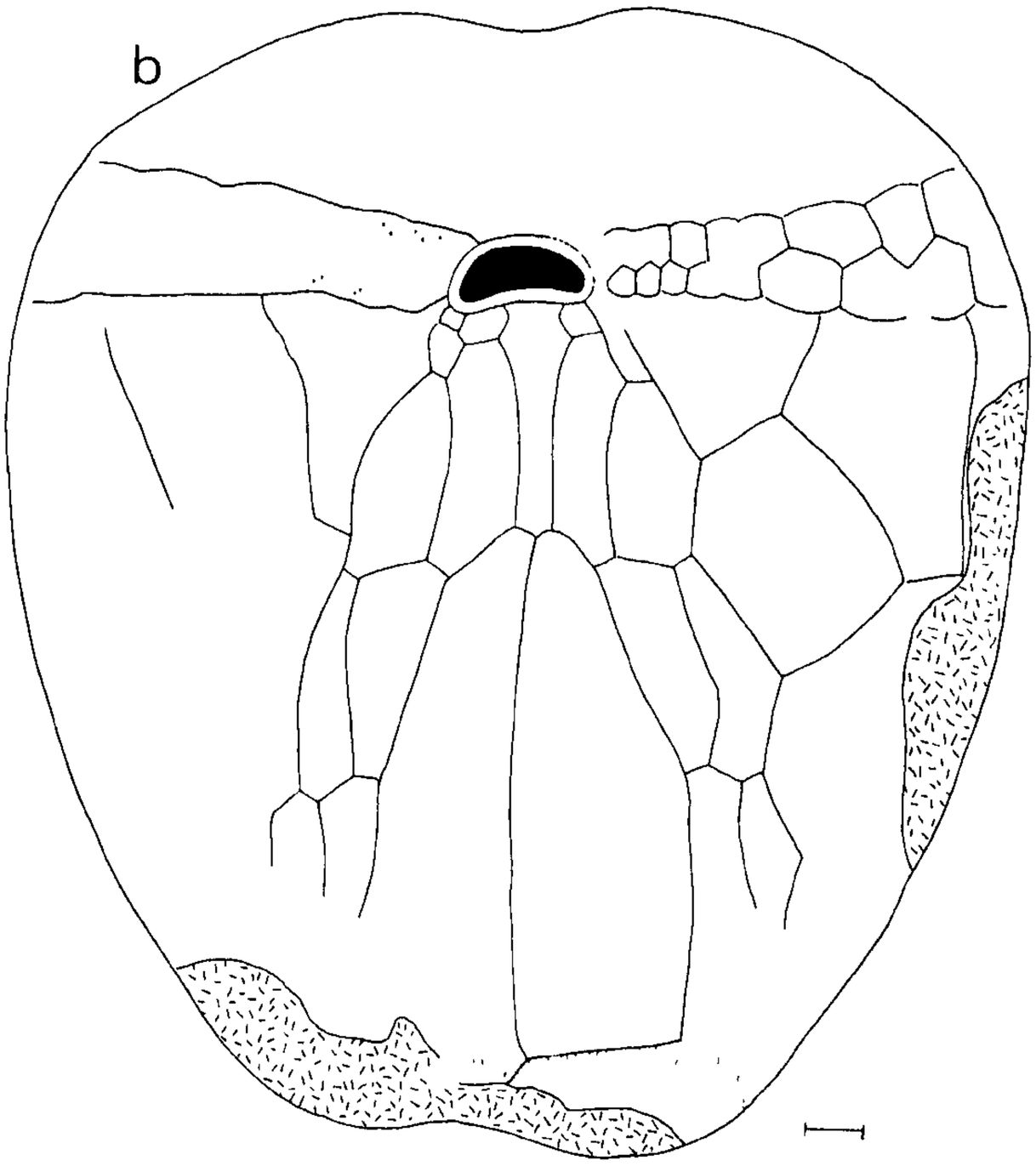

Maastrichtian
Palaeocene
Lower
Upper
Danian
Thanetian
Ma
Mb
Mc
Md
Pa
Pb
Pc
Pd
B. lanceolata
B. occidentalis
B. junior
B. casimirovensis
P. pusilla
P. pseudomenardi
Micraster schroederi
Micraster aturicus
Micraster grimmensis
Micraster sp.
Mokotibaster hourcqi
Mokotibaster nobilis
Mokotibaster trangahyensis
Mokotibaster amnicus
Mokotibaster nicklesi
Mokotibaster? gregalis
Pseudogibbaster akkajensis
Pseudogibbaster tercensis
Pseudogibbaster depressus
Diplodetus americanus
Diplodetus duponti
Diplodetus nutrix
Diplodetus gauthieri
Diplodetus parvistella
Diplodetus coloniae
Diplodetus? sp. indet.
Ovulaster zignoanus
Ovulaster auberti

Figure 3.35. Camera lucida drawings of *Cyclaster aturicus* (Seunes). a, BMNH EE6068, Danian of Navarra, Spain, apical view. b & c, PI 509/55, Danian of the Northern Caucasus; b, oral view; c, apical disc plating. a & b, scale bars = 2 mm. c, scale bar = 1 mm.


a


b

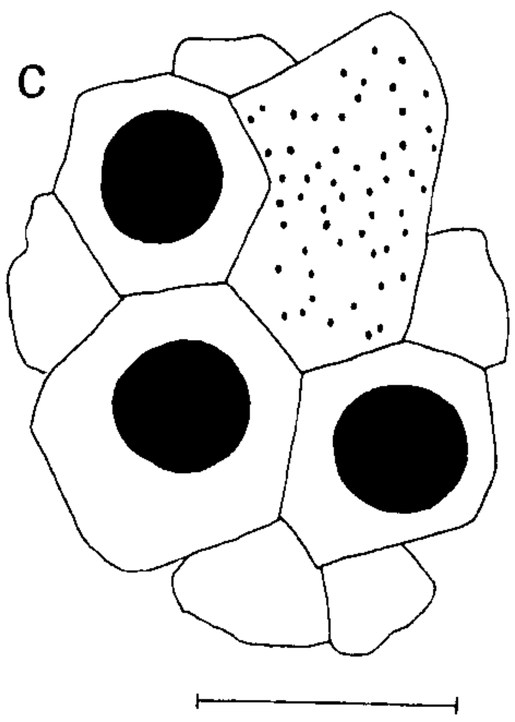

c

Figure 3.36. Camera lucida drawings of *Cyclaster pfenderae* Lambert, MNHN (Lambert Collection) no specimen number, Lower Maastrichtian of northwest Madagascar; a, apical view; b, oral surface; c, apical disc plating. a & b, scale bars = 2 mm. c, scale bar = 1 mm.

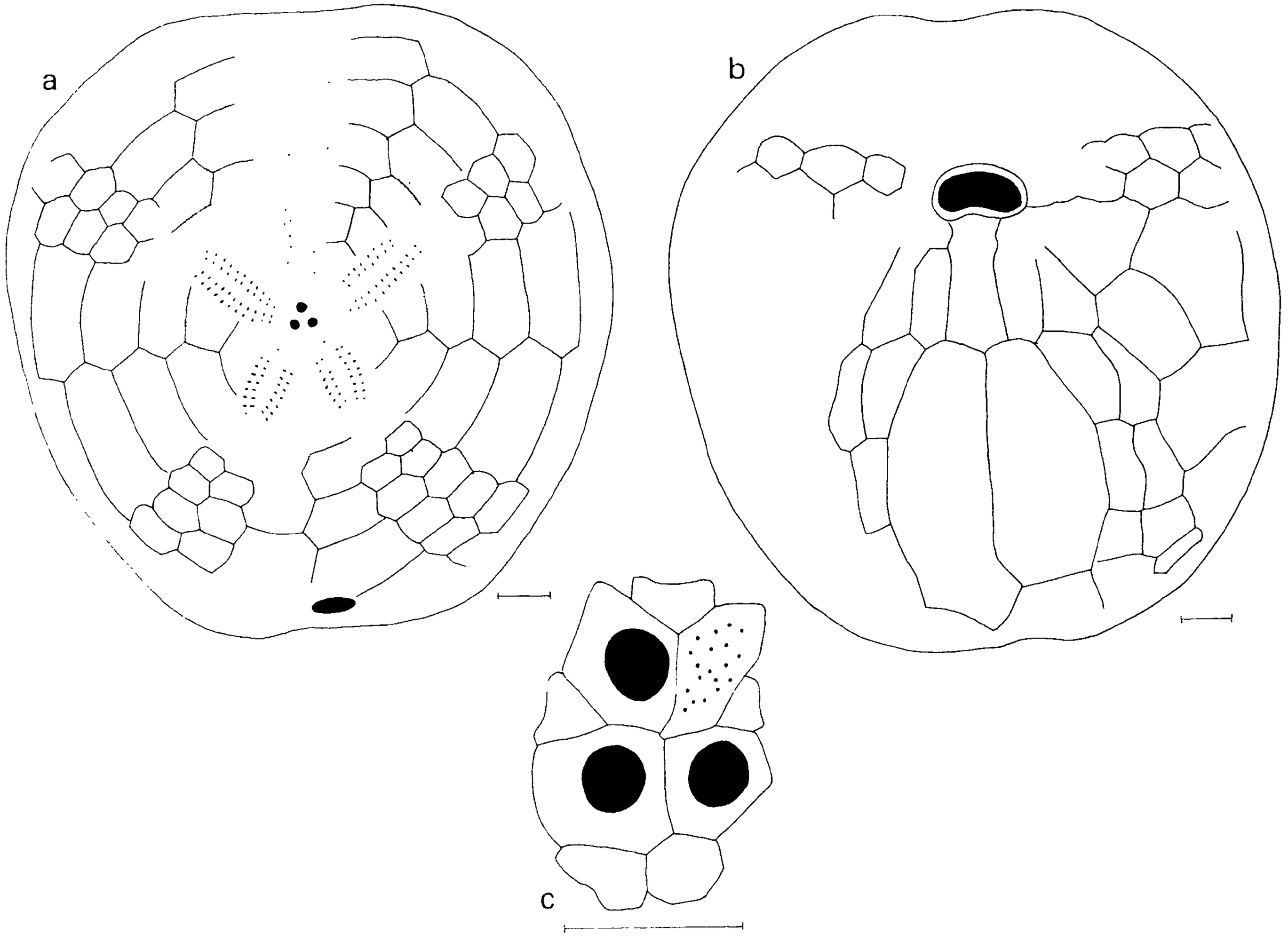

a
b
c

Figure 3.37. Camera lucida drawings of *Cyclaster galei* Jeffery, BMNH EE5575 (HOLOTYPE), Uppermost Maastrichtian of Mangyshlak, Kazakhstan; a, apical view; b, oral view; c, apical disc plating. a & b, scale bars = 2 mm. c, scale bar = 1 mm.

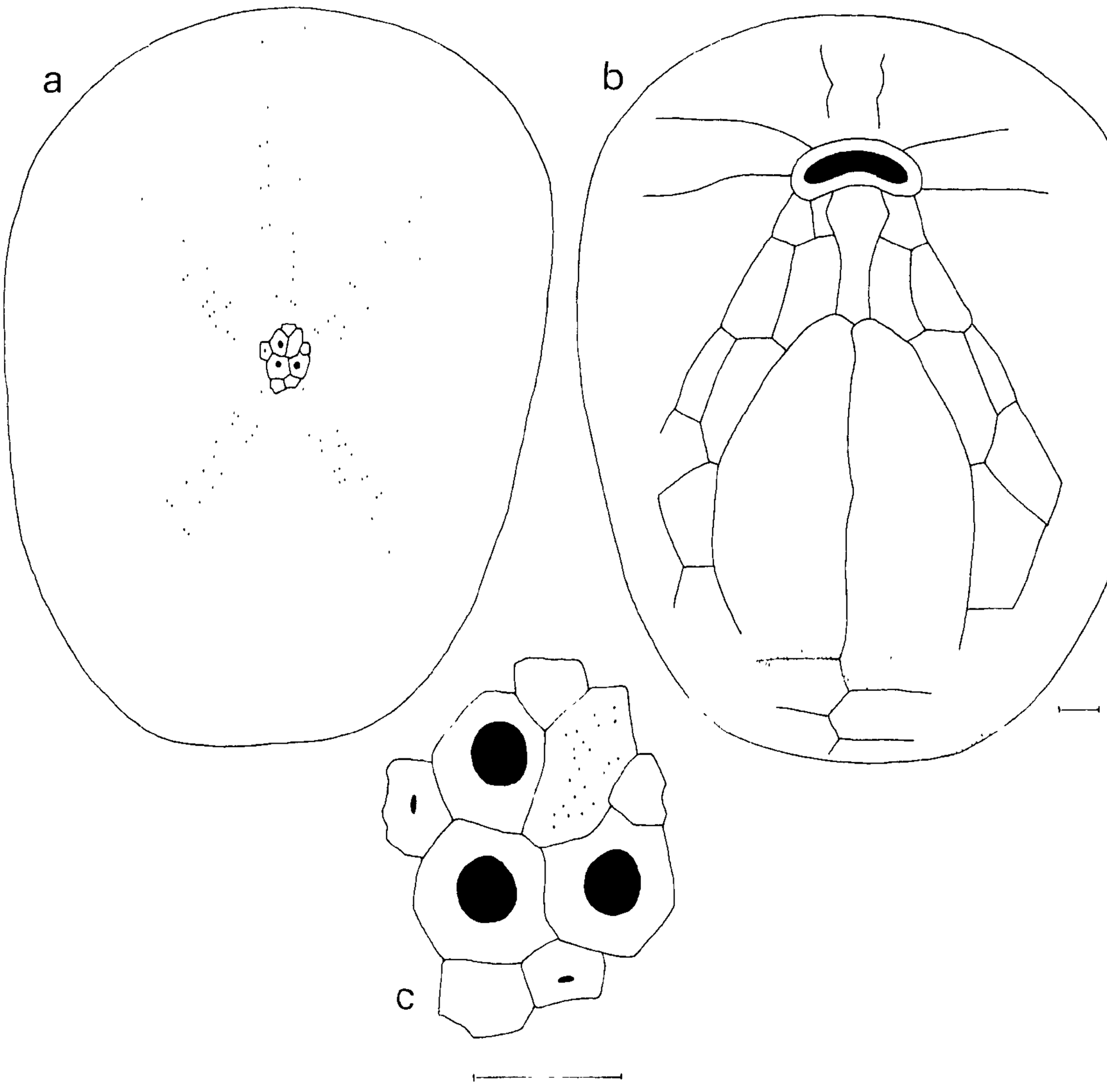
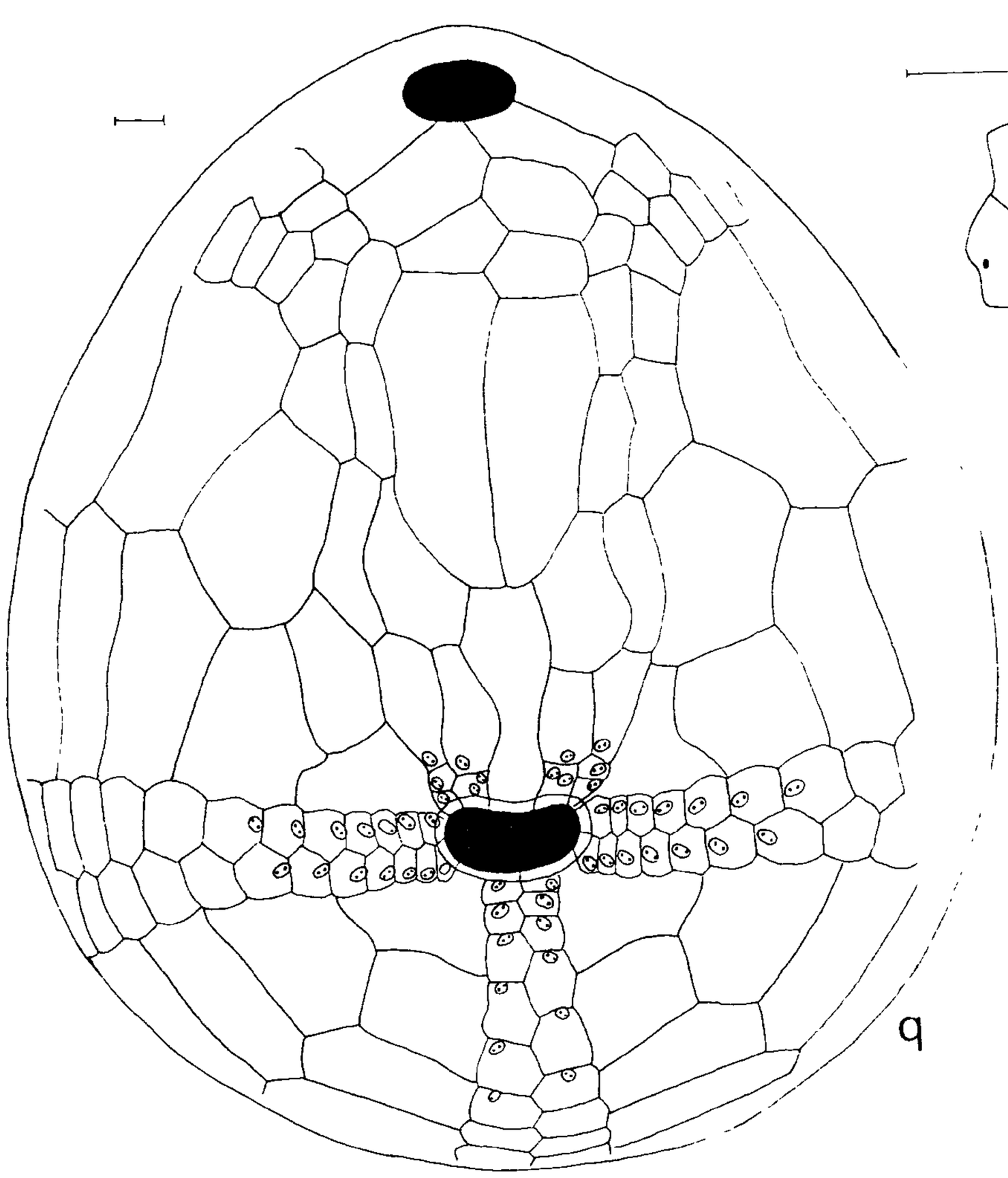
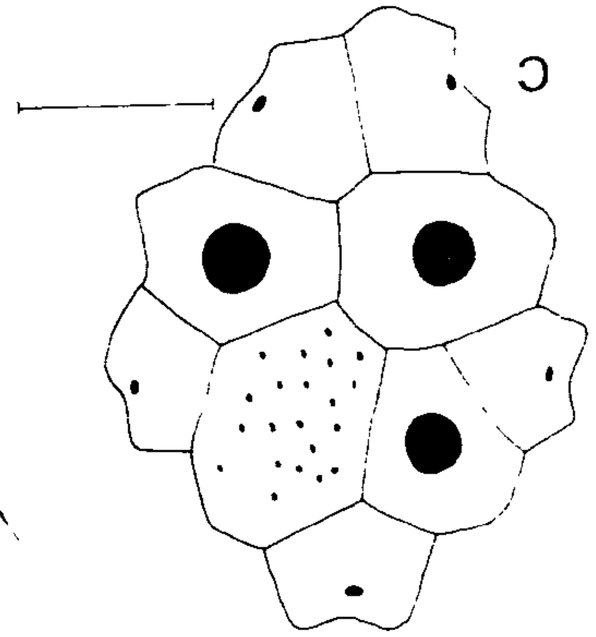

a
b
c

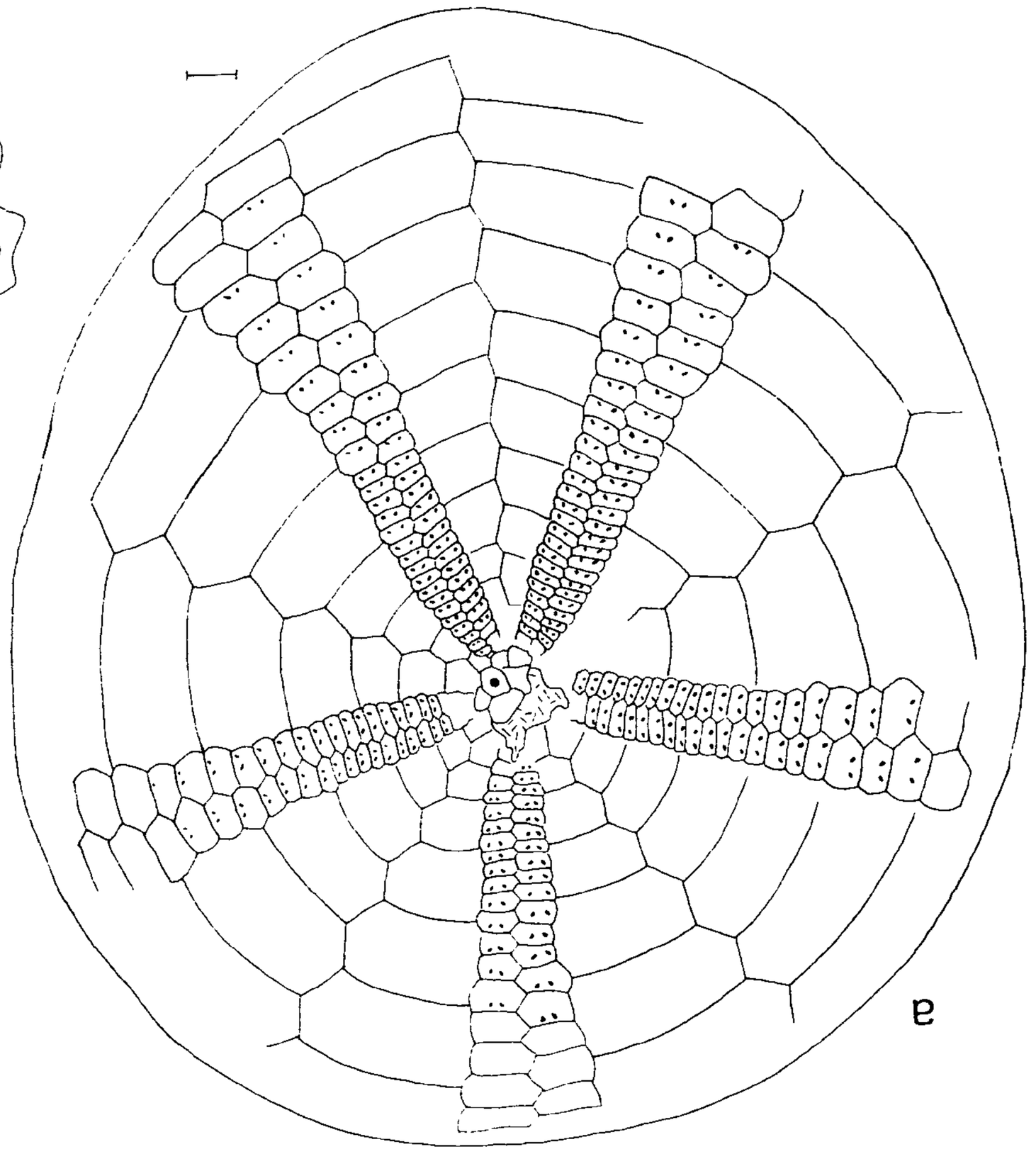
Figure 3.38. Camera lucida drawings of *Isaster aquitanicus* (Grateloup). a & b, specimen in box with PI 1945/1; a, apical view; b, oral view. c, BMNH EE6069, apical disc plating. a & b, scale bars = 2 mm. c, scale bar = 1 mm.



b

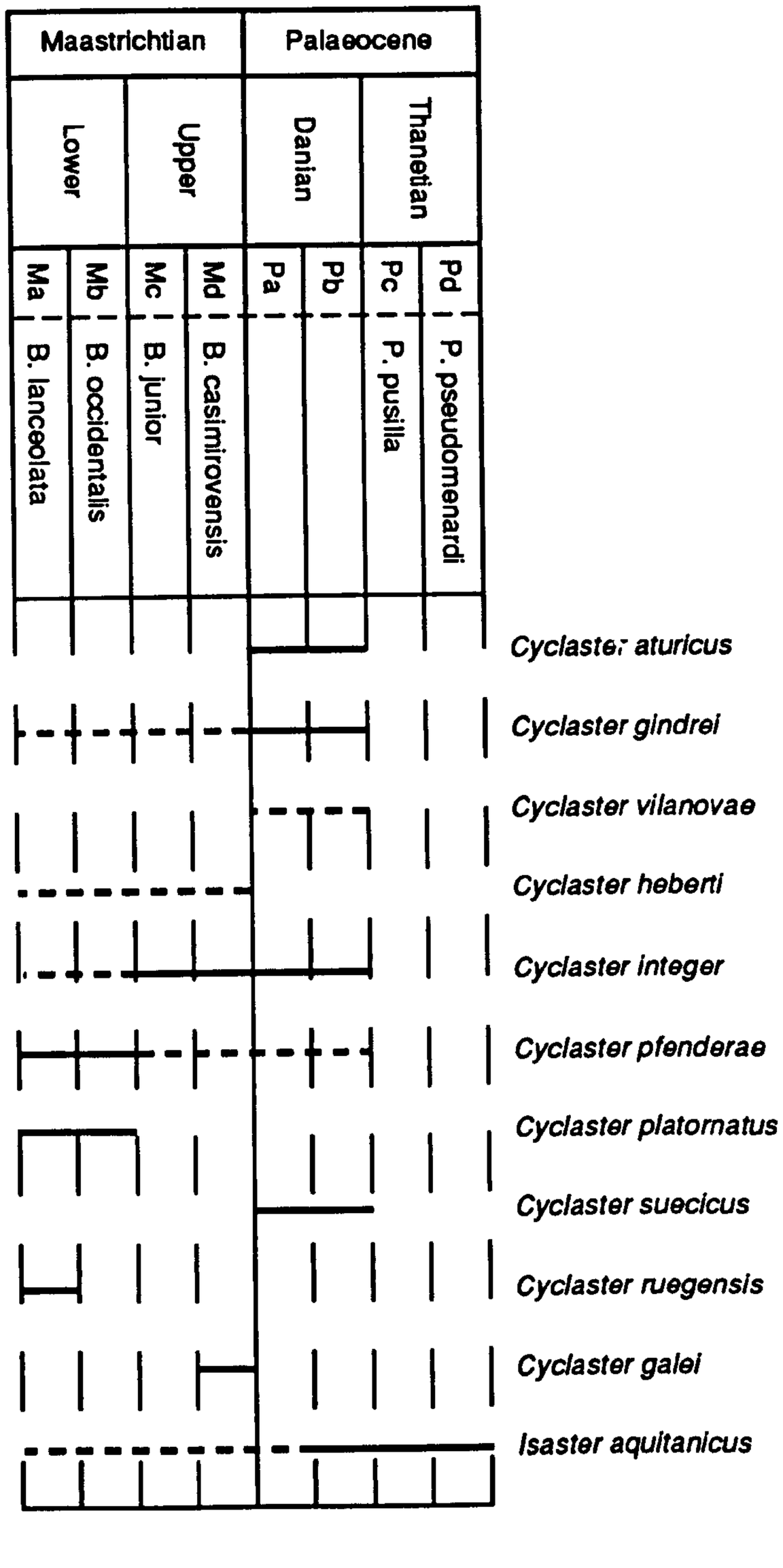


c



a

Figure 3.39. Range chart for Maastrichtian and Palaeocene three-gonopored micrasterid species. See Figure 3.2 for explanation of symbols.


Maastrichtian
Palaeocene
Lower
Upper
Danian
Thanetian
Ma
Mb
Mc
Md
Pa
Pb
Pc
Pd
B. lanceolata
B. occidentalis
B. junior
B. casimirovensis
P. pusilla
P. pseudomenardi
Cyclaster aturicus
Cyclaster gindrei
Cyclaster vilanovae
Cyclaster heberti
Cyclaster integer
Cyclaster pfenderae
Cyclaster platornatus
Cyclaster suecicus
Cyclaster ruegensis
Cyclaster galei
Isaster aquitanicus

Family BRISSIDAE Gray, 1855

Diagnosis. Paired ambulacra petaloid. Apical system ethmophract to ethmolytic with two to four gonopores. Plastron with symmetrical sternal plates. Peripetalous and subanal fascioles. Large tubercles generally contained within peripetalous fasciole.

Remarks. Brissids differ from micrasterids primarily in the structure of the plastron and in the style of tuberculation (see section on *Cyclaster*). In addition, although some genera included in the brissids have ethmophract apical systems, no taxa referred to the micrasterids have ethmolytic apical discs.

Genus EUPATAGUS Agassiz *in* Agassiz & Desor, 1847

[Type species *Eupatagus valenciennesi* Agassiz *in* Agassiz & Desor, 1847, by SD of Pomel, 1883]

Synonym. *Protobrissus* Lambert, 1907a (type species *Protobrissus mortenseni* Lambert, 1907a). *non Protobrissus* Moskvin & Poslavskaya, 1959; Poslavskaya & Moskvin, 1960; Gongadze, 1979 (= *Pseudogibbaster* Moskvin, 1983).

Diagnosis. Test ovoid, low. Paired ambulacra form flush petals. Apical system anteriorly positioned; ethmolytic with four gonopores. Primary tubercles on apical surface contained within fasciole.

Eupatagus mortenseni Lambert, 1907a

(Figure 3.40)

1907a *Protobrissus mortenseni* Lambert, p. 719, pl. 25, figs 17-20.

1975 *Eupatagus (Protobrissus) mortenseni* (Lambert); Plaziat *et al.*, p. 638, pl. 1, fig. 9, text fig. 10.

Occurrence. Lower to Mid Thanetian of the French and Spanish Pyrenees (Lambert 1907a; Plaziat *et al.* 1975) (MNHN).

Diagnosis. Outline almost rectangular with very slight frontal depression. Paired ambulacra form narrow petals, subequal in length. Petals reach 60% distance to ambitus

in plan view. Large periproct. Large tubercles on apical surface sparse and poorly developed.

Remarks. The type specimen of this species (and the genus *Protobrissus*) was originally believed to have an ethmophract apical system. On these grounds, *Protobrissus* was treated as a synonym of *Diplodetus* by Fischer (1966). However, examination of new material from the Pyrenees and a re-examination of the holotype (Plaziat *et al.* 1975) show it to be ethmolytic. My own inspection of the holotype confirms this. *Eupatagus* is characterized by having a low test, petaloid ambulacra and an ethmolytic apical system, coupled with subanal and peripetalous fascioles. Since these features are all present in the type of *Protobrissus*, the two genera are treated as synonyms.

Eupatagus skourensis **(Lambert, 1937)**

1937 *Brissoides skourensis* Lambert, p. 87, pl. 3, figs 12-14.

1957 *Brissoides skourensis* Lambert; Gauthier, p. 110, 122.

1970 *Eupatagus* sp. ex. gr. *skourensis* Lambert; Roman, p. 73.

Occurrence. Upper Thanetian of Morocco (Lambert 1937; Gauthier 1957). Upper Palaeocene of Angola (Roman 1970).

Diagnosis. Ovate with shallow frontal notch. Paired ambulacra form long, broad, straight, somewhat depressed petals reaching 90% distance to ambitus in plan view. Large periproct. Enlarged tubercles on apical surface poorly developed and sparse.

Remarks. Distinguished from *E. mortenseni* by its longer, broader petals reaching almost to the ambitus and by its smaller periproct.

Figure 3.40. Camera lucida drawings of *Eupatagus mortenseni* (Lambert), MNHN no specimen number (HOLOTYPE), Danian of the French Pyrenees; a, apical view; b; oral view; c, apical disc plating. a & b, scale bars = 2 mm. c, scale bar = 1 mm.

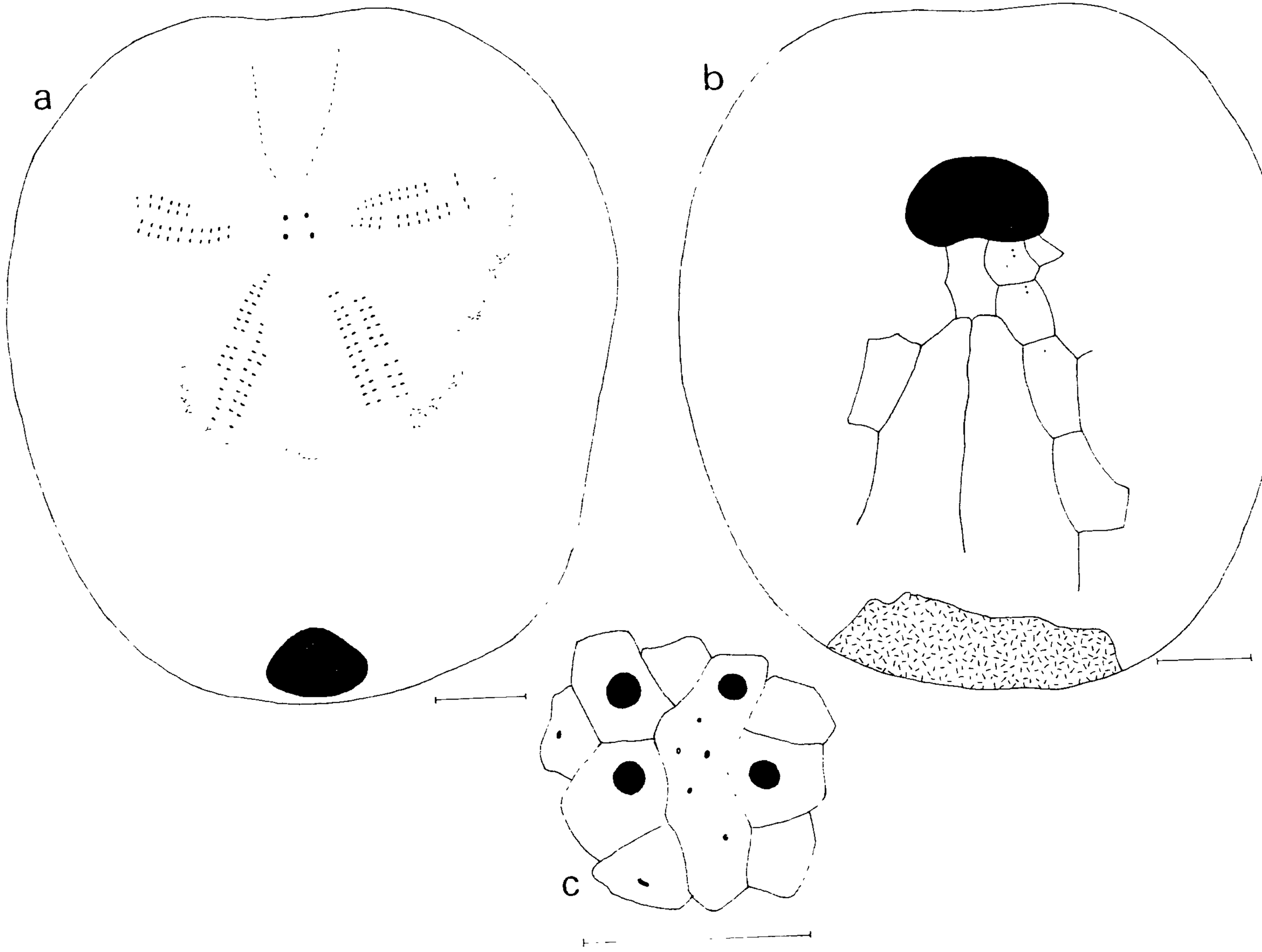
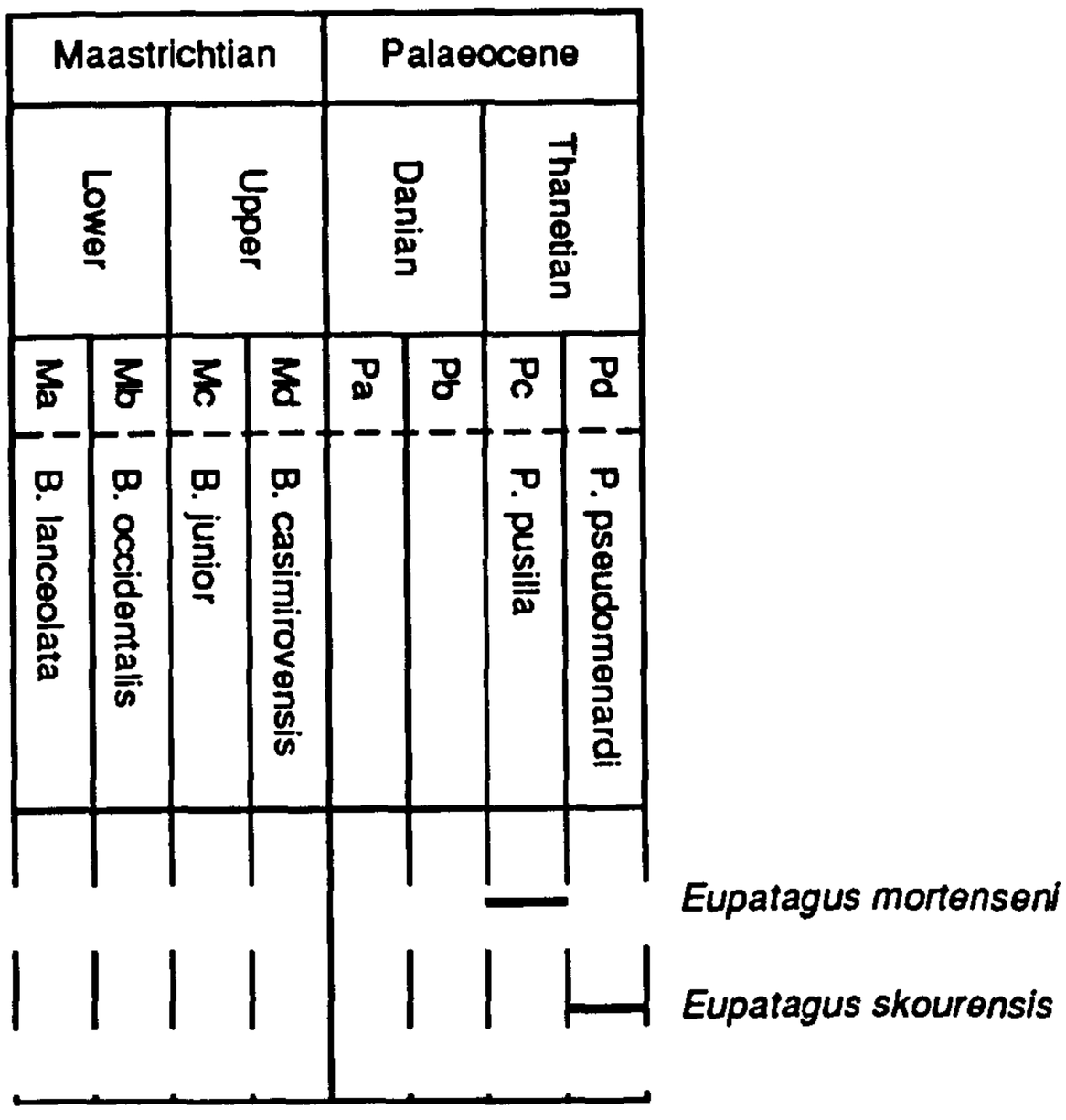

a
b
c

Figure 3.41. Range chart for Maastrichtian and Palaeocene brissid species. See Figure 3.2 for explanation of symbols.


Maastrichtian
Palaeocene
Lower
Upper
Danian
Thanetian
Ma
Mb
Mc
Md
Pa
Pb
Pc
Pd
B. lanceolata
B. occidentalis
B. junior
B. casimirovensis
P. pusilla
P. pseudomenardi
Eupatagus mortenseni
Eupatagus skourensis

Suborder HEMIASTERINA Fischer, 1966

Family HEMIASTERIDAE Clark, 1917

Emended diagnosis. Petaloid paired ambulacra. Ethmophract to transitional apical system. Peripetalous fasciole only.

Remarks. The hemiasterids have generally been characterized as having a peripetalous fasciole and no other fascioles. Consequently, the family has included taxa with both ethmophract and ethmolytic apical systems. The presence or absence of fascioles and the structure of the apical system are both highly variable characters and any classification based on these characters will produce paraphyletic groupings. However in an attempt to allow easy identification of Maastrichtian and Palaeocene spatangoids with peripetalous fascioles using dichotomous keys, taxa with ethmolytic apical discs are transferred to the schizasterids and the familial diagnosis of the hemiasterids has been emended to reflect this.

KEY TO MAASTRICHTIAN & PALAEOCENE GENERA

1 Bulging plates with deeply sunken sutures.....*Leiostomaster*

Non-bulging plates with flush sutures.....2

2 Frontal groove not indenting ambitus.....*Hemiaster*

Frontal groove indenting ambitus.....3

3 Anterior petals 3 to 4 times longer than posterior;

trapezoidal peripetalous fasciole.....*Leymeriaster*

Subequal petals; oval peripetalous fasciole.....4

4 Very broad, bowed, shallow petals.....*Mecaster*

Distinctly sunken, narrow, straight petals.....*Gregoryaster*

Genus HEMIASTER Agassiz *in* Agassiz & Desor, 1847

[Type species *Spatangus bufo* Brogniart *in* Cuvier, 1822, by SD of Savin, 1903]

Synonyms. *Bolbaster* Pomel, 1883 (type species *Spatangus prunella* Lamarck, 1816); *Integraster* Lambert & Thiéry, 1924 (type species *Hemiaster ligeriensis* d'Orbigny, 1854).

Diagnosis. Ovate to circular test. Wedge-shaped to globular in profile. Unpaired ambulacrum straight-sided. Paired ambulacra petaloid - narrow and parallel sided to broad and bowed. Apical system ethmophract; positioned 45-65% of test length from anterior margin. Peristome 20-25% of test length from anterior margin. Peripetalous fasciole hardly indents between petals.

Remarks. *Hemiaster* has frequently been split into a number of subgenera. Many of these have ethmolytic apical systems and are here transferred to the schizasterids. Of the ethmophract species, those with ovate tests and narrow, parallel sided petals have previously been assigned to *Hemiaster (Bolbaster)*. However, the characters used to differentiate *Hemiaster (Hemiaster)* and *Hemiaster (Bolbaster)*, cited by Neraudeau (1994), are not substantive and are commonly size related. The two subgenera are thus synonymized.

Other ethmophract spatangoids with a peripetalous fasciole, such as *Cyclaster* and *Diplodetus*, also possess a subanal fasciole. All other spatangoids with peripetalous fascioles have ethmolytic apical systems.

KEY TO MAASTRICHTIAN & PALAEOCENE GENERA

1 Broad sunken, unpaired ambulacrum; coarse aboral tuberculation.....2

Narrow unpaired ambulacrum; fine tuberculation.....3

2 Apical system 50-55% of test length from anterior.....*H. wetherbyi*

Apical system 60-65% of test length from anterior.....*H. parastatus*

3 Narrow, parallel sided paired ambulacra.....4

Broad, bowed paired ambulacra.....6

4 Anterior petals two times longer than posterior.....*H. prunella*

Anterior petals 1.2-1.3 times longer than posterior.....5

5 Circular test; peripetalous fasciole almost marginal towards anterior.....*H. nucula*

Elongate test; peripetalous fasciole restricted to apical surface.....*H. koninckanus*

6 Apical system with L-shaped posterior genital plates separating posterior ocular plates.....*H. hattaensis*

Standard ethmophract apical system 7

7 Anterior petals sub-parallel to frontal groove and three to four times longer than posterior petals.....*H. madagascariensis*

Anterior petals divergent and twice as long as posterior.....8

8 Parallel sided frontal groove; elongate peripetalous fasciole....*H. stella*

Bowed frontal groove; circular fasciole.....*H. paronai*

Hemiaster prunella **(Lamarck, 1816)**

(Plate 10, figures 1-4; Figure 3.42)

1909 *Hemiaster prunella* (Lamarck); Lambert, p. 24.

1911 *Hemiaster prunella* (Lamarck); Lambert, p. 53.

1926 *Hemiaster* sp. Brünnich Nielsen, p. 13.

1927 *Hemiaster* sp. Ravn, p. 345.

1927 *Hemiaster prunella* (Lamarck); Lambert, p. 50.

1935b *Hemiaster (Bolbaster) prunella* (Lamarck); Smiser, p. 86, pl. 7, fig. 9.

1959 *Hemiaster inkermanensis* de Loriol; Moskvin & Poslavskaya, p. 292, pl. 26, fig. 8.

1973 *Hemiaster (Bolbaster) batalleri* Lambert; Radig, p. 61, pl. 10, figs 4-7.

1987 *Hemiaster (Bolbaster) prunella* (Lamarck); van der Ham *et al.*, p. 33, pl. 20, fig. 3.

1992 *Hemiaster (Bolbaster) batalleri* Lambert; Gallemí, p. 344.

1992 *Hemiaster (Bolbaster)* gr. *prunella* (Lamarck); Gallemí, p. 347.

1992 *Hemiaster (Bolbaster)* sp. gr. *prunella* (Lamarck); Gallemí, p. 350.

1996 *Hemiaster (Bolbaster) prunella*; Wilmsen *et al.*, fig. 7.

Occurrence. Upper Maastrichtian Calcaire à *Baculites* of Normandy, France (Lambert 1909). Lower Maastrichtian of Tremp (Lambert 1927; Gallemí 1992) (PUAB) and Cabo

de Lata Formation of Santander, Spain (Wilmsen *et al.* 1996) (BMNH). Lower Maastrichtian Olazaguthia Formation of Navarra, Spain (Radig 1973) (BMNH). Lower Maastrichtian Lanaye Chalk and Upper Maastrichtian Kunrade and Meerssen Chalks of the Maastricht area (Lambert 1911; Smiser 1935b; van der Ham *et al.* 1987) (NMM). Mid to Upper Danian Saltholm Limestone of Denmark (Brünnich Nielsen 1926; Ravn 1927). Mid Danian Faxe Limestone of Denmark (DGFMM) and Danian Kangilia Formation of East Greenland (DGFMM). Lower to Mid Danian of the northern Caucasus (Moskvin & Poslavskaya 1959).

Diagnosis. Ovate outline and globular profile with highest point central. Truncate posterior. Unpaired ambulacrum narrow. Paired ambulacra form narrow, parallel sided petals. Anterior petals about twice as long as posterior. Anterior petals diverge at 120 degrees; posterior at 75 degrees. Anterior column of pores narrower than posterior. Peripetalous fasciole ovate; longer than wide.

Remarks. Most similar to *H. koninckanus*. *H. prunella* is distinguished by its shorter, broader horizontal outline, its proportionally shorter posterior petals and its vertically truncate posterior surface. *H. prunella*, *H. koninckanus* and *H. nucula* differ from other Maastrichtian and Palaeocene species of *Hemiaster* in having narrow, parallel sided petals.

Hemiaster koninckanus d'Orbigny, 1854

1854 *Hemiaster koninckanus* d'Orbigny, p. 250, pl. 885.
1861 *Hemiaster angustipneustes* Desor; Cotteau & Triger, p. 318, 434, pl. 53, figs 5-11.
1934 *Hemiaster angustipneustes* Desor; Tzankov, p. 215, pl. 2, fig. 5.
1984 *Hemiaster koninckanus* d'Orbigny; van der Ham, p. 169, fig. 1.
1987 *Hemiaster koninckanus* d'Orbigny; van der Ham *et al.*, p. 33, pl. 20, fig. 2.

Occurrence. Lower Maastrichtian Lanaye Chalk and Upper Maastrichtian Kunrade and Nekum Chalks of the Maastricht area (van der Ham 1984; van der Ham *et al.* 1987) (NMM). Lower Maastrichtian Upper Chalk of Bulgaria (Tzankov 1934). Lower Maastrichtian Olazaguthia Formation of Navarra, Spain (BMNH).

Diagnosis. Elongate, globular test (width 85-90% of length) with highest point towards

posterior. Test keeled between apical system and posterior. Posterior surface concave with small overhang above periproct. Narrow parallel-sided paired ambulacra, shallowly sunken. Anterior pair 1.2 to 1.3 times longer than posterior.

Remarks. Differs from *H. prunella* most noticeably in have proportionally longer posterior petals and a somewhat more elongate test. *H. nucula* has a similar petal arrangement to *H. koninckanus* but differs in having a low profile with the highest point central and a circular horizontal outline.

Hemiaster nucula Desor *in* Agassiz & Desor, 1847

1847	*Hemiaster nucula* Desor *in* Agassiz & Desor, p. 122.
1854	*Hemiaster nucula* Desor; d'Orbigny, p. 259, pl. 891.
1909	*Hemiaster neustriae* Desor; Lambert, p. 25, pl. 1, figs 20-23.
1909	*Hemiaster nucula* Desor; Lambert, p. 26, pl. 1, figs 24-26.

Occurrence. Upper Maastrichtian Calcaire à *Baculites* of Normandy, France (Lambert 1909).

Diagnosis. Circular horizontal outline and depressed profile with highest point central. Narrow ambulacra. Paired ambulacra form parallel sided petals. Anterior pair 1.2-1.3 times longer than posterior. Peripetalous fasciole almost marginal towards anterior.

Remarks. Most similar to *H. prunella* and *H. koninckanus*. Differs from both these species in having a more depressed profile and a peripetalous fasciole that is almost marginal towards the anterior. Differs additionally from *H. prunella* in having proportionally longer posterior petals and from *H. koninckanus* in having its highest point subcentral rather than posterior.

Hemiaster stella (Morton, 1830)

1830	*Spatangus stella* Morton, p. 245, pl. 3, fig. 11.
1834	*Spatangus stella* Morton, p. 78, pl. 3, fig. 18.
1877	*Hemiaster nasutulus* Cotteau, p. 65, pl. 6, figs 19-20.
1893	*Hemiaster stella* (Morton); Clark, p. 84, pl. 44, fig. 1

1897 *Hemiaster tamulicus* Kossmat, p. 61, 96, pl. 10, fig. 5.

1899 *Hemiaster(?) aquisgranensis* Schlüter, p. 123, pl. 10, figs 1-2.

1907a *Hemiaster punctatus* var. *garumnica* Lambert, p. 720 [*nomen nudum*].

1907a *Hemiaster punctatus* var. *arizensis* Lambert, p. 721 [*nomen nudum*].

1907a *Hemiaster punctatus* var. *spissa* Lambert, p. 721 [*nomen nudum*].

1908a *Hemiaster (Leucaster) lamberti* Cottreau, p. 173, pl. 5, fig. 3, text fig. 15.

1911 *Hemiaster rutoti* Lambert, p. 52, pl. 3, figs 3, 5.

1915 *Hemiaster stella* (Morton); Clark, p. 93, pl. 48, fig. 2.

1922 *Hemiaster madagascariensis* forma A Cottreau, p. 118, pl. 2, figs 1-3, 6.

1930 *Hemiaster madagascariensis* Cottreau; Besairie, p. 229, pl. 26, fig. 12.

1933a *Hemiaster hawkinsi* Lambert, p. 22, pl. 4, fig. 19.

1936 *Hemiaster heteropneustes* Lambert, p. 28, pl. 4, figs 20-22.

1959 *Hemiaster stella* (Morton); Cooke, p. 67, pl. 28, figs 10-14.

1975 *Hemiaster garumnicus* Lambert; Plaziat *et al.*, p. 643, fig. 10.

1979 *Hemiaster (Bolbaster) hawkinsi* Lambert; Tanaka *et al.*, p. 32, pl. 1, fig. 4, text figs 5-8.

1979 *Hemiaster (Bolbaster)* cf. *madagascariensis* Cottreau; Tanaka *et al.*, p. 33, pl. 1, fig. 5.

1985 *Hemiaster aquisgranensis* Schlüter; van der Ham, p. 147, figs 1-4.

1987 *Hemiaster aquisgranensis* Schlüter; van der Ham *et al.*, p. 33, pl. 20, fig. 1.

1992 *Hemiaster aquisgranensis* Schlüter; van der Ham & van Birgelen, p. 150, pl. 4, fig. 6.

1996 *Hemiaster (Bolbaster) madagascariensis* Cottreau; Greyling, p. 32, figs 8-10.

Occurrence. Upper Thanetian Vincentown Sand of New Jersey, USA (Morton 1830, 1834; Clark 1893, 1915; Cooke 1959). Lower Maastrichtian Vijlen and Lanaye Chalks and Upper Maastrichtian Kunrade Chalk of the Maastricht area (Schlüter 1899; Lambert 1911; van der Ham 1985; van der Ham *et al.* 1987; van der Ham & van Birgelen 1992). Upper Danian of Denmark and Palaeocene Agatdal Formation of East Greenland (DGFMM). Lower to Mid Thanetian of the French Pyrenees (Cotteau 1877; Lambert 1907a; Plaziat *et al.* 1975). Lower Maastrichtian St. Lucia Formation of Zululand (Greyling 1996). Maastrichtian and Danian of northwestern Madagascar (Cottreau 1908a; Lambert 1933a; Collignon 1968; Besairie 1971; Tanaka *et al.* 1979). Maastrichtian of eastern (Besairie 1930) and southwestern (Lambert 1936; Besairie 1971) Madagascar. Maastrichtian and Danian of southwestern, northwestern and eastern Madagascar (Cottreau 1922; Besairie 1971). Upper Maastrichtian *Trigonoarca* beds, Ariyalur Group of southern India (Kossmat 1897).

Diagnosis. Ovate test up to 80 mm long. Truncate posterior. Unpaired ambulacrum long and narrow. Paired ambulacra form broad, sunken, bowed petals. Anterior petals

flexuous distally and about twice as long as posterior. Anterior pair diverge at 90 degrees; posterior at 80 degrees. Apical system at mid-length. Mouth labiate with thickened rim. Oval peripetalous fasciole.

Remarks. Specimens referred to *H. aquisgranensis* and *H. rutoti* are far larger than those previously assigned to *H. stella*. However, there are no other morphological characters to separate the species and they are therefore synonymized.

H. stella differs from *H. paronai* and *H. madagascariensis* in having the apical system more anteriorly positioned. In addition, *H. stella* differs from *H. madagascariensis* in its less strongly flexed anterior petals and proportionally longer posterior petals and from *H. paronai* in its more flexuous anterior petals and elongate rather than circular peripetalous fasciole.

Hemiaster paronai Checchia-Rispoli, 1921

(Figure 3.43)

?1913 *Cyclaster berberus* de Stefani, p. 265, pl. 23, figs 7-8.
?1913 *Cyclaster beduinus* de Stefani, p. 266, pl. 23, fig. 9.
1914 *Hemiaster* sp. indet. Checchia-Rispoli, p. 307, pl. 1, fig. 9.
1921 *Hemiaster paronai* Checchia-Rispoli, p. 27, pl. 8, fig. 24, pl. 9, figs 14-18.
1933 *Hemiaster paronai* Checchia-Rispoli, p. 8, pl. 2, figs 1-8.
1967 *Hemiaster punctatus* Devriès, p. 194, pl. 6, figs 34-41.
1967 *Hemiaster regulusanus* Devriès, p. 194, pl. 6, figs 42-44.
1995 *Hemiaster paronai* Checchia-Rispoli; Smith, p. 233, pl. 33, figs 1-4, text fig. 81.

Occurrence. Mid to Upper Maastrichtian Lower Tar Member (Al Gharbiyah Formation) of Tripolitania, Libya (de Stefani 1913; Checchia-Rispoli 1914, 1921, 1933). Early Upper Maastrichtian Simsima Formation of UAE/Oman (Smith 1995). Upper Maastrichtian Besni Formation of Central Turkey (Devriès 1967).

Diagnosis. Approximately circular horizontal outline. Inflated test (height about 75% of test length). Posterior face outwardly truncate so that periproct is visible from above. Unpaired ambulacrum in bowed groove with adjoining interambulacra forming keels. Paired ambulacra form broad, bowed petals. Anterior petals diverge at 90 degrees and

are twice as long as posterior which diverge at 120 degrees. Short labral plate. Apical disc at 60% of test length from anterior. Circular peripetalous fasciole.

Remarks. Distinguished from *H. stella* by its broader petals, more posterior apical system and circular peripetalous fasciole. Differs from *H. madagascariensis* in having proportionally longer posterior petals and more divergent, less flexuous anterior petals.

Hemiaster hattaensis Ali, 1989
(Plate 10, figures 5-7)

1989 *Hemiaster hattaensis* Ali, p. 409, fig. 6(5-8).

1995 *Hemiaster hattaensis* Ali; Smith, p. 232, pl. 32, figs 5-8, text fig. 81.

Occurrence. Early Upper Maastrichtian Simsima Formation of UAE/Oman (Ali 1989; Smith 1995).

Diagnosis. Elongate oval test. Broad, bowed petals. Distally flexuous anterior petals diverge at 85-90 degrees and are 2.5 to 3 times longer than posterior. Short labral plate. Ethmophract apical system posterior of mid-length. Posterior genital plates L-shaped extending backwards and separating posterior oculars. Broad plastron and short labral plate. Oval peripetalous fasciole.

Remarks. Easily distinguished from other Maastrichtian and Palaeocene species of *Hemiaster* on the basis of its apical disc structure.

Hemiaster madagascariensis Cottreau, 1922

1903 *Hemiaster* sp. Lambert, p. 87, pl. 3, figs 6-8.

1906 *Hemiaster* sp. Lambert *in* Boule & Thevenin, p. 53, pl. 2, fig. 6.

1922 *Hemiaster madagascariensis* forma B Cottreau, p. 118, pl. 2, figs 4-5, 7-8.

Occurrence. Maastrichtian of southwestern Madagascar (Lambert 1903; Lambert *in* Boule & Thevenin 1906). Maastrichtian and Danian of southwestern, northwestern and eastern Madagascar (Cottreau 1922; Besairie 1971).

Diagnosis. Ovate horizontal outline and wedge-shaped profile. Paired ambulacra form

bowed, sunken petals. Strongly flexed anterior petals are 3 to 4 times longer than posterior, diverge at 65 degrees and are subparallel to the frontal groove. Posterior petals diverge at 120 degrees. Apical system 60% of test length from anterior margin.

Remarks. Most similar to *H. stella* and *H. paronai* from which it may be distinguished by its strongly flexed anterior petals which are subparallel to the frontal groove and proportionally shorter posterior petals.

Hemiaster parastatus (Morton, 1833)

1830 *Spatangus cormarinum?* Parkinson; Morton, p. 250, pl. 3, fig. 10.
1833 *Spatangus parastatus* Morton, p. 294.
1834 *Spatangus parastatus* Morton, p. 77, pl. 3, fig. 21.
1858 *Hemiaster? humphreysanus* Meek & Hayden, p. 147.
1893 *Hemiaster parastatus* (Morton); Clark, p. 83, pl. 45, fig. 1.
1893 *Hemiaster humphreysanus* Meek & Hayden; Clark, p. 88, pl. 48, fig. 1.
1915 *Hemiaster parastatus* (Morton); Clark, p. 92, pl. 48, fig. 1.
1915 *Hemiaster humphreysanus* Meek & Hayden; Clark, p. 95, pl. 49, fig. 2.
1953 *Hemiaster humphreysanus* Meek & Hayden; Cooke, p. 30, pl. 12, figs 1-4.
1959 *Hemiaster parastatus* (Morton); Cooke, p. 67, pl. 28, figs 15-20.

Occurrence. Lower Maastrichtian Upper Pierre Shale of Wyoming and Nacotach Sand of Arkansas. Lower to Mid Maastrichtian Ripley Formation of Mississippi. Upper Thanetian Vincentown Sand of New Jersey, USA (Cooke 1959).

Diagnosis. Highest posteriorly. Very broad unpaired ambulacrum fairly deep at apex, shallows towards ambitus. Anterior petals about three times longer than posterior, diverging at 90 degrees. Posterior petals diverge at 90 to 100 degrees. Apical system positioned at 60-65% of test length from anterior margin. Peristome at about 20% of test length from anterior margin. Coarse tuberculation on apical surface.

Remarks. The Maastrichtian specimens previously assigned to *H. humphreysanus* have slightly less divergent petals. Most similar to *H. wetherbyi*, but differs in having a more posteriorly positioned apical system, more divergent posterior petals and more flexuous anterior petals.

Hemiaster wetherbyi de Loriol, 1888

1888 *Hemiaster wetherbyi* de Loriol, p. 391, pl. 17, figs 5-6.

1909 *Hemiaster lacunosus* Slocum, p. 10, pl. 2, figs 1-7.

1915 *Hemiaster bexari* Clark, p. 89, pl. 46, fig. 1.

1916 *Hemiaster delawarensis* Clark, p. 751, pl. 47, figs 11-14.

1941 *Hemiaster benhurensis* Stephenson, p. 67, pl. 7, figs 8-10.

1953 *Hemiaster wetherbyi* de Loriol; Cooke, p. 31, pl. 12, figs 17-18.

1953 *Hemiaster delawarensis* Clark; Cooke, p. 35, pl. 14, figs 6-9.

Occurrence. Lower Maastrichtian Saratoga Chalk and Nacotach Sand of Arkansas and Lower Maastrichtian Mount Laurel Sand of Delaware, USA. Lower to Mid Maastrichtian Ripley Formation of Mississippi and Mid to Upper Maastrichtian Prarie Bluff Chalk of Alabama. Mid to Upper Maastrichtian Corsicana Marl of Texas, USA (Cooke 1953).

Diagnosis. Broad, sunken unpaired ambulacrum. Paired ambulacra form broad, straight petals. Anterior petals twice as long as posterior. Anterior diverge at 100 degrees; posterior at 80 degrees. Apical system at 50-55% test length from anterior margin. Peristome one third test length from anterior margin; non-labiate. Broad peripetalous fasciole. Coarse aboral tuberculation.

Remarks. Most similar to *H. parastatus* from which it differs in having a less anterior apical system, more equal petals and a less labiate peristome.

Hemiaster sp. indet.

1923 *Hemiaster* sp. Spengler, p. 7.

Occurrence. Lower Maastrichtian of Assam, India (GSI).

Remarks. Ethmophract apical system and peripetalous fasciole allow generic identification. Broad, bowed petals make this specimen most similar to *H. stella, H. madagascariensis, H. hattaensis* and *H. paronai.* Poor preservation prevents specific identification.

Hemiaster sp. Indet.

1935 *Micraster* sp. Kongiel, p. 39, pl. 5, figs 2-3.
1936 *Hemiaster vistulensis* Kongiel, p. 5.

Occurrence. Lower to Mid Danian Siwak of southeastern Poland (Kongiel 1935, 1936).

Remarks. Poorly preserved, crushed specimen is certainly a *Hemiaster* and may be a representative of the *H. stella* group.

Hemiaster sp. Indet.

1962 *Hemiaster uwajimensis* Morishita, p. 114, pl. 1, figs 1-7.
1968 *Hemiaster uwajimensis* Morishita; Nisiyama, p. 196, pl. 18, figs 2, 5, 9.

Occurrence. Maastrichtian Miyakura (Furushiroyama) formation of Japan.

Remarks. Too poorly preserved to allow specific identification.

Juvenile *Hemiaster*

1887 *Peroniaster cotteaui* Gauthier *in* Peron, p. 390, pl. 7, figs 1-7.
1920b *Pusillaster dallonii* Lambert, p. 159, pl. 1, fig. 20.
1932 *Pusillaster dallonii* Lambert, p. 78.
1978b *Peroniaster cotteaui* Gauthier; Kutscher, p. 1023, pl. 1.

Occurrence. Lower Maastrichtian Rügener Schreibkreide of the Isle of Rügen (Kutscher 1978b). Maastrichtian of Oran, Algeria (Lambert 1920b, 1932). Also from the Campanian of Reims, France (Gauthier *in* Peron 1887).

Remarks. Very small individuals starting to develop gonopores. Specific identification not possible.

Genus LEIOSTOMASTER Lambert, 1920b

[Type species *Leiostomaster gentili* Lambert, 1920b, by OD]

Diagnosis. Test has bulging plates and no distinct frontal groove. Paired ambulacra form deeply sunken, short petals. Apical system ethmophract with four gonopores. Peristome non-labiate.

Remarks. Both *Leiostomaster* and the Campanian genus *Vomeraster* have depressed sutures and bulging plates. *Vomeraster* is distinguished by its distinctly labiate mouth and exceptionally coarse tuberculation covering the whole of the test.

Leiostomaster gentili Lambert, 1920b

(Plate 10, figures 8-11; Figure 3.44)

1920b	*Leiostomaster gentili* Lambert, p. 163, pl. 1, figs 15-19.
1932	*Leiostomaster gentili* Lambert, p. 112.

Occurrence. Maastrichtian of Oran, Algeria (Lambert 1920b, 1932) (MNHN).

Diagnosis. Almost circular in horizontal outline with deeply sunken paired petals. Apical system anterior of mid-length.

Leiostomaster bigoneti (Cotteau, 1888)

1888	*Hemiaster bigoneti* Cotteau, p. 116, pl. 14, figs 4-8.
1920b	*Leiostomaster bigoneti* (Cotteau); Lambert, p. 163.
1932	*Leiostomaster bigoneti* (Cotteau); Lambert, p. 112.

Occurrence. Maastrichtian of Constantine, Algeria (Cotteau 1888; Lambert 1932).

Diagnosis. Elongate horizontal outline with apical system situated at mid-length. Paired ambulacra form very broad, shallow petals.

Remarks. Differs from *L. gentili* in having shorter, broader petals and a more anterior mouth.

Genus LEYMERIASTER Lambert *In* Lambert & Thiéry, 1924

[Type species *Hemiaster leymeriei* Agassiz *in* Agassiz & Desor, 1847, by OD]

(Plate 11, figures 1-3)

Diagnosis. Subhexagonal in horizontal outline. Unpaired ambulacrum sunken at apex, shallows towards ambitus. Paired ambulacra form bowed petals. Anterior petals flexuous and 3 to 5 times longer than posterior. Transitional apical system with madreporite separating posterior genitalplates but not posterior ocular plates; four gonopores. Madreporite separates posterior genital plates but not posterior oculars. Peripetalous fasciole trapezoidal and indented between anterior and posterior petals.

Remarks. Distinguished from other hemiasterids by its unequal petals and trapezoidal peripetalous fasciole.

KEY TO MAASTRICHTIAN SPECIES

1 Test highest anterior of apical system; unpaired ambulacrum bordered by keeled interambulacra.....*L. eluvialis*

Test highest behind apical system; unpaired ambulacrum bordered by smoothly rounded interambulacra.....2

2 Sharply keeled between apex and periproct; peripetalous fasciole convex around anterior of test.....*L. sexangulatus*

No sharp keel between apex and periproct; peripetalous fasciole straight across anterior of test.....*L. maestrichtensis*

Leymeriaster maestrichtensis (Schlüter, 1897)

(Figure 3.45)

1897 *Hemiaster maestrichtensis* Schlüter, p. 32, pl. 2, figs 3-4.

1935b *Brissopneustes maestrichtensis* Lambert; Smiser, p. 85, pl. 8, fig. 2.

1987 *Hemiaster maestrichtensis* Schlüter; van der Ham *et al.*, p. 33, pl. 21, fig. 1.

Occurrence. Upper Maastrichtian Kunrade, Nekum and Meerssen Chalks of the Maastricht area (Schlüter 1897; Smiser 1935b; van der Ham *et al.* 1987) (NMM).

Diagnosis. Test as broad as long. Highest immediately behind apical system. Anterior petals 4 to 5 times longer than posterior. Broad peripetalous fasciole is straight across anterior of test, between ends of anterior petals.

Remarks. Differs from *L. eluvialis* in lacking interambulacral keels bordering the frontal groove. In addition, *L. maestrichtensis* has less flexed petals and a peripetalous fasciole that is straight rather than concave across the anterior of the test. *L. maestrichtensis* differs from *L. sexangulatus* in having a less angular horizontal profile, a less carinate unpaired interambulacrum and a straight rather than convex peripetalous fasciole anteriorly.

Leymeriaster eluvialis van der Ham, 1995

1987 *Hemiaster* sp. van der Ham *et al.*, p. 33, pl. 21, fig. 2.

1995 *Hemiaster (Leymeriaster) eluvialis* van der Ham, p. 156, pls 1-3, text-figs 3-4.

Occurrence. Lower Maastrichtian Lanaye Chalk (van der Ham 1995). Upper Maastrichtian Kunrade Chalk (van der Ham *et al.* 1987) and Nekum Chalk (van der Ham 1995). All from the Maastricht area (NMM).

Diagnosis. Test slightly broader than long and tapers posteriorly. Highest point anterior of apical system. Unpaired ambulacrum bordered by sharply keeled interambulacra. Anterior petals very strongly bowed. Peripetalous fasciole cuts back anteriorly to give concave portion on anterior slope of test.

Remarks. Differs from both *L. maestrichtensis* and *L. sexangulatus* in having distinct keels adjoining the unpaired ambulacrum, more strongly flexed anterior petals and its highest point anterior of the apical system.

Leymeriaster sexangulatus (d'Orbigny, 1854)

1854 *Hemiaster sexangulatus* d'Orbigny, p. 256, pl. 889.

1873 *Hemiaster sexangulatus* d'Orbigny; Stoliczka, p. 18, pl. 3, fig. 6.

1897 *Hemiaster sexangulatus* Stoliczka; Kossmat, p. 106.

1971 *Hemiaster* aff. *sexangulatus* d'Orbigny; Akkus, p. 16.

Occurrence. Upper Maastrichtian *Trigonoarca* Beds, Ariyalur Group of southern India (d'Orbigny 1854; Stoliczka 1973; Kossmat 1897). Lower Maastrichtian Ulupinar Formation of Turkey (Akkus 1971).

Diagnosis. Angular hexagonal horizontal outline with widest point at mid-length. Highest point posterior of apical system. Test strongly keeled between apex and periproct. Peripetalous fasciole convex across anterior margin.

Remarks. Most similar to *L. maestrichtensis* from which it differs in having a distinct keel on the posterior apical surface and a peripetalous fasciole that is convex across the anterior of the test.

Genus MECASTER Pomel, 1883

[Type species *Hemiaster fournelli* Deshayes i*n* Agassiz & Desor, 1847, by OD]

Diagnosis. Low test. Shallow, subequal petals. Transitional apical system with madreporite separating posterior genital plates but not posterior ocular plates; situated at mid-length.

Remarks. Differs from *Hemiaster* in having a transitional rather than ethmophract apical system and in having broad, subequal petals. Differs from *Leymeriaster* in having a low test, oval peripetalous fasciole and subequal petals.

Mecaster fournell Deshayes *In* Agassiz & Desor, 1847

(Plate 11, figures 4-7; Figure 3.46)

1847 *Hemiaster fourneli* Deshayes *in* Agassiz & Desor, p. 17.

1881 *Hemiaster fourneli* Deshayes; Cotteau *et al.*, p. 58, 132, 149, pl. 2, figs 1-8.

1914 *Hemiaster sanfilippoi* Checchia-Rispoli, p. 306, pl. 1, fig. 10.

1933 *Hemiaster fourneli* Checchia-Rispoli, p. 10, pl. 1, fig. 8.

1939 *Hemiaster messai* Airaghi, p. 262, pl. 10, figs 4-5.

?1939 *Periaster subsexangulatus* Airaghi, p. 263, pl. 10, figs 2-3.

1939 *Periaster zinai* Airaghi, p. 265, pl. 10, fig. 6.

1959 *Hemiaster oliveirai* Santos & Cunha, p. 13, pl. 3, figs 1-4.

1981 *Linthia oliveirai* (Santos & Cunha); Brito, p. 574, pl. 3, figs 7-9.

1981 *Hemiaster* cf. *fourneli* Amard *et al.*, p. 46.

Occurrence. Lower Maastrichtian of Constantine (*Cotteau* et al. 1881) and the eastern Tademait Plateau (Amard *et al.* 1981), Algeria. Mid to Upper Maastrichtian Lower Tar Member (Al Gharbiyah Formation) of Tripolitania, Libya (Checchia-Rispoli 1914, 1933; Airaghi 1939). Upper Maastrichtian Gramame Formation of northeastern Brazil (Santos & Cunha 1959; Brito 1981).

Diagnosis. Low profile with highest point immediately behind apical system and periproct visible in apical view. Broad shallow frontal notch. Broad unpaired ambulacrum, widening distally. Petals broad and bowed, shallow. Anterior pair 1.2 to 1.3 times longer than posterior. Anterior petals diverge at 115-120 degrees and reach almost whole distance to ambitus. Posterior diverge at 60-70 degrees and extend 75% distance to ambitus. Long, triangular labral plate.

Mecaster victoris (Lambert 1932)

1932 *Hemiaster victoris* Lambert, p. 127, pl. 4, figs 18-19.

1967 *Hemiaster* sp. Devriès, p. 194, pl. 6, figs 45-47.

1989 *Periaster subsexangulatus* Airaghi; Ali, p. 410, fig. 5(8).

1995 *Mecaster victoris* (Lambert); Smith, p. 236, pl. 34, figs 4-7, text figs 82-84.

Occurrence. Campanian of Algeria (Lambert 1932). Upper Maastrichtian Besni Formation of Central Turkey (Devriès 1967). Early Upper Maastrichtian Simsima Formation of UAE / Oman (Ali 1989; Smith 1995).

Diagnosis. Similar to *M. fourneli* but with narrower, parallel-sided petals. Anterior petals in *M. victoris* are more divergent (140-150 degrees) and the plastronal suture is offset to the right.

Genus GREGORYASTER Lambert, 1907b

[Type species *Pericosmus coranguinum* Gregory, 1892, by OD]

Diagnosis. Large test with truncate posterior. Sunken, long, narrow, subequal petals. Ethmophract apical system with four gonopores. Peripetalous fasciole.

Remarks. Easily distinguished from other hemiasterids by its cordate outline and long, straight, narrow petals.

Gregoryaster jacobi (Besairie & Lambert, 1930)

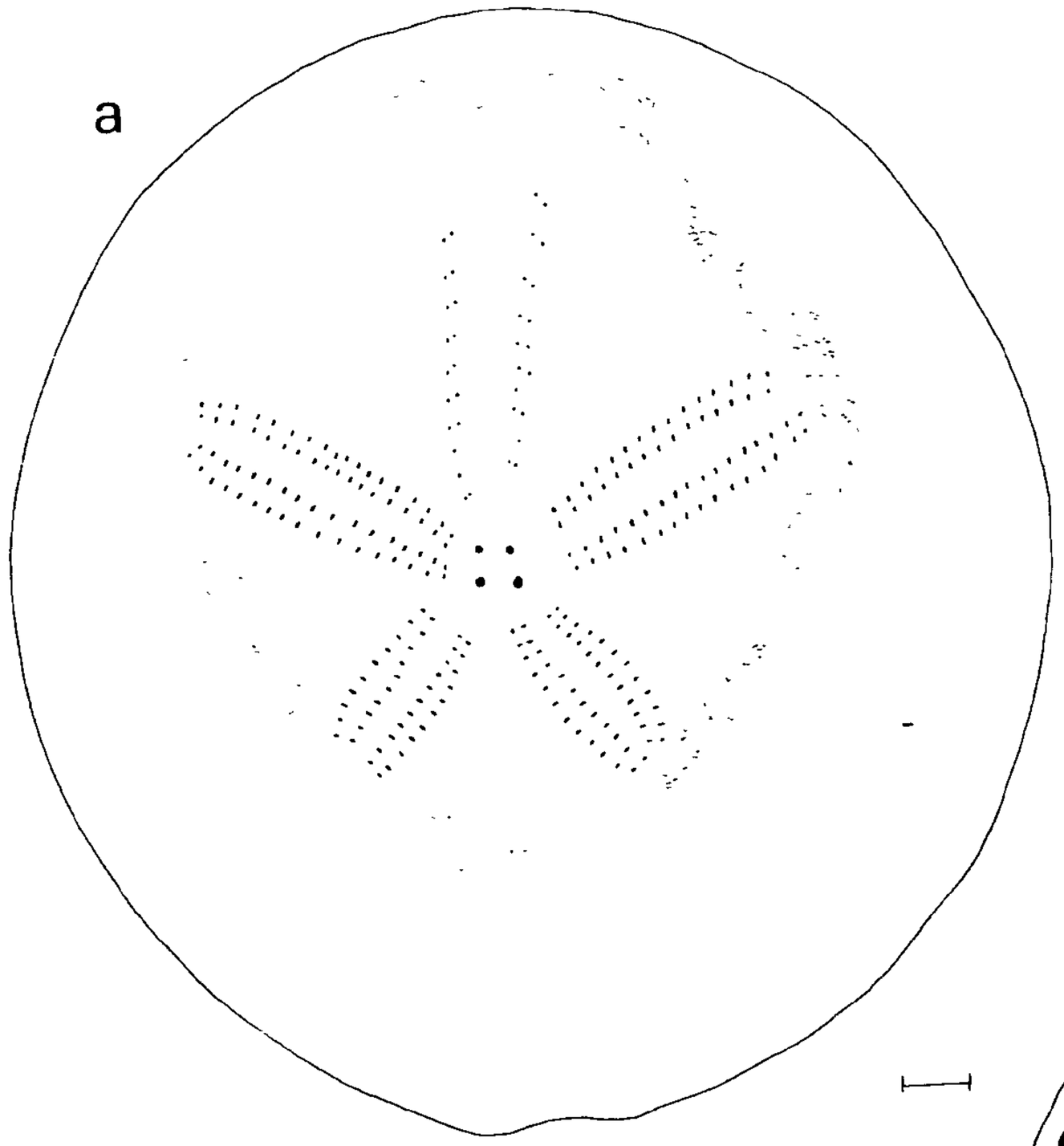
1930	*Hemiaster jacobi* Besairie & Lambert, p. 109, pl. 9, figs 2-3.
1933a	*Hemiaster narindensis* Lambert, p. 24, text fig. 2.
1990	*Hemiaster jacobi* Besairie & Lambert; Cooper & Greyling, p. 412, fig. 2.

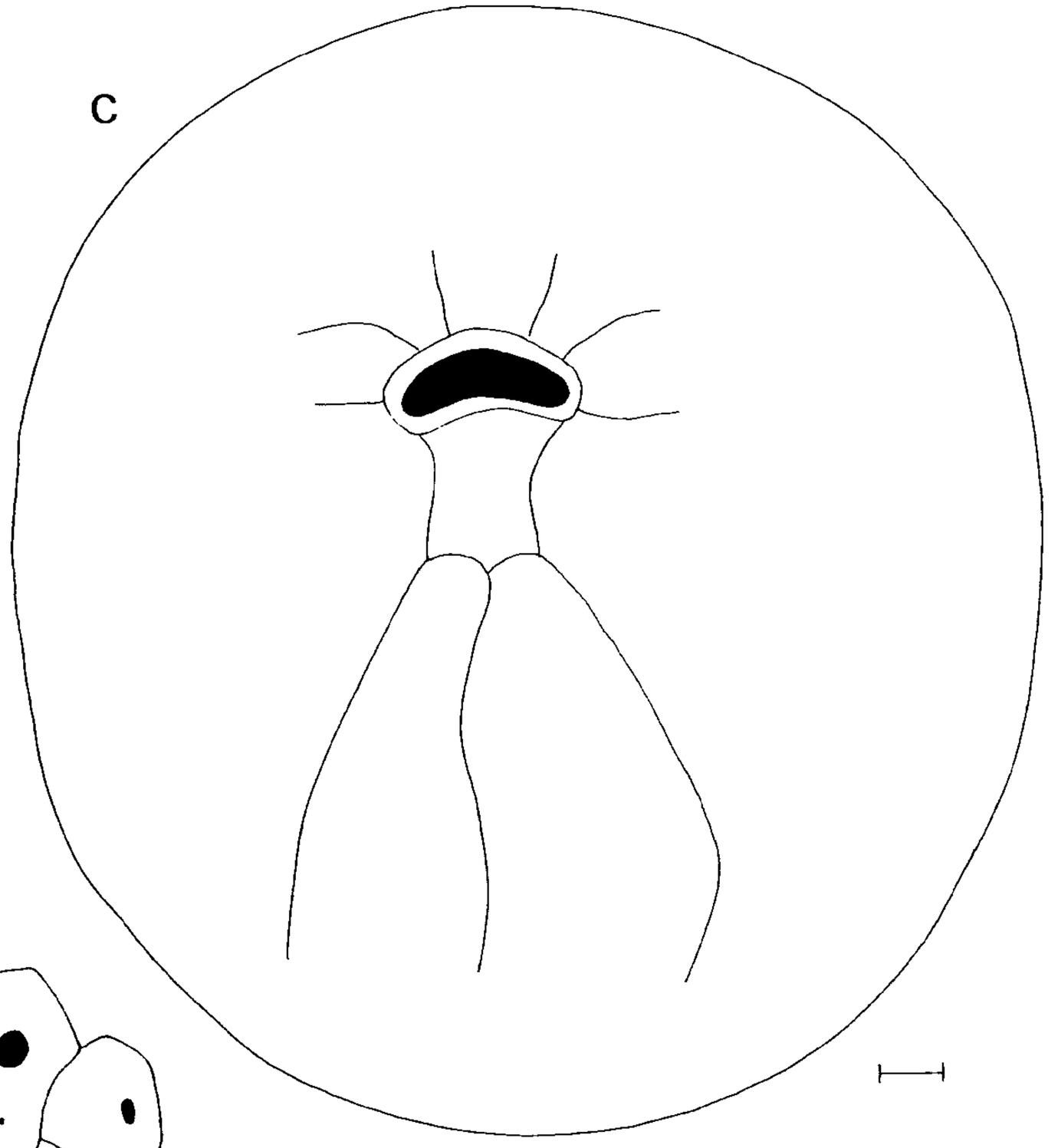
Occurrence. Campanian of northernmost Madagascar (Besairie & Lambert 1930). Lower Maastrichtian of northwestern Madagascar (Besairie 1971). Danian of northwest Madagascar (Lambert 1933a). Lower Maastrichtian St. Lucia Formation of Zululand (Cooper & Greyling 1990).

Diagnosis. Large cordate test; commonly broader than long with distinct frontal notch. Paired ambulacra form straight, narrow petals. Anterior pair diverge at 125-130 degrees and are about 1.5 times longer than posterior petals. Ethmophract apical system situated at mid-length. Narrow, indistinct peripetalous fasciole. Densely packed, sunken tubercles over upper surface of test.

Remarks. *Gregoryaster jacobi* is similar in overall appearance to *Paraster expansus*. However, *G. jacobi* may be differentiated by its ethmophract rather than ethmolytic apical system, its lack of latero-anal fasciole and its less sharply defined frontal groove. In addition, *G. jacobi* has distinctive aboral tuberculation.

Figure 3.42. Camera lucida drawings of *Hemiaster prunella* (Lamarck), Upper Maastrichtian Meerssen Chalk of Maastricht. a & b, NMM MK3147; a, apical view; b, apical disc plating. c, NMM MK817, oral view. Scale bars = 1 mm.


a


c

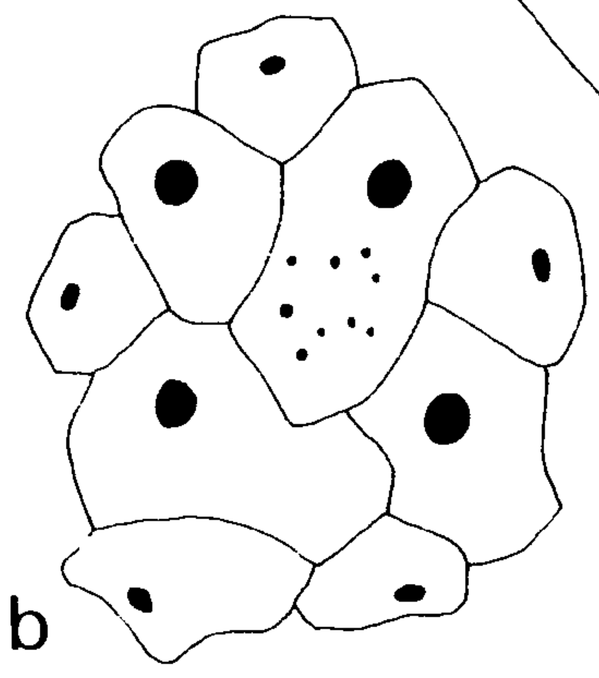
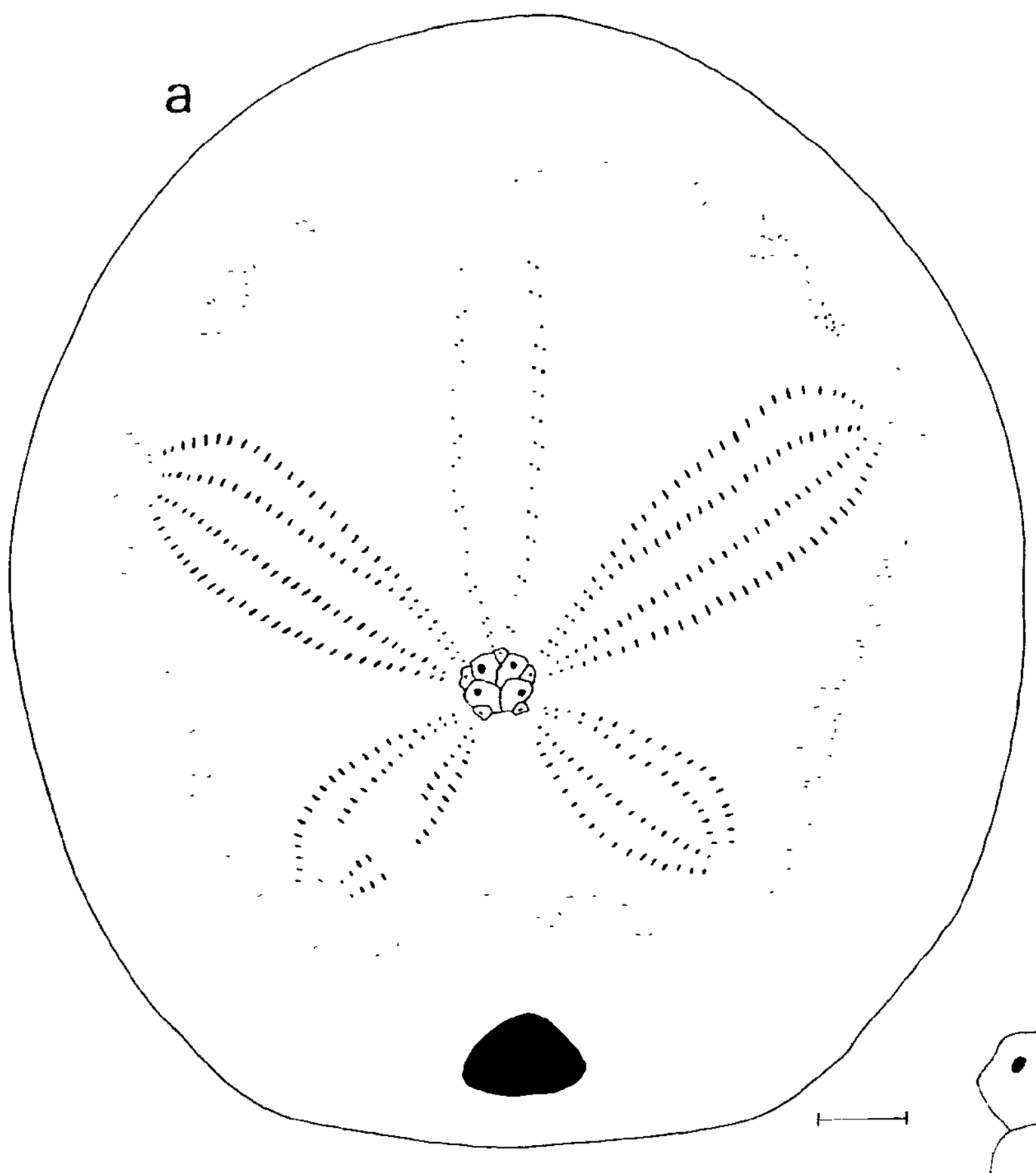
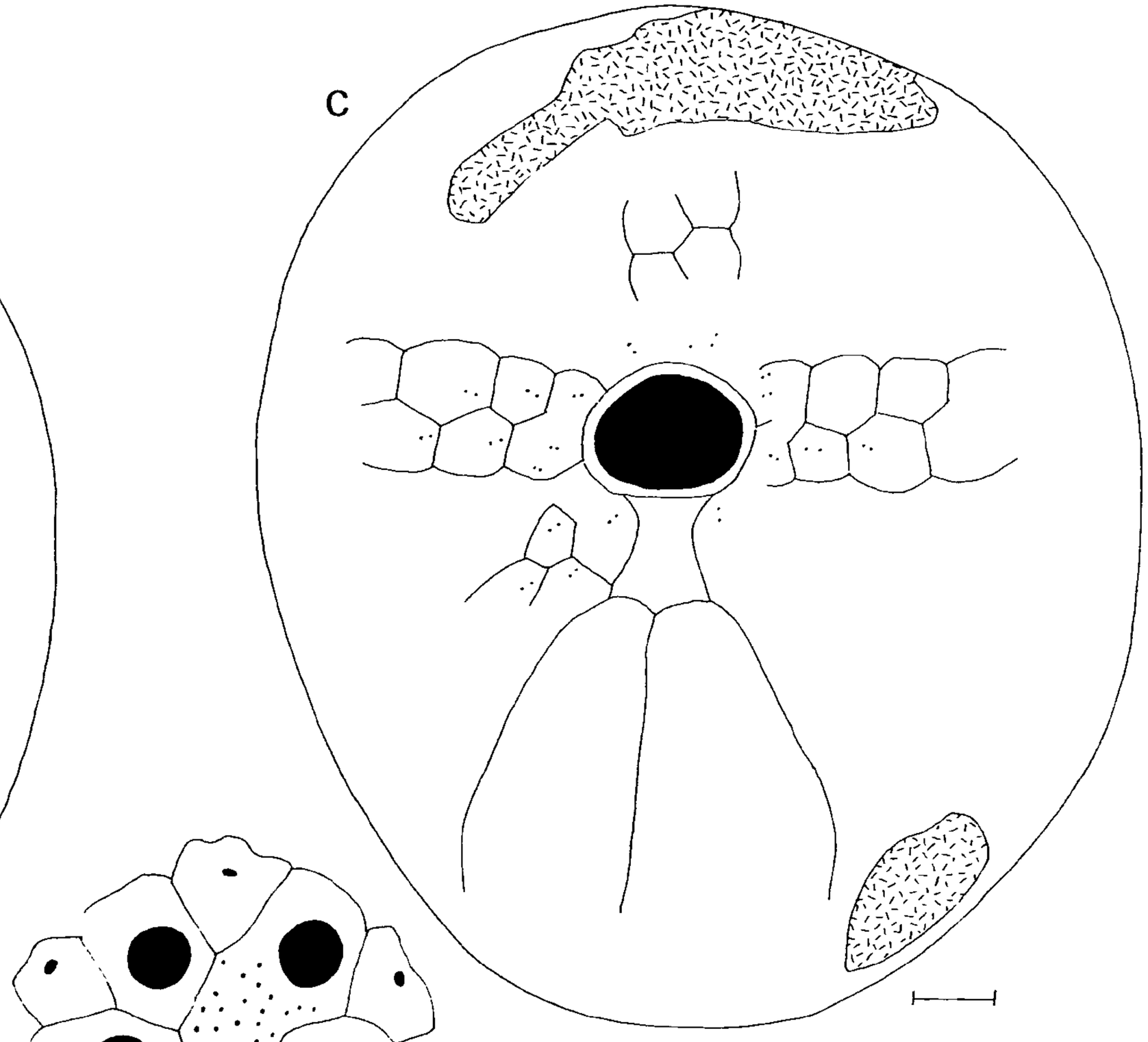

b

Figure 3.43. Camera lucida drawings of *Hemiaster paronai* Checchia-Rispoli, Maastrichtian of Tripolitania, Libya. a & b, URGM i76; a, apical view; b, apical disc plating. c, URGM i75, oral view. a & c, scale bars = 2 mm. b, scale bar = 1 mm.


a


c

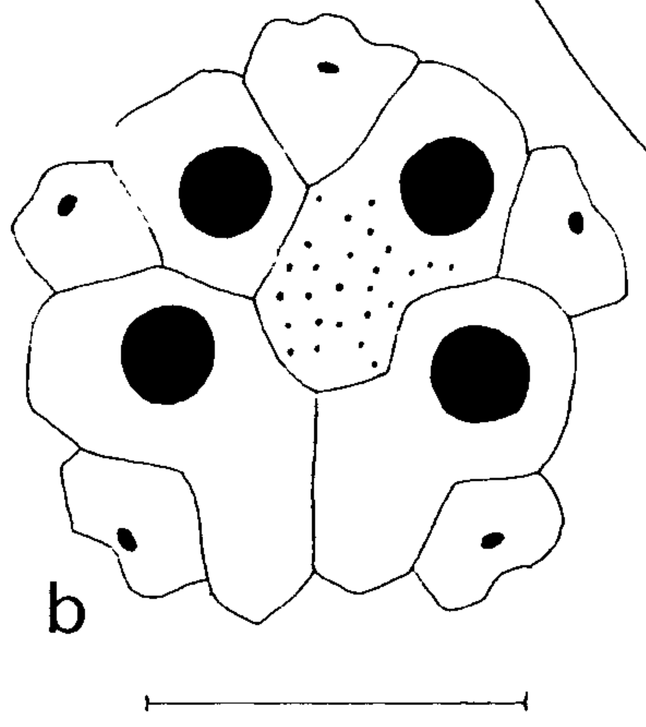
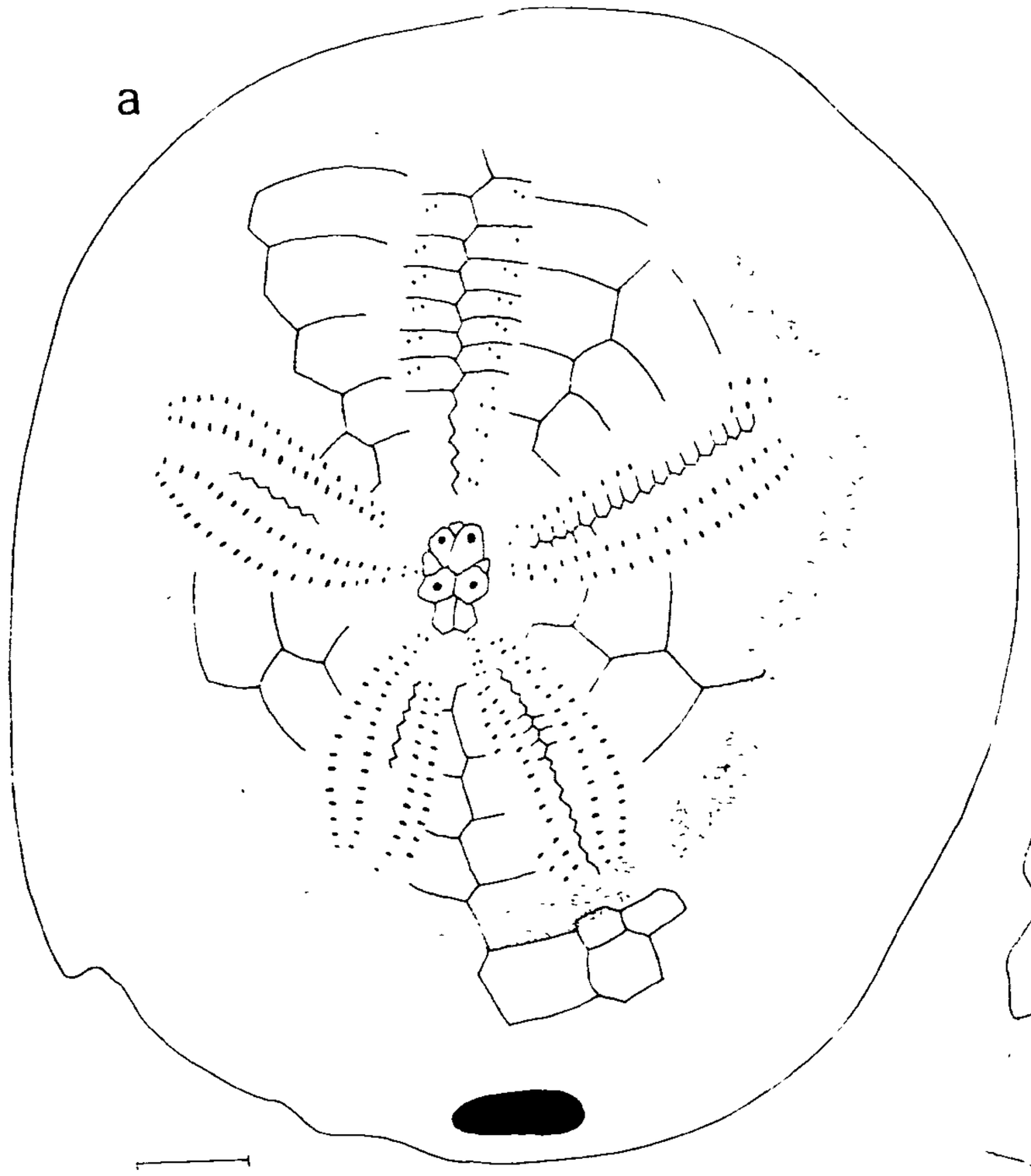
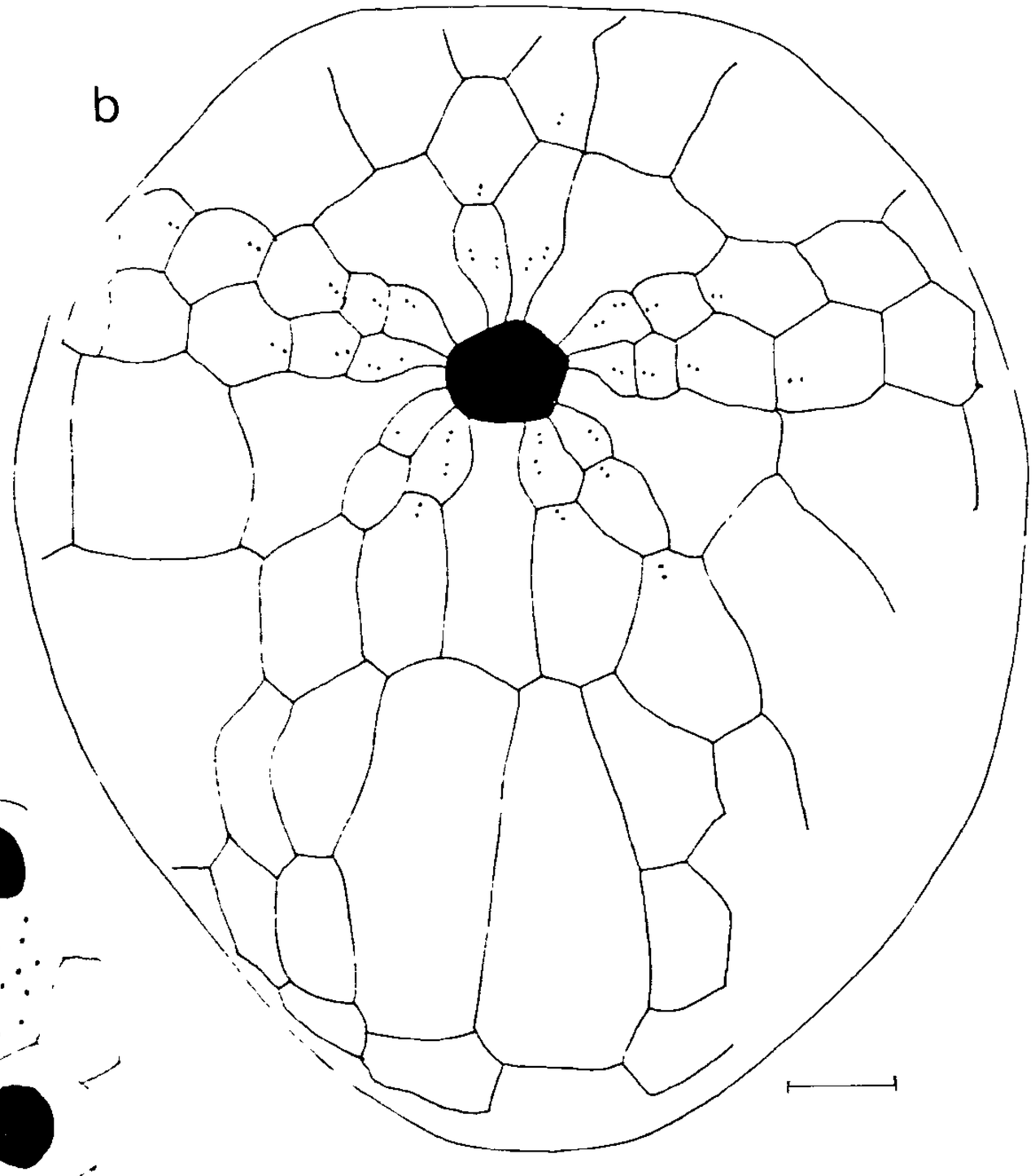

b

Figure 3.44. Camera lucida drawings of *Leiostomaster gentili* Lambert, MNHN no specimen number, Maastrichtian of Oran, Algeria; a, apical view; b, oral view; c, apical disc plating. a & b, scale bars = 2 mm. c, scale bar = 1 mm.


a


b

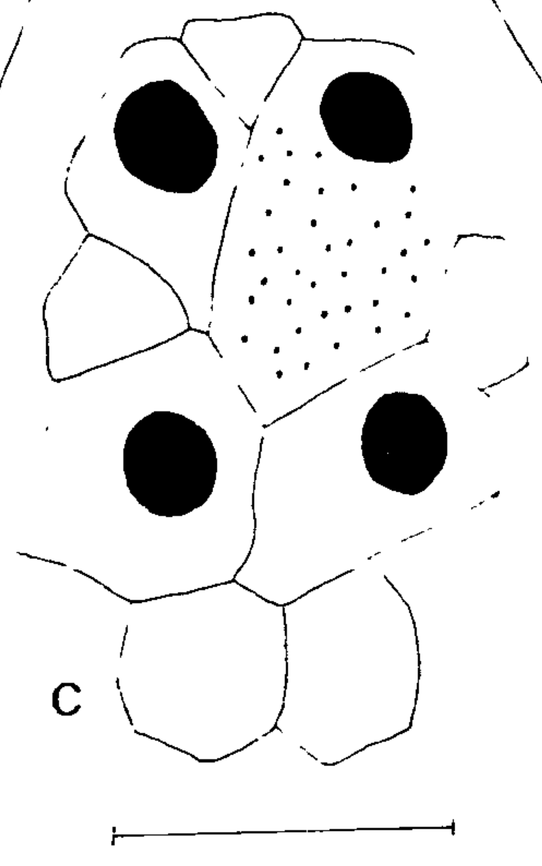
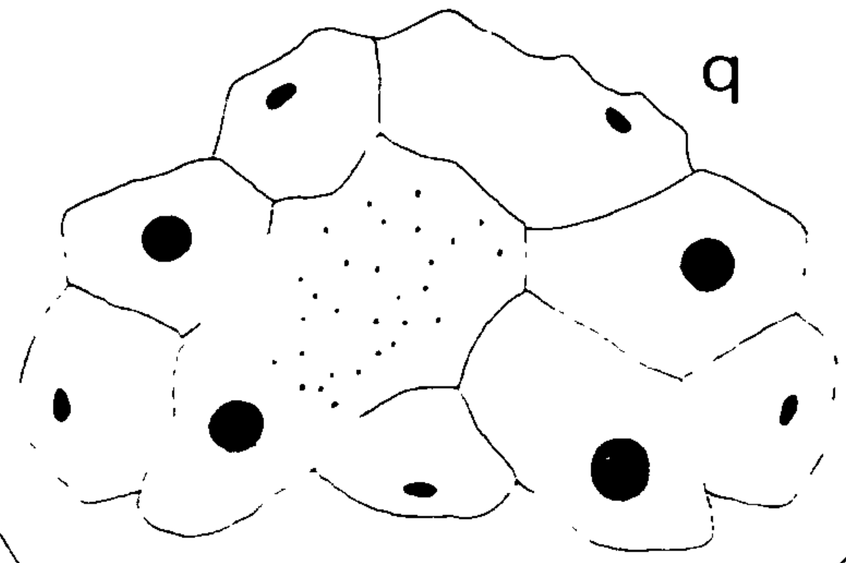
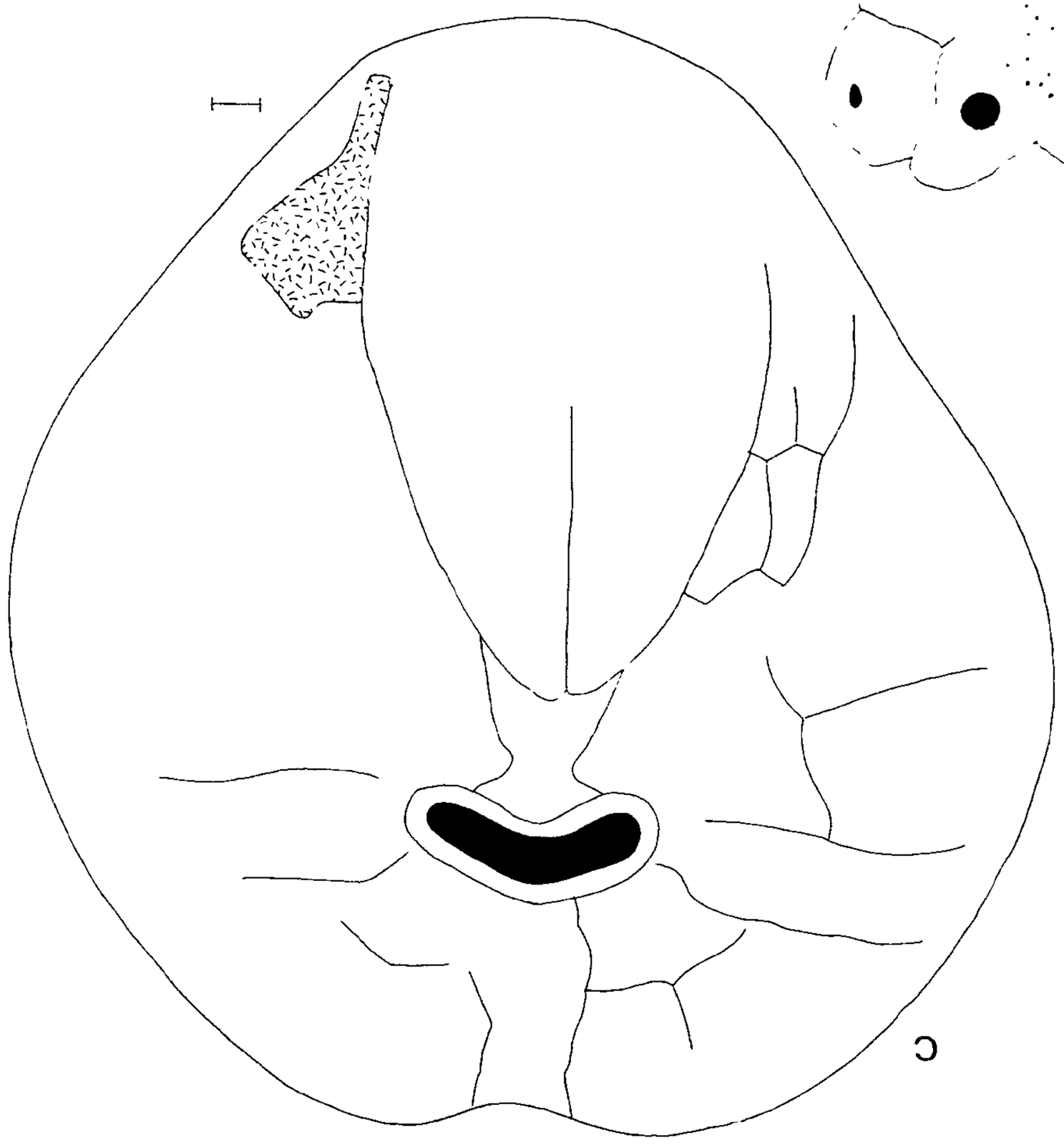

c

Figure 3.45. Camera lucida drawings of *Leymeriaster maestrichtensis* (Agassiz), Upper Maastrichtian Nekum or Meerssen Chalk of Maastricht. a & b, NMM MM538; a, apical view; b, apical disc plating. c, NMM MM066, oral view. Scale bars = 1 mm.


q


c

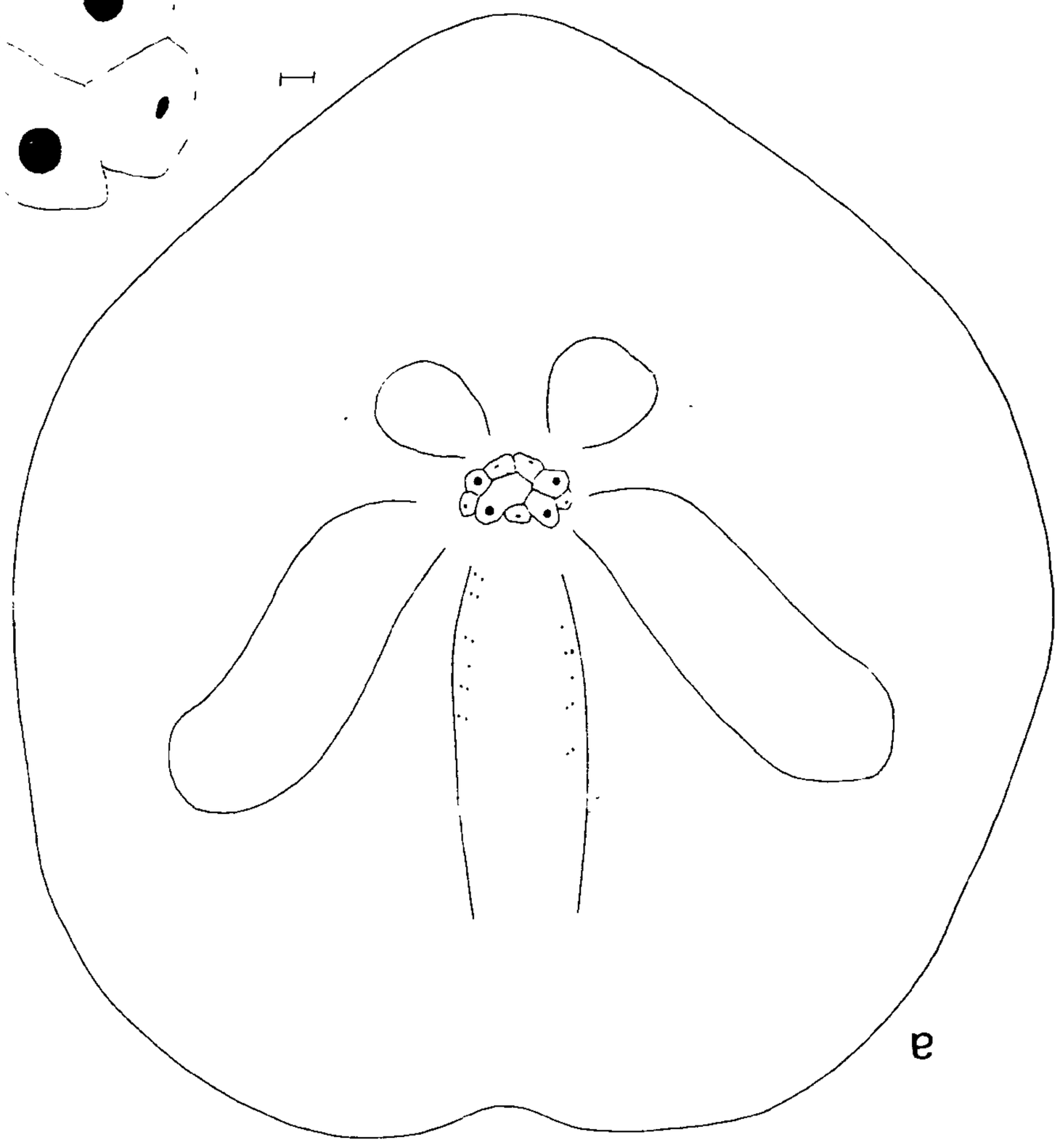
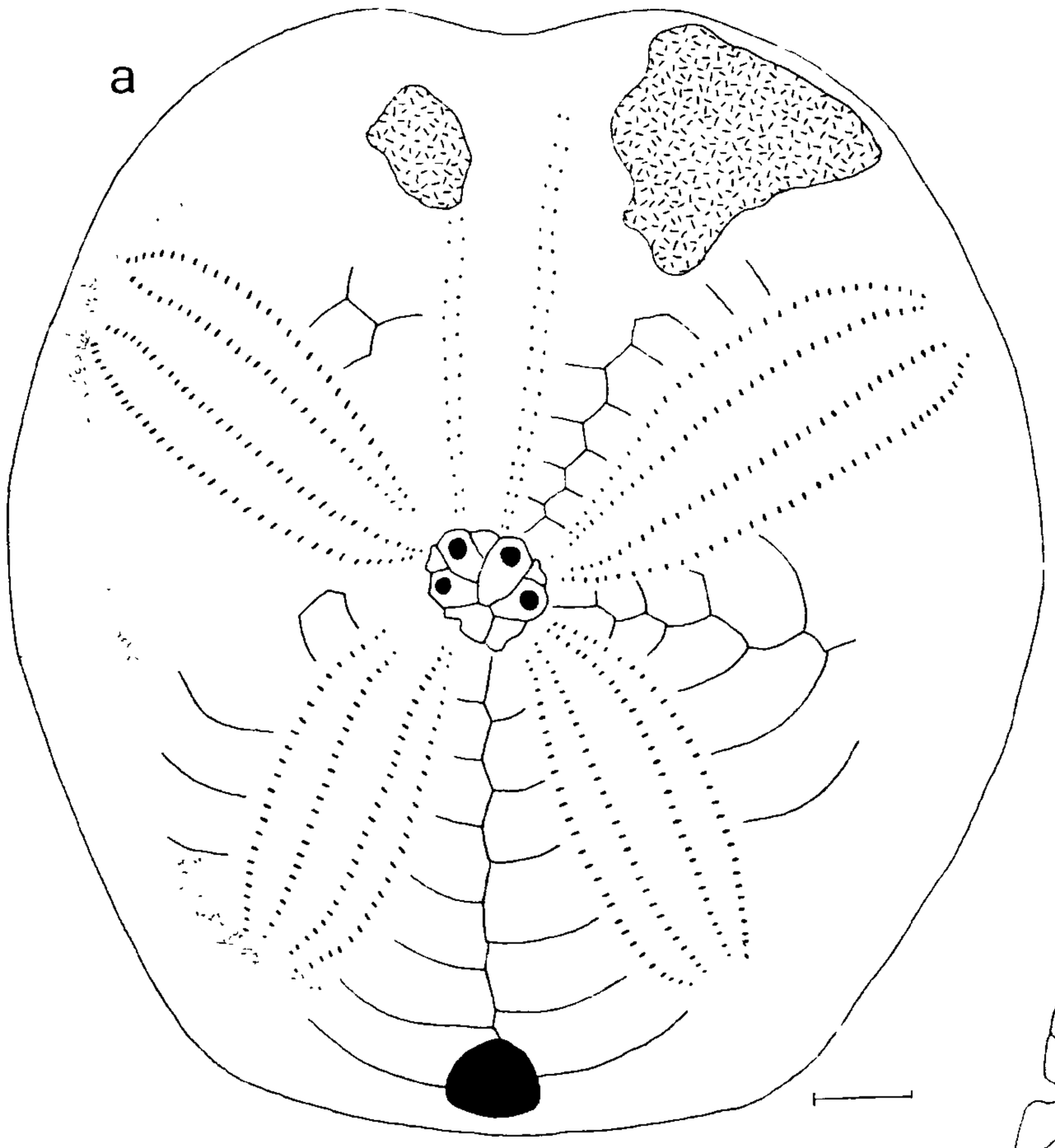
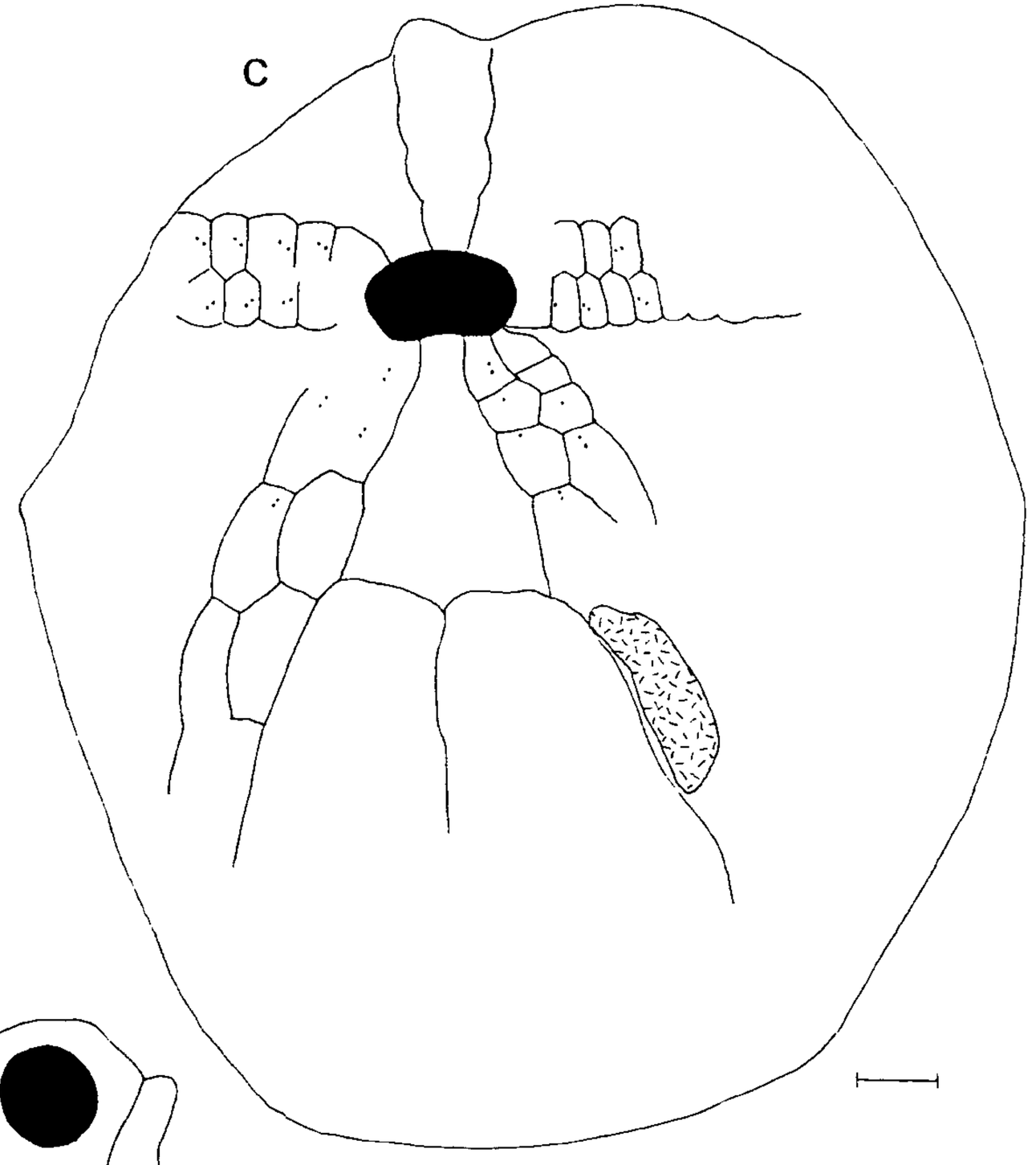

a

Figure 3.46. Camera lucida drawings of *Mecaster fourneli* (Deshayes), Maastrichtian of Tripolitania, Libya. a & b, URGM i82c; a, apical view; b, apical disc plating. c, URGM i82a, oral view. a & c, scale bars = 2 mm. b, scale bar = 1 mm.


a


c

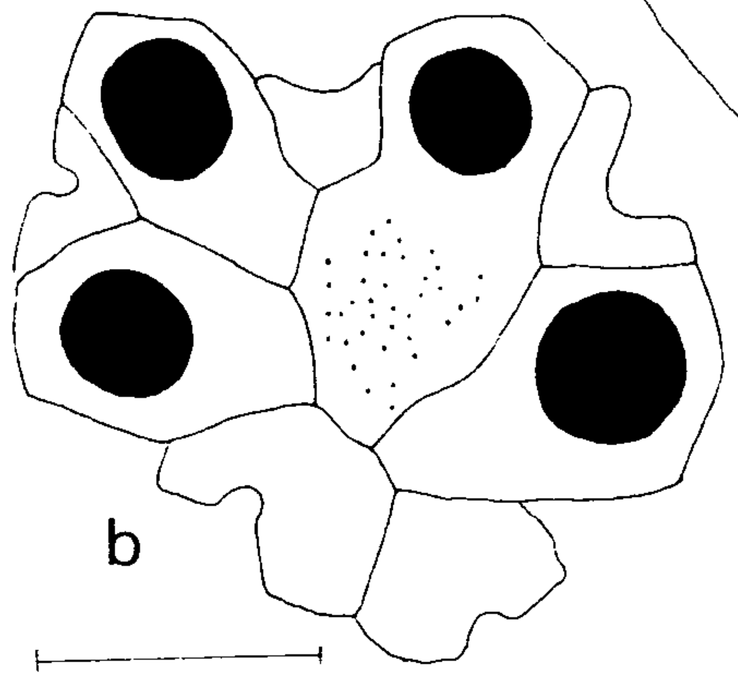
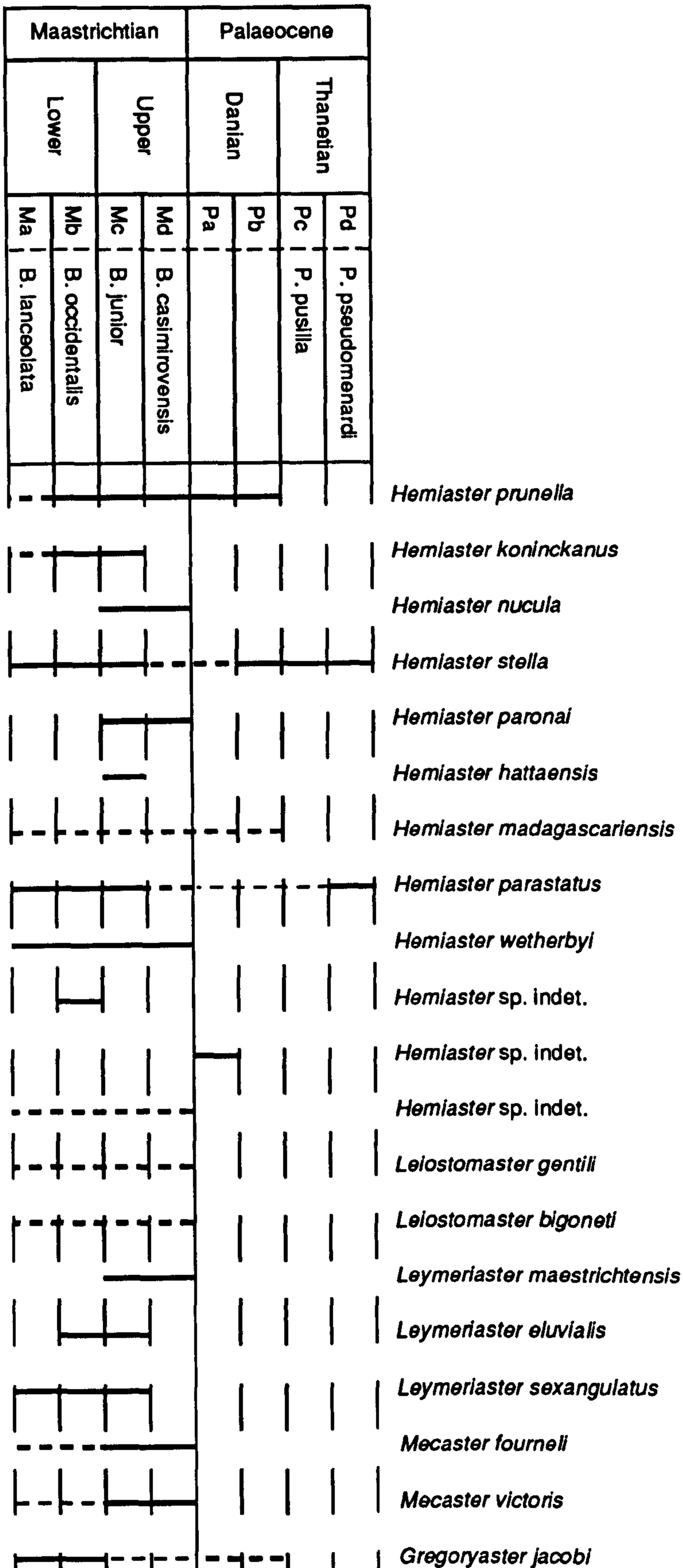

b

Figure 3.47. Range chart for Maastrichtian and Palaeocene hemiasterid species. See Figure 3.2 for explanation of symbols.


Maastrichtian
Palaeocene
Lower
Upper
Danian
Thanetian
Ma
Mb
Mc
Md
Pa
Pb
Pc
Pd
B. lanceolata
B. occidentalis
B. junior
B. casimirovensis
P. pusilla
P. pseudomenardi
Hemiaster prunella
Hemiaster koninckanus
Hemiaster nucula
Hemiaster stella
Hemiaster paronai
Hemiaster hattaensis
Hemiaster madagascariensis
Hemiaster parastatus
Hemiaster wetherbyi
Hemiaster sp. indet.
Hemiaster sp. indet.
Hemiaster sp. indet.
Leiostomaster gentili
Leiostomaster bigoneti
Leymeriaster maestrichtensis
Leymeriaster eluvialis
Leymeriaster sexangulatus
Mecaster fourneli
Mecaster victoris
Gregoryaster jacobi

Family SCHIZASTERIDAE Lambert *in* Doncieux, 1905

Emended diagnosis. Petaloid paired ambulacra. Apical system ethmolytic with two to four gonopores. Short broad labrum followed by symmetrical sternal plates. Peripetalous fasciole.

Remarks. Commonly with short broad labrum followed by symmetrical sternal plates and latero-anal fasciole.

Schizasterids have traditionally been characterized as possessing both peripetalous and latero-anal fascioles. However, some taxa generally included in this family, either lose the latero-anal fasciole during ontogeny or lack it entirely (McNamara & Philip 1980; McNamara 1985). The above diagnosis reflects the transitory nature of the latero-anal fasciole.

KEY TO MAASTRICHTIAN & PALAEOCENE GENERA

1 Apical system with four gonopores.....2

Apical system with two or three gonopores.....10

2 Large nodules in ambulacra adjoining plastron.....*Tessieria*

No large nodules.....3

3 Paired ambulacra flush.....4

Paired ambulacra sunken.....5

4 Peripetalous and latero-anal fascioles; peripetalous fasciole extends onto oral surface anteriorly.....*Prenaster*

Peripetalous fasciole only; restricted to aboral surface.....*Mauritanaster*

5 Peripetalous fasciole only.....6

Peripetalous and latero-anal fascioles.....8

6 Apical system 30-40% of test length from anterior.....*Holcopneustes*

Apical system at least 50% of test length from anterior.....7

7 Very deep, broad frontal groove often with vertical sides.....*Proraster*

Shallow frontal groove without vertical walls.....*Trachyaster*

8 Posterior petals less than 80% length of anterior.....*Paraster*

Posterior petals at least 80% length of anterior.....*Linthia*

9 Apical system with three gonopores.....10

Apical system with two gonopores.....11

10 Test circular; petals narrow and straight; peripetalous

and sub-anal fascioles.....*Pseudolinthia*

Test elongate; anterior petals strongly flexuous;

peripetalous fasciole only.....*Brisaster*

11 Peripetalous fasciole only.....*Opissaster*

Peripetalous and latero-anal fascioles.....*Abatus*

Genus LINTHIA Desor, 1853

[Type species *Linthia insignis* Desor, 1853, by OD]

Diagnosis. Paired ambulacra form long, straight, subequal petals. Apical system ethmolytic with four gonopores. Peripetalous fasciole indents between petals. Latero-anal fasciole.

Remarks. *Linthia* is most similar to *Paraster*, from which it differs in having long, straight petals with the anterior pair at least one and a half times longer than the posterior. *Linthia* is sometimes confused with *Schizaster*. However the two are easily distinguished since *Schizaster* has very short posterior petals, distinctly flexuous anterior petals and only two gonopores.

KEY TO MAASTRICHTIAN & PALAEOCENE SPECIES

1 Test heart-shaped with a pointed posterior in horizontal

outline; unpaired ambulacrum widens distally.....*L. andrussovi*

Test not pointed posteriorly; unpaired ambulacrum

with parallel sides.....2

2 Anterior petals diverge at 140 degrees or more.....*L. houzeaui*

Anterior petals diverge at less than 140 degrees.....3

3 Apical system at one third test length from anterior.....*L. brodermanni*

Apical system at mid-length.....4

4 Unpaired ambulacrum flush at apex.....*L. sudanensis*

Unpaired ambulacrum sunken at apex.....*L. payeni*

Linthia payeni Coquand, 1880

1880 *Linthia payeni* Coquand, p.260.

1881 *Linthia payeni* Coquand; Cotteau *et al.*, p. 134, 151, pl. 12, figs 3-8.

1939 *Linthia payeni* Coquand; Airaghi, p. 265.

?1981 *Linthia* cf. *medjesensis* Peron & Gauthier; Amard *et al.*, p. 46.

Occurrence. Lower Maastrichtian of Constantine (Coquand 1880; Cotteau *et al.* 1881) and ?eastern Tademait Plateau (Amard *et al.* 1981), Algeria (BMNH, MNHN). Mid to Upper Maastrichtian Lower Tar Member, Al Gharbiyah Formation of Tripolitania, Libya (Airaghi 1939).

Diagnosis. Distinct carina posterior of apical system. Broad, unpaired ambulacrum depressed at apex. Adjoining interambulacra form pinched keels. Broad, sunken petals of approximately equal lengths.

Remarks. The pinched anterior interambulacra and broad, equal length petals make this easy to distinguish from other species of *Linthia.*

Linthia sudanensis (Bather, 1904)

(Plate 12, figures 1-3; Figure 3.48)

1904 *Hemiaster sudanensis* Bather, p. 299, pl. 11, figs 6-13.

1908b *Hemiaster (Linthia) sudanensis* Bather; Cottreau, p. 553.

1914 *Linthia chargensis beadnelli* Fourtau, p. 93, pl. 8, fig. 10.

1914 *Schizaster dowsoni* Fourtau, p. 96, pl. 8, fig. 11.

1925 *Hemiaster* sp. indet. Currie, p. 74, pl. 9, fig. 7.

1927 *Linthia*? n. sp. Currie, p. 437.

1931 *Linthia sudanensis* (Bather), Lambert & Pérébaskine, p. 476.

1931 *Linthia sudanenis brevipetala* Lambert *in* Lambert & Pérébaskine, p. 476, pl. 38, fig. 12.

1934 *Linthia desioi* Airaghi, p. 73, pl. 5, figs 12 -14.

1943 *Linthia hargisensis* Currie, p. 27.

1957 *Schizaster (Paraster) duroensis* Kier, p. 885, pl. 106, figs 11-14.

?1995 ?*Linthia sudanensis* (Bather); Smith, p. 236, pl. 33, figs 9-11, text figs 84-85.

Occurrence. Thanetian limestone of Nigeria (Bather 1904) (BMNH) and Sudan (Cottreau 1908b; Lambert & Pérébaskine 1931). Palaeocene Lower Auradu Limestone of Somalia (Currie 1925, 1927, 1943; Kier 1957) (BMNH) and Lower Palaeocene of Sirtica, Libya (Airaghi 1934) (BMNH). ?Early Upper Maastrichtian Simsima Formation of UAE / Oman (Smith 1995) (BMNH). Upper Thanetian Tarwan Chalk of the Libyan Desert, Egypt (Fourtau 1914).

Diagnosis. Test elongate. Frontal groove deepens to ambitus. Paired ambulacra form long straight petals - only slightly sunken. Anterior about one and a half times longer than posterior. Anterior petals diverge at 110-120 degrees. Large tubercles along edges of frontal groove.

Remarks. Specimens referred to *L. desioi* have a less inflated test with the widest point a little more anterior. However, within the large BMNH collections of *L. sudanensis*, there are depressed forms (indistinguishable from the types of *L. desioi*) and inflated forms along with all intermediates. The two species are thus synonymized.

L. sudanensis is most similar other elongate species of Linthia - *L. houzeaui*, *L. brodermanni* and *L. payeni*. Both *L. houzeaui* and *L. brodermanni* have a more anterior apical disc. In addition, *L. houzeaui* has far more divergent anterior petals and *L. brodermanni* has a deeper frontal notch and more deeply sunken petals. *L. sudanensis* differs from *L. payeni* in having smoothly rounded interambulacra adjoining the frontal groove.

Linthia houzeaui Cotteau, 1879

1879 *Linthia houzeaui* Cotteau, p. 10, pl. 1, figs 27-29.

1935b *Linthia houzeaui* Cotteau; Smiser, p. 87, pl. 8, fig. 3.

1989 *Linthia houzeaui* Cotteau, Roman, p. 303, pl. 1, figs 7, 9-10.

Occurrence. Montian Calcaire grossier de Mons of Mons, Belgium (Cotteau 1879; Smiser 1935b). Dano-Montian Calcaire de Vigny of the Paris Basin (Roman 1989).

Diagnosis. Elongate test. Paired petals of approximately equal lengths, slightly sunken. Anterior petals are somewhat flexuous and diverge at 140 degrees.

Remarks. Most similar to *L. brodermanni* from which it differs in having a far shallower frontal notch and less depressed petals. In addition, *L. houzeaui* differs from all Maastrichtian and Palaeocene species of *Linthia* in having shallow, very widely diverging anterior petals.

Linthia brodermanni Sanchez Roig, 1949

1949 *Linthia brodermanni* Sanchez Roig, p. 263, pl. 49, figs 2-4.

1949 *Linthia alta* Sanchez Roig, p. 266, pl. 49, figs 3-5.

?1949 *Linthia cretacica* Sanchez Roig, p. 264, pl. 47, figs 1-3.

1949 *Micraster elevatus* Sanchez Roig, p. 218, pl. 47, figs 4-5.

1949 *Hemiaster lamberti* Sanchez Roig, p. 238, pl. 35, figs 7-8.

1952 *Linthia collignoni* Tessier, p. 308, pl. 18, figs 14-18.

1984 *Linthia brodermanni* Sanchez Roig; Kier, p. 73, pls 37-39, text figs 27-28.

Occurrence. Early Upper Maastrichtian of Cuba (Sanchez Roig 1949; Kier 1984). Palaeocene of Senegal (Tessier 1952).

Diagnosis. Elongate test narrowing to posterior. Highest point central. Parallel sided frontal groove. Petals shallowly sunken; both pairs approximately equal in length. Apical system anterior.

Remarks. *L. brodermanni* is most similar to *L. houzeaui* and *L. sudanensis* but differs in having more deeply sunken petals and a more sharply defined frontal notch. Additionally, *L. houzeaui* has more divergent anterior petals and *L. sudanensis* has a far less anterior apical system.

Linthia andrussovi Bajarunas *in* Weber, 1949

1994 *Linthia andrussovi* Bajarunas; Markov, p. 62, pl. 2, fig. 4, text fig. 17.

Occurrence. Thanetian of Mangyshlak (Markov 1994) (Pl).

Diagnosis. Test heart-shaped with pointed posterior. Unpaired ambulacrum widens distally. Adjoining interambulacra form pinched keels. Paired ambulacra form narrow petals. Posterior pair about 80% length of anterior.

Remarks. Easily distinguished from other species of *Linthia* on the basis of its posteriorly pointed horizontal outline, narrow petals and distally widening frontal groove.

Linthia? sp. indet.

1959 *Linthia? prima* Cooke, p. 70, pl. 43, figs 1-4.

Occurrence. Lower Danian Clayton Formation of Georgia, USA.

Remarks. Represented by single internal mould with small pieces of test attached. Apical system ethmolytic with four gonopores. Paired ambulacra form long, straight, subequal petals. On the basis of the apical disc structure and petal arrangement, this specimen is tentatively assigned to *Linthia*. Poor preservation prevents specific identification.

Genus PARASTER Pomel, 1869

[Type species *Schizaster gibberulus* Agassiz *in* Agassiz & Desor, 1847, by OD]

Diagnosis. Test subcircular in horizontal outline. Paired ambulacra form straight petals; posterior pair distinctly shorter than anterior. Ethmolytic apical system with four gonopores. Peripetalous and latero-anal fascioles.

Remarks. *Paraster* is considered by some authors to form a subgenus of *Schizaster*. *Schizaster* is generally characterized as having only two gonopores, although arguments

continue as to whether *Schizaster studeri*, the type species of *Schizaster*, has two or four gonopores. The types of both *Paraster* and *Linthia* definitely have four gonopores. In addition, *Linthia* and *Paraster* both have straight paired petals in contrast to the strongly flexuous anterior petals that characterize *Schizaster*. In light of this, *Schizaster* and *Paraster* are separated and *Paraster* given full generic status. However, without access to type material for *Schizaster*, *Paraster* and *Linthia* it is not possible to determine the true affinities of *Paraster*.

Paraster differs from *Linthia* in having a more circular horizontal outline and paired petals of unequal length.

KEY TO MAASTRICHTIAN & PALAEOCENE SPECIES

1 Narrow paired petals; anterior petal width 20% of petal length.....*P. brevipetalus*

Anterior petal width greater than 20% of petal length.....2

2 All interambulacra form sharp carinae on apical surface.....*P. variabilis*

Not all interambulacra from sharp carinae.....3

3 Apical system anterior.....*P. canaliculatus*

Apical system at mid-length or posterior.....4

4 Parallel-sided frontal groove with very sharp edges.....*P. expansus*

Interambulacra adjoining frontal groove smoothly rounded.....5

5 Highest point central; anterior petals 1.5 times longer than posterior.....*P. sindensis*

Test highest posteriorly; anterior petals 2 times longer than posterior.....6

6 Low flat-based test with sharp carina between apex and periproct.....*P. chargensis*

Globular test with convex oral surface; slight or no posterior carina.....*P. indicus*

Paraster sindensis (Duncan & Sladen, 1882a)

1882a *Linthia sindensis* Duncan & Sladen, p. 18, pl. 4.
1915 *Linthia alabamensis* Clark, p. 153, pl. 71, figs 1-2.
1933a *Linthia sindensis* Duncan & Sladen; Lambert, p. 26, pl. 4, fig. 16.
1959 *Linthia alabamensis* Clark; Cooke, p. 69, pl. 29, figs 5-7.
1987 *Linthia* sp. 2 van der Ham *et al.*, p. 33, pl. 23, fig. 1.
1988 *Linthia* sp. van der Ham, p. 155, pl. 9, figs 1-5.
1994 *Linthia spiennensis* Schlüter; Markov, p. 56, pl. 1, fig. 1, text fig. 15.
1994 *Linthia bajsarensis* Markov, p. 58, pl. 1, fig. 3, pl. 2, figs 1-3, text figs 15-16.

Occurrence. Lower Danian *Cardita beaumonti* beds of Sind, Pakistan (Duncan & Sladen 1882a) (BMNH, GSI). Danian of northwest Madagascar (Lambert 1933a; Besairie 1971). Lower Danian Clayton Formation and Upper Danian Wills Point Formation (Midway Group) of Alabama, Arkansas and Texas, USA (Cooke 1959). Montian of the Transcaspian and Upper Maastrichtian of Turkmenia (Markov 1994) (PI). Danian Guelhem Chalk of the Maastricht area (van der Ham *et al.* 1987; van der Ham 1988) (NMM).

Diagnosis. Low test with flat base and highest point central. Upper surface smoothly rounded with no posterior carina. Anterior petals 1.5 times longer than posterior. Apical system at mid-length.

Remarks. Most similar to *P. variablis* from which it differs in having a smoothly rounded apical surface with shallow petals and no interambulacral keels. *P. sindensis* also resembles *P. chargensis*, but differs in having its highest point central and no keel between the apical system and periproct. *P. sindensis* differs additionally from both these species in having proportionally longer posterior petals.

Paraster chargensis (Wanner, 1902)

1902 *Hemiaster chargensis* Wanner, p. 108, pl. 15, figs 12-13.
1902 *Hemiaster chargensis* Wanner; Quaas, p. 165.
1933 *Linthia paronai* Checchia-Rispoli, p. 11, pl. 1, figs 5-7.
1957 *Schizaster (Paraster) hunti* Kier, p. 882, pl. 106, figs 5-7.
1969 *Hemiaster chargensis* Wanner; Hassan, p. 15.

?1980 *Schizaster (Paraster) carinatus* McNamara & Philip, p. 50, text fig. 1.

Occurrence. Danian Dakhla Formation of Chargeh and Dachel Oases, Egypt (Quaas, 1902). Upper Thanetian Tarwan Chalk of Dakhla Oasis, Egypt (Hassan 1969). Mid to Upper Maastrichtian Al Gharbiyah Formation of Tripolitania, Libya (Checchia-Rispoli 1933) (URGM). Palaeocene Lower Auradu Series of northern Somalia (Kier 1957). ?Palaeocene Pirie and Cashin Calcarenites of the Carnarvon Basin, Western Australia (McNamara & Philip 1980).

Diagnosis. Test is low with flat base. Highest point posterior. Sharply carinate behind apical system. Petals quite deeply sunken. Anterior petals about two times longer than posterior petals. Apical system at mid-length.

Remarks. Distinguished from *P. sindensis* and *P. variabilis* by its posteriorly positioned highest point. In addition, *P. chargensis* differs from *P. sindensis* in having proportionally shorter posterior petals and a very sharp keel between the apical system and periproct. *P. variabilis* has coarse, pustular tuberculation on the apical surface and deeply sunken petals with sharply keeled interambulacra between.

Paraster variabilis (Slocum, 1909)

1909 *Linthia variabilis* Slocum, p. 12, pl. 3, figs 1-1, text fig. 1.
1915 *Linthia variabilis* Slocum; Clark, p. 99, pl. 54, fig. 1.
1941 *Linthia variabilis* Slocum?; Stephenson, p. 68, pl. 8, figs 1-5.
1953 *Linthia variabilis* Slocum; Cooke, p. 36, pl. 14, figs 18-25.
1981 *Linthia romani* Brito, p. 576, pl. 3, figs 1-6.

Occurrence. Upper Maastrichtian Gramame Formation of northeastern Brazil (Brito 1981). Lower Maastrichtian Nacotach Sand, Mid Maastrichtian Peedee Formation, Mid to Upper Maastrichtian Prairie Bluff Chalk and Corsicana Marl of Mississippi, North Carolina, Arkansas and Texas, USA (Cooke 1953) (BMNH).

Diagnosis. Test has flat base and is highest centrally. Very deeply sunken petals with interambulacra forming sharp carinae in between. Posterior petals about half length of anterior. Apical system at mid-length. Pustular tuberculation on upper surface.

Remarks. Most similar to other low, flat-based forms of *Paraster* - *P. sindensis* and *P. chargensis*. *P. variabilis* differs from both these species (as well as the remaining Maastrichtian and Palaeocene species of *Paraster*) in having very sharp carinae between the deeply sunken petals and in having pustular tuberculation on the apical surface. Differs additionally from *P. chargensis* in having the highest point central and from *P. sindensis* in having proportionally shorter posterior petals.

Paraster canaliculatus (Cotteau, 1877)

1877	*Hemiaster canaliculatus* Cotteau, p. 66, pl. 6, figs 21-25.
1877	*Schizaster antiquus* Cotteau, p. 67, pl. 6, figs 26-28.
1891	*Dipneustes aturicus* Arnaud; Cotteau, p. 153, pl. 19, figs 11-13.
1907a	*Linthia canaliculata* (Cotteau); Lambert, p. 721.
?1928	*Linthia caraibensis* Jeannet, p. 17, pl. 2, figs 1-3, pl. 6, figs 4-6.
?1975	*Linthia caraibensis* Jeannet; Kugler & Caudri, p. 376.
1975	*Linthia canaliculata* (Cotteau); Plaziat *et al.*, p. 638, p. 643.

Occurrence. Lower to Mid Thanetian of the French (Cotteau 1877, 1891; Lambert 1907a; Plaziat *et al.* 1975) and Spanish Pyrenees (Plaziat *et al.* 1975) (BMNH, MNHN)). Upper Cretaceous of Cuba (BMNH) - precise age uncertain. ?Upper Danian Soldado Formation Bed 2 of Soldado Rock, Trinidad (Jeannet 1928; Kugler & Caudri 1975).

Diagnosis. Globular profile with highest point posterior. Carinate between apex and anus. Petals short (reaching only about 50% of distance to ambitus) and deeply sunken. Posterior petals less than one half length of anterior. Apical system anterior.

Remarks. Both *P. canaliculatus* and *P. indicus* are somewhat globular in profile. However, *P. canaliculatus* differs in having a more anterior apical system and shorter, straighter paired petals. Its anterior apical system also distinguishes it from all other Maastrichtian and Palaeocene species of *Paraster*.

Paraster indicus (Duncan & Sladen, 1882b)

(Plate 12, figures 4-7; Figure 3.49)

1882b	*Linthia indica* Duncan & Sladen, p. 82, pl. 20, figs 1-8.
1933a	*Periaster inconstans* Lambert, p. 25, pl. 4, fig. 15.
1959	*Linthia collignoni* Tessier; Roman & Gorodiski, p. 53, pl. 3, figs 30-32.
?1959	*Linthia* sp. Roman & Gorodiski, p. 53, pl. 3, figs 33-35.
1973	*Schizaster (Paraster) rougeriei* Tessier & Roman, p. 158, pl. 2, figs 8-16.
1979	*Linthia (Linthia) inconstans* Tanaka *et al.*, p. 39, pl. 2, figs 4-5, pl. 3, fig. 1, text fig. 11.
1979	*Linthia (Linthia) madagascarensis* Tanaka *et al.*, p. 41, pl. 3, figs 2-4, text fig. 12.
1979	*Linthia (Linthia)*? sp. Tanaka *et al.*, p. 43, pl. 3, fig. 6, text fig. 13.
1979	*Hemiaster (Mecaster) majungensis* Tanaka *et al.*, p. 36, pl. 2, fig. 1, text fig. 9.
?1979	*Abatus*? sp. Tanaka *et al.*, p. 37, pl. 2, fig. 3, text fig. 10.

Occurrence. Upper Thanetian Ranikot Series of Sind, Pakistan (Duncan & Sladen 1882b) (BNMH, GSI). Maastrichtian to Danian of northwestern Madagascar (Lambert 1933a; Besairie 1971; Tanaka *et al.* 1979) (BMNH, MNHN). Mid to Upper Thanetian Fresco lower beds 2 to 5 of the Ivory Coast (Tessier & Roman 1973). ?Palaeocene of Diourbel, Senegal (Roman & Gorodiski 1959) (MNHN).

Diagnosis. Circular to hexagonal horizontal outline with highest point posterior. Inflated plastron, especially in larger specimens. Petals sunken. Anterior petals somewhat flexuous distally. Posterior petals half length of anterior petals or shorter. Apical system at mid-length.

Remarks. Specimens referred to *Linthia indica* and *Schizaster (Paraster) rougerieri* are smaller and more globular. However they are identical in petal structure and are thus treated as synonyms.

Tanaka *et al.* (1979) assigned a single specimen from northwestern Madagascar to *Abatus*? sp. on the basis of its three gonopores. In all other respects the specimen is identical to specimens referred to *Linthia inconstans* by the same authors. Photographs of the specimen in question show it to be somewhat damaged and with some sediment cover in the apical region. Since the number of gonopores cannot be determined with certainty, I have tentatively grouped this specimen with *Linthia inconstans*.

Differs from *P. canaliculatus* in having a broader, flatter apical surface with the

apical system at mid-length and distally flexuous anterior petals.

Paraster brevipetalus (Markov, 1994)

1994 *Linthia brevipetala* Markov, p. 61, pl. 1, fig. 2, text fig. 15.

Occurrence. Montian of Mangyshlak, Kazakhstan (PI).

Diagnosis. Highest point of test central. Broad, smoothly domed upper surface. No posterior carina on upper surface. Paired ambulacra form very narrow paired petals. Anterior pair two times longer than posterior. Apical system at mid-length.

Remarks. Easily distinguished from other Maastrichtian and Palaeocene species of *Paraster* on the basis of its very narrow paired ambulacra.

Paraster expansus (Forbes 1848)

1848 *Brissus expansus* Forbes, p. 160, pl. 19, fig. 7.

1848 *Brissus rana* Forbes, p. 161, pl. 19, fig. 5.

1897 *Hemiaster rana* (Forbes); Kossmat, p. 106.

Occurrence. Maastrichtian *Trigonoarca* beds of the Ariyalur Group of southern India (Forbes 1848; Kossmat 1897) (BMNH).

Diagnosis. Sharp, parallel sided (but not keeled) frontal groove extends from apex to mouth. Broad, smoothly rounded apical surface with no keel between apex and periproct. Anterior petals about 1.5 times longer than posterior.

Remarks. Most similar to *P. brevipetala* from which it differs in having broader petals, proportionally longer posterior petals and a sharp sided frontal groove.

Paraster sp. Indet.

1979 "*Schizaster*" sp. Asgaard, tables 1 & 2 (pars).

Occurrence. Upper Danian of Denmark (Asgaard 1979) and southern Sweden (DGFMM). Danian Kangilia Formation of East Greenland (DGFMM).

Diagnosis. Circular outline. Depressed profile with truncate posterior. Anterior petals diverge at 115 degrees and are slightly flexuous distally. Anterior petals are between 1.6 and 2 times longer than posterior petals. Peripetalous fasciole embayed between paired petals.

Remarks. Specimens have a circular horizontal outline, four gonopores in the ethmolytic apical system and anterior petals 1.5 to 2 times longer than posterior. Thus they are clearly referrable to *Paraster* rather than *Schizaster*. However, the material is too incompletely known to refer it to any named species with certainty.

Genus TESSIERIA Collignon, 1949

[Type species *Tessieria senegalensis* Collignon, 1949, by OD]

Diagnosis. Inflated upper surface. Large nodules on ambulcral plates adjoining plastron. Paired ambulacra form well-developed sunken petals - anterior pair reach ambitus. Apical system ethmolytic with four gonopores. Peripetalous fasciole indents between petals. Latero-anal fasciole.

Remarks. Distinguished from all other schizasterids by the large nodules on the oral surface.

Tessieria senegalensis Collignon, 1949

(Figure 3.50)

1949 *Tessieria senegalensis* Collignon, p. 263, pl. 9a, figs 1-5, text figs 1-2.

1952 *Tessieria senegalensis* Collignon; Tessier, p. 307, pl.18, figs 19-20.

Occurrence. Upper Maastrichtian of Senegal (Collignon 1949; Tessier 1952) (MNHN).

Diagnosis. As generic diagnosis.

Genus PRORASTER Lambert In Grosouvre, 1901

[Type species *Proraster atavus* Arnaud *in* Cotteau 1883, by OD]

Synonym. *Sanfilippaster* Checchia-Rispoli, 1932 (type species *Proraster geayi* Cottreau, 1908a).

Diagnosis. Frontal groove with vertical or overhanging walls, deeply indenting anterior margin. Anterior petals strongly flexuous; longer than posterior. Apical system ethmolytic with four gonopores, situated posterior of mid-length. Short labral plate. Peripetalous but no latero-anal fasciole.

Remarks. Most similar to *Brisaster* and *Schizaster*. Differs from *Brisaster* in having four rather than three gonopores and from *Schizaster* in having four rather than two gonopores and no latero-anal fasciole. Differs from *Trachyaster* in having a far more deeply sunken frontal groove.

KEY TO MAASTRICHTIAN & PALAEOCENE SPECIES

1	Elongate test	2
	Almost circular horizontal outline	3
2	Interambulacral keels adjoining frontal groove converge towards anterior; apical disc >60% test length from anterior	*P. geayi*
	Interambulacral keels do not converge distally; apical system at 50% test length from anterior	*P.? alveolatus*
3	Apical system at mid-length	4
	Apical system at 60% of test length from anterior	*P.* sp.
4	Anterior petals 2 times longer than posterior	*P. atavus*
	Anterior petals 1.5 times longer than posterior	*P. herrerae*

Proraster atavus Arnaud *in* Cotteau, 1883

1883	*Proraster atavus* Arnaud *in* Cotteau, p. 223, pl. 12, figs 5-9.
1893	*Hemiaster dalli* Clark, p. 89, pl. 48, fig. 2.

1895 *Opissaster centrosus* Cotteau & Gauthier, p. 45, pl. 7, figs 10-15.

1915 *Hemiaster dalli* Clark, p. 90, pl. 47, fig. 1.

1923 *Hemiaster* sp. (or spp.) indet. Hawkins, p. 206 (pars?).

1924 *Hemiaster* sp. indet. Hawkins, p. 316, pl. 18, fig. 3.

1927 *Proraster atavus* (Arnaud); Lambert, p. 50, pl. 3, fig. 23.

1934 *Hemiaster siboneyensis* Weisbord, p. 201, pl. 22, figs 7-9.

1941 *Hemiaster dalli* Clark; Stephenson, p. 63, pl. 6, figs 1-4.

1949 *Hemiaster siboneyensis* Weisbord; Sanchez Roig, p. 237.

1953 *Proraster dalli* (Clark); Cooke, p. 36, pl. 15, figs 1-5.

1984 *Hemiaster siboneyensis* Weisbord; Kier, p. 17, pl. 8, figs 5-7.

1993 *Hemiaster* sp. or spp. Donovan, p. 101, fig. 12.

1993 *Hemiaster* sp. Donovan & Lewis, p. 187.

Occurrence. Senonian of southeastern France (Arnaud *in* Cotteau 1883). Lower Maastrichtian of Tremp, Spain (Lambert 1927) (BMNH). Lower Maastrichtian Rudist Limestones of Jamaica (Hawkins 1923, 1924; Donovan 1993; Donovan & Lewis 1993) (BMNH). Upper Cretaceous of Cuba (Weisbord 1934; Sanchez Roig 1949; Kier 1984) (BMNH) - precise age uncertain. Mid to Upper Maastrichtian Corsicana Marl of Texas, USA (Cooke 1953). Senonian (Campanian or Maastrichtian) of Louristan, Iran (Cotteau & Gauthier 1895).

Diagnosis. Test almost as broad as long. Highest (60% of test length) immediately behind apical system. Unpaired ambulacrum in broad groove from apex to mouth with sharp bordering interambulacral keels. Pore-pairs uniserial. Anterior petals distally flexuous and twice as long as posterior. Both pairs diverge at about 90 degrees. Apical disc at 50-55% of test length from anterior. Complete peripetalous fasciole.

Remarks. Differs from *P. herrerae* in having proportionally shorter posterior petals and a shallower frontal notch. Differs from *Proraster* sp. from the Palaeocene of Denmark of Denmark and East Greenland in having proportionally longer posterior petals and a more anteriorly positioned apical system.

Proraster herrerae (Lambert & Sanchez Roig *In* Sanchez Roig, 1926)

1926 *Opissaster herrerae* Lambert & Sanchez Roig *in* Sanchez Roig, p. 126, pl. 40, figs 1-2, pl. 41, fig. 3.

1949 *Opissaster herrerae* Lambert & Sanchez Roig; Sanchez Roig, p. 244.

1953 *Hemiaster gonzalezmunozi* Sanchez Roig, p. 170, pl. 11, figs 3-4.

1984 *Hemiaster? (Trachyaster) gonzalezmunozi* Sanchez Roig; Kier, p. 18, pl. 7, figs 1-3.

1984 *Hemiaster (Trachyaster) herrerae* (Lambert & Sanchez Roig); Kier, p. 18, pl. 7, figs 4-8, pl. 8, fig. 1.

Occurrence. Late Cretaceous of Cuba (Sanchez Roig 1926, 1949, 1953; Kier 1984) - precise age uncertain. Maastrichtian of Jamaica (BMNH).

Diagnosis. Test almost as broad as long and somewhat inflated. Unpaired ambulacrum in broad groove from apex to mouth with sharp bordering interambulacral keels. Pore-pairs uniserial. Anterior petals distally flexuous and about 1.5 times longer than posterior. Both pairs diverge at about 90 degrees. Apical disc at 50-55% of test length from anterior.

Remarks. Most similar to *P. atavus* but with a deeper frontal notch and proportionally longer posterior petals. Differs from *P.* sp. in having proportionally longer posterior petals and a more anteriorly positioned apical system.

Proraster geayi Cottreau, 1908a

(Plate 12, figures 8-11; Figure 3.51)

?1895 *Opissaster morgani* Cotteau & Gauthier, p. 43, pl. 7, figs 6-9.

1908a *Proraster geayi* Cottreau, p. 170, pl. 4, fig. 5, text fig. 13.

1922 *Proraster geayi* Cottreau, p. 117, pl. 2, fig. 9.

1932 *Sanfilippaster geayi* (Cottreau); Checchia-Rispoli, p. 313, pl. 1.

1994 *Proraster magnus* Markov, p. 66, pl. 3, fig. 1, text fig. 18.

?1994 *Neoproraster usakensis* Markov, p. 83, pl. 4, fig. 2, text fig. 24.

1995 *Proraster geayi* Cottreau; Smith, p. 238, pl. 34, figs 1-3, 8.

Occurrence. Maastrichtian of eastern Madagascar (Cottreau 1908a, 1922; Besairie 1971) (MNHN). Early Upper Maastrichtian Simsima Formation of UAE / Oman (Smith 1995) (BMNH). Mid to Upper Maastrichtian Al Gharbiyah Formation (Lower Tar Member) of Tripolitania, Libya (Checchia-Rispoli 1932) (URGM). Upper Maastrichtian and ?Montian of Mangyshlak, Kazakhstan (Markov 1994) (PI). ?Maastrichtian of Louristan, Iran (Cotteau & Gauthier 1895).

Diagnosis. Test low with broad flat upper and lower surfaces. Unpaired ambulacrum

very deeply sunken with overhanging interambulacral keels which converge towards anterior. Pore-pairs arranged biserially. Anterior petals about three times longer than posterior, running subparallel to frontal groove and flexuous distally. Posterior petals diverge at 120 to 160 degrees. Apical system about 60% of test length from anterior. Peristome opens vertically into frontal groove. Very broad complete peripetalous fasciole.

Remarks. Both *Opissaster morgani* and *Neoproraster usakensis* represent small, juvenile specimens that have the characteristic flexed anterior petals sub-parallel to the frontal groove and widely diverging posterior petals of *Proraster geayi* but lack the convergent anterior interambulacral keels. In addition, *Neoproraster usakensis* was originally described as possessing just three gonopores. However, preparation of the type specimen revealed a fourth gonopore. Both species are tentatively synonymized with *Proraster geayi*.

Easily distinguished by its posterior apical disc, sub-parallel anterior paired ambulacra and very divergent posterior petals. Large specimens also have characteristic distally convergent interambulacral keels.

Proraster sp.

1979 "*Schizaster*" sp. Asgaard, tables 1 & 2 (pars).

Occurrence. Late Danian and Thanetian of Denmark and East Greenland (DGFMM).

Diagnosis. Circular to slightly elongate oval horizontal outline. Highest posteriorly. Very deep frontal groove with adjacent interambulacra forming sharp keels. Unpaired ambulacrum with pore-pairs positioned at edges of plates beneath keel. Paired ambulacra form well developed, sunken cruciform petals. Anterior petals are 3 to 4 times longer than posterior petals. Apical system at about 60% of test length from anterior. Narrow peripetalous fasciole.

Remarks. Most similar to *P. atavus* and *P. herrerrae*. Differs in having proportionally shorter posterior petals and a more posteriorly positioned apical system.

Proraster? alveolatus (Duncan & Sladen, 1882b)

1882b *Schizaster alveolatus* Duncan & Sladen, p. 87, pl. 20, figs 10-13.

Occurrence. Upper Thanetian Ranikot Limestone of Sind, Pakistan (GSI).

Diagnosis. Elongate test; highest immediately behind apical system. Deep frontal groove with vertical walls, shallowing to ambitus. Anterior petals flexuous and twice as long as posterior. Anterior petals diverge at about 90 degrees; posterior at about 60 degrees. Apical system at mid-length. Broad peripetalous and no latero-anal fasciole.

Remarks. The schizasteriform petals and broad peripetalous fasciole allow this species to be assigned to either *Proraster* or *Brisaster*. However, the only known specimen lacks the apical disc and so generic determination is somewhat tentative. *P.? alveolatus* is most similar to *P. herrerae* but differs in having a broader, shallower frontal notch.

Genus TRACHYASTER Pomel, 1869

[Type species *Trachyaster globosus* Pomel, 1869, by OD]

Diagnosis. Broad unpaired ambulacrum sunken adapically and shallowing towards ambitus. Paired ambulacra form bowed petals. Anterior petals flexuous and about twice as long as posterior. Labral plate triangular. Apical disc ethmolytic with four gonopores. Peripetalous fasciole hardly indents between anterior and posterior petals.

Remarks. *Trachyaster* is distinguished from *Holcopneustes* in having a narrower unpaired ambulacrum, more posterior apical disc and less sunken, unequal, shorter petals. It differs from *Proraster* in having a less distinct frontal groove.

Trachyaster oldhami (Noetling, 1897)

(Figure 3.52)

1897 *Hemiaster oldhami* Noetling, p. 36, pl. 8, figs 4-7.

Occurrence. Maastrichtian Bed 4 of the Mari Hills, Baluchistan (GSI).

Diagnosis. Subcircular to hexagonal horizontal outline with slight frontal notch. Highest immediately behind apical system. Anterior petals 1.2 times longer than posterior; flexuous distally and diverging at 120 degrees. Posterior petals diverge at 60 to 65 degrees. Mouth 25-30% of test length from anterior margin.

Trachyaster sp. Indet.

Occurrence. Lower Maastrichtian reworked nodules in the Kangilia Formation of East Greenland (DGFMM).

Diagnosis. Ovate horizontal outline. Inflated upper and lower surfaces. Frontal groove shallow at apex and flush by ambitus. Anterior paired ambulacra flexuous distally, diverging at 125 to 130 degrees. Anterior petals only slightly longer than posterior. Apical system 50% of test length from the anterior margin. Long, narrow labral plate.

Remarks. Material too poorly preserved to assign to a named species with any certainty.

Genus HOLCOPNEUSTES Lambert, 1933a

[Type species *Holcopneustes narindensis* Lambert, 1933a, by OD]

Diagnosis. Test angular in horizontal outline with widest point at mid-length. Distinct frontal groove extending to peristome. Petals long and subequal; deeply sunken. Anterior pair somewhat flexuous. Apical system 30-40% test length from anterior; ethmolytic with four gonopores. Long labral plate. Peripetalous fasciole only.

Remarks. Most similar to *Trachyaster*, from which it differs in having a more anterior apical system, more deeply sunken, longer, subequal petals and a narrower anterior ambulacrum. Differs from *Mauritanaster* in having a more inflated test with deeply sunken petals.

Holcopneustes cristatus (Stollczka 1873)

(Plate 13, figures 1-3; Figure 3.53)

1873	*Hemiaster cristatus* Stoliczka, p. 17, pl. 3, figs 2-5.
1930	*Mecaster (Hemiaster) cristatus* Stoliczka; Besairie, p. 231, pl. 23, fig. 9.
1933a	*Holcopneustes narindensis* Lambert, p. 24, pl. 4, figs 8-10.
1973	*Linthia ghiroboensis* Tessier & Roman, p. 157, pl. 2, figs 4-7.

Occurrence. Upper Maastrichtian Trigonoarca beds of the Ariyalur Group, southern India (Stoliczka 1873). Maastrichtian (Besairie 1930) to Danian (Besairie 1930; Lambert 1933a; Besairie 1971) of northwest Madagascar. Mid to Upper Thanetian Fresco Bed 5 of the Ivory Coast (Tessier & Roman 1973).

Diagnosis. Subconical in profile with very steep anterior, truncate posterior and flat base. Anterior petals diverge at 120-130 degrees and reach 75-76% distance to ambitus. Posterior petals diverge at 45-55 degrees and reach 51-52% distance to ambitus. Apical system at 31-38% test length from anterior margin.

Holcopneustes indicus (Stollczka, 1873)

1873	*Hemiaster indicus* Stoliczka, p. 16, pl. 2, figs 6-7, pl. 3, fig. 1.
1873	*Hemiaster rana* (Forbes); Stoliczka, p. 15, pl. 2, figs 4-5.
1873	*Hemiaster tuberosus* Stoliczka, p. 12, pl. 1, figs 3-6.
1873	*Hemiaster pullus* Stoliczka, p. 18, pl. 2, figs 8-9.
1882b	*Linthia* sp. Duncan & Sladen, p. 85, pl. 20, fig. 5.
1897	*Hemiaster pullus* Stoliczka; Kossmat, p. 61, 96, pl. 10, fig. 6.
1897	*Hemiaster blanfordi* Noetling, p. 35, pl. 8, fig. 3.
1908a	*Hemiaster boulei* Cottreau, p. 171, pl. 3, fig. 8, text fig. 14.

Occurrence. Upper Maastrichtian *Trigonoarca* beds (Ariyalur Group) of southern India (Stoliczka 1873, Kossmat 1897). Maastrichtian of Baluchistan (Noetling 1897). Upper Thanetian Ranikot Series of Sind, Pakistan (Duncan & Sladen 1882b). Danian of northwest Madagascar (Cottreau 1908a; Besairie 1971).

Diagnosis. Domed profile with rounded base. Very sharp keel between apical system and periproct. Anterior petals diverge at 95 to 115 degrees and extend 85-86% of

distance to ambitus. Posterior petals diverge at 50-70 degrees and reach 65-67% of distance to ambitus. Apical system at 37-40% of test length from anterior.

Remarks. Very similar to *H. cristatus*. Differs in lateral profile and in having less divergent anterior petals and proportionally longer anterior and posterior petals.

Genus PRENASTER Desor, 1853

[Type species *Prenaster alpinus* Desor, 1853, by OD]

(see Plate 13, figures 8-11)

Diagnosis. Anterior sulcus faint or absent. Apical system anterior - ethmolytic with four gonopores. Paired ambulacra of approximately equal length or posterior pair longer. Peripetalous fasciole extends onto oral surface anteriorly. Latero-anal fasciole.

Remarks. *Prenaster* differs from the majority of schizasterids in lacking a well developed frontal groove and deeply sunken petals. It is most similar to *Parabrissus*. However, *Parabrissus* differs in having greatly reduced pores in the anterior portion of the anterior petals. Pores in the petals of *Prenaster* are all of equal size. In addition, the presence of a subanal fasciole in *Parabrissus* has not been confirmed.

Prenaster oviformis Duncan & Sladen, 1882b

(Figure 3.54)

1882b *Prenaster oviformis* Duncan & Sladen, p. 90, pl. 19, figs 1-6.

Occurrence. Upper Thanetian Ranikot Series of Sindh, Pakistan (GSI).

Diagnosis. Test ovate with convex anterior margin. Paired ambulacra of approximately equal length, slightly sunken with anterior pair flexuous and strongly divergent. Posterior petals straight. Apical system placed very anteriorly.

Remarks. This is the first record of a pre-Eocene *Prenaster*. *Prenaster* contains numerous nominal species, many of which are virtually indistinguishable from one another. Indeed, several names have been erected for species with petals of equal length and

strongly divergent anterior petals (*P. alpinus*, *P. arabicus*, *P. jutieri*, *P. oviformis*). Inspection of type material may show all these species to be synonymous.

Genus MAURITANASTER Lambert, 1920b

[Type species *Mauritanaster gentili* Lambert, 1920b, by OD]

Diagnosis. Low ovate test with broad upper and lower surfaces. Paired ambulacra form long, almost flush, subequal petals reaching most of distance to ambitus. Anterior petals widely divergent. Long labral plate. Apical system ethmolytic with four gonopores. Mouth hardly labiate. Peripetalous fasciole passes beyond ends of petals. Coarse, heterogeneous tuberculation.

Remarks. Easily recognized by its long, straight, superficial petals and coarse tuberculation.

Mauritanaster gentili Lambert, 1920b

(Figure 3.55)

?1902 *Micraster* sp. Quaas, p. 165, pl. 31, figs 18-19.
1920b *Mauritanaster gentili* Lambert, p. 22, pl. 2, figs 12-13.
1932 *Mauritanaster gentili* Lambert, p. 54, pl. 2, figs 19-20.
1957 *Mauritanaster gentili* Lambert; Gauthier, p. 96, 103, 105, 108, 110, 113, 122.

Occurrence. Upper Thanetian of Morocco (Lambert 1920b, 1932; Gauthier 1957) (MNHN). ?Danian Dakhla Formation of Egypt (Quaas 1902).

Diagnosis. Low test with broad, shallow frontal groove. Large teardrop shaped periproct accounts for 32-42% of test height.

Remarks. *Micraster* sp. Quaas is based on an internal mould of a spatangoid with a broad, shallow frontal notch and long, subequal petals. Although strictly speaking indeterminate, the specimen is most similar in shape and general appearance to *Mauritanaster gentili*.

Mauritanaster mirabilis (Peron & Gauthier *in* Cotteau *et al.*, 1881)

(Plate 11, figures 8-11)

1881 *Hemiaster mirabilis* Peron & Gauthier *in* Cotteau *et al.*, p. 145, pl. 14, figs 1-5.

Occurrence. Maastrichtian of Constantine, Algeria (BMNH).

Remarks. Differs from *M. gentili* in lacking a frontal notch and in having a smaller periproct taking up only 25% of test height. In addition, *M. mirabilis* shows sexual dimorphism in gonopore size.

Mauritanaster konglell sp. nov.

Holotype. DGFMM 1937.194. One other specimen with no specimen number.

Occurrence. Mid to Late Danian Saltholm Limestone of Denmark (DGFMM).

Diagnosis. Ovoid test with truncate anterior and posterior. Very shallow, broad frontal groove traceable to peristome. Highest posteriorly. Paired ambulacra form slightly depressed, straight, rudimentary petals. Anterior petals diverge at 155 degrees. Very short labrum. Peristome semicircular and non-labiate. Narrow marginal fasciole runs just above periproct.

Remarks. Distinguished from *M. gentili* and *M. mirabilis* by its more rudimentary, less sunken paired petals and lower peripetalous fasciole.

Genus BRISASTER Gray, 1855

[Type species *Brissus fragilis* Düben & Koren, 1844, by OD]

Diagnosis. Paired ambulacra unequal in length. Anterior pair flexuous distally. Apical system ethmolytic with three gonopores. Peripetalous fasciole. Latero-anal fasciole present in juveniles and absent in adults.

Remarks. Most similar to *Tripylus*, *Abatus* and *Pseudolinthia* but differing from these genera by losing its latero-anal fasciole through ontogeny and in having less equal, more

flexuous petals. Differs additionally from *Tripylus* and *Pseudolinthia* in having anterior petals that reach the peripetalous fasciole and from Maastrichtian and Palaeocene species of *Abatus* in having three rather than two gonopores.

Brisaster micropetalus Markov, 1994

(Figure 3.56)

1994 *Brisaster micropetalus* Markov, p. 69, pl. 3, figs 2-4, text fig. 19.
1994 *Brisaster latus* Markov, p. 72, pl. 3, fig. 6, text fig. 19.
1994 *Neoproraster bajarunasi* Markov, p. 85, pl. 4, fig. 3, text fig. 24.

Occurrence. Danian to Thanetian of the Mangyshlak Peninsula, Kazakhstan (Markov 1994) (PI).

Diagnosis. Elongate test with sharp frontal notch and truncate posterior. Anterior ambulacrum bordered by vertical walls. Paired ambulacra petaloid. Anterior pair strongly flexuous, diverging at 70 degrees and 3-4 times longer than posterior. Labral plate short and broad. Apical system at 55-65% of test length from anterior margin. Non-perforate madreporite long and narrow. Peristome faces anteriorly.

Genus PSEUDOLINTHIA Markov, 1994

[Type species *Pseudolinthia triporata* Markov, 1994, by OD]

Diagnosis. Paired ambulacra form straight petals. Posterior pair about half as long as anterior. Apical system ethmolytic with three gonopores (madreporite not perforated). Peripetalous and latero-anal fascioles. Anterior petals do not reach peripetalous fasciole.

Remarks. See below for comparison to *Tripylus*. Differs from *Abatus* in having a shallower frontal notch, anterior petals that do not reach the peripetalous fasciole and a latero-anal fasciole even in large specimens. *Brisaster* differs in having flexuous anterior petals and a latero-anal fasciole that disappears during ontogeny. Differs from *Linthia* and *Paraster* in having only three gonopores and additionally from *Linthia* in having paired petals of unequal lengths.

Pseudolinthia triporata Markov, 1994

(Figure 3.57)

1994 *Pseudolinthia triporata* Markov, p. 80, pl. 4, fig. 1, text fig. 23.

1994 *Brisaster moskvini* Markov, p. 68, pl. 3, fig. 5, text fig. 19.

Occurrence. Danian of the Mangyshlak Peninsula, Kazakhstan (Markov 1994) (Pl).

Diagnosis. Test as broad as long with distinct frontal notch. Paired petals narrow and straight. Posterior pair approximately half length of anterior. Peripetalous fasciole distant from ends of anterior petals.

Remarks. *P. triporata* is very similar to Recent specimens referred to the genus *Tripylus*. Both have anterior petals that do not reach the peripetalous fasciole. Both have three gonopores in an ethmolytic apical system. However, *P. triporata* has narrow paired petals whilst species of *Tripylus* show sexual dimorphism with females having far more sunken petals forming marsupia in which juveniles are sheltered during development. Markov records over 30 specimens of *Pseudolinthia triporata*, all with narrow, shallow petals. It may be (but it seems unlikely) that all these specimens represent males of a sexually dimorphous species. Until "female" specimens are discovered *Pseudolinthia triporata* is best retained in its own genus.

Genus ABATUS Troschel, 1851

[Type species *Spatangus (Tripylus) carvernosus* Philippi, 1845, by OD]

Diagnosis. Unpaired ambulacrum subpetaloid. Paired ambulacra form deeply sunken broad petals. Anterior pair somewhat flexuous distally and reach peripetalous fasciole. Apical system with three (or less commonly two) gonopores. Latero-anal fasciole present in juveniles but absent in adults.

Remarks. *Abatus* is most similar to *Tripylus* but may be differentiated by having anterior petals which reach the peripetalous fasciole and by the loss of the latero-anal fasciole in adults. In addition, *Tripylus* has a less distinct frontal groove. Maastrichtian and Palaeocene specimens here assigned to *Abatus* have only two gonopores and are thus

easily distinguished from *Pseudolinthia*.

***Abatus*? *pseudoviviparus* (Lambert, 1933a)**

1933a *Tripylus pseudoviviparus* Lambert, p. 27, pl. 4, figs 1-7.

1933a *Tripylus antonibensis* Lambert, p. 28, pl. 4, figs 12-14.

Occurrence. Maastrichtian to Danian of northwest Madagascar (Lambert 1933a; Besairie 1971).

Diagnosis. Test with distinct frontal notch and subpetaloid unpaired ambulacrum. Paired ambulacra form broad, deeply sunken petals. Juveniles are preserved within the petals of some specimens. Anterior petals flexuous distally. Apical system with two gonopores. Latero-anal fasciole very narrow and sinuous; missing in largest specimens.

Remarks. In Lambert's original description, nothing is mentioned about the distance between the peripetalous fasciole and the ends of the anterior petals. In addition, Mortensen (1951, p. 276) claims that species of *Tripylus* always have three (rather than two) gonopores. These facts together with the presence of a distinct frontal notch and a narrow to non-existent latero-anal fasciole have led me to tentatively assign these specimens to *Abatus* rather than *Tripylus*.

Genus OPISSASTER Pomel, 1883

[Type species *Opissaster polygonalis* Pomel, 1883, by OD]

Diagnosis. Test ovate to hexagonal in horizontal outline. Highest between apical system and posterior. Paired ambulacra form well-developed bowed, sunken petals. Anterior petals two to three times longer than posterior. Short, broad labral plate. Apical disc ethmolytic with two gonopores (genital plates 2 and 3 are non-perforate). Peripetalous fasciole oval.

Remarks. Most similar in general appearance to *Hemiaster* from which it differs in having an ethmolytic apical system with only two gonopores.

KEY TO PALAEOCENE SPECIES

1 Distinct frontal notch at ambitus.....2

Frontal notch virtually absent at ambitus.....*O. elongatus*

2 Straight anterior petals; shallow broad frontal groove.....*O. schweinfurthi*

Strongly flexuous anterior petals; deep sharp frontal groove.....*O. somaliensis*

Opissaster elongatus (Duncan & Sladen, 1882b)

(Figure 3.58)

1882b *Hemiaster elongatus* Duncan & Sladen, p. 78, pl. 19, figs 7-15.

1943 *Hemiaster elongatus* Duncan & Sladen; Davies, p. 70.

Occurrence. Late Thanetian Upper Khairabad Limestone of the Ranikot Series, Pakistan (Duncan & Sladen 1882b; Davies 1943) (GSI).

Diagnosis. Test longer than wide; oval or hexagonal in horizontal outline with no frontal notch. Paired ambulacra form shallow, bowed petals. Anterior petals twice as long as posterior and flexuous distally, diverging at about 90 degrees. Apical disc at 55-60% of test length from the anterior margin. Apical system shows sexual dimorphism in gonopore size.

Remarks. Two species appear to be represented in the specimens assigned to *O. elongatus* in the collections of the Geological Survey of India. However, there are only five specimens in total and the two specimens which exhibit a more polygonal outline and slightly more anterior apical disc are much smaller than the remaining specimens. The differences could well represent intraspecific ontogenetic variations.

Easily distinguished from other species of *Opissaster* by its convex anterior margin and more posteriorly positioned apical system.

Opissaster schweinfurthi (de Loriol, 1883)

1883 *Hemiaster schweinfurthi* de Loriol, p. 34, pl. 8, figs 3-5.

1913 *Hemiaster schweinfurthi* de Loriol; Fourtau, p. 51.

?1933a *Distefanaster pygmeus* Lambert, p. 25, pl. 4, fig. 18.

1957 *Opissaster auraduensis* Kier, p. 876, pl. 105, figs 3-5, text-fig. 15a.

Occurrence. Palaeocene Lower Auradu Series of Somalia (Kier 1957). Lower Palaeocene of Tripolitania, Libya (BMNH). Late Thanetian of Egypt (de Loriol 1883; Fourtau 1913). ?Danian of eastern Madagascar (Lambert 1933a).

Diagnosis. Low domed profile. Narrow frontal groove extends from apex to peristome. Flexuous anterior petals diverge at 100 degrees and are about twice as long as posterior. Apical disc at mid-length. Peristome accounts for 20-25% of test width.

Remarks. Somali specimens referred to *O. auradensis* are somewhat lower in profile with narrower paired ambulacra and less divergent posterior petals. These differences are small, however, and fall close to the range of variation exhibited by de Loriol's types.

Distinguished from *O. somaliensis* by its lower profile, shallower frontal notch and larger mouth.

Opissaster somaliensis Currie, 1925

(Plate 13, figures 5-7)

1925 *Opissaster somaliensis* Currie, p. 71, pl. 10, figs 8-12, text-fig. 14.

1957 *Opissaster somaliensis* Currie; Kier, p. 877.

Occurrence. Palaeocene Lower Auradu Series of Somalia (Currie 1925; Kier 1957) (UGHM).

Diagnosis. Broad frontal groove is shallow adapically but deepens towards ambitus and peristome. Anterior paired petals very flexuous. Mouth occupies 10-15% of test width.

schizasterid gen. & sp. indet.

1949 *Linthia avilensis* Sanchez Roig, p. 264, pl. 32, figs 2-3.

1984 *Linthia? avillensis* Sanchez Roig; Kier, p. 72, pl. 40, figs 5-7.

Occurrence. Early Upper Maastrichtian of Cuba.

Remarks. Assigned to schizasterids on account of ethmolytic apical system and short, broad labral plate. Generic identification impossible, however, since number of gonopores and presence of fascioles uncertain.

Juvenile schizasterid

1987 *Linthia? breviusculus* (d'Orbigny); van der Ham *et al.*, p. 33.

1988 *Linthia? breviuscula* (d'Orbigny); van der Ham, p. 155, pl. 9, figs 6-8.

Occurrence. Danian Geulhem Chalk of the Maastricht area (van der Ham *et al.* 1987; van der Ham 1988) (NMM).

Remarks. Ethmolytic apical system allows placement within the schizasterids. However, as the gonopores have not opened and no tuberculation is preserved, generic identification is impossible. The small size of the specimen (8 mm long) suggests that this is a juvenile.

Family PERICOSMIDAE Lambert *in* Doncieux, 1905

Diagnosis. Petaloid paired ambulacra. Ethmolytic apical system with two to four gonopores. Peripetalous and marginal fascioles.

Genus KERTASTER Poslavskaya & Solovjev, 1964

[Type species *Kertaster termiri* Poslavskaya & Solovjev, 1964, by OD]

Diagnosis. Apical system with two gonopores - genital plates 1 and 4 perforated. Paired ambulacra form short, straight petals.

Kertaster termiri Poslavskaya & Solovjev, 1964

(Figure 3.59)

1934 *Kertaster termiri* Bajarunas (ms).

1964 *Kertaster termiri* Poslavskaya & Solovjev, p. 183, pl. 37, fig. 4, text fig. 230.

Occurrence. Thanetian of Mangyshlak, Kazakhstan (Poslavskaya & Solovjev 1964) (Pl).

Diagnosis. Broad, distinct anterior sulcus. Flat base and domed upper surface. Paired petals of approximately equal length. Anterior reach halfway to ambitus in plan view; posterior about a third of the distance to the ambitus. Apical system somewhat anterior.

Remarks. *Kertaster termiri* is the earliest recorded pericosmid. All other taxa referred to this family are from Eocene or younger strata.

Figure 3.48. Camera lucida drawings of *Linthia sudanensis* (Bather), BMNH EE2262, Thanetian Limestone of Niger; a, apical view; b, oral view; c, apical disc plating. a & b, scale bars = 2 mm. c, scale bar = 1 mm.

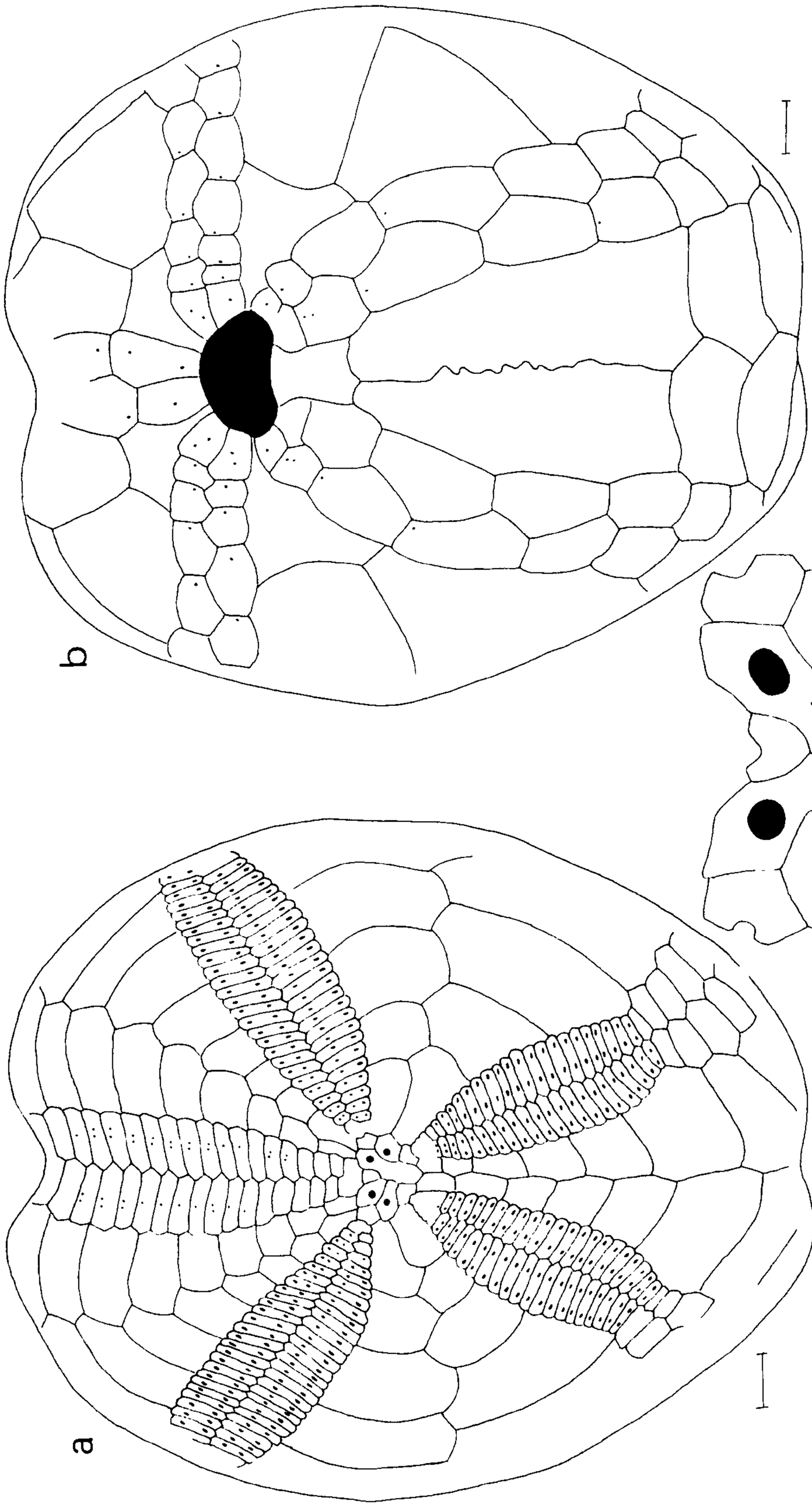
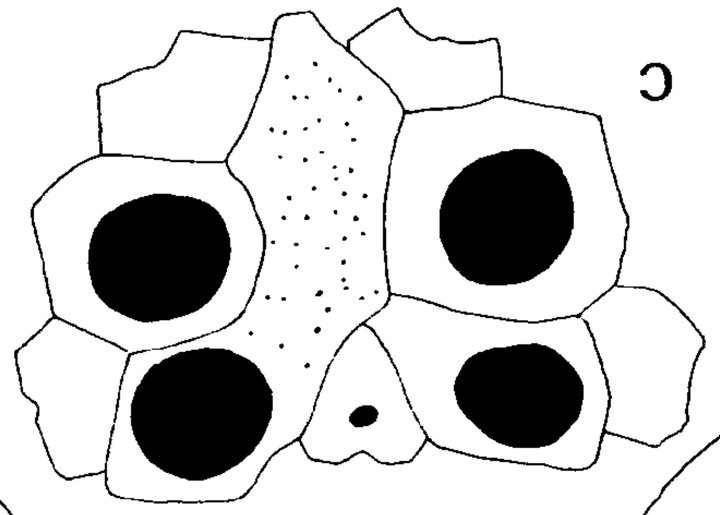
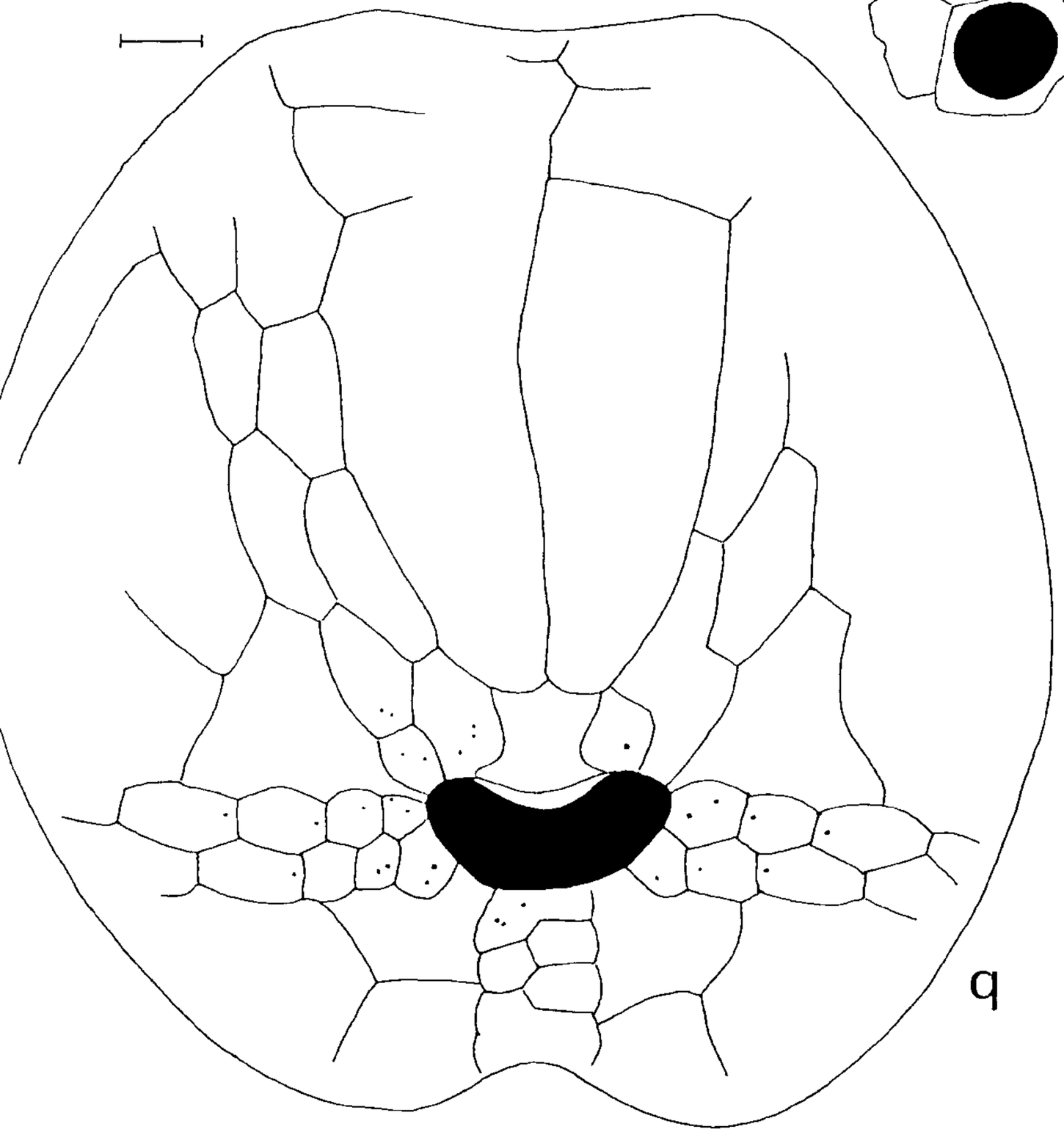

b
c
a

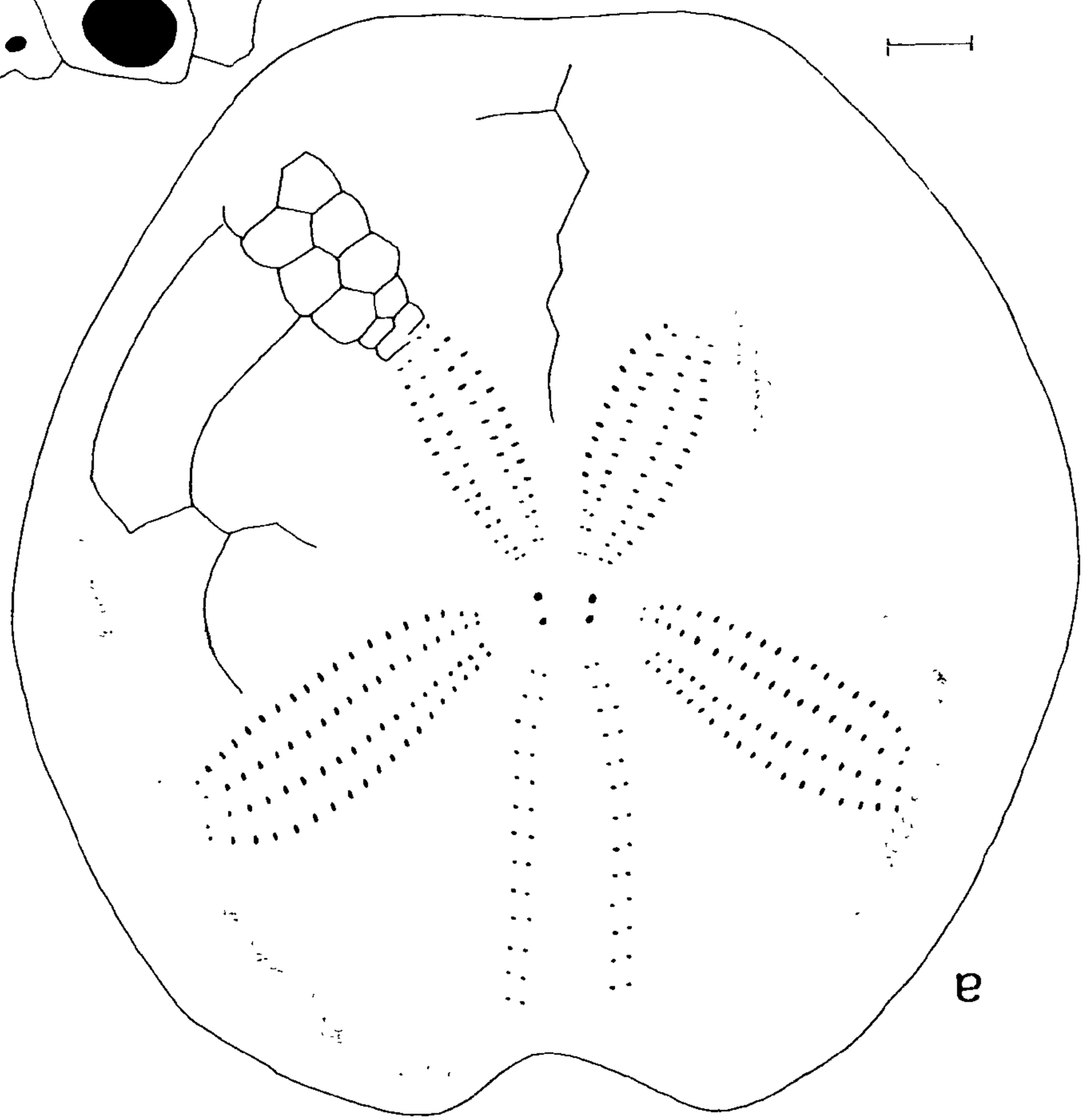
Figure 3.49. Camera lucida drawings of *Paraster indicus* (Duncan & Sladen), BMNH E20094, Danian of northwest Madagascar; a, apical view; b, oral view; c, apical disc plating. a & b, scale bars = 2 mm. c, scale bar = 1 mm.



c

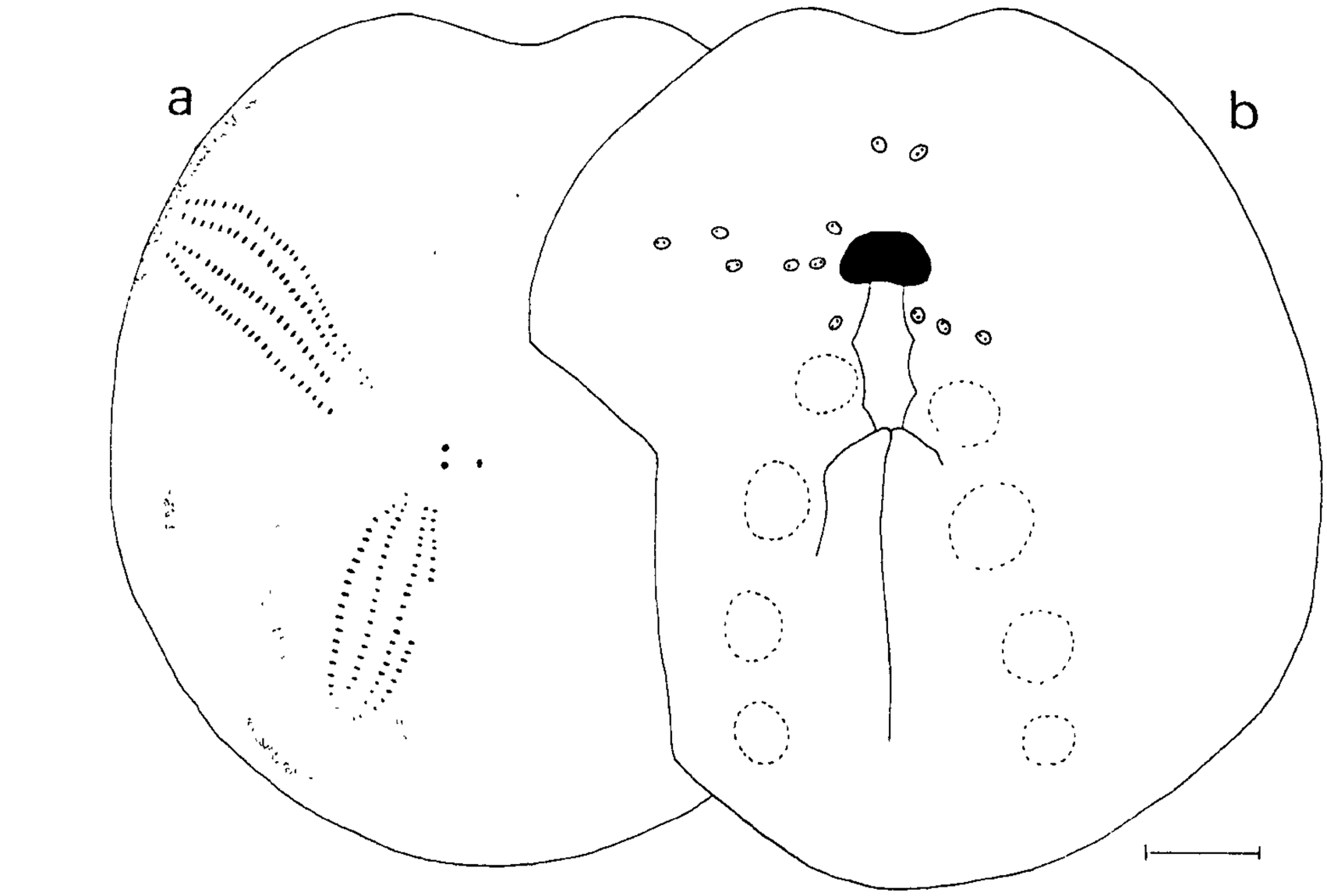


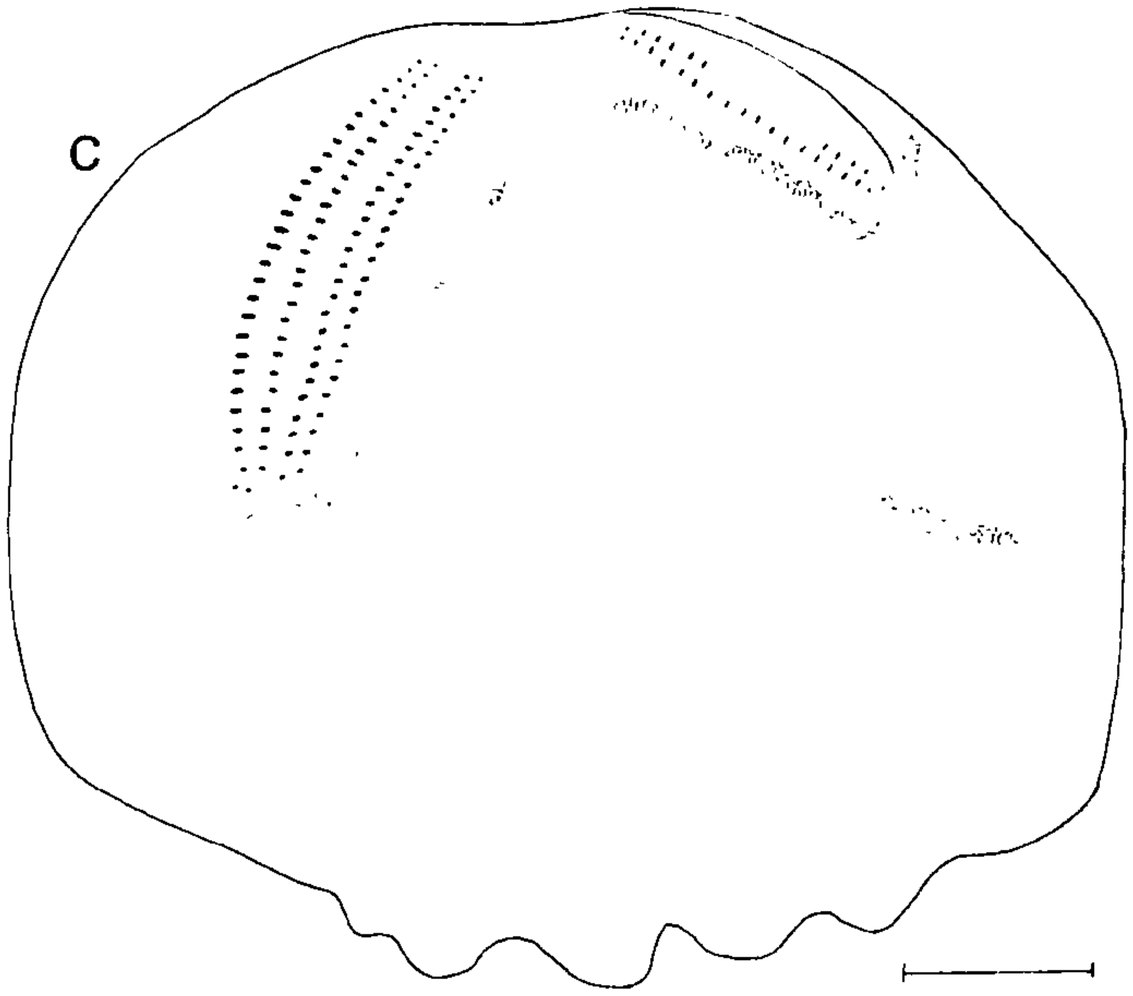
b



a

Figure 3.50. Camera lucida drawings of *Tessieria senegalensis* Gorodiski, MNHN R06304 (HOLOTYPE), Maastrichtian of Senegal; a, apical view; b, oral view; c, lateral view; d, apical disc plating. a-c, scale bars = 5 mm. d, scale bar = 1 mm.


a
b


c

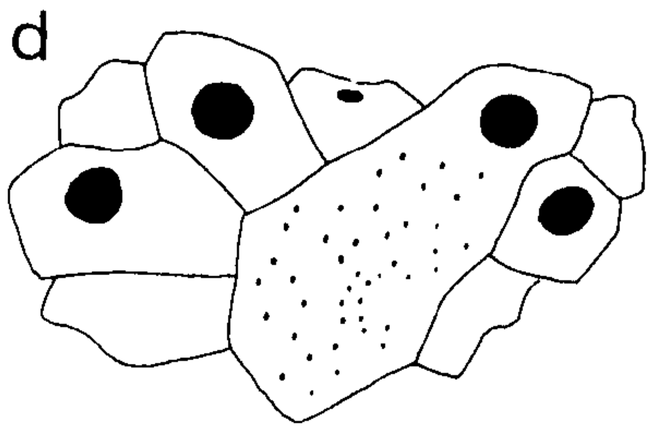
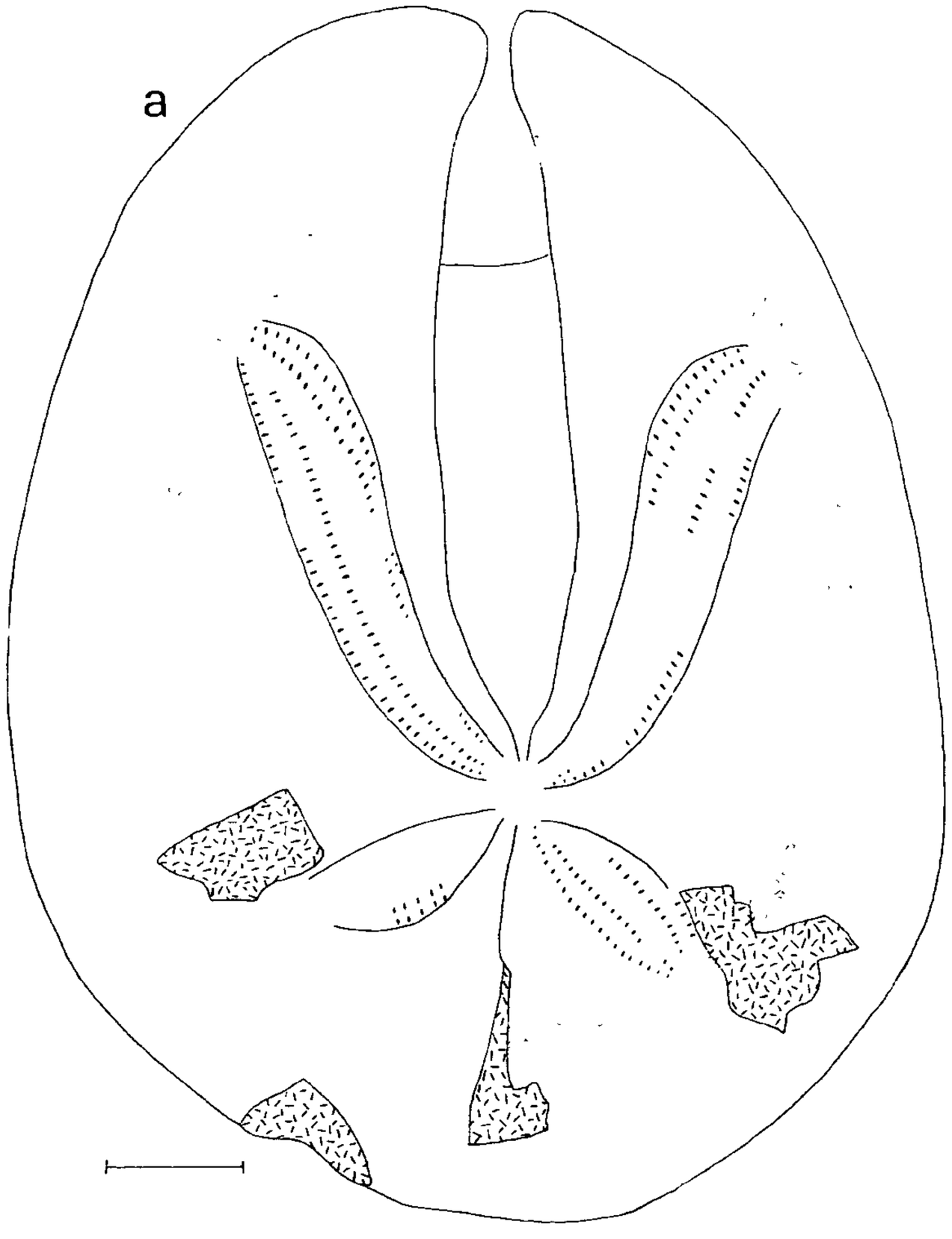
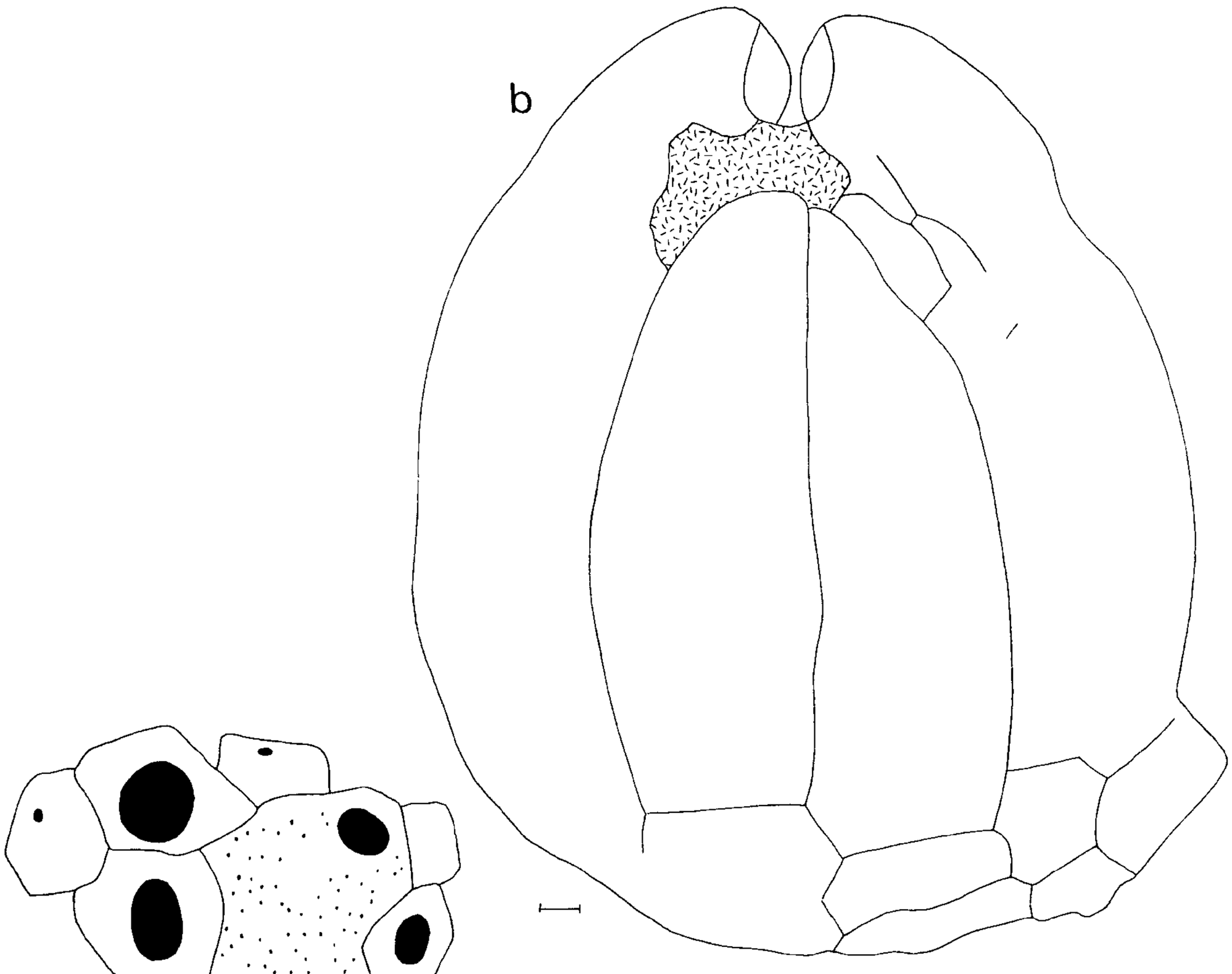

d

Figure 3.51. Camera lucida drawings of *Proraster geayi* Cottreau. a, URGM i45, Maastrichtian of Tripolitania, Libya, apical view. b, PI 4351/547, Upper Maastrichtian of Mangyshlak, Kazakhstan, oral view. c, MNHN R62301, Maastrichtian of eastern Madagascar, apical disc plating. a, scale bar = 5 mm. b, scale bar = 2 mm. c, scale bar = 1 mm.


a


b

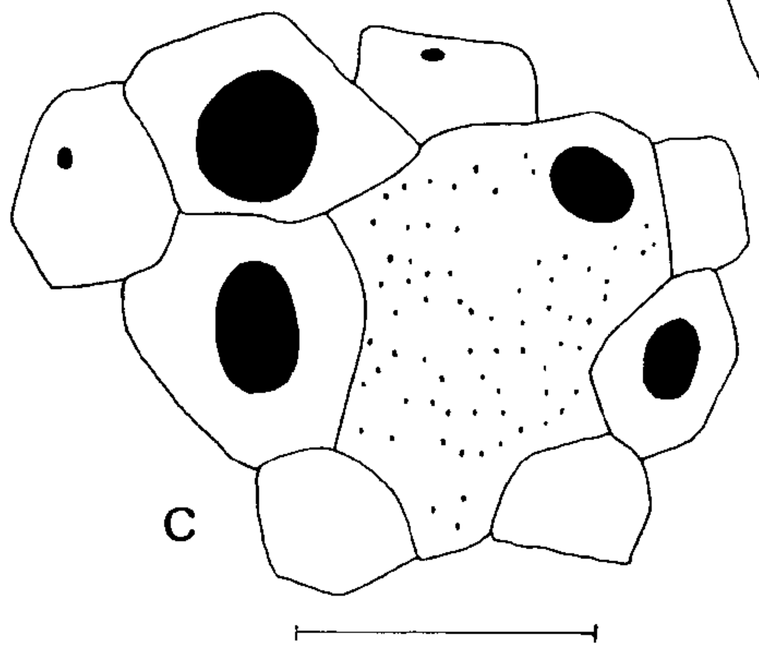
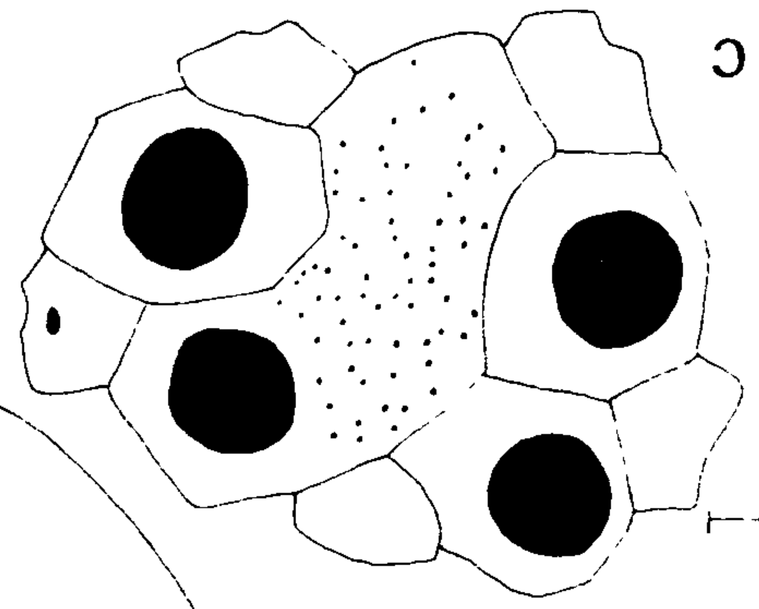
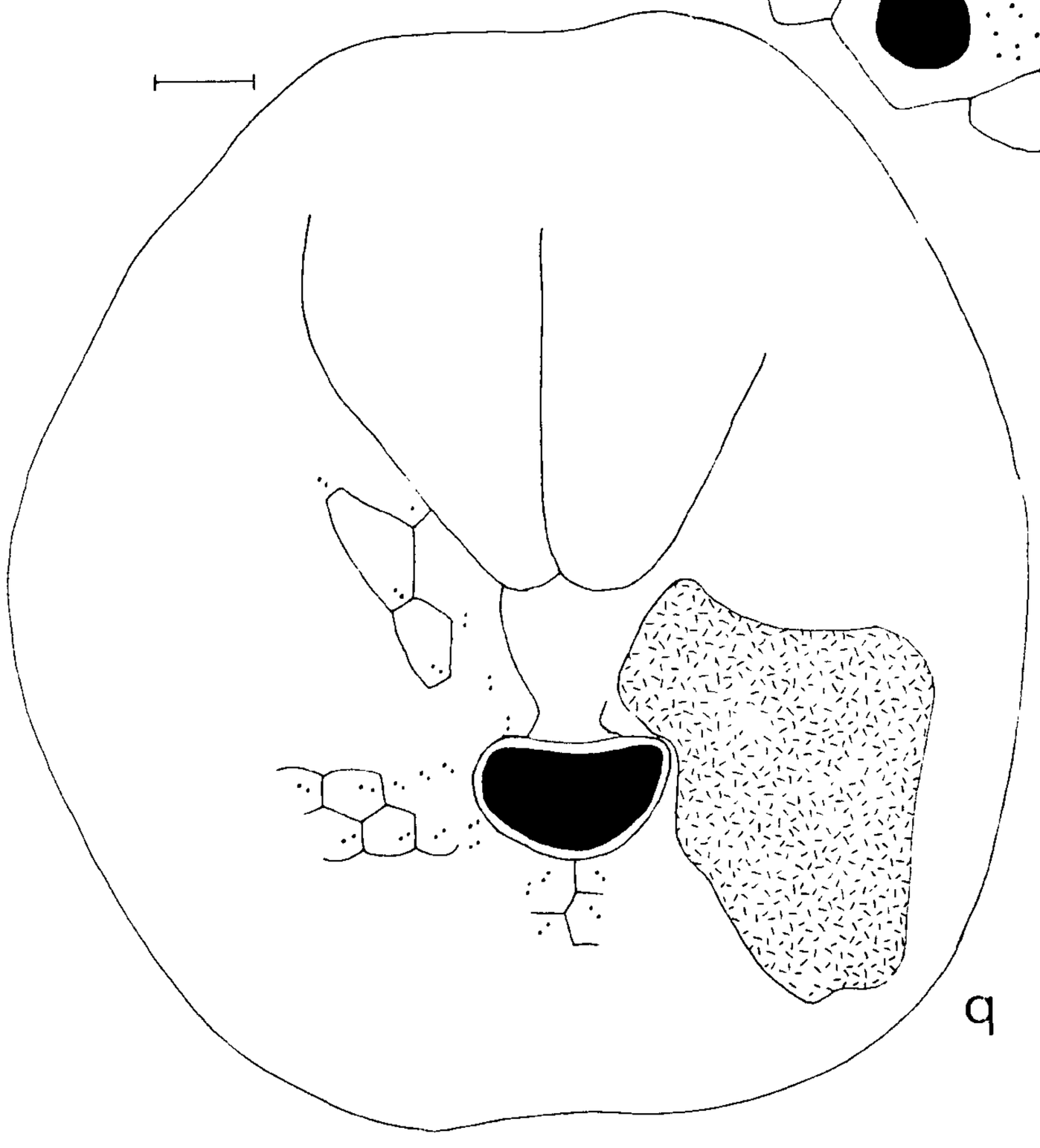

c

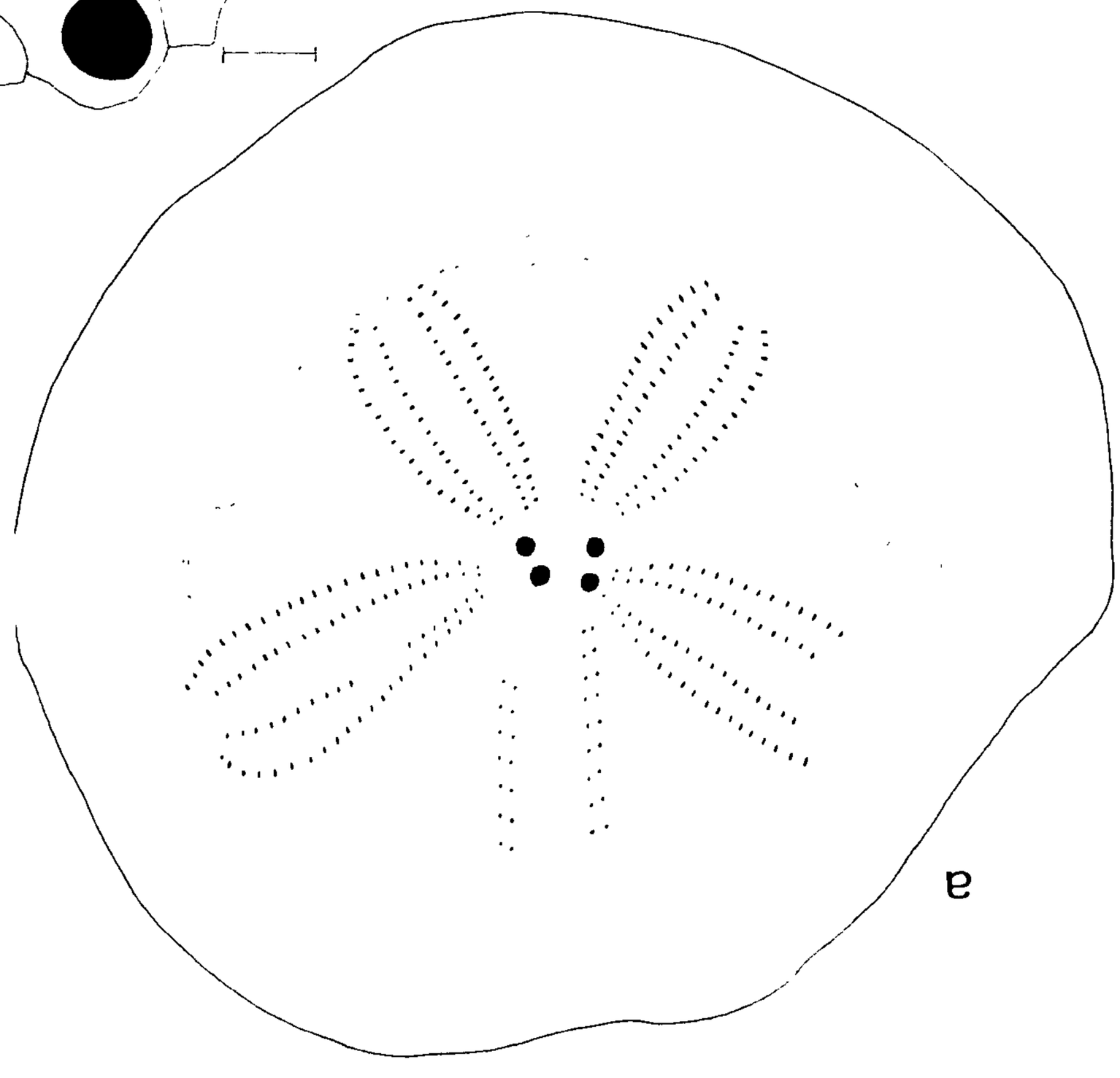
Figure 3.52. Camera lucida drawings of *Trachyaster oldhami* (Noetling), Maastrichtian of Baluchistan. a & b, GSI 3001 (PARATYPE); a, apical view; b, oral view. c, GSI 3000 (PARATYPE), apical disc plating. a & b, scale bars = 2 mm. c, scale bar = 1 mm.



c

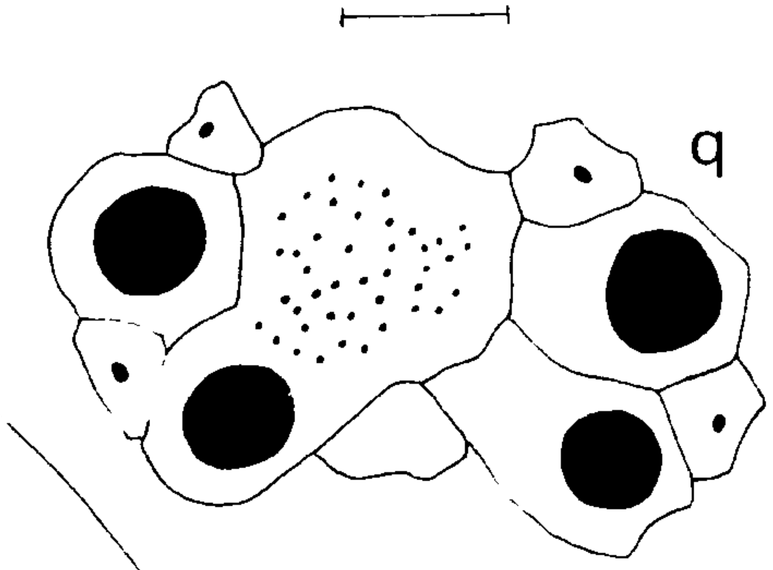


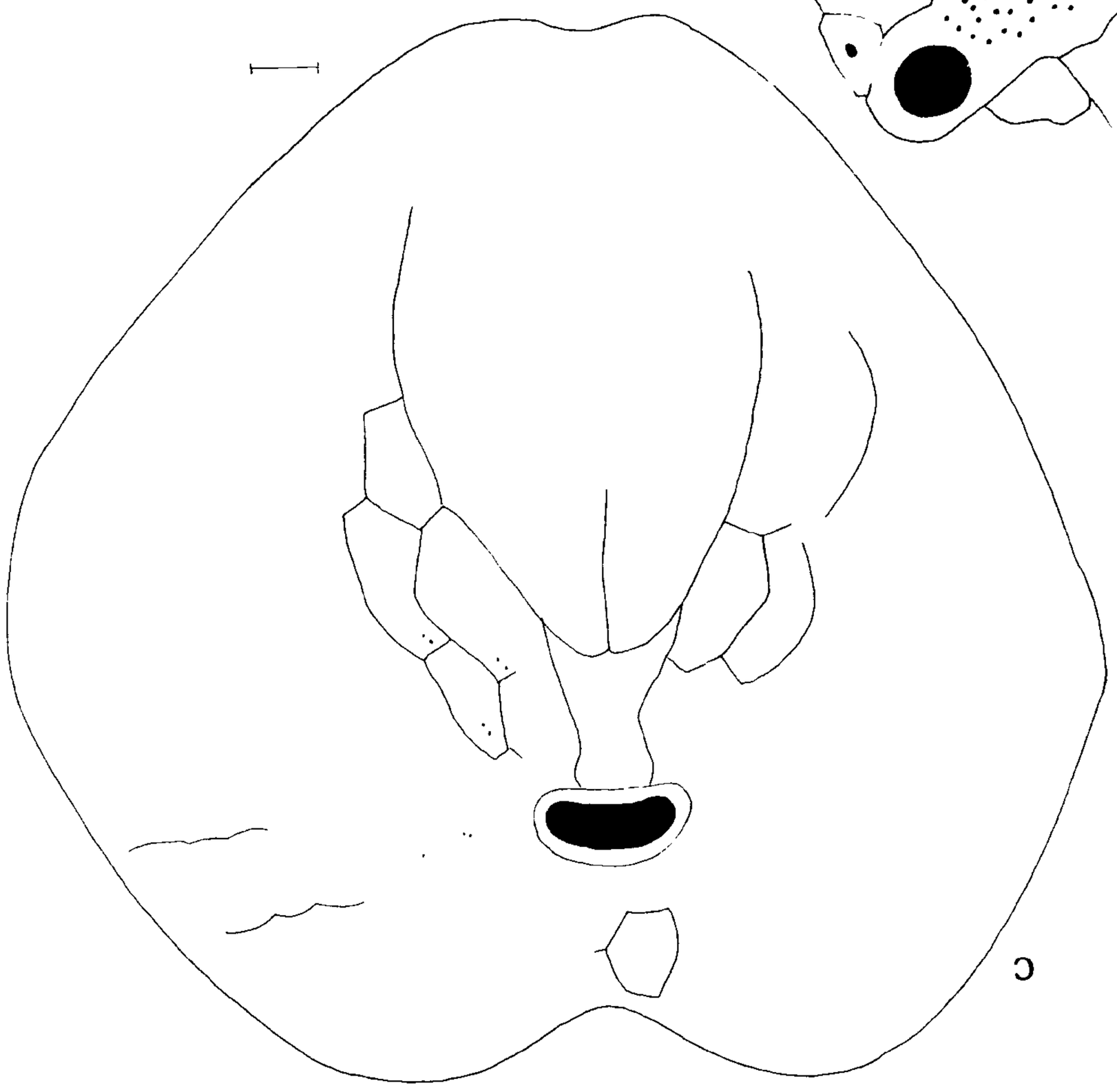
q



a

Figure 3.53. Camera lucida drawings of *Holcopneustes cristatus* (Stoliczka). a & b, MNHN no specimen number, Danian of northwest Madagascar; a, apical view; b, apical disc plating. c, GSI 1650 (PARATYPE), Maastrichtian Ariyalur Group of southern India, oral view. a, scale bar = 5 mm. b, scale bar = 1 mm. c, scale bar = 2 mm.


q


c

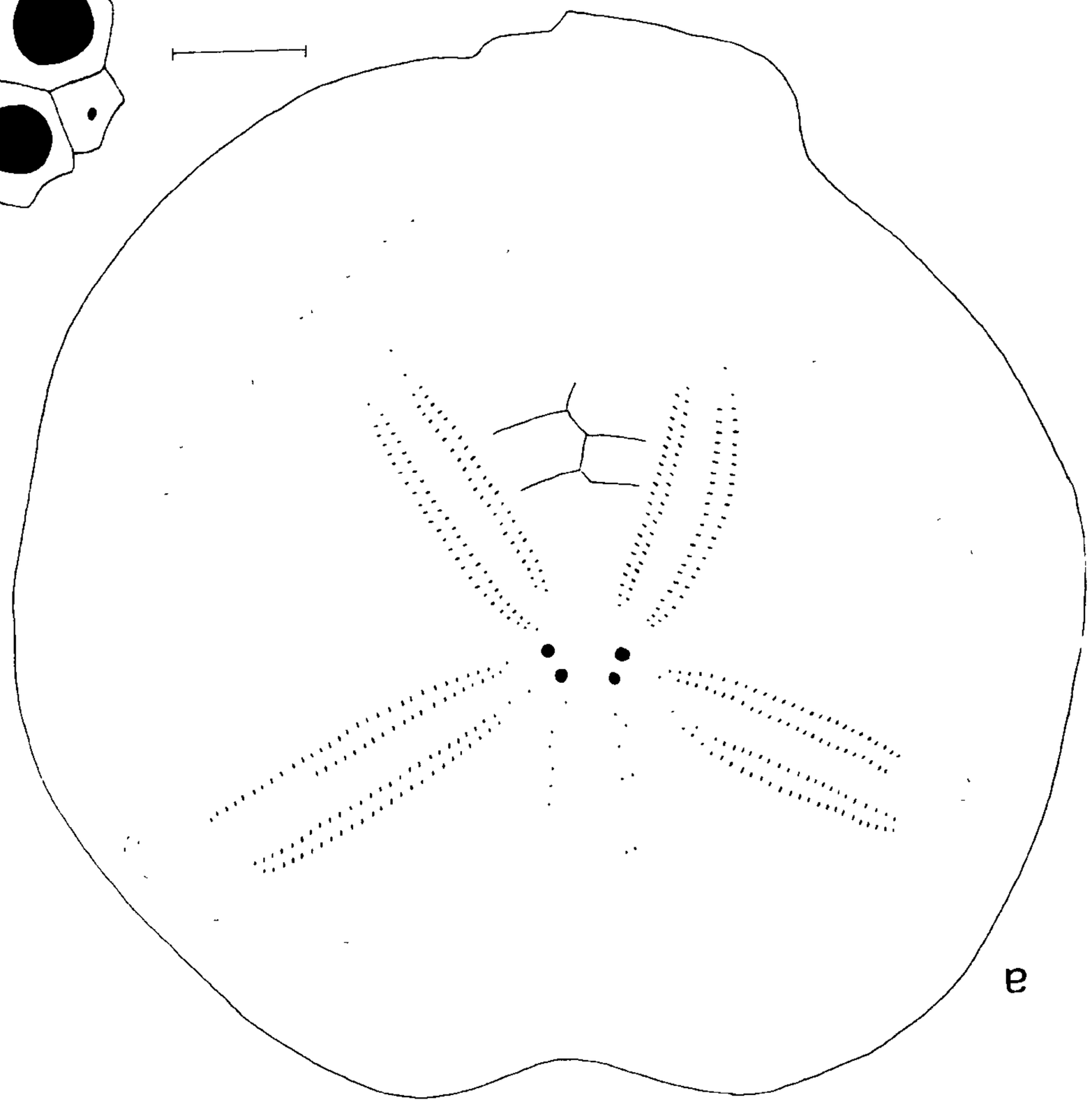
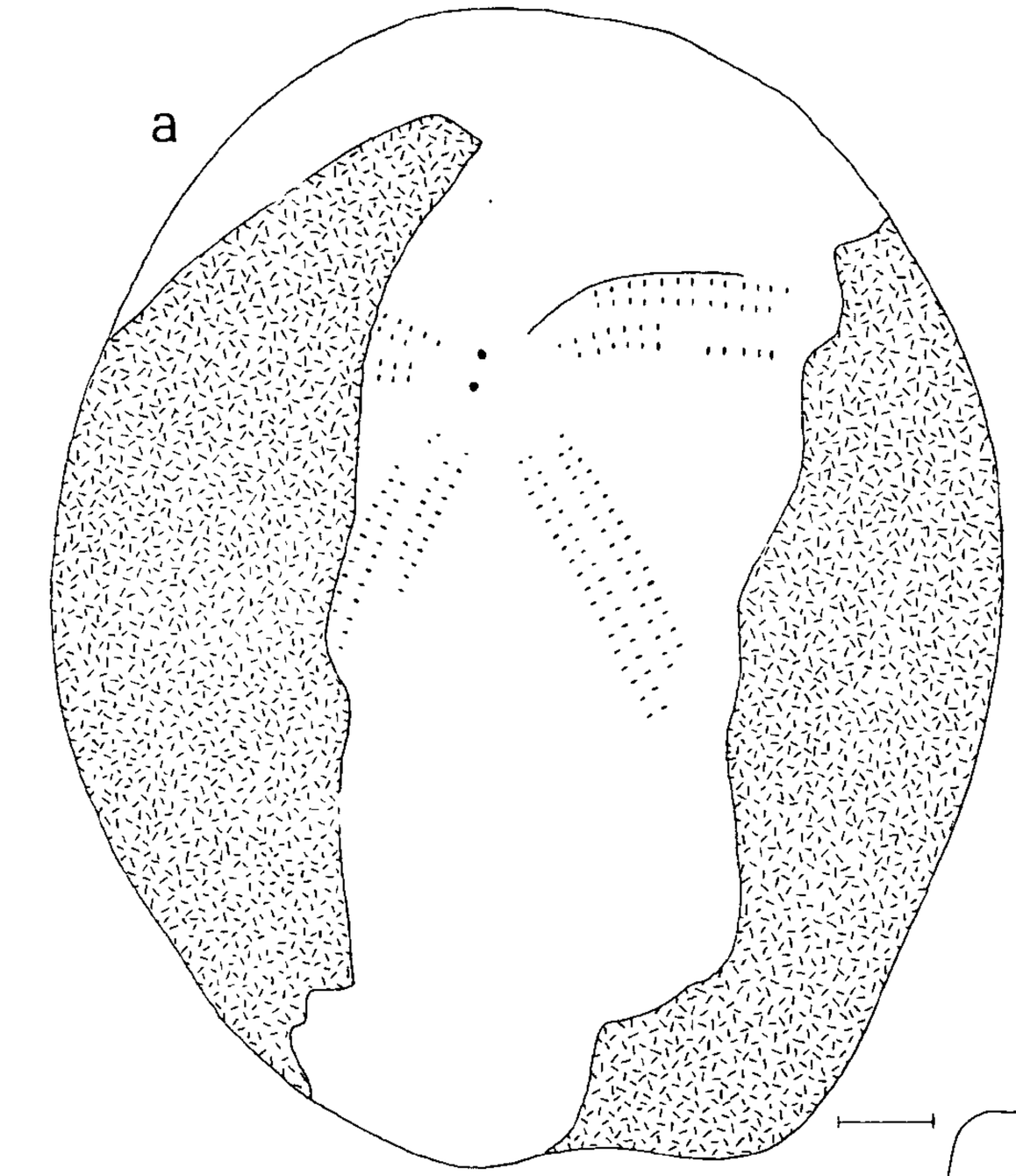
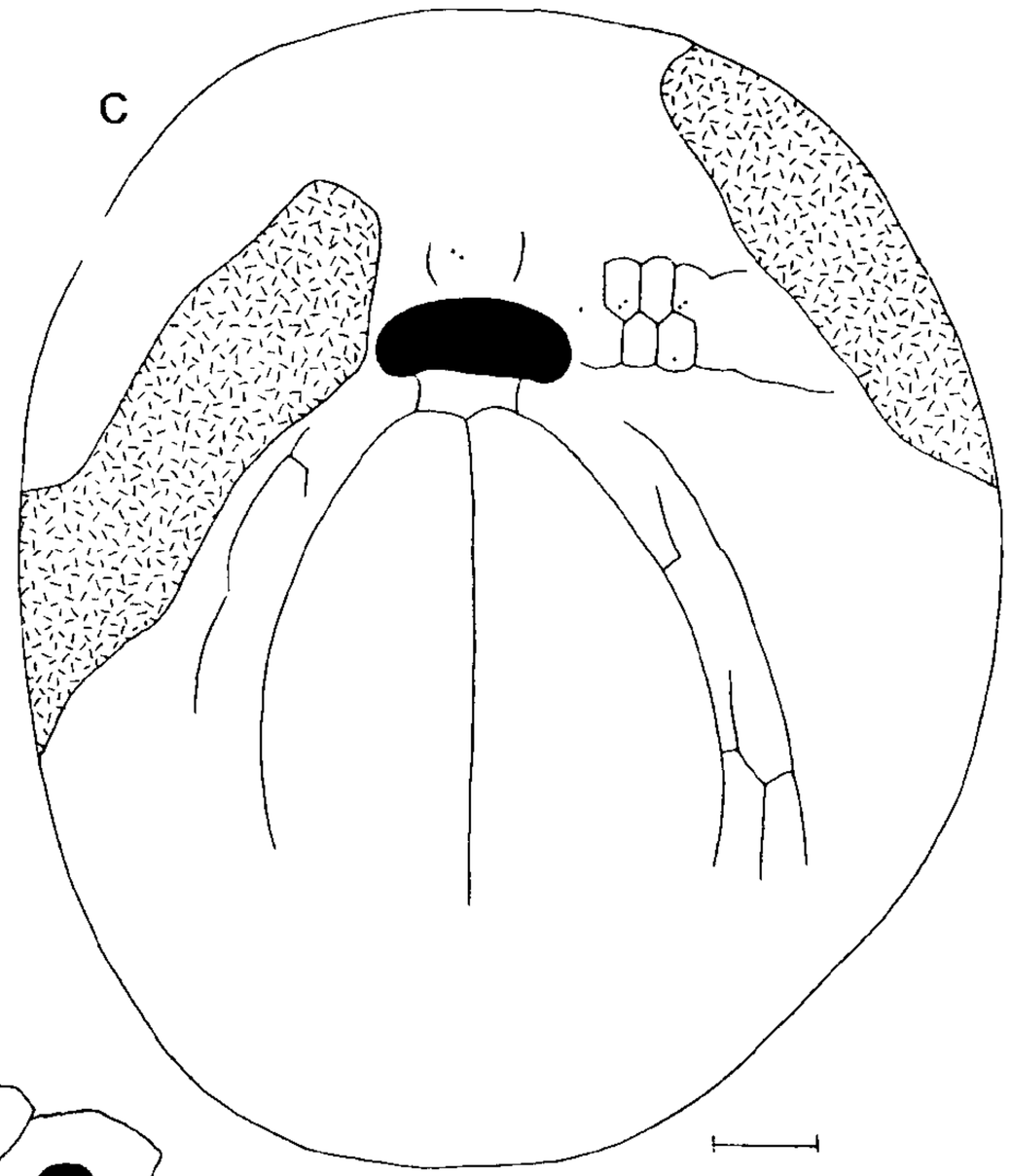
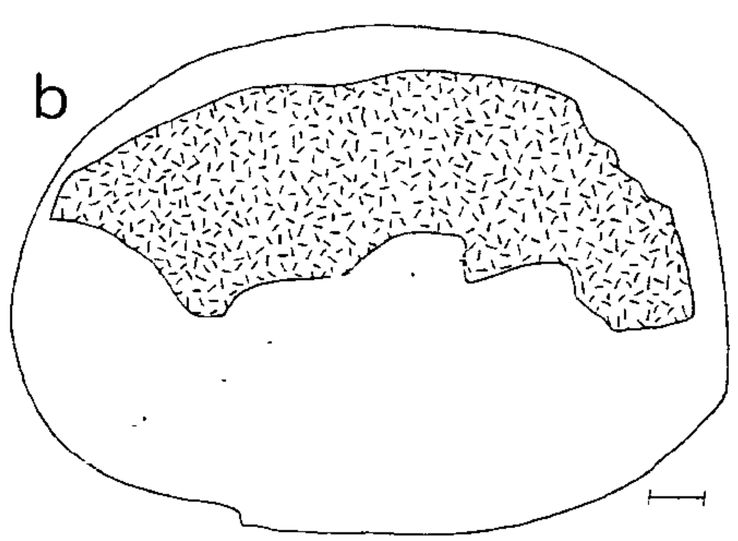
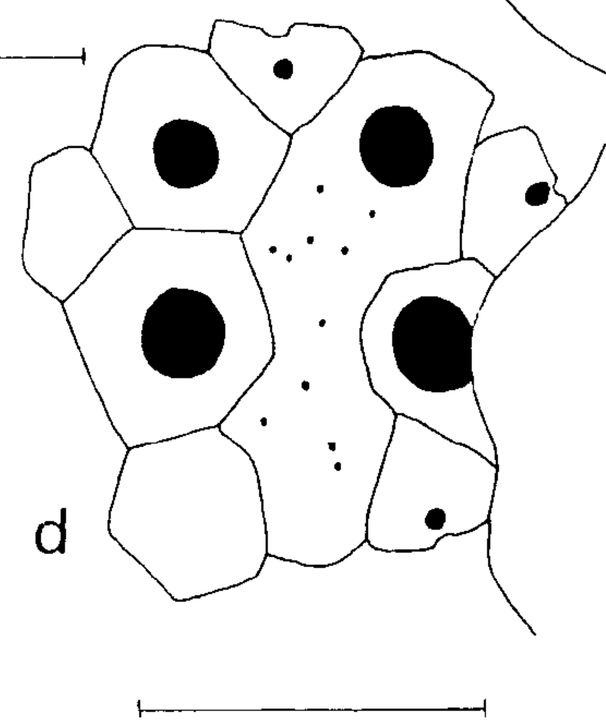

a

Figure 3.54. Camera lucida drawings of *Prenaster oviformis* Duncan & Sladen, Thanetian Ranikot Series of Pakistan. a & b, GSI 2572 (PARATYPE); a, apical view; b, lateral view. c-e, GSI 2573 (PARATYPE); c, oral view; d, apical disc plating; e, posterior view. a-c & e, scale bars = 2 mm. d, scale bar = 1 mm.


a


c


b


d

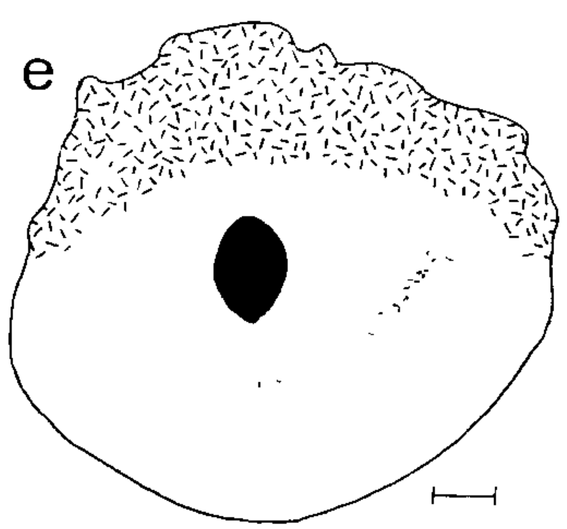
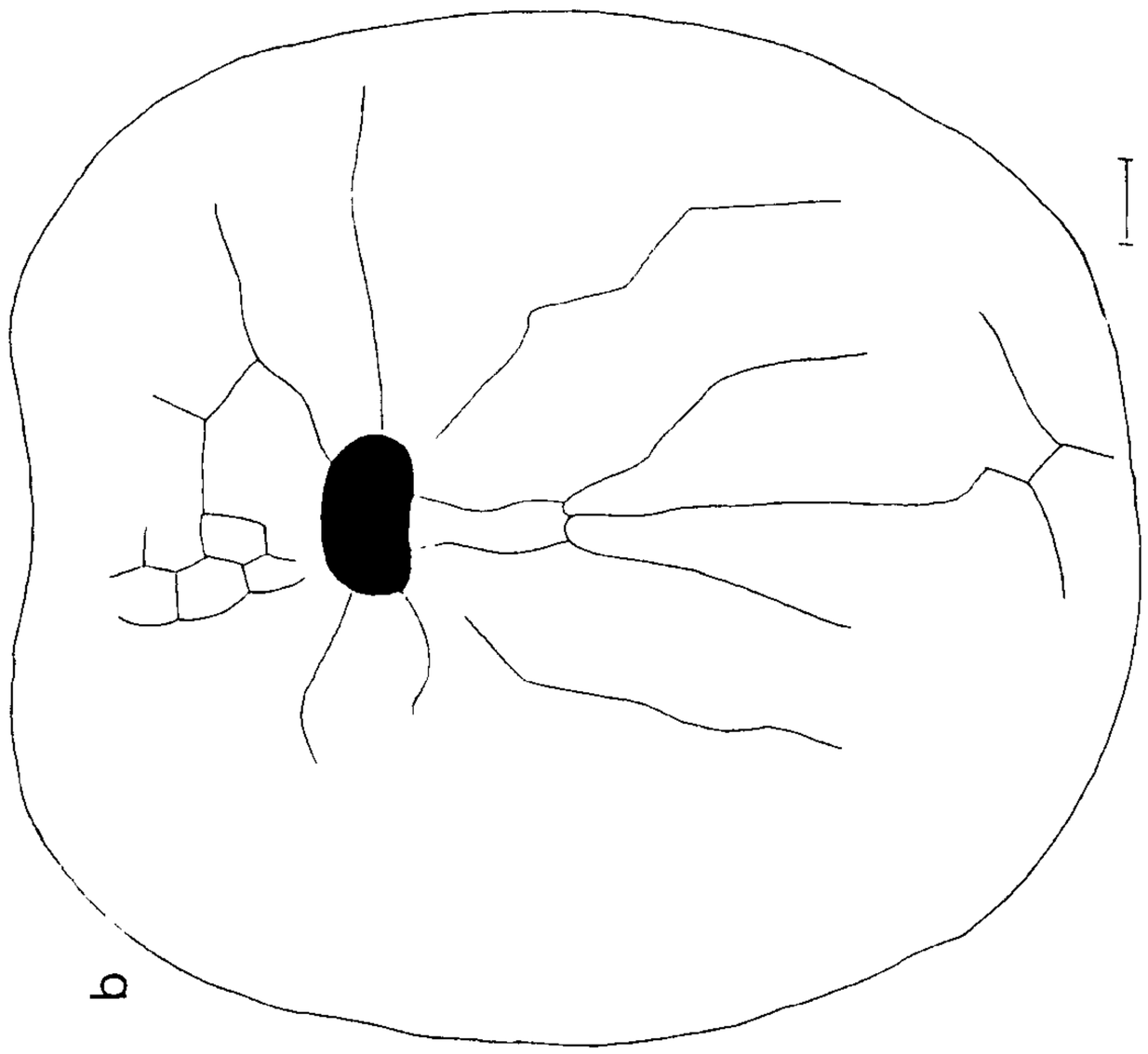
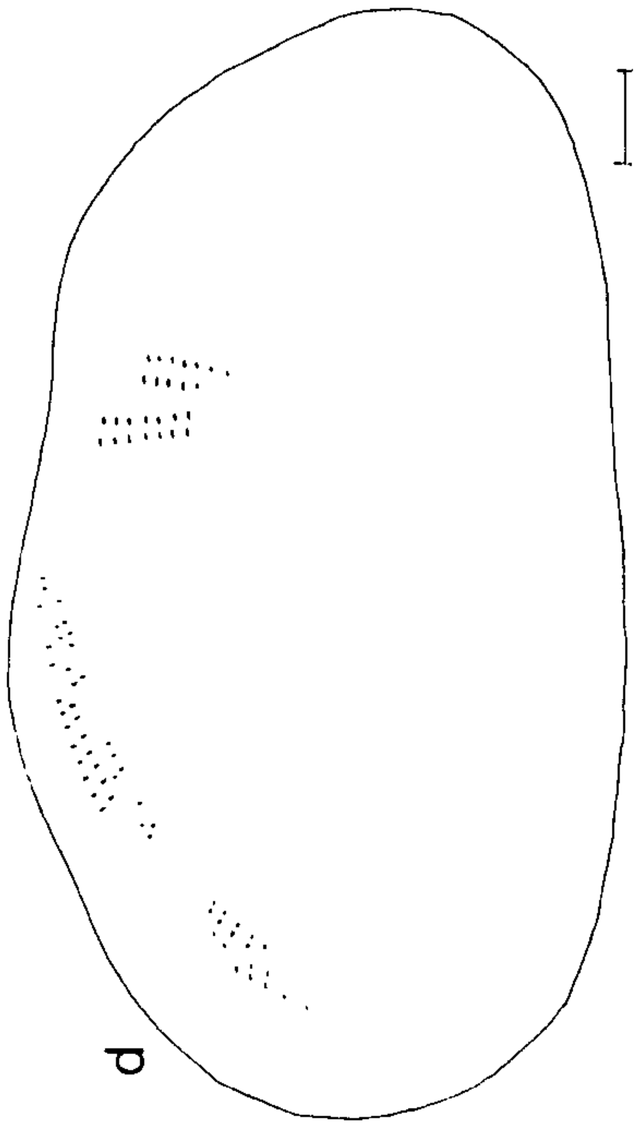

e

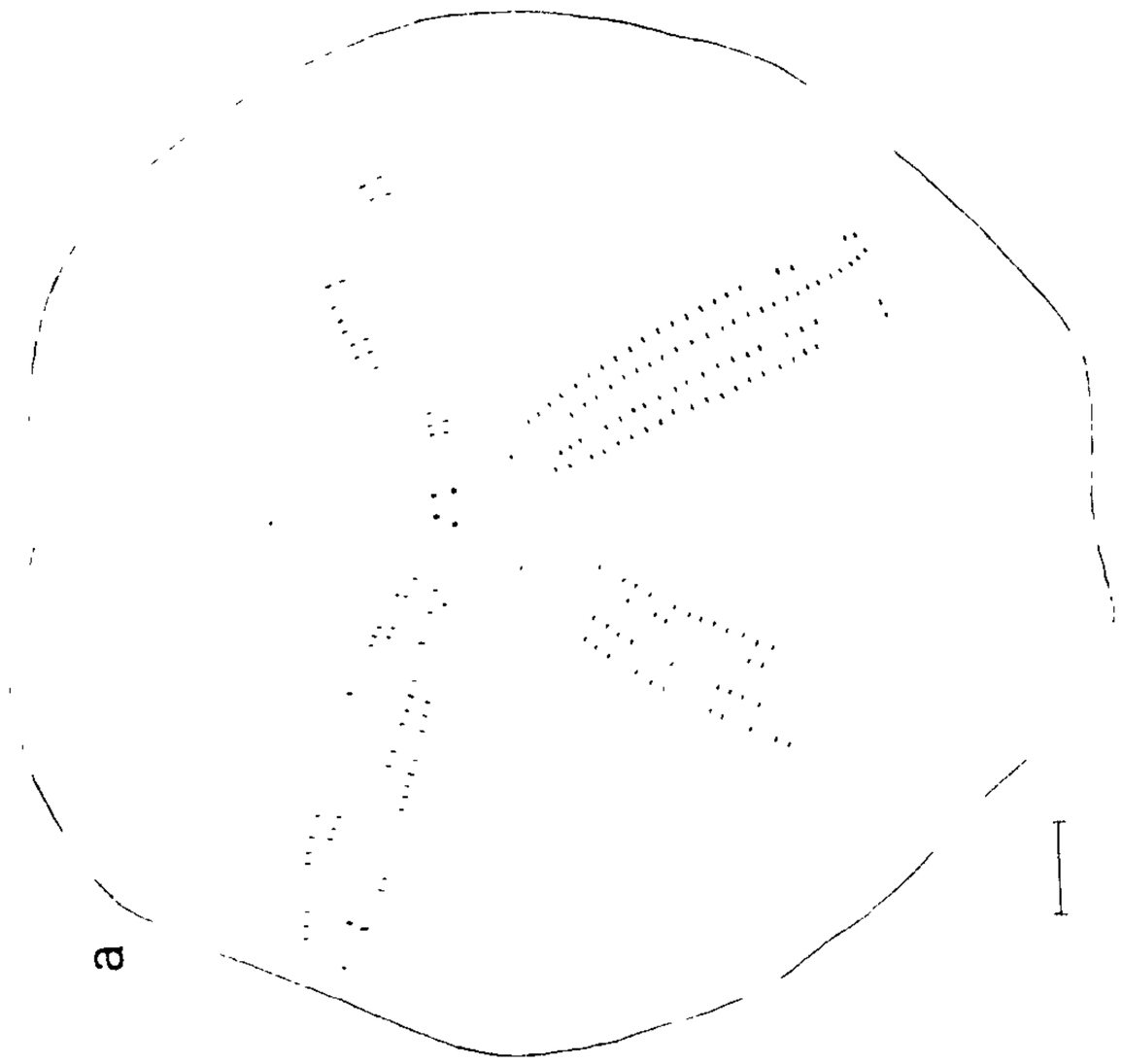
Figure 3.55. Camera lucida drawings of *Mauritanaster gentili* Lambert, MNHN no specimen number, Thanetian of Morocco; a, apical view; b, oral view; c, apical disc plating; d, lateral view. a, b & d, scale bars = 3 mm. c, scale bar = 1 mm.



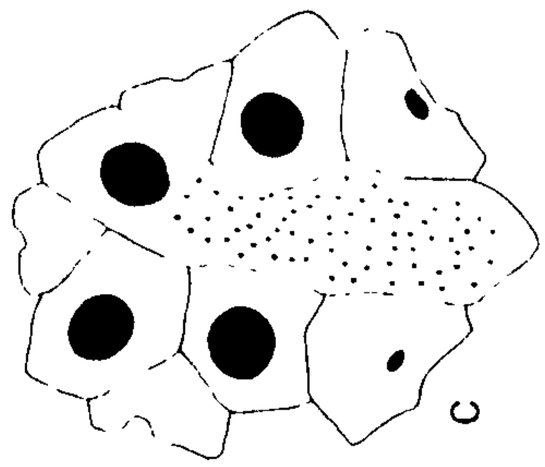
b



d

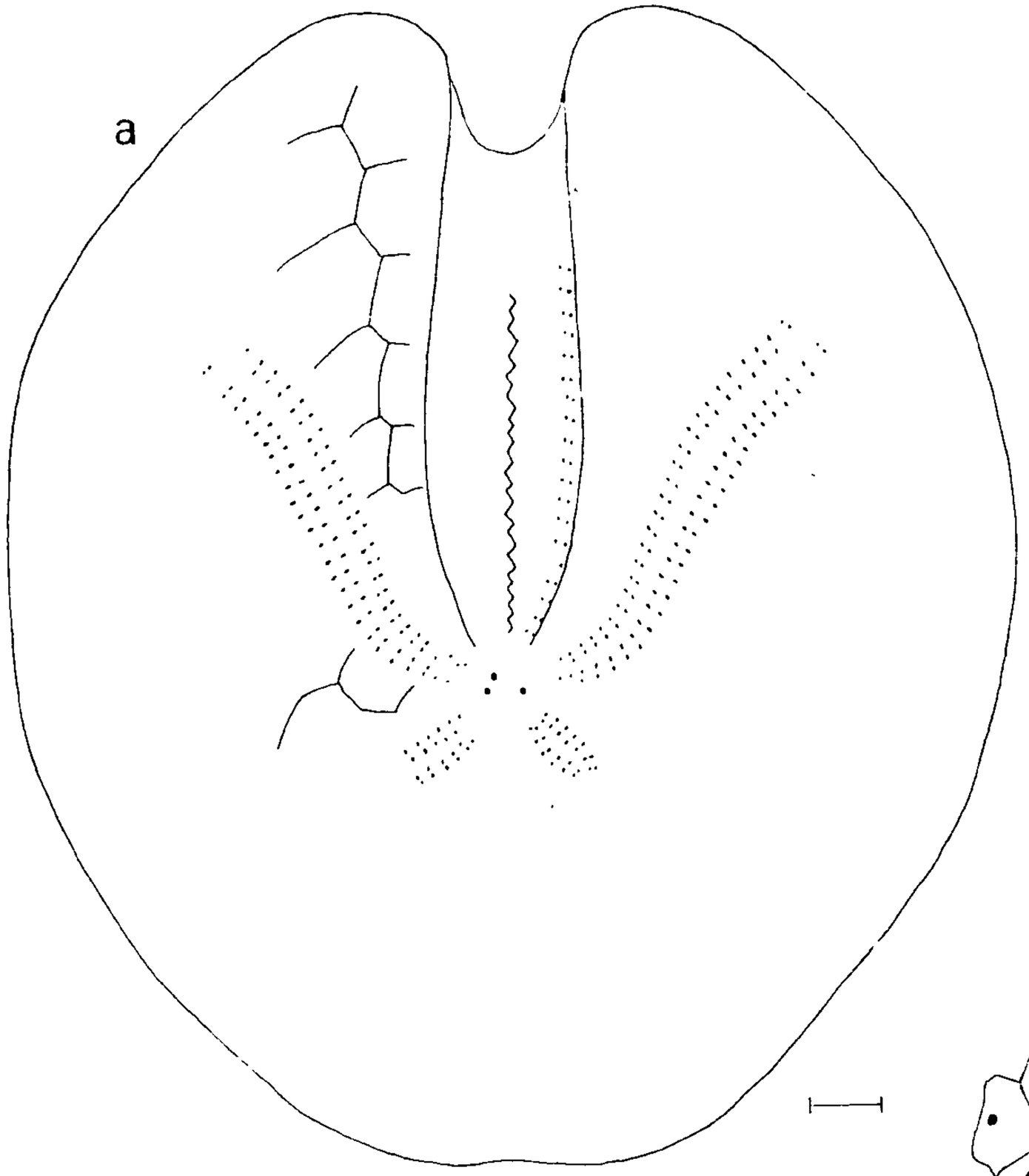


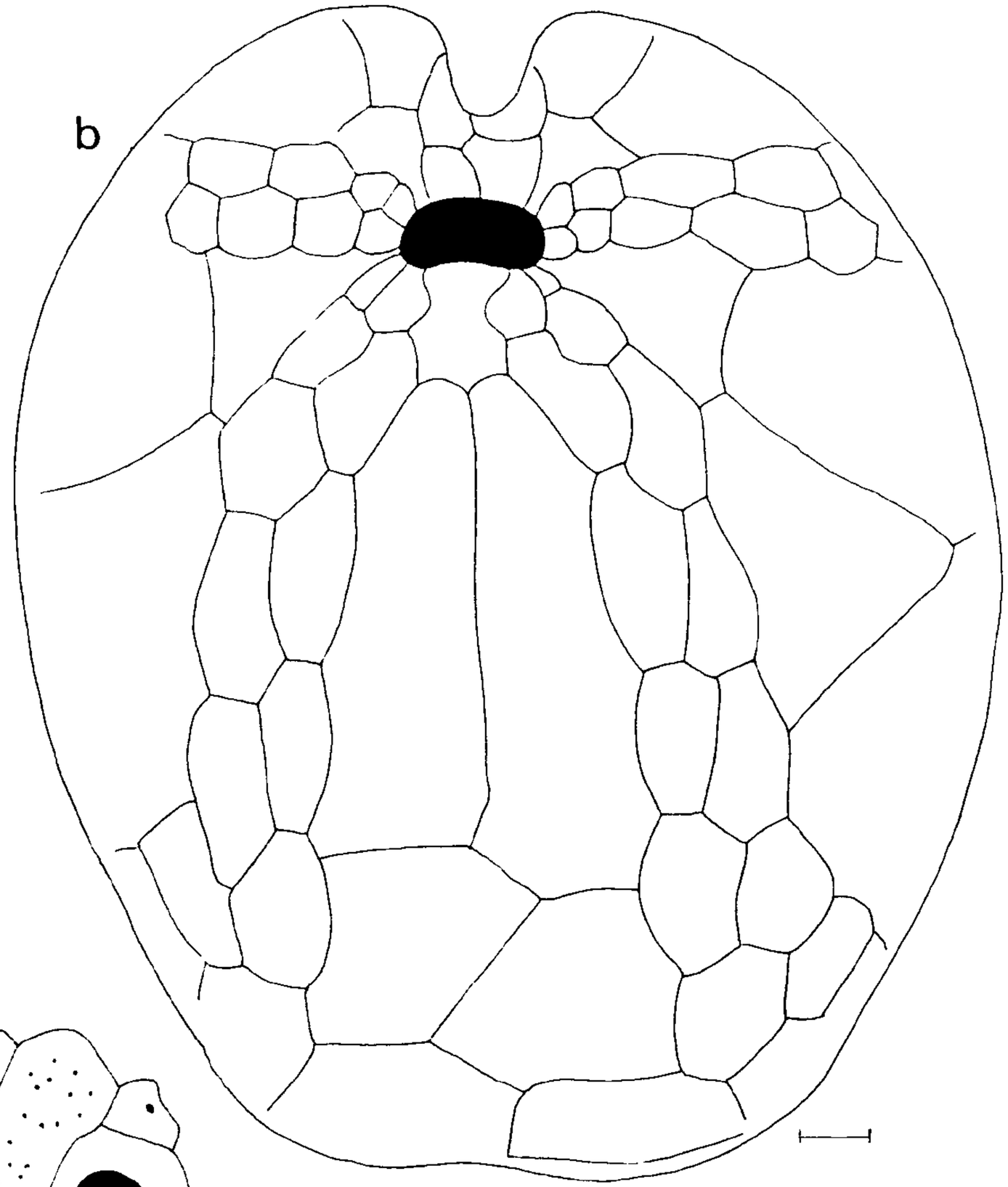
a



c

Figure 3.56. Camera lucida drawings of *Brisaster micropetalus* Markov. a, PI 4351/388, Thanetian of Mangyshlak, Kazakhstan, apical view. b & c, PI 4351/330, Danian of Mangyshlak, Kazakhstan; b, oral view; c, apical disc plating. a & b, scale bars = 2 mm. c, scale bar = 1 mm.


a


b

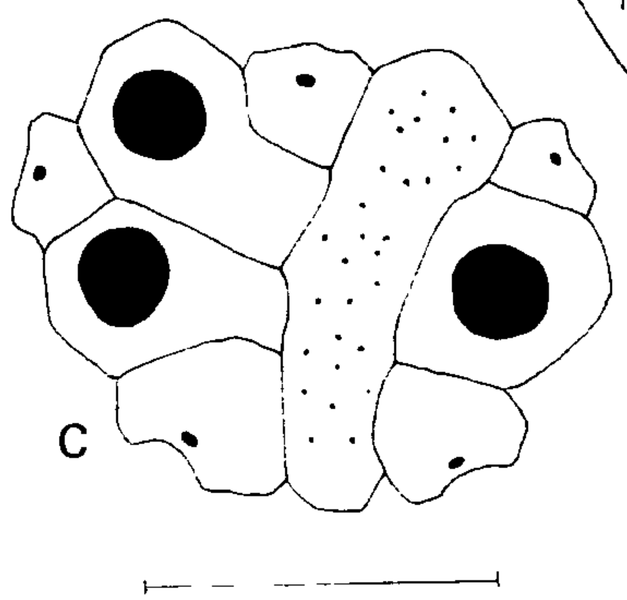

c

Figure 3.57. Camera lucida drawings of *Pseudolinthia triporata* Markov, PI 4351/362 (HOLOTYPE), Danian of Mangyshlak, Kazakhstan; a, oral view; b, apical disc plating; c, apical view. a & c, scale bars = 5 mm. b, scale bar = 1 mm.

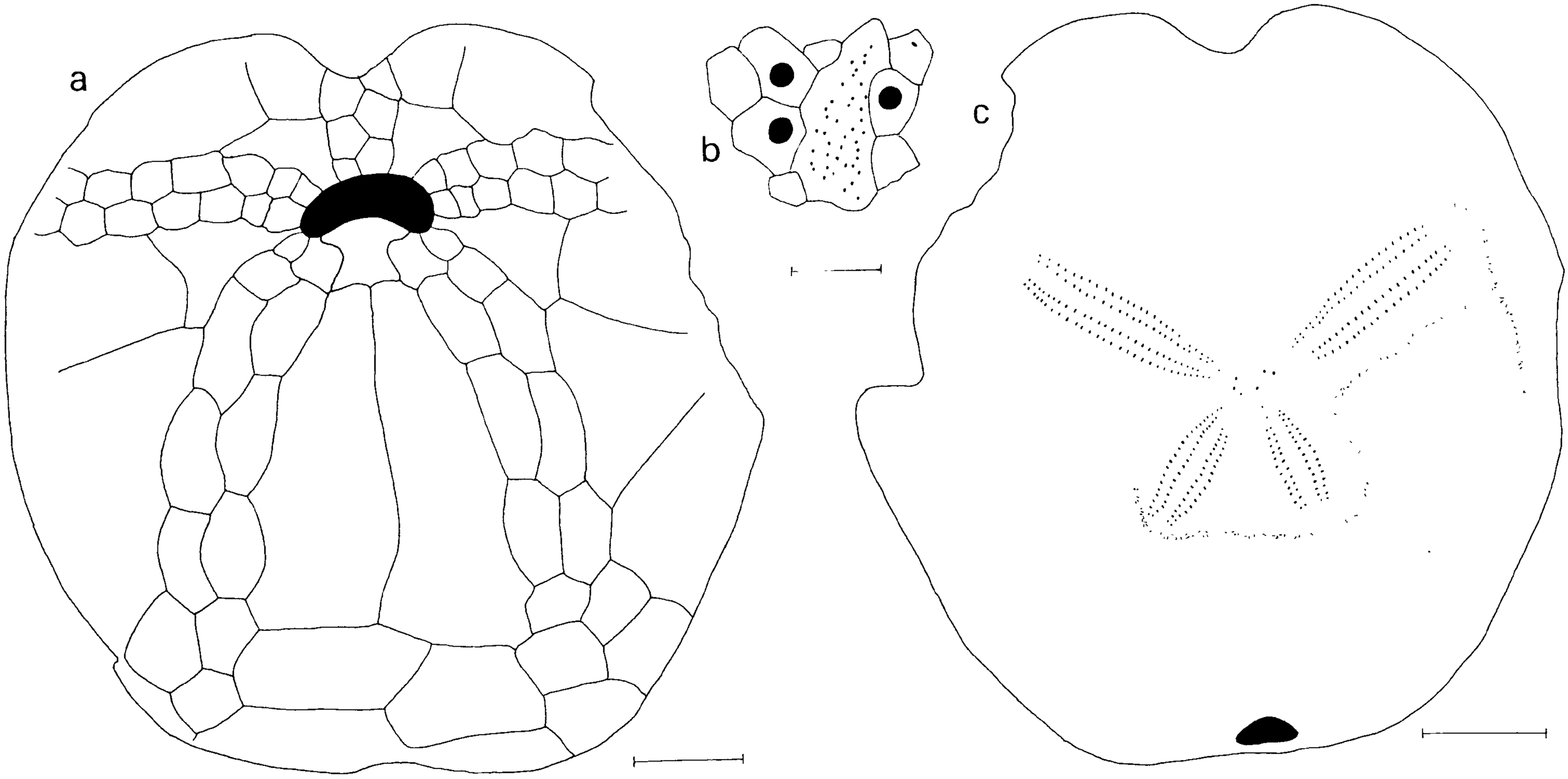
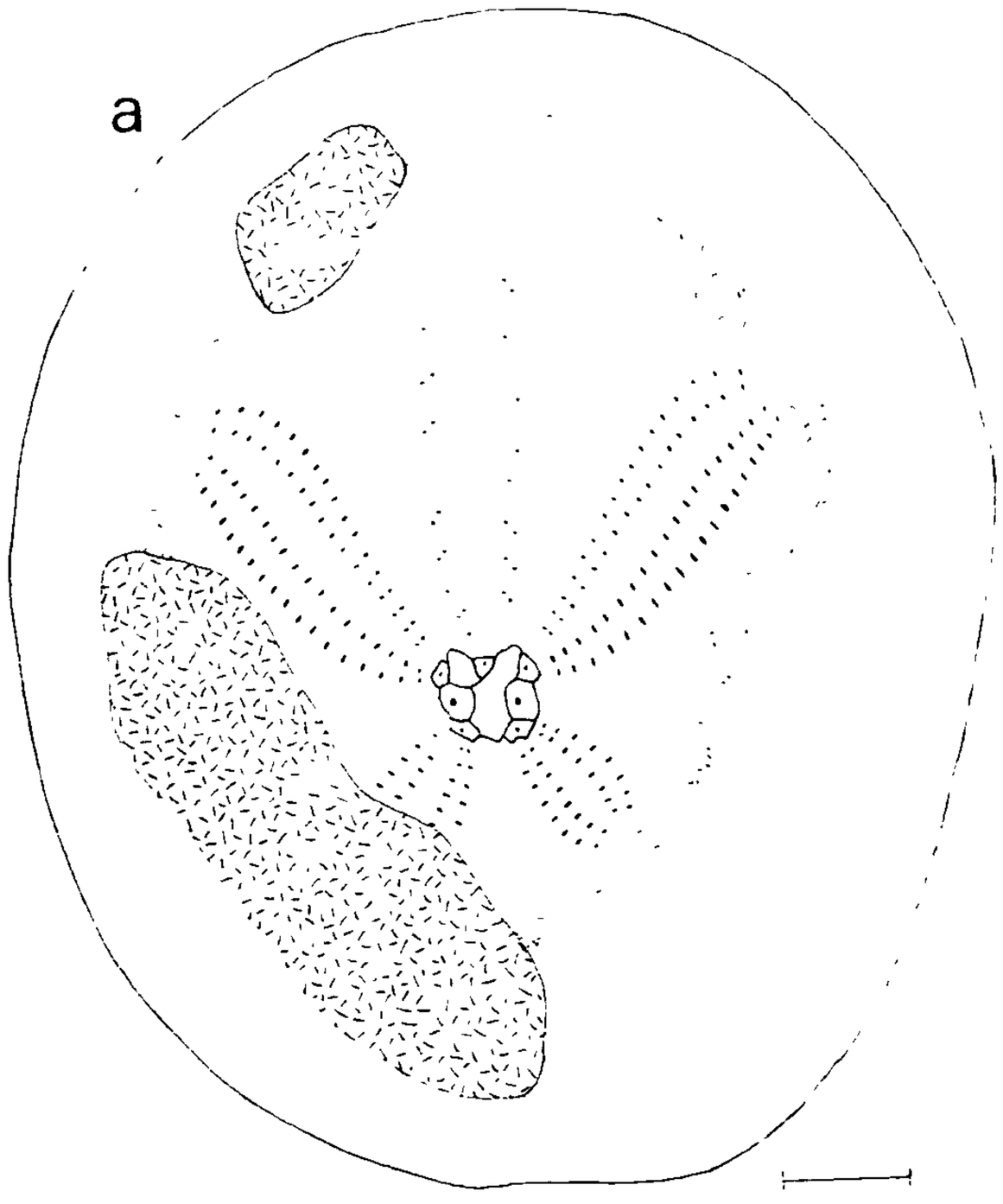
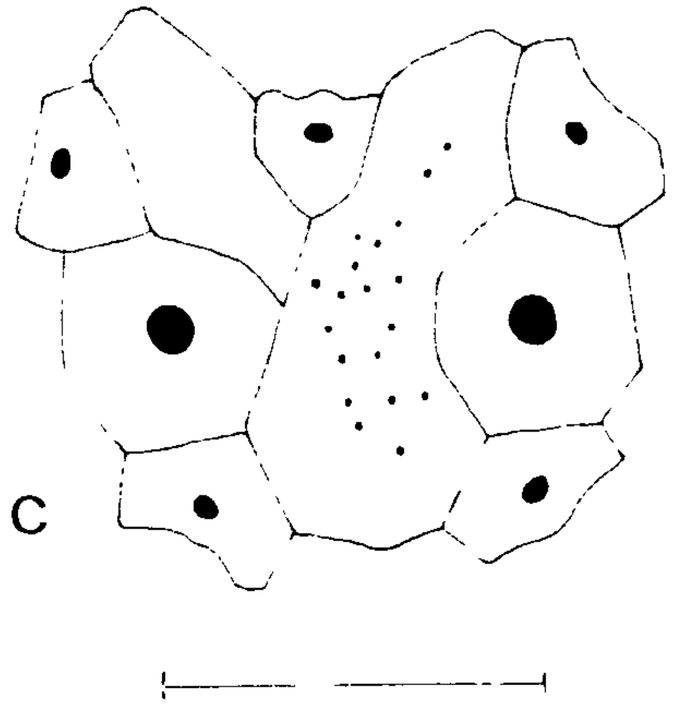

a
b
c

Figure 3.58. Camera lucida drawings of *Opissaster elongatus* (Duncan & Sladen), GSI 2575 (PARATYPE), Thanetian Ranikot Series of Pakistan; a, apical view; b, oral view; c, apical disc plating. a & b, scale bars = 2 mm. c, scale bar = 1 mm.


a


C

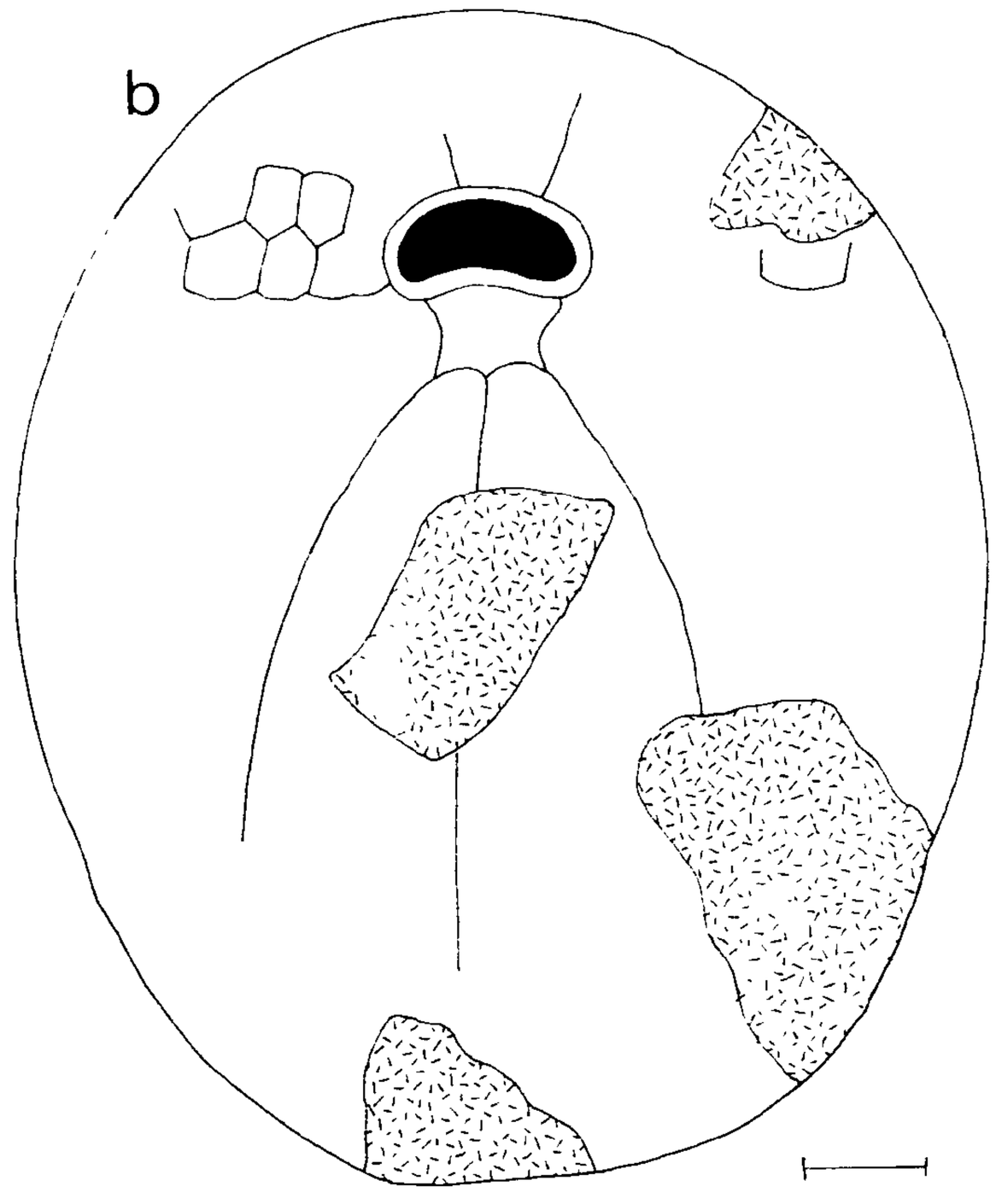
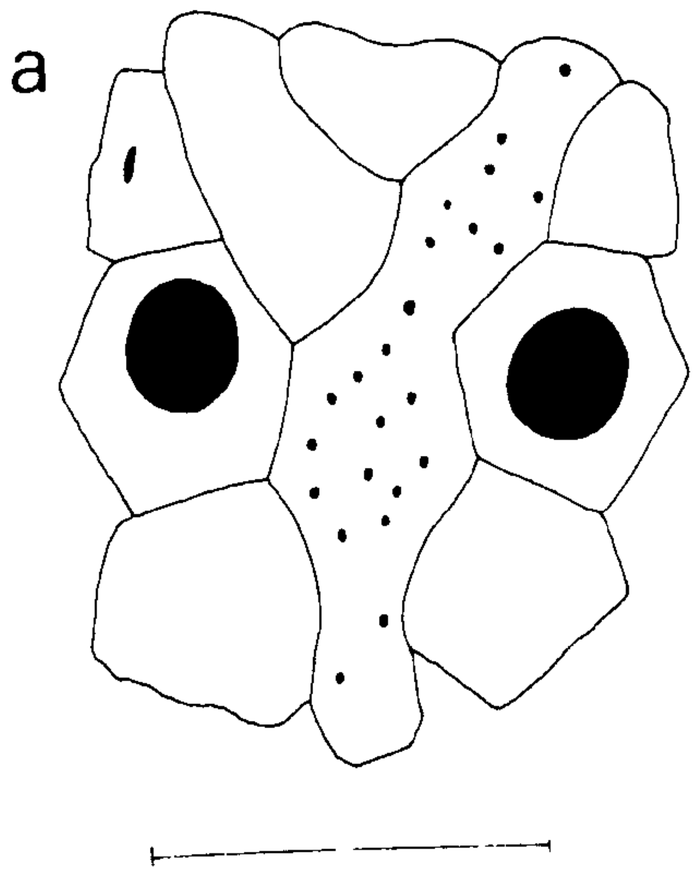

b

Figure 3.59. Camera lucida drawings of *Kertaster termiri* Poslavskaya & Moskvin, PI no specimen number, Thanetian of Mangyshlak, Kazakhstan; a, apical view; b, apical disc plating. a, scale bar = 2 mm. b, scale bar = 1 mm.


a

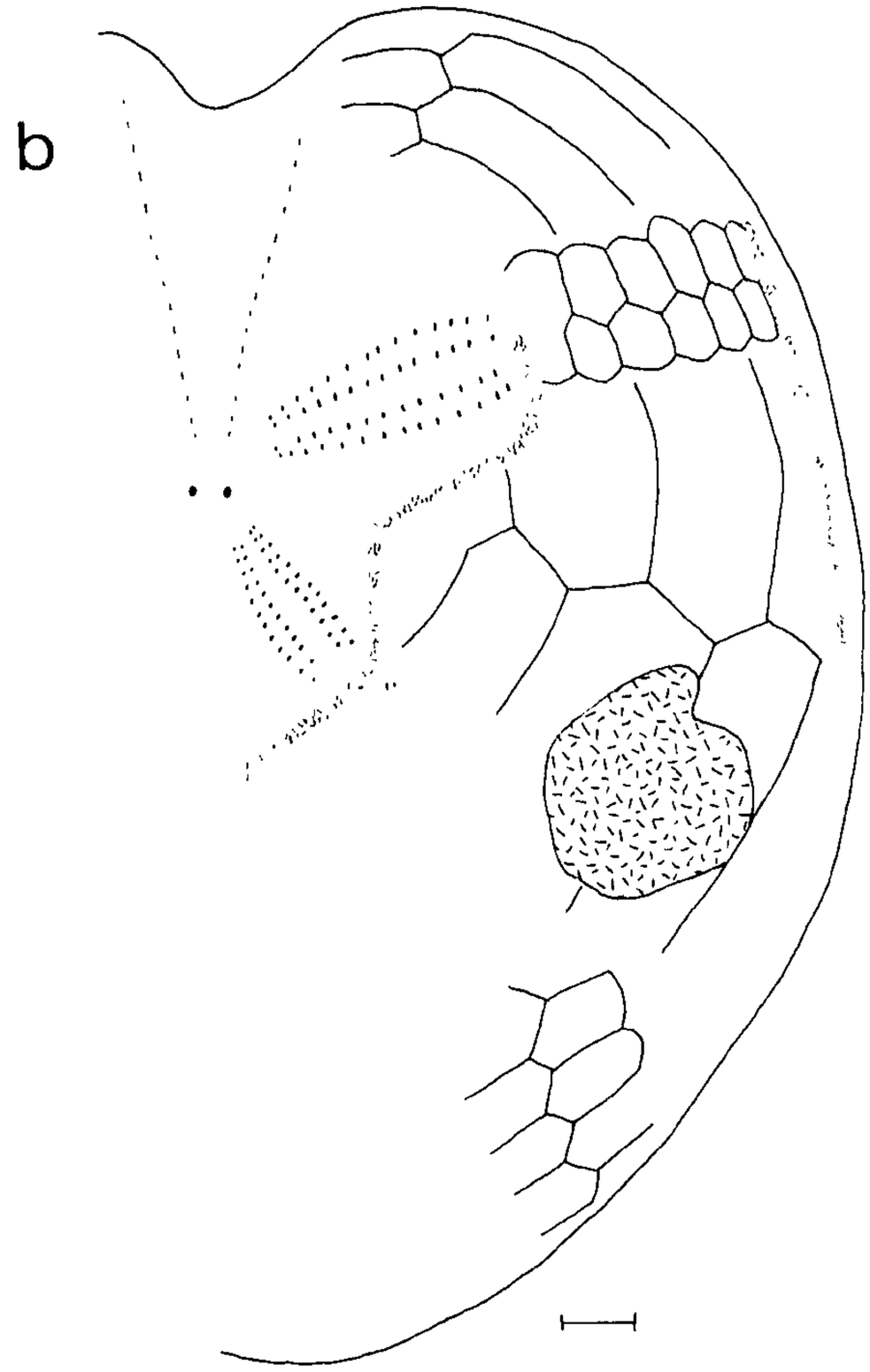

b

Figure 3.60. Range chart for Maastrichtian and Palaeocene species of *Linthia*, *Paraster* and *Tessieria*. See Figure 3.2 for explanation of symbols.

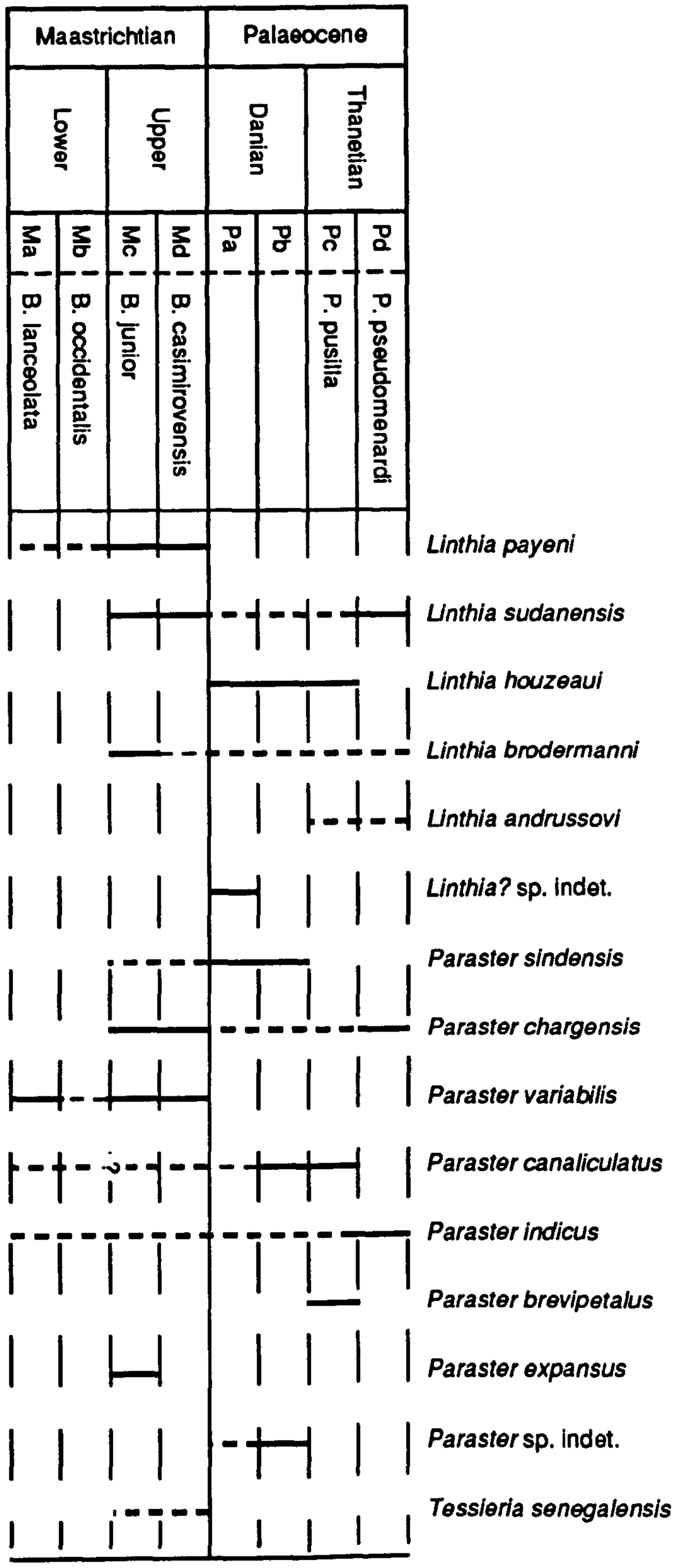
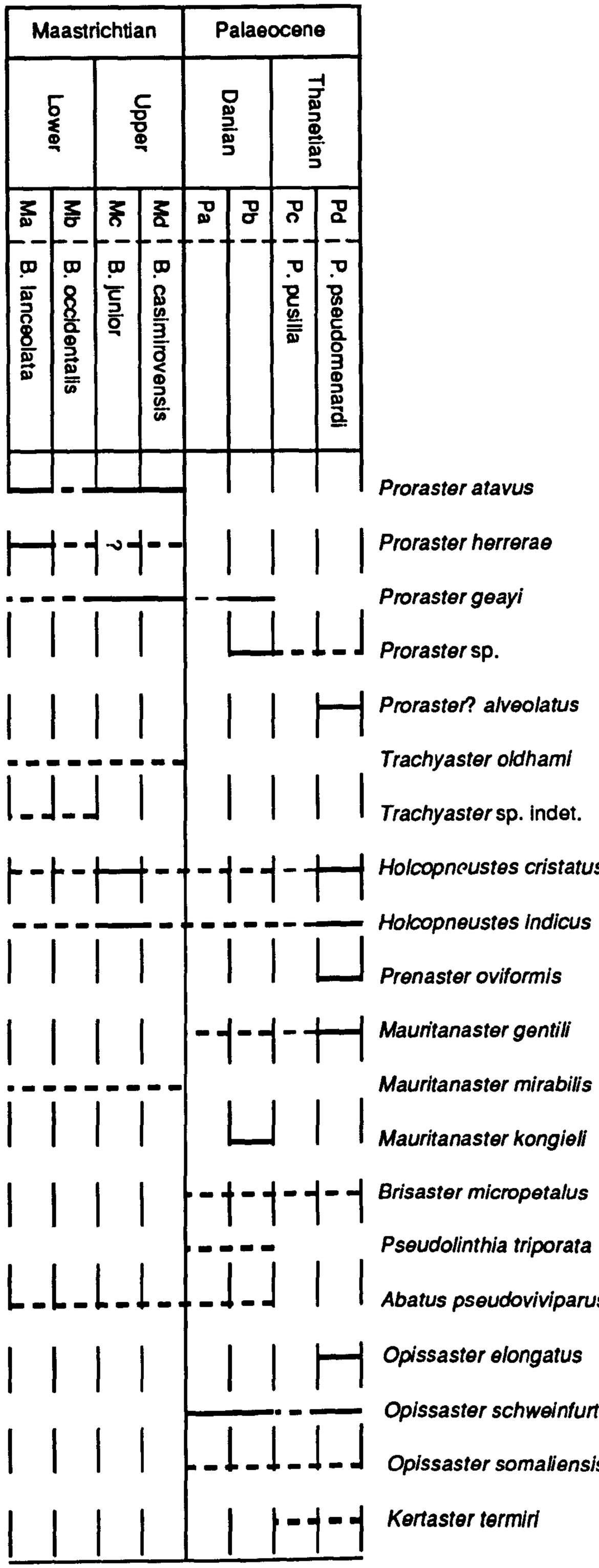

Maastrichtian
Palaeocene
Lower
Upper
Danian
Thanetian
Ma
Mb
Mc
Md
Pa
Pb
Pc
Pd
B. lanceolata
B. occidentalis
B. junior
B. casimirovensis
P. pusilla
P. pseudomenardi
Linthia payeni
Linthia sudanensis
Linthia houzeaui
Linthia brodermanni
Linthia andrussovi
Linthia? sp. indet.
Paraster sindensis
Paraster chargensis
Paraster variabilis
Paraster canaliculatus
Paraster indicus
Paraster brevipetalus
Paraster expansus
Paraster sp. indet.
Tessieria senegalensis

Figure 3.61. Range chart for Maastrichtian and Palaeocene pericosmid and schizasterid species, excluding species of *Linthia*, *Paraster* and *Tessieria*. See Figure 3.2 for explanation of symbols.


Maastrichtian
Palaeocene
Lower
Upper
Danian
Thanetian
Ma
Mb
Mc
Md
Pa
Pb
Pc
Pd
B. lanceolata
B. occidentalis
B. junior
B. casimirovensis
P. pusilla
P. pseudomenardi
Proraster atavus
Proraster herrerae
Proraster geayi
Proraster sp.
Proraster? alveolatus
Trachyaster oldhami
Trachyaster sp. indet.
Holcopneustes cristatus
Holcopneustes indicus
Prenaster oviformis
Mauritanaster gentili
Mauritanaster mirabilis
Mauritanaster kongieli
Brisaster micropetalus
Pseudolinthia triporata
Abatus pseudoviviparus
Opissaster elongatus
Opissaster schweinfurthi
Opissaster somaliensis
Kertaster termiri

Family CORASTERIDAE Lambert *in* Lambert & Thiéry, 1924

Diagnosis. Paired ambulacra non-petaloid to sub-petaloid. Apical system ethmophract. Non-labiate mouth. Peripetalous fasciole.

Remarks. Wagner & Durham (1966) included *Coraster* as *incertae sedis* in connection with the holasteroids. However, its amphisternous plastron and ethmophract apical system confirm its position within the spatangoids.

Homoeaster was placed in the palaeostomatids by Fischer (1966), along with *Palaeostoma* and *Leiostomaster*. Both *Palaeostoma* and *Leiostomaster* have well developed petaloid paired ambulacra that reach the peripetalous fasciole and are, in my view, more properly placed within the hemiasterids.

The corasterids differ from the hemiasterids, from which they are almost certainly derived, in possessing a non-labiate mouth, non- to sub-petaloid paired ambulacra and a more oblique peripetalous fasciole.

KEY TO MAASTRICHTIAN & PALAEOCENE GENERA

1 Apical system ethmophract with 3 gonopores
(genital plate 4 not perforated).....*Orthaster*
Apical system ethmophract with 4 gonopores.....2

2 Test hemispherical with flattened oral surface;
non-labiate, ambulacral plates low..... .....*Homoeaster*
Test gibbous; ambulacral plates high.....*Coraster*

Genus CORASTER Cotteau, 1886

[Type species *Coraster vilanovae* Cotteau, 1886, by OD]

Diagnosis. Test gibbous. All ambulacra non-petaloid with small, round pores. Ambulacral plates high. Apical system ethmophract with four gonopores. Mouth anteriorly positioned. Peripetalous fasciole passes close behind apical system and ambitally

towards anterior of test.

Remarks. *Coraster* differs from *Orthaster* in having all four genital plates perforated. *Coraster* and *Homoeaster* both have ethmophract apical systems with four gonopores. However, *Coraster* differs from *Homoeaster* in having a gibbous lateral profile, high ambulacral plates and the peripetalous fasciole passing closer to the apical system.

Coraster vilanovae Cotteau, 1886

(Plate 14, figures 1-4; Figure 3.62)

1886 *Coraster vilanovae* Cotteau, p. 70, pl. 9, figs 1-4.
1888 *Coraster marsooi* Seunes, p. 806, pl. 29, fig. 2.
1888 *Coraster sphaericus* Seunes, p. 807, pl. 29, fig. 3
1888 *Coraster munieri* Seunes, p. 808, pl. 29, fig. 4.
1892 *Coraster vilanovae* Cotteau, Nicklès, p. 115.
1892 *Coraster marsooi* Seunes; Nicklès, p. 115.
1892 *Coraster munieri* Seunes; Nicklès, p. 115.
1899 *Coraster vilanovae* Cotteau; Anthula, p. 61, pl. 2, fig. 5.
1927 *Coraster vilanovae* Cotteau; Böhm, p. 195, pl. 12, fig. 6.
1927 *Coraster frechi* Böhm, p. 195, pl. 12, fig. 5.
1931 *Coraster vilanovae* Cotteau; Lambert, p. 8, pl. 1, fig. 16.
1931 *Coraster alapliensis* Lambert, p. 9, pl. 1, figs 10-11.
1934 *Coraster vilanovae* Cotteau; Tzankov, p. 210.
1940 *Coraster* cf. *sphaericus* Seunes; Rouchadze, p. 170, pl. 1, fig. 4.
1940 *Coraster munieri* Seunes; Rouchadze, p. 170.
1959 *Coraster vilanovae* Cotteau; Moskvin & Poslavskaya, p. 278, pl. 18, fig. 5, text fig. 89.
1959 *Coraster sphaericus* Seunes; Moskvin & Poslavskaya, p. 278, pl. 18, fig. 6, text fig. 90.
1959 *Coraster ansaltensis* Poslavskaya; Moskvin & Poslavskaya, p. 279, pl. 18, fig. 7, text fig. 91.
1960 *Coraster vilanovae* Cotteau; Poslavskaya & Moskvin, p. 65, pl. 4, fig. 1, text fig. 15.
1960 *Coraster sphaericus* Seunes; Poslavskaya & Moskvin, p. 65, pl. 4, fig. 2, text fig. 16.
1960 *Coraster ansaltensis* Poslavskaya; Poslavskaya & Moskvin, p. 66, pl. 4, fig. 3, text fig. 17.
1964 *Coraster vilanovae* Cotteau; Poslavskaya & Solovyev, p. 183, pl. 34, fig. 9.
1975 *Coraster* cf. *sphaericus* Seunes; Plaziat *et al.*, p. 637, pl. 1, fig. 7.
1979 *Coraster* cf. *vilanovae* Cotteau; Gongadze, p. 117, pl. 27, fig. 1.
1979 *Coraster sphaericus* Seunes; Gongadze, p. 119, pl. 27, fig. 2.
1979 *Coraster ansaltensis* Poslavskaya; Gongadze, tables 1 & 2.
1982 *Coraster urmanensis* Moskvin, p. 106, pl. 10, figs 4-5.
1995 *Coraster vilanovae* Cotteau; Gallemí *et al.*, table 1.
1995 *Coraster* sp. Gallemí *et al.*, table 1.

Occurrence. Danian (Cotteau 1886; Nicklès 1892; Gallemí *et al.* 1995) and Maastrichtian Quipar-Jorquera Formation (Gallemí *et al.* 1995) of Alicante, Spain (BMNH, MGB). Danian *Coraster* beds of Navarra, Spain (BMNH). Danian of French (Seunes 1888) and Spanish Pyrenees (Plaziat *et al.* 1975). Early Maastrichtian Upper Chalk of Bulgaria (Tzankov 1934; Mileva-Ilieva 1995). Maastrichtian Marnes de Bartine (Lambert 1931) and Danian of northwest Turkey (Böhm 1927; Lambert 1931) (BMNH). Lower to Upper Maastrichtian of the Transcaspian (Poslavskaya & Moskvin 1960) (PI). Lower Maastrichtian to Upper Danian of Georgia (Rouchadze 1940; Poslavskaya & Moskvin 1960; Gongadze 1979) (PI) and the northern Caucasus (Moskvin & Poslavskaya 1959; Poslavskaya & Moskvin 1960) (PI). Maastrichtian (Anthula 1899) and Upper Palaeocene (Moskvin 1982) of Dagestan (PI).

Diagnosis. Globular, commonly spherical test with no or slight frontal groove. Posterior truncate to somewhat undercut. Position of mouth extremely variable, from almost marginal to about one quarter test length from the anterior margin.

Remarks. Previously named species of *Coraster* are distinguished from one another on subtleties of shape, distinctness and depth of the frontal groove and position of the mouth. Within populations, however, representatives of all these varieties form gradational series and thus these nominal species are treated as synonyms.

Coraster beneharnicus Seunes, 1888

1888 *Coraster beneharnicus* Seunes, p. 804, pl. 29, fig. 1.

1975 *Coraster beneharnicus* Seunes; Plaziat *et al.*, p. 635, pl. 1, figs 1-6, text figs 6, 8.

Occurrence. Danian of the French (Seunes 1888) and Spanish (Plaziat *et al.* 1975) Pyrenees. Danian of Navarra, Spain (BMNH).

Diagnosis. Elongate horizontal outline and gibbous profile. Weak subanal heel. Broad and shallow frontal groove which deepens on the oral surface and reaches mouth. Mouth at about one quarter test length from the anterior margin.

Remarks. Differs from *C. vilanovae* in its more angular and elongate test, its weak subanal heel and in the frontal groove extending to the mouth. Although *C. vilanovae*

covers a wide gradational series of morphologies, specimens referred to *C. beneharnicus* fall outside this range with no intermediate forms. *C. beneharnicus* merits recognition as a separate species.

Genus ORTHASTER Moskvin, 1982

[Type species *Orthaster dagestanensis* Moskvin, 1982, by OD]

Synonym. *Ornithaster* Poslavskaya & Moskvin, 1960; Poslavskaya & Solovyev, 1964. *non Ornithaster* Cotteau, 1886 (= *Homoeaster* Pomel, 1883).

Diagnosis. Test globular with shallow frontal groove. All ambulacra non-petaloid with small, round pores. Apical system ethmophract with three gonopores (genital plate 4 not perforated). Peripetalous fasciole passes immediately behind apical system.

Remarks. *Orthaster* is easily distinguished from *Coraster* in having only three gonopores in the apical system.

Orthaster dagestanensis Moskvin, 1982

(Figure 3.63)

1959 *Ornithaster munieri* Seunes; Moskvin & Poslavskaya, p. 276, pl. 18, fig. 1, text fig. 86.

1960 *Ornithaster munieri* Seunes; Poslavskaya & Moskvin, p. 63, pl. 3, fig. 5, text fig. 13.

1960 *Ornithaster marsooi* Seunes; Poslavskaya & Moskvin, p. 63, pl. 3, fig. 6, text fig. 14.

1979 *Ornithaster beneharnicus* Seunes; Gongadze, p. 113, pl. 26, figs 2-3.

1979 *Ornithaster munieri* Seunes; Gongadze, p. 114, pl. 26, fig. 4.

1979 *Ornithaster* cf. *marsooi* Seunes; Gongadze, p. 116, pl. 26, fig. 5.

1982 *Orthaster dagestanensis* Moskvin, p. 103, pl. 10, fig. 1.

1982 *Orthaster okhliensis* Moskvin, p. 105, pl. 10, fig. 3.

Occurrence. Lower to Upper Danian of Georgia (Poslavskaya & Moskvin 1960; Gongadze 1979) and the northern Caucasus (Moskvin & Poslavskaya 1959; Poslavskaya & Moskvin 1960) (Pl). Upper Palaeocene of Dagestan (Moskvin 1982) (Pl).

Diagnosis. Inflated upper and lower surfaces. Marginally positioned mouth.

Orthaster alievi Moskvin, 1982

1959 *Ornithaster alapliensis* (Lambert); Moskvin & Poslavskaya, p. 275, pl. 18, fig. 10, text fig. 85.

1964 *Ornithaster alapliensis* (Lambert); Poslavskaya & Solovyev, pl. 34, fig. 8, text fig. 219b.

1982 *Orthaster alievi* Moskvin, p. 104, pl. 10, fig. 2.

Occurrence. Campanian of Dagestan (Moskvin 1982) (PI). Lower to Upper Maastrichtian of the northern Caucasus and Kopet Dag (Moskvin & Poslavskaya 1959; Poslavskaya & Solovjev 1964) (PI).

Diagnosis. Differs from *O. dagestanensis* in its flatter oral surface, less distinct frontal groove and more posteriorly positioned mouth.

Genus HOMOEASTER Pomel, 1883

[Type species *Homoeaster tunetanus* Pomel, 1883, by OD]

Synonyms. *Physaster* Pomel, 1883 (type species *Echinospatagus inflatus* d'Orbigny, 1854); *Ornithaster* Cotteau, 1886 (type species *Ornithaster evaristei* Cotteau, 1886); *Inflataster* Anthula, 1899 (type species *Inflataster abichi* Anthula, 1899); *Cottreaucorys* Lambert, 1920b (type species *Homoeaster blayaci* Cottreau *in* Blayac & Cottreau, 1909).

Diagnosis. Inflated apical surface and flat oral surface. No frontal groove. Paired ambulacra non-petaloid to sub-petaloid. Apical system anteriorly positioned, ethmophract with four gonopores. Mouth circular, non-labiate, downward facing. Peripetalous fasciole.

Remarks. *Ornithaster* was erected for specimens with small, round pores in the paired petals, *Homoeaster* for forms with comma-shaped pores. Since small specimens tend to have small, circular pores and larger forms more elongate pores, it seems that the character is purely related to age. *Homoeaster* and *Ornithaster* are synonymized. *Cottreaucorys* is characterized by have a pronounced subanal heel. Specimens previously referred to this genus do form distinct populations but the character (based purely on the shape of the test) is not of generic value. In all other respects, *Cottreaucorys* is identical to *Homoeaster* and the two are treated as synonymous.

Homoeaster differs from *Coraster* and *Orthaster* in its hemispherical lateral profile,

in completely lacking a frontal groove and in having lower ambulacral plates. In *Homoeaster*, the mouth is less anteriorly positioned and downward facing. *Homoeaster* differs additionally from *Orthaster* in having four gonopores in the apical system.

KEY TO MAASTRICHTIAN SPECIES

1 Distinct subanal heel.....*H. blayaci*
Truncated posterior.....2

2 Paired ambulacra subpetaloid with elongate pores.....*H. auberti*
Paired ambulacra non-petaloid.....*H. tunetanus*

Homoeaster tunetanus Pomel 1883

(Plate 14, figures 5-8; Figure 3.64)

1883 *Homoeaster tunetanus* Pomel, p. 44.
1886 *Ornithaster evaristei* Cotteau, p. 72, pl. 9, figs 5-8.
1892 *Ornithaster evaristei* Cotteau; Nicklès, p. 115.
1892 *Homoeaster tunetanus* Pomel; Gauthier, p. 45, pl. 2, figs 3-10.
1892 *Homoeaster discrepans* Gauthier, p. 48, pl. 4, fig. 13.
1899 *Inflataster abichi* Anthula, p. 63, pl. 2, fig. 6.
1909 *Homoeaster tunetanus* Pomel; Cottreau *in* Blayac & Cottreau, p. 430.
1924 *Homoeaster tunetanus* Pomel; Dalloni, p. 118.
1927 *Ornithaster cordiformis* Böhm, p. 196, pl. 12, fig. 3.
1927 *Physaster abichi* (Anthula); Böhm, p. 197.
1932 *Homeaster tunetanus* Pomel; Lambert, p. 99.
1934 *Ornithaster cordiformis* Böhm; Tzankov, p. 212.
1934 *Physaster abichi* (Anthula); Tzankov, p. 213.
1940 *Physaster abichi* (Anthula); Rouchadze, p. 170.
1959 *Homoeaster tunetanus* Pomel; Moskvin & Poslavskaya, p. 274, pl. 18, fig. 1.
1959 *Homoeaster abichi* (Anthula); Moskvin & Poslavskaya, p. 274, pl. 18, fig. 2.
1960 *Homoeaster tunetanus* Pomel; Poslavskaya & Moskvin, p. 60, pl. 3, fig. 1, text fig. 10.
1960 *Homoeaster evaristei* (Cotteau); Poslavskaya & Moskvin, p. 61, pl. 3, fig. 2, text fig. 11.
1960 *Homoeaster abichi* (Anthula); Poslavskaya & Moskvin, p. 61, pl. 3, figs 3-4, text fig. 12.
1979 *Homoeaster abichi* (Anthula); Gongadze, p. 111, pl. 26, fig. 1.
1979 *Homoeaster* cf. *tunetanus* Pomel; Gongadze, p. 110, pl. 25, fig. 4.
1983 *Homoeaster* ? n. sp. afl. *tuneatus* Pomel; Schulz, p. 718, text fig. 3.

1995 *Homoeaster tunetanus* Pomel; Mileva-Ilieva, p. 239.

1995 *Ornithaster? evaristei* Cotteau; Gallemí *et al.*, table 1.

1995 *Ornithaster?* sp. Gallemí *et al.*, table 1.

Occurrence. Maastrichtian Quipar-Jorquera Formation (Gallemí *et al.* 1995) and Danian (Cotteau 1886; Nicklès 1892; Gallemí *et al.* 1995) of Alicante, Spain (BMNH, MGB). Lower Maastrichtian Upper Chalk (Tzankov 1934) and Mezdra Formation (Mileva-Ilieva 1995) of Bulgaria. Lower Maastrichtian *Inoceramus* Marls of Bavaria (Schulz 1983). Lower Maastrichtian and Lower to Upper Danian of the Northern Caucasus (Moskvin & Poslavskaya 1959; Poslavskaya & Moskvin 1960) (PI). Lower to Upper Danian of the Crimea (Moskvin & Poslavskaya 1959) (PI). Maastrichtian of Dagestan (Anthula 1899). Maastrichtian (Rouchadze 1940; Poslavskaya & Moskvin 1960; Gongadze 1979) and Lower to Upper Danian (Poslavskaya & Moskvin 1960; Gongadze 1979) of Georgia. Maastrichtian of Constantine (Blayac & Cottreau 1909; Lambert 1932) and Oran, Algeria (Dalloni 1924; Lambert 1932) (MNHN). Danian Kangilia Formation of East Greenland (DGFMM) and Danian of northwest Turkey (Böhm 1927) (BMNH). Maastrichtian of Mozambique (BMNH). Maastrichtian or Palaeocene of Senegal (BMNH).

Diagnosis. Paired ambulacra made up of round or comma-shaped pores. Posterior obliquely truncate.

Remarks. Gauthier (1892) recorded this species from the Maastrichtian of Tunisia. However, these deposits have been shown to be Coniacian on the basis of microfossil data (Zagbib-Turki 1987).

Homoeaster auberti (Gauthier, 1892)

1892 *Lambertiaster auberti* Gauthier, p. 32, pl. 3, figs 4-15.

1909 *Lambertiaster auberti* Gauthier; Cottreau *in* Blayac & Cottreau, p. 425.

1924 *Homoeaster auberti* (Gauthier); Dalloni, p. 117.

1924 *Homoeaster* nov. sp. Dalloni, p. 117.

1924 *Ornithaster* nov. sp. Dalloni, p. 118.

1925 *Homoeaster petalodes* Lambert *in* Lambert & Thiéry, p. 429, pl. 11, figs 7-8.

1932 *Homeaster auberti* (Gauthier); Lambert, p. 75, 99.

1932 *Homeaster petalodes* Lambert, p. 76.

Occurrence. Maastrichtian of Constantine (Blayac & Cottreau 1909; Lambert 1932) and Oran, Algeria (Dalloni 1924; Lambert & Thiéry 1925; Lambert 1932). Maastrichtian Marnes de Bartine of northwest Turkey (MNHN).

Diagnosis. Differs from *H. tunetanus* in having subpetaloid paired ambulacra, made up of elongate pores.

Remarks. Also recorded from the Maastrichtian of northern Tunisia by Gauthier (1892). However, microfaunal evidence from his localities show the strata to be Coniacian in age (Zagbib-Turki 1987).

Homoeaster blayaci Cottreau *in* Blayac & Cottreau, 1909

1909	*Homoeaster blayaci* Cottreau *in* Blayac & Cottreau, p. 428, pl. 14, figs 7-19, text fig. 2.
1932	*Cottreaucorys blayaci* (Cottreau); Lambert, p. 76.
1971	*Cottreaucorys (Homoeaster) blayaci* (Cottreau); Akkus, p. 16.

Occurrence. Maastrichtian of Constantine, Algeria (Blayac & Cottreau 1909; Lambert 1932) (MNHN) and Lower Maastrichtian Ulupinar Formation of Central Turkey (Akkus 1971).

Diagnosis. Differs from *H. tunetanus* in having a very pronounced subanal heel.

Homoeaster sp. Indet.

1968	*Cottreaucorys (Cordastrum) sulcatus* Nisiyama, p. 175, pl. 18, figs 10-11, pl. 20, fig. 2, text fig. 65.

Occurrence. Maastrichtian Miyakura (Furushiroyama) formation of Japan.

Remarks. Definitely a member of this genus but too poorly preserved to allow specific identification.

Family AEROPSIDAE Lambert, 1896

Diagnosis. Elongate test. Broad anterior ambulacrum, petaloid with enlarged pores. Paired ambulacra non-petaloid. Apical system ethmophract or ethmolytic with two or four gonopores. Peripetalous fasciole.

Remarks. In erecting the aeropsids, Lambert included a large number of fossil and Recent taxa with both holasteroid and spatangoid affinities which were, according to Mortensen (1950, p. 326), " a real balderdash that does not deserve a critical revision". Mortensen himself included just three genera in the aeropsids - *Aeropsis*, *Aceste* and *Cottreaucorys* (here treated as a synonym of *Homoeaster* and a member of the palaeostomatids). It seems probable that the aeropsids are very closely related to the palaeostomatids and that both groups are ultimately derived from the hemiasterids. Until now, no fossils have been referred to the aeropsids with any degree of certainty and derivation of this family has remained unresolved. A new specimen from the Danian of Spain is the first unequivocal fossil aeropsid, and extends the range of the family by some 60 million years. Phylogenetic analysis of spatangoid genera will clarify from where this new genus and the remainder of the aeropsids are derived.

Genus SPHENASTER nov.

[Type species *Sphenaster larumbensis* sp. nov.]

Etymology. From *sphenos* - a wedge.

Diagnosis. Narrow wedge-shaped test. Broad unpaired ambulacrum with enlarged pore-pairs. Non-petaloid paired ambulacra. Ethmophract apical disc with two gonopores. Peripetalous fasciole passes immediately behind apical system and low down anteriorly. Enlarged tubercles along edges of unpaired ambulacrum.

Remarks. The new genus is most similar to *Aeropsis* from which it differs in having a wedge-shaped (rather than cylindrical) test with an obliquely truncate posterior, a less anterior apical system and a number of enlarged tubercles on the apical surface. *Aceste* differs in having an ethmolytic apical system, a deeply sunken frontal groove leading to

the mouth, single pores in the paired ambulacra and uniform tuberculation. *Sphenaster* is flat across the anterior margin and possesses a mouth which is flush with the test and pore-pairs in all ambulacra.

Sphenaster larumbensis sp. nov.

(Plate 14, figs 9-13; Figure 3.65)

Etymology. Larumbe - the locality at which the type specimen was found.

Holotype. Holotype and only known specimen BMNH EE6073.

Occurrence. Danian *Coraster* beds of Larumbe near Pamplona, Spain (BMNH).

Description. The single available specimen measures 14.6 mm in length and 8.4 mm in width (58% of test length). In horizontal outline, the test is an elongate pentagon. It is flat across the anterior margin, broadens to the widest point (approximately two thirds of test length from the anterior margin) and narrows to the rounded posterior. Maximum height is 10.3 mm (71% of test length), midway along the test. In profile, the test is wedge-shaped sloping gently to the anterior from the apical system and with a somewhat gibbous lower surface. The posterior is oblique with a very slight subanal heel.

The paired ambulacra are flush and non-petaloid with tiny, inconspicuous pore-pairs. By contrast, the unpaired ambulacrum is very slightly sunken and contains enlarged pore-pairs presumably an adaptation for respiration. Pore-pairs are obliquely positioned and diminish in size towards the anterior margin of the test.

The plastron is amphisternous with a long narrow labral plate followed by two equally long, narrow sternal plates. The suture between these plates runs along the midline of the test.

The ethmophract apical system is positioned 39% of test length from the anterior margin. It has two large genital plates each with a gonopore, and five small ocular plates. A small number of hydropores are present on the madreporite.

The peristome is circular or rounded pentagonal with no rim. It measures 1.7 mm in diameter (20% of maximum test width), is situated 21% of test length from the anterior margin and is flush with the test. Although the oral surface of the test is damaged, it is

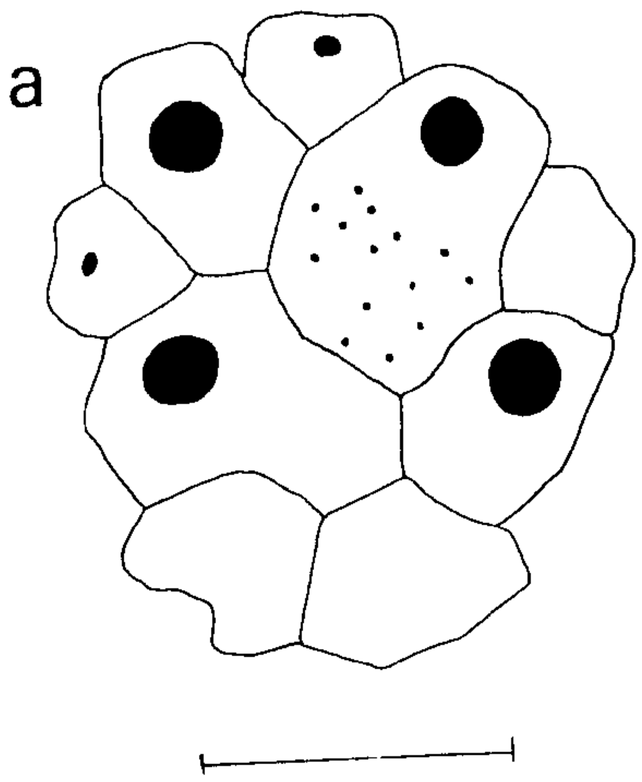
clear that the labral plate does not extend over the mouth.

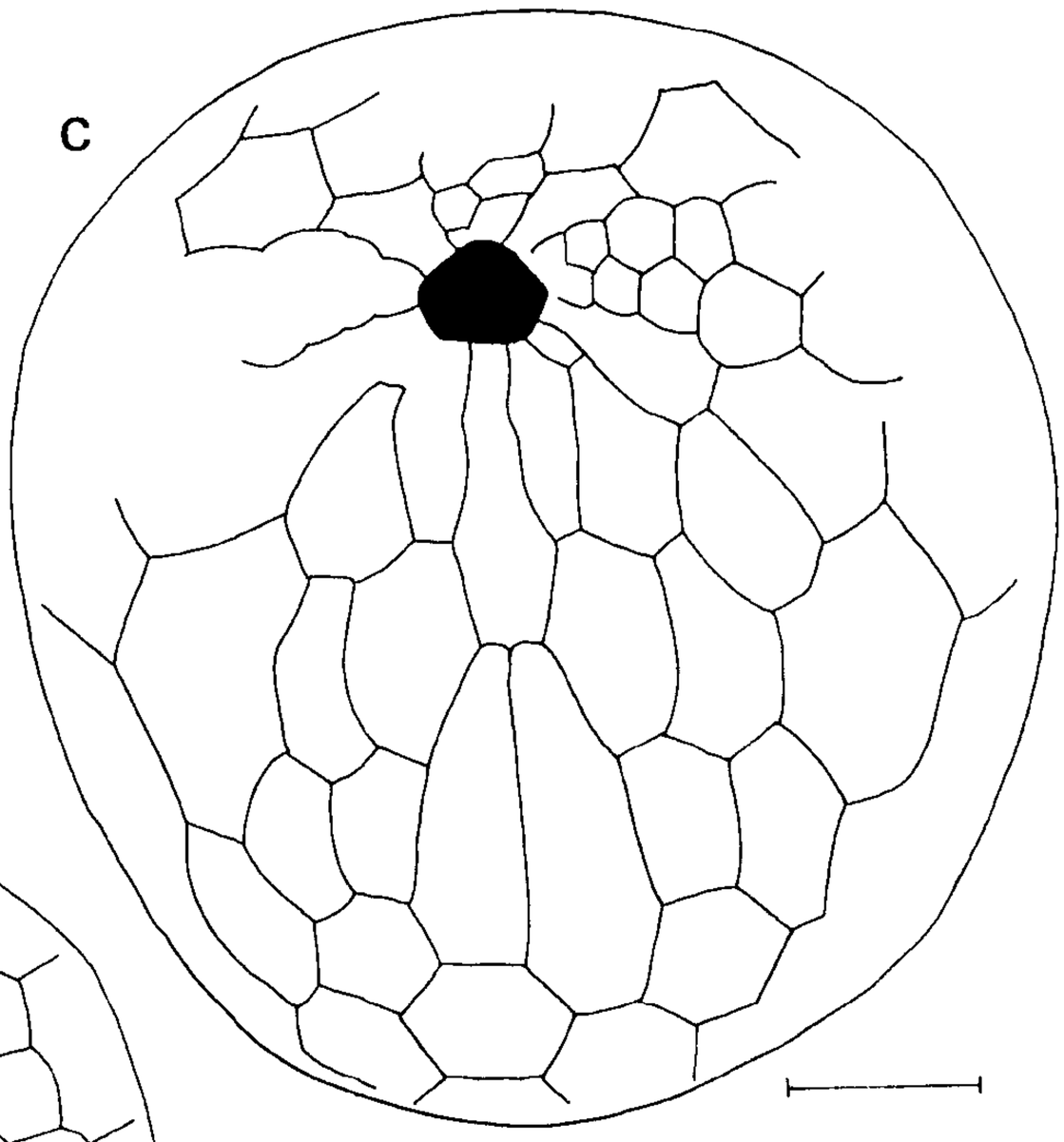
The periproct is also circular and measures 2.0 mm in diameter. It is positioned high on the oblique posterior of the test, 52% of test height from the base.

A distinct peripetalous fasciole is positioned high on the test. It passes immediately behind the apical system and crosses the anterior margin at the ambitus. At its broadest point, the fasciole is 8 miliaries wide. The fasciole becomes less distinct towards the anterior where a number of small tubercles are incorporated.

Tubercles are perforate and crenulate and are fairly densely distributed over the aboral surface of the test with scattered miliaries in between. The largest tubercles are positioned on the anterior margin at the end of the frontal ambulacrum, and on the posterior below the periproct. Tubercles are most densely packed around the periproct. Overall, the test has a somewhat granular appearance. On the oral surface, tubercles are far sparser and on the whole larger than on the upper surface. The largest tubercles are situated on the plastron.

Figure 3.62. Camera lucida drawings of *Coraster vilanovae* Cotteau. a, MGB RM523 (TOPOTYPE), Danian of Alicante, Spain, apical disc plating. b, PI no specimen number, Danian of the northern Caucasus, lateral view. c, BMNH EE6070, Maastrichtian Quipar-Jorquera Formation of El Sacarest, Alicante, Spain, oral view. a, scale bar = 1 mm. b & c, scale bars = 2 mm.


a


c

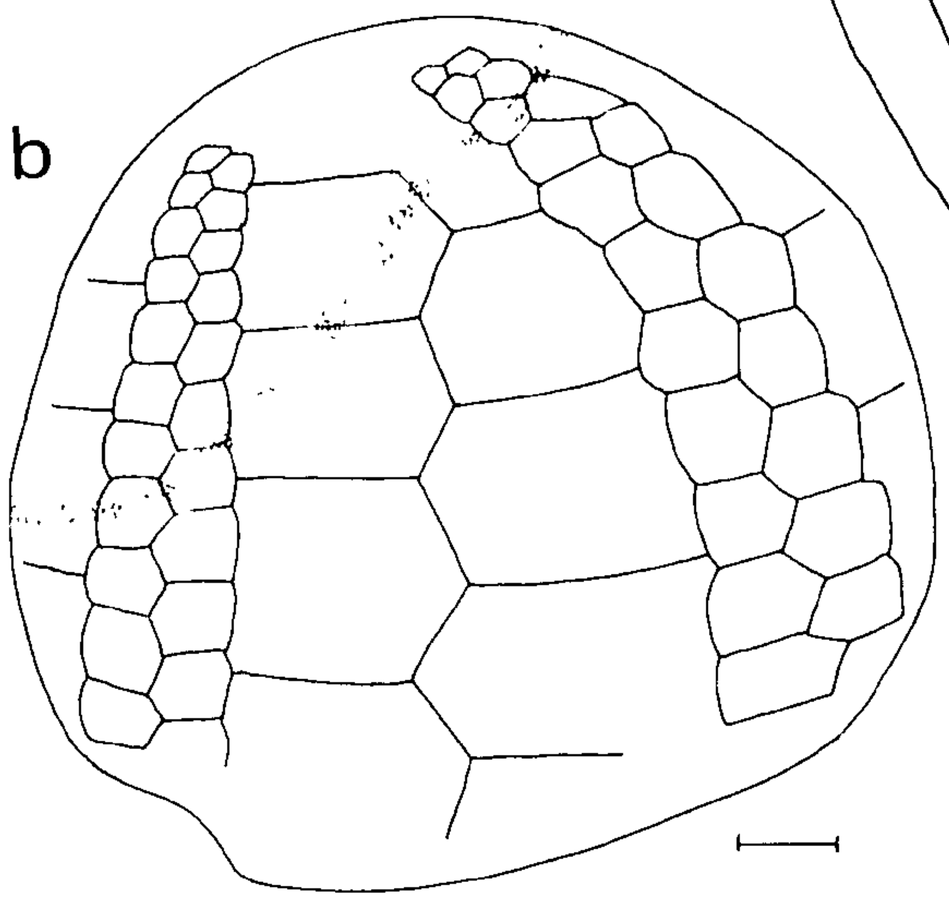
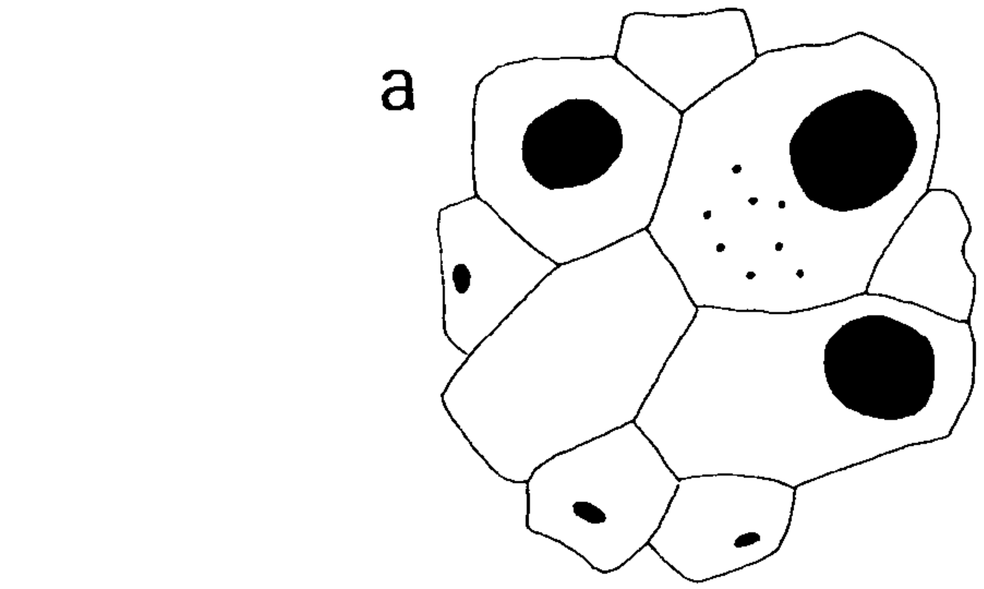
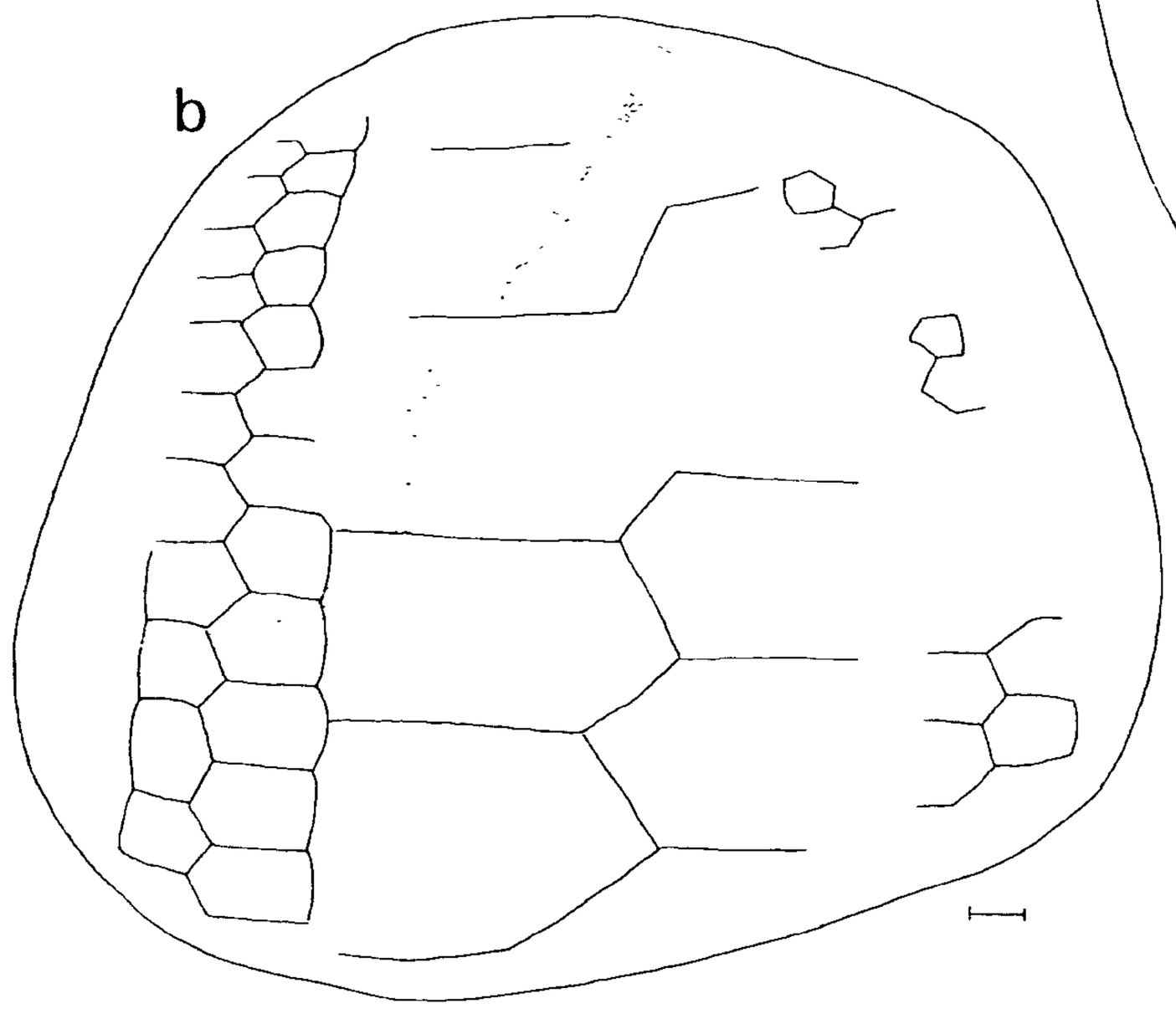

b

Figure 3.63. Camera lucida drawings of *Orthaster dagestanensis* Moskvin, PI 3939/1 (HOLOTYPE), Upper Palaeocene of Dagestan; a, apical disc plating; b, lateral view; c, oral view. Scale bars = 1 mm.


a


b

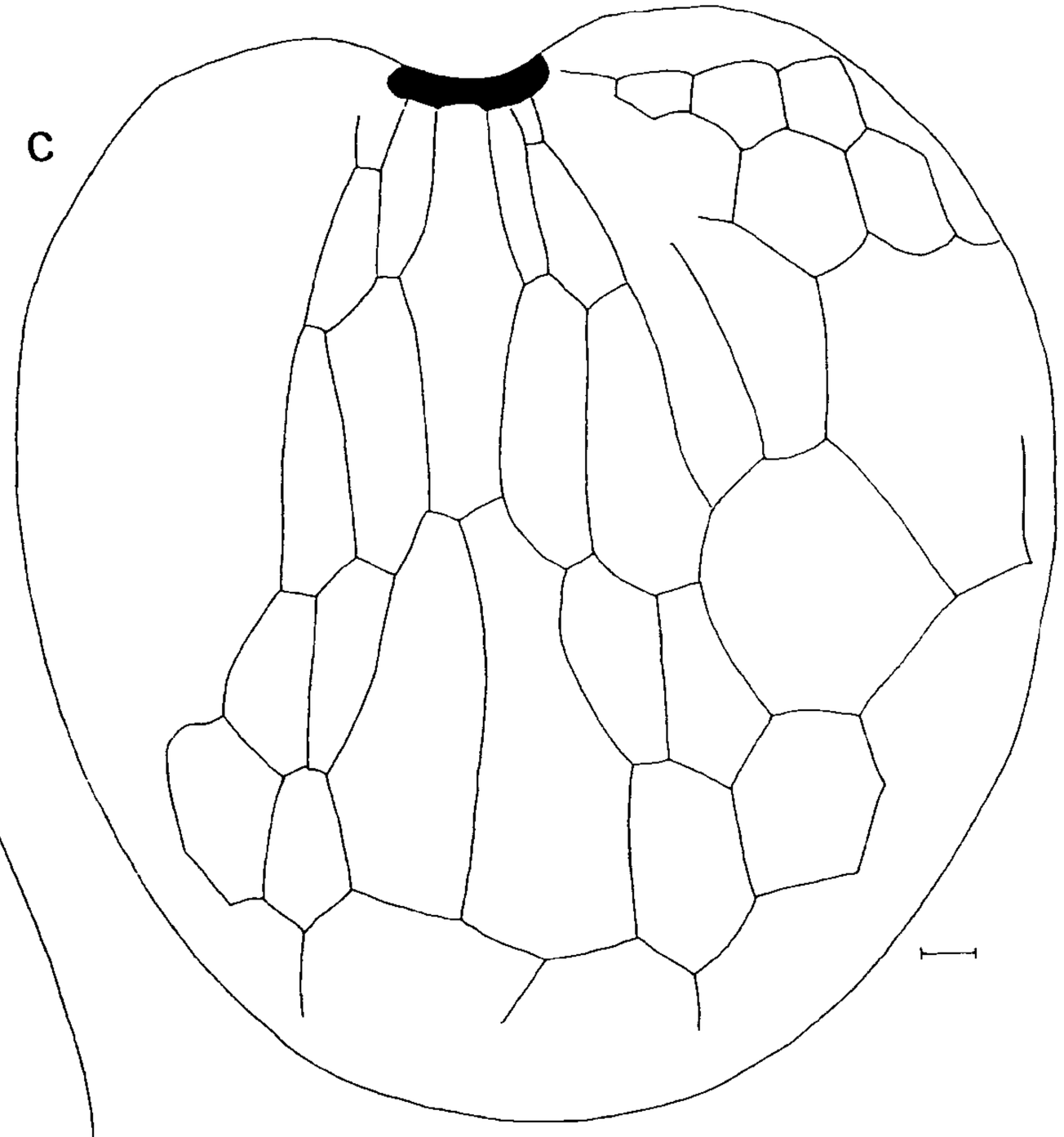
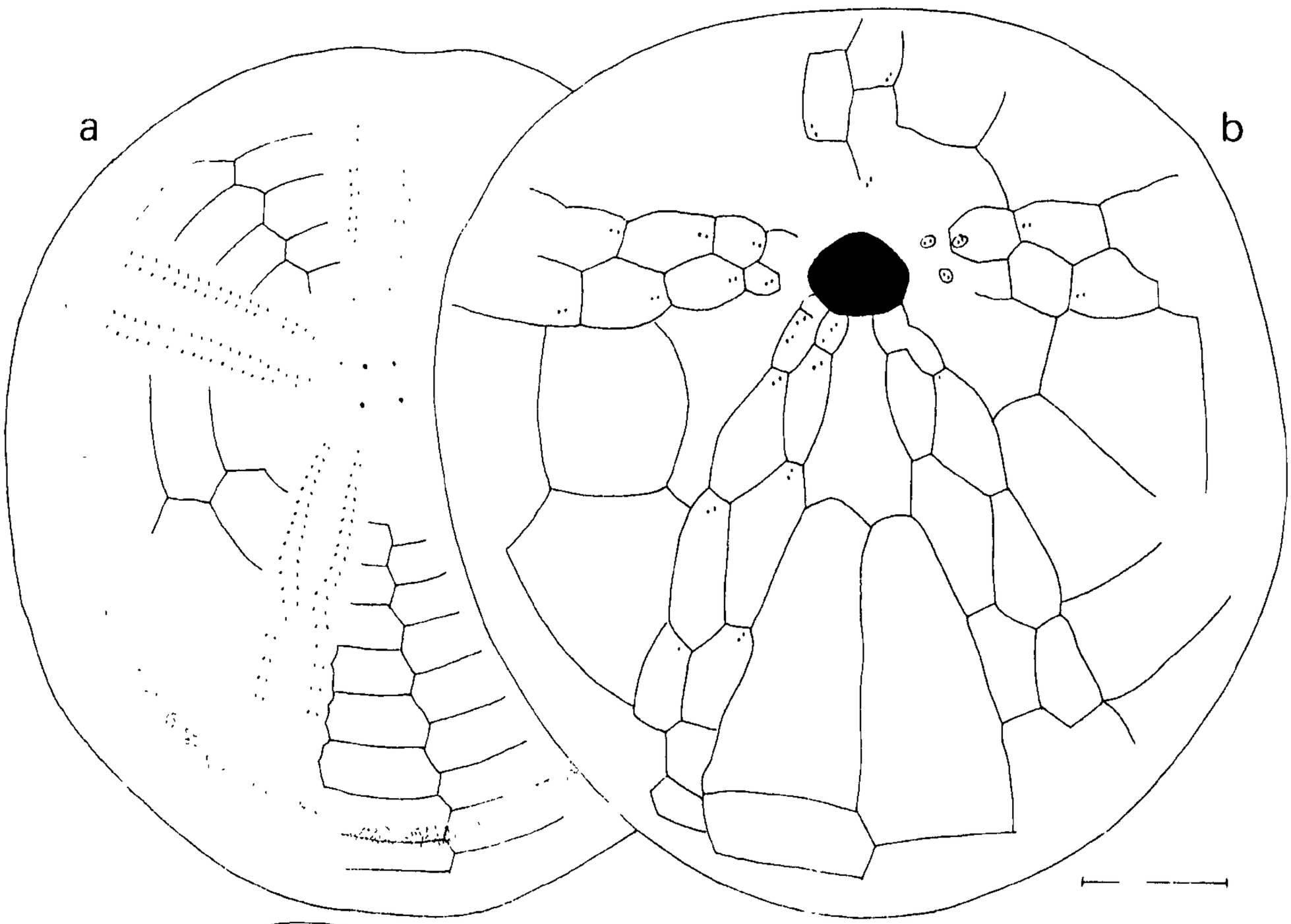
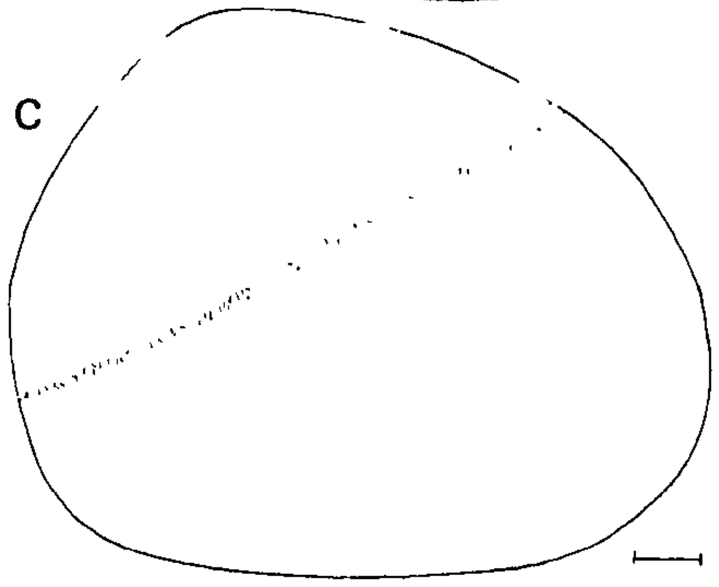

c

Figure 3.64. Camera lucida drawings of *Homoeaster tunetanus* Pomel. a & b, MNHN no specimen number, Maastrichtian of Oran, Algeria; a, apical view; b, oral view. c, PI 418n/52 1, Maastrichtian of the northern Caucasus, lateral view. d, BMNH EE6071, Maastrichtian Quipar-Jorquera Formation of El Sacarest, Alicante, Spain, apical disc plating. a & b, scale bars = 5 mm. c, scale bar = 2 mm. d, scale bar = 1 mm


a
b


c

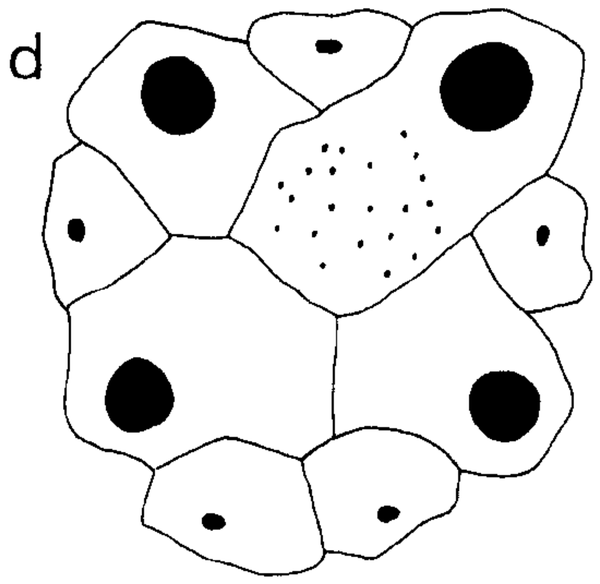
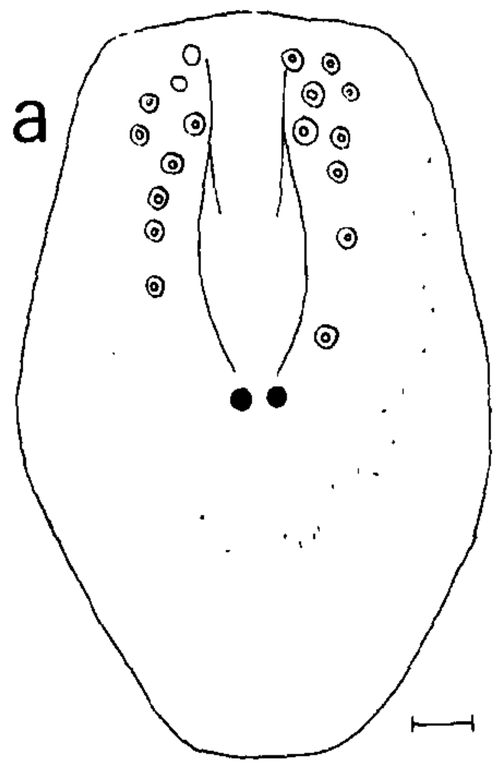
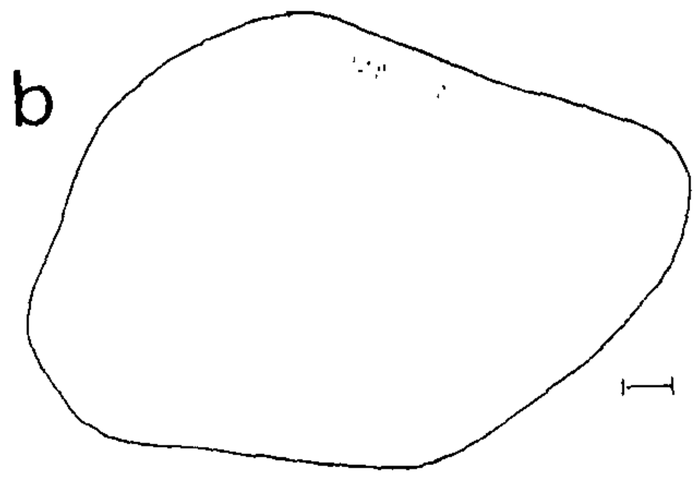
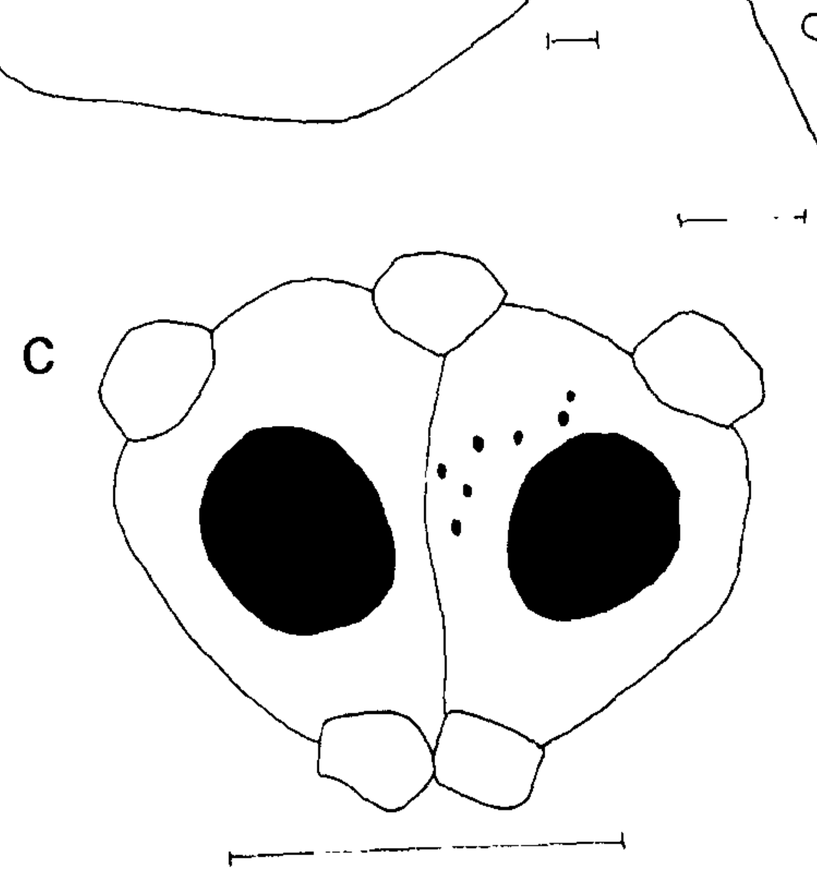

d

Figure 3.65. Camera lucida drawings of *Sphenaster larumbensis* sp. nov., BMNH EE6073 (HOLOTYPE), Danian *Coraster* beds of Navarra, Spain; a, apical view; b, lateral view; c, apical disc plating; d, oral view. Scale bars = 1 mm.


a


b


c

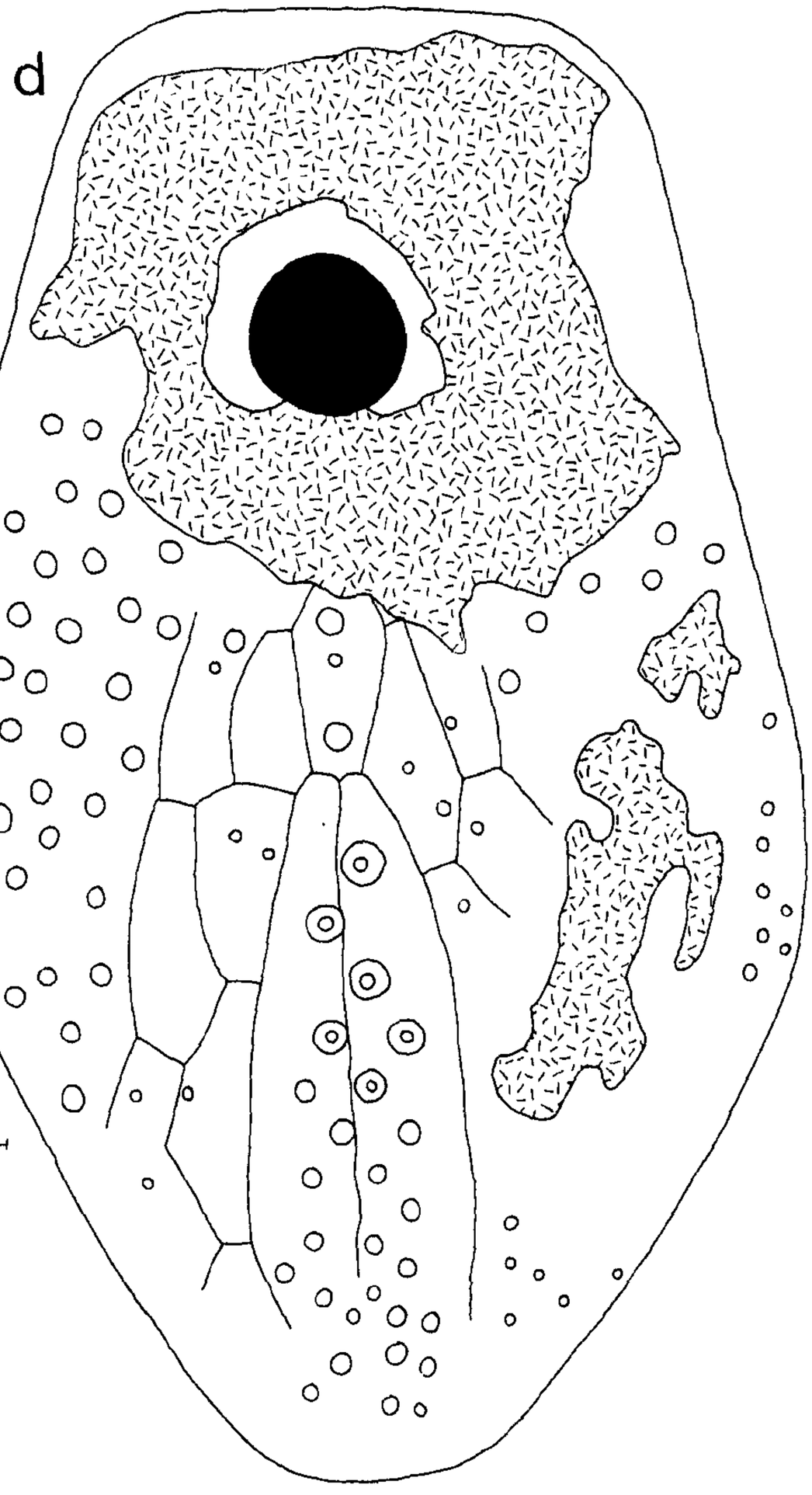
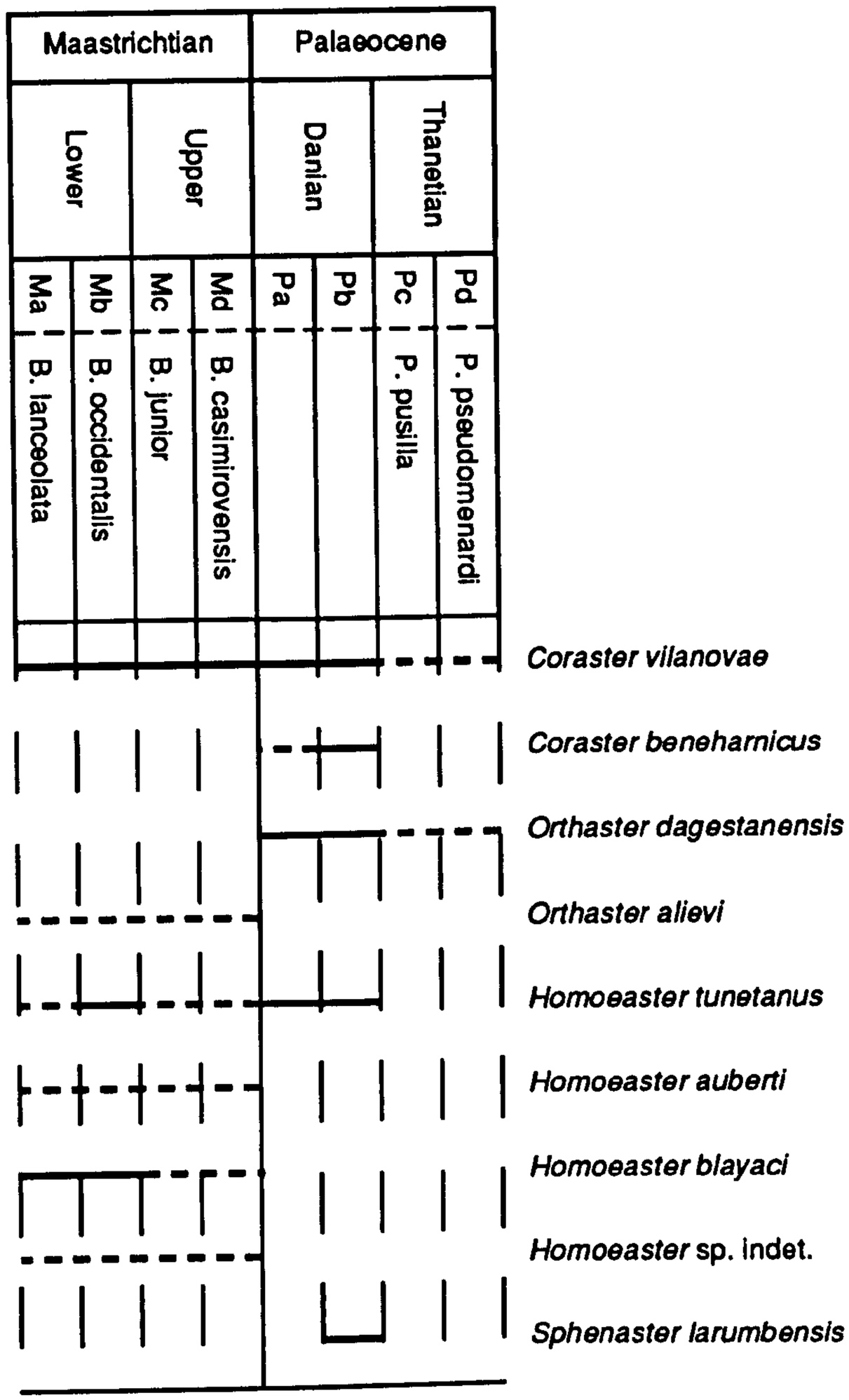

d

Figure 3.66. Range chart for Maastrichtian and Palaeocene corasterid and aeropsid species. See Figure 3.2 for explanation of symbols.


Maastrichtian
Palaeocene
Lower
Upper
Danian
Thanetian
Ma
Mb
Mc
Md
Pa
Pb
Pc
Pd
B. lanceolata
B. occidentalis
B. junior
B. casimirovensis
P. pusilla
P. pseudomenardi
Coraster vilanovae
Coraster beneharnicus
Orthaster dagestanensis
Orthaster alievi
Homoeaster tunetanus
Homoeaster auberti
Homoeaster blayaci
Homoeaster sp. indet.
Sphenaster larumbensis

Family SOMALIASTERIDAE Wagner & Durham, 1966

Diagnosis. Paired ambulacra form long petals with large numbers of pores. Plastron meridosternous but approaches amphisternous condition. Labral and sternal plates may be disjunct. Apical system compact - ethmophract or ethmolytic. Peripetalous fasciole.

Remarks. The two orders of atelostomate echinoids, the Holasteroida and the Spatangoida, are distinguished from each other by differences in apical disc and plastron plating. Holasteroids are characterized by having a meridosternous plastron and an elongate apical disc with the anterior and posterior genital plates separated from each other by ocular plates II and IV meeting at the midline. Spatangoids, on the other hand, have an amphisternous plastron and a compact apical system. The systematic position of taxa with different combinations of these characters (so called aberrant taxa) is more problematic (e.g. Jeffery 1997a).

All genera assigned to the somaliasterids have compact apical systems, petaloid paired ambulacra and plastrons that are meridosternous but which approach an amphisternous condition. The genus *Somaliaster* Hawkins has, at different times, been referred to the hemiasterid spatangoids (Hawkins 1935, Mortensen 1950), the palaeopneustid spatangoids (Maccagno 1941), the stenonasterid holasteroids (Joysey 1954, Kier 1957) and the somaliasterid holasteroids (Wagner & Durham 1966, Kier 1972). Whether this family should be placed in the holasteroids or spatangoids is still a matter of some debate (David 1988). However, a phylogenetic analysis with unequivocal representatives of both orders (see Chapter 4) demonstrates that the somaliasterids are derived from the spatangoids.

KEY TO MAASTRICHTIAN & PALAEOCENE GENERA

1	Apical system with 2 gonopores	2
	Apical system with 4 gonopores	3
2	Apical system ethmophract; petals virtually flush	*Iraniaster*
	Apical system ethmolytic; petals sunken	*Pseudiraniaster*

3 Apical system ethmolytic;

test with rounded horizontal outline.....*Leviechinus*

Apical system ethmophract

test with angular, rectangular horizontal outline.....*Brightonia*

Genus IRANIASTER Cotteau & Gauthier, 1895

[Type species *Iraniaster morgani* Cotteau & Gauthier, 1895, by OD]

Synonyms. *Somaliaster* Hawkins, 1935 (type species *Somaliaster magniventer* Hawkins, 1935).

Diagnosis. Widest point at mid-length. Apical system ethmophract or ethmolytic with four gonopores. Plastron meridosternous - disjunct in larger specimens.

Remarks. *Iraniaster* differs from *Leviechinus* and *Brightonia* in having four gonopores in the apical system. Further, while the plastron in disjunct in all examined specimens of *Leviechinus* and *Brightonia*, it is not disjunct in small specimens of *I. morgani* nor in specimens of *I. douvillei*.

Iraniaster morgani Cotteau & Gauthier, 1895

(Plate 15, figures 1-4; Figure 3.67)

1895 *Iraniaster morgani* Cotteau & Gauthier, p. 28, pl. 4, figs 1-12.

Occurrence. Senonian (probably Maastrichtian) of Iran (Cotteau & Gauthier 1895) (BMNH).

Diagnosis. Distinct frontal notch. Anterior right of test extends beyond left. Low domed upper surface and slightly convex lower surface. Paired ambulacra form virtually flush petals with equally elongate pores. Anterior petals diverge at 100 degrees, posterior at 75 degrees. Plastron meridosternous (approaching orthosternous) with labral and sternal plates disjunct in larger specimens (> about 35 mm length). Two post-sternal plates approximately equal in size and symmetrically placed. Apical system ethmophract with

four gonopores. Narrow peripetalous fasciole does not indent between petals.

Iraniaster douvillei Cotteau & Gauthier, 1895

(Figure 3.68)

1895 *Iraniaster douvillei* Cotteau & Gauthier, p. 30, pl. 5, figs 1-6.
1935 *Somaliaster magniventer* Hawkins, p. 53, pl. 7, figs 2-3, text figs 8-14.
1941 *Somaliaster magniventer* Hawkins; Maccagno, p. 89, pl 11, figs 1-9, 12, text figs 1-3.
1941 *Somaliaster magniventer* var. *Checchiai* Maccagno, p. 93, pl. 11, figs 10-11.
1954 *Somaliaster magniventer* Hawkins; Joysey, p. 45, text fig. 1.

Occurrence. Senonian (probably Maastrichtian of Iran) (Cotteau & Gauthier 1895) and Maastrichtian of Somalia (Hawkins 1935; Maccagno 1941) (BMNH, UGHM).

Diagnosis. Differs from *I. morgani* in higher, more gibbous profile; shallower frontal groove; non-disjunct plastron even in large specimens; anterior and posterior petals more widely divergent (anterior 110-120 degrees; posterior 85-90 degrees); less distinct peripetalous fasciole.

Genus PSEUDIRANIASTER nov.

Diagnosis. Paired ambulacra form long, straight sunken petals. Apical system ethmolytic with four gonopores. Plastron meridosternous with labral and sternal plates disjunct. narow peripetalous fasciole does not indent behind anterior petals.

Remarks. Most similar to *Iraniaster*, from which it differs in having an ethmolytic apical system and more deeply sunken paired ambulacra. The petals of *Pseudiraniaster* are also more deeply sunken than those of either *Leviechinus* or *Brightonia*. In addition, both *Leviechinus* and *Brightonia* have only two gonopores in the apical system.

Pseudiraniaster omanensis sp. nov.

(Plate 15, figures x-y; Figure 3.69)

Types. Holotype BMNH E82606. Four other paratypes BMNH E82603-E82605, E82607.

Occurrence. Maastrichtian of Oman (BMNH).

Diagnosis. Inflated upper surface, flat base. Broad, shallow frontal groove. Paired ambulacra form long, straight, sunken petals. Anterior pair diverge at 140 degrees; posterior at 60 degrees. Plastron (where visible) disjunct in specimens of all sizes. Apical system ethmolytic with four gonopores.

Remarks. Most similar to *Iraniaster morgani* and *Iraniaster douvillei*, but differs in having an ethmolytic apical system and sunken petals, the anterior pair of which are very divergent.

Genus LEVIECHINUS Kier, 1957

[Type species *Pericosmus gregoryi* Currie, 1927, by OD]

Diagnosis. Broad heart-shaped test. Apical system ethmolytic with two gonopores. Disjunct meridosternous plastron approaching amphisternous structure.

Remarks. Differs from *Brightonia* in having an ethmolytic apical system and in having the plastron more nearly amphisternous in structure. In addition, the mouth is more anteriorly placed in *Brightonia*. The two genera also differ in horizontal outline. *Leviechinus* is cordate whilst *Brightonia* is approximately rectangular.

Leviechinus gregoryi (Currie, 1927)

(Plate 15, figures x-y; Figure 3.70)

1927 *Pericosmus gregoryi* Currie, p. 430, text fig. 7.

1943 *Pericosmus gregoryi* Currie, p. 26, pl. 4, fig. 5, text fig. 10.

1957 *Leviechinus gregoryi* (Currie); Kier, p. 874, pl. 104, figs 14-16, text fig. 14.

Occurrence. Palaeocene Lower Auradu Series of Somalia (Currie 1927, 1943; Kier 1957) (BMNH, UCSM).

Diagnosis. Broad flat upper and lower surfaces curving steeply at margins. Petals flush in small specimens, slightly sunken in larger specimens. Pore-pairs slit-like and equally elongate. Anterior petals diverge at 130 degrees; posterior at 80 degrees. Plastron strictly

speaking meridosternous (i.e. plastron is followed by a single large sternal plate) but plate 3 extends nearly as far towards the anterior as plate 2. Labral and sternal plates disjunct. Apical system ethmolytic with two gonopores; posterior genital plates perforate. Peripetalous fasciole preserved only in some specimens.

Genus BRIGHTONIA Kier, 1957

[Type species *Brightonia macfadyeni* Kier, 1957, by OD]

Diagosis. Test rectangular, widest anteriorly. Ethmophract apical system with two gonopores. Disjunct meridosternous plastron approaching amphisternous structure.

Brightonia macfadyeni Kier, 1957

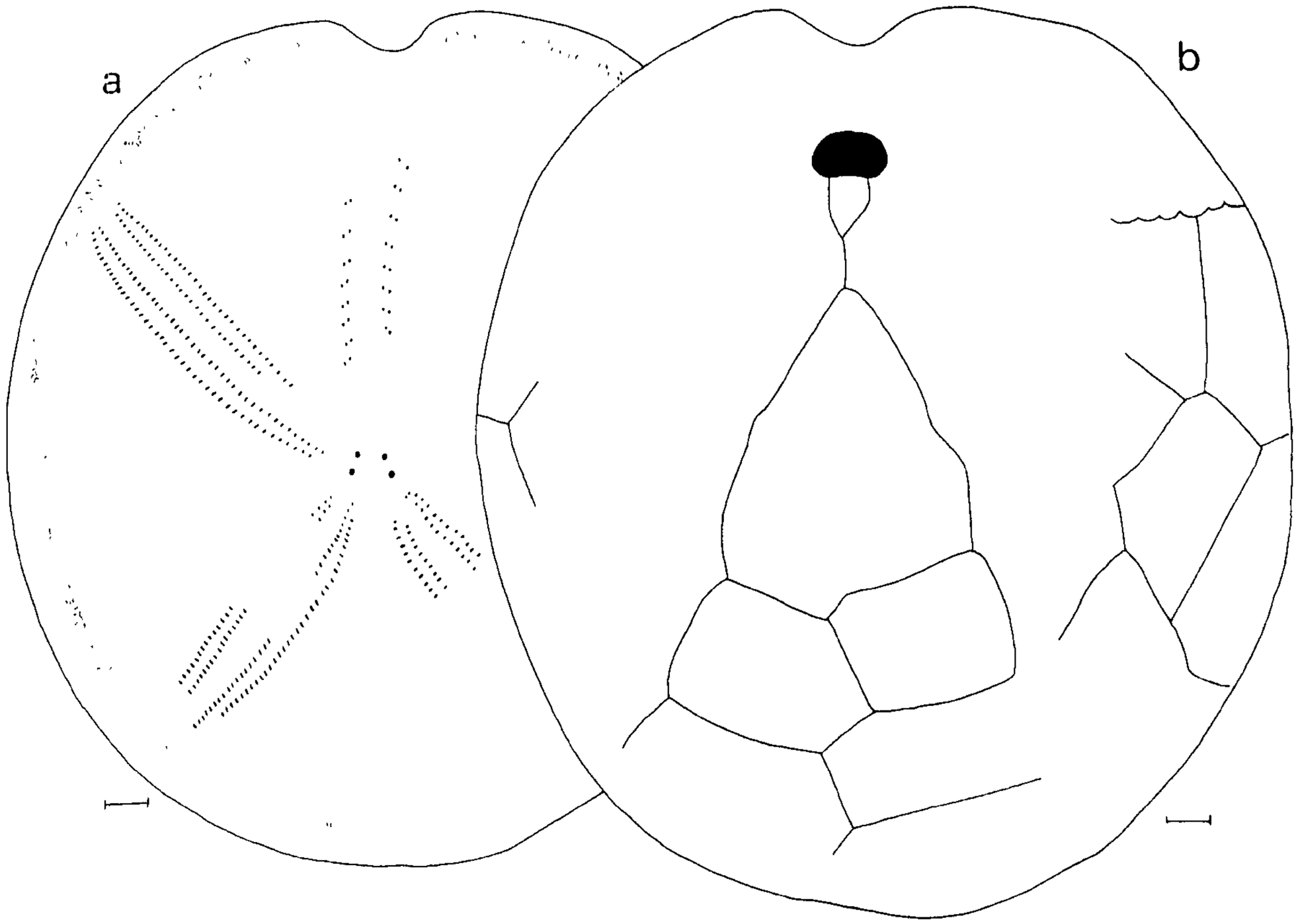
(Figure 3.71)

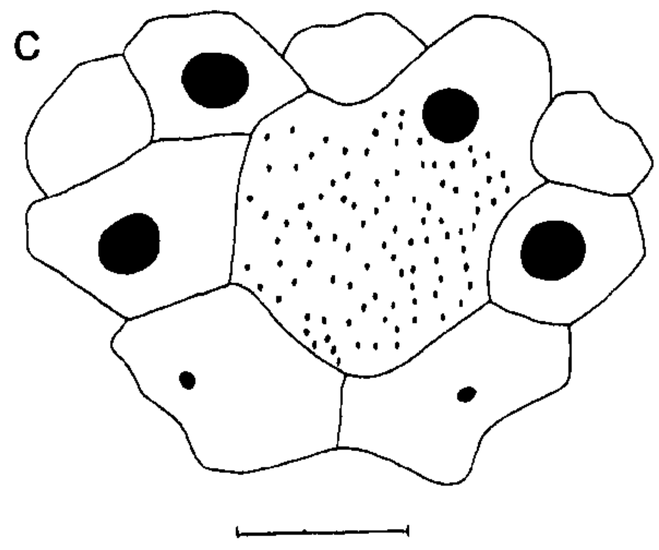
1957 *Brightonia macfadyeni* Kier, p. 872, pl. 104, figs 12-13, text fig. 13.

Occurrence. Palaeocene Lower Auradu Series of Somalia (UCSM).

Diagnosis. Test approximately rectangular in horizontal outline with flat anterior margin. Pores in paired ambulacra equally elongated. Labral and sternal plates separated by ambulacra meeting at mid-line. Plastron meridosternous but approaches amphisternous arrangement as plate 3 extends more than half way along plate 2. Apical system ethmophract with two gonopores - genital plates 1 and 4 perforated. Rudimentary peripetalous fasciole.

Figure 3.67. Camera lucida drawings of *Iraniaster morgani* Cotteau & Gauthier, "Senonian" of Louristan, Persia. a, BMNH E17327, apical view. b & c, BMNH E17324; b, oral view; c, apical disc plating. d, BMNH E17326, lateral view. a, b & d, scale bars = 2 mm. c, scale bar = 1 mm.


a
b


c

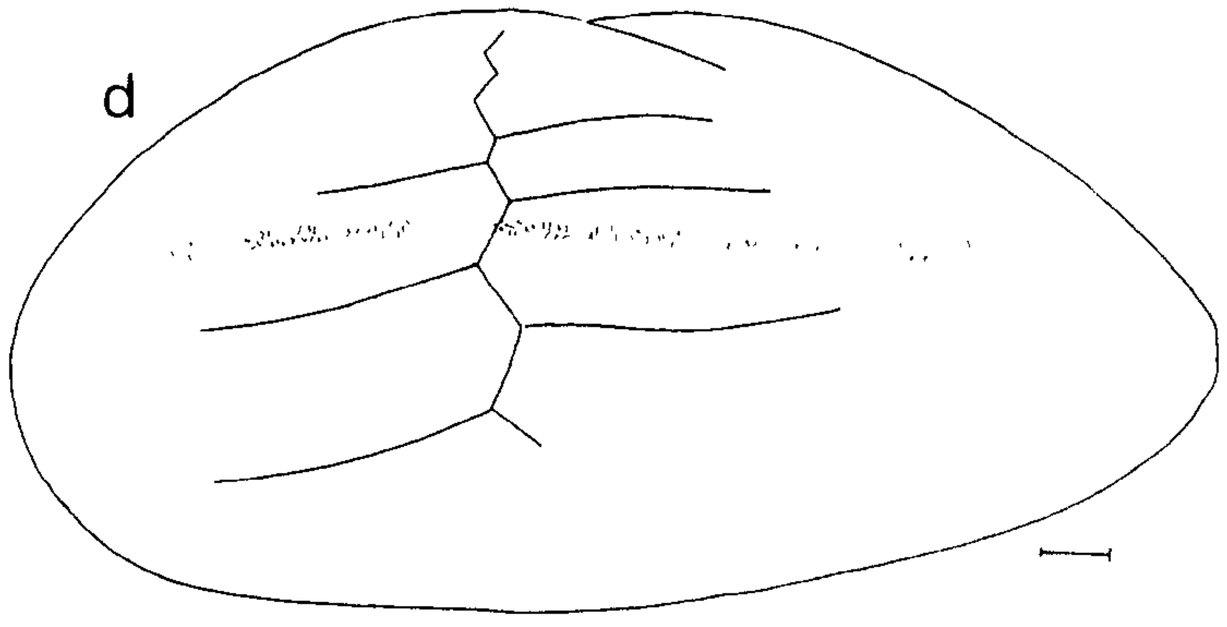
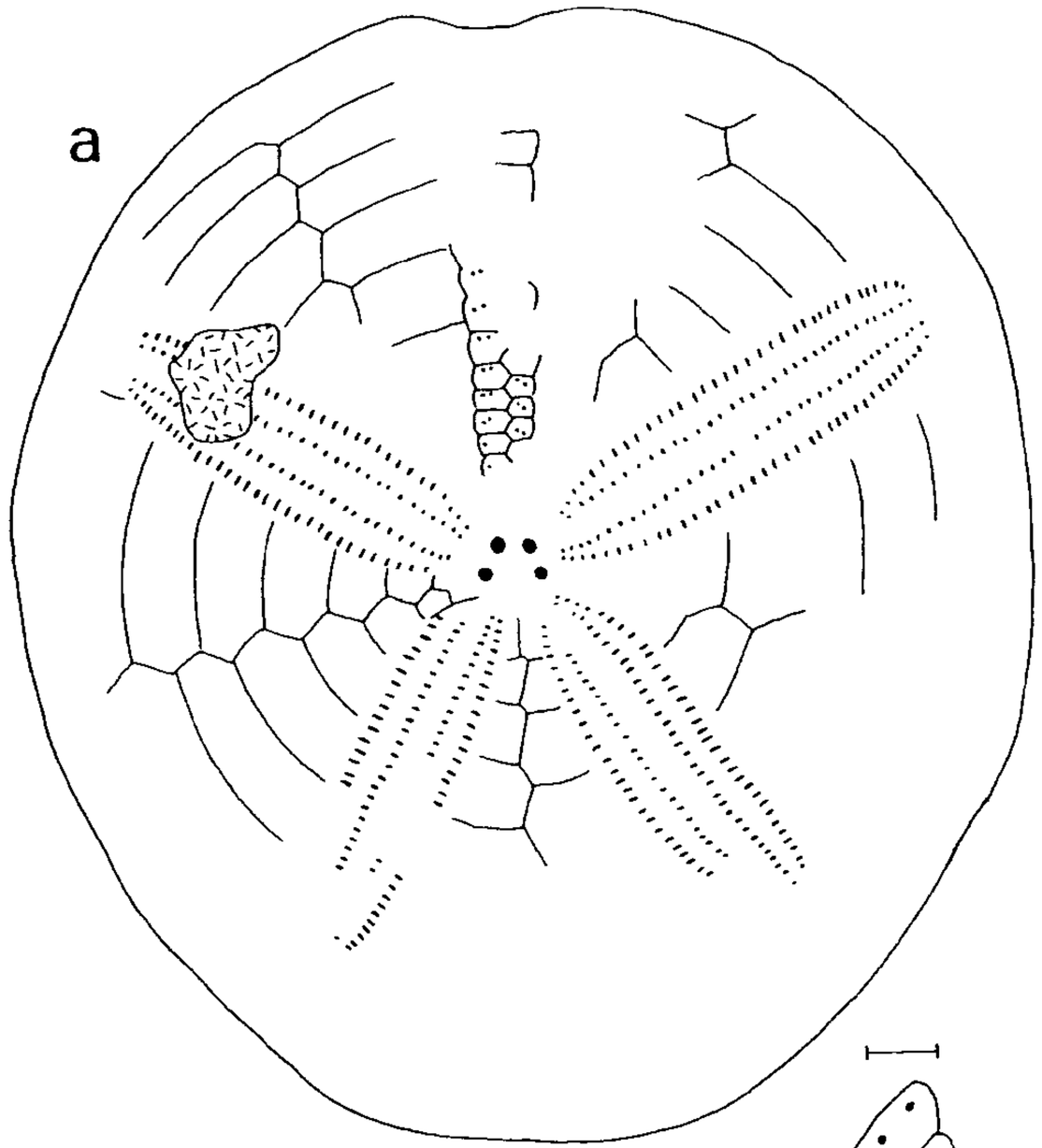
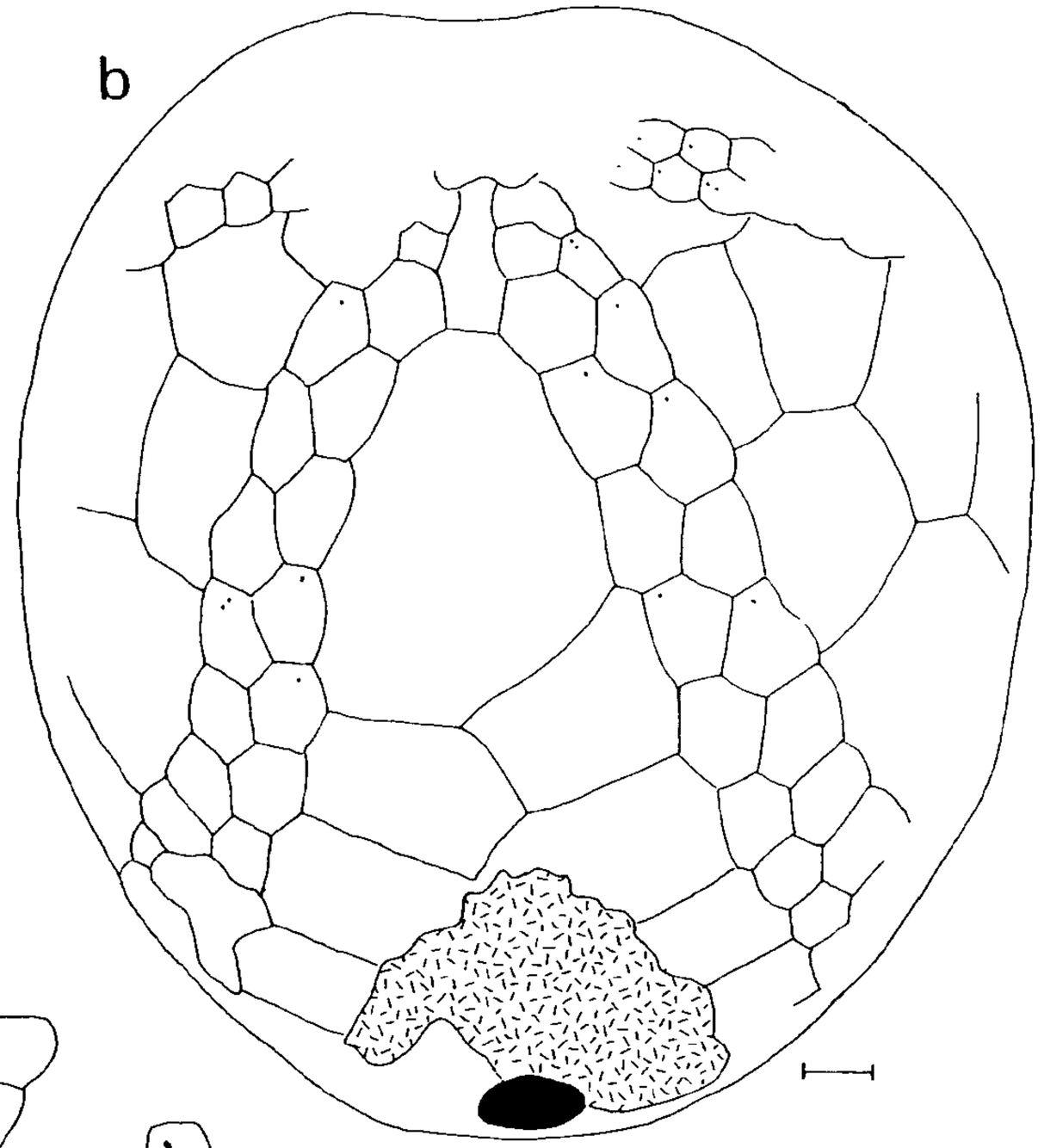

d

Figure 3.68. Camera lucida drawings of *Iraniaster douvillei* Cotteau & Gauthier, "Senonian" of Somalia. a & b, UGHM E325; a, apical view; b, oral view. c, BMNH E43775, apical disc plating. a & b, scale bars = 2 mm. c, scale bar = 1 mm.


a


b

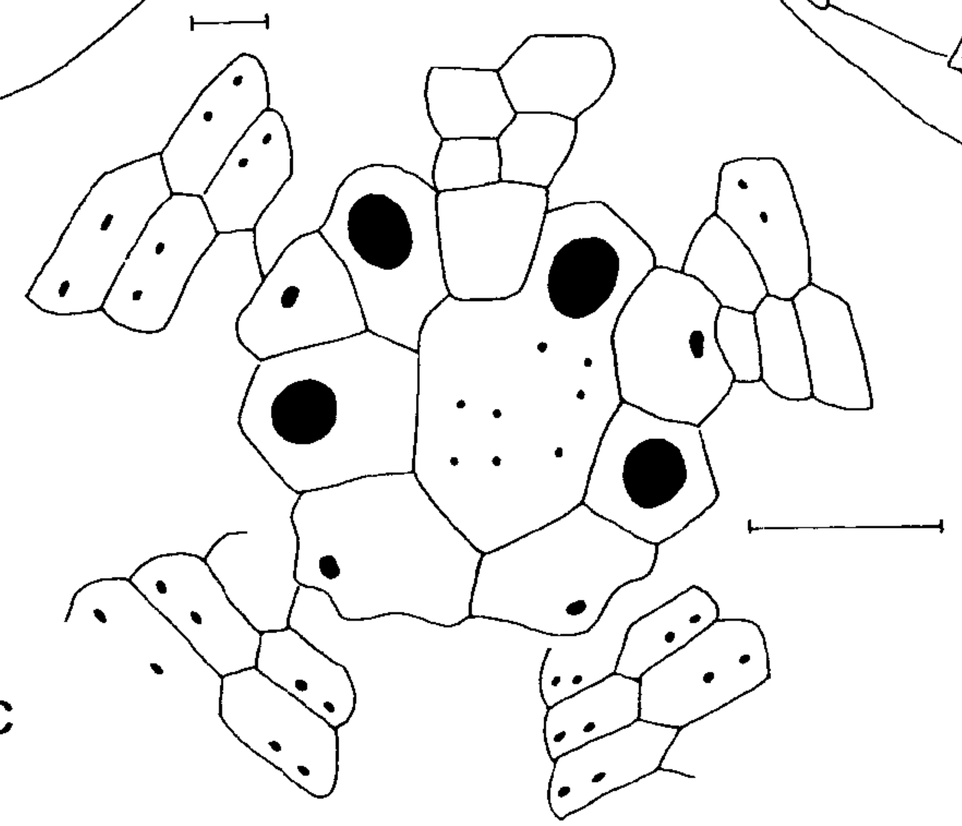

c

Figure 3.69. Camera lucida drawings of *Pseudiraniaster omanensis* sp. nov., Maastrichtian of Oman. a, BMNH E82606 (HOLOTYPE), apical view. b & c, BMNH E82603 (PARATYPE); b, apical disc plating; c, oral view. a, scale bar = 2 mm. b, scale bar = 1 mm. c, scale bar = 5 mm.

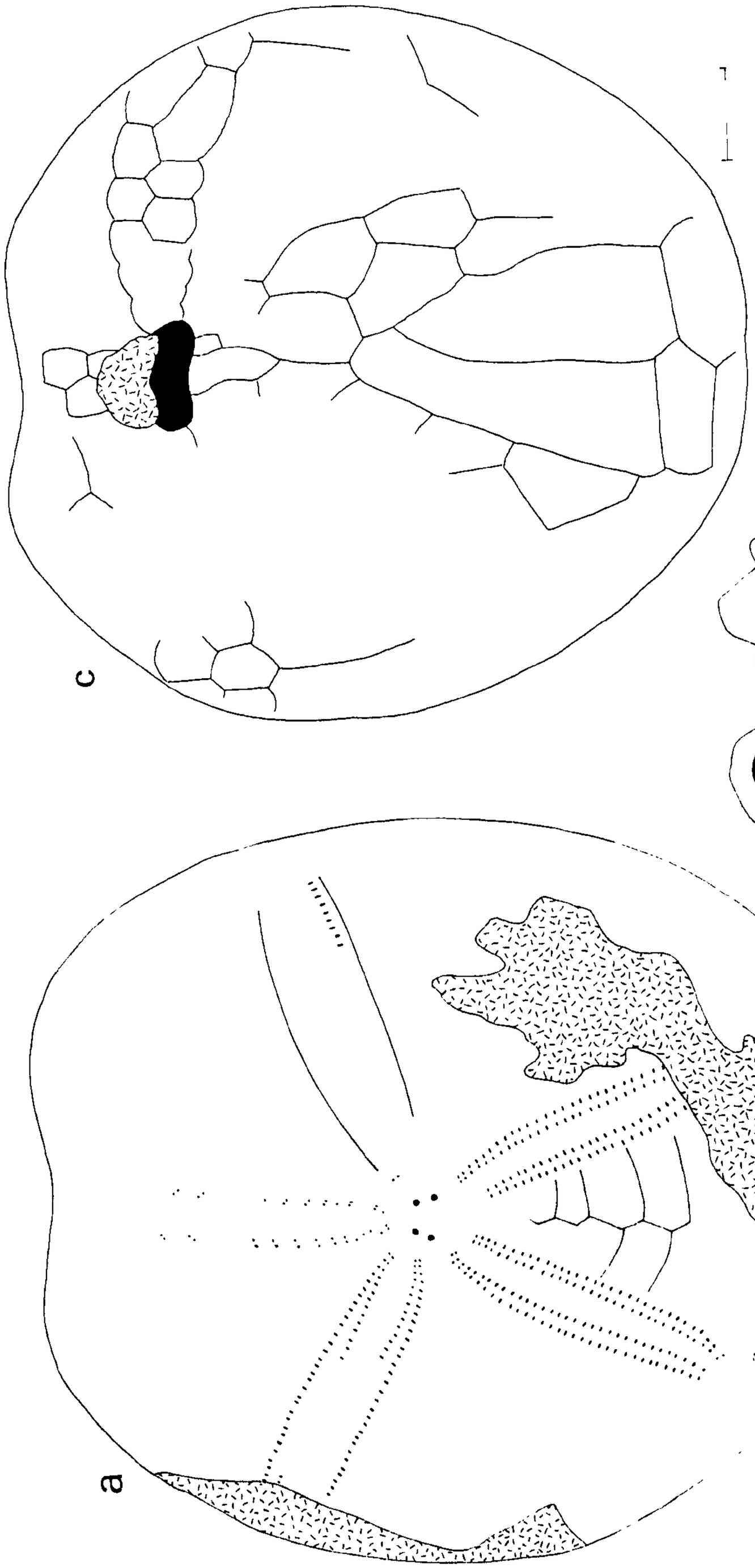
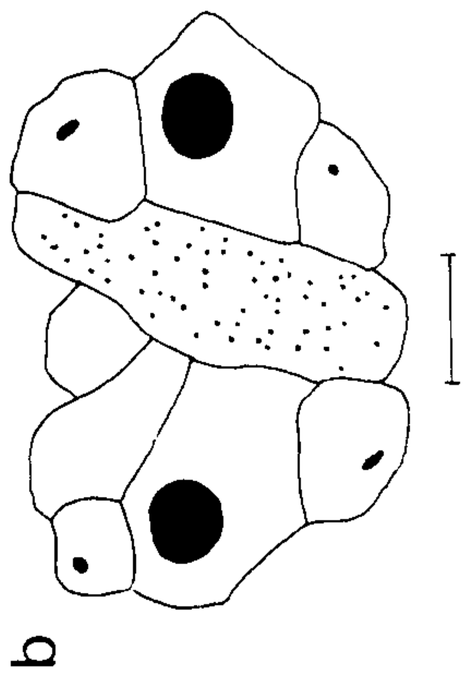
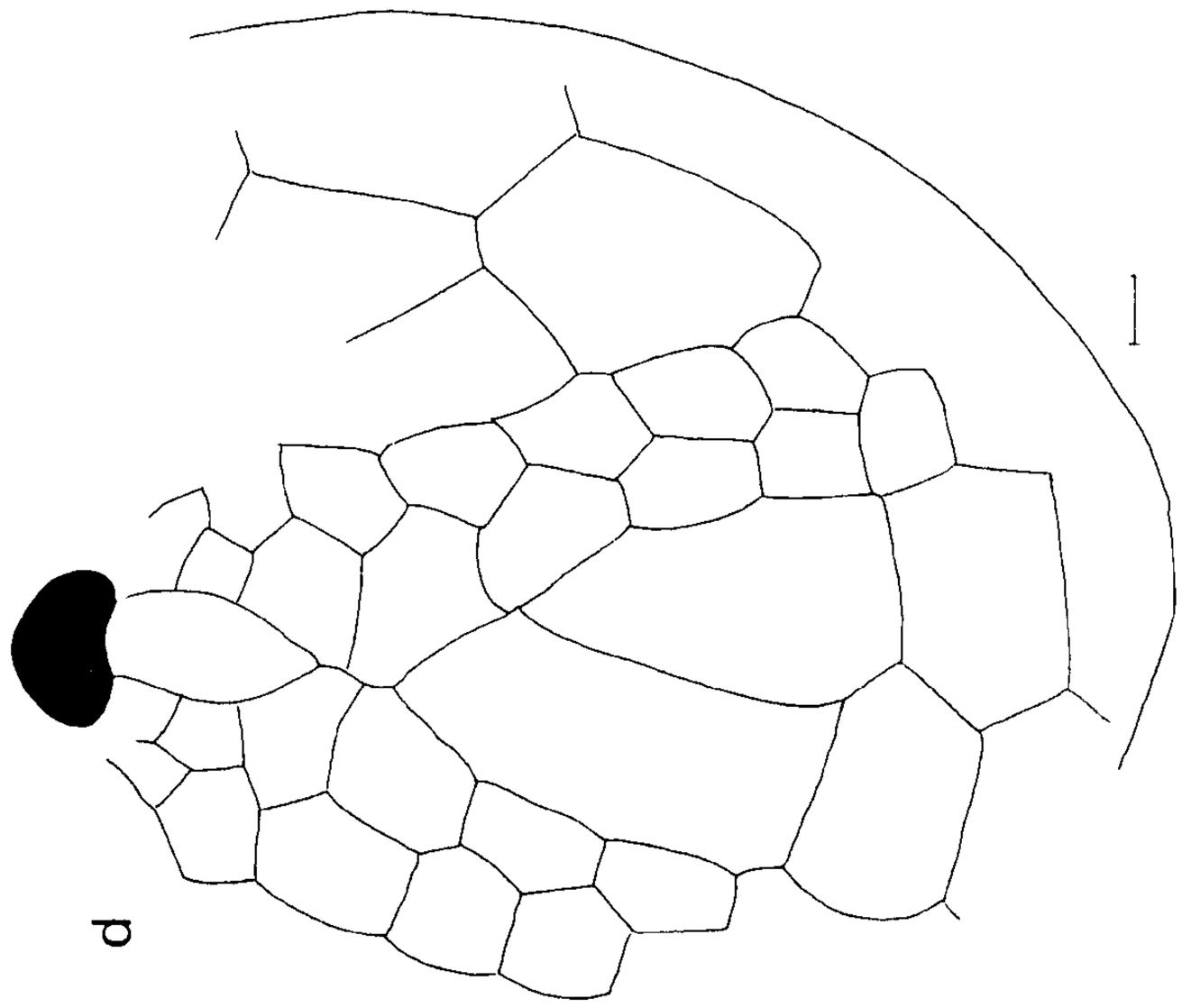

c
b
a

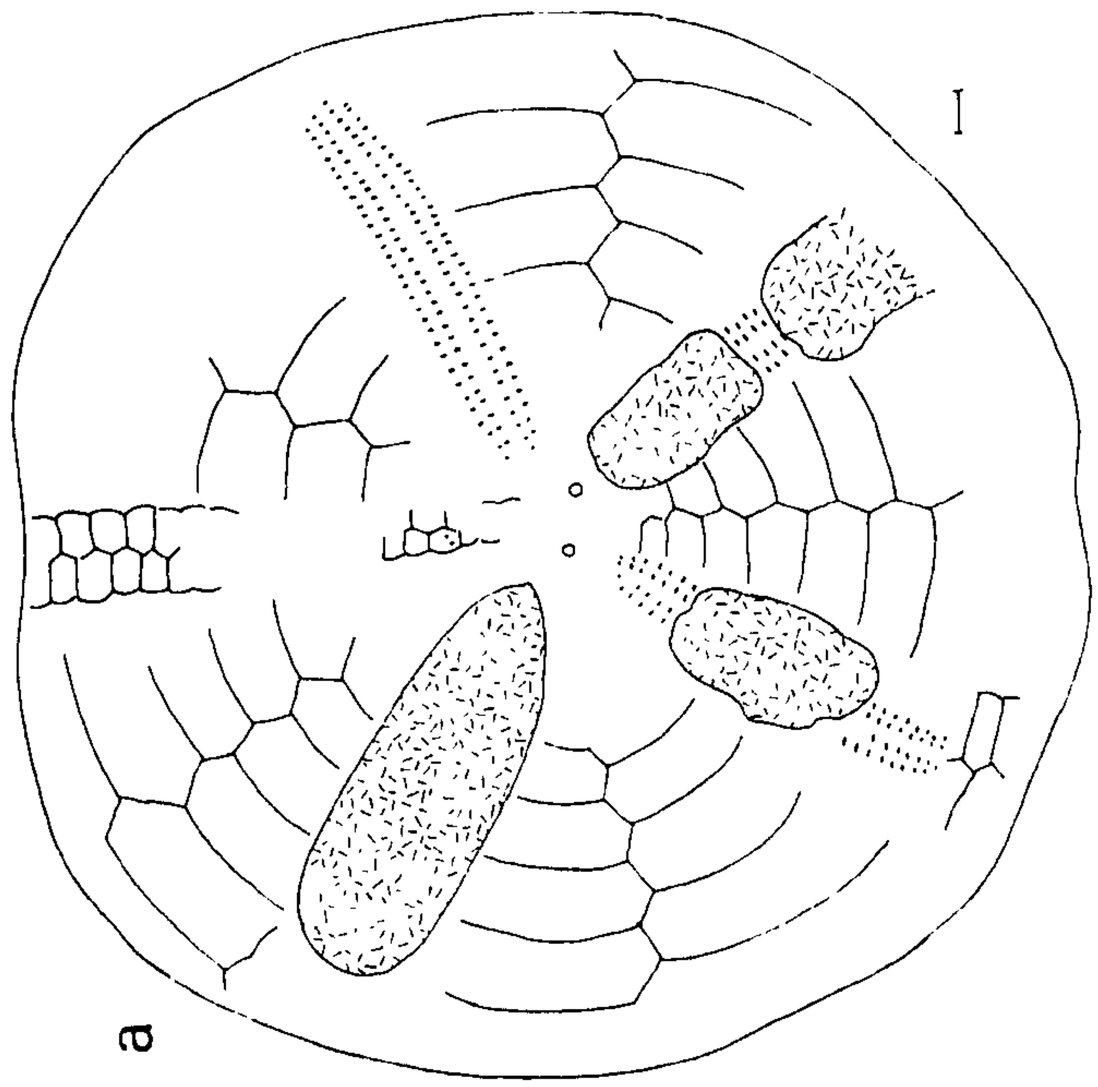
Figure 3.70. Camera lucida drawings of *Leviechinus gregoryi* (Currie), Palaeocene Lower Auradu Series of Somalia. a-c, BMNH E18080 (HOLOTYPE); a, apical view; b, apical disc plating; c, lateral view. d, UCSM, C3050, oral view. a, c & d, scale bars = 2 mm. b, scale bar = 1 mm.



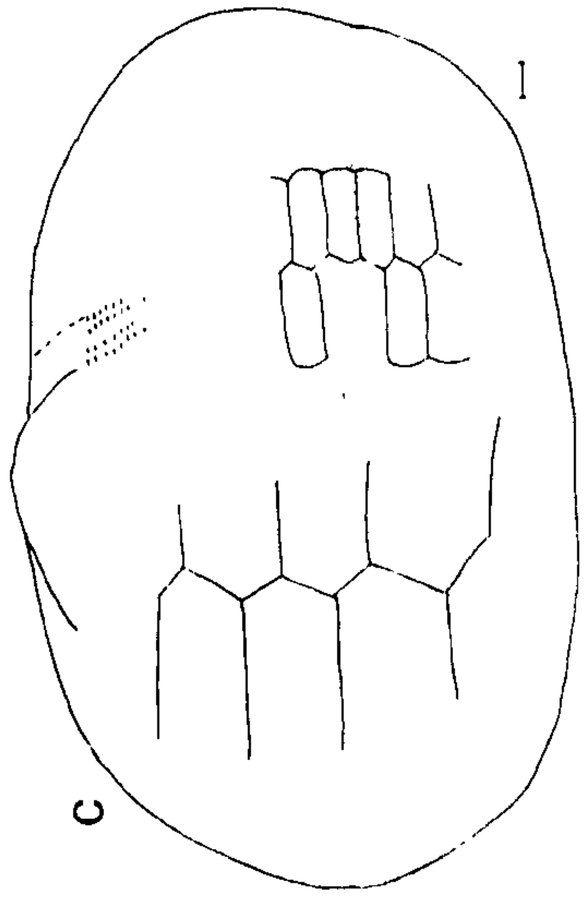
b



d

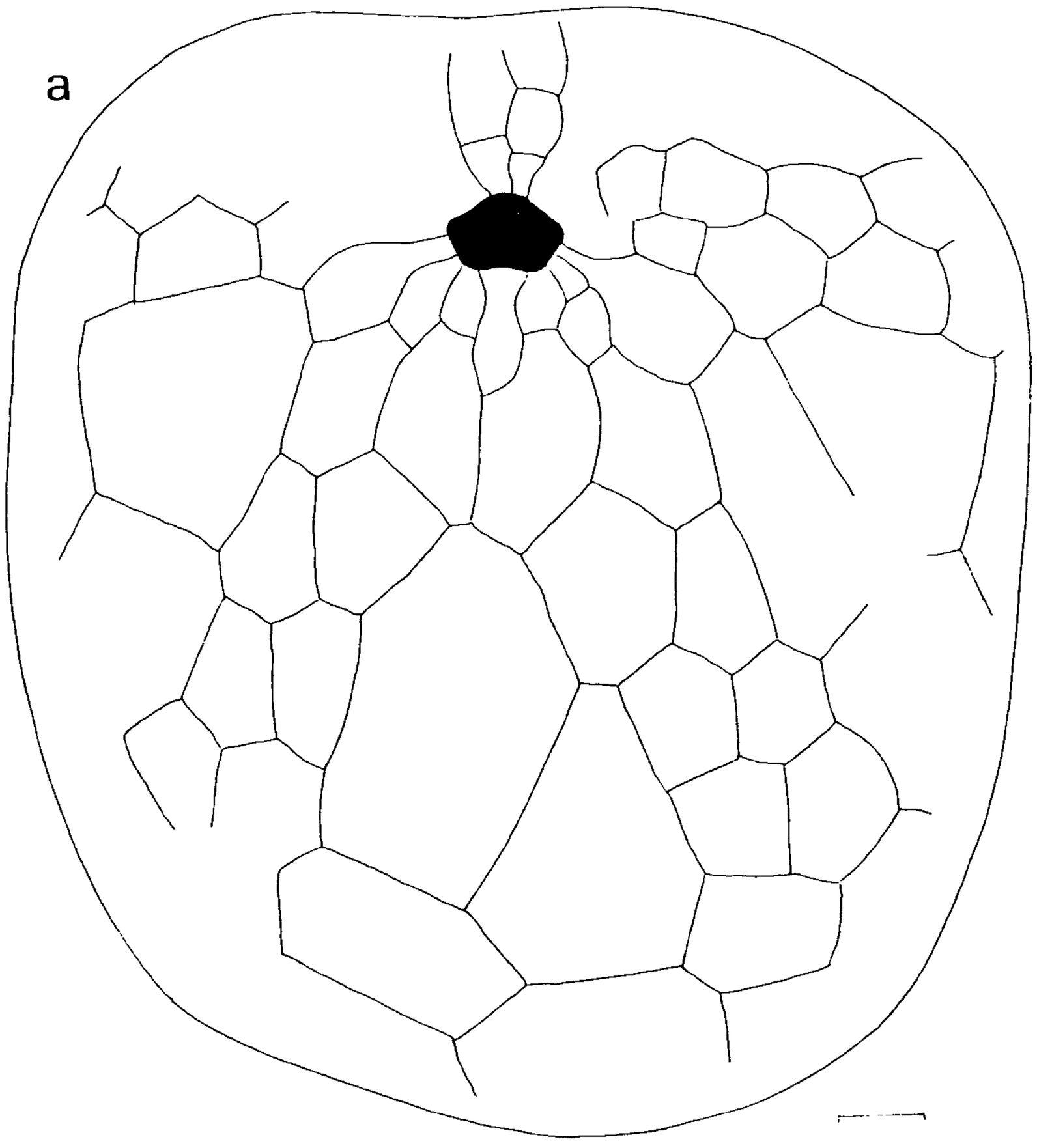


a



c

Figure 3.71. Camera lucida drawings of *Brightonia macfadyeni* Kier, Palaeocene Lower Auradu Series of Somalia. a, UCSM C3055, oral view. b, UCSM C3059, apical disc plating. a, scale bar = 2 mm. b, scale bar = 1 mm.


a

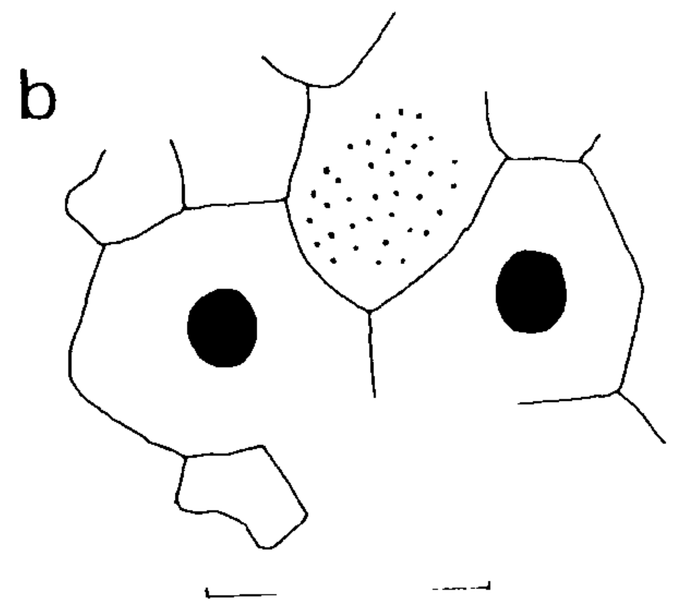
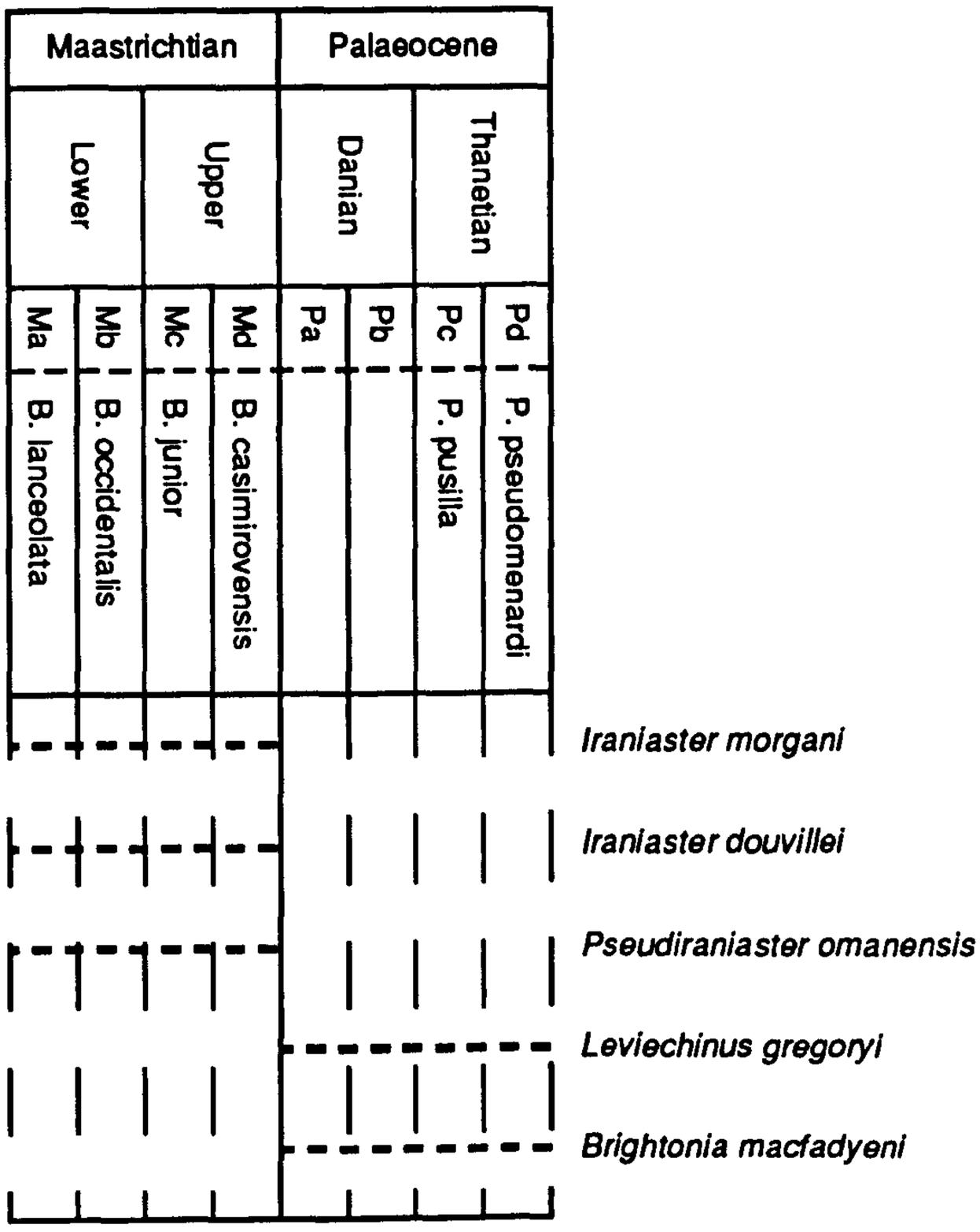

b

Figure 3.72. Range chart for Maastrichtian and Palaeocene somaliasterid species. See Figure 3.2 for explanation of symbols.


Maastrichtian
Palaeocene
Lower
Upper
Danian
Thanetian
Ma
Mb
Mc
Md
Pa
Pb
Pc
Pd
B. lanceolata
B. occidentalis
B. junior
B. casimirovensis
P. pusilla
P. pseudomenardi
Iraniaster morgani
Iraniaster douvillei
Pseudiraniaster omanensis
Leviechinus gregoryi
Brightonia macfadyeni

Indeterminate spatangolds.

Material too poorly preserved to allow identification:

1950 *Micraster vistulensis* Kongiel, p. 318, pl. 2, figs 5-8.

Occurrence. Maastrichtian glauconitic sandstone of southeastern Poland.

Remarks. Worn specimen with posterior portion of test damaged. Apical system ethmophract. Most similar in overall appearance to *Diplodetus coloniae.*

1935 *Micraster duponti* Lambert; Kongiel, p. 39, pl. 5, fig. 1.

Occurrence. Mid Danian Siwak of southeastern Poland.

Remarks.

1881 *Hemiaster antillensis* Cotteau, p. 31, pl. 3, figs 1-4.
1949 *Trachyaster antillensis* (Cotteau); Sanchez Roig, p. 243.
1984 *Hemiaster antillensis* Cotteau; Kier, p. 19.

Occurrence. Early Upper Maastrichtian of Cuba (Cotteau 1881; Sanchez Roig 1949; Kier 1984) (BMNH).

Remarks. The types of this species are housed at the Natural History Museum, London. Neither specimen has the apical system visible or any trace of tuberculation preserved. Consequently, generic identification is impossible.

1933b *Hemiaster batalleri* Lambert, p. 187, pl. 1, figs 14-16.

Occurrence. Maastrichtian of Barcelona, Spain.

Remarks. The type of this species is a worn specimen with an ethmophract apical system but no fascioles preserved. Consequently it is indeterminate. Material subsequently assigned to *H. batalleri* is transferred to *H. prunella.*

1993 *Hemifaorina? rex* McNamara, p. 333, figs 1-2.

Occurrence. Thanetian Kings Park Formation of Western Australia.

Diagnosis. Circular horizontal outline with indistinct frontal notch. Paired ambulacra form broad, bowed petals. Anterior pair three times longer than posterior. Apical system ethmolytic with four gonopores. No tuberculation preserved.

Remarks. Since fascioles are not preserved, the generic position of the material cannot be determined with any degree of certainty and it is considered indeterminate. Specimens assigned to *Hemifaorina? rex* are most similar to *Hemiaster stella*, but differ in possessing an ethmolytic rather than an ethmophract apical system.

1979 *Hemiaster (Mecaster) boulei* Tanaka *et al.*, p. 35, pl. 3, fig. 7.

Occurrence. Danian Formation C10 of northwestern Madagascar.

Remarks. No fascioles preserved. The photographs accompanying the description are inadequate to allow identification.

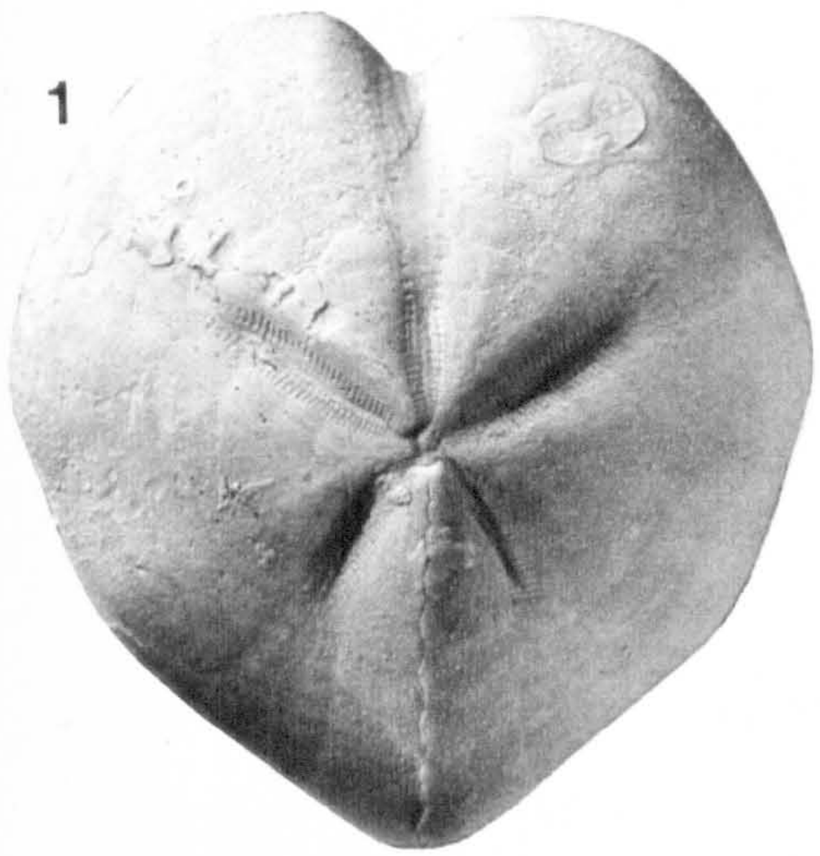
Table 3.3. Indeterminate spatangoid taxa recorded from Maastrichtian and Palaeocene deposits. Material unavailable for study. Descriptions and / or illustrations inadequate to allow even generic identification.

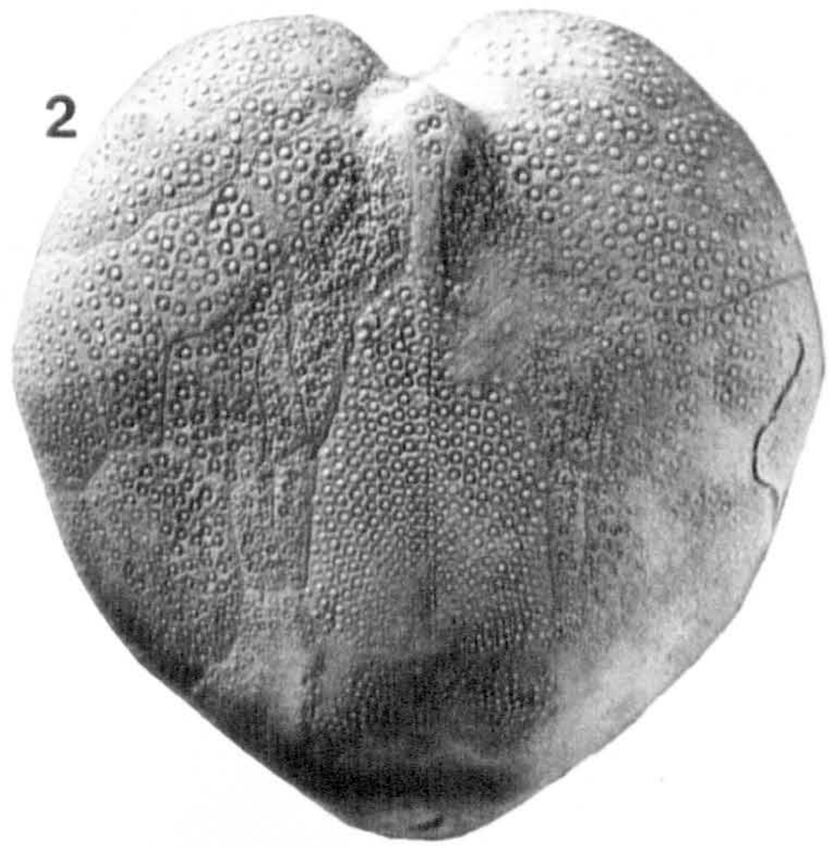
Taxon	Reference	Age	Locality
Micraster transcaspius	Gongadze 1979	Lower - Upper Maas.	Georgia
Micraster sp.	Ravn 1927	Lower Danian Bryozoan Limestone; Mid - Upper Danian Saltholm Limestone	Denmark
Micraster sp.	Brünnich Nielsen 1926	Mid - Upper Danian Saltholm Limestone	Denmark
Micraster sp.	Hassan 1969	Upper Thanetian Esna Shale	Egypt
Micraster sp.	Akkus 1971	Lower Maas. Ulupinar Fm.	Turkey
Cyclaster sp.	Ravn 1927	Lower Danian Bryozoan Limestone	Denmark
Isopneustes gindrei	Tzankov 1934	Lower Maas. Upper Chalk	Bulgaria
Hemiaster aff. *amygdala*	Akkus 1971	Lower Maas. Ulupinar Fm.	Turkey
Hemiaster nasutulus	Nicklès 1892	Maastrichtian	Spain
Hemiaster nasutulus	Gongadze 1979	Upper Maas.	Georgia
Hemiaster cf. *regulusi*	Rouchadze 1940	Maastrichtian	Georgia
Hemiaster cf. *regulusi*	Gongadze 1979	Lower - Upper Maas.	Georgia
Hemiaster sp.	Das Gupta 1920	Early Upper Maas.	India
Hemiaster sp.	Amard *et al.* 1981	Lower Maas. c6a	Algeria
Hemiaster sp.	Duncan & Sladen 1882	Thanetian Ranikot Fm.	Pakistan
Hemiaster sp.	Besairie 1930	Upper Maas. Craie d'Andrafiavelo	Madagascar
Hemiaster? sp.	Kugler & Caudri 1975	?Palaeocene Soldado Fm.	Trinidad
Linthia sp.	Kugler & Caudri 1975	Palaeocene Soldado Fm.	Trinidad
Linthia sp. 1	van der Ham *et al.* 1987	Upper Maas. Nekum Chalk	Maastricht area
Schizaster schlosseri	Traub 1938	Thanetian	Austria
Schizaster sp. indet.	Traub 1938	Mid Palaeocene	Austria
Trachyaster minutus	Sanchez Roig 1949	Upper Cretaceous?	Cuba
Trachyaster simpaticus	Sanchez Roig 1949	Upper Cretaceous?	Cuba
Homoeaster sp.	Sanchez Roig 1949	Upper Cretaceous?	Cuba

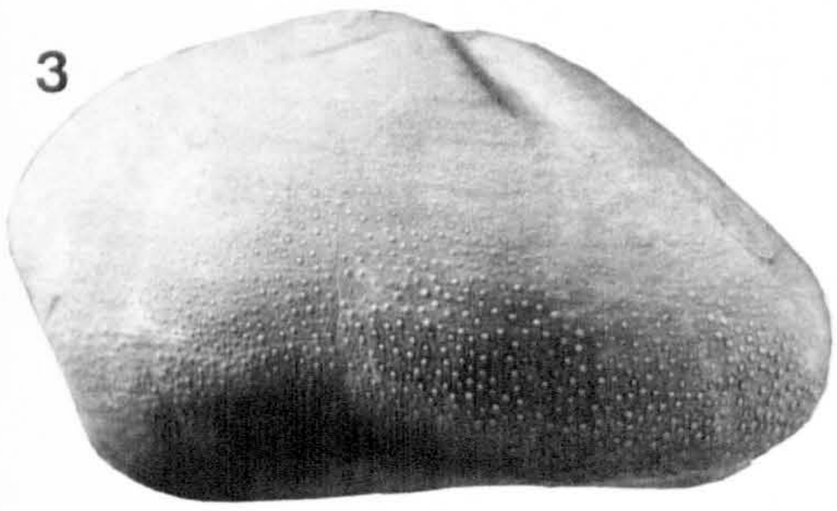
PLATE 7

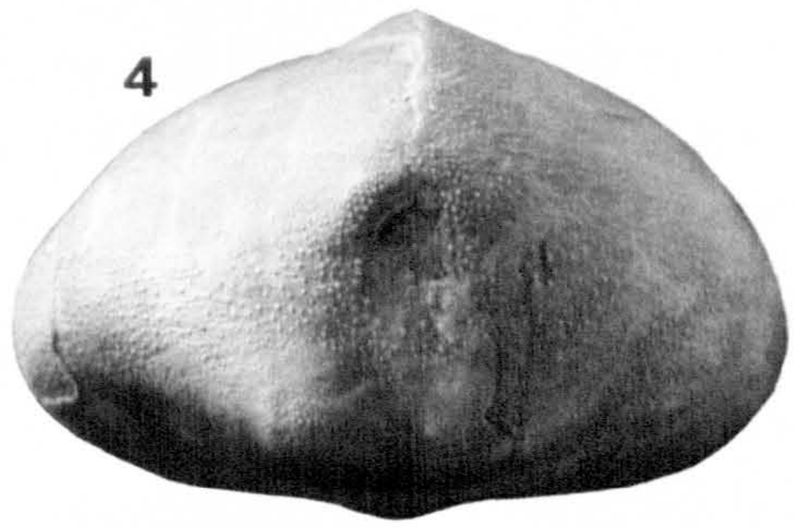
Figs 1-4. *Micraster schroederi* Stolley, BMNH E75824, Campanian of northern Germany. 1, apical view; 2, oral view; 3, lateral view; 4, posterior view. All x1.

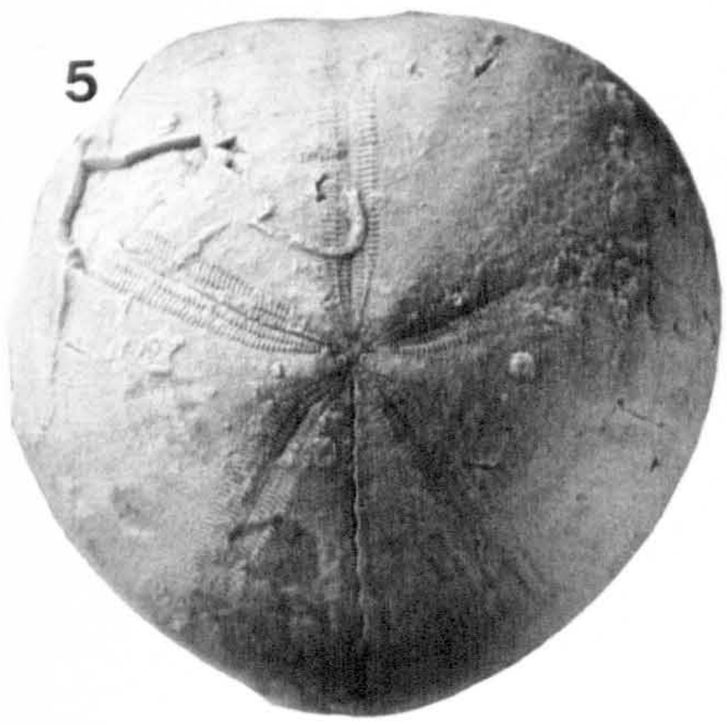
Figs 5-8. *Mokotibaster hourcqi* Lambert, BMNH E79094, Lower Maastrichtian of northwest Madagascar (TOPOTYPE). 1, apical view; 2, oral view; 3, lateral view; 4, posterior view. All x1.

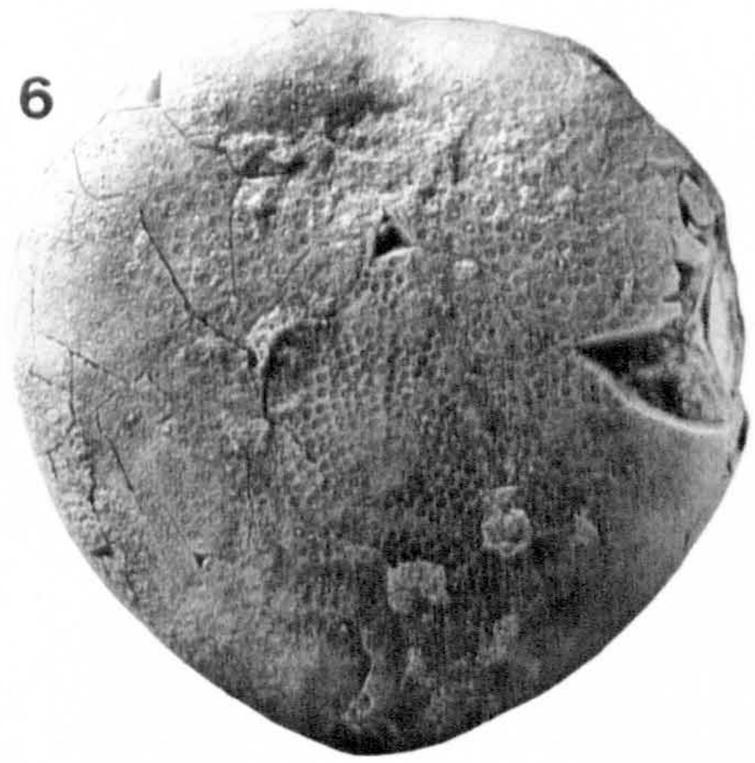

1

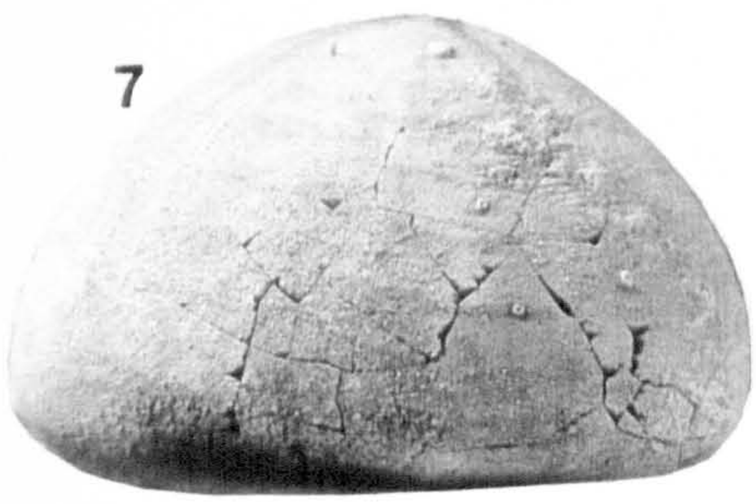

2


3


4


5


6


7

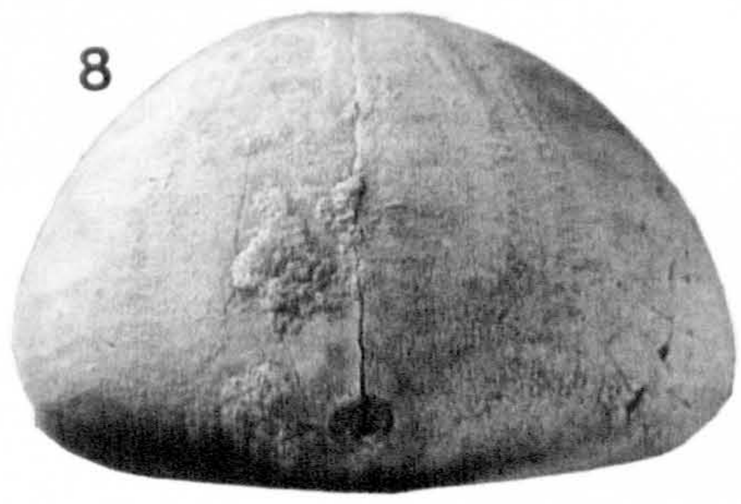

8

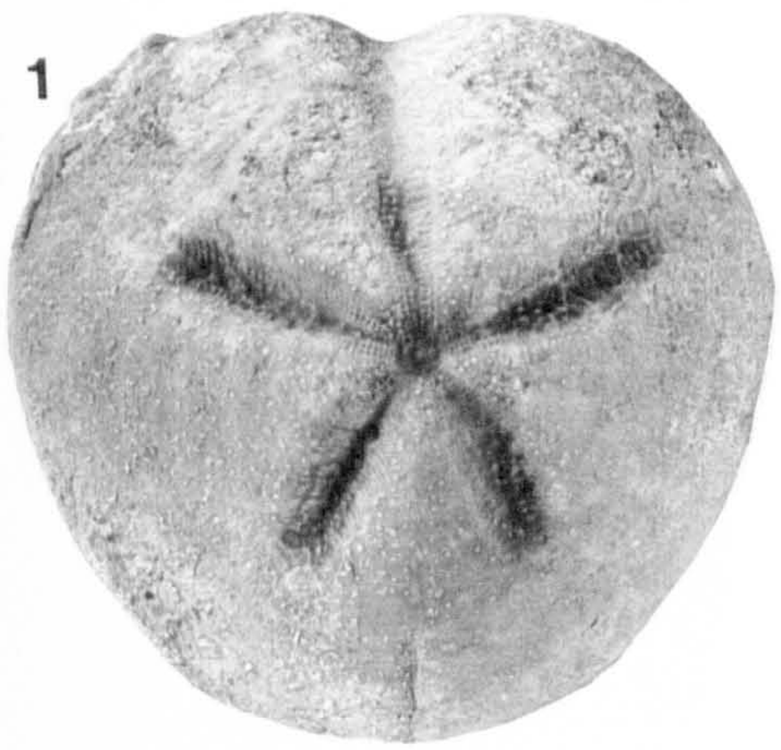
PLATE 8

Figs 1-4. *Pseudogibbaster tercensis* (Cotteau), BMNH EE6067, locality. 1, apical view; 2, oral view; 3, posterior view; 4, lateral view. All x1.

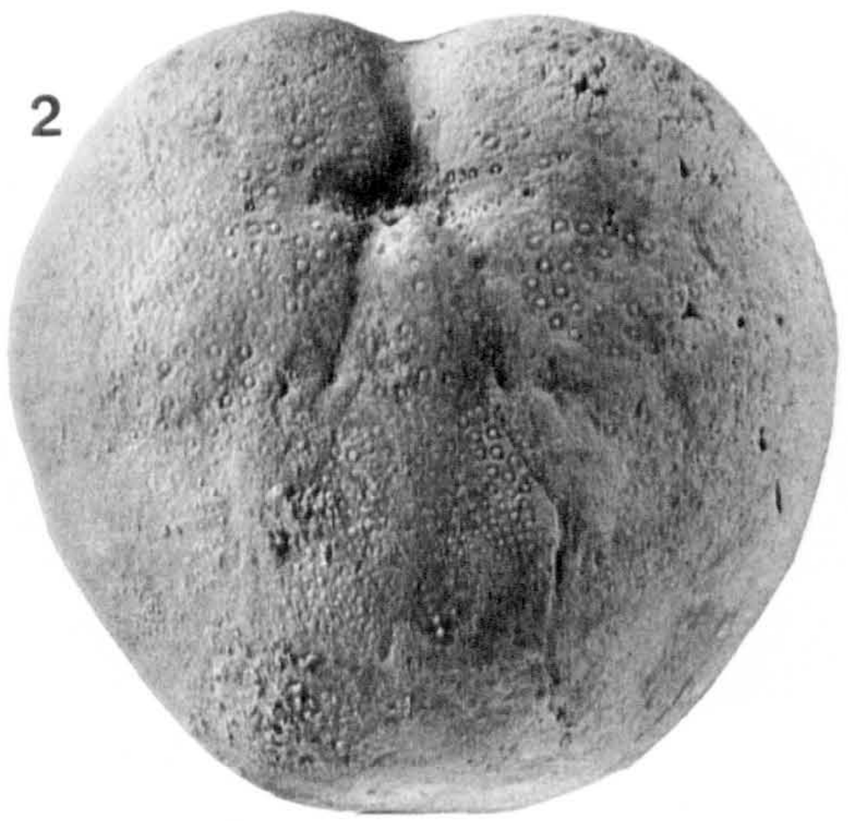
Figs 5-7. *Diplodetus americanus* (Stephenson), USNM 76285 (HOLOTYPE), Mid Maastrichtian Corsicana Marl of Texas, USA. 5, apical view; 6, oral view; 7, lateral view. All x2.

Figs 8-11. *Cyclaster integer* (Seunes), Danian of the Mangyshlak Peninsula, Kazakhstan. 8-9, BMNH EE5597. 8, apical view; 9, oral view. 10-11, BMNH EE5585. 10, lateral view; 11, posterior view. All x2.

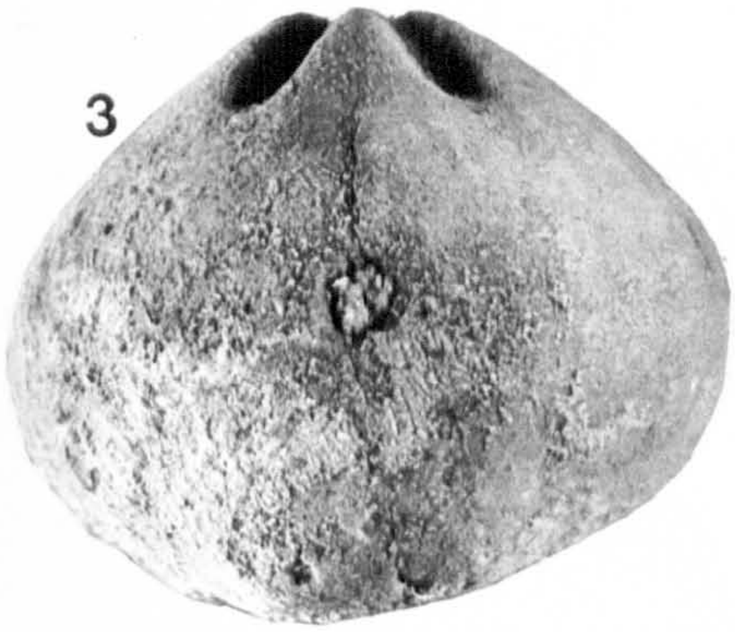
1



2



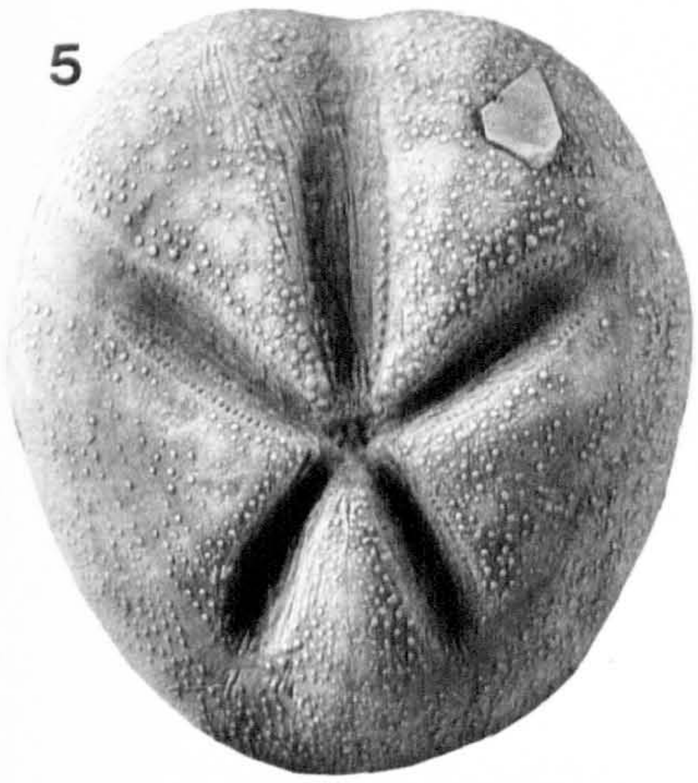
3



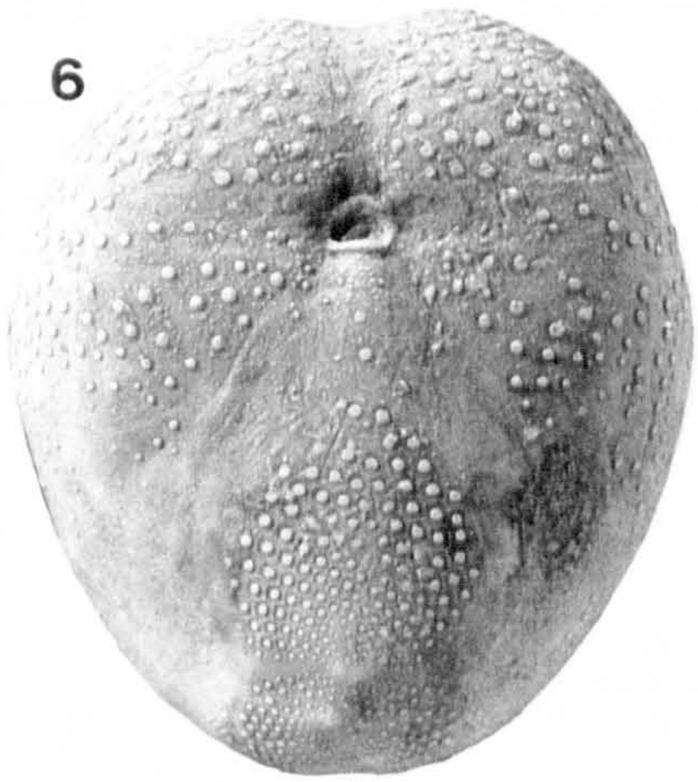
4



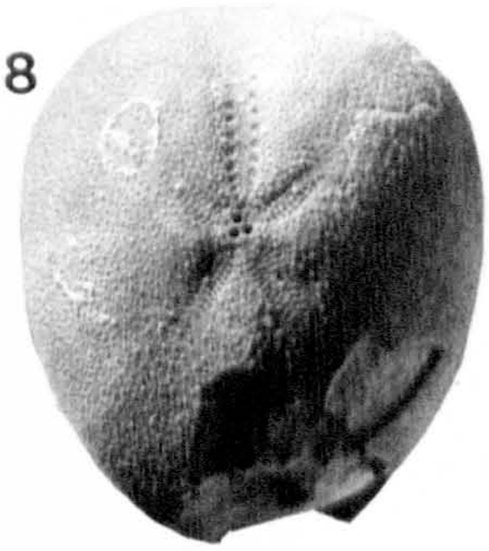
5



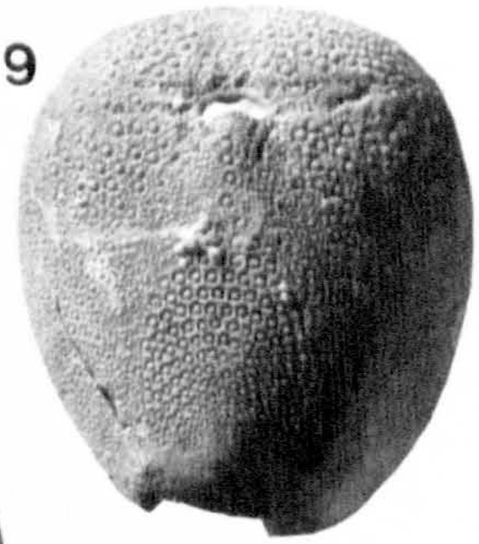
6



8



9



10



7



11

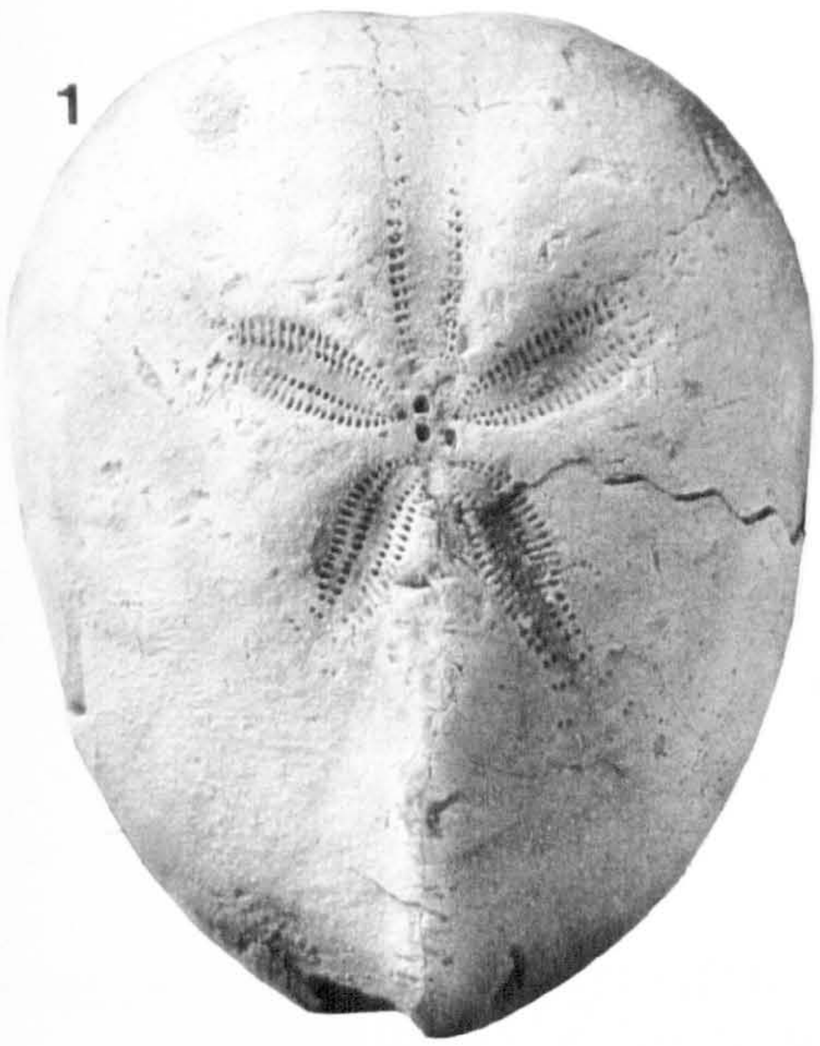


PLATE 9

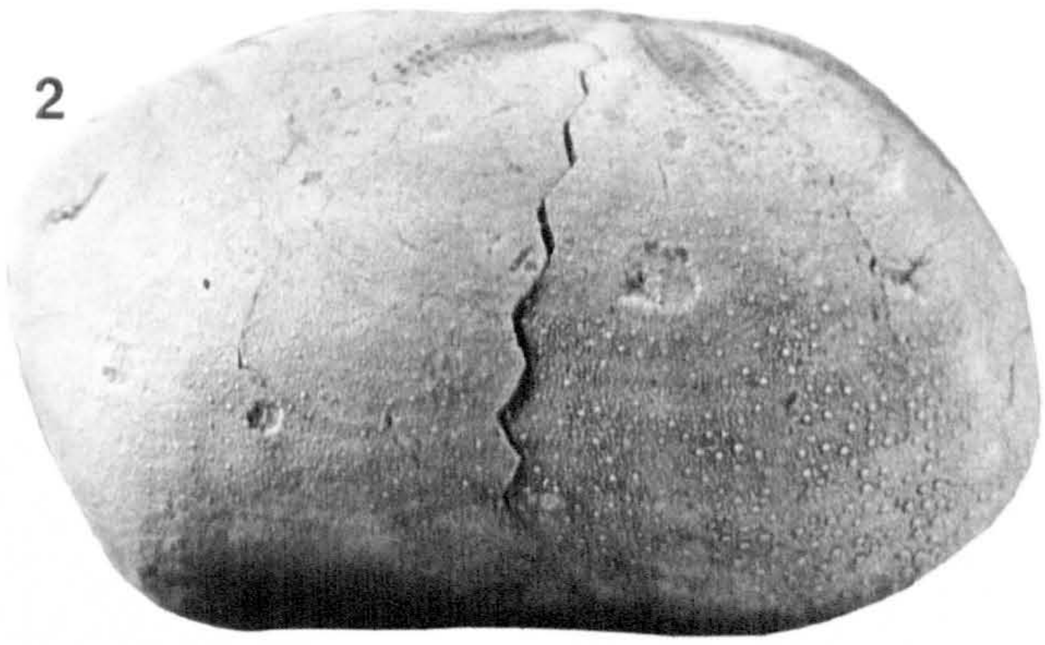
Figs 1-3. *Cyclaster aturicus* (Seunes), BMNH EE6068, Danian of Navarra, Spain. 1, apical view; 2, lateral view; 3, oral view. All x2.

Figs 4-7. *Isaster aquitanicus* (Grateloup), BMNH EE6069, Late Thanetian of Navarra, Spain. 4, lateral view; 5, posterior view; 6, apical view; 7, oral view. All x1 1/2.

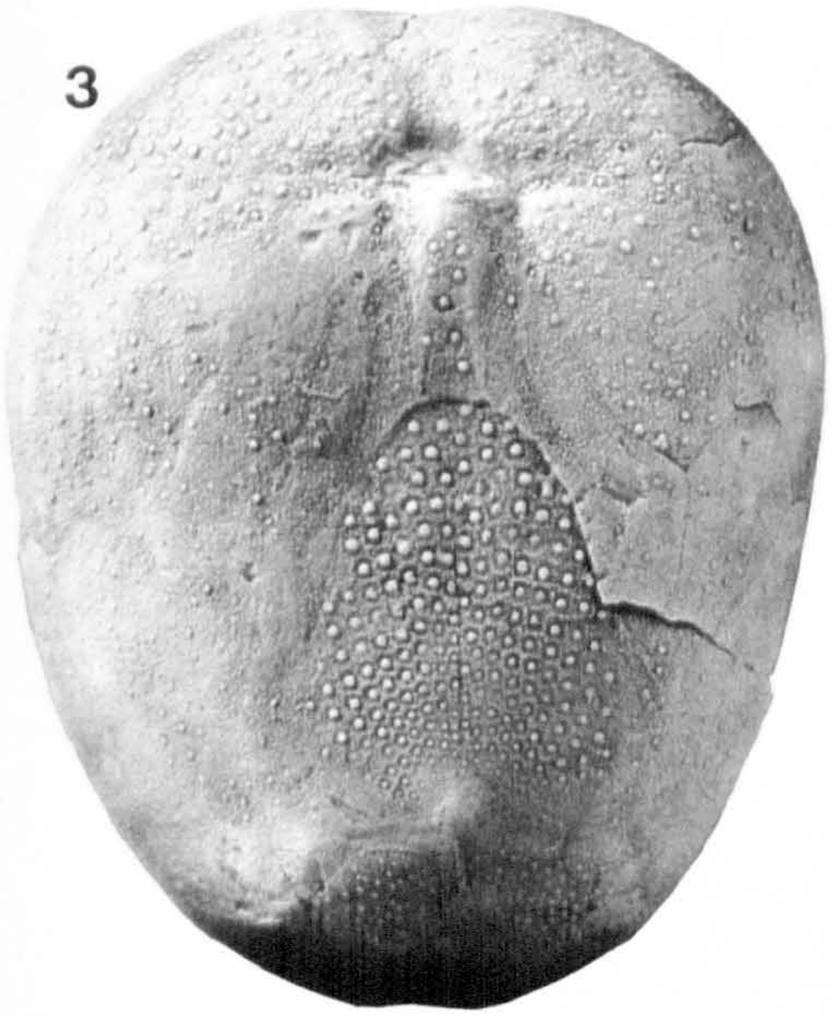
1



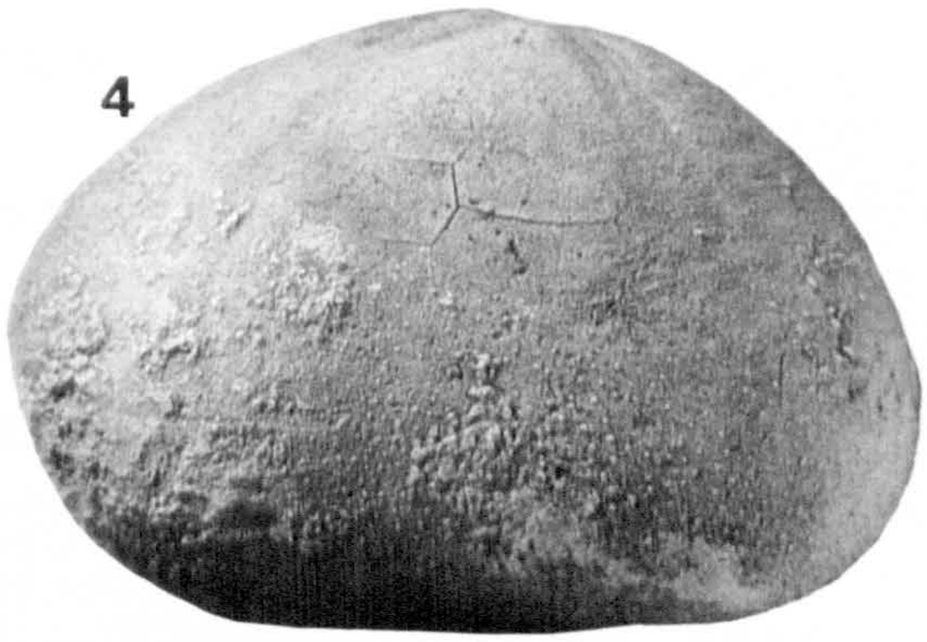
2



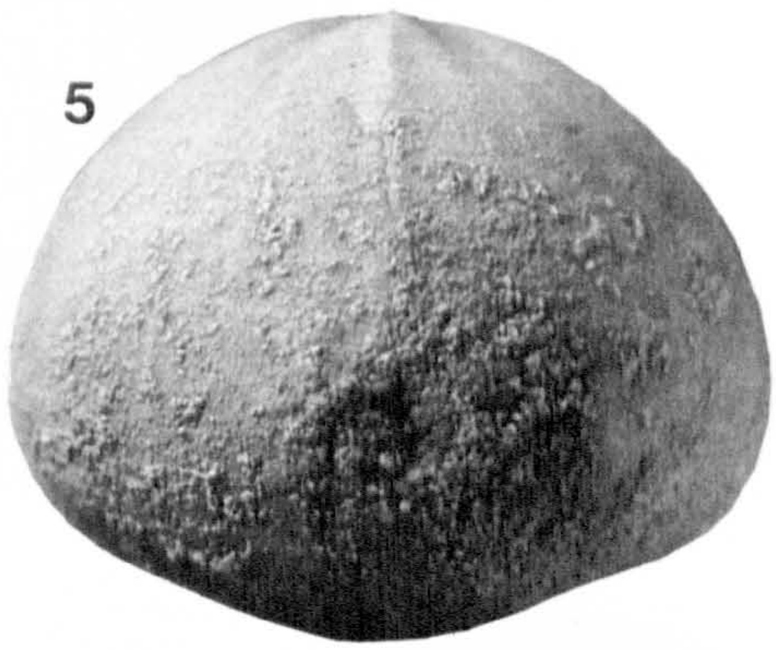
3



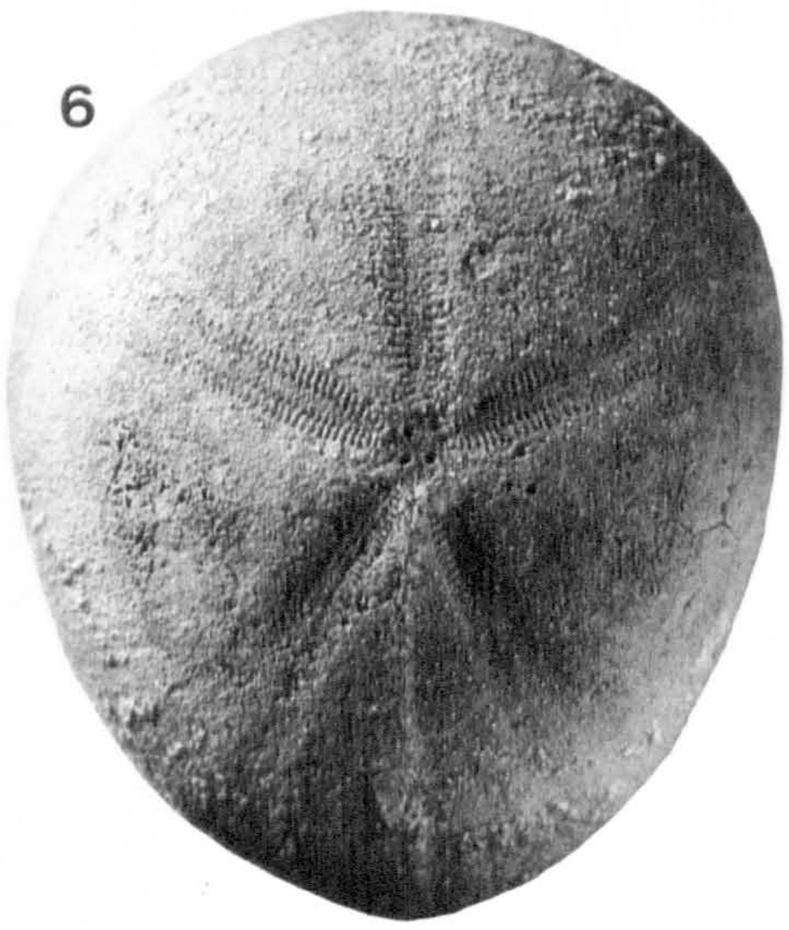
4



5



6



7

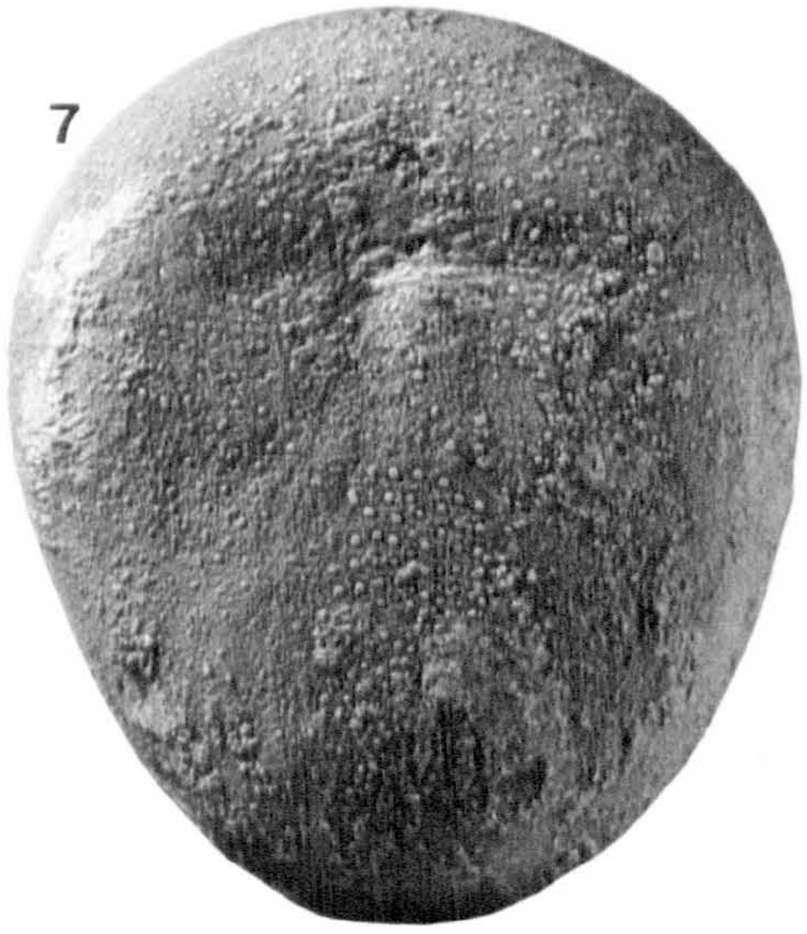
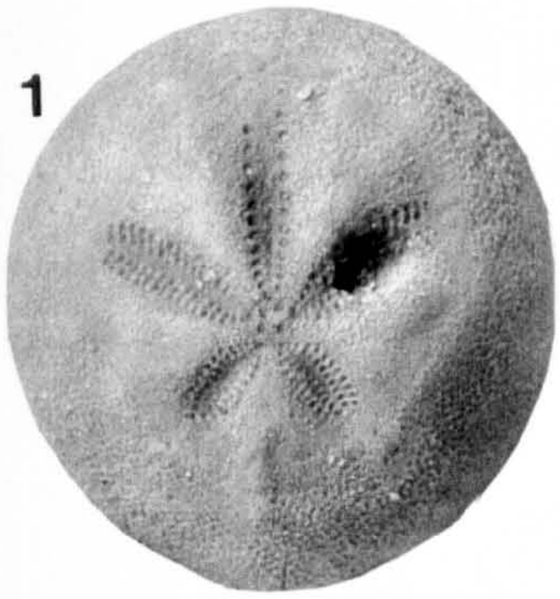


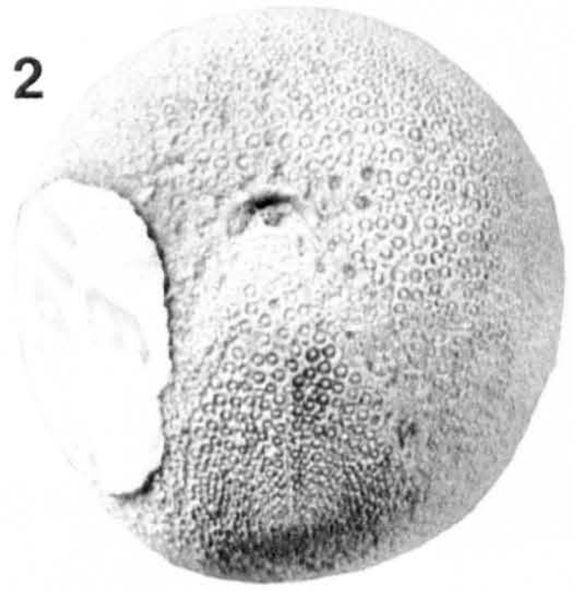
PLATE 10

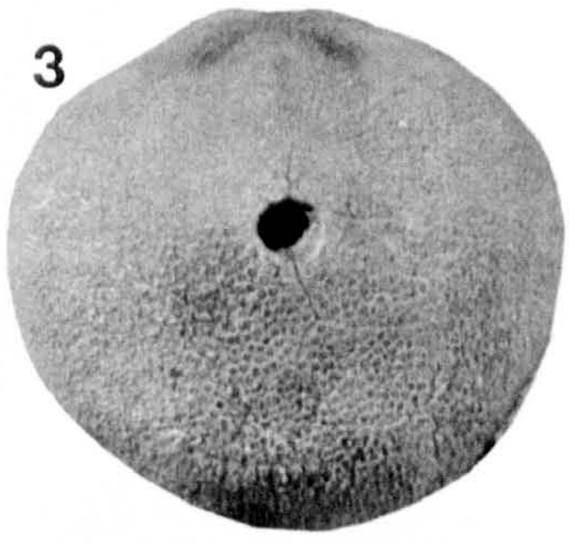
Figs 1-4. *Hemiaster prunella* (Lamarck), BMNH E11090, Upper Maastrichtian Meerssen Chalk of Maastricht, the Netherlands. 1, apical view; 2, oral view; 3, posterior view; 4, lateral view. All x3.

Figs 5-7. *Hemiaster hattaensis* Ali, BMNH EE4060, Early Upper Maastrichtian Simsima Formation of UAE/Oman. 5, apical view; 6, oral view; 7, lateral view. All x2.

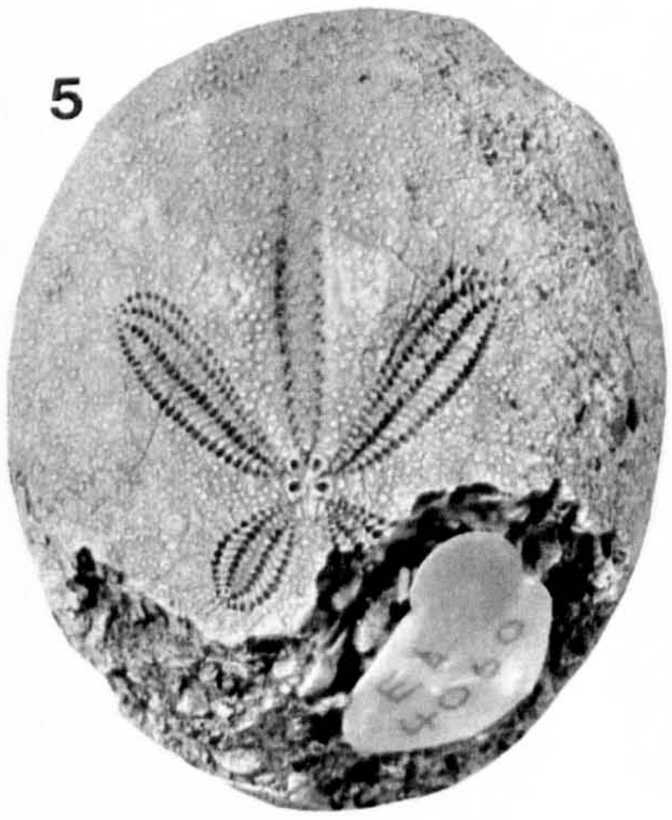
Figs 8-11. *Leiostomaster gentili* Lambert, BMNH E45372, Maastrichtian of Constantine, Algeria. 8, apical view; 9, oral view; 10, posterior view; 11, lateral view. All x2.

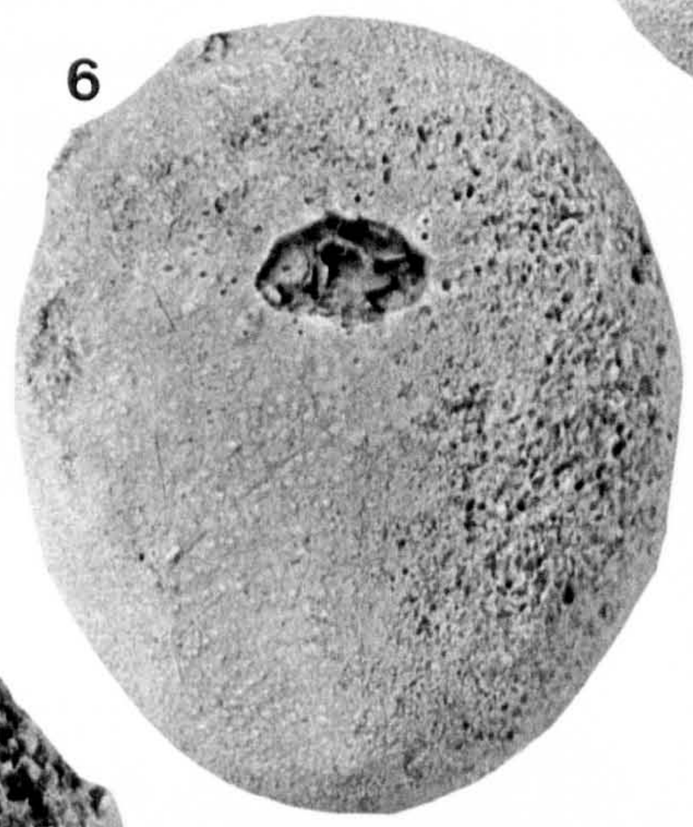

1


2

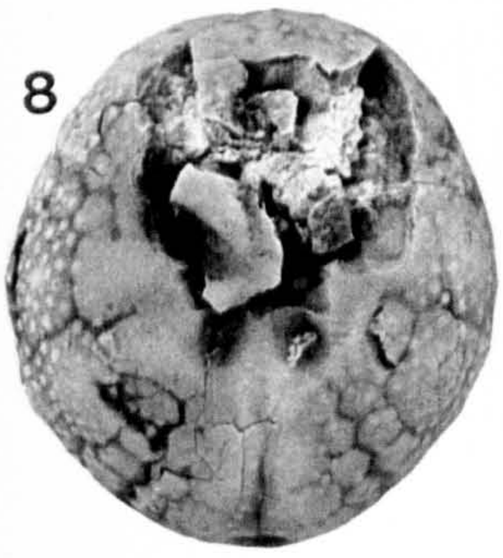

3

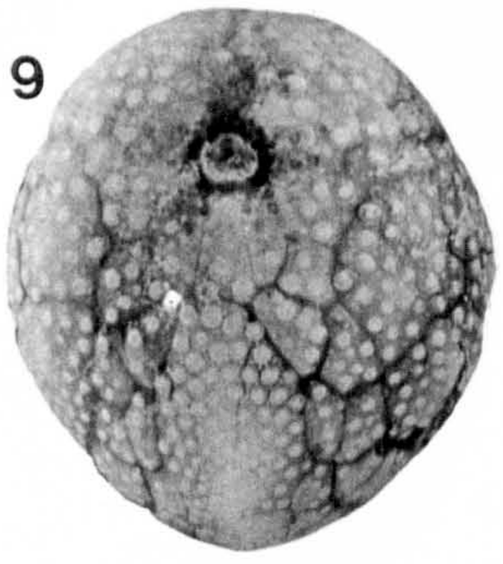

4

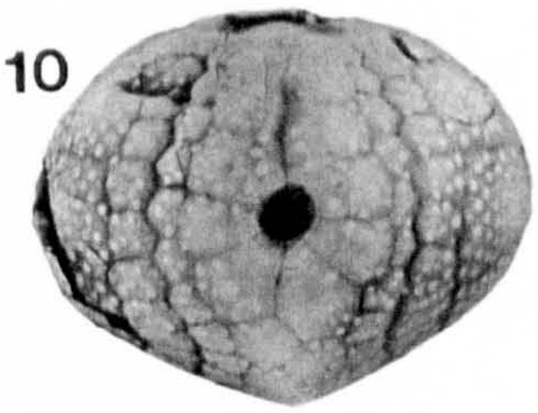

5


6


7


8


9


10

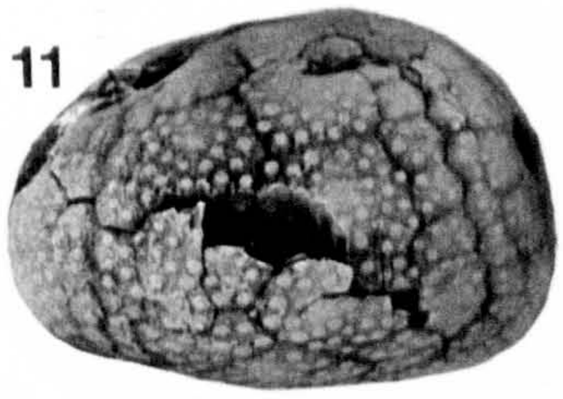
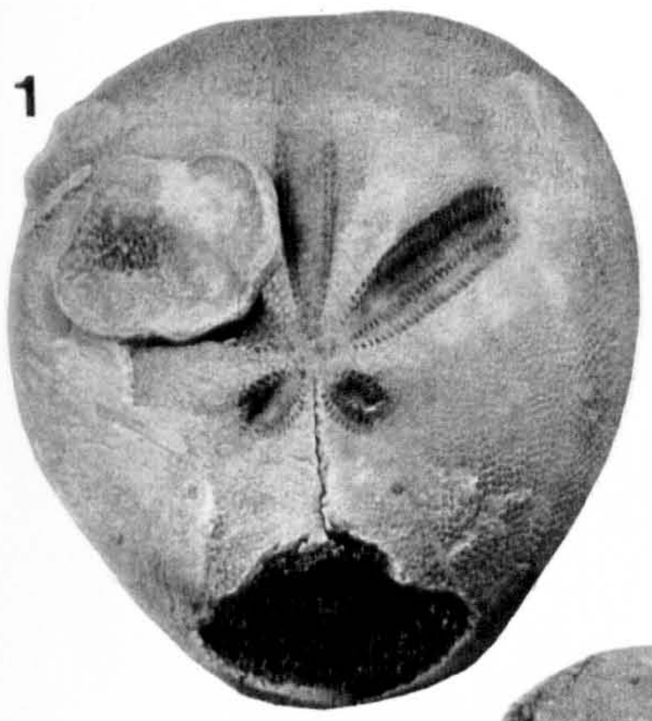

11

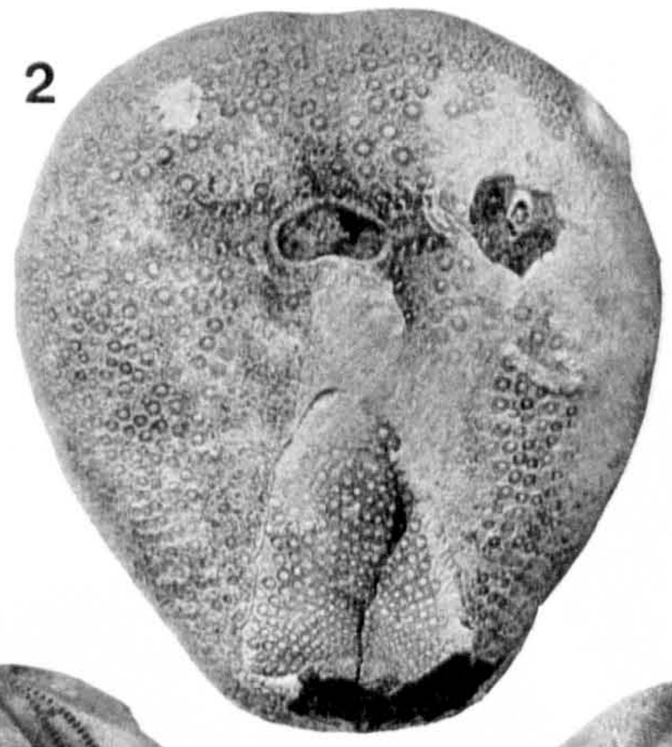
PLATE 11

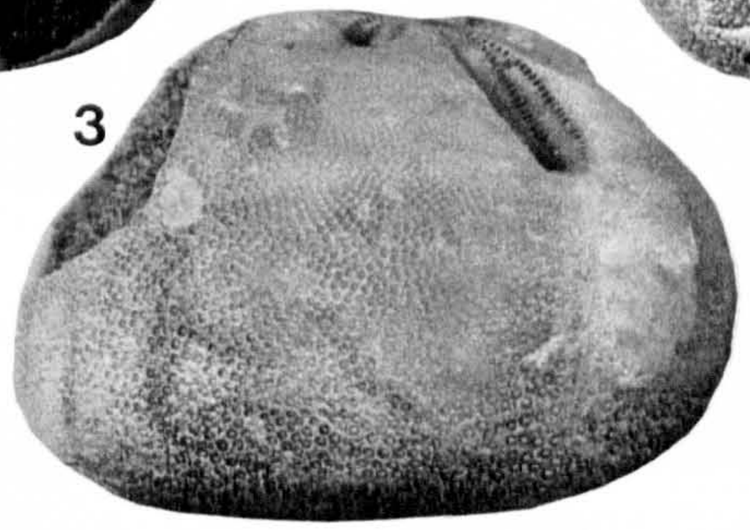
Figs 1-3. *Leymeriaster leymeriei* (Agassiz), BMNH E45372, Turonian of Sarthe, France. 1, apical view; 2, oral view; 3, lateral view. All x2

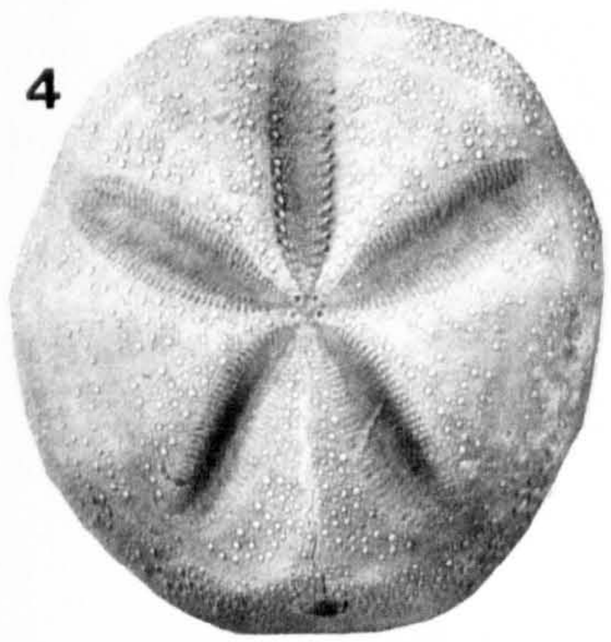
Figs 4-7. *Mecaster fourneli* (Deshayes), BMNH E4034, Maastrichtian of Constantine, Algeria. 4, apical view; 5, lateral view; 6, oral view; 7, posterior view. All x2.

Figs 8-11. *Mauritanaster mirabilis* (Peron & Gauthier), BMNH E3657, Maastrichtian of Constantine, Algeria. 8, apical view; 9, oral view; 10, posterior view; 11, lateral view. All x2.

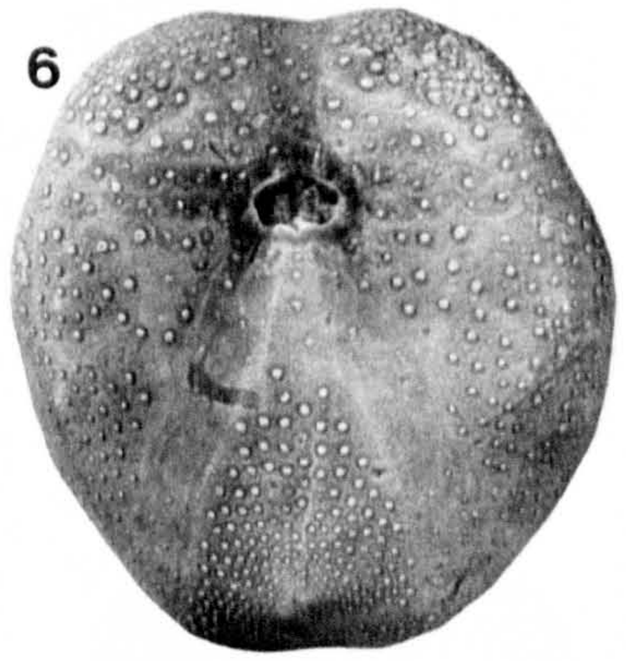

1

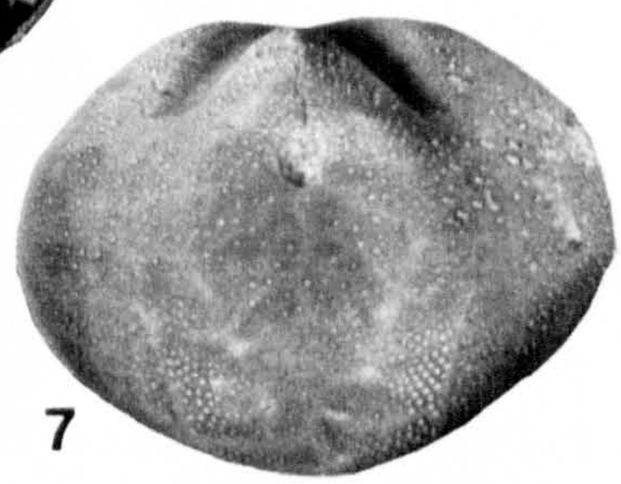

2

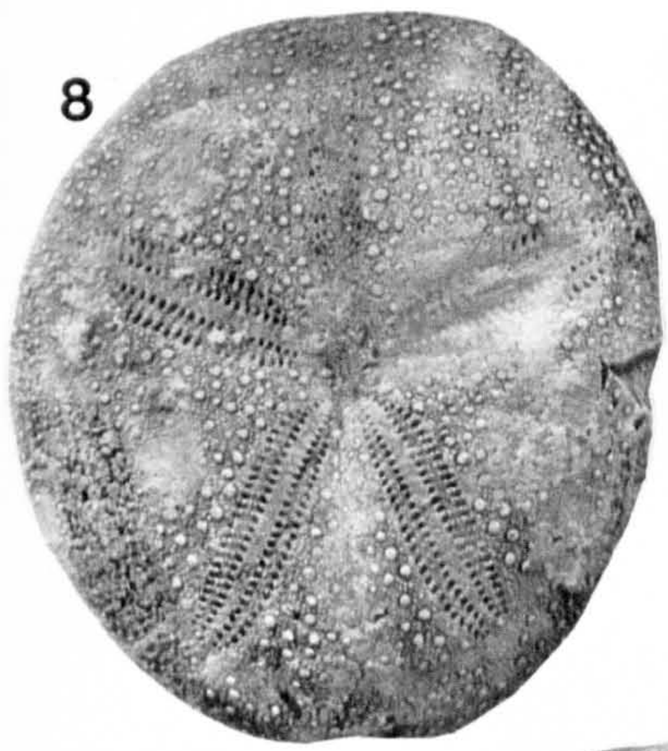

3

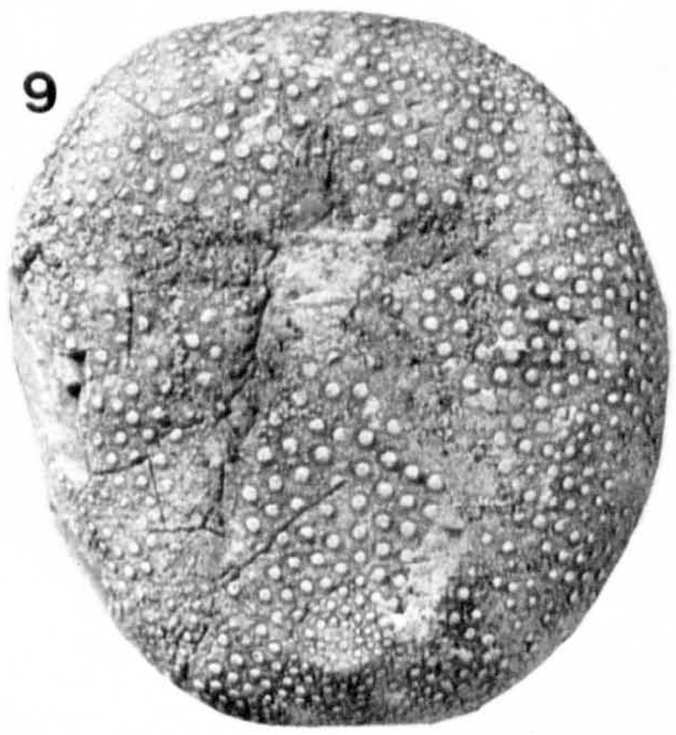

4

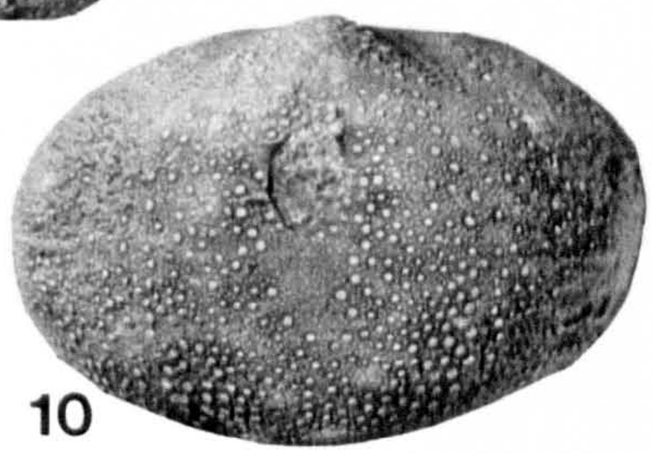

5


6


7


8


9


10

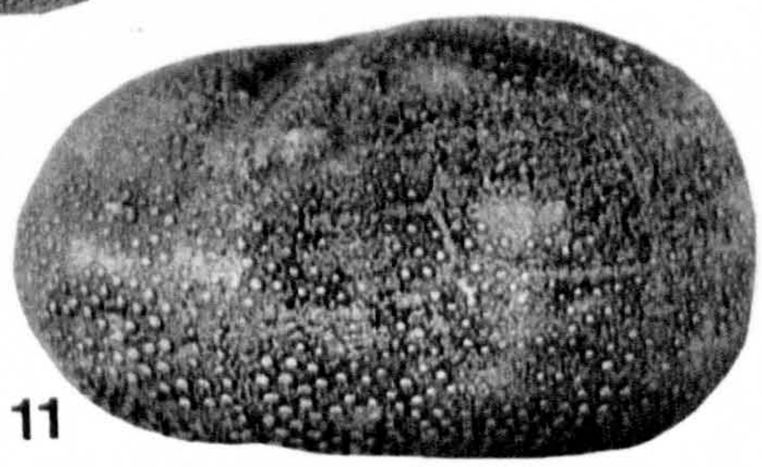

11

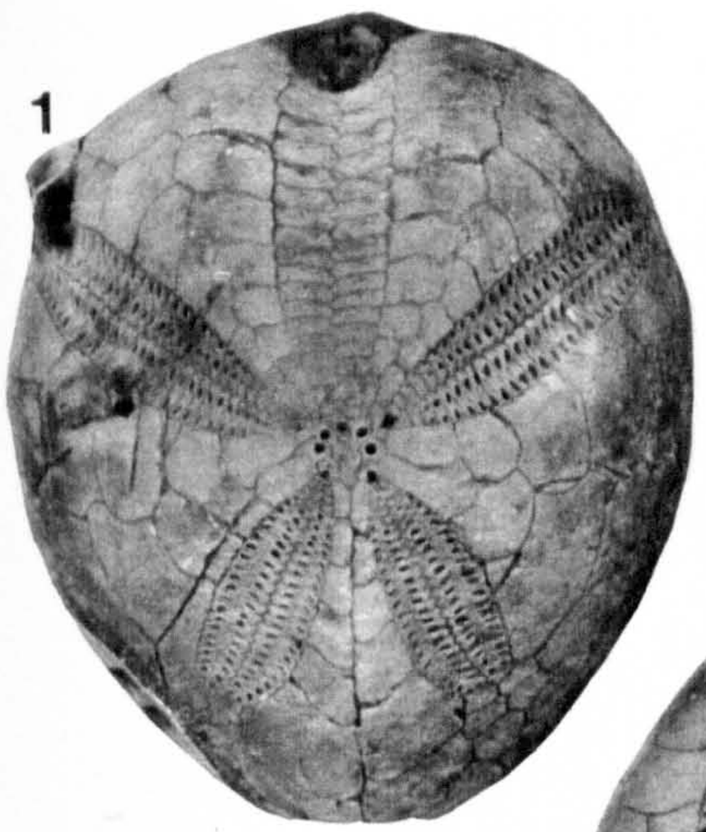
PLATE 12

Figs 1-3. *LInthia sudanensis* (Bather), BMNH EE2262, Thanetian Limestone of Niger. 1, apical view; 2, oral view; 3, lateral view. All x2.

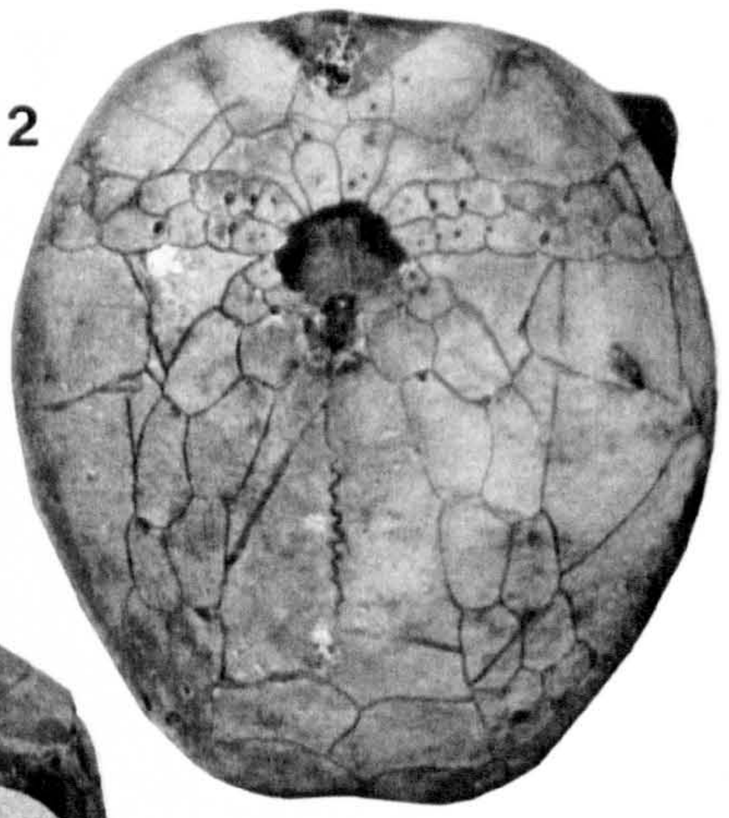
Figs 4-7. *Paraster indicus* (Duncan & Sladen), BMNH E730, Thanetian Ranikot Series of Sind, Pakistan. 4, apical view; 5, lateral view; 6, oral view; 7, posterior view. All x2$^{1}/_{2}$.

Figs 8-11. *Proraster geayi* Cottreau, BMNH E79710, Campanian of Oman. 8, apical view; 9, oral view; 10, lateral view; 11, anterior view. All x1.

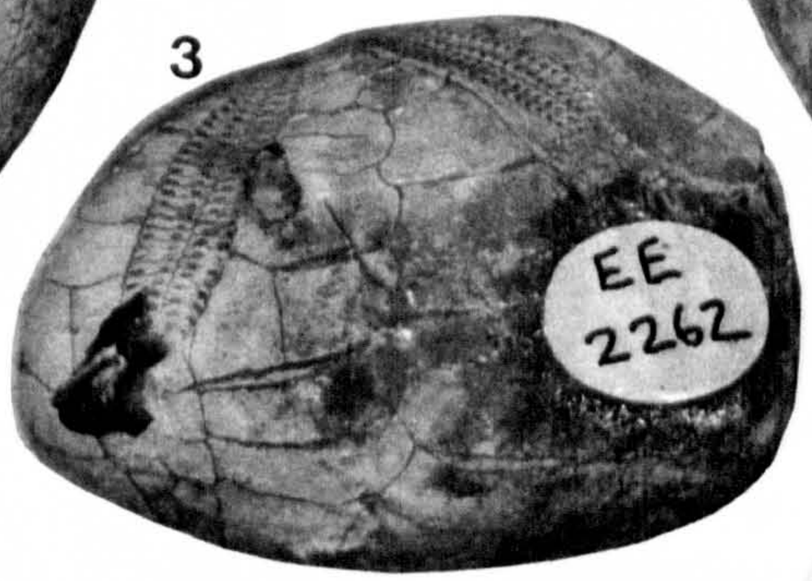
1



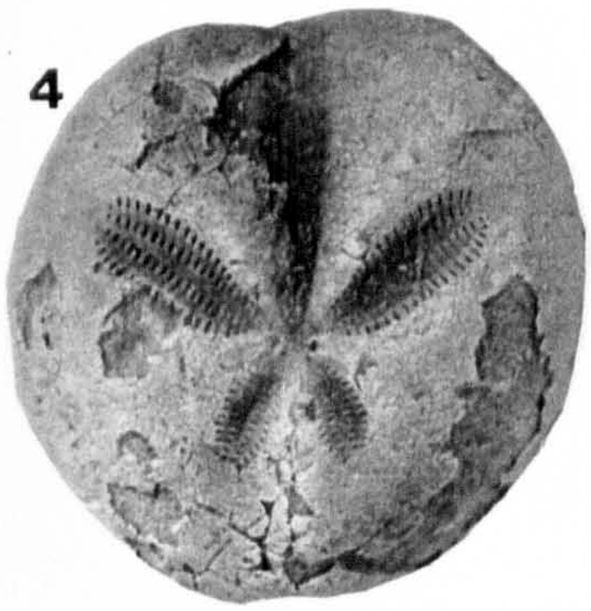
2



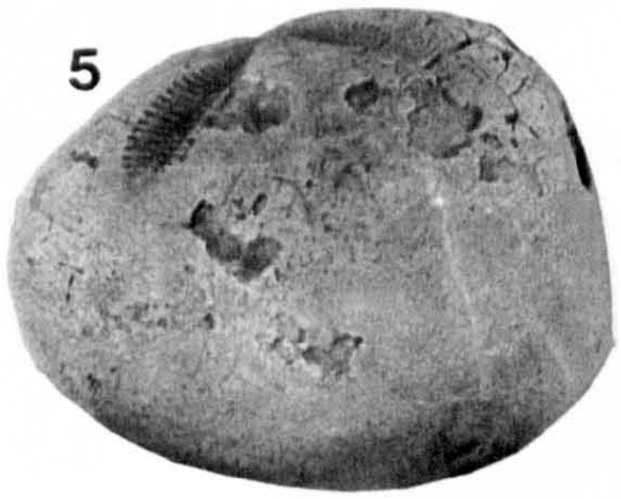
3



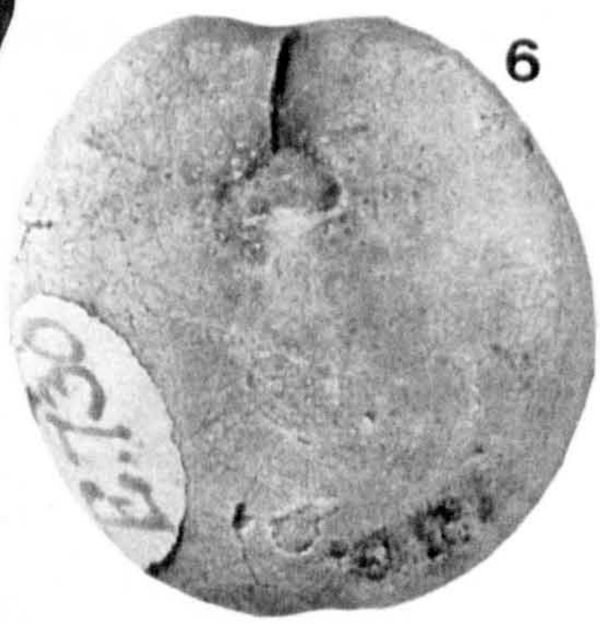
4



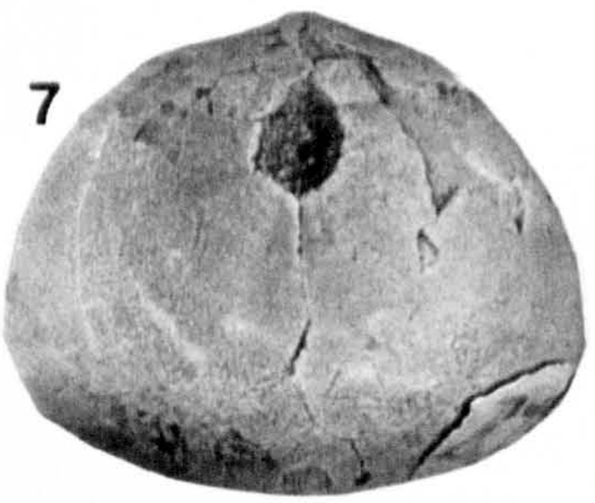
5



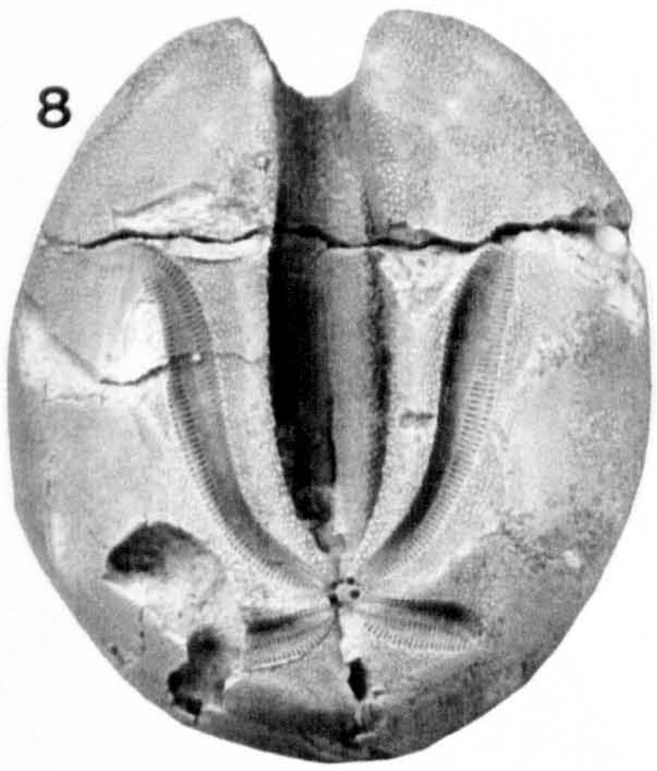
6



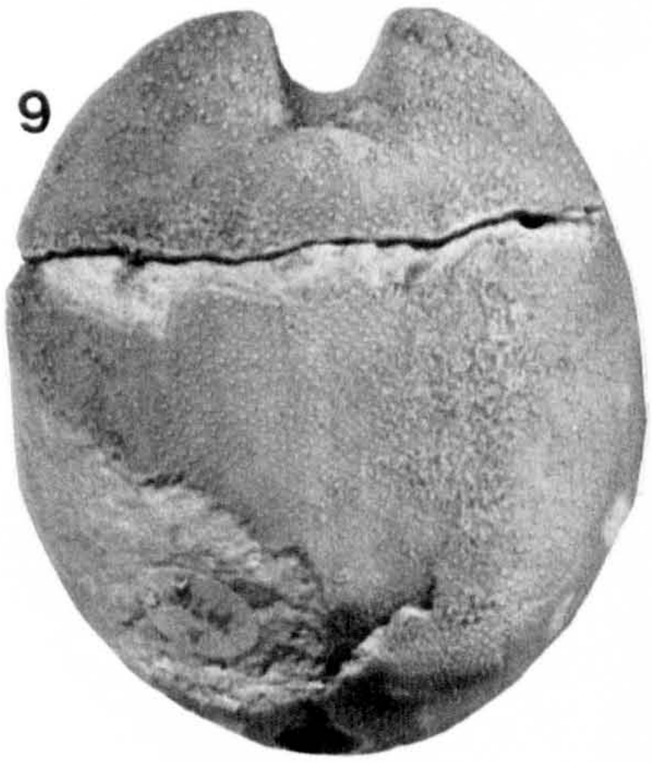
7



8



9



10



11

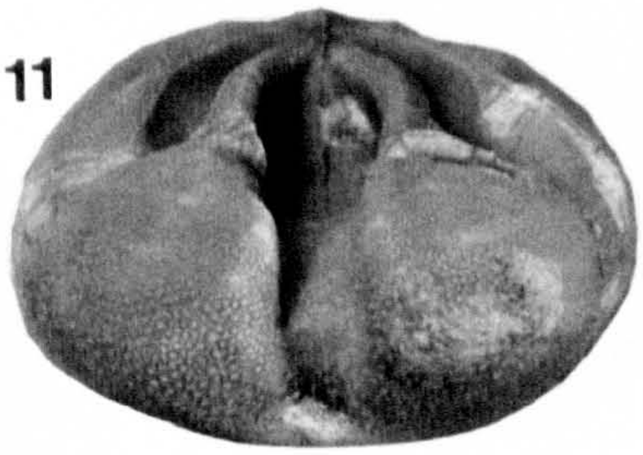


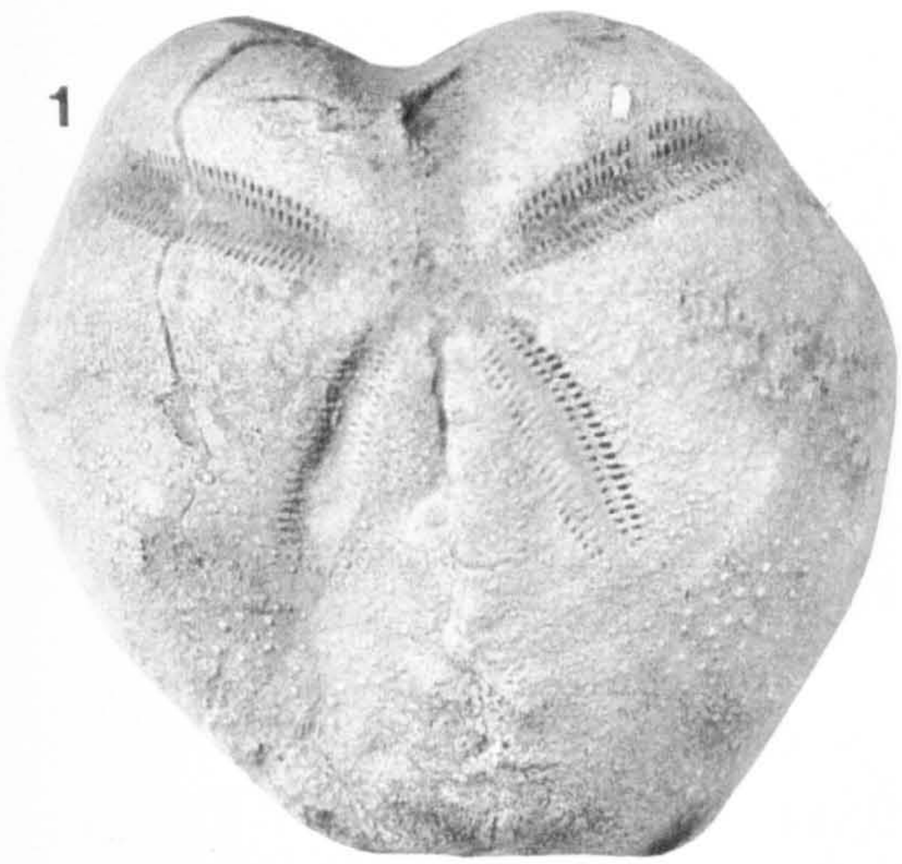
PLATE 13

Figs 1-3. *Holcopneustes cristatus* (Stoliczka), E20097 (TOPOTYPE), Danian of northwest Madagascar. 1, apical view; 2, oral view; 3, lateral view. All x2.

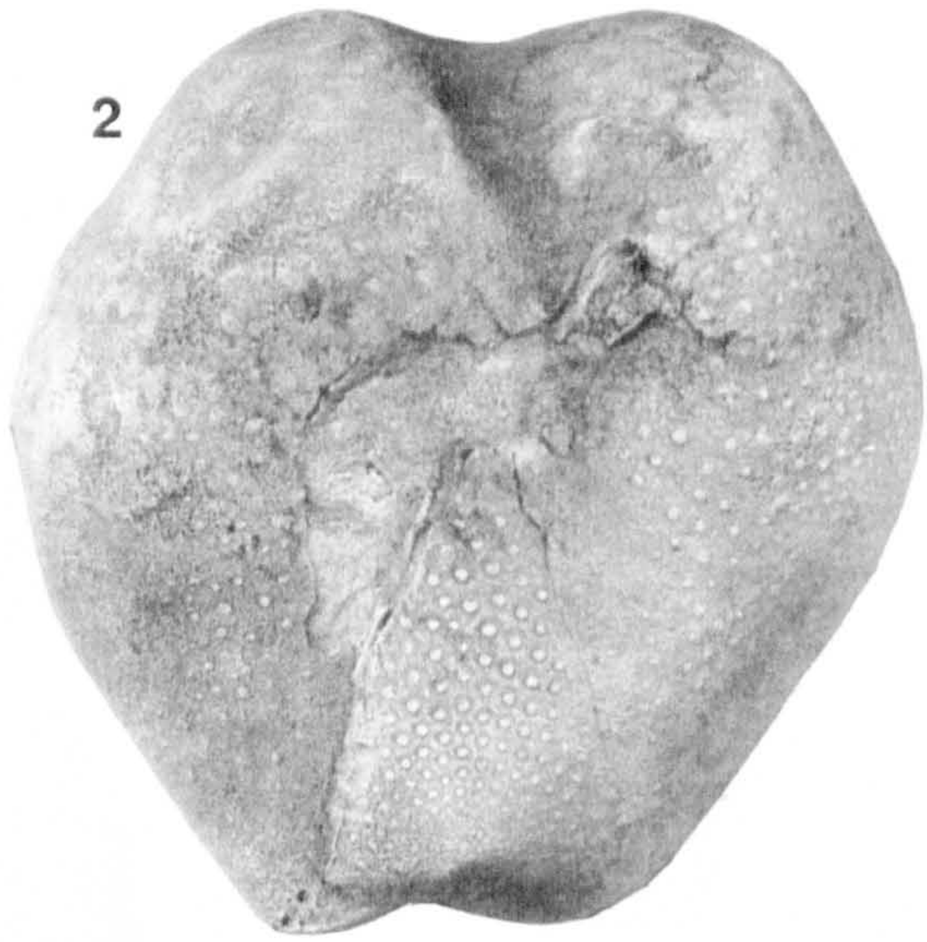
Figs 4-7. *Opissaster somaliensis* Currie, UGHM E772 (TOPOTYPE), Palaeocene Lower Auradu Series of Somalia. 4, apical view; 5, anterior view; 6, oral view; 7, lateral view. All x2.

Figs 8-11. *Prenaster* sp., BMNH E76200, Eocene of Alicante, Spain. 8, lateral view; 9, apical view; 10, posterior view; 11, oral view. All x2.

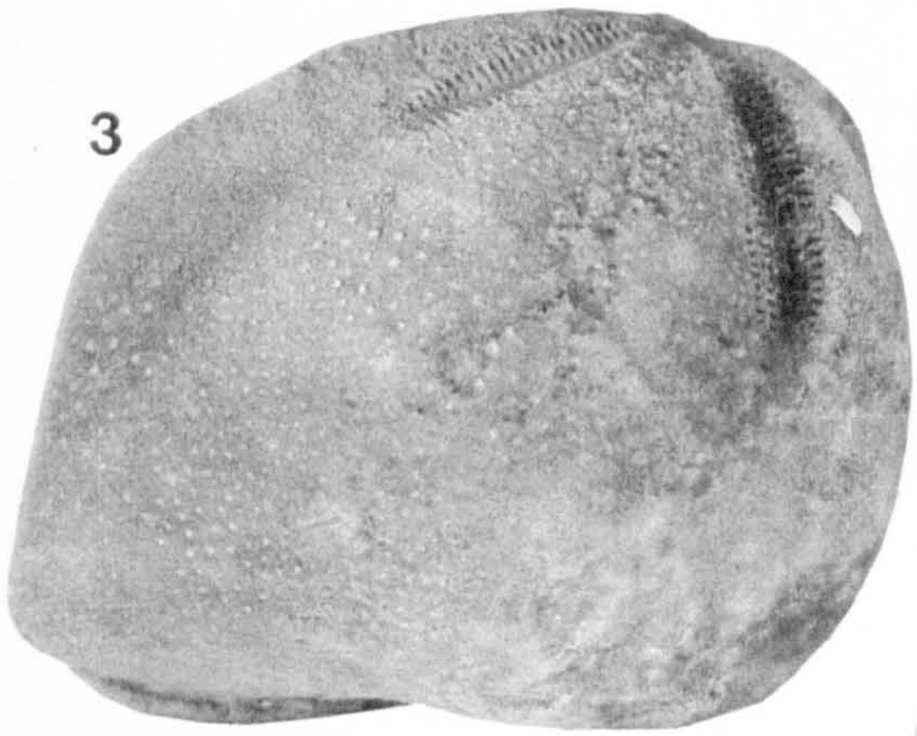
1



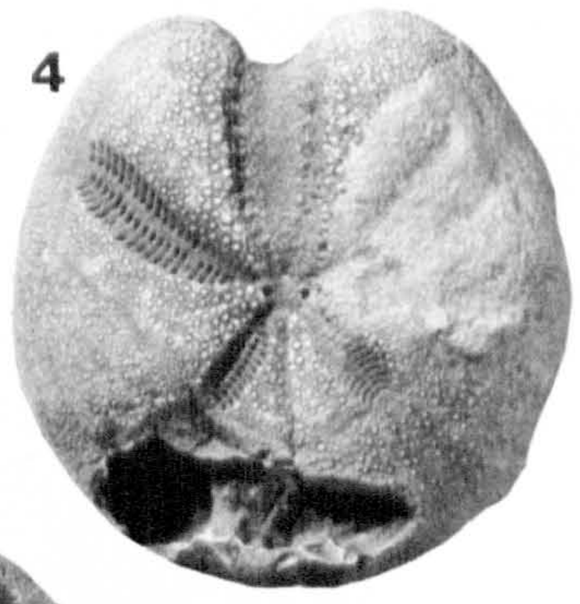
2



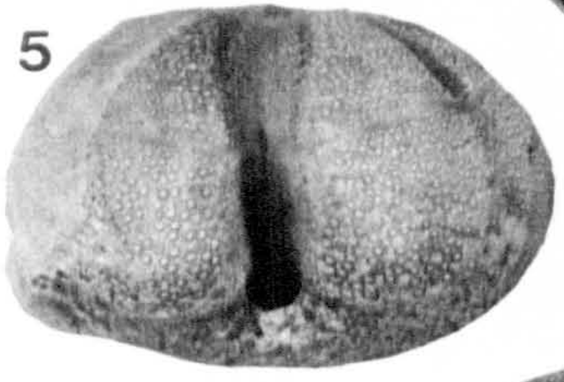
3



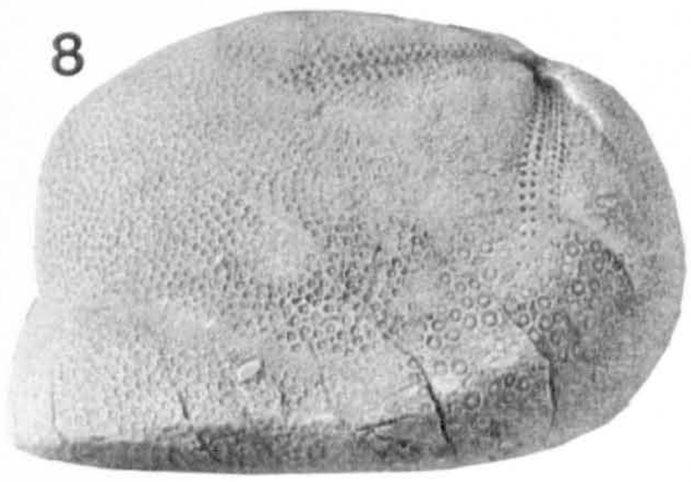
4



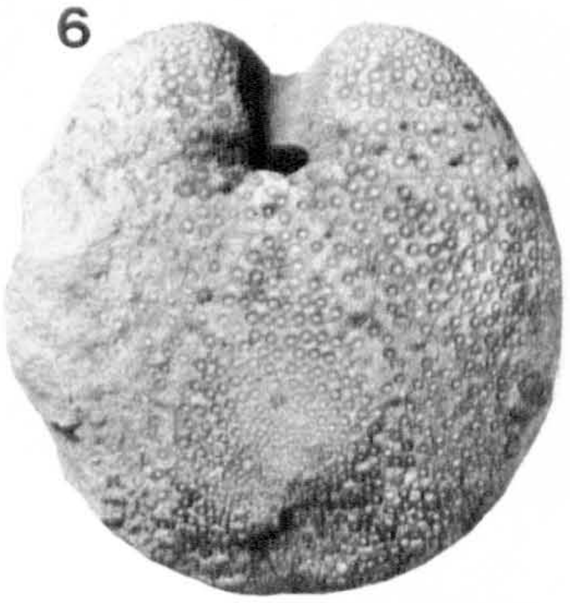
5



8



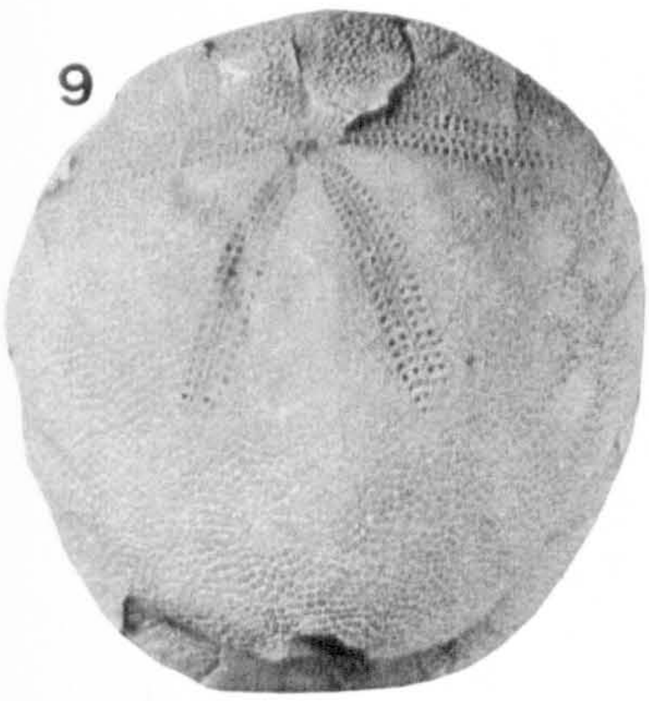
6



7



9



10



11

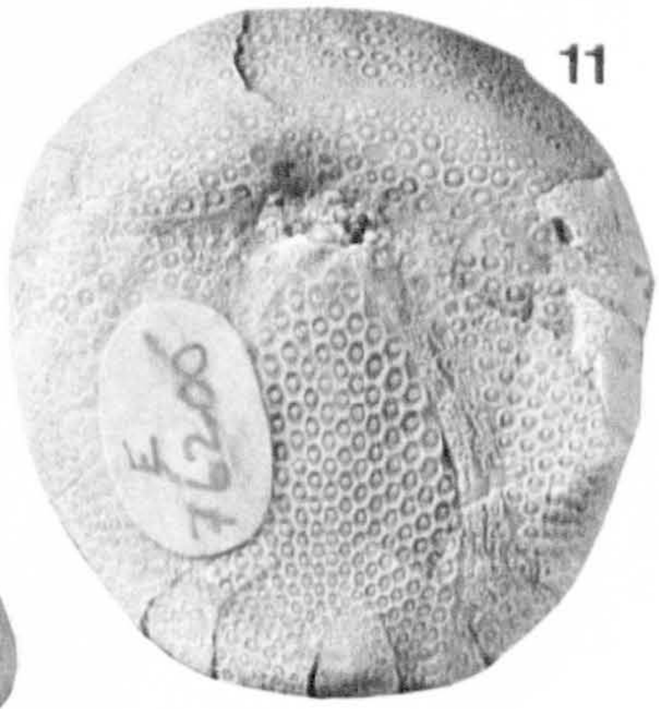


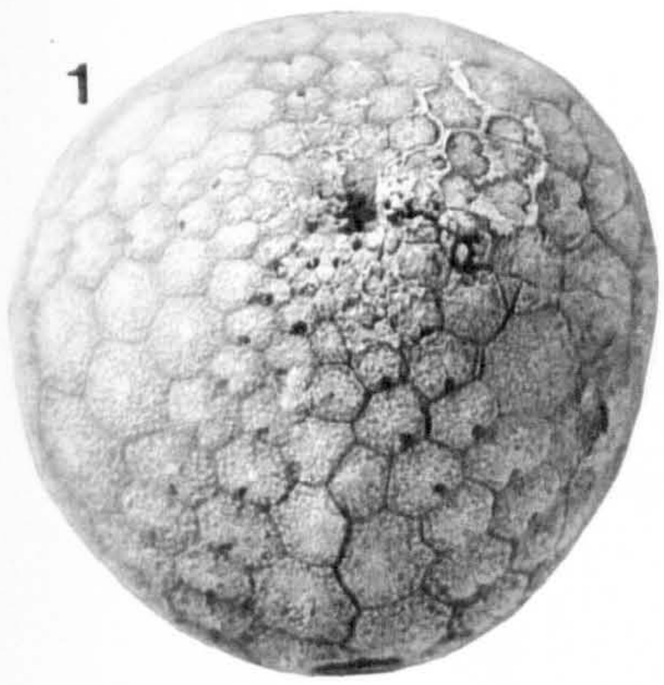
PLATE 14

Figs 1-4. *Coraster vilanovae* Cotteau, BMNH EE6074, Danian *Coraster* beds of Navarra, Spain. 1, apical view; 2, oral view; 3, posterior view; 4, lateral view. All x3.

Figs 5-8. *Homoeaster tunetanus* Pomel, Maastrichtian Quipar-Jorquera Formation of Alicante, Spain. 5-6, BMNH EE6072; 5, apical view; 6, posterior view. 7-8, BMNH EE6071; 7, oral view; 8, lateral view. All x2.

Figs 9-13. *Sphenaster larumbensis* sp. nov., BMNH EE6073, Danian *Coraster* beds of Navarra, Spain. 9, apical view; 10, oral view; 11, lateral view; 12, anterior view; 13, posterior view. All x4.

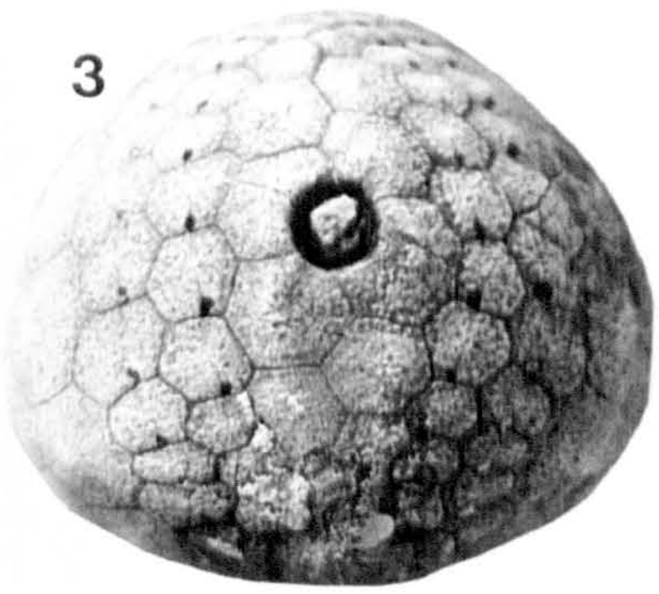
1



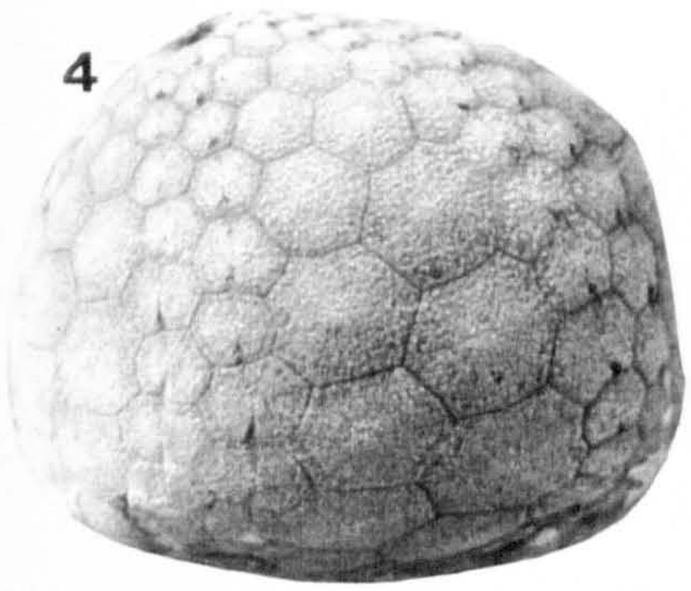
2



3



4



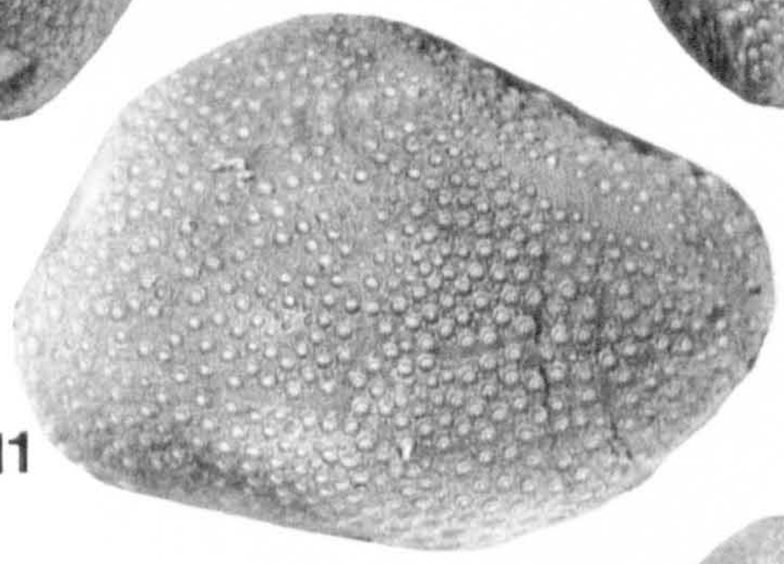
9



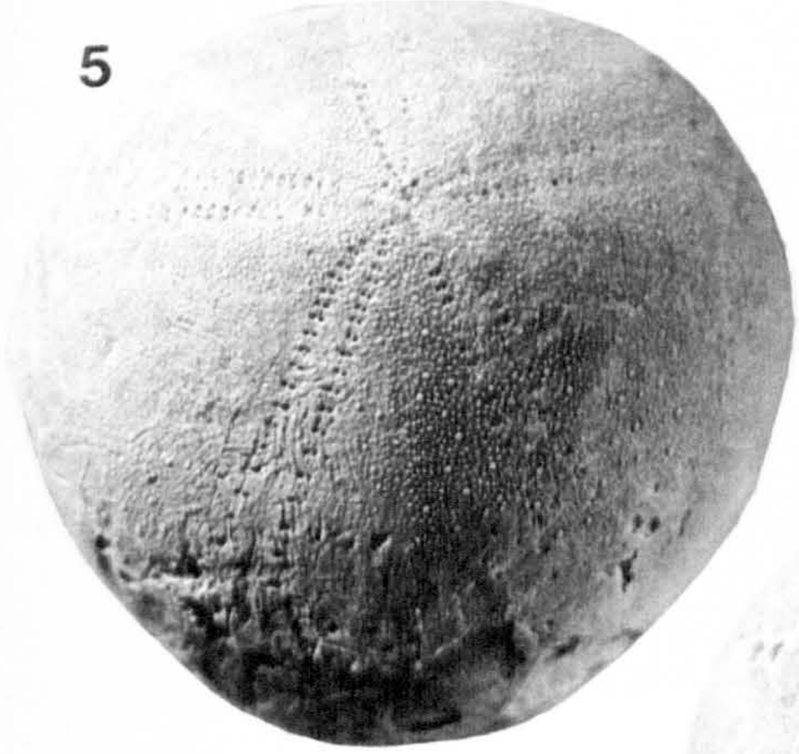
10



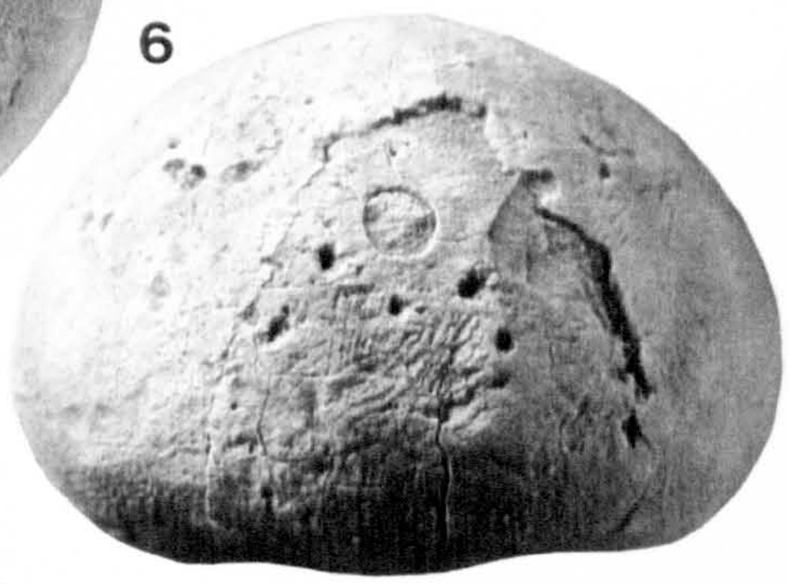
11



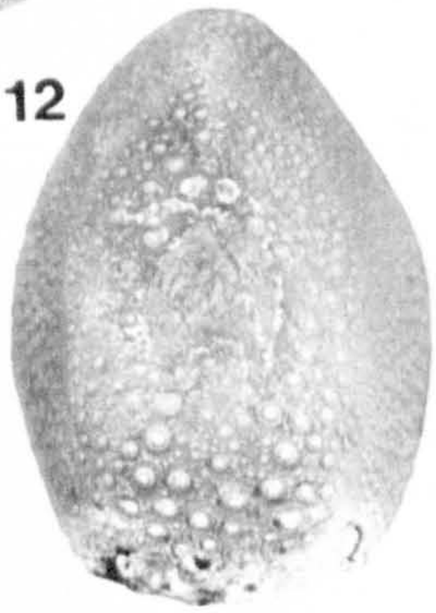
5



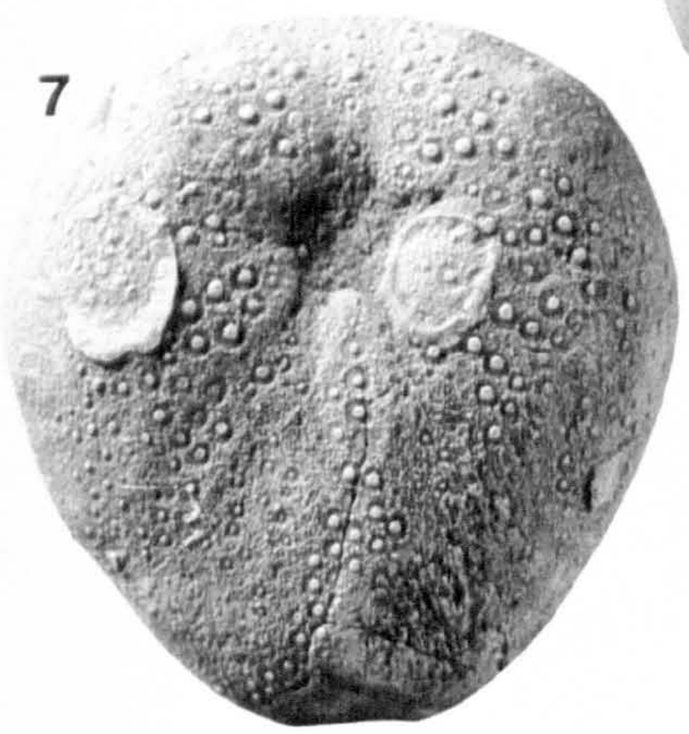
6



12



7



8



13

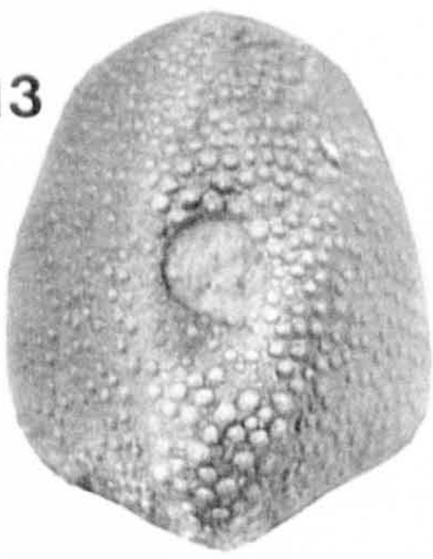


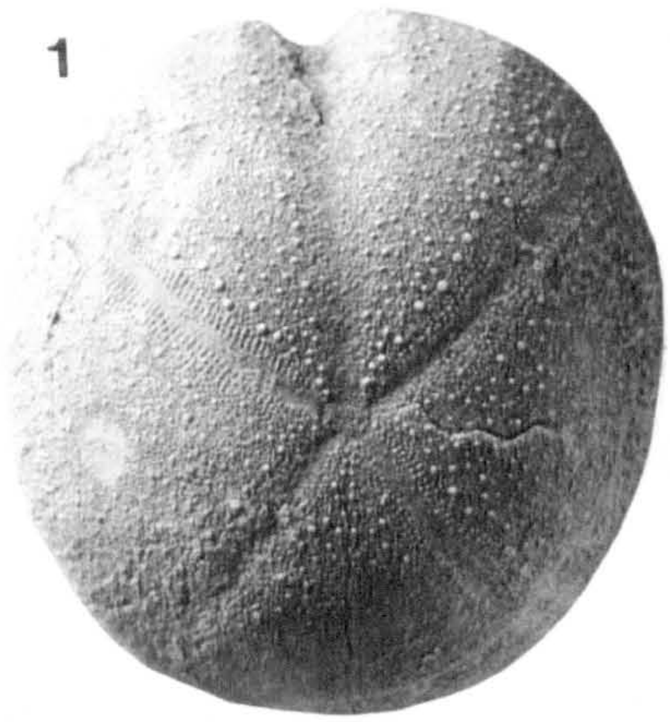
PLATE 15

Figs 1-4. *Iraniaster morgani* Cotteau & Gauthier, Senonian of Louristan, Iran. 1-2, BMNH E17326; 1, apical view; 2, posterior view. x1½. 3-4, BMNH E17324; 3, oral view; 4, lateral view. x1.

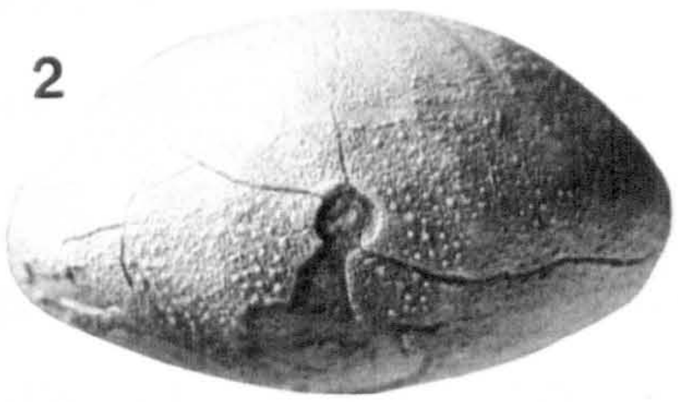
Figs 5-7. *Pseudiraniaster omanensis* sp. nov., BMNH E82606 (HOLOTYPE), Maastrichtian of Oman. 5, apical view; 6, oral view; 7, lateral view. All x1½.

Figs 8-9. *Leviechinus gregoryi* (Currie), BMNH E18080 (HOLOTYPE), Palaeocene Lower Auradu Series of Somalia. 8, apical view; 9, lateral view. All x1.

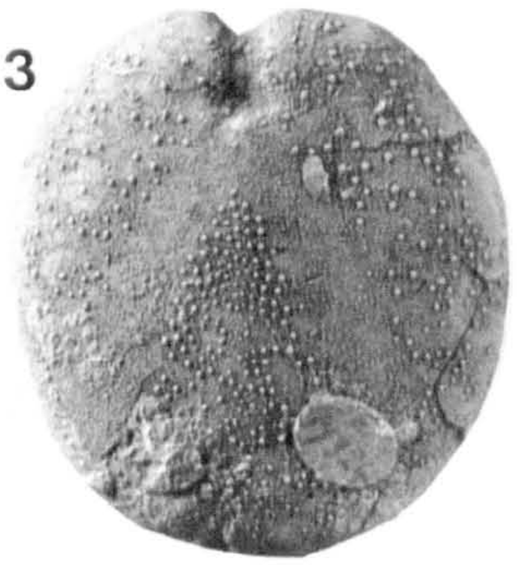
1



2



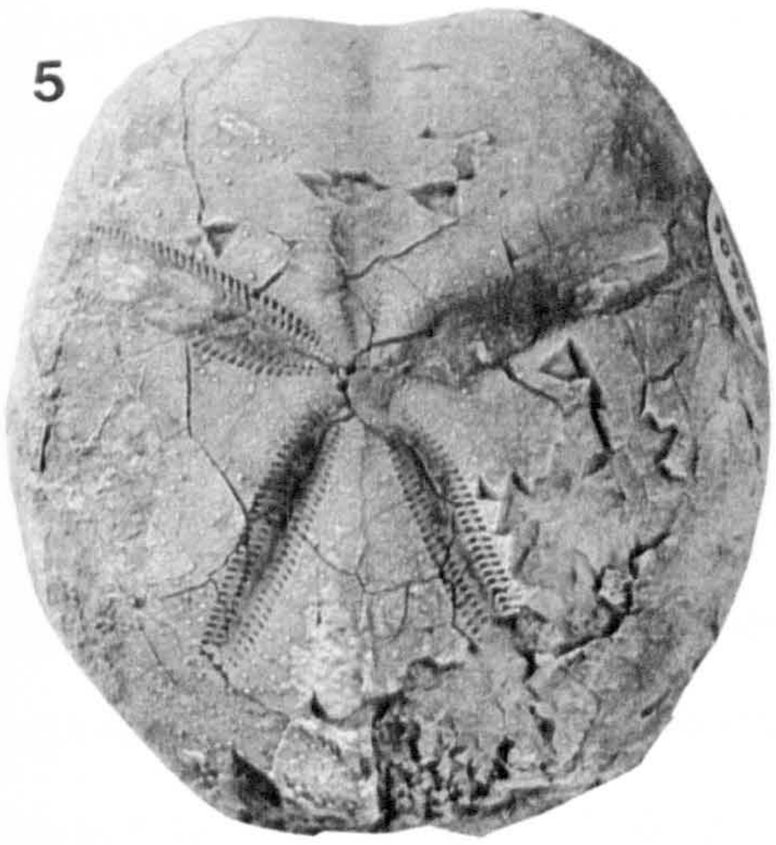
3



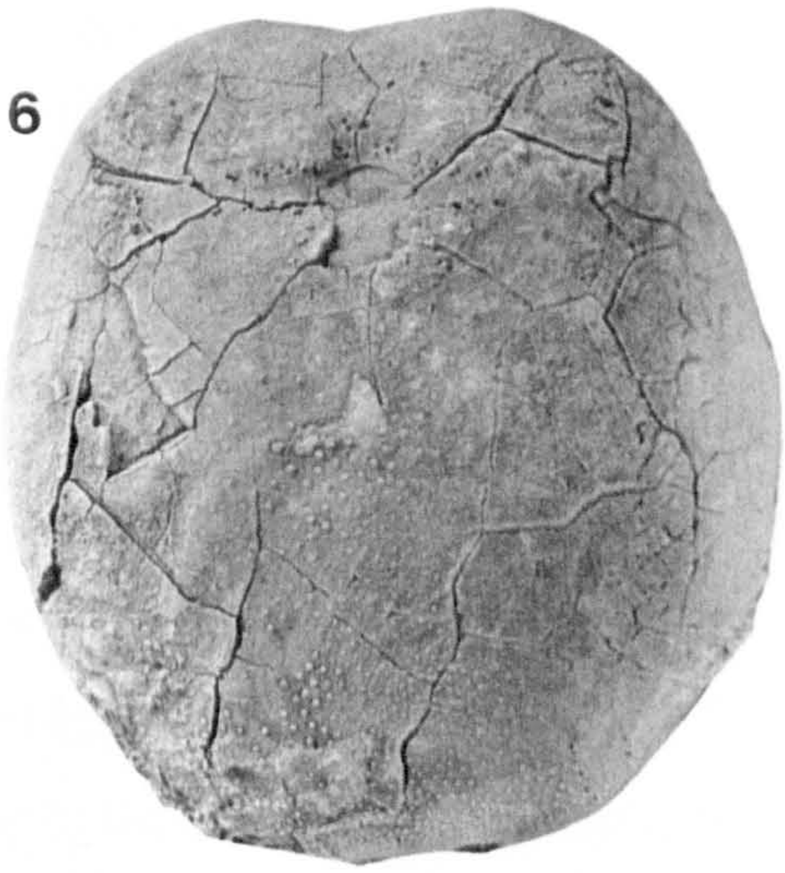
4



5



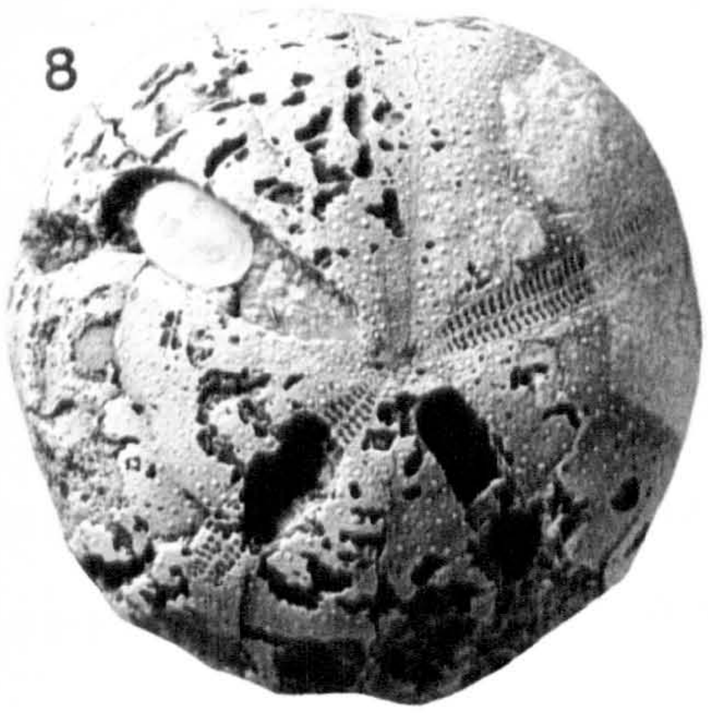
6



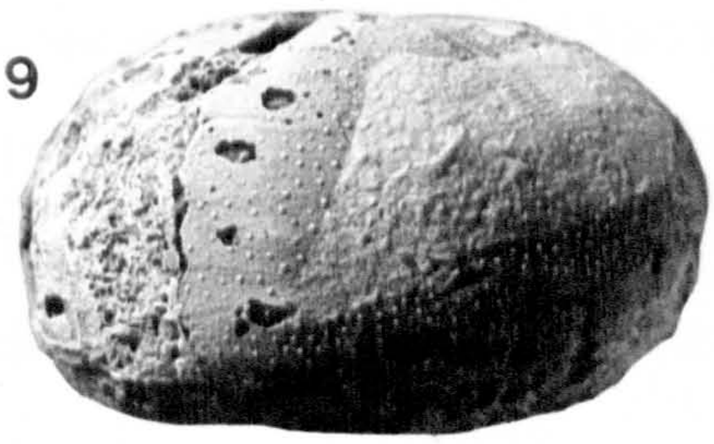
7



8



9



CHAPTER 4

PHYLOGENETIC ANALYSES OF MAASTRICHTIAN AND PALAEOCENE ATELOSTOMATE ECHINOIDS

The occurrence of numerous non-monophyletic taxa in the literature indicates that traditional taxonomic practice, resting on the idiosyncrasies of the individual taxonomist, does not always reflect genuine biological groupings and processes. For example, the last appearance of a non-monophyletic taxon in the fossil record may correspond to a true biological extinction. Equally, it may just reflect a change in nomenclature, or pseudoextinction, and obscure lineage continuity. Thorough phylogenetic analysis may lead to a reduction in the number of apparent extinctions by allowing inferences about the survival of clades to be made. Jeffery (1997b) gives the example of the irregular echinoid *Conulus* which becomes extinct at the end of the Maastrichtian but has the Palaeocene genus *Neoglobator* as a sister group.

It is now widely recognized that rates and patterns of extinction in the fossil record can be more reliably determined within a robust phylogenetic framework (MacLeod 1996a; Jablonski 1997; MacLeod *et al.* 1997; Jeffery 1997b; Jeffery & Smith, in press), and the construction of secure phylogenies has been identified as a major area for future research (e.g. MacLeod *et al.* 1997). As yet, no modern generic level phylogenies are available for atelostomate echinoids and so cladistic analyses of Maastrichtian and Palaeocene holasteroids and spatangoids have been carried out to determine the phylogenetic relationships between taxa and thus ascertain which clades survived the K-T event.

Methods.

To resolve the phylogenetic relationships between Maastrichtian and Palaeocene atelostomate echinoids, cladistic analyses have been carried out using morphological characters compiled for all species examined as part of the taxonomic revision, as well as for those species where there are unambiguous descriptions and illustrations in the

literature. Following David (1988) and Mooi & David (1996), the chosen characters are based, wherever possible, on structural differences in test architecture rather than on "softer" characters such as overall size.

Generic level analyses have been performed on the holasteroids and spatangoids in addition to more detailed species level analyses on subsets (ie. clades) identified by the generic analyses.

Measurements for metric characters were made using electronic callipers and rounded to 0.1 mm. Gap analysis (Archie 1985) was used to define the boundaries of metric characters. Only metric characters with more than two character states were ordered.

Missing data has been coded as a question mark. Question marks have also been used in generic level analysis when the character state varies within and between members of a genus. Species level analyses have been carried out where it is thought that this practise may have blurred any phylogenetic signal. Generic analyses use characters that are common in traditional taxonomies for distinguishing between genera, whilst the species level analyses use additional characters which may be variable within genera.

The phylogenetic analyses have been carried out using the Macintosh application PAUP 3.1.1 (Swofford 1993) which uses the principle of parsimony to search for and construct trees where character congruence is maximised. These maximally parsimonious trees are by definition also those with the smallest number of character transformations along their branches (minimum length trees). Accelerated transformation (ACCTRAN) was used for character state optimization. ACCTRAN maximises synapomorphies at each node and emphasizes reversals.

Where multiple solutions were produced, characters were reweighted according to the rescaled consistency index derived from the original unweighted analysis, and the search repeated (Farris 1988; Smith 1994). Reweighting characters in this way leads to maximum weight being given to characters showing no homoplasy and homoplaseous characters being down-weighted according to the number of times they have evolved. In all instances, except the generic level analysis of the Hemiasterina, this approach resulted

in one of the original trees being selected.

Bootstrapping was carried out to test the strength of the phylogenetic signal (Felsenstein 1985; Smith 1994). This process involves picking characters at random from the character matrix to create a dataset of the same dimensions as the original. The most parsimonious solution for this new dataset is then determined. The process is repeated and the results compared to the solution obtained from the original dataset. The higher the bootstrap percentage, the more times that node was present in the trees from the randomly constructed datasets and the stronger phylogenetic signal exists. Bootstrap percentages for this analysis were based on 1000 replicates.

Holasteroid generic level analysis.

Eighteen genera of Maastrichtian and Palaeocene holasteroids were included in the analysis. The indeterminate holasteroids *Corechinus* and *Ganbirretia* were excluded since adequate morphological diagnoses are lacking. In traditional phylogenetic schemes (e.g. Ernst 1972), *Hagenowia* is derived from the Campanian *Infulaster*. *Infulaster* is thus included in this analysis. *Holaster* was added as an outgroup.

Table 4.1. Characters used in the generic level phylogenetic analysis of holasteroids. Asterisks indicate ordered characters.

1	Marginal fasciole: 0 = absent; 1 = present.
2	Subanal fasciole: 0 = absent; 1 = present.
3*	Position of apical system: 0 = >40% TL from anterior margin; 1 = 20-40% TL; 2 = <20% TL.
4	Number of gonopores: 0 = 4; 1 = 3; 2 = 2.
5	Supplementary gonopores in ocular plates: 0 = absent; 1 = present.
6	Posterior ocular and genital plates: 0 = in contact; 1 = disjunct.
7	Fused plates in apical system: 0 = absent; 1 = present.
8	Plastron: 0 = not protosternous; 1 = protosternous.
9	Plastron: 0 = not metasternous; 1 = metasternous.
10	Plastron: orthosternous - 1st paired poststernal plates symmetrical: 0 = not symmetrical; 1= symmetrical.
11	Plastron: orthosternous - 2nd pair of post sternal plates symmetrical: 0 = not symmetrical; 1 = symmetrical.
12	Labrum and sternum: 0 = not separated; 1 = separated.
13	Rostral plate: 0 = absent; 1 = present.
14	Shape of labral plate: 0 = broadens posteriorly; 1 = tapers posteriorly.
15	Shape of sternal plate: 0 = triangular; 1 = pentagonal; 2 = elongate hexagonal; 3 = short hexagonal.
16	Labral plate extends to which ambulacral plate?: 0 = 2nd; 1 = 3rd.
17	Sternal plate extends to which ambulacral plate?: 0 = 3rd; 1 = 4th; 2 = 5th or higher.
18	Anterior rostrum: 0 = absent; 1 = present.
19	Frontal groove: 0 = none - slight depression; 1 = distinct frontal groove.
20	Anterior interambulacra form: 0 = no sharp keels; 1 = sharp keels.
21	Subanal heel: 0 = absent; 1 = weakly developed; 2 = distinct bilobed heel.
22	Position of anus: 0 = inframarginal; 1 = on truncate posterior; 2 = supramarginal.
23	Anus: 0 = flush with test; 1 = in depression.
24	Mouth: 0 = not in groove; 1 = in distinct but shallow groove; 2 = in deep, sharp groove.
25*	Position of mouth: 0 = >25% TL from anterior margin; 1 = 18-25% TL; 2 = <18% TL.
26	Mouth faces: 0 = forward; 1 = downward.
27	Shape of mouth: 0 = circular; 1 = transversely elongate.
28	Thickness of test: 0 = thin; 1 = average; 2 = thick.
29	Large tubercles on apical surface: 0 = absent; 1 = large tubercles present; 2 = very large, sunken tubercles present.
30	Large tubercles around ambitus: 0 = absent; 1 = large tubercles present.
31	Pores single beyond ends of paired petals: 0 = paired pores; 1 = single pores.
32	Paired ambulacra: 0 = non-petaloid; 1 = petaloid.
33	Number of ambulacral plates adjacent to each interambulacral plate: 0 = 3 or more; 1 = up to 2.
34	Pore position on plates: 0 = adoral centre; 1 = central; 2 = outer edge.
35	Structure of interambulacra near mouth: 0 = all amphiplacous; 1 = interambulacra 1 and 4 meridoplacous; 2 = all meridoplacous.

The 35 characters used in the cladistic analysis of holasteroid genera are shown in Table 4.1 and a character matrix is given in Table 4.2.

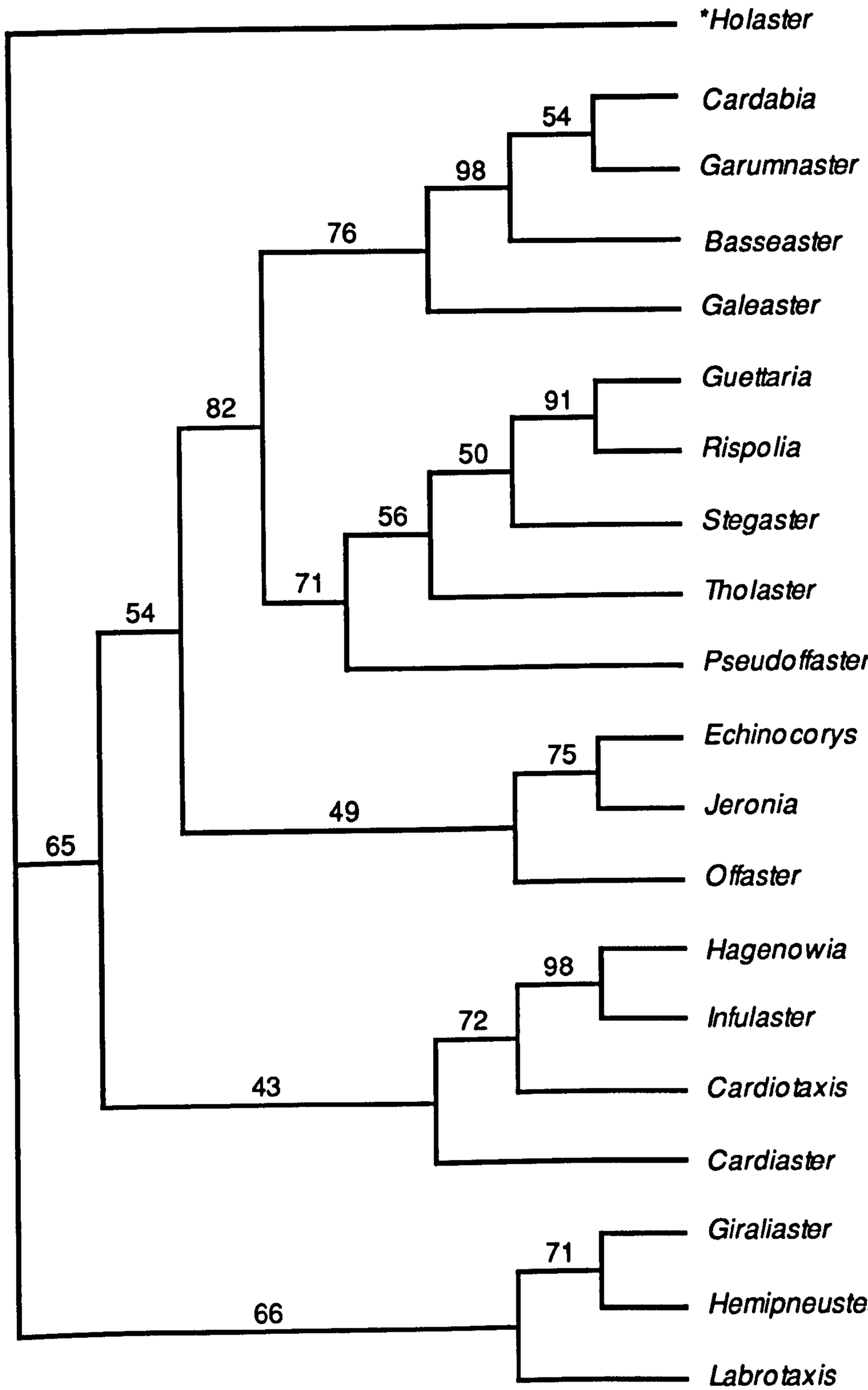
Table 4.2. Character matrix for the 18 Maastrichtian and Palaeocene holasteroid genera plus *Infulaster* and the outgroup *Holaster* (indicated by an asterisk).

**Holaster*	0000000000	0000000010	0100111100	01020
Basseaster	0110010001	1001201000	1200011000	00102
Cardabia	0111000001	1011201000	1200011000	00101
Cardiaster	1000000000	0000300011	0100101110	01021
Cardiotaxis	1000000010	0000300010	0100200000	0102?
Echinocorys	0000000000	0001100000	0000111200	00000
Galeaster	01100?1001	1?0120001?	1101200000	00101
Garumnaster	0111000001	1001201000	1200011000	00102
Giraliaster	0100000100	0000000011	0100111110	1102?
Guettaria	1000100001	1001201010	2112100221	01021
Hagenowia	1022011010	0101312111	1202200000	00???
Hemipneustes	000000?100	0000000011	0110111110	01020
Jeronia	0011000000	000???000	0000111201	0011?
Labrotaxis	0010000100	0000001010	0100111100	01020
Offaster	1000000000	0001101000	0100211100	00101
Pseudoffaster	1000000001	1001200010	0102200121	00101
Rispolia	1010000001	1000201010	2112100210	01021
Stegaster	0000000001	1?01200010	211210020?	00101
Tholaster	0000000001	10012??010	2202000221	0010?
Infulaster	1020000010	00013??111	1101100000	000?1

A heuristic search (replicated 25 times with random taxon addition) produced two most parsimonious solutions which differ only in the relative positions of *Basseaster*, *Garumnaster* and *Cardabia*. By reweighting the characters using the rescaled consistency index and rerunning the analysis, one of these trees was chosen. The resulting tree, which has a consistency index of 0.674 and a retention index of 0.834, is shown in Figure 4.1.

The holasteroid genera form four major clades, each of which can be easily distinguished on the basis of plastron architecture. Orthosternous taxa form two distinct groups, the thick tested stegasterids and thin tested genera with subanal fascioles: *Basseaster*, *Garumnaster*, *Cardabia* and *Galeaster*. Each clade corresponds to one of the holasteroid families outlined in the taxonomic revision in Chapter 3. Bootstrap support is moderate to high for most branches.

Figure 4.1. Cladogram for Maastrichtian and Palaeocene holasteroid genera plus *Infulaster*. Bootstrap support percentages based on 1000 replicates are indicated for each internal branch.


*Holaster
Cardabia
54
Garumnaster
98
Basseaster
76
Galeaster
Guettaria
91
Rispolia
82
50
Stegaster
56
Tholaster
71
Pseudoffaster
54
Echinocorys
75
Jeronia
49
Offaster
65
Hagenowia
98
Infulaster
72
Cardiotaxis
43
Cardiaster
Giraliaster
71
Hemipneustes
66
Labrotaxis

Stegasterid species level analysis.

Many of the taxa included in the generic level analysis of holasteroids are monospecific or contain only a small number of Maastrichtian and Palaeocene species. However, since the stegasterids form a specious clade, a species level analysis was carried out to resolve phylogenetic relationships within the group. In addition to the Maastrichtian and Palaeocene stegasterids, *Sanchezaster habanensis* from the Eocene of Cuba was included in the analysis. It appears to represent the sister taxon of *Stegaster cotteaui*. On inspection of the generic level analysis of holasteroids, *Echinocorys scutata* was chosen as an outgroup. The 29 characters used in the analysis are given in Table 4.3. The data matrix is given in Table 4.4.

Table 4.3. Characters used in the species level phylogenetic analysis of stegasterids. Asterisks indicate ordered characters.

1	Supplementary gonopores in ocular plates II and IV: 0 = absent; 1 = present.
2	Supplementary gonopores in ocular plate III: 0 = absent; 1 = present.
3	Plastron: 0 = not orthosternous; 1 = orthosternous.
4	Labrum and sternum: 0 = not separated; 1 = separated.
5	Shape of labral plate: 0 = broadens posteriorly; 1 = tapers posteriorly.
6	Shape of sternal plate: 0 = pentagonal; 1 = hexagonal.
7	Ambulacrum III: 0 = not differentiated; 1 = differentiated.
8	Pore shape in paired ambulacra: 0 = round; 1 = slightly elongate, placed *en chevron*; 2 = elongate.
9	Pore position in paired ambulacra: 0 = centre of plate; 1 = adoral centre of plate; 2 = outer edge of plate.
10	Ambulacral pores: 0 = double; 1 = single.
11	Number of ambulacral plates adjacent to each interambulacral plate: 0 = >3; 1 = >1, <3; 2 = 1.
12	Ambulacral plates: 0 = wider than high; 1 = higher than wide.
13	Shape of *mouth*: 0 = circular; 1 = transversely elongate.
14	Mouth: 0 = not in groove; 1 = in sharp, parallel-sided groove.
15	Mouth faces: 0 = downwards; 1 = forwards.
16*	Distance of mouth from anterior margin: 0 = >25% TL; 1 = 18-25% TL; 2 = <18% TL.
17	Anterior interambulacra form: 0 = no sharp keels; 1 = sharp keels.
18	Test shape in profile: 0 = gibbous; 1 = flat-based.
19	Test shape in horizontal outline: 0 = circular; 1 = elongate.
20	Distance of widest point *from* anterior margin: 0 = >60% of TL; 1 = 40-60% of TL; 2 = <40% of TL.
21	Height as a percentage of TL: 0 = <50%; 1 = >50%.
22	Large tubercles apically: 0 = present; 1 = absent.
23	Large tubercles along anterior interambulacra: 0 = present; 1 = absent.
24	Large tubercles in ring around test: 0 = present; 1 = absent.
25	Large tubercles low down anteriorly: 0 = present; 1 = absent.
26	Marginal fasciole: 0 = present; 1 = absent.
27	Test: 0 = not thick-tested; 1 = thick-tested.
28	Subanal heel: 0 = absent; 1 = weakly developed; 2 = distinct bilobed heel.
29	Position of anus: 0 = inframarginal: 1 = on truncate posterior; 2 = supramarginal.

Table 4.4. Character matrix for the ten Maastrichtian and Palaeocene stegasterid taxa plus *Sanchezaster habanensis* and the outgroup *Echinocorys scutata* (indicated by an asterisk).

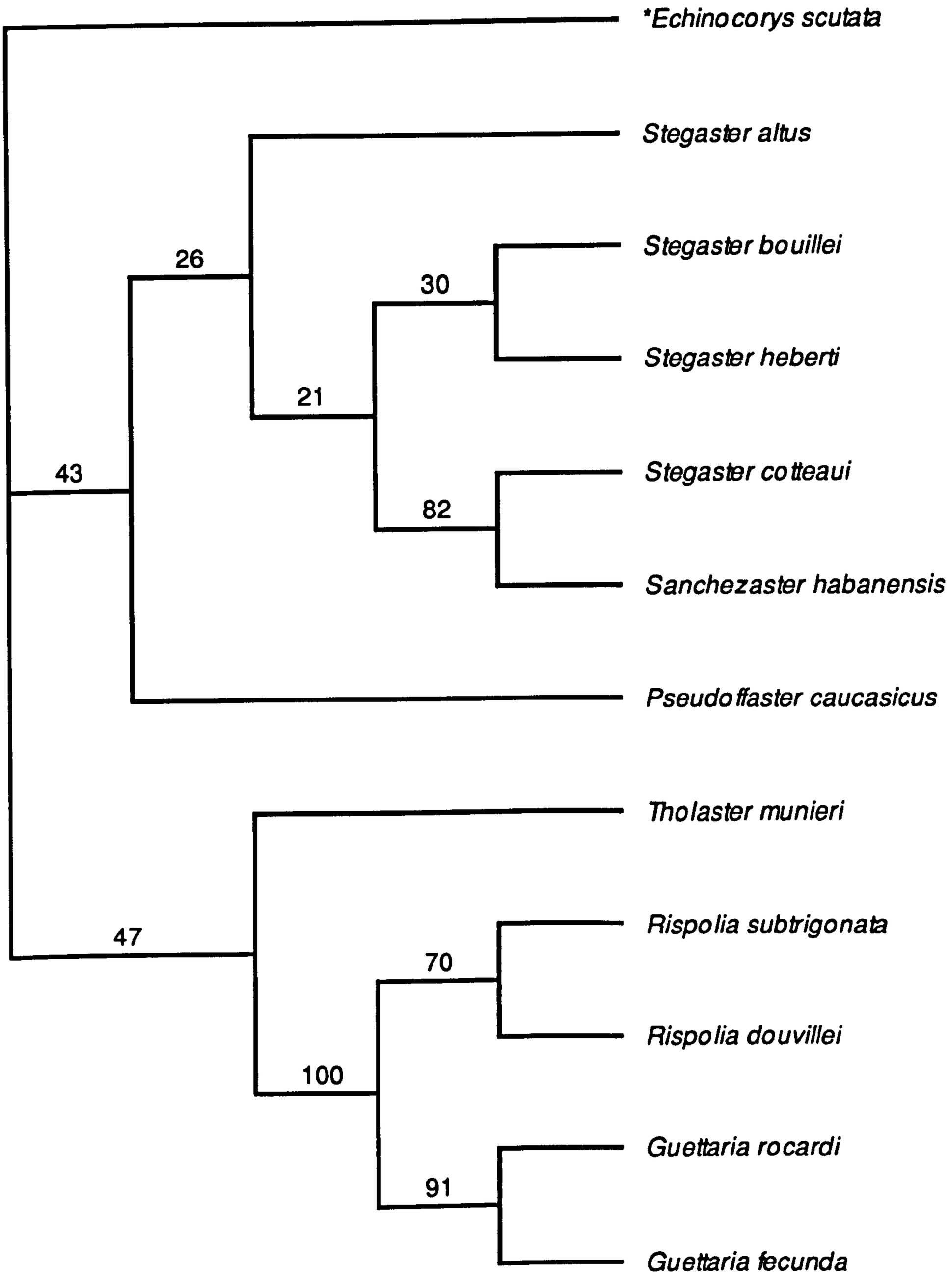
**Echinocorys scutata*	0000100010	1010010112	100000100
Guettaria rocardi	1010111220	0001110112	100111121
Guettaria fecunda	1110111220	0001110112	110111121
Pseudoffaster caucasicus	0010110010	2001120001	111111?01
Rispolia subtrigonata	0010011220	0001110112	110001121
Rispolia douvillei	0010011220	0011111112	111001121
Stegaster altus	0010110010	2001110101	100000111
Stegaster bouillei	0010110110	1001110111	000010111
Stegaster cotteaui	0011110010	2101110101	000000111
Stegaster heberti	0010110010	1001110101	000000111
Tholaster munieri	0010110010	2001100110	011000122
Sanchezaster habanensis	0011110001	2101110101	000001001

A branch and bound search produced just one most parsimonious solution (Figure 4.2) with a consistency index of 0.901 and a retention index of 0.891. *Sanchezaster habanensis* and *Stegaster cotteaui* were found to be sister taxa.

Although the species and genus level analyses do not produce exactly the same arrangement of stegasterid taxa, they differ only in the position of the *Stegaster* clade. *Stegaster* is a specious genus containing some taxa which have previously been assigned to separate genera (e.g. *Stegaster bouillei* was considered to be the type species of *Seunaster*). Consequently, *Stegaster* includes taxa that encompass a variety of character states (e.g. only *Stegaster cotteaui* has a disjunct plastron). It is possible that coding such characters as "uncertain" in the generic analysis obscures phylogenetic signal.

Bootstrap support is moderate for most branches. This is to expected since many nodes are supported by two or three characters at most.

Figure 4.2. Cladogram for Maastrichtian and Palaeocene stegasterid species plus *Sanchezaster habanensis*. The outgroup, *Echinocorys scutata*, is indicated by an asterisk. Bootstrap support percentages based on 1000 replicates are indicated for each internal branch.


*Echinocorys scutata
Stegaster altus
Stegaster bouillei
Stegaster heberti
Stegaster cotteaui
Sanchezaster habanensis
Pseudoffaster caucasicus
Tholaster munieri
Rispolia subtrigonata
Rispolia douvillei
Guettaria rocardi
Guettaria fecunda
26
30
21
43
82
47
70
100
91

Spatangoid generic level analysis.

After scoring as many characters as possible for the generic level analysis of spatangoids, there were still too few characters to unambiguously resolve the phylogeny of all spatangoid taxa. The large number of spatangoid genera made it necessary to divide the spatangoids into Micrasterina and Hemiasterina for the generic level analysis. The same set of 52 characters was used for both analyses to simplify the task of character scoring (Table 4.5), although this led to the inclusion of a number of redundant characters (characters which are constant in all genera of the Micrasterina or Hemiasterina) in each analysis. Data matrices for the two analyses are given in Tables 4.6 and 4.7.

Table 4.6. Character matrix for Maastrichtian and Palaeocene genera of Micrasterina and the outgroup *Toxaster* (indicated by an asterisk).

***Toxaster**	0001000000	0001111000	1101100010	0110110002	1000002000	11
Micraster	0001000100	0001111001	2012200010	0120110002	1001001011	12
Mokotibaster	0001000100	0001111000	1101100010	11?0220002	1101001011	11
Pseudogibbaster	0001000100	0001111000	1111200010	0120110002	1101001111	12
Ovulaster	0000000100	0002211000	0100000000	0000000001	0101000110	10
Habanaster	0200000100	0012211000	0100000000	0000000001	0101001111	10
Diplodetus	0001?11100	0001111000	1101200010	0120110001	1001002010	11
Cyclaster	0101?11100	0011111000	1101100010	0110110001	1001002010	02
Isaster	0101000000	0011111000	1100100010	0110110001	1001001010	02
Eupatagus	2000111100	0011?11000	1101100?0	0110110001	1100002000	10

A branch and bound search of the Micrasterina resulted in a single most parsimonious solution with a consistency index of 0.892 and a retention index of 0.858 (Figure 4.3). In this tree, the three- and four-gonopored micrasterids form separate distinct clades. These two clades are more closely related to each other than either is to the single included brissid genus *Eupatagus*. The Eocene *Habanaster* is found to be sister group of the Maastrichtian *Ovulaster*. Bootstrap support is moderate for the separation of the micrasterids from *Eupatagus* and for the division of the three- and four-gonopored micrasterids.

Table 4.5. Characters used in the generic level phylogenetic analysis of Micrasterina and Hemiasterina. Asterisks indicate ordered characters.

1	Apical disc: 0 = ethmophract; 1 = transitional; 2 = ethmolytic.
2	Number and position of gonopores: 0 = 4; 1 = 3 (madreporite lacking pore); 2 = 3 (genital plate 4 lacking pore); 3 = 2.
3	Apical system: 0 = without fused plates; 1 = with fused plates.
4*	Position of apical system, as % of TL from anterior: 0 = <38; 1 = 38-60; 2 = >60.
5	Peripetalous fasciole: 0 = absent; 1 = present.
6	Peripetalous fasciole: 0 = does not reach oral surface; 1 = reaches oral surface.
7	Peripetalous fasciole: 0 = not indented; 1 = strongly indented behind anterior petals.
8	Subanal fasciole: 0 = absent; 1 = present.
9	Latero-anal fasciole: 0 = absent; 1= present.
10	Marginal fasciole: 0 = absent; 1 = present.
11	Plastron: 0 = not disjunct; 1 = disjunct.
12	Labrum in contact with: 0 = 2 sternal plates; 1 = 1 sternal plate.
13	Shape of labral plate: 0 = broadens posteriorly; 1 = tapers posteriorly.
14*	Relative length:width of labral plate: 0 = <1.2; 1 = 1.2-3.1; 2 = >3.1.
15*	Relative length:width of sternal plates: 0 = <2.0; 1 = 2.0-3.2; 2 = >3.2.
16	Sternal plates: 0 = asymmetric; 1 = symmetrical.
17	Sternal plates: 0 = unequal sized; 1 = equal sized.
18*	Angle between first and second sternal plates: 0 = <10; 1 = 10-50; 2 = >50.
19	Lumps along edges of plastron: 0 = absent; 1 = present.
20	Position of mouth, as % of TL from anterior: 0 = >15; 1 = <15.
21*	Extent of labral projection as % of mouth length: 0 = <15; 1 = 15-50; 2 = >50.
22	Rim around mouth: 0 = absent; 1 = present.
23	Mouth: 0 = does not open into groove; 1 = opens into groove.
24	Depth of frontal groove at ambitus: 0 = no groove; 1 = shallow; 2 = deep.
25	Depth of frontal groove at apex: 0 = flush; 1 = shallow; 2 = deeply sunken.
26	Breadth of anterior ambulacrum: 0 = narrower than or equal to paired ambulacra; 1 = broader than paired ambulacra.
27	Anterior ambulacrum: 0 = without vertical walls; 1 = with vertical walls.
28	Pores in unpaired ambulacrum: 0 = in single column; 1 = in two columns.
29	Pores in frontal ambulacrum: 0 = not closely packed; 1 = closely packed.
30	Unpaired ambulacrum: 0 = non-petaloid; 1 = petaloid.
31	Shape of pores in unpaired ambulacrum: 0 = round; 1 = elongate.
32	Paired ambulacra: 0 = non-petaloid; 1 = petaloid.
33	Paired ambulacra: 0 = flush; 1 = slightly sunken; 2 = deeply sunken.
34	Relative length of anterior:posterior paired petals: 0 = <1.6; 1 = >1.6.
35	Anterior paired ambulacra - % distance to ambitus: 0 = <66; 1 = >66.
36	Posterior paired ambulacra - % distance to ambitus: 0 = <68; 1 = >68.
37	Paired ambulacra: 0 = parallel sided 1 = bowed.
38	Paired ambulacra: 0 = straight; 1 = distally flexuous.
39	Pore zone narrower or broader than area between: 0 = narrower; 1 = broader.
40	Pore-pairs in paired ambulacra: 0 = widely spaced; 1 = medium spacing; 2 = very closely spaced.
41	Shape of pores in paired ambulacra: 0 = round; 1 = elongate.
42	Divergences of anterior petals: 0 = <130 degrees; 1 = >130 degrees.
43	Granulation between pore-pairs in ambulacral column: 0 = absent; 1 = present.
44	Tuberculation: 0 = not micrasterid style; 1 = micrasterid style.
45	Tuberculation: 0 = not pustulous; 1 = pustulous.
46	Sutures between plates: 0 = indistinct; 1 = deep and distinct.
47	Highest point of test: 0 = anterior; 1 = central; 2 = posterior.
48	Shape in profile: 0 = flat base; 1 = strongly inflated lower surface.
49	Number of angles in horizontal outline at posterior of test: 0 = 2; 1 = 1.
50	Horizontal outline: 0 = longer than broad; 1 = broader than long.
51	Widest point of test: 0 = anterior; 1 = central; 2 = posterior.
52	Posterior truncation on test: 0 = outward; 1 = vertical; 2 = undercut.

Table 4.7. Character matrix for Maastrichtian and Palaeocene genera of Hemiasterina and the outgroup *Toxaster* (indicated by an asterisk).

**Toxaster*	0001000000	0001111000	1101100010	0110110002	1000002000	11
Hemiaster	0001111000	0001011000	11001?0010	011121?001	1000002010	11
Leiostomaster	0001111000	0001011000	0000100010	0111111001	1000112010	11
Mecaster	1001111000	0001111000	1101200010	0120221012	1100002001	10
Leymeriaster	1001112000	0000111000	1101200010	0121211112	1000002011	00
Gregoryaster	1001112000	0001111000	2112200010	0120210002	1000002011	10
Linthia	2001112010	0000111000	1102200010	0120221021	1000002010	11
Paraster	2001112010	0000111000	1102200010	0121211111	1000002011	11
Tessieria	2001112010	0011111010	1102100000	0120221112	1000002110	11
Proraster	2002111000	0000111000	0012311110	0121211102	1000002010	11
Trachyaster	2001111000	0001111000	1101110000	0110211011	1000002011	11
Holcopneustes	2000111000	0001111000	1112110010	0120210002	1100000001	10
Prenaster	2000132010	0000111000	1100000000	0110210002	1100002010	11
Mauritanaster	2000111000	0001111000	1101100010	0110220002	1100101010	11
Brisaster	2102112000	0000111000	0012311010	0121211102	1000002010	11
Pseudolinthia	2101112010	0000111000	1112301010	0121210002	1000002011	11
Abatus	2301112010	0000111000	1102310010	0121211112	1000002011	11
Opissaster	2301112000	0000111000	0???1?0010	0121211101	1000002010	11
Kertaster	2300112001	0000111000	1012100010	0120110001	1000000010	12
Coraster	0000121000	0011111001	0101000000	0000000000	0100001111	12
Orthaster	0200121000	0012111001	0101000000	0000000000	0100001111	12
Homoeaster	0000121000	0001111000	0101000010	0000000001	0100001011	00
Sphenaster	0310121000	0012211000	0000010011	0000000001	0100101110	20
Iraniaster	1001111000	1111000200	1001000010	0110220002	1010001010	12
Pseudiraniaster	2001111000	1111101100	1001000010	0110220002	1010002010	12
Leviechinus	2301111000	1111001100	1001000010	0110220002	1010001011	12
Brightonia	0301111000	1111001100	1001000010	0110210002	1010001000	12

A heuristic search of the Hemiasterina (replicated 25 times with random taxon addition) produced 67 equally parsimonious trees. By reweighting the characters using the rescaled consistency index and rerunning the analysis, the number of solutions was reduced to two trees with a consistency index of 0.658 and a retention index of 0.800. These two trees differ only in the position of the corasterid clade which groups either with *Hemiaster* and *Leiostomaster* or with the somaliasterids. Traditional taxonomies (e.g. Fischer 1966) which place *Leiostomaster* with the corasterids support the first of these alternatives. This solution is shown in Figure 4.4, and clearly illustrates the paraphyletic nature of the hemiasterids and schizasterids as currently diagnosed. Much of this problem arises because of the variability of apical disc structure and fasciole placement. Cladistic analysis with extant hemiasterids and schizasterids is necessary to fully resolve the phylogeny of these groups.

However, the tree presented in Figure 4.4 is adequate for the purposes of this

thesis, since it is possible to determine sister group relationships for those genera restricted to the Maastrichtian and subsequently, when the tree is plotted against stratrigraphy, which clades survived into the Tertiary. Bootstrap support is low for most branches with the exception of the corasterid and somaliasterid clades. This is not unexpected since most nodes are supported by small numbers of character changes.

Figure 4.3. Cladogram for Maastrichtian and Palaeocene micrasterid and brissid spatangoid genera (Micrasterina) plus *Habanaster*. The outgroup, *Toxaster*, is indicated by an asterisk. Bootstrap support percentages based on 1000 replicates are indicated for each internal branch.

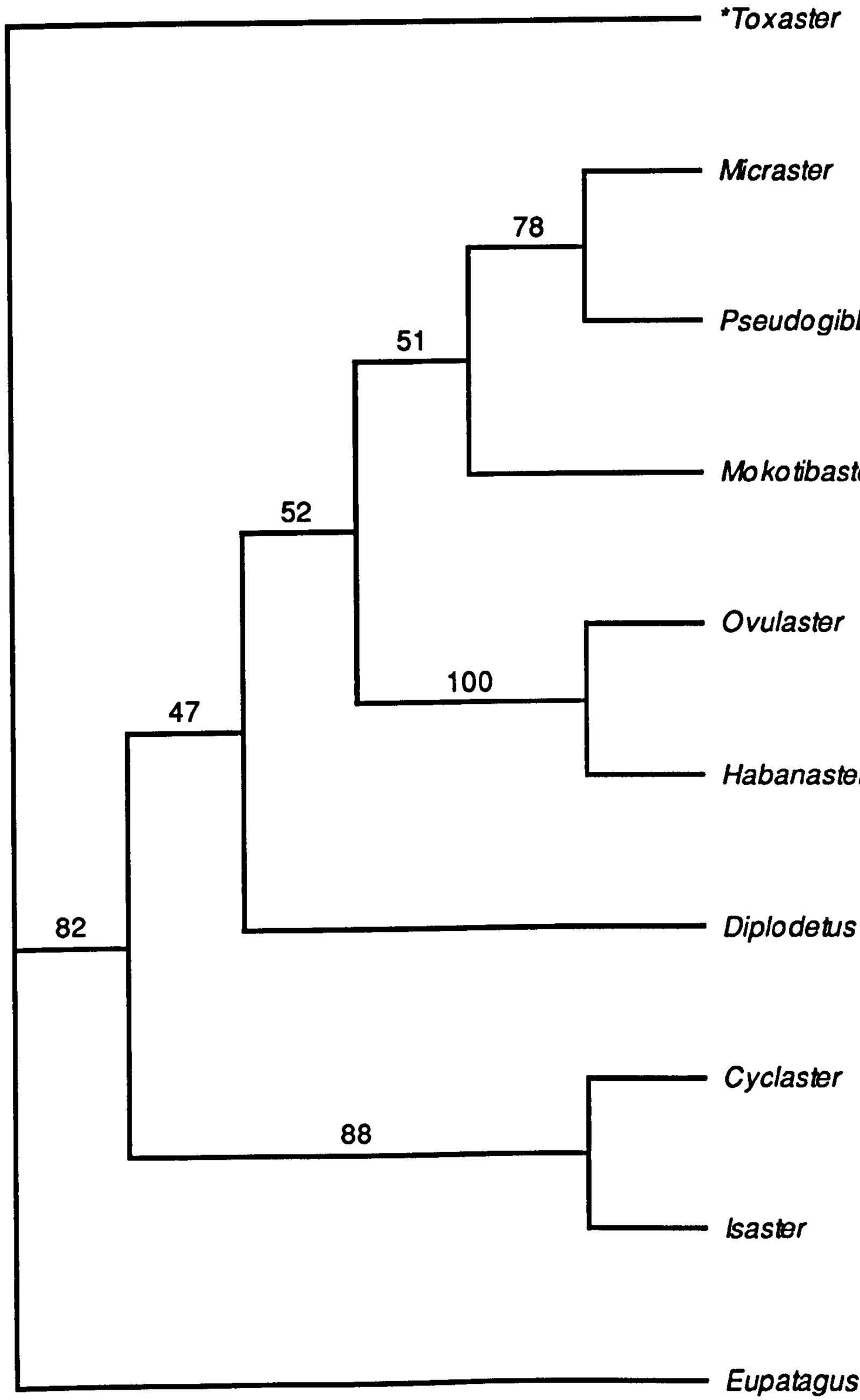
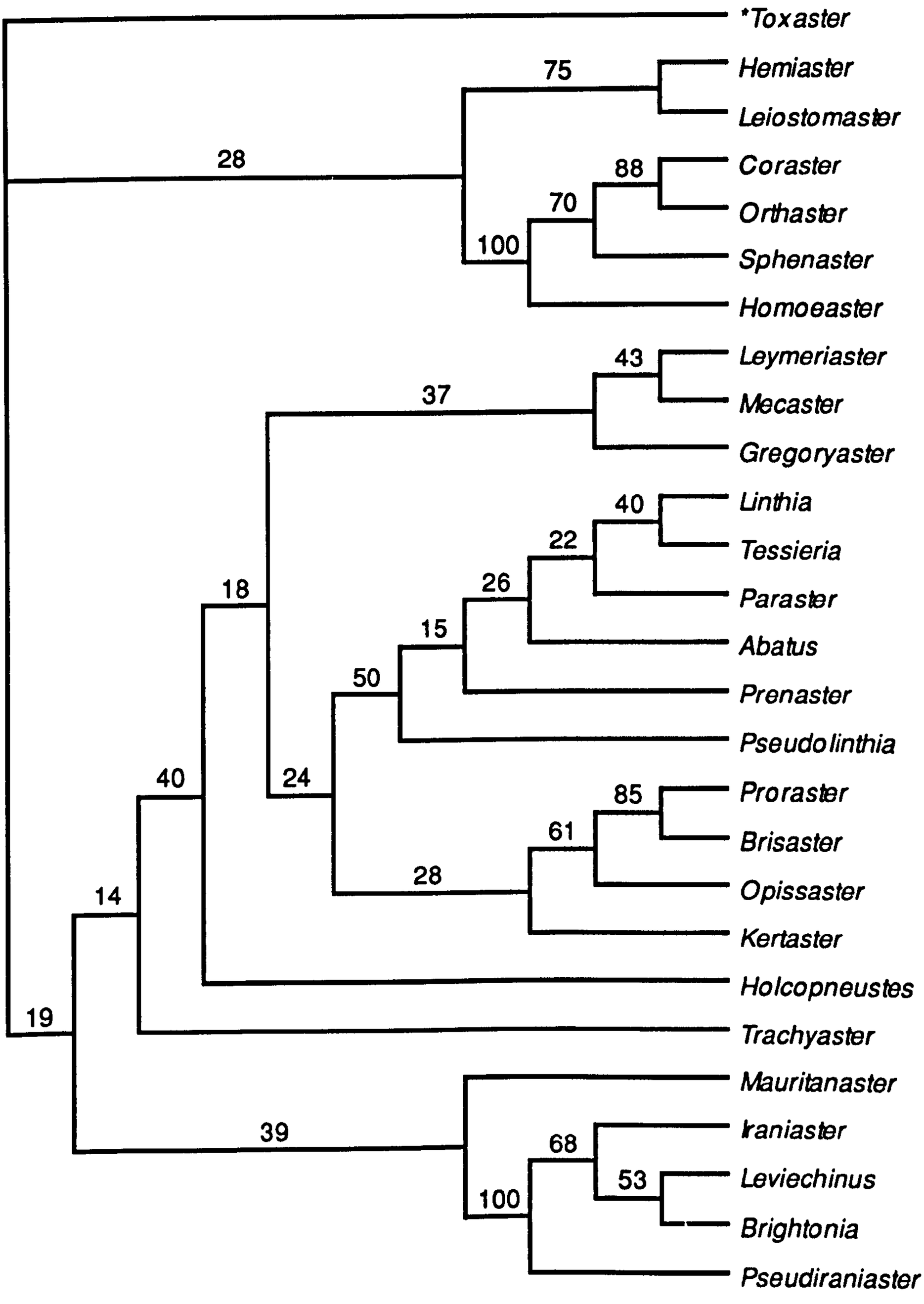

*Toxaster
Micraster
78
Pseudogibbaster
51
Mokotibaster
52
Ovulaster
100
47
Habanaster
82
Diplodetus
Cyclaster
88
Isaster
Eupatagus

Figure 4.4. Cladogram for Maastrichtian and Palaeocene hemiasterid, schizasterid, pericosmid, corasterid, aeropsid and somaliasterid spatangoid genera (Hemiasterina). The outgroup, *Toxaster*, is indicated by an asterisk. Bootstrap support percentages based on 1000 replicates are indicated for each internal branch.


*Toxaster
Hemiaster
Leiostomaster
Coraster
Orthaster
Sphenaster
Homoeaster
Leymeriaster
Mecaster
Gregoryaster
Linthia
Tessieria
Paraster
Abatus
Prenaster
Pseudolinthia
Proraster
Brisaster
Opissaster
Kertaster
Holcopneustes
Trachyaster
Mauritanaster
Iraniaster
Leviechinus
Brightonia
Pseudiraniaster
75
28
88
70
100
43
37
40
22
18
26
15
50
24
85
61
28
40
14
19
39
68
53
100

Micrasterid species level analysis.

Maastrichtian and Palaeocene micrasterids with four gonopores and petaloid paired ambulacra were included in this analysis with *Micraster leskei* as an outgroup. The 31 characters used in the cladistic analysis are given in Table 4.8. A character matrix is given in Table 4.9.

Table 4.8. Characters used in the species level phylogenetic analysis of micrasterids. Asterisks indicate ordered characters.

1	Width as % of TL: 0 = <94; 1 = >94.
2	Shape in plan view: 0 = heart shaped; 1 = round subcordate; 2 = elongate subcordate; 3 = ovate.
3	Height as % of TL: 0 = <50; 1 = >50.
4	Angle of posterior truncation: 0 = undercut; 1 = vertical; 2 = outwardly truncate.
5	Position of highest point: 0 = central; 1 = posterior.
6	Shape of anterior profile: 0 = convex; 1 = concave.
7*	Shape of anterior margin: 0 = convex-flat; 1 = slightly notched; 2 = deeply notched.
8	Frontal groove: 0 = deepens towards ambitus; 1 = shallows towards ambitus.
9*	% of unpaired ambulacral length in which pores closely spaced: 0 = <46; 1 = 46-69; 2 = >69.
10	Pores in anterior ambulacrum: 0 = round; 1 = elongate.
11*	Divergence of anterior paired petals: 0 = <120; 1 = 120-135; 2 = >135 degrees.
12*	% length to ambitus of anterior paired petals: 0 = <53; 1 = 53-75; 2 = >75.
13	% length to ambitus of posterior paired petals: 0 = <62; 1 = >62.
14	Relative length of anterior to posterior petals: 0 = <1.3; 1 = >1.3.
15	Sunkeness of petals: 0 = virtually flush; 1 = sunken; 2 = deeply sunken.
16	Shape of pores in paired petals: 0 = inner circular, outer elongate; 1 = elongate.
17	Width of poriferous zone: 0 = narrower; 1 = equal; 2 = broader than zone between.
18*	Width of anterior petals as % of anterior petal length: 0 = <31; 1 = 31-39; 2 = >39.
19*	Relative length to width of labral plate: 0 = <1.7; 1 = 1.7-2.5; 2 = >2.5.
20	Shape of labral plate: 0 = broadens posteriorly; 1 = tapers posteriorly.
21	Plastron suture: 0 = central; 1 = offset to right.
22*	Extent of labral projection as % of mouth length: 0 = <15; 1 = 15-50; 2 = >50.
23	Peristomal rim: 0 = absent; 1 = present.
24	Width of mouth as % of test width: 0 = <20; 1 = >20.
25*	Distance of peristome from anterior: 0 = <19% TL; 1 = 19-27% TL; 2 = >27% TL.
26	Mouth: 0 = not invaginated; 1 = invaginated.
27	Peripetalous fasciole: 0 = absent; 1 = crowded miliaries at ends of petals; 2 = incomplete.
28	Subanal fasciole: 0 = absent; 1 = present.
29	Aboral tuberculation: 0 = uniform; 1 = large tubercles around apex.
30*	Distance of apical system from anterior margin as % of TL: 0 = <38; 1 = 38-51; 2 = >51.
31*	Height of periproct from base as % of test height: 0 = <35; 1 = 35-52; 2 = >52.

A heuristic search (replicated 25 times with random taxon addition) produced 22 most parsimonious trees. Reweighting the characters using the rescaled consistency index and rerunning the analysis resulted in one of these solutions being chosen. The resulting tree, which has a consistency index of 0.581 and a retention index of 0.783, is

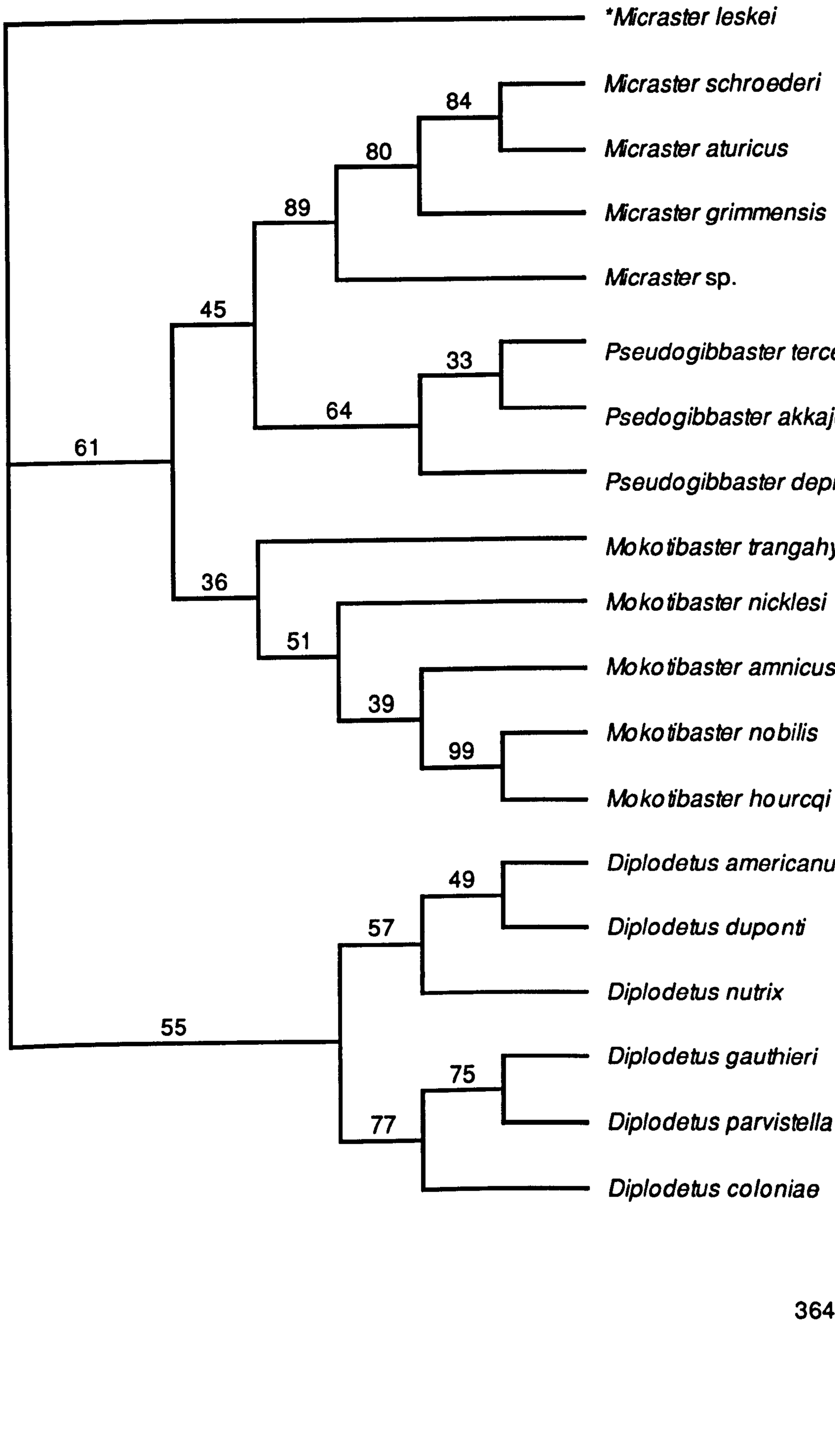
shown in Figure 4.5. It is identical to the 50% majority rule consensus tree.

The micrasterid genera recognized in the taxonomic analysis all form separate clades. However, bootstrap percentages are generally low since most nodes are supported by small numbers of character changes.

Table 4.9. Character matrix for Maastrichtian and Palaeocene micrasterid species and the outgroup *Micraster leskei* (indicated by an asterisk).

**Micraster leskei*	0211001110	0001110010	0110100101	2
Diplodetus americanus	0211102110	0110210011	0110102111	2
Diplodetus coloniae	0311100120	2100110100	1010100100	2
Diplodetus duponti	?010102110	1101211000	0110101111	2
Diplodetus gauthieri	1312100120	0000111???	0101202111	2
Diplodetus nutrix	0212101110	1101200010	0110200111	2
Diplodetus parvistella	0302100110	0001110100	0110201101	2
Micraster aturicus	1010012000	0110101011	0200010102	?
Micraster grimmensis	1010002000	1101112001	1200010101	1
Micraster schroederi	1010002000	0101101021	0200010101	1
Micraster sp.	1011002?0	1001211??0	1???0?0101	1
Mokotibaster amnicus	1010001110	0210110110	1100100101	1
Mokotibaster hourcqi	111?001121	1210011000	0000000000	0
Mokotibaster nicklesi	1011001?0	2210110210	?00100?100	?
Mokotibaster nobilis	1110001111	1210011100	1010100001	0
Mokotibaster trangahyensis	1011001100	1110100000	0000100101	2
Pseudogibbaster akkajensis	1111001110	2100210110	0010110101	2
Pseudogibbaster depressus	1111001110	2101210020	0010110101	1
Pseudogibbaster tercensis	1111001110	2100210011	0110110101	2

Figure 4.5. Cladogram for Maastrichtian and Palaeocene species of four-gonopored, petaloid micrasterids. The outgroup, *Micraster leskei*, is indicated by an asterisk. Bootstrap support percentages based on 1000 replicates are indicated for each internal branch.


*Micraster leskei
Micraster schroederi
Micraster aturicus
Micraster grimmensis
Micraster sp.
Pseudogibbaster tercensis
Psedogibbaster akkajensis
Pseudogibbaster depressus
Mokotibaster trangahyensis
Mokotibaster nicklesi
Mokotibaster amnicus
Mokotibaster nobilis
Mokotibaster hourcqi
Diplodetus americanus
Diplodetus duponti
Diplodetus nutrix
Diplodetus gauthieri
Diplodetus parvistella
Diplodetus coloniae
84
80
89
45
33
64
61
36
51
39
99
49
57
55
75
77

Cyclaster *and* Isaster *species level analysis.*

Cyclaster and *Isaster* are the only two spatangoids with an ethmophract apical system lacking only the gonopore in the madreporite. *Isaster* was included in the analysis to determine from where amongst Maastrichtian and Palaeocene species of *Cyclaster* it was derived. *Micraster leskei* was added as an outgroup.

Table 4.10 gives the 24 characters which were used in the cladistic analysis. Table 4.11 is the character matrix for the ten species of *Cyclaster* included in the analysis, plus *Isaster* and the outgroup.

Table 4.10. Characters used in the cladistic analysis of species of *Cyclaster* and *Isaster*. Ordered characters are indicated by asterisks.

1	Width of test as % of test length: 0 = <75; 1 = >75.
2	Shape in plan view: 0 = rectangular; 1 = tapered; 2 = ovate.
3	Height of test as % of test length: 0 = <55; 1 = >55.
4*	Anterior margin: 0 = convex; 1 = flat to slightly notched; 2 = distinctly notched.
5*	Divergence of anterior paired petals: 0 = <100; 1 = 100-120; 2 = >120 degrees.
6*	% length to ambitus of anterior paired petals: 0 = <40; 1 = 40-60; 2 = >60.
7*	% length to ambitus of posterior paired petals: 0 = <35; 1 = 35-48; 2 = >48.
8	Relative length of anterior to posterior petals: 0 = <1.2; 1 = >1.2.
9	Sunkeness of petals: 0 = virtually flush; 1 = noticeably depressed.
10	Pores in paired petals: 0 = small and circular; 1 = circular anteriorly & elongate posteriorly; 2 = elongate.
11	Width of poriferous zone: 0 = narrower; 1 = equal; 2 = broader than area between pore zones.
12	Posterior upper surface: 0 = non-carinate; 1 = carinate.
13	Relative length to width of labral plate: 0 = <2.5; 1 = >2.5.
14	Shape of labral plate: 0 = not tapered posteriorly; 1 = tapered posteriorly.
15	Extent of labral projection as % of mouth length: 0 = <33; 1 = >33.
16	Peristome rim: 0 = narrow; 1 = prominent.
17	Width of mouth as % of test width: 0 = <16; 1 = >16.
18	Position of mouth as % of test length: 0 = <20; 1 = >20.
19	Mouth: 0 = not invaginated; 1 = invaginated.
20	Peripetalous fasciole: 0 = absent; 1 = incomplete; 2 = complete.
21	Subanal fasciole: 0 = absent; 1 = present.
22	Tuberculation: 0 = normal; 1 = pustular.
23	Position of apical disc as % of TL: 0 = <40; 1 = >40.
24	Number of gonopores: 0 = 4; 1 = 3.

A branch and bound search produced two equally parsimonious solutions, differing only in the position of *Cyclaster heberti*. One solution best fits the stratigraphy. The same tree (Figure 4.6) is selected by reweighting the characters using the rescaled consistency index and rerunning the analysis. The resulting tree has a consistency index

of 0.789 and a retention index of 0.845.

The *Cyclaster* species form three clades, which could be considered as subgenera. Each of these three clades can be easily distinguished on the basis of overall test morphology:

rectangular - *suecicus*, *galei* and *ruegensis*

These three species are characterised by their short petals of equal length, generally with small round pores. The peripetalous fasciole is either absent or just visible posteriorly. The test has non pustular tuberculation.

ovate - *platornatus* and *pfenderae*

The petals of these two species are well developed and sunken with elongate pores. The peripetalous fasciole is complete. Tests have pustular tuberculation (most obvious in *C. pfenderae*).

tapered or **"coffin-shaped"** - *integer*, *vilanovae*, *gindrei*, *aturicus* and *heberti*

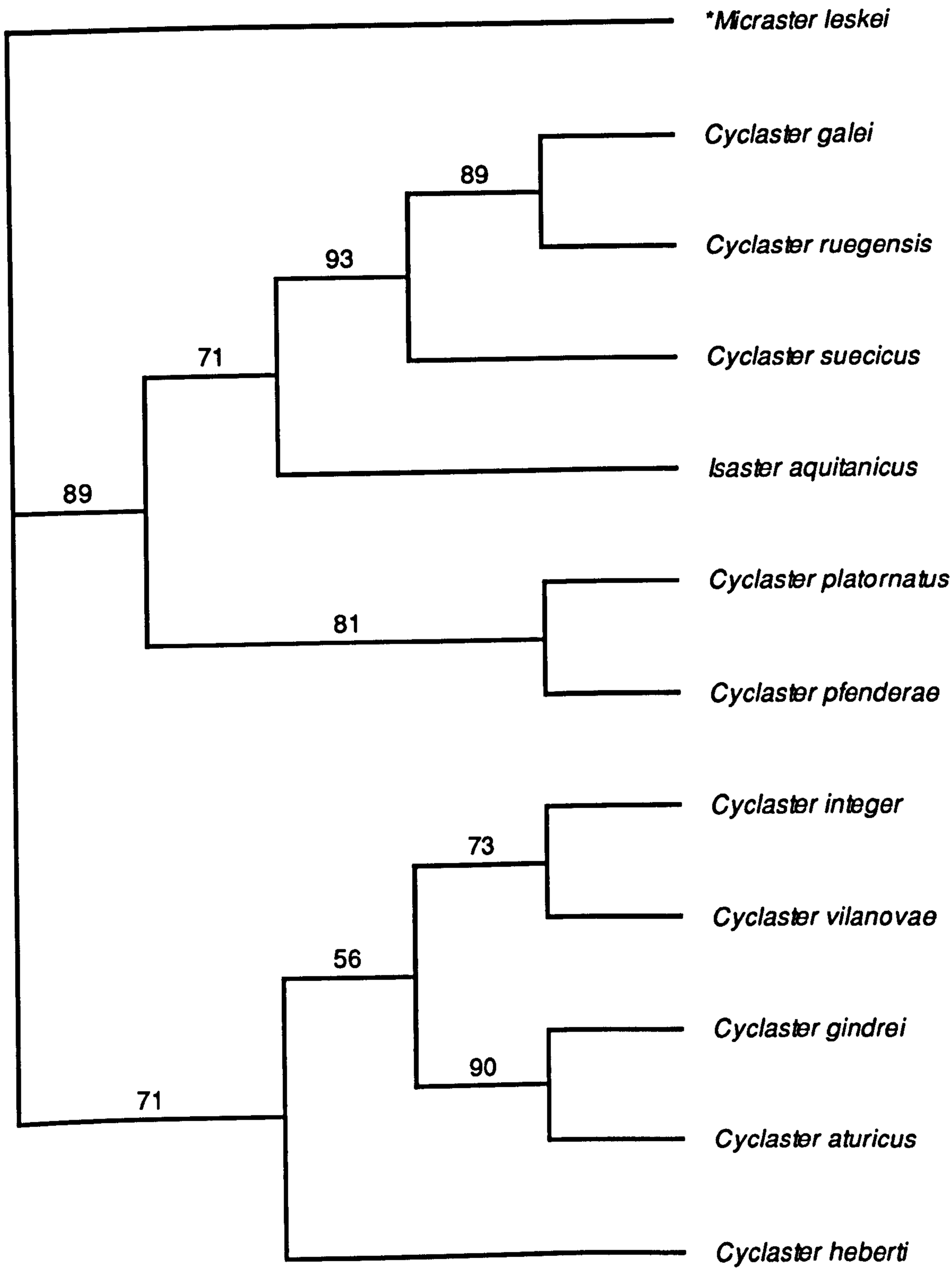
These five taxa have well developed petals with elongate pores. Development of the peripetalous fasciole varies within the group. Tuberculation is uniformly non-pustular. *C. gindrei* and *C. aturicus* (forms with distinct frontal grooves and anterior apical systems) group together.

Isaster aquitanicus is the sister taxon of the rectangular species of *Cyclaster*. Bootstrap support is high for most branches.

Table 4.11. Character matrix for the ten species of *Cyclaster* plus *Isaster* and the outgroup *Micraster leskei* (indicated by an asterisk).

**Micraster leskei*	1111111112	0100000100	1010
Cyclaster aturicus	1112211012	2111100000	1001
Cyclaster galei	0000000000	0001111011	1011
Cyclaster gindrei	1112210102	211000000?	1001
Cyclaster heberti	1101111112	2111110102	1011
Cyclaster integer	1111111001	1111101002	1011
Cyclaster pfenderae	1210111112	2000010102	1111
Cyclaster platornatus	1200000112	2000011102	1111
Cyclaster ruegensis	1000100000	0000?00100	1011
Cyclaster suecicus	1010211000	0010011100	1011
Cyclaster vilanovae	1111111012	2111001001	1011
Isaster aquitanicus	1210222002	2001000100	0011

Figure 4.6. Cladogram for Maastrichtian and Palaeocene species of Cyclaster plus *Isaster aquitanicus*. Bootstrap support percentages based on 1000 iterations are indicated for each internal branch.


*Micraster leskei
Cyclaster galei
89
Cyclaster ruegensis
93
Cyclaster suecicus
71
Isaster aquitanicus
89
Cyclaster platornatus
81
Cyclaster pfenderae
Cyclaster integer
73
Cyclaster vilanovae
56
Cyclaster gindrei
90
71
Cyclaster aturicus
Cyclaster heberti

Taxonomic position of the somaliasterids.

The systematic position of the somaliasterids has long been a source of confusion since they possess a combination of the characters usually considered diagnostic for placement in either the holasteroids or spatangoids. All genera assigned to the somaliasterids have a compact apical system and slightly sunken petaloid paired ambulacra which are closed distally, typical of spatangoids. However, they also possess a meridosternous plastron, characteristic of the holasteroids. Taxonomic position is therefore somewhat uncertain. In fact, *Somaliaster* itself has, at different times, been referred to the hemiasterid spatangoids (Hawkins 1935, Mortensen 1950), the palaeopneustid spatangoids (Maccagno 1941), the stenonasterid holasteroids (Joysey 1954, Kier 1957) and the somaliasterid holasteroids (Wagner & Durham 1966, Kier 1972). A phylogenetic analysis with unequivocal representatives of both orders has been carried out to determine the true taxonomic position of these so-called "aberrant taxa".

The characters chosen for the analysis (Table 4.12) relate to plastron and apical disc structure and petal morphology, since these are the traits typically used for the differentiation of holasteroids and spatangoids. Only easily scored fasciole characters were added since resolution within the holasteroids and spatangoids was unnecessary for this analysis.

All five Maastrichtian and Palaeocene species of somaliasterid were included in the analysis along with representatives of each of the five holasteroid clades. A number of taxa from the Micrasteridae and Hemiasterinae were also included. The disasterid echinoid *Pygomalus analis* was added as an outgroup. A character matrix is given in Table 4.13.

A branch and bound search produced ten equally parsimonious trees. Re-weighting the characters using the rescaled consistency index and rerunning the analysis resulted in a single tree (Figure 4.7). The consistency index for this tree is 0.794 and the retention index is 0.916. *Mauritanaster* is the immediate sister group of the somaliasterids.

Bootstrapping based on 1000 iterations indicates that although many internal branches within the holasteroids and spatangoids are not strongly supported in this analysis, the dichotomy between holasteroids and spatangoids and the grouping of somaliasterids with spatangoids is very strongly supported.

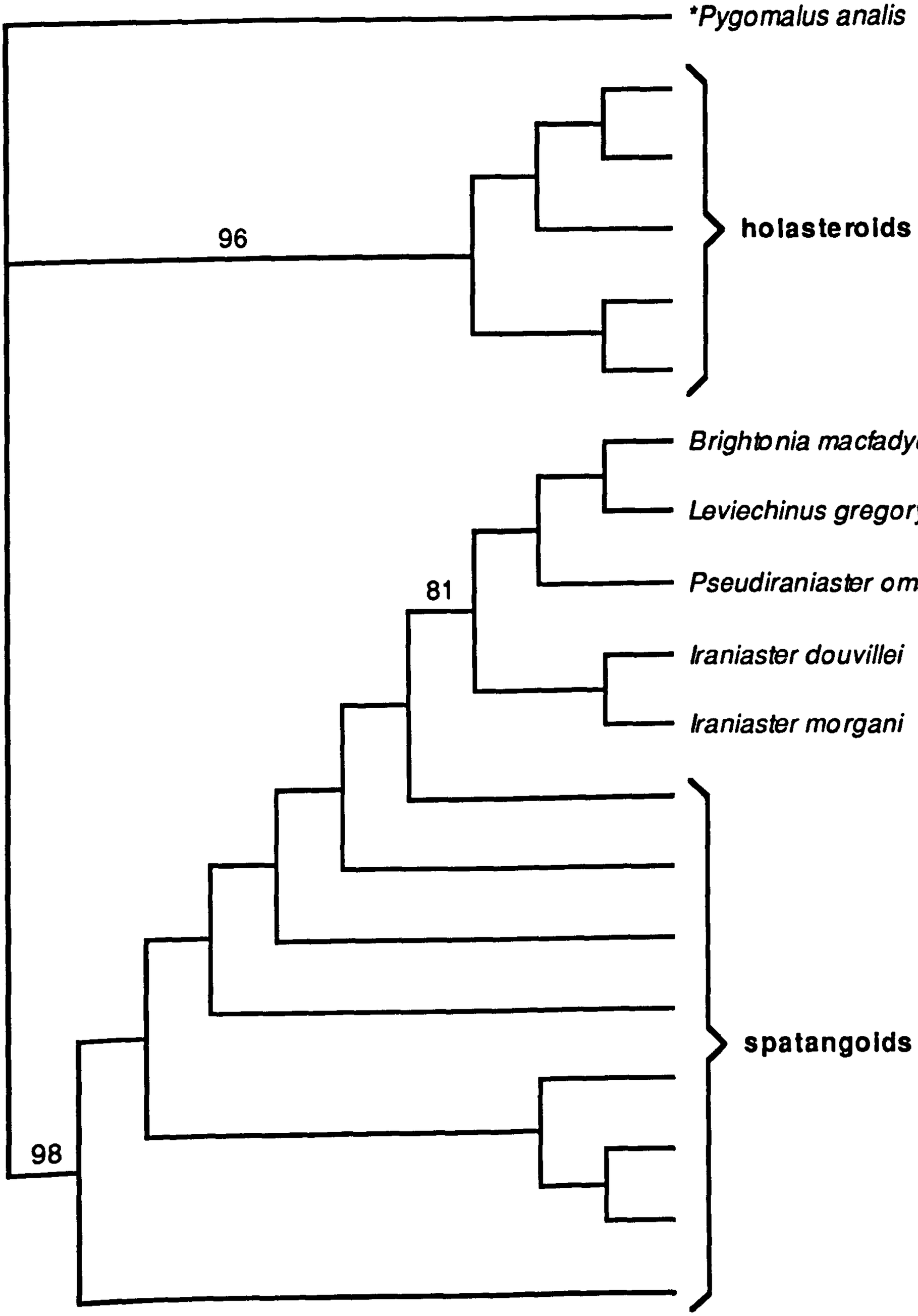
Table 4.12. Characters used in the cladistic analysis of somaliasterids with representatives of the holasteroids and spatangoids.

1	Number of gonopores: 0 = 4; 1 = 3; 2 = 2.
2	Supplementary gonopores in ocular plates: 0 = absent; 1 = present.
3	Apical system: 0 = elongate; 1 = compact.
4	Apical system: 0 = posterior genital plates in contact; 1 = madreporite separates posterior genital plates.
5	Apical system: 0 = posterior ocular plates in contact; 1 = madreporite separates posterior ocular plates.
6	Apical system: 0 = posterior ocular plates in contact with posterior genital plates; 1 = posterior ocular plates disjunct from posterior genital plates.
7	Marginal fasciole (above anus): 0 = absent; 1 = present.
8	Peripetalous fasciole (below anus): 0 = absent; 1 = present.
9	Subanal fasciole: 0 = absent; 1 = present.
10	Latero-anal fasciole: 0 = absent; 1= present.
11	Number of interambulacral plates adjoining labrum: 0 = 1; 1 = 2.
12	Labral and sternal plates: 0 = in contact; 1 = disjunct.
13	Angle between line through mouth and anus and suture between first and second post-labral plates: 0 = <40 degrees; 1 = 40-90 degrees.
14	First and second post-labral plates: 0 = not symmetrical; 1 = symmetrical.
15	Second and third post-labral plates: 0 = not symmetrical; 1 = symmetrical.
16	First and second post-labral plates: 0 = not equal sized; 1 = equal sized.
17	Second and third post-labral plates: 0 = not equal sized; 1 = equal sized.
18	Paired ambulacra: 0 = non-petaloid; 1 = distally open sub-petaloid; 2 = distally closed petaloid.
19	Paired ambulacra: 0 = flush; 1 = sunken.
20	Paired ambulacra: 0 = non- or sub-petaloid; 1 = parallel-sided; 2 = bowed.
21	Pore shape in paired ambulacra: 0 = round in both columns; 1 = anterior and posterior columns differentiated.
22	Width of poriferous zone: 0 = non- or sub-petaloid; 1 = narrower; 2 = broader than zone between.
23	Relative length of posterior to anterior petals: 0 = non- or sub-petaloid; 1 = >0.8; 2 = <0.8.

Table 4.13. Character matrix for the five somaliasterid species plus five holasteroids and eight spatangoids. The outgroup *Pygomalus analis* is indicated by an asterisk.

**Pygomalus analis*	0000010000	1000000000	000
Cardiaster granulosus	0000001000	0010001100	110
Echinocorys scutata	0000000000	0010001000	000
Galeaster bertrandi	00000?0010	0?10101000	000
Guettaria rocardi	0100001000	0010101100	110
Labrotaxis faxensis	0000000000	0010011100	110
Brightonia macfadyeni	2010000100	0100010211	221
Iraniaster douvillei	0011000100	0010001211	221
Iraniaster morgani	0011000100	0?10001211	221
Leviechinus gregoryi	2011100100	0100010211	221
Pseudiraniaster omanensis	0011100100	0100010211	221
Coraster vilanovae	0010000100	1001010000	000
Cyclaster vilanovae	1010000110	1001010211	231
Hemiaster prunella	0010000100	1001010211	232
Linthia sudanensis	0011100101	1001010212	221
Mauritanaster gentili	0011100100	1001010211	221
Mecaster fourneli	0011000100	1001010212	231
Micraster schroederi	0010000010	1001010211	232
Opissaster elongatus	2011100100	1001010212	232

Figure 4.7. Cladogram for Maastrichtian and Palaeocene species of somaliasterid plus representatives of the Holasteroida and Spatangoida. Bootstrap support percentages based on 1000 replicates are indicated for selected internal branches.


*Pygomalus analis
holasteroids
96
Brightonia macfadyeni
Leviechinus gregoryi
Pseudiraniaster omanensis
81
Iraniaster douvillei
Iraniaster morgani
spatangoids
98

CHAPTER 5

ATELOSTOMATE EXTINCTION AT THE CRETACEOUS-TERTIARY BOUNDARY

Estimates of extinction intensity vary widely among previous studies of echinoids at the Cretaceous-Tertiary boundary, from the low local extinction rates recognized within the Danish sections (Asgaard 1979; Gravesen 1979) to the high levels calculated from global compilations (e.g. Roman 1984; see Chapter 2). Previous authors agree, however, that holasteroids suffered more substantial losses than spatangoids at the end of the Cretaceous.

Atelostomate extinction in the Maastrichtian and Danian.

The global generic-level extinction of atelostomate echinoids at the end of the Cretaceous, calculated from the raw unstandardized data, is 65% (28 out of 43 genera). This value is similar to other estimates calculated from compendia of occurrences (63% for bivalves (Raup & Jablonksi 1993); 70% for echinoids (Roman 1984)). However, taxonomic revision substantially reduces the size of the atelostomate dataset through synonymization. Even taking into account recent taxonomic revisions of this group (e.g. Kier 1972, 1984), 28% of generic names were found to be superfluous, whilst 52% of species names were removed. The effect of this standardization on estimates of extinction rate is outlined below.

The range charts for Maastrichtian and Palaeocene species of atelostomate echinoid given in Chapter 3 illustrate that of the 92 species present in the upper Maastrichtian, only 27 survive into the Tertiary. This equates to a species extinction level of 71 per cent. The dependence of individual species on the continuity of particular facies types coupled with facies changes at the end of the Cretaceous (see Chapter 1) account for the large size of this extinction estimate. These difficulties may be minimised by looking instead at generic extinction rates.

Figures 5.1, 5.2 and 5.3 show the holasteroid and spatangoid generic level

phylogenies computed in Chapter 4 plotted against stratigraphy. From these figures it is possible to determine which clades survived the end-Cretaceous event and which became extinct.

Of the 40 genera of atelostomate echinoid present during the Maastrichtian, only 14 (9 holasteroids and 5 spatangoids) have no post-Cretaceous representatives. This corresponds to a world-wide generic extinction level for atelostomate echinoids of 35 per cent over this time period. If the two genera known only from lower Maastrichtian strata are excluded (*Offaster* and *Hagenowia*), the extinction level is reduced to 32 per cent. These figures are comparable to the global generic extinction rate of 33-37 per cent estimated by Jeffery & Smith (in press) for all echinoids at the Cretaceous-Tertiary boundary, but are rather lower than previous estimates of 70 per cent (Roman 1984) and 57 per cent (McKinney 1995) calculated from global compilations of taxonomic occurrences. The data also show that a further bout of extinction occurred at the end of the Danian (Early Palaeocene). Of the 32 atelostomate clades present in Danian strata, nine (28 per cent) fail to survive into the Thanetian (Late Palaeocene). The magnitude of this second pulse of extinction illustrates why the debate on whether to place the Mesozoic-Caenozoic boundary at the beginning or end of the Danian, based on macrofossil stratigraphy, raged for 150 years. The recognition of a major microfaunal turnover at the end of the Maastrichtian influenced the decision to make the Maastrichtian the final stage of the Cretaceous.

Figure 5.1. Stratigraphic distribution of Maastrichtian and Palaeocene holasteroid genera (thick lines) and inferred phylogenetic tree (thin lines) based on the cladogram presented in Chapter 4. Thin dashed lines indicate presence of sister taxon in stage above or below. Thick dashed lines represent stratigraphic uncertainty, where taxon cannot be asigned to substage. See Figure 3.2 for explanation of symbols.

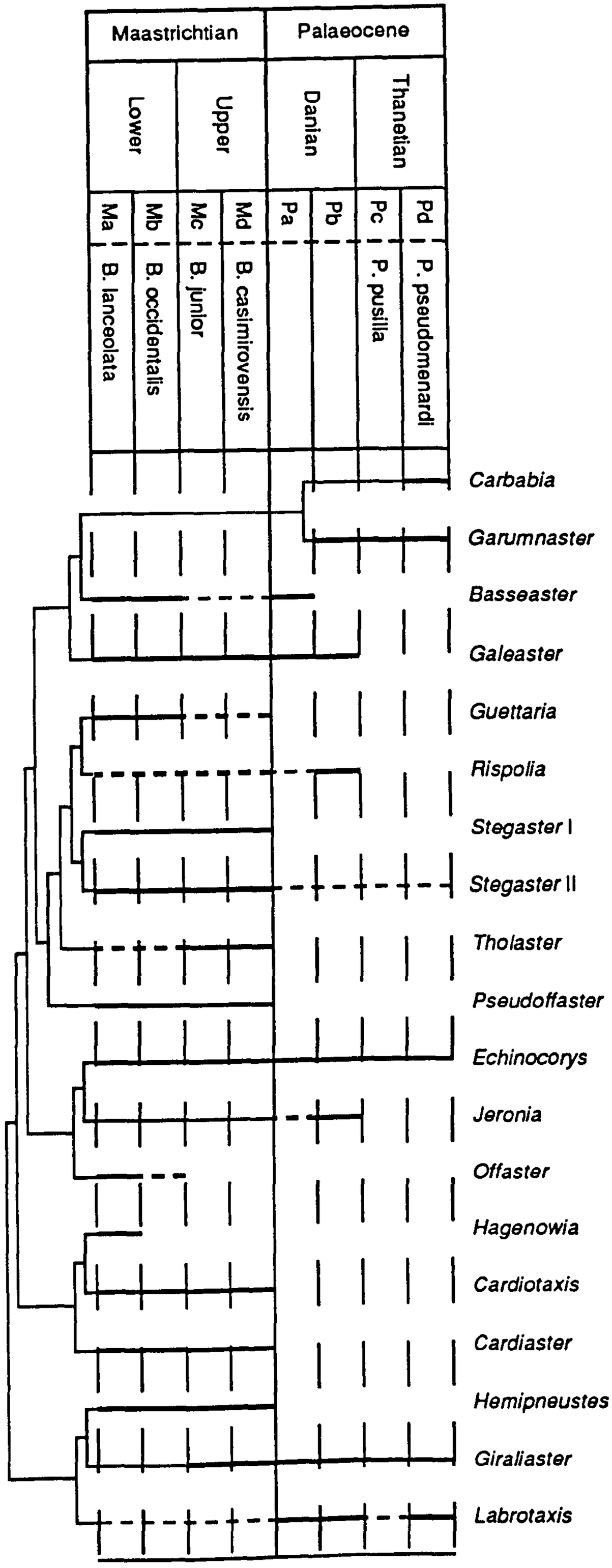

Maastrichtian
Palaeocene
Upper
Lower
Danian
Thanetian
Md
Mc
Mb
Ma
Pb
Pa
Pc
Pd
B. casimirovensis
B. junior
B. occidentalis
B. lanceolata
P. pusilla
P. pseudomenardi
Carbabia
Garumnaster
Basseaster
Galeaster
Guettaria
Rispolia
Stegaster I
Stegaster II
Tholaster
Pseudoffaster
Echinocorys
Jeronia
Offaster
Hagenowia
Cardiotaxis
Cardiaster
Hemipneustes
Giraliaster
Labrotaxis

Figure 5.2. Stratigraphic distribution of Maastrichtian and Palaeocene genera of the Micrasterina (thick lines) and inferred phylogenetic tree (thin lines) based on the cladogram presented in Chapter 4. Thin dashed lines indicate presence of sister taxon in stage above or below. Thick dashed lines represent stratigraphic uncertainty, where taxon cannot be assigned to substage. See Figure 3.2 for explanation of symbols.

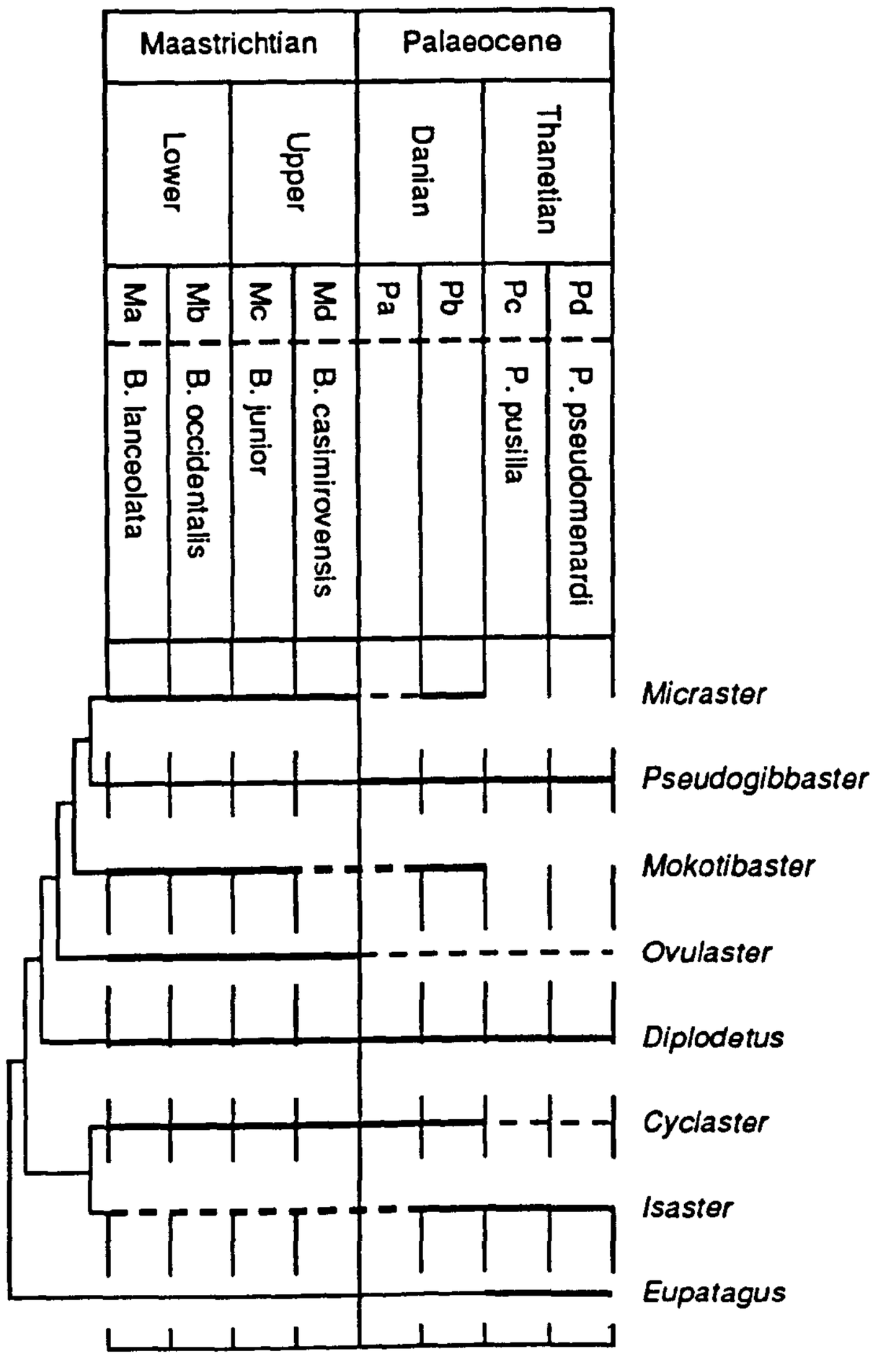
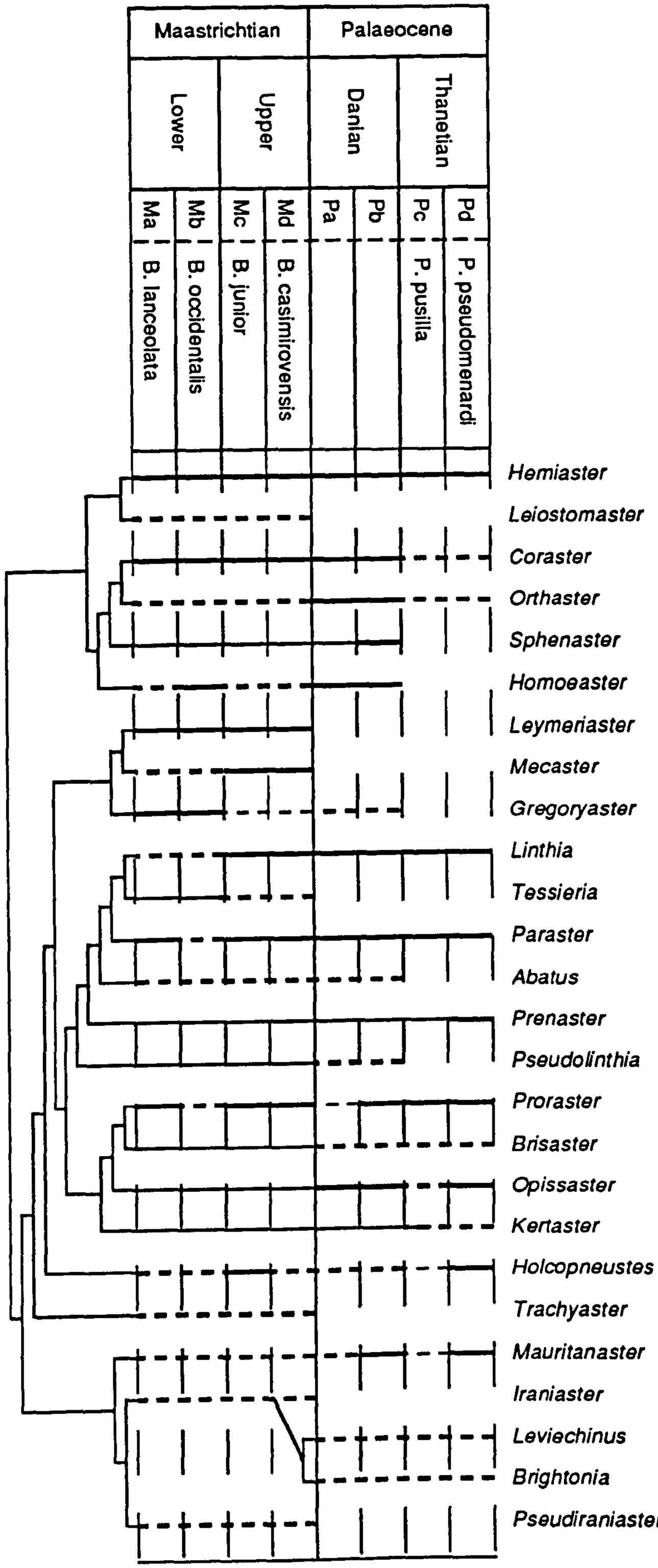

Maastrichtian
Palaeocene
Lower
Upper
Danian
Thanetian
Ma
Mb
Mc
Md
Pa
Pb
Pc
Pd
B. lanceolata
B. occidentalis
B. junior
B. casimirovensis
P. pusilla
P. pseudomenardi
Micraster
Pseudogibbaster
Mokotibaster
Ovulaster
Diplodetus
Cyclaster
Isaster
Eupatagus

Figure 5.3. Stratigraphic distribution of Maastrichtian and Palaeocene genera of the Hemiasterina (thick lines) and inferred phylogenetic tree (thin lines) based on the cladogram presented in Chapter 4. Thin dashed lines indicate presence of sister taxon in stage above or below. Thick dashed lines represent stratigraphic uncertainty, where taxon cannot be assigned to substage. See Figure 3.2 for explanation of symbols.


Maastrichtian
Palaeocene
Lower
Upper
Danian
Thanetian
Ma
Mb
Mc
Md
Pa
Pb
Pc
Pd
B. lanceolata
B. occidentalis
B. junior
B. casimirovensis
P. pusilla
P. pseudomenardi
Hemiaster
Leiostomaster
Coraster
Orthaster
Sphenaster
Homoeaster
Leymeriaster
Mecaster
Gregoryaster
Linthia
Tessieria
Paraster
Abatus
Prenaster
Pseudolinthia
Proraster
Brisaster
Opissaster
Kertaster
Holcopneustes
Trachyaster
Mauritanaster
Iraniaster
Leviechinus
Brightonia
Pseudiraniaster

Atelostomate extinction and taxonomy.

Despite being lower than previously published extinction estimates, it still appears that a sizable proportion of atelostomate echinoids became extinct at the end of the Cretaceous. Could this be an artefact of taxonomic practise, with clades including fewest Maastrichtian species being most prone to extinction? Figure 5.4 shows survivorship plotted against the number of Maastrichtian species in each clade. All clades containing three or more species were grouped in one category to reduce the number of cells with expected values of less than five. Figure 5.4a shows the **number** of clades surviving whilst Figure 5.4b shows the **proportion** of clades surviving. These figures indicate that the extinction rate is roughly constant for all taxa, monospecific to speciose, and thus that survival at the end of the Cretaceous was independent of species diversity within each clade. This result is supported by a chi-squared (X^2) test which indicates that extinction is not significantly correlated with the number of Maastrichtian species included in a clade (Table 5.1) and corroborates previous work on molluscan extinctions at the K-T boundary (Jablonski 1986a, 1989, 1995; McClure & Bohonak 1995). In addition, since a completely random pattern of extinction would lead to higher extinction rates within the least specious clades, this result demonstrates that survival at the K-T was non-random.

Table 5.1. Summary statistics of contingency tables testing the independence of extinction with regard to taxonomy.

factor	degrees of freedom	X^2	P
number of species in a genus	2	0.89	0.641
higher taxonomic placement	1	5.293	0.021

If extinction at the end of the Cretaceous was selective rather than random, what are the common factors that link the survivors? Possible correlates fall into two main categories (Table 5.2) which will be explored in Chapters 6 and 7.

Table 5.2. Possible correlates to atelostomate echinoid survivorship at the end of the Cretaceous.

geographic & environmental	biological
geographic range	life position in sediment
absolute geographic distribution	larval strategy
water depth	feeding strategy
sedimentary environment	

Atelostomate extinction and higher taxonomy.

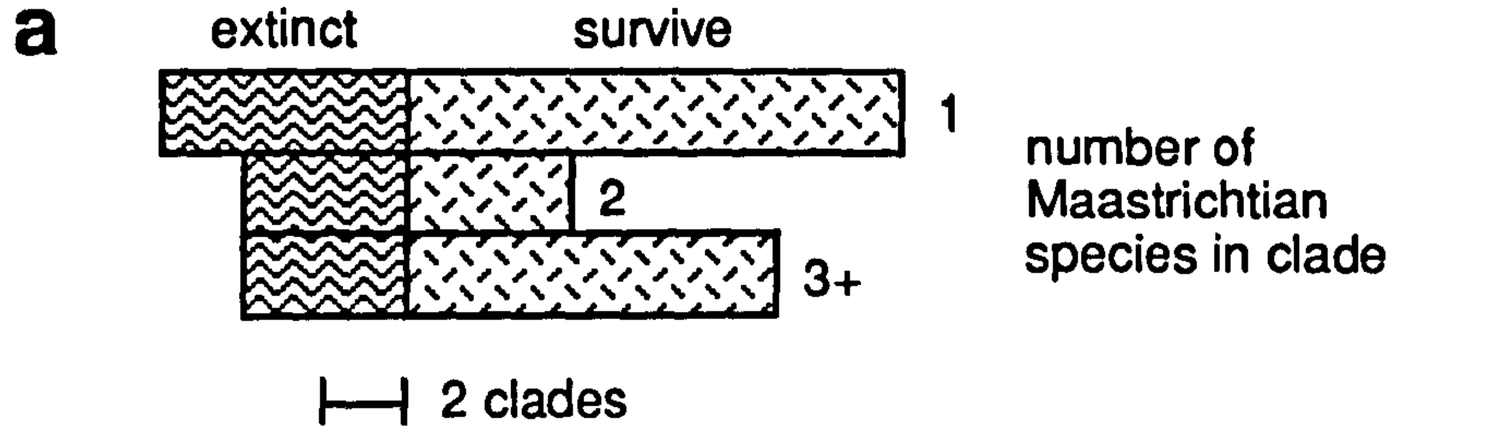
Before exploring the biological, geographical and environmental factors that may have had a bearing on survivorship at the end of the Cretaceous, the effect of taxonomic hierarchy on the K-T extinctions should be investigated.

Of the 16 holasteroid genera present during the Maastrichtian, only seven survive into the Palaeocene. This corresponds to an extinction rate of 56 per cent. In contrast, 19 of the 24 Maastrichtian spatangoid clades are also present in Palaeocene strata, representing an extinction rate of just 21 per cent. These differential extinction levels are shown diagrammatically in Figure 5.5. A X^2-test for independence suggests that extinction is significantly correlated with higher taxonomic grouping (Table 5.1).

Although the contrast between holasteroid and spatangoid extinction levels has been noted by previous authors, it is still a surprising result which has not been adequately explained. Holasteroids and spatangoids are sister taxa with a broadly similar appearance and life-style. Because of their phylogenetic relationship and the fact that they suffered such different fates at the K-T boundary, holasteroids and spatangoids offer a means of testing hypotheses about end-Cretaceous scenarios.

The differential extinction levels have been attributed to the better adaptation of spatangoids for infaunal living (Roman 1984). Certainly, the disparate fates of the holasteroids and spatangoids are linked to the biological differences between these groups and an explanation for the more severe holasteroid losses will be sought in Chapter 7.

Figure 5.4. Atelostomate survivorship plotted against number of species in each clade. a, histogram showing number of clades surviving; b, proportion of clades surviving.


a
extinct
survive
1
2
3+
number of
Maastrichtian
species in clade
2 clades

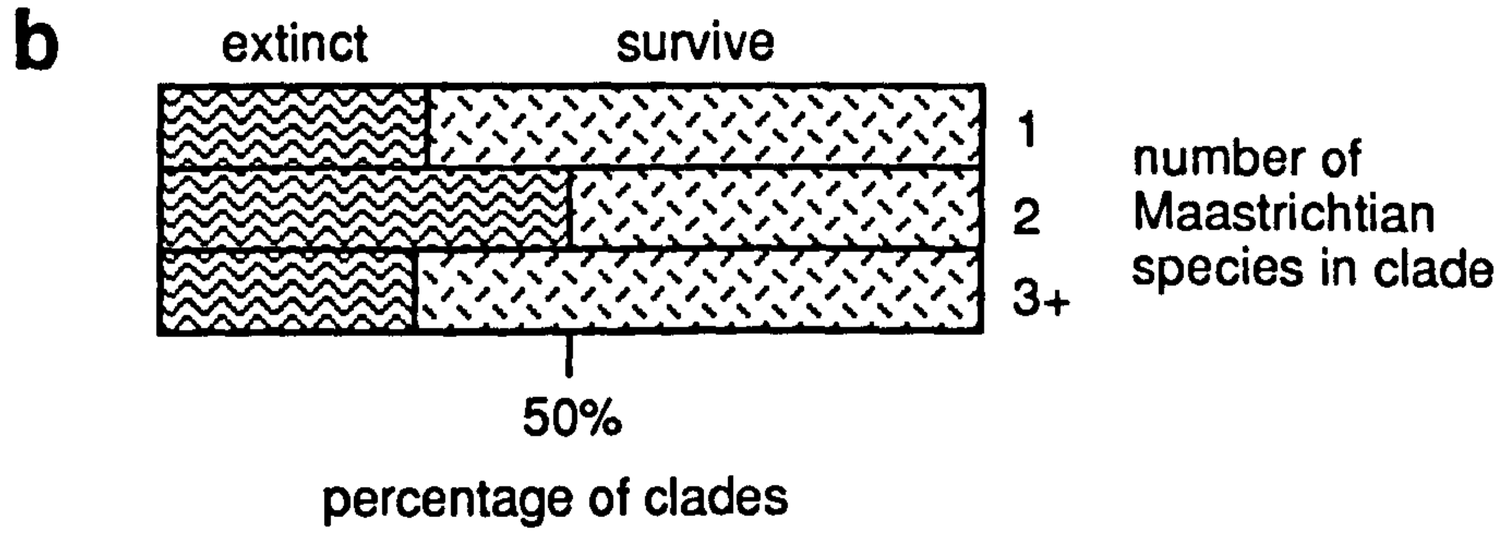
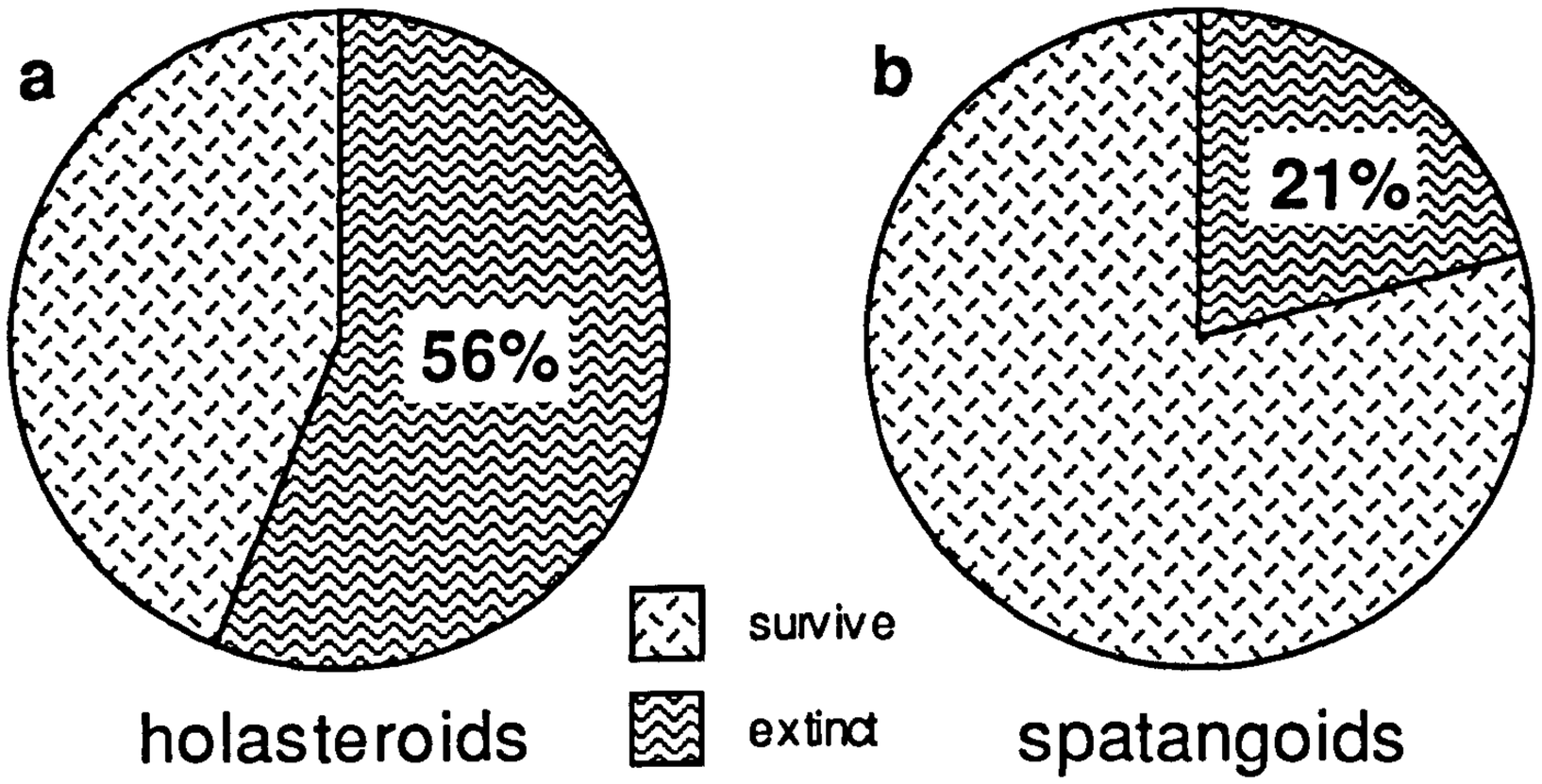

b
extinct
survive
1
2
3+
number of
Maastrichtian
species in clade
50%
percentage of clades

Figure 5.5. Generic extinction levels at the end of the Cretaceous in a, holasteroids and b, spatangoids.


a
56%
b
21%
survive
extinct
holasteroids
spatangoids

CHAPTER 6

ATELOSTOMATE EXTINCTION AND GEOGRAPHICAL AND ENVIRONMENTAL CORRELATES

In Chapter 5, I demonstrated that atelostomate clades containing small numbers of species are no more prone to extinction at the end of the Cretaceous than species rich lineages. Similar patterns have been recorded for bivalves at the end of the Cretaceous (Jablonski 1989, 1991, 1995, 1996; McClure & Bohonak 1995), corals (Sorauf & Pedder 1986) and ammonoids (House 1985) in the Late Devonian and end-Cambrian trilobites (Westrop 1989). Erwin (1989b, 1990) documents the only exception to this general trend. The observation that species richness had no effect on survivorship implies that species extinctions were not entirely random but that these species had something in common that made them all more susceptible to the environmental stresses operating in the terminal Cretaceous (Raup 1995). So what are the common biologic, ecologic or geographic characteristics that enhance the chance of survival?

Methods.

Many patterns of survivorship selectivity have been proposed in the vast mass extinction literature but few have been tested empirically. Notable exceptions include work on K-T bivalve faunas (Raup & Jablonski 1993; Jablonski & Raup 1995; McClure & Bohonak 1995). In this and the following chapter, I shall explore patterns of survivorship selectivity in end-Cretaceous atelostomate echinoids using chi-squared tests of contingency tables, an approach that has already proved its worth in other studies of extinction selectivity (McKinney 1985; McClure & Bohonak 1995; Lessa & Fariña 1996). Two sets of analyses were carried out. The first cross-classifying each of the possible correlates with the extinct-survive status of the genera, and the second testing for association between possible correlative factors and whether the taxa are holasteroids or spatangoids. Sample sizes for

these tests ranged from 39 to 90 and, where appropriate, categories were chosen to minimize the number of cells with expected values of less than five. Exact *p*-values for all statistics were found using Microsoft EXCEL.

Geographic range.

Widespread taxa are commonly believed to be more resistant to extinction than those with narrow geographic ranges during periods of background and mass extinction. This pattern has been documented for Cambrian trilobites (Westrop 1989, 1991), Late Ordovician taxa (Sheehan *et al.* 1996), end-Permian gastropods (Erwin 1989a, b, 1990), end-Cretaceous bivalves and gastropods (Jablonski 1986a, 1989, 1991, 1995; Jablonski & Raup 1995), foraminifera (Keller 1996) and other taxa at the K-T boundary (Sheehan *et al.* 1996). In marked contrast, a widespread geographic distribution does not appear to have acted as a buffer to extinction during the Late Devonian mass extinction (McGhee 1996). Presence in a large number of provinces is also an indicator of abundance and it has been suggested that the most common taxa were also the most resilient (Keller 1996). However, this is not supported by analysis of bivalves at the end-Cretaceous mass extinction (McClure & Bohonak 1995).

Determining palaeogeographic ranges.

A number of different methods of estimating geographic range exist (see Emlet 1995). For this study geographic range was determined as (i) the number of degrees of palaeolongitude between a clade's two most distant occurrences plotted onto a palaeogeographic reconstruction (see Appendix 1); (ii) the number of degrees palaeolatitude between a clade's most northerly and southerly occurrences; (iii) the number of regions and (iv) the number of localities in which a taxon occurs. Details of total palaeogeographic range for all Maastrichtian clades using each of these approaches are given in Appendix 4. Range size was split into categories, chosen to minimize the number of cells in the contingency tables with expected values of less than five. Regions were chosen to be of approximately

equal size.

Atelostomate survivorship and geographic range.

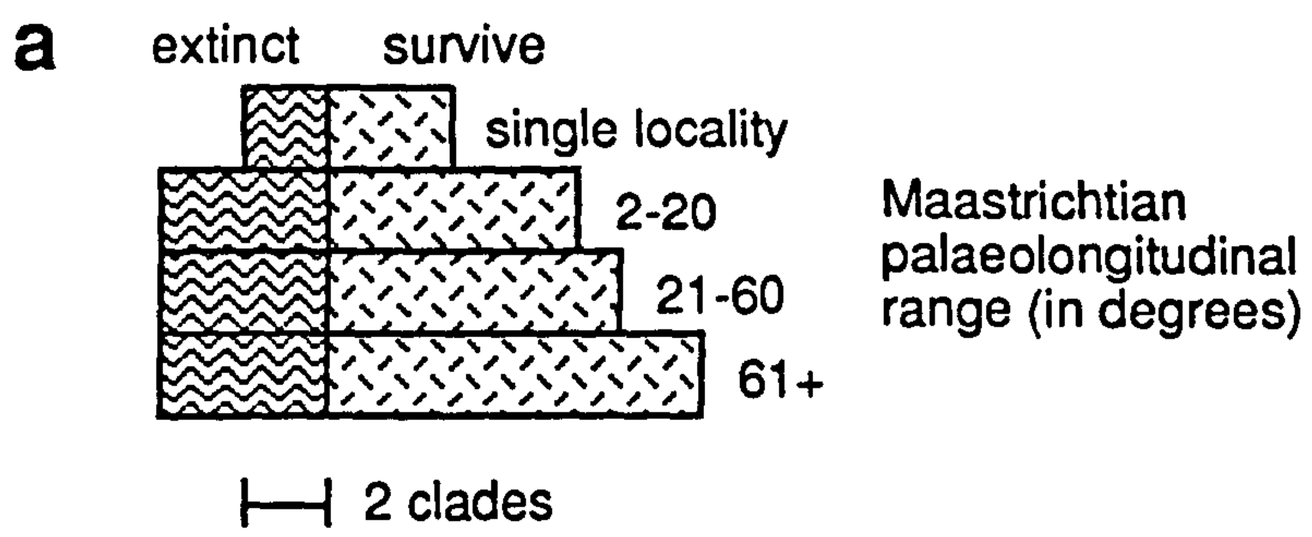
The numbers and proportions of taxa surviving or going extinct in each category for total longitudinal and latitudinal ranges are shown in Figures 6.1 and 6.2 respectively. Survivorship is plotted against number of regions and number of localities in Figures 6.3 and 6.4. Chi-squared tests indicate that survival into the Tertiary is independent of the size of geographic range (however measured) (Table 6.1), with narrowly and widely distributed taxa experiencing not significantly different levels of extinction. In addition, there is no correlation between size of geographic range and atelostomate higher taxonomy (Table 6.2).

This result contradicts earlier studies of preferential survivorship of widespread taxa at times of mass extinction. However, it can be explained in terms of the data used for analysis. In contrast to all previous work, this study uses a phylogenetic framework, identifying lineage rather than taxonomic continuity. All synoptic compilations contain a proportion of superfluous names of taxa often known only from a single locality or stratigraphic horizon. The exclusion of these taxa through taxonomic standardization combined with the construction of a phylogenetically based dataset reduces the number of endemic pseudoextinctions. In addition the pattern of selectivity could be an artefact since widespread taxa are likely to be more common and thus better sampled.

Table 6.1. Summary statistics of contingency tables testing the independence of extinction with regard to possible geographical correlates.

factor	degrees of freedom	X^2	p
total longitudinal range	3	0.259	0.967
total latitudinal range	3	3.443	0.328
number of regions	2	2.145	0.342
number of localities	3	0.178	0.981
absolute longitude	3	1.146	0.766
absolute latitude	2	0.148	0.929
latitudinal tolerance	2	3.118	0.210

Figure 6.1. Atelostomate survivorship plotted against total longitudinal range. a, histogram showing number of clades surviving; b, proportion of clades surviving.


a
extinct
survive
single locality
2-20
21-60
61+
Maastrichtian
palaeolongitudinal
range (in degrees)
2 clades

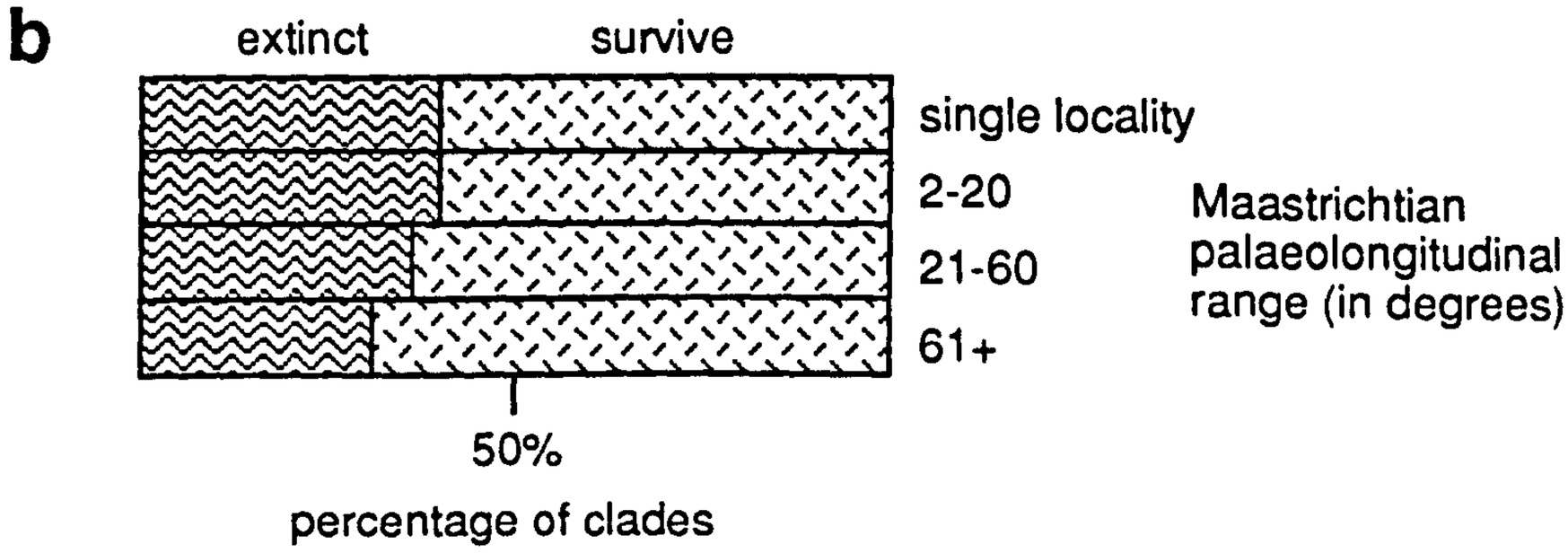
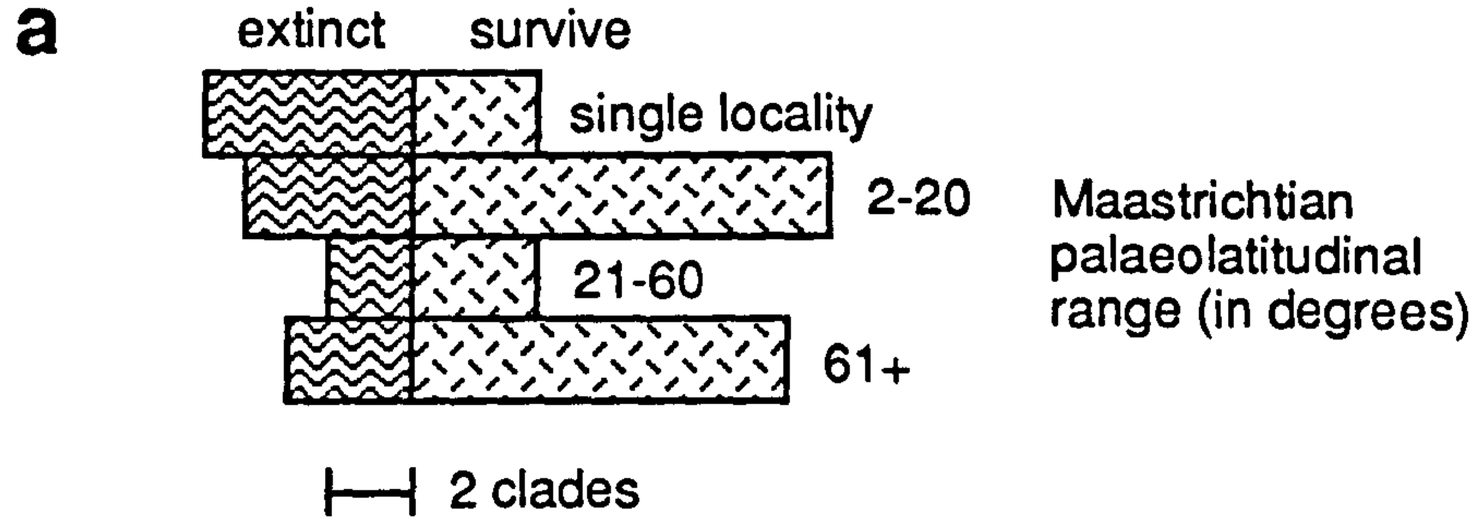

b
extinct
survive
single locality
2-20
21-60
61+
Maastrichtian
palaeolongitudinal
range (in degrees)
50%
percentage of clades

Figure 6.2. Atelostomate survivorship plotted against total latitudinal range. a, histogram showing number of clades surviving; b, proportion of clades surviving.


a
extinct
survive
single locality
2-20
21-60
61+
Maastrichtian
palaeolatitudinal
range (in degrees)
2 clades

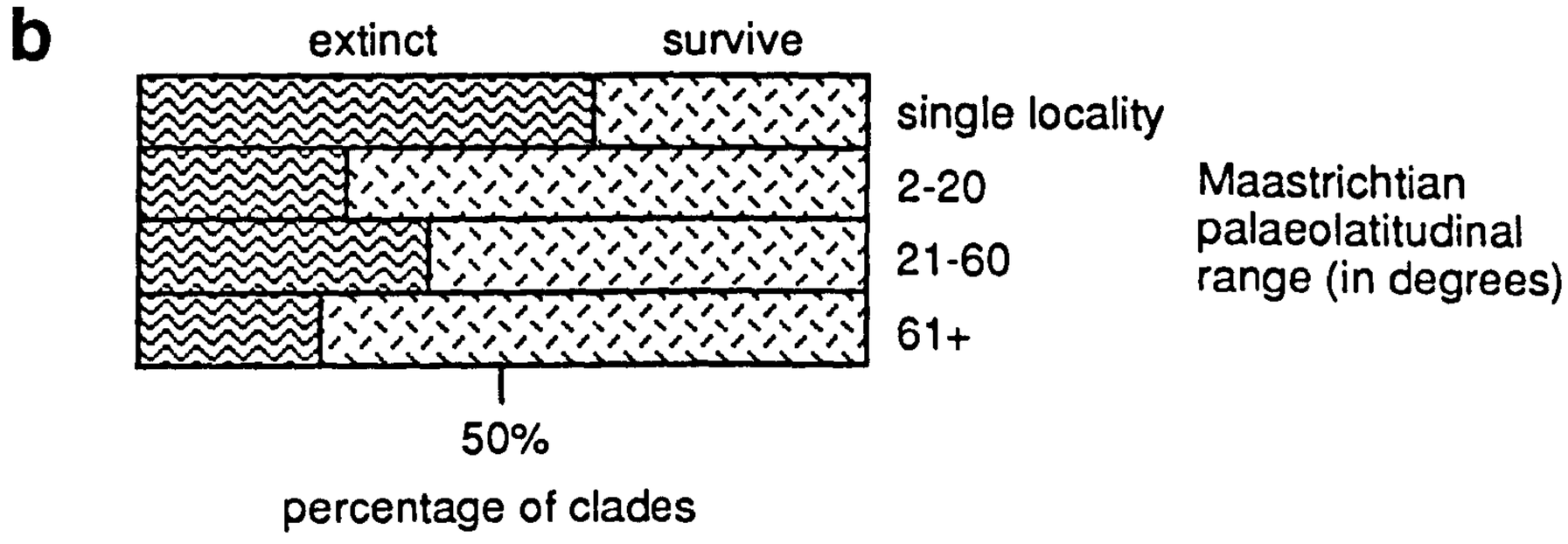
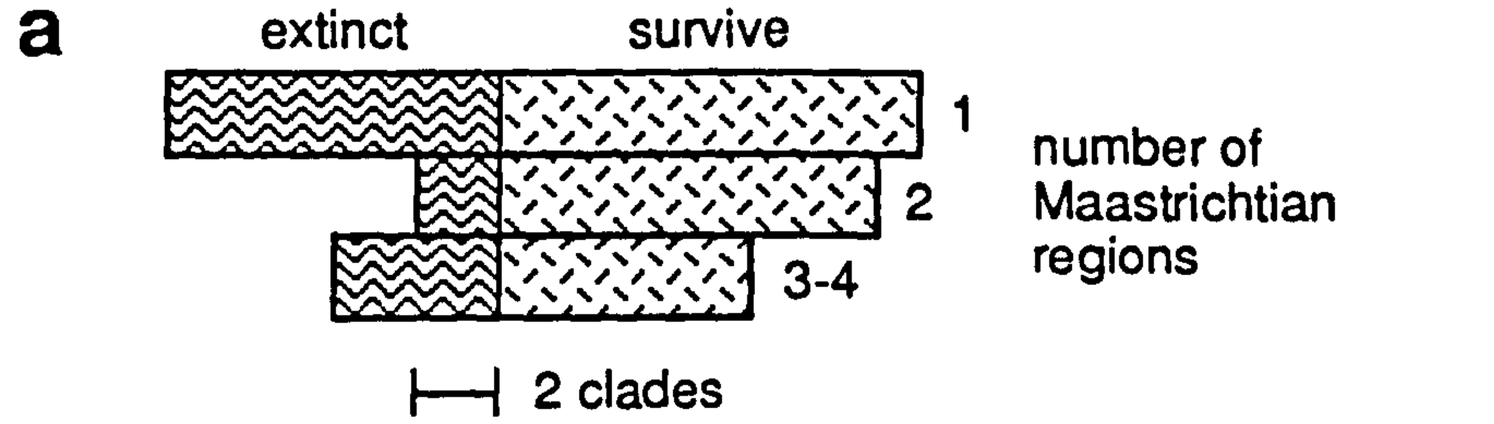

b
extinct
survive
single locality
2-20
21-60
61+
Maastrichtian
palaeolatitudinal
range (in degrees)
50%
percentage of clades

Figure 6.3. Atelostomate survivorship plotted against number of regions. a, histogram showing number of clades surviving; b, proportion of clades surviving.


a
extinct
survive
1
2
3-4
number of
Maastrichtian
regions
2 clades

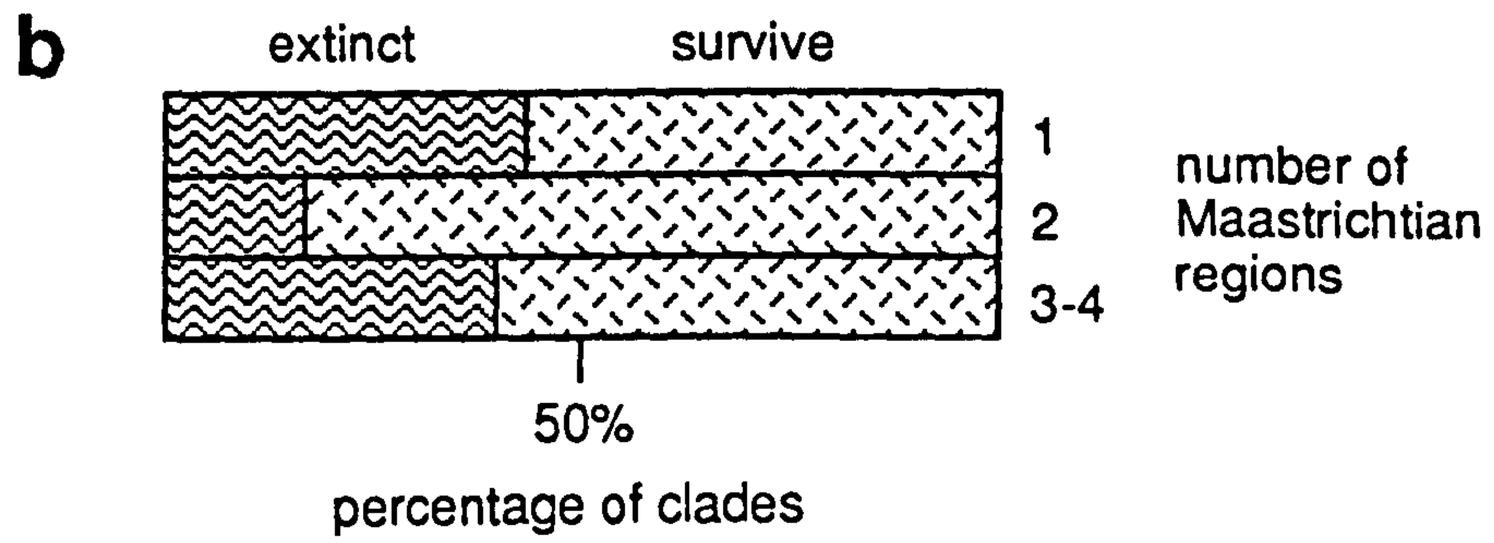
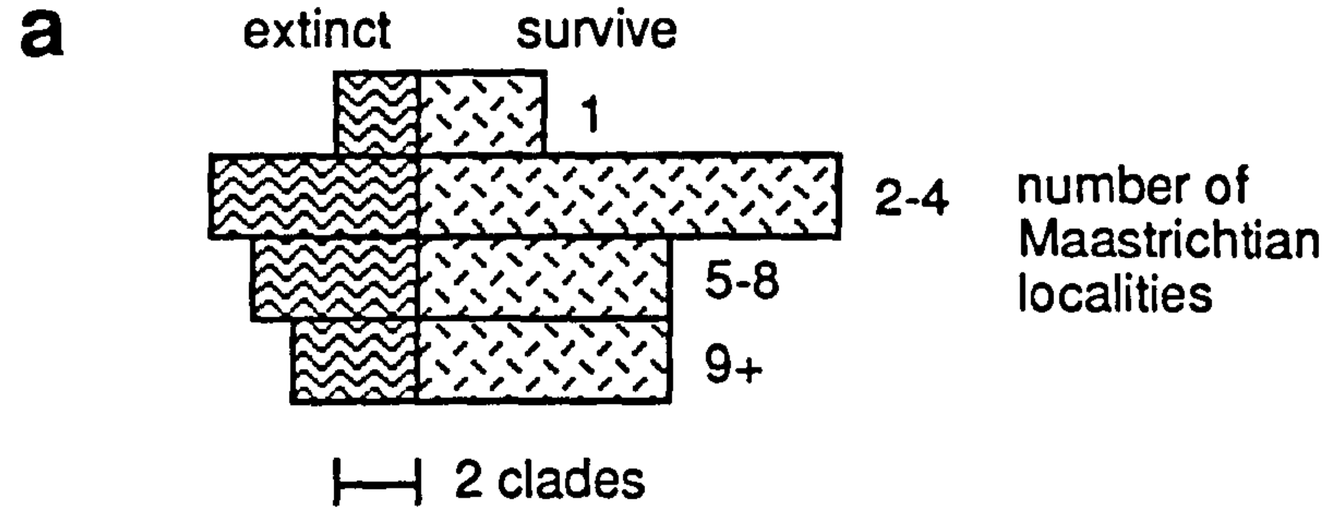

b
extinct
survive
1
2
3-4
number of
Maastrichtian
regions
50%
percentage of clades

Figure 6.4. Atelostomate survivorship plotted against number of localities. a, histogram showing number of clades surviving; b, proportion of clades surviving.


a
extinct
survive
1
2-4
5-8
9+
number of Maastrichtian localities
2 clades

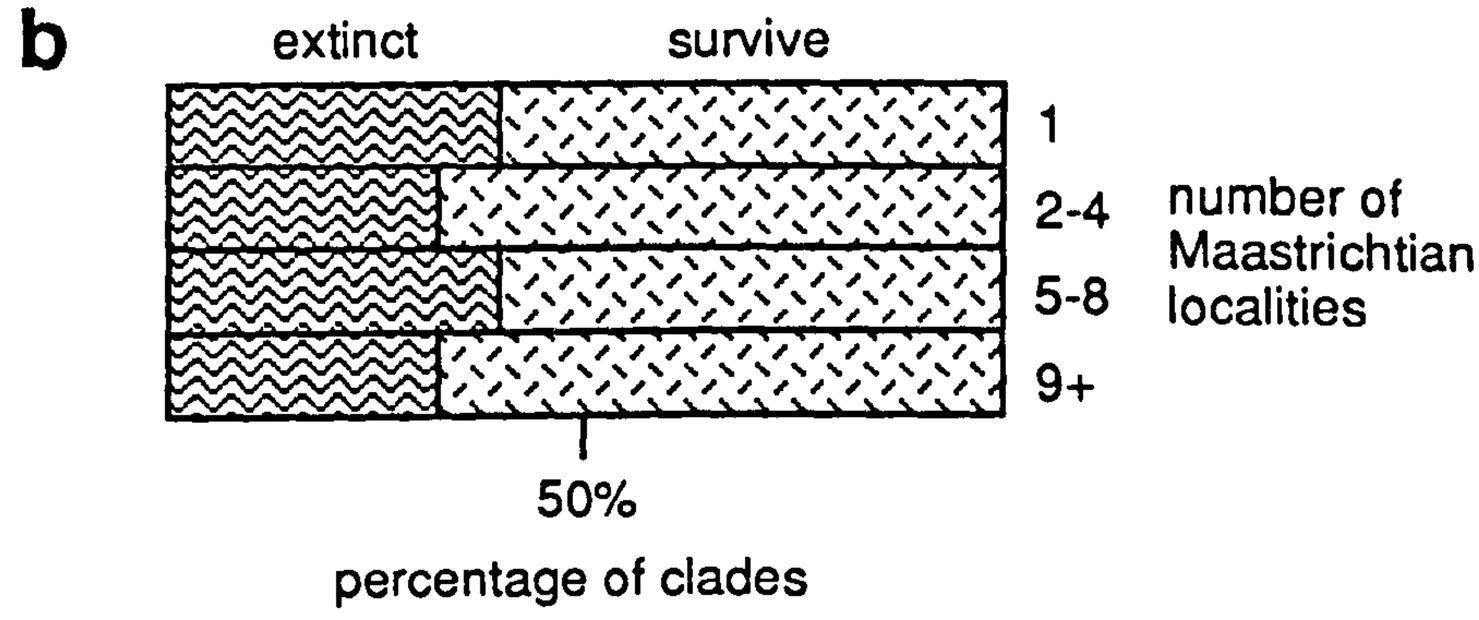

b
extinct
survive
1
2-4
5-8
9+
number of Maastrichtian localities
50%
percentage of clades

Table 6.2. Summary statistics of contingency tables testing the independence of atelostomate higher taxonomy with regard to possible geographical correlates.

factor	degrees of freedom	X^2	p
total longitudinal range	3	2.424	0.489
total latitudinal range	3	2.016	0.569
number of regions	2	0.864	0.649
number of localities	3	0.881	0.830
absolute longitude	3	1.603	0.659
absolute latitude	2	2.277	0.320
latitudinal tolerance	2	0.332	0.847

Absolute geographic distribution.

It has been suggested that taxa show different levels of extinction susceptibility at times of mass extinction depending on their absolute geographic distribution with low latitude faunas generally considered to be the least resilient. This pattern has been demonstrated for foraminifera (Keller *et al.* 1993; Keller 1996; MacLeod & Keller 1994), dinoflagellates (Elliot *et al.* 1994) and corals (Rosen & Turnsek 1989) at the K-T boundary and for taxa during the Late Devonian mass extinction (McGhee 1996). The opposite pattern of high extinction levels in high latitudes is documented for the Late Ordovician extinction which is thought to have been caused by a glaciation event (Sheehan *et al.* 1996). Calcareous nannoplankton extinctions, on the other hand, show no latitudinal bias at the end of the Cretaceous (Pospichal 1996). Bivalves too show fairly uniform extinction intensities at all palaeolatitudes (and palaeolongitudes) if rudists are excluded from the analysis (Raup & Jablonski 1993). Including the rudists, which are restricted to tropical carbonate platform facies, produces a pattern of elevated extinction in low latitudes (and west of 30 degrees west) (Raup & Jablonski 1993) supporting the suggestion that the preponderance of endemic taxa in the tropics could in itself explain the latitudinal patterns (Jablonski 1995).

Determining absolute geographic distribution.

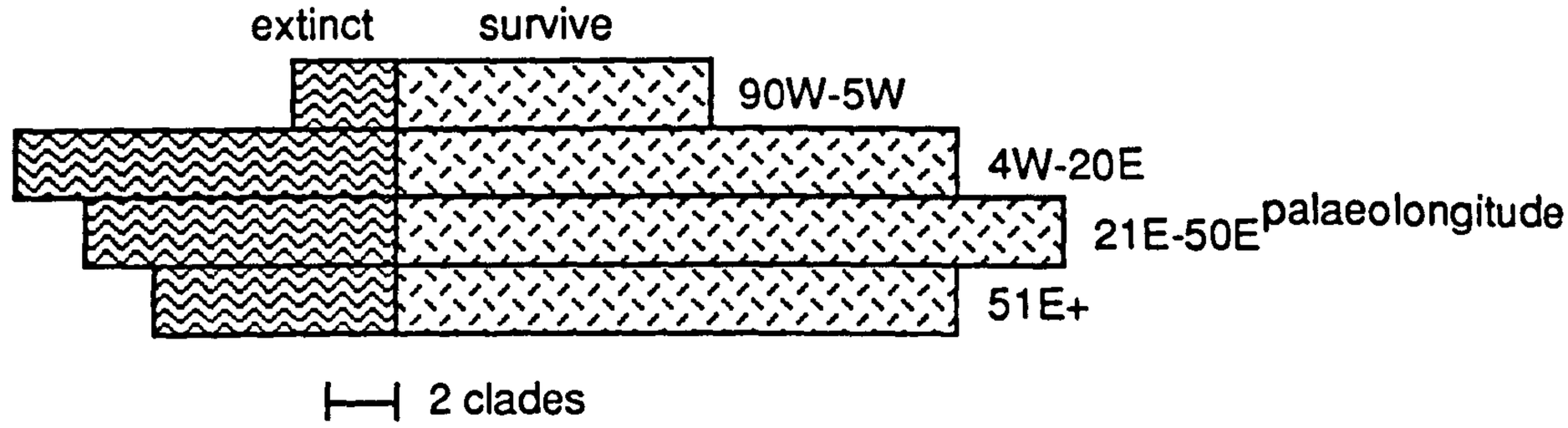
All localities yielding fossil atelostomate echinoids were plotted onto a palaeogeographical reconstruction and from this palaeolatitudes and palaeolongitudes

were calculated (see Appendix 1) for each Maastrichtian clade. Limits of categories for chi-squared tests were chosen using gap analysis. Occurrence in two latitudinal or longitudinal categories was not taken as evidence of occurrence in intermediate categories. In order to investigate the association of latitude and extinction intensity, northern and southern latitudes were combined. In addition, the effect of latitudinal tolerance on extinction was explored. Latitudinal tolerance was defined as the palaeolatitudinal range with northern and southern latitudes combined. Data on the absolute geographical distribution of all Maastrichtian clades of atelostomate is given in Appendix 4.

Atelostomate extinction and absolute geographical distribution.

Atelostomate survivorship is plotted against absolute palaeolongitude in Figure 6.5 and against absolute palaeolatitude in Figure 6.6. Figure 6.7 shows the numbers and proportions of taxa surviving and going extinct partitioned according to latitudinal tolerance. Chi-squared tests indicate that atelostomate survivorship at the end of the Cretaceous is not significantly correlated with any of these factors (Table 6.1) supporting claims that extinction at that time was globally uniform (Raup & Jablonski 1993). In addition, absolute geographic distribution and latitudinal tolerance is not tied to atelostomate higher taxonomy (Table 6.2).

Figure 6.5. Atelostomate survivorship plotted against absolute longitude. a, histogram showing number of clades surviving; b, proportion of clades surviving.


a
extinct
survive
90W-5W
4W-20E
21E-50E
51E+
palaeolongitude
2 clades

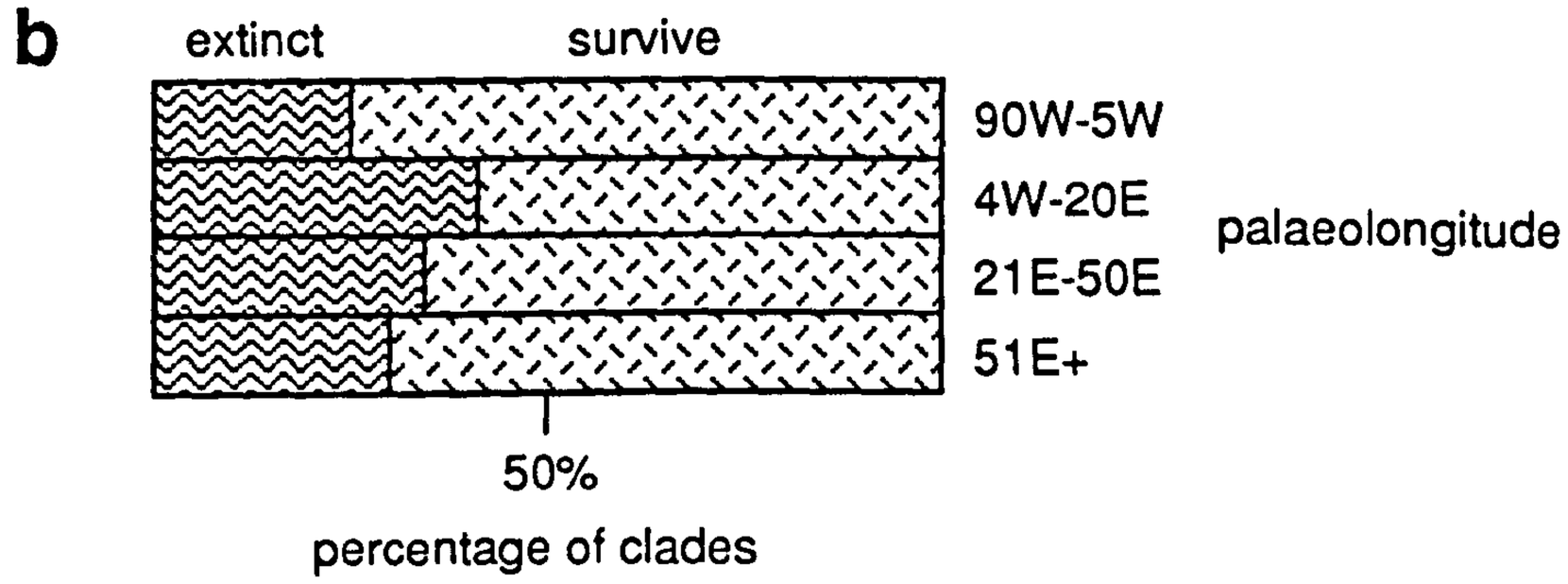
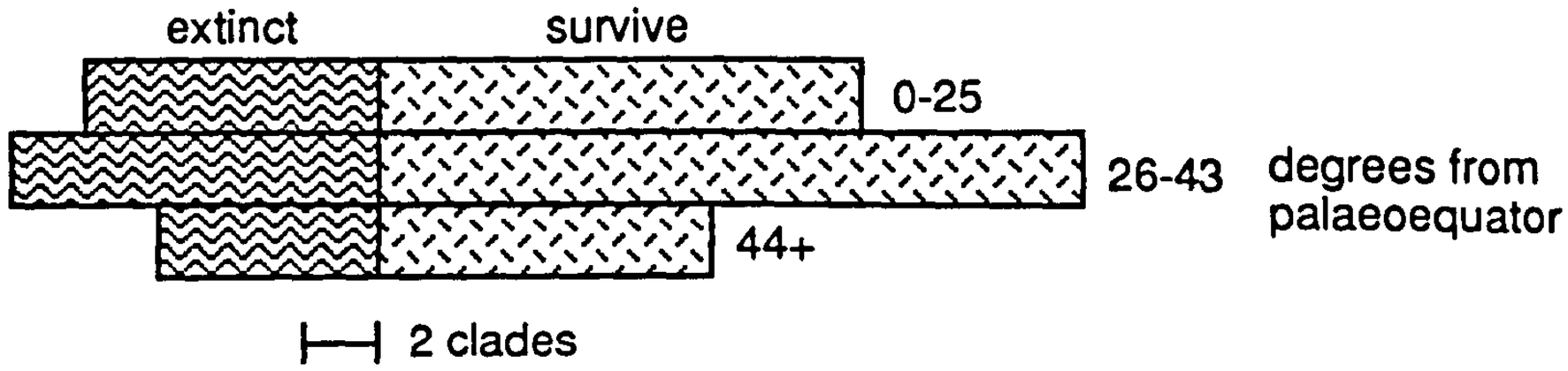

b
extinct
survive
90W-5W
4W-20E
21E-50E
51E+
palaeolongitude
50%
percentage of clades

Figure 6.6. Atelostomate survivorship plotted against absolute latitude (combining northern and southern latitudes). a, histogram showing number of clades surviving; b, proportion of clades surviving.


a
extinct
survive
0-25
26-43
44+
degrees from palaeoequator
2 clades

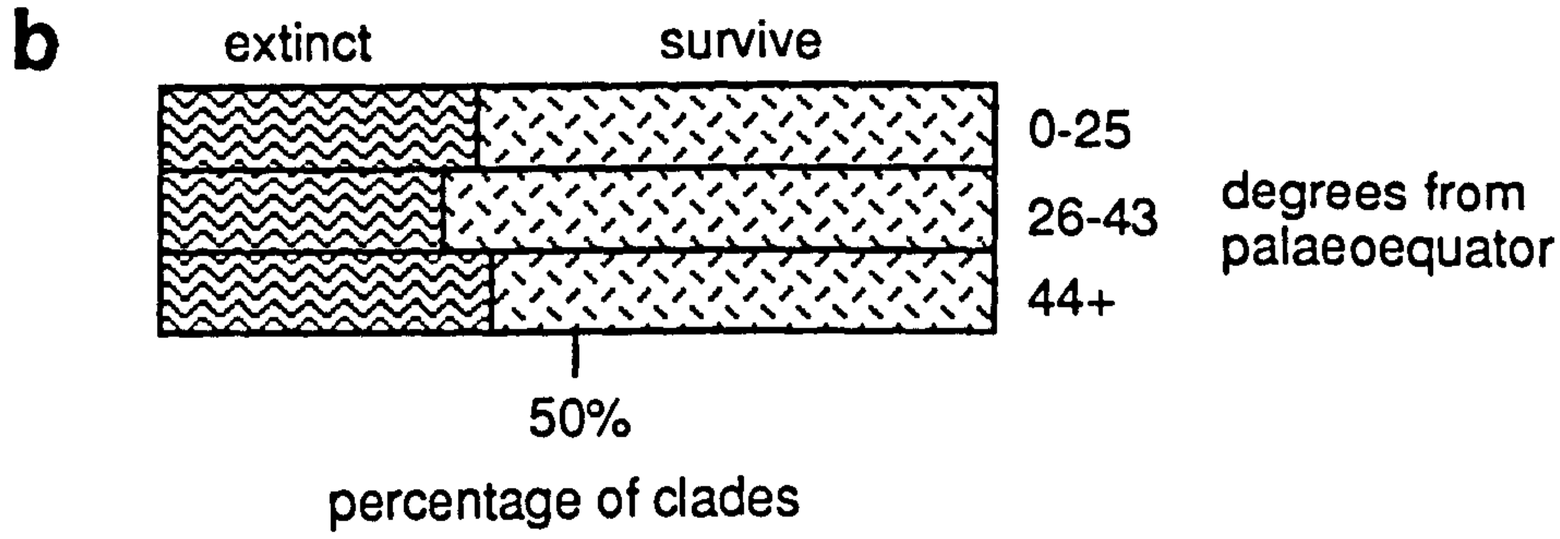
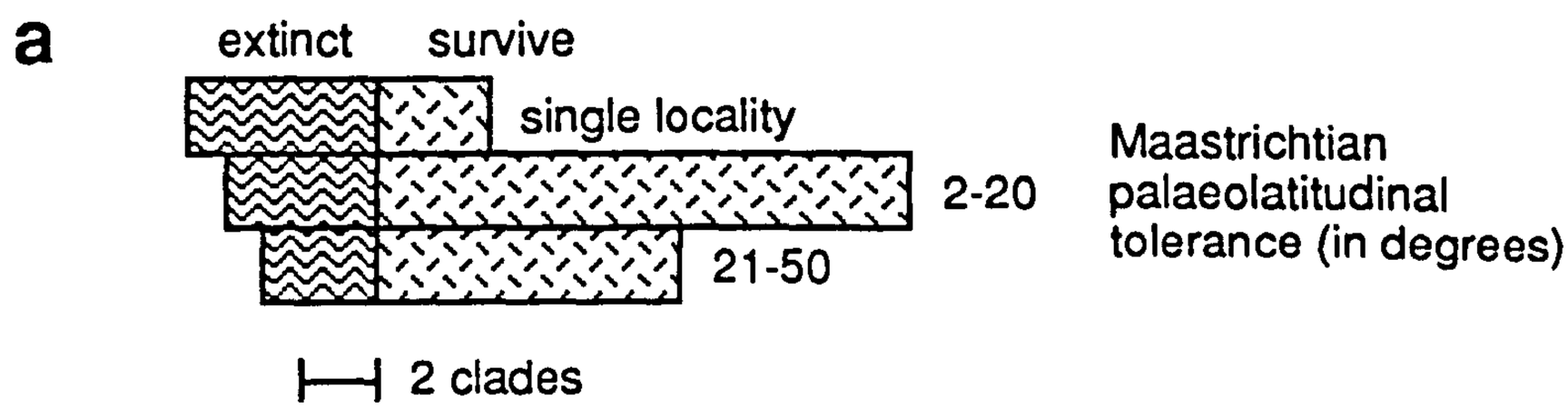

b
extinct
survive
0-25
26-43
44+
degrees from palaeoequator
50%
percentage of clades

Figure 6.7. Atelostomate survivorship plotted against latitudinal tolerance. a, histogram showing number of clades surviving; b, proportion of clades surviving.


a
extinct
survive
single locality
2-20
21-50
Maastrichtian
palaeolatitudinal
tolerance (in degrees)
2 clades
b
extinct
survive
single locality
2-20
21-50
Maastrichtian
palaeolatitudinal
tolerance (in degrees)
50%
percentage of clades

Water depth.

It has been suggested that deep water taxa experienced lower levels of extinction than shallow water taxa (Sorauf & Pedder 1986; McGhee 1996 for the Late Devonian; Erwin 1996 for the Permian-Triassic boundary; Kaiho 1994 for K-T foraminifera) and that genera with broad depth ranges were less severely effected (Westrop 1989 for end-Cambrian trilobites; Erwin 1989a, b, 1990 for end-Permian gastropods) during times of mass extinction. For the Frasnian-Famennian event, the increased levels of extinction in deep water taxa have been ascribed to "a massive disruption of the upper oceanic water habitat" (McGhee 1996, p. 121), perhaps caused by an asteroid impact (Sorauf & Pedder 1986; McGhee 1996) or a rapid decline in ocean temperature (Sorauf & Pedder 1986). At the Permian-Triassic boundary, major sea level fluctuations combined with large-scale vulcanism could have led to the preferential survival of deep sea and depth tolerant taxa (Erwin 1996). In contrast, no correlation between extinction level and bathymetric distribution has been found in bivalves at the Cretaceous-Tertiary boundary (Jablonski & Raup 1995; Jablonski 1996; McClure & Bohonak 1995) or for marine invertebrates during the Palaeozoic mass extinctions (Sepkoski 1987).

Inferring water depth.

Independent data from general sedimentological and faunal studies were used to identify palaeodepth preferences of Maastrichtian and Palaeocene echinoid communities (see Appendix 2). Data on water depth preferences for the taxa included in this analysis are given in Appendix 5.

Atelostomate extinction and water depth.

Figure 6.8 shows the numbers and proportions of taxa surviving and going extinct in each depth category. Figure 6.9 shows the same for depth tolerance (number of depth zones occupied). Chi-squared tests suggest that atelostomate survivorship at the end of the Cretaceous was independent of both palaeodepth inhabited and the breadth of the

bathymetric range (Table 6.3) corroborating the results of previous analyses of the marine invertebrate macrofauna at the K-T boundary. In addition, neither factor is significantly associated with atelostomate higher taxonomy (Table 6.4).

Table 6.3. Summary statistics of contingency tables testing the independence of extinction with regard to possible environmental correlates.

factor	degrees of freedom	X^2	p
sediment type	3	1.706	0.636
number of sediment types	2	0.279	0.870
water depth	2	0.252	0.882
number of depth zones	2	0.301	0.860

Table 6.4. Summary statistics of contingency tables testing the independence of atelostomate higher taxonomy with regard to possible environmental correlates.

factor	degrees of freedom	X^2	p
sediment type	3	2.242	0.524
number of sediment types	2	1.037	0.595
water depth	2	2.038	0.361
number of depth zones	2	2.193	0.334

Figure 6.8. Atelostomate survivorship plotted against water depth. a, histogram showing number of clades surviving; b, proportion of clades surviving.

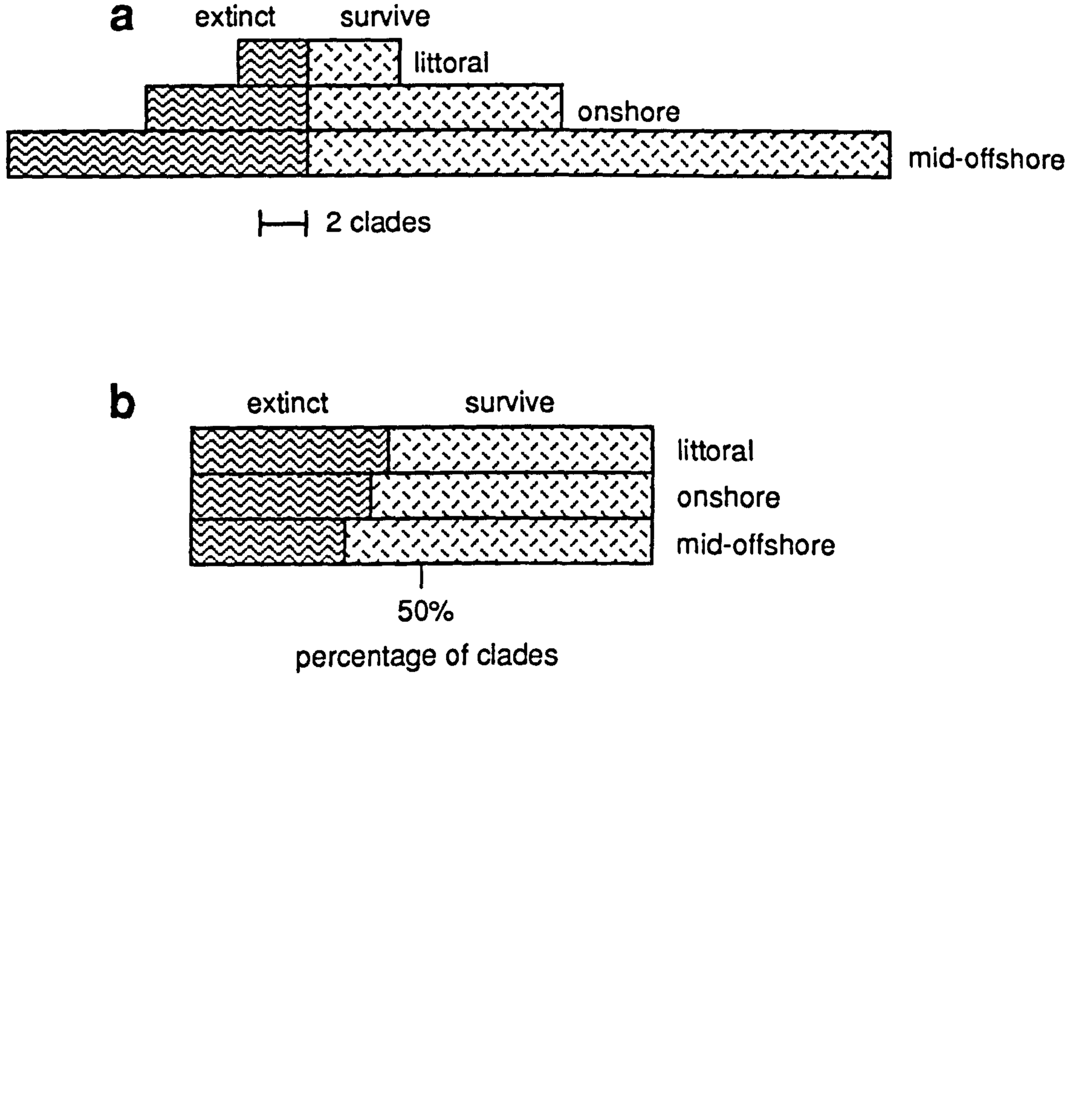
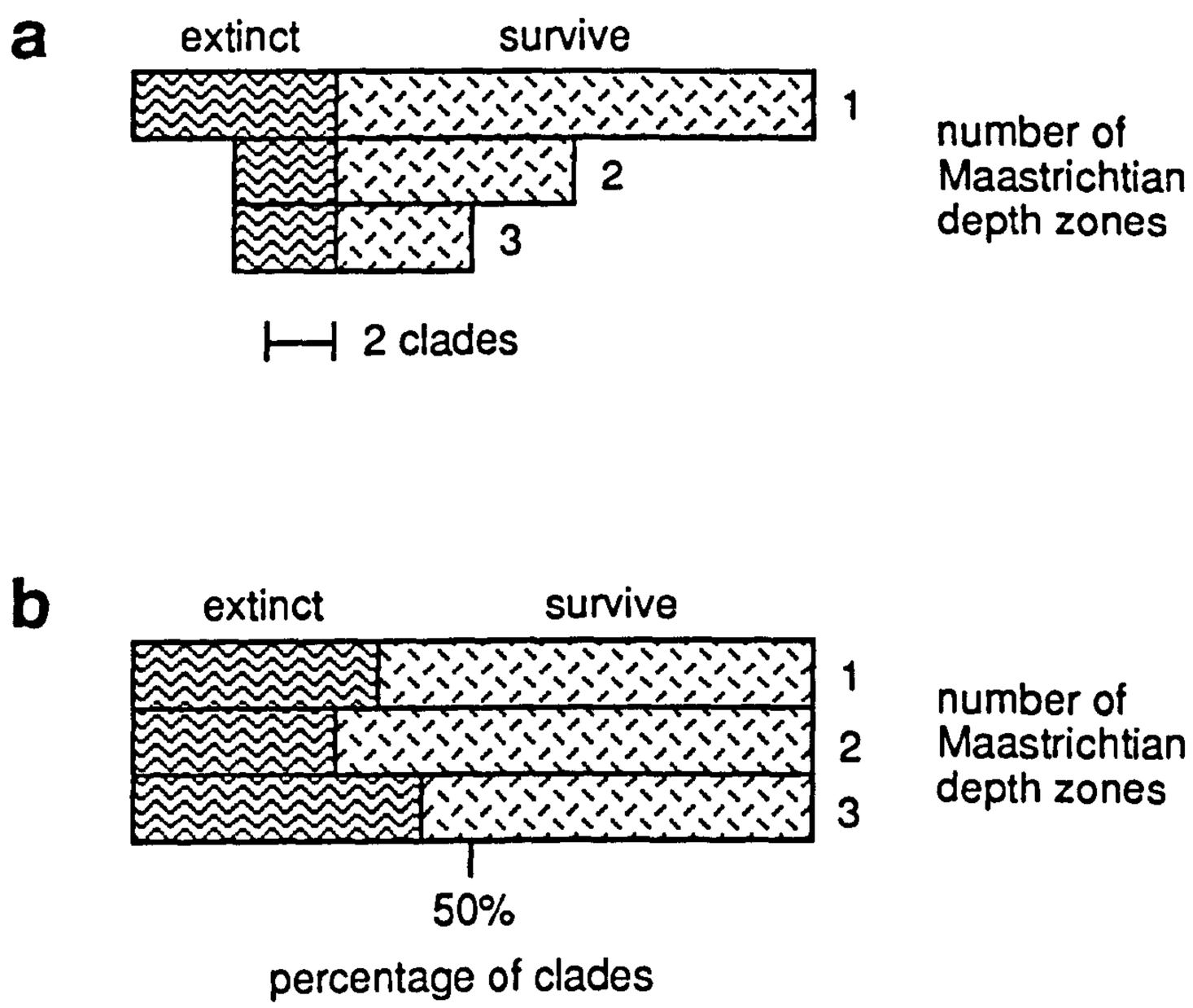

a
extinct
survive
littoral
onshore
mid-offshore
2 clades
b
extinct
survive
littoral
onshore
mid-offshore
50%
percentage of clades

Figure 6.9. Atelostomate survivorship plotted against number of depth zones occupied. a, histogram showing number of clades surviving; b, proportion of clades surviving.


a
extinct
survive
1
2
3
number of
Maastrichtian
depth zones
2 clades
b
extinct
survive
1
2
3
number of
Maastrichtian
depth zones
50%
percentage of clades

Sedimentary environment.

Recent and fossil echinoids are known from a wide range of marine habitats, from shallow coastal waters to the deep sea, and from rocky substrates to unconsolidated sediment. However, it is clear that echinoid species exhibit marked substrate preferences (Smith 1984; Carter *et al.* 1989; Carter & Hamza 1994) and the nature of the substratum is thought to strongly influence the local distribution of echinoid taxa (Smith 1984).

As far as I am aware, there has been no previous work on survivorship selectivity and substrate preferences of pre-mass extinction faunas *per se*. This is surprising since other marine invertebrates require specific sedimentary habitats (Koch 1995). However, since substrate type is generally linked to water depth and latitude, tests for association between survivorship and latitude or depth also provide indirect information on correlation between sedimentary environments and extinction intensities. For example, Raup & Jablonski (1993) found that by excluding carbonate platform dwelling rudists from their analysis there was no significant difference between extinction intensities at different latitudes. Low latitude extinctions amongst echinoids can be largely explained by the virtual disappearance of carbonate platform facies in the Danian (Smith & Jeffery, in press).

Inferring echinoid substrate preferences.

Inspection of sediment within, and adhering to the outside of, echinoid tests is the easiest way of determining the substrate preferences of fossil echinoids. For atelostomates, sediment preferences may also be ascertained from the functional morphology of the adult test, since the presence and position of fascioles and the density of tuberculation give an indication of the grade of sediment in which the animal could live.

Since the majority of specimens examined for this project come from well characterized lithological units, the substratum preferences for each genus were gathered from general sedimentological and faunal studies of each stratigraphic unit (Appendix 2). Sediment type was divided into four categories based on grain size and calcareous content: chalk / marl, calcarenite / sandy limestone, sand / gravel and silt / mud. Data on sedimentary environments

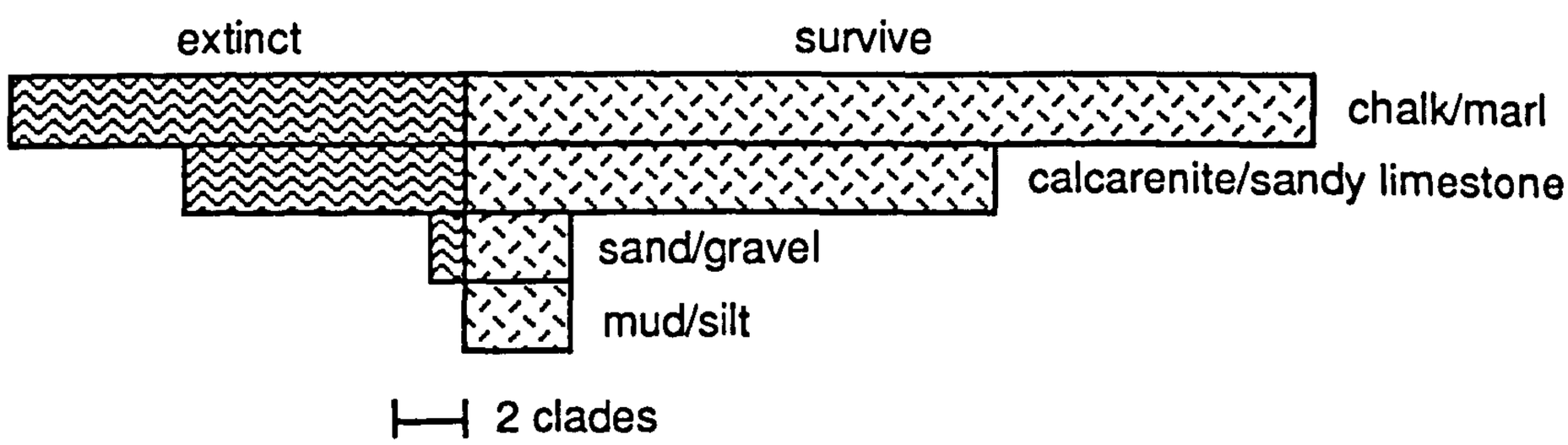
of the genera included in this analysis are given in Appendix 5.

Atelostomate extinction and sedimentary environment.

Two analyses were carried out - the first to test the association of extinction with sediment type and the second to test for the possible correlation of extinction and sedimentary tolerance (i.e. number of lithofacies occupied). Figure 6.10 shows the numbers and proportions of taxa going extinct partitioned by the nature of the substrate and the results of chi-squared tests for independence are given in Table 6.3. Despite small observed and expected values in the sand / gravel and silt / mud categories which inflated the value of X^2, atelostomate survivorship at the end of the Cretaceous is not significantly correlated with substrate preference. In an attempt to overcome the problems associated with small expected values, presence in three and four lithofacies were combined and a chi-squared test indicates that survivorship is also independent of substrate tolerance (Table 6.4). Figure 6.11 shows the numbers and proportions of taxa surviving into the Tertiary plotted against number of sediment types occupied.

These results appear to contradict previous studies which have shown end-Cretaceous marine invertebrate extinctions to be concentrated in carbonate platform habitats (Sohl 1987; Rosen & Turnsek 1989; Raup & Jablonski 1993; Jablonski 1995, 1996; Smith & Jeffery, in press). However, very few Maastrichtian atelostomate echinoids are known from carbonate platform settings but *Hemipneustes*, the only genus known exclusively from this habitat, does go extinct.

Figure 6.10. Atelostomate survivorship plotted against sediment type. a, histogram showing number of clades surviving; b, proportion of clades surviving.


a
extinct
survive
chalk/marl
calcarenite/sandy limestone
sand/gravel
mud/silt
2 clades

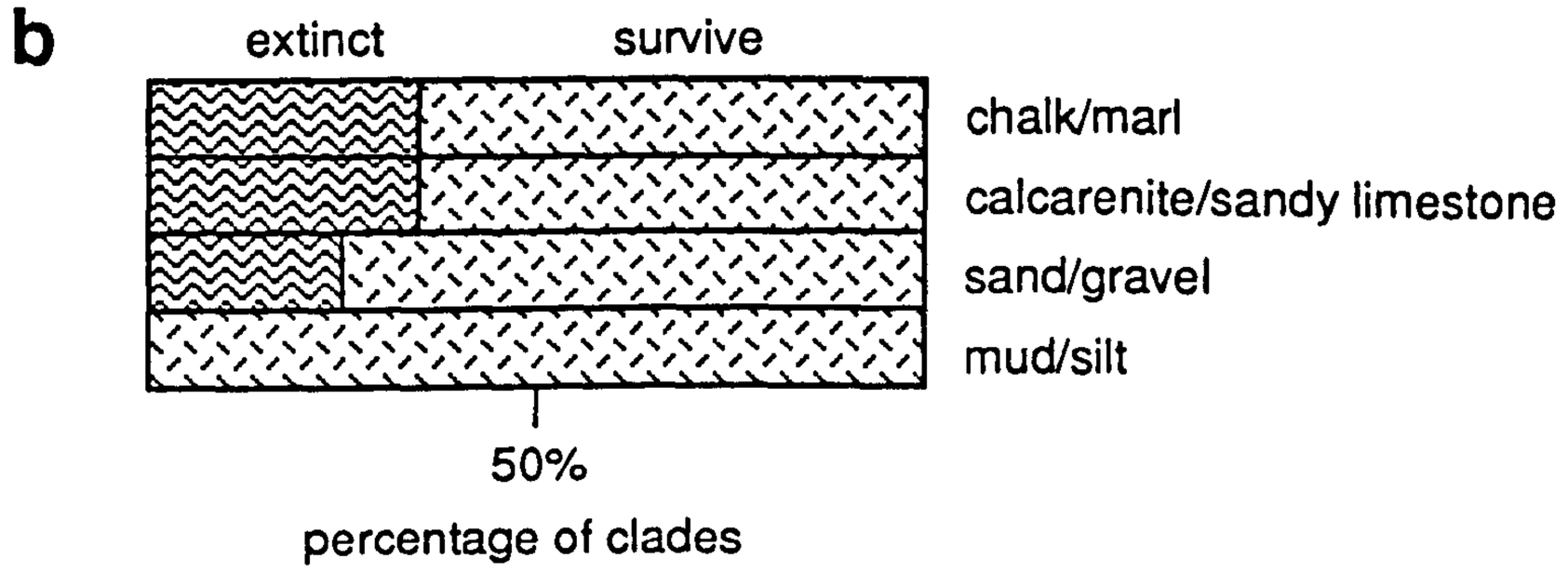
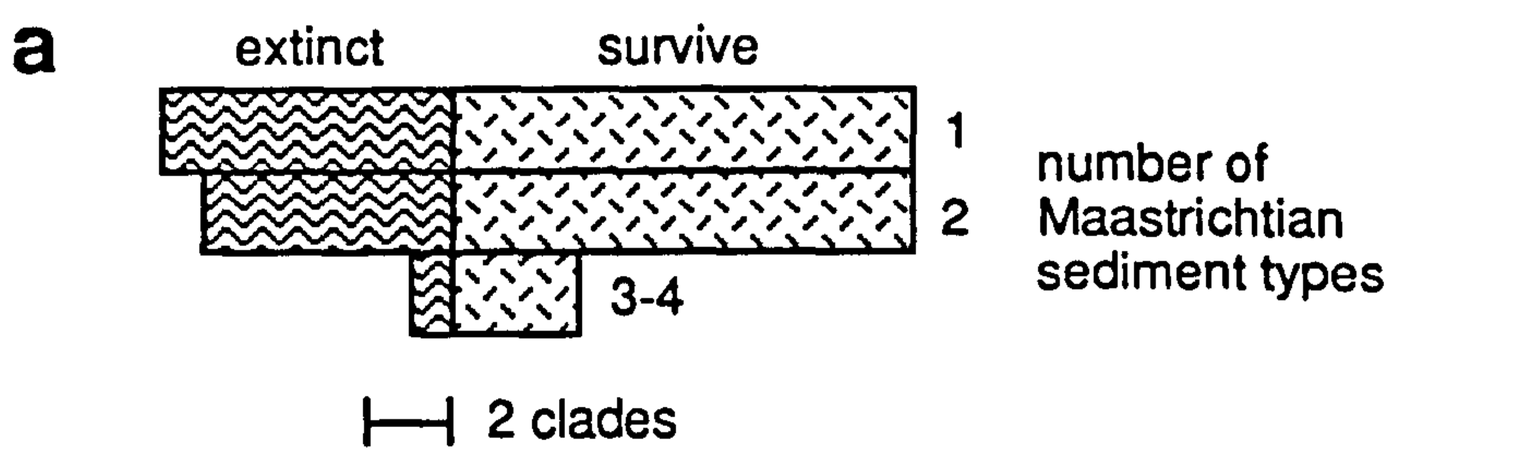
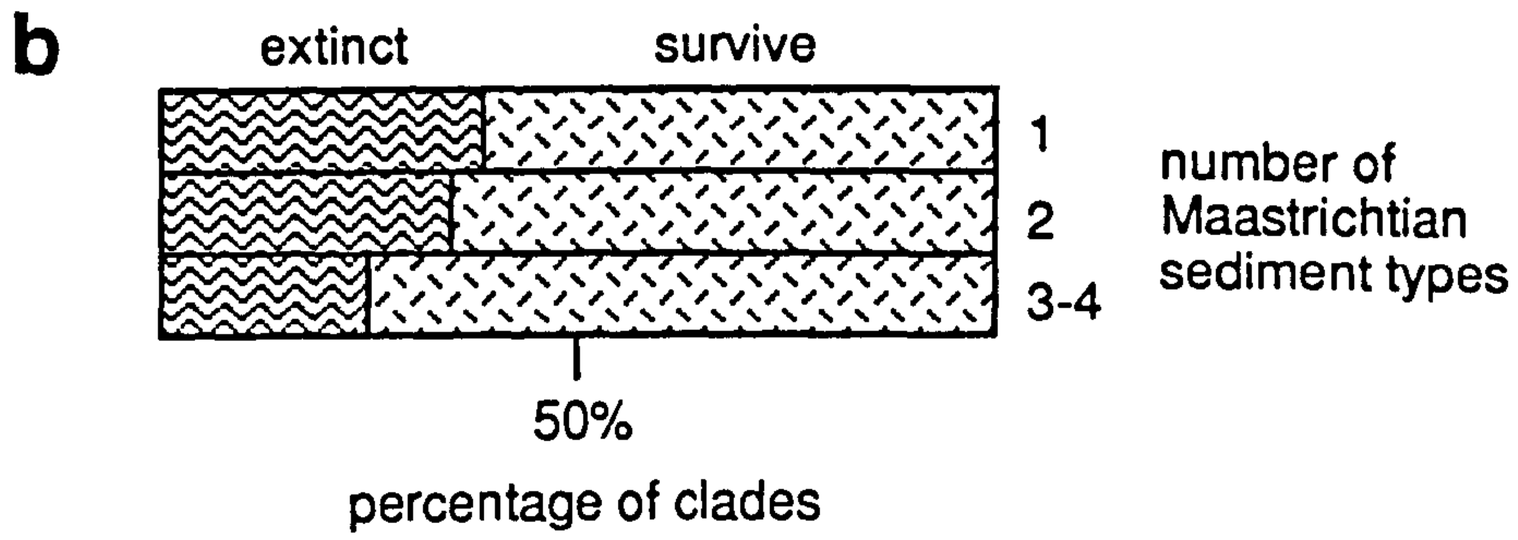

b
extinct
survive
chalk/marl
calcarenite/sandy limestone
sand/gravel
mud/silt
50%
percentage of clades

Figure 6.11. Atelostomate survivorship plotted against sedimentary tolerance. a, histogram showing number of clades surviving; b, proportion of clades surviving.


a
extinct
survive
1
2
3-4
number of
Maastrichtian
sediment types
2 clades


b
extinct
survive
1
2
3-4
number of
Maastrichtian
sediment types
50%
percentage of clades

CHAPTER 7

ATELOSTOMATE EXTINCTION AND BIOLOGICAL CORRELATES

The analyses in Chapter 6 demonstrate that atelostomate survivorship at the end of the Cretaceous was independent of geographic and environmental factors. The same approach is used in this chapter to explore the possible correlation of extinction with the biological factors listed in Table 5.2. In addition, chi-squared tests of independence are used to ascertain whether each biological factor is correlated with atelostomate higher taxonomy and thus to explore why holasteroids were more severely depleted at the Cretaceous-Tertiary boundary.

Life-position in sediment.

A number of studies have suggested that infaunal taxa are more resistant to extinction during background times than those living epifaunally since they are buffered against environmental stresses and perturbations (Kauffman 1978; Stanley 1986). In contrast, no significant difference in extinction rates between infauna and epifauna has been found for end-Cretaceous bivalves (Jablonski & Raup 1995; McClure & Bohonak 1995). However, it should be noted that Jablonski & Raup (1995) excluded rudists from their global analysis.

Methods of inferring burrowing habit in atelostomes.

The burrowing habits of fossil and Recent heart urchins may be inferred in a number of ways. For spatangoids, the shape of the test in lateral profile gives an indication of the sediment type and depth of burial (Kanazawa 1992). For holasteroids and spatangoids, the density of tuberculation on the aboral surface and the presence of large tubercles along the edges of the unpaired ambulacrum also provide information on the animal's ability to burrow (Smith 1980a), since dense spine cover prevents sediment choking the test and larger spines along the frontal groove provide space for tunnel-

building tube feet to function. Fascioles are made up of miliary spines that produce mucus which is used to coat the upper surface of the test and prevent it from becoming clogged with sediment. Hence, the presence of aboral fascioles indicates an infaunal habit. Finally, large pores in the unpaired ambulacrum for funnel-building tube feet or subanally for tunnel-building tube feet also provide evidence of a burrowing mode of life (Smith 1980b). Data on burrowing habit for Maastrichtian and Palaeocene atelostomate echinoids are given in Appendix 5. For this study, taxa considered to be semi-infaunal and aborally exposed were included in the epifaunal category, since they would have been subject to similar levels of environmental stress as fully epifaunal taxa.

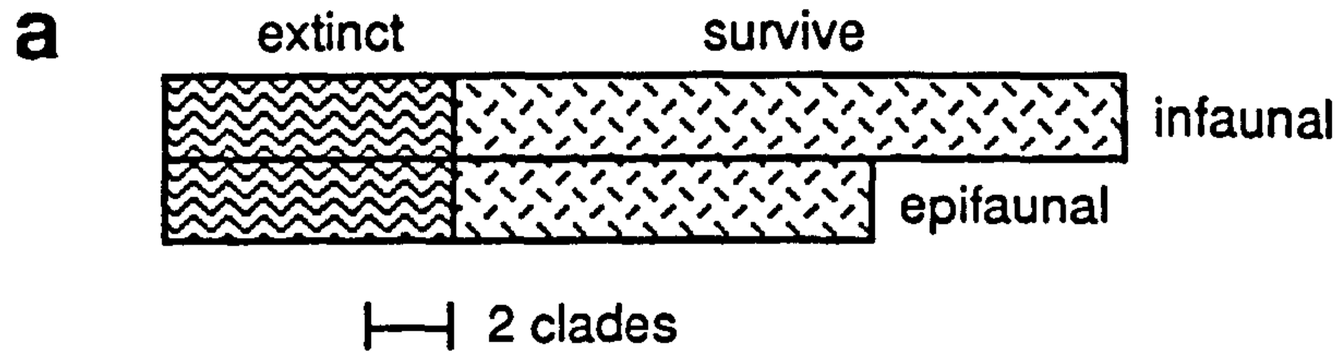
Atelostomate extinction and life-position in the sediment.

The numbers and proportions of infaunal and epifaunal taxa surviving or becoming extinct at the end of the Cretaceous are shown in Figure 7.1. A chi-squared test suggests that atelostomate survival at the end of the Cretaceous was not correlated with life-position in the sediment (Table 7.1). However, there is a significant correlation between burrowing habit and atelostomate higher taxonomy (i.e. significantly more holasteroids are epifaunal than is expected) (Table 7.2). This result goes some way towards explaining why ability to burrow has often been cited as the reason why spatangoids preferentially survived the K-T event.

Table 7.1. Summary statistics of contingency tables testing the independence of extinction with regard to possible biological correlates.

factor	degrees of freedom	X^2	p
life-position in sediment	1	0.496	0.481
larval strategy	1	2.393	0.122
feeding strategy	1	5.119	0.024

Figure 7.1. Atelostomate survivorship plotted against burrowing habit. a, histogram showing number of clades surviving; b, proportion of clades surviving.


a
extinct
survive
infaunal
epifaunal
2 clades

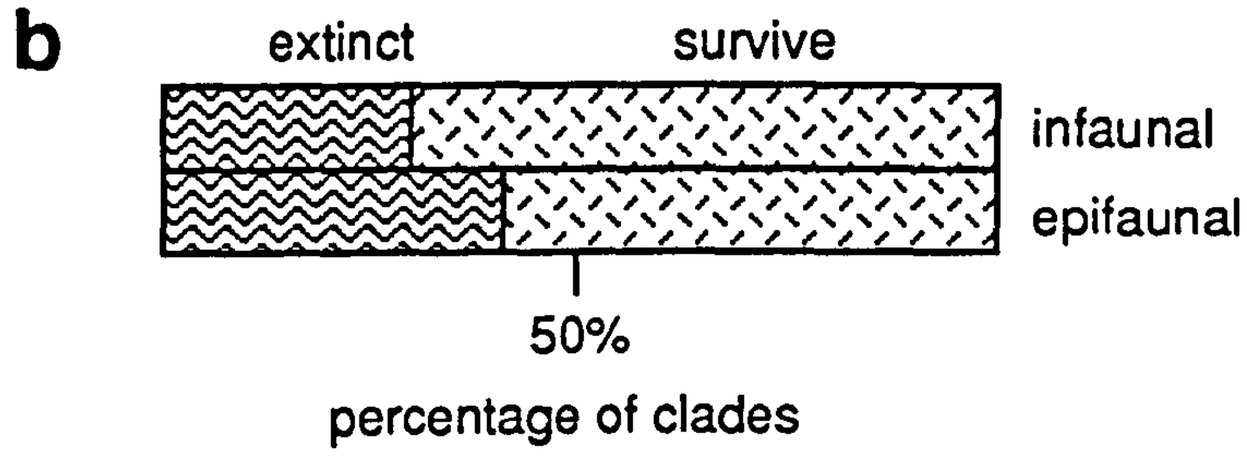

b
extinct
survive
infaunal
epifaunal
50%
percentage of clades

Table 7.2. Summary statistics of contingency tables testing the independence of higher taxonomy with regard to possible biological correlates.

factor	degrees of freedom	X^2	p
life-position in sediment	1	11.526	<0.001
larval strategy	1	2.963	0.085
feeding strategy	1	17.419	<0.001

Larval strategy.

Reproductive strategy within marine invertebrates can be broadly divided into three types - planktotrophic, lecithotrophic, and brooded - although many taxa show developmental patterns that are intermediate between, or a combination of, these three primary modes. Planktotrophs produce large numbers of small eggs that hatch into free-swimming larvae dependent on particulate matter for their nutrition to reach metamorphosis. These larvae are capable of surviving for prolonged periods in the plankton and have the capacity for widespread dispersal (Strathmann 1985, 1990). For non-planktotrophs, the nutritional burden of development rests with the parents since both lecithotrophic and brooded larvae do not feed during development but rely on nutrient reserves in the large yolk-rich eggs from which they hatch. Such taxa have a very much lower dispersal potential since lecithotrophic larvae are either non-pelagic or have only a brief planktonic existence whereas the eggs of brooders are retained by the parent throughout development to the juvenile stage.

Almost nothing is known about the evolutionary history of developmental patterns in marine invertebrates, yet it is widely accepted that reproductive strategy is closely linked with a number of biogeographic and macroevolutionary correlates such as geographic range, species longevity and survival at mass extinction events (Jackson 1974; Shuto 1974; Scheltema 1977; Hansen 1978, 1980, 1982, 1983; Jablonski 1982, 1986b; Erwin 1990; Gili & Martinell 1994; Emlet 1995). Non-planktotrophs are thought to be less susceptible during mass extinctions because they are not dependent on phytoplankton for their nutrition, and therefore a crash in oceanic productivity would have little effect on them. In fact, larval strategy has been proposed as the explanation for the survival of the nautiloids (with a lecithotrophic larval stage) and the demise of the

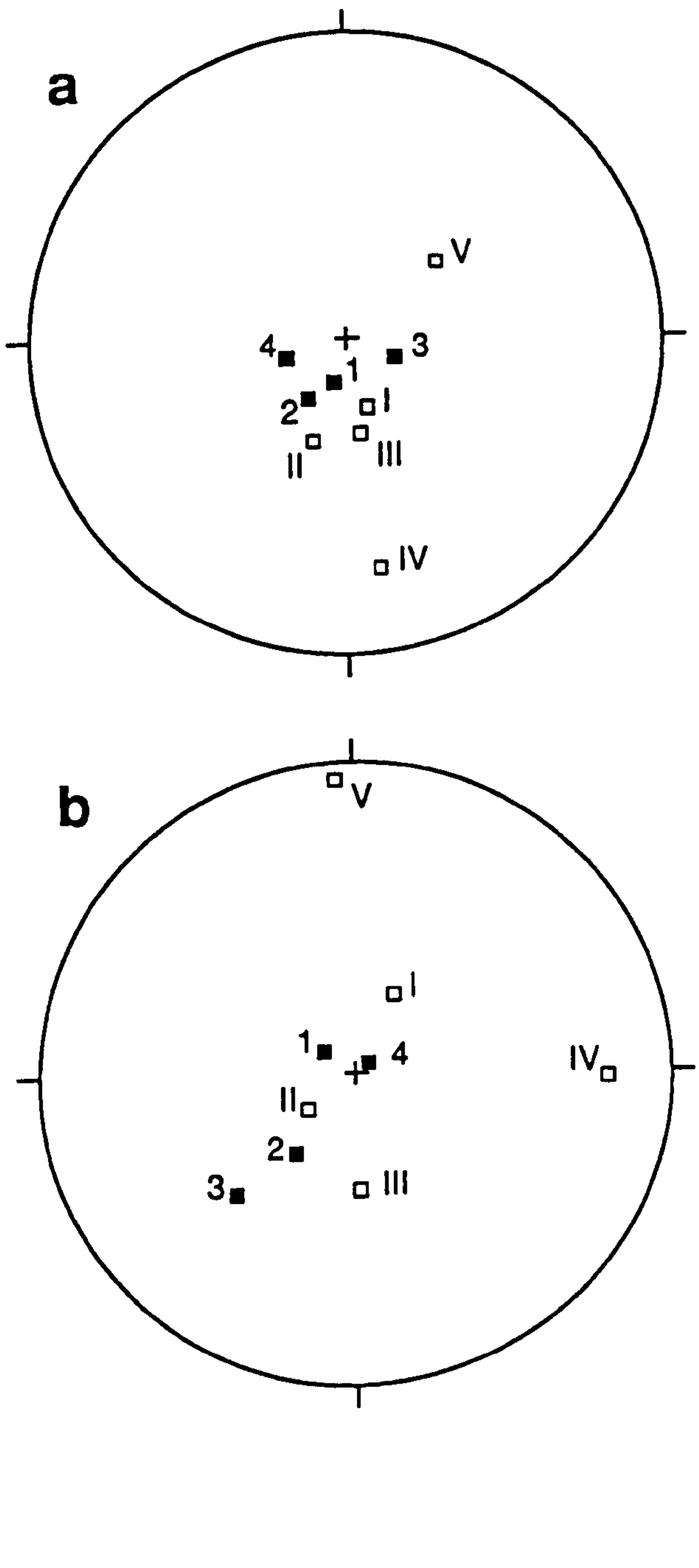
ammonites (with a planktotrophic larval stage) at the end of the Cretaceous (Landman 1984; Kennedy 1989, 1993; Gallagher 1991; Sheehan *et al.* 1996), the persistence of trilobites with a benthonic larval stage during the Late Ordovician (Chatterton & Speyer 1989) and the decimation of bivalves and brachiopods at the end-Permian mass extinction (Erwin 1990). However, no correlation between survivorship and larval type has been found for taxa during the Late Devonian (McGhee 1996) or for gastropod molluscs at the K-T boundary (Jablonski 1986a, b; Valentine & Jablonski 1986).

Methods of inferring non-planktotrophy in echinoids.

Echinoids are unusual among marine invertebrates in that developmental mode (planktotrophy vs. non-planktotrophy) can be deduced simply and unambiguously from the adult skeleton. Three methods of inference are known, applicable to both Recent and fossil taxa. Brooded development may be recognized by the presence of depressed areas, or marsupia, on the adult test where offspring are sheltered during development (Kier 1967, 1969; McNamara 1994). To date, marsupial structures have been identified in at least 20 species of fossil echinoid (Lambert 1933; Kier 1969; Philip & Foster 1971; Roman 1983; Blake & Zinsmeister 1991; McNamara & Barrie 1993; Jagt & van der Ham, 1994) and 28 Recent taxa (Philip & Foster 1971). Extreme sexual dimorphism in gonopore size (Kier 1967, 1969; Emlet 1989) can also be used to infer non-planktotrophy in sea urchins since in some taxa the female has bigger gonopores to accommodate the large yolky eggs produced. The third method hinges on the fact that calcite skeletal rods in feeding larvae determine the orientation of optic axes in adult genital plates (see Appendix 3). Thus developmental mode may be inferred from the orientations of crystallographic axes in the calcite of apical disc plates (Emlet 1985, 1988, 1989) (Figure 7.2).

Data on developmental mode for this study were either gathered from the published literature or inferred by using the methods outlined above. In common with earlier studies (Emlet 1990, 1995), taxa judged to have non-feeding larvae according to the crystallographic and gonopore dimorphism criteria were assigned to the lecithotrophic category. Only those species with obvious brood structures were considered to be marsupiate.

Figure 7.2. Stereographic projections of C-axis orientations of apical disc plates in fossil echinoids. Genital plate traces are represented by solid squares; ocular plate traces by open squares. A: *Cyclaster vilanovae* (Cotteau) (BMNH EE4361-9) - a non-planktotroph: B: *Hemipneustes persicus* Cotteau and Gauthier (BMNH EE4098) - a planktotroph. For irregular echinoids, crystallographic orientation of genital plate 3 is critical in inferring planktotrophy. For non-planktotrophs, the trace is almost perpendicular whereas for planktotrophs, the trace falls in the lower left quadrant.


a
V
4
3
1
2
I
II
III
IV
b
V
I
1
4
IV
II
2
3
III

Atelostomate extinction and larval strategy.

The inferred larval strategy for all Maastrichtian and Palaeocene atelostomate genera is given in Appendix 5. The number and proportion of planktotrophic and non-planktotrophic clades becoming extinct at the end of the Cretaceous are shown in Figure 7.3. Despite the fact that no non-planktotrophs become extinct, a chi-squared test for independence suggests that survivorship is not significantly correlated with reproductive strategy at the end of the Cretaceous (Table 7.1). However, the non-significant result is related in part to the very small number of lecithotrophs and brooders present in the Maastrichtian. The value of X^2 is larger although still not significant if all Maastrichtian and Palaeocene echinoids are included (Smith & Jeffery, in press). In addition, although there are no non-planktotrophic holasteroids in the Maastrichtian or Palaeocene, larval strategy is not significantly correlated with atelostomate higher taxonomy (Table 7.2).

Why are there so few Maastrichtian lecithotrophs?

Several lines of evidence suggest that planktotrophy is the plesiomorphic developmental pattern among the echinoids and has subsequently been lost in a number of lineages (Strathmann 1985; Wray 1996). It is estimated that a non-planktotrophic mode of larval development has been independently evolved a minimum of 20 times by the reduction of complex larval structures (Wray 1995a).

Non-planktotrophic echinoids are widely recognized in Tertiary strata. However, within the published literature there are no reports of pre-Campanian brooding echinoids, and only two examples of sexual dimorphism in gonopore size have been recorded (Smith *et al.* 1988; Néraudeau 1993). Crystallographic analysis of apical disc plates indicates that both of these taxa are in fact planktotrophs (Emlet, pers. comm. 1997). Thus, gonopore dimorphism does not always distinguish between planktotrophs and non-planktotrophs. However, in a survey of late Cretaceous and early Tertiary taxa (see Appendix 3), all echinoids inferred to be lecithotrophs using crystallographic criteria do show dimorphism in gonopore size. Extreme gonopore dimorphism therefore provides a good first approximation of developmental mode. Examination of the comprehensive collections at the Natural History Museum, London found no pre-Campanian taxa with

extreme gonopore dimorphism.

C-axis orientations of echinoid apical disc plates have previously been determined for a number of fossil (including Jurassic and Cretaceous) taxa (Kirchner 1929; Lucas 1953; Devriès 1954; Jesionek-Szymanska 1959; Raup 1965; Emlet, unpublished). These all show C-axis orientations characteristic of a planktotrophic larval stage. No pre-Campanian lecithotrophs have been found using crystallographic criteria. Consequently, the shift to a non-feeding mode of larval development is a geologically recent phenomenon.

The shift to a non-feeding mode of development is thought to be an irreversible process (Strathmann 1978; Hansen 1983; Wray 1996), and it has been implicitly assumed that switches to non-planktotrophy have occurred randomly scattered through geological time. However, the reasons for shifts in developmental mode and the factors responsible for driving such shifts remain largely obscure. The demonstration of coordinated switches in developmental mode would provide strong evidence for global environmental change, but until now, the documentation of first occurrences in the fossil record has never been attempted.

First occurrences of non-planktotrophy in echinoids.

The taxonomic and temporal distribution of first occurrences of non-feeding development in echinoid orders is illustrated in Figure 7.4. Non-planktotrophy evolved independently in nine clades from five orders within the last 10 m.y. of the Cretaceous (Table 7.3). These five orders diverged well before the Cretaceous (Smith *et al.* 1995). For the two orders showing multiple first occurrences of non-planktotrophy in the late Cretaceous, traditional phylogenetic schemes (e.g. Kier 1962; Moore 1966) and unpublished cladograms support the independence of these shifts. Nearest sister groups for all six clades within the cassiduloids and spatangoids are demonstrably planktotrophic, indicating that these shifts to non-planktotrophy represent independent replicate transformations. In marked contrast to today's distribution of non-planktotrophic echinoids, lecithotrophy and brooding evolved over wide palaeolatitudinal and depth ranges (Figure 7.5) from shallow- water carbonate platforms to deeper-water chalk basins during the late Campanian and Maastrichtian.

Table 7.3. First occurrences of lecithotrophy and brooding in echinoids during the late Campanian and Maastrichtian. Sister taxa are shown in parentheses. Asterisks indicate those taxa where developmental mode was inferred using crystallographic criteria.

lineage	first genera showing nonplanktotrophic development	age	locality	developmental mode
Cidaroida	*Almucidaris*	E. Maastrichtian	Antarctic & Spain	brooding
Arbacioida	*Goniopygus**	L. Maastrichtian	Netherlands	brooding
	[*Goniopygus* sp.]*			planktotrophy
Phymosomatoida	*Thylechinus*	L. Campanian	North Africa	brooding
	[*Glyphopneustes*]*			planktotrophy
Cassiduloida	*Oolopygus*	L. Maastrichtian	Netherlands, France, Belgium & southern India	lecithotrophy
	[*Catopygus*]			planktotrophy
	Rhynchopygus	L. Maastrichtian	Netherlands	lecithotrophy
	[*Procassidulus*]			planktotrophy
Spatangoida	*Cyclaster**	E. Maastrichtian	western Europe	lecithotrophy
	[*Isaster*]*			planktotrophy
	*Diplodetus**	L. Maastrichtian	USA	lecithotrophy
	[*Micraster*]*			planktotrophy
	*Mauritanaster**	Maastrichtian	Algeria	lecithotrophy
	[*Iraniaster*]*			planktotrophy
	*Abatus**	Maastrichtian	Madagascar	brooding
	[*Linthia*]*			planktotrophy

Global environmental change and the shift to non-planktotrophy in echinoids.

The near-simultaneous adoption of lecithotrophic and brooded development in many independent echinoid lineages near the end of the Cretaceous over a wide geographic range shows that this shift in life-history strategy was driven by some extrinsic factor. Available evidence suggests that a similar pattern is true for some molluscan groups since the earliest undisputed incidence of non-planktotrophy reported in bivalves and gastropods is also from the end of the Cretaceous (Campanian and Maastrichtian) (Jablonski 1982, 1986b).

Two environmental factors could be responsible for driving this change: decreasing temperature or changing nutrient predictability. Extant taxa with different larval strategies are non-randomly distributed, and a significant correlation between decreasing planktotrophy and increasing latitude and depth has been demonstrated for Recent echinoids (Emlet *et al.* 1987; Emlet 1990) and molluscs (Thorson 1950; Jackson 1974; Jablonski 1978). For example, of the 28 extant brooding echinoid species, 25 are known from polar (predominantly Antarctic) waters (Philip & Foster 1971). This correlation has led

to the suggestion that the presence of marsupiate echinoids in the fossil record is indicative of low oceanic temperatures (Foster 1974; Rowe & Vail 1982). Non-planktotrophic development is thought to be advantageous in polar regions (and deep seas) where cold-water conditions prevail and there is extreme seasonality in primary productivity (Thorson 1950).

Although the Cretaceous is often interpreted as a time of warm, equable climate, an increasing amount of evidence suggests that the Maastrichtian was neither as warm nor as equable as commonly characterized. In fact, stable isotope data from low to mid (Lecuyer *et al.* 1993; Oberhänsli 1986) and mid to high latitudes (Barrera 1994; D'Hondt & Lindinger 1994; Ditchfield *et al.* 1994) indicate that a long-term cooling trend occurred though the Campanian and Maastrichtian. The cooling rate increased during the Maastrichtian when the trend culminated in the lowest temperatures of the late Cretaceous (Barrera 1994). Palaeobotanical data (Wolfe & Upchurch 1987) also provide evidence of cooling over this interval.

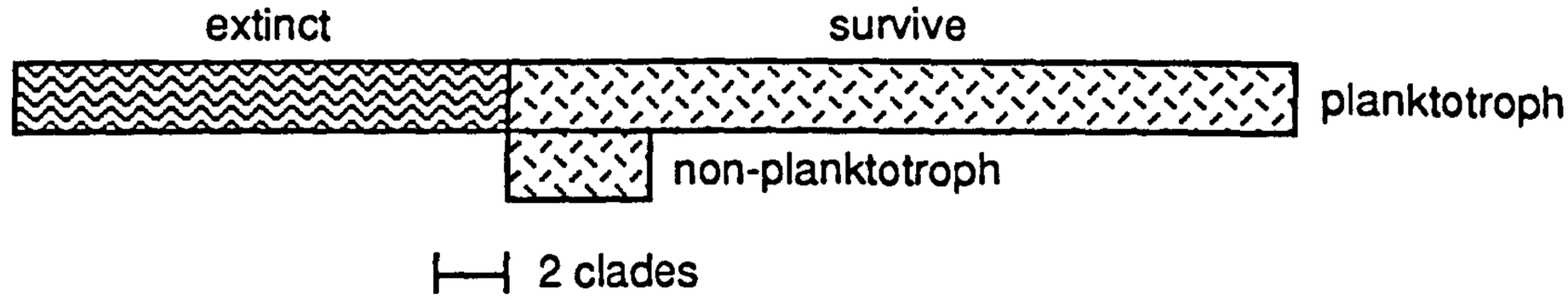
The existence of brooding spatangoid echinoids in the Danian has been regarded as evidence for global cooling at the Cretaceous-Tertiary boundary (Fischer 1963). However, fossil marsupiate echinoids have been found in subtropical carbonate-platform conditions (Roman 1983), and the distribution of first occurrences of non-planktotrophy in echinoids during the late Campanian and Maastrichtian demonstrates no latitudinal pattern (Figure 7.5). Thus, the shift in developmental strategy cannot be attributed to temperature alone.

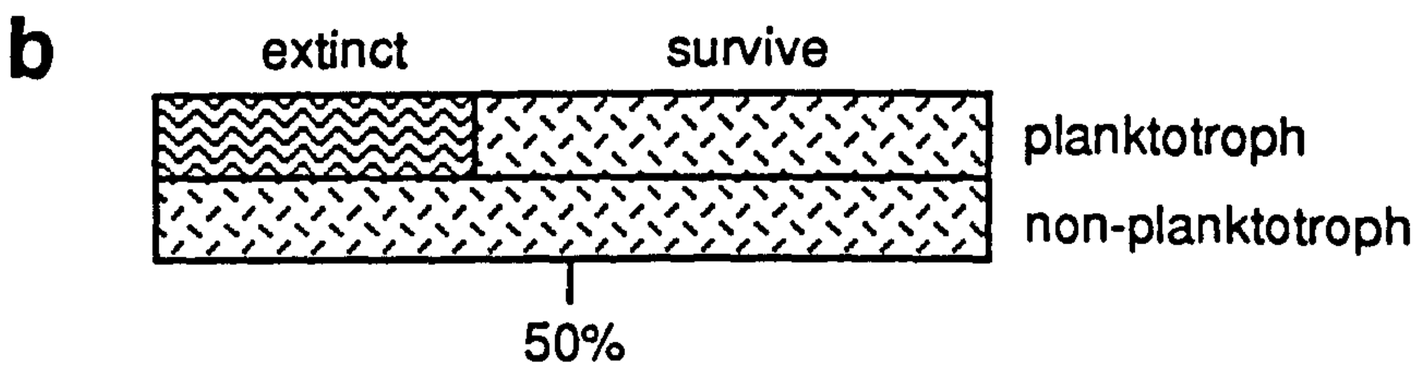
Apart from temperature, tropical and polar regions differ in one other important aspect. Primary production is fairly uniform throughout the year in tropical environments. In contrast, polar regions are characterized by a markedly seasonal pattern of primary production. Research into the distribution of marine invertebrates in Antarctic waters reveals that the extreme seasonality of food supply may be more influential than low temperatures on the life-history of marine organisms (Clarke 1988, 1990). This finding has resulted in an alternative interpretation for the high incidence of non-planktotrophic marine invertebrates at high latitudes (Thorson 1950; McNamara 1994; Poulin & Féral 1996) - the availability of food, which may be due to seasonality or variations in primary productivity.

In a nutrient-limited environment, the planktotrophic need to feed is a definite disadvantage and non-planktotrophy may act as an "insurance against fluctuations in phytoplankton abundance" (Wray 1995b, p. 435), since the nutritional demands of non-planktotrophic larvae are met by the yolk-rich eggs from which they hatch.

Determining the intensity of seasonality in the fossil record may well prove difficult. Nevertheless, evidence for at least a degree of seasonality in low latitudes at the end of the Cretaceous comes from cyclicity in stable isotope ratios in rudist bivalves (Steuber 1996). In addition, fluctuations in primary productivity have been reported for the Maastrichtian interval (Barrera & Keller 1994). The discovery that many echinoid clades independently evolved non-planktotrophy in the latest Cretaceous provides compelling evidence for a marked increase in the fluctuation of nutrient supply in marine environments and adds to the growing evidence for environmental instability in the period leading up to the end of the Cretaceous.

Figure 7.3. Atelostomate survivorship plotted against larval strategy. a, histogram showing number of clades surviving; b, proportion of clades surviving.





percentage of clades

Figure 7.4. Stratigraphic range chart for major post-Jurassic echinoid clades. First occurrences of non-planktotrophic development are represented by solid rectangles. Patterned band indicates period from late Campanian to Maastrichtian.

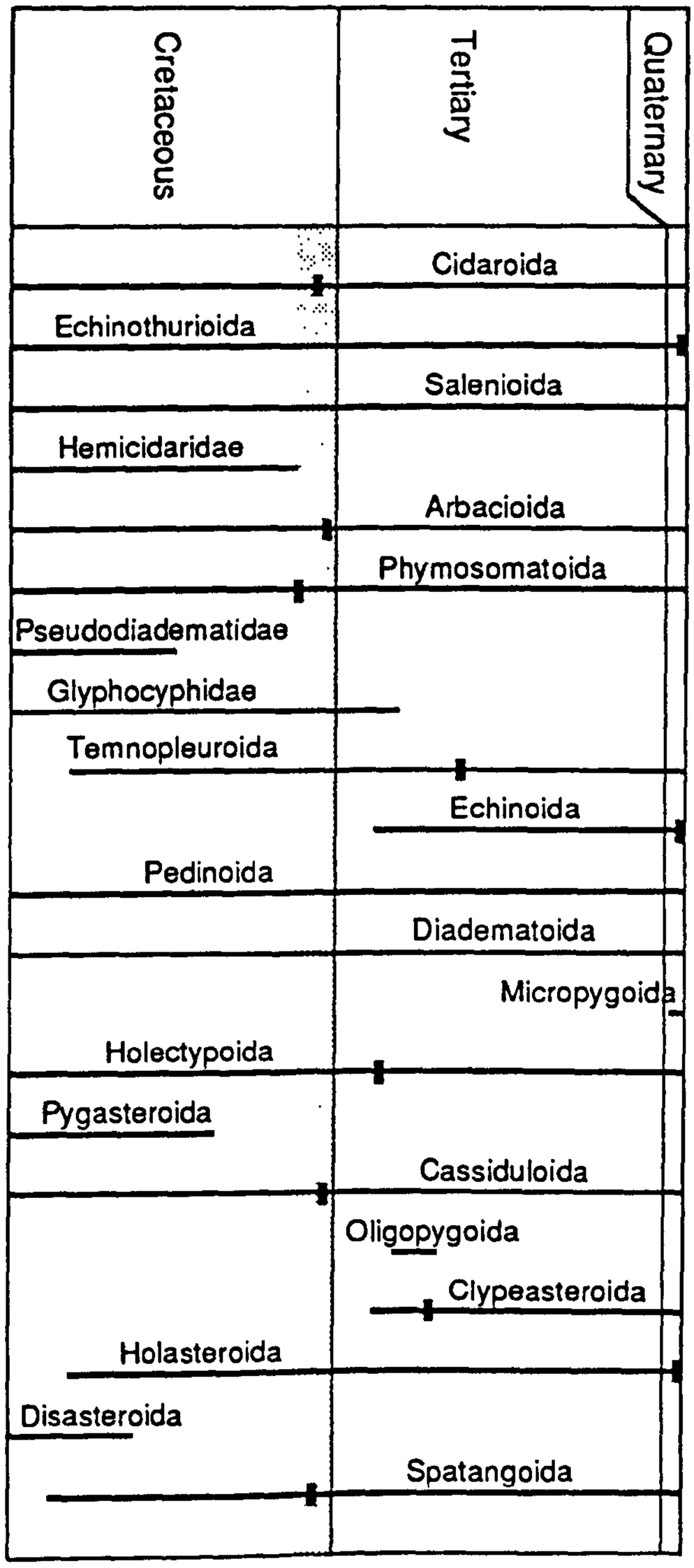
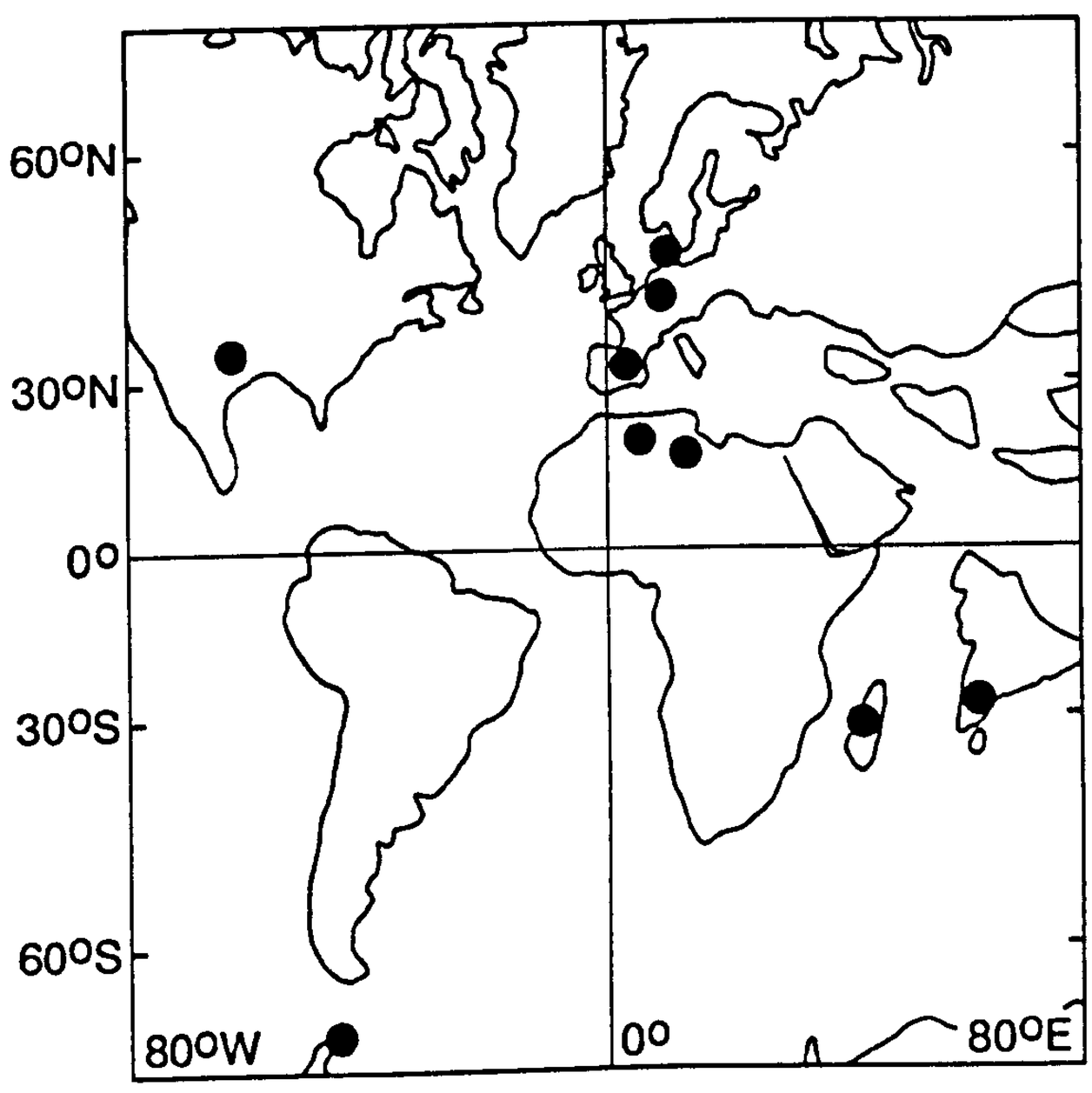

Quaternary
Tertiary
Cretaceous
Cidaroida
Echinothurioida
Salenioida
Hemicidaridae
Arbacioida
Phymosomatoida
Pseudodiadematidae
Glyphocyphidae
Temnopleuroida
Echinoida
Pedinoida
Diadematoida
Micropygoida
Holectypoida
Pygasteroida
Cassiduloida
Oligopygoida
Clypeasteroida
Holasteroida
Disasteroida
Spatangoida

Figure 7.5. First occurrences of lecithotrophy and brooding in late Campanian and Maastrichtian echinoids plotted onto Maastrichtian geography. Occurrences are equally divided between temperate and tropical latitudes.


60°N
30°N
0°
30°S
60°S
80°W
0°
80°E

Feeding strategy.

Feeding strategy is often cited as a correlate to preferential survivorship at the Cretaceous-Tertiary boundary with detritivores showing significantly lower extinction rates than those taxa which rely on primary productivity (McKinney 1985, 1987; Sheehan & Hansen 1986; Rhodes & Thayer 1991; Ward *et al.* 1991; Jablonski & Raup 1995; Jablonski 1996; Sheehan *et al.* 1996). A similar pattern is seen during the end-Permian mass extinction (Erwin 1989b, 1996). The correlation between extinction level and deposit and suspension feeding at the end of the Cretaceous is often explained in terms of a catastrophic collapse of phytoplankton production brought about by global darkness caused by a bolide impact (Sheehan & Hansen 1986; Paul & Mitchell, 1994; Sheehan *et al.* 1996). However, deposit feeders are more dependent on the input of organic matter from surface waters than commonly recognized (Jablonski & Raup 1995; Levinton 1996) since they rely on the rain of phytodetritus for their nutrition. In fact, many detritivores live in environments that are nutrient stressed for much of the year since nutrient supply to the sea floor fluctuates with the seasonality of phytoplankton production. In addition, among deposit feeding bivalves the low overall extinction rate is due to extremely low extinction levels in just two groups, the Nuculoida and the Lucinoidea (Jablonski & Raup 1995). Thus the preferential survivorship exhibited by these groups is attributable to factors other than, or in addition to, the dichotomy between deposit and suspension feeding (Jablonski 1996; Levinton 1996). In contrast, McClure & Bohonak (1995) found no correlation between extinction level and feeding strategy in bivalves at the end of the Cretaceous and no association between trophic mode and preferential survivorship has been identified for taxa during the Late Ordovician (Sheehan *et al.* 1996) or Late Devonian (McGhee 1996) mass extinctions.

Inferring feeding strategy in atelostomate echinoids.

All irregular echinoids are deposit feeders which collect detritus from the sea floor. However, depending on the collection strategy employed, they may be subdivided into bulk or selective detritivores. Bulk detritivores shovel vast quantities of surface sediment directly into the mouth in order to extract the small amount of organic material. They may be

recognized by the deep, sharp frontal groove leading directly to the mouth and the lack of enlarged pores around the mouth. Taxa adopting this strategy are often associated with deep sea, oligotrophic settings (Jeffery & Smith, in press). Selective detritivores on the other hand, have specialized pencillate tube feet around the mouth which they use to pick up and manipulate small particles of detrital material (Smith 1980b). Large perioral pores are evidence of the existence of such tube feet in life.

Atelostomate extinction and feeding strategy.

Details of feeding strategies in Maastrichtian and Palaeocene atelostomates are given in Appendix 5. There are no bulk detritivores among the spatangoids, and a chi-squared test demonstrates that feeding strategy and atelostomate higher taxonomy are significantly correlated (Table 7.2).

Figure 7.6 shows the numbers and proportions of bulk and selective detritivores surviving into the Tertiary. A chi-squared test for independence indicates that survivorship is significantly correlated with feeding strategy, with bulk detrivores (and thus holasteroids) more severely affected (Table 7.1), suggesting that atelostomate extinction at the end of the Cretaceous was nutrient driven. Moreover, since echinoids drastically curtail growth when faced with extrinsic food limitation (Lawrence 1987, p. 253), this result is corroborated by the observation that most Danian echinoids are substantially smaller than their Maastrichtian precursors (Figure 7.7). This concurs with the prediction that the survivors of a nutrient driven extinction event will be small (Paul & Mitchell 1994) and parallels the reduction in shell size in bivalves at the K-T boundary noted by Hayami (1997).

Nevertheless, these conclusions appear to be at odds with the fact that extinction is not significantly correlated with larval feeding strategy (i.e. planktotrophy vs. non-planktotrophy). However, the amount of phytodetritus reaching the sea floor decreases with depth and thus a reduction in phytoplankton abundance which would be of insufficient proportions to decimate planktotrophic larvae in the upper water column, could still lead to the curtailment of the rain of phytodetrital material to the sea floor and the subsequent starvation of detritivores in deep sea oligotrophic settings, and would explain

the observed pattern of selective extinction in the benthic adult rather than the planktonic larval stage.

Figure 7.6. Atelostomate survivorship plotted against feeding stategy. a, histogram showing number of clades surviving; b, proportion of clades surviving.

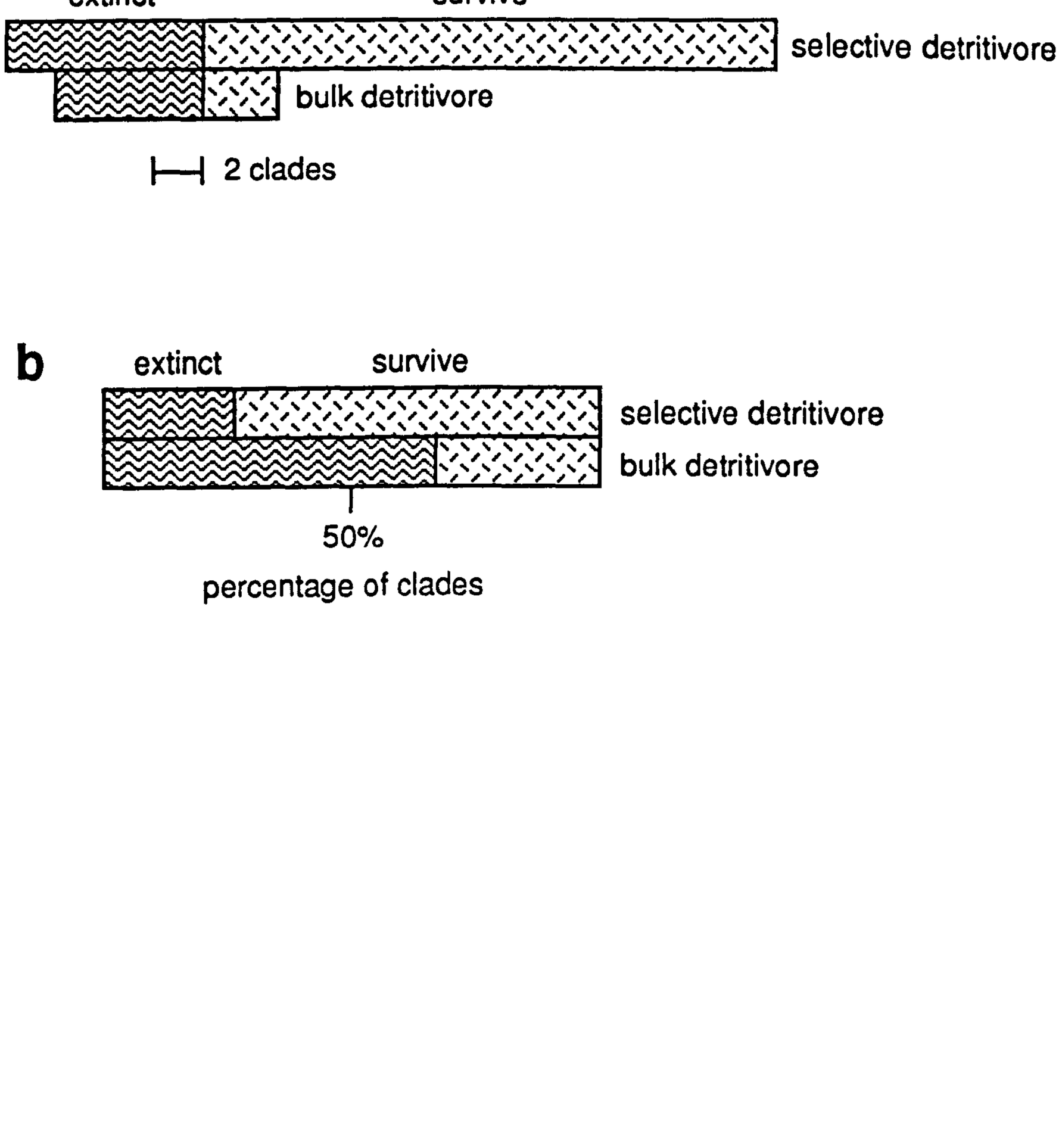
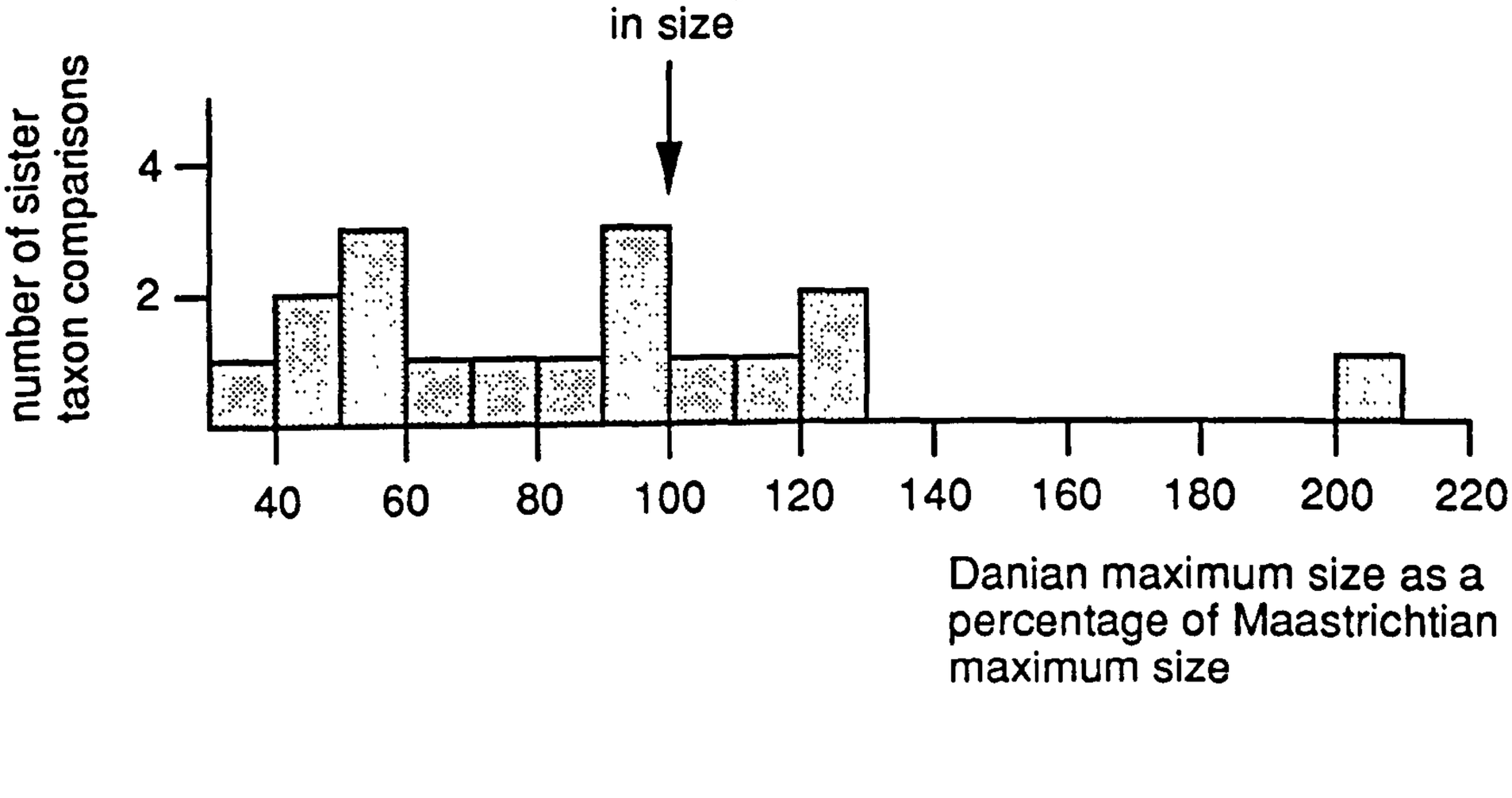

a
extinct
survive
selective detritivore
bulk detritivore
2 clades
b
extinct
survive
selective detritivore
bulk detritivore
50%
percentage of clades

Figure 7.7. Histogram of Danian maximum test size as a percentage of Maastrichtian maximum test size for surviving clades.


no change
in size
number of sister taxon comparisons
4
2
40
60
80
100
120
140
160
180
200
220
Danian maximum size as a percentage of Maastrichtian maximum size

PAGE NUMBERING AS ORIGINAL

CHAPTER 8

CAN WE TELL WHAT HAPPENED AT THE CRETACEOUS-TERTIARY BOUNDARY?

Size of the extinction event.

Previous estimates of global extinction intensity at the Cretaceous-Tertiary boundary have suggested generic levels of 70% for echinoids (Roman 1984) and 63% for bivalves (Raup & Jablonski 1993). My own estimate of global generic level extinction for atelostomate echinoids calculated from the raw non-standardized data gives a very similar result (65%). However, a nomenclatural revision (Chapter 3) and subsequent phylogenetic analysis (Chapter 4) substantially reduces this estimate to 35%, underlining the amount of error that taxonomic inconsistencies can contribute to any regional or global analysis. This result suggests that similar treatment of other datasets could lead to analogous reductions in the magnitude of extinction level estimates for other groups and provides justification for the taxonomic standardization (Jeffery 1997b) and phylogenetic approaches (MacLeod 1996a; Jablonski 1997; MacLeod *et al.* 1997; Jeffery & Smith, in press) that have been advocated in theory but rarely applied in practice. This should prove a fertile area for future research.

Selectivity of the extinction event.

It has been demonstrated by this and many previous studies that mass extinction events are non-random and that victims and survivors are not arbitrary samples of the pre-extinction biota. Instead there are biological, ecological and geographical correlates common to survivors. Many differing patterns of extinction selectivity have been documented for different taxonomic groups at the same extinction horizon, and for different mass extinction events. However, many studies appear to show selectivity patterns that are common to mass extinction events (see Chapters 6 & 7) but that do not occur during times of background extinction. This has resulted in the proposal that alternating macroevolutionary regimes operate during times of background and mass extinction

(Jablonski 1986a, b, 1989, 1991, 1995, 1996; Johansen 1989). Others authors find no evidence of a quantitative dichotomy between background and mass extinctions (McKinney 1987; Raup & Boyajian 1988; Raup 1995).

The most recent investigations of extinction selectivity, that have relied on statistical analysis rather than anecdotal evidence (Raup & Jablonski 1993; Jablonski & Raup 1995; McClure & Bohonak 1995; see also Chapters 6 & 7), have shown very few recognizable selectivity patterns for the marine invertebrate macrofauna at the Cretaceous-Tertiary boundary. Results of this type have led some authors to suggest that selectivity occurs when extinction rates are low but not when levels are high (McClure & Bohonak 1995; Raup 1995).

My own analysis of atelostomate echinoids over the Cretaceous-Tertiary boundary indicates that there was no statistically significant correlation between extinction and any geographical or environmental characteristics and that similar levels of extinction were experienced in all geographic, depth and sedimentary settings. Widespread taxa were not more resilient than more restricted forms and low latitude faunas were not more severely effected. These results attest to the global scale of the mass extinction event (Jablonski & Raup 1995). Furthermore, extinction risk was not significantly influenced by larval mode or infaunal / epifaunal habit. However, atelostomate survivorship at the K-T boundary is correlated with feeding strategy. Other studies (Sheehan & Hansen 1986; Rhodes & Thayer 1991; Ward *et al.* 1991; Jablonski & Raup 1995; Sheehan *et al.* 1996) have also shown survivorship to be associated with trophic mode with detritivores showing significantly lower extinction rates than those taxa which rely on primary productivity. However all heart urchins are detritivores and it is the dichotomy between bulk detritivores, generally found in deep sea oligotrophic settings, and selective detritivores, common in less nutrient stressed environments, that is associated with differential survivorship at the end of the Cretaceous.

This result suggests that among atelostomate echinoids at least, extinction at the K-T boundary was nutrient driven. Elevated extinction rates among bulk detritivores would have followed a decrease in nutrient supply to deep sea oligotrophic environments, and are consistent with a collapse of phytoplankton productivity at the K-T boundary

(whatever its cause). From this analysis, there is no evidence of an alternation of macroevolutionary regimes between times of background and mass extinction. Further research on selectivity within a phylogenetic framework is needed to determine whether this holds for other taxonomic groups and at other extinction horizons.

What happened at the K-T boundary?

It has been argued that deducing the causes of extinction events in the fossil record is fundamental to the understanding of evolutionary processes and the long term dynamics of biodiversity (Banerjee & Boyajian 1996). The recognition of patterns of survivorship selectivity is thought to provide clues to the causes of mass extinctions (Raup 1986; Raup & Jablonski 1993; Jablonski & Raup 1995; Smith & Jeffery, in press). We are moving away from explaining individual aspects of extinction events (e.g. Cys 1967 on the inability of dinosaurs to hibernate) towards interpretations which explain the whole pattern of biotic collapse. Even so, a plethora of "killing mechanisms" have been proposed as causes of mass extinction events, and the K-T boundary event in particular (see Chapter 1), but linking extinction patterns to potential forcing factors is difficult because of the nature of complex biological systems (Jablonski 1996, 1997). For example, "a single 'forcing factor' might have radically different effects depending on the state of the system at the time of perturbation, and a single extinction pattern might be equally consistent with a host of potential forcing factors" (Jablonski 1997, p. 354).

Sedimentological and geochemical evidence for an impact at the end of the Cretaceous is overwhelming (Glen 1994; MacLeod 1996a) and it is now generally accepted that there was a bolide impact at or near the stratigraphic K-T boundary. In addition, a mass extinction did occur at the end of the Cretaceous (see MacLeod 1996a for a discussion of this point). For some workers the K-T debates are largely over (Ward 1995a, b) whilst for others there is still uncertainty about the role played by an impact (Rigby *et al.* 1994; MacLeod 1996a; Sims 1997). Nevertheless, the globally uniform intensity of the event, demonstrated by the lack of geographical selectivity patterns, attests to its magnitude and rules out the involvement of mechanisms with purely latitudinal or regional effects (Raup & Jablonski 1993).

However, not all Maastrichtian extinctions are coincident with the Cretaceous-Tertiary boundary (Marshall & Ward 1996; Jablonski 1997). For example, inoceramid bivalves had disappeared long before the end of the Maastrichtian (MacLeod 1994; MacLeod *et al.* 1996; Marshall & Ward 1996), a number of ammonites went extinct before the K-T boundary in the Biscay region (Marshall & Ward 1996), and two atelostomate echinoid genera included in this study (*Offaster* and *Hagenowia*) are known only from the Lower Maastrichtian.

These extinctions, together with evidence of deteriorating climate (Barrera 1994; Huber *et al.* 1995), sea level fluctuations (Haq 1991) and flood basalt volcanism (Courtillot *et al.* 1996) during the Maastrichtian as well as the coordinated switch of several clades of echinoid to a non-planktotrophic larval mode (see Chapter 7) suggest that the uppermost Cretaceous was a time of increasing (wholly terrestrial) environmental instability. Several authors see the biotic crisis at the end of the Cretaceous as the superposition of a catastrophic bolide impact on an already stressed fauna (Keller 1996; MacLeod 1996a). Even those who believe that the majority of taxa involved in the K-T mass extinction were killed by an impact and resulting atmospheric and climatic effects (see Chapter 1) accept that it was not the only cause of extinctions during the Maastrichtian. Until finer stratigraphic resolution and the application of confidence intervals to stratigraphic ranges (e.g. Marshall 1995; Marshall & Ward 1996) allow a more precise determination of extinction patterns and until robust patterns of selectivity are known for other taxonomic groups, I do not think it will be possible to say with certainty what role each of the possible multiple causes played in the demise of some atelostomate echinoids (and all dinosaurs) at the end of the Cretaceous. Integration of the atelostomate dataset with information on other echinoid orders would produce a more comprehensive account of selectivity patterns in the marine benthic realm.

When the dust settles.....

There have been plenty of suggestions for prospective extinction research (Ward 1995b). As well as the taxonomic revision, phylogenetic analysis and subsequent search for survivorship correlates in large datasets advocated above, I suggest that

future research would benefit from focusing on patterns of recovery in the aftermath of mass extinction. Some work to this end has already been attempted (Hansen 1988; Hart 1996). Evidence that the K-T event was severe and protracted comes from the small size of individuals well into the Danian (see Chapter 7) and the continuing high levels of extinction in the early Palaeocene (see Chapter 5). Mass extinctions often cause the sudden and rapid demise of successful well adapted species, providing opportunities for new species to flourish (Raup 1995; Erwin 1996). Documentation and analysis of biotic rebound on both ecological and evolutionary timescales will lead to greater appreciation of the effects and perhaps the causes of mass extinctions.

Another, perhaps less glamorous, suggested area for future research is the documentation of extinction patterns at less pervasive extinction events such as the Cenomanian-Turonian boundary. Analysis of such intermediate extinction levels would permit determination of whether all extinction events differ only quantitatively or whether threshold effects separate distinct macroevolutionary regimes.

Finally, the observation that a non-planktotrophic developmental pattern first evolved, and was independently adopted, in nine clades over a broad taxonomic and latitudinal range immediately prior to the Cretaceous-Tertiary boundary strongly suggests that changes in life history and developmental mode are primarily driven by extrinsic, global environmental factors (see Chapter 7). However, evidence that the same suite of environmental factors are associated with the switch to non-planktotrophy at other times in the past is necessary to produce a convincing case. Thus, a fruitful area for future research is the investigation of the post-Cretaceous record of echinoids, when non-planktotrophy arose in many more lineages, in order to determine precisely when and where non-planktotrophic modes of development evolved. By searching for underlying patterns, it will be possible to ascertain whether or not changes in developmental mode are indeed linked with environmental factors.

REFERENCES

Agassiz, L. 1836. Prodrome d'une monographie des Radiaires ou Échinodermes. *Mémoires de la Société des Sciences Naturelles de Neuchâtel* **1**, 168-199.

Agassiz, L. & Desor, E. 1846-47. *Catalogue raisonné des familles, des genres et des espèces de la classe des échinodermes.* Martinet, Paris, 167 pp.

Airaghi, C. 1934. Echinidi Paleogenici della Sirtica e del Fezzan Orientale. *Missione Scientifica della Reale Accademia d'Italia a Cufra* **3**, 61-81.

Airaghi, C. 1939. Echinidi Cretacici e Terziari della Regione di Orfella e della Sirtica. *Annali del Museo Libico di Storia Naturale* **1**, 253-286, pls 10-12.

Akkus, M.F. 1971. Geologic and stratigraphic investigation of the Darende-Balaban Basin (Malatya, ESE Turkey). *Bulletin of the Mineral Research and Exploration Institute of Turkey* **76**, 1-54.

Ali, M.S.M. 1989. Late Cretaceous echinoids from Gebel El Rowdah, Hatta area, U.A.E. *Neues Jahrbuch für Geologie, Paläontologie und Mineralogie Abhandlungen* **177**, 393-412.

Alvarez, L.W., Alvarez, W., Asaro, F. & Michel, H.V. 1980. Extraterestrial cause for the Cretaceous-Tertiary extinction. *Science* **208**, 1095-1108.

Amard, B., Collignon, M. & Roman, J. 1981. Étude stratigraphique et paléontologique du Crétacé superieur et Paléocène du Tinrhert-W et Tademait-E (Sahara Algérien). *Documents des Laboratoires de Geologie, Lyon; Hors Serie* **6**, 15-173.

Anthula, D.J. 1899. Über die Kreidefossilien des Kaukasus. *Beiträge zur Paläontologie und Geologie Österreich-Ungarns und des Orients* **12**, 55-102, pls 2-7.

Archie, J.W. 1985. Methods for coding variable morphological features for numerical taxonomic analysis. *Systematic Zoology* **34**, 326-345.

Asgaard, U. 1979. The irregular echinoids and the boundary in Denmark. *In* Birkelund, T. & Bromley, R.G. (eds), *Cretaceous-Tertiary Boundary Events Symposium I: The Maastrichtian and Danian of Denmark.* University of Copenhagen, 74-77.

Aziz, S.A. & Badve, R.M. 1990. Occurrence of *Hemipneustes* Agassiz (echinoid) from Tiruchirapalli Cretaceous, Tamil Nadu, India. *Journal of the Geological Society of India* **36**, 326-330.

Banerjee, A. & Boyajian, G. 1996. Changing biologic selectivity of extinction in the foraminifera over the past 150 m.y. *Geology* **24**, 607-610.

Barrera, E. 1994. Global environmental changes preceding the Cretaceous-Tertiary boundary: Early-late

Maastrichtian transition. *Geology* **22**, 877-880.

Barrera, E. & Keller, G. 1994. Productivity across the Cretaceous-Tertiary boundary in high latitudes. *Geological Society of America Bulletin* **106**, 1254-1266.

Bather, F.A. 1904. Eocene echinoids from Sokoto. *Geological Magazine; New Series; Decade 5* **1**, 292-304, pl. 11.

Besairie, H. 1930. Recherches géologiques a Madagascar. *Bulletin de la Société d'Histoire Naturelle de Toulouse* **60** (2), 272 pp.

Besairie, H. 1971. Geologie de Madagascar I: Les terrains sedimentaires. *Madagascar Annales Géologiques du Service des Mines* **35**, 1-463, pls 1-89.

Besairie, H. & Lambert, J. 1930. Notes sur quelques échinides de Madagascar et du Zululand. *Bulletin de la Société Géologique de France, 4th Series* **30**, 107-117.

Blake, D.B. & Zinsmeister, W.J. 1991. A new marsupiate cidaroid echinoid from the Maastrichtian of Antarctica. *Palaeontology* **34**, 629-635.

Blayac, J. 1912. Esquisse géologiques du bassin de la Seybouse et de quelques régions voisines. *Bulletin du Service de la Carte Géologique de l'Algérie; 2nd Series* **6**, 490 pp., 5 pls.

Blayac, J. & Cottreau, J. 1909. Échinides Maëstrichtiens de Bordj-Sabath (Algérie). *Bulletin de la Société Géologique de France; 4th Series* **9**, 416-430, pl. 14.

Böhm, J. 1927. Beitrag zur Kenntnis der Senonfauna der Bithynischen Halbinsel. *Palaeontographica* **69**, 187-222, pls 11-18.

Boule, M. 1899. Note sur de nouveaux fossiles secondaires de Madagascar. *Bulletin du Muséum d'Histoire Naturelle* **5**, 130-134.

Boule, M. & Thevenin, A. 1906. Paléontologie de Madagascar 1, Fossiles de la côte orientale. *Annales de Paléontologie* **1**, 43-59, pls 1-2.

Bouillé, R. de. 1873. Paléontologie de Biarritz et des quelques autres localités des Basses Pyrénées. *Congrès Scientifique de France* **39**, 427-450.

Brito, I.M. 1981. Os Equinóides Fósseis do Brasil 3: Espatangóides, exceto Hemiasteridae. *Anais da Academia Brasileira de Ciências* **53**, 569-578.

Bromley, R.G., Jensen, M. & Asgaard, U. 1995. Spatangoid echinoids: deep-tier trace fossils and chemosymbiosis. *Neues Jahrbuch für Geologie, Paläontologie und Mineralogie Abhandlungen* **195**, 25-35.

Brünnich Nielsen, K. 1926. Kalken paa Saltholm. *Danmarks geologiske Undersøgelse; 4th Series* **1** (20), 23 pp.

Brünnich Nielsen, K. 1942. *Martinosigra elongata* n. g. et n. sp. A new echinoid from the white chalk of Denmark. *Meddelelser fra Dansk Geologisk Forening* **10**, 159-166.

Carter, B.D., Beisel, T.H., Branch, W.B. & Mashburn, C.M. 1989. Substrate preferences of Late Eocene (Priabonian/Jacksonian) echinoids of the eastern Gulf Coast. *Journal of Paleontology* **63**, 495-503.

Carter, B.D. & Hamza, F. 1994. Substrate preferences and biofacies distributions of Egyptian Eocene echinoids. *Palaios* **9**, 237-253.

Casey, R. 1960. A new echinoid from the Lower Cretaceous (Albian) of Kent. *Palaeontology* **3**, 260-264.

Catullo, T.A. 1827. Saggio di Zoologia fossile. Padova, 348 pp., 8 pls.

Chabaglian, J. 1959. Le Paléocène dans l'ouest du Sénégal. Étude paléontologique. *Annales de la Faculté des Sciences (Dakar)* **4**, 133-187, pls 1-4.

Chatterton, B.D.E. & Speyer, S.E. 1989. Larval ecology, life history strategies, and patterns of extinction and survivorship among Ordovician trilobites. *Paleobiology* **15**, 118-132.

Checchia-Rispoli, G. 1914. Sopra alcuni Echinidi del Cretaceo superiore della Tripolitania raccolti dal cav. Ignazio Sanfilippo. *Giornale de Scienze Naturali ed Economiche* **30**, 297-310, pl. 1.

Checchia-Rispoli, G. 1921. Fauna del Neocretacico della Tripolitania: Echinidi. *Memorie per servire alla Descrizione della Carta Geologica d'Italia* **8** (2), 1-31, pls 7-9.

Checchia-Rispoli, G. 1931. Sopra alcuni Spatagoidi Maestrichtiano della Tripolitania. *Bollettino del Royal Ufficio Geologico d'Italia* **56** (5), 1-14, pl. 1.

Checchia-Rispoli, G. 1932. "*Sanfilippaster*", nuovo genere di Echinide del Cretaceo superiore. *Atti della Reale Accademia Nazionale dei Lincei; 6th Series* **15**, 313-316.

Checchia-Rispoli, G. 1933. Echinidi Cretacei della Tripolitania. *Bollettino del Royal Ufficio Geologico d'Italia* **58** (9), 1-14, pls 1-2.

Clark, H.L. 1917. Hawaiian and other Pacific Echini. *Memoirs of the Museum of Comparative Zoology* **46** (2), 81-284, pls 144-161.

Clark, W.B. 1893. The Mesozoic Echinodermata of the United States. *Bulletin of the United States Geological Survey* **97**, 207 pp.

Clark, W.B. 1916. Systematic paleontology of the Upper Cretaceous deposits of Maryland. *In Maryland Geological Survey: Upper Cretaceous*. John Hopkins Press, Baltimore, 343-986.

Clark, W.B. & Twitchell, M.W. 1915. The Mesozoic and Cenozoic echinodermata of the United States. *Monographs of the United States Geological Survey* **54**, 341 pp.

Clarke, A. 1988. Seasonality in the Antarctic marine environment. *Comparative Biochemistry and*

Physiology **90B**, 461-473.

Clarke, A. 1990. Temperature and evolution: Southern Ocean cooling and the Antarctic marine fauna. *In* Kerry, K.R. & Hempel, G. (eds), *Antarctic ecosystems: Ecological change and conservation.* Springer, Berlin, 9-22.

Claus, C.F.W. 1876-80. *Grundzüge der Zoologie.* Marburg & Leipzig. 3rd edition, 1254 pp. (1876). 4th edition, **2**, 522 pp. (1880).

Collignon, M. 1949. *Tessieria*, nouveau genre d'échinide du Maëstrichtien du Sénégal (*Tessieria senegalensis*, sp. nov.). *Bulletin de la Société Géologique de France; 5th Series* **19**, 263-268, pl. 9a.

Collignon, M. 1968. Le Crétacé superieur de Madagascar. *Geological Survey of India Memoir* **2**, 320-334.

Collignon, M. & Lambert, J. 1928. Espèces nouvelles d'échinides fossiles établies par Paul Thiéry. *Bulletin de la Société Géologique de France; 4th Series* **28**, 261-272, pls 20-21.

Cooke, C.W. 1953. American Upper Cretaceous Echinoidea. *Geological Survey Professional Paper* **254-A**, 44 pp., 16 pls.

Cooke, C.W. 1959. Cenozoic Echinoids of Eastern United States. *Geological Survey Professional Paper* **321**, 106 pp., 43 pls.

Cooper, M.R. & Greyling, E.H. 1990. A spatangoid echinoid from the Upper Cretaceous (Maastrichtian) of Zululand. *South African Journal of Geology* **93**, 412-416.

Coquand, H. 1862. Géologie et paléontologie de la region sud de la province de Constantine. *Mémoires de la Société d'Émulation de la Provence* **2**, 1-342, 35 pls.

Coquand, H. 1880. Études supplémentaires sur la paléontologie algérienne faisant suite a la description géologique et paléontologique de la region sud de la province de Constantine. *Bulletin de l'Académie d'Hippone* **15**, 449 pp.

Cotteau, G. 1863. Échinides fossiles des Pyrénées. *Congrès Scientifique de France; 28me session (Bordeaux)*, 165-320, pls 1-9.

Cotteau, G. 1874. Note sur les échinides crétacés de la province du Hainaut. *Bulletin de la Société Géologique de France; 3rd Series* **2**, 638-660.

Cotteau, G. 1877. Description des Échinides de la Colonie du Garumnien. *Annales des Sciences Géologiques* **9**, 55-72, pls 4-7.

Cotteau, G. 1879. Description des échinides du Calcaire Grossier de Mons. *Mémoires couronnés et Mémoires des Savants Étrangers publiés par l'Académie Royale des Sciences, des Lettres et des*

Beaux-Arts de Belgique **42**, 12 pp., 1 pl.

Cotteau, G. 1881. Description des échinides fossiles de l'île de Cuba. *Annales de la Société Géologique de Belgique* **9** (Memoir 4) 1-49, pls 1-4.

Cotteau, G. 1883. Échinides Jurassiques, Crétacés et Tertaires du sud-ouest de la France. *Annales de la Société des Sciences Naturelles de la Charente-Inférieure* **19**, 45-253, 12 pls.

Cotteau, G. 1884. Échinides nouveaux ou peu connus; 2nd series, 3rd article. *Bulletin de la Société Zoologique de France* **9**, 328-342, pls 8-10.

Cotteau, G. 1886. Échinides nouveaux ou peu connus; 2nd series, 5th article. *Bulletin de la Société Zoologique de France* **11**, 708-728.

Cotteau, G. 1888. Échinides nouveaux ou peu connus; 2nd series, 7th article. *Mémoires de la Société Zoologique de France* **1**, 253-269.

Cotteau, G. 1889. Échinides crétacés de Madagascar. *Bulletin de la Société Zoologique de France* **14**, 87-89.

Cotteau, G. 1891. Échinides nouveaux ou peu connus; 2nd series, 10th article. *Mémoires de la Société Zoologique de France* **4**, 620-633.

Cotteau, G. 1892a. Notice sur l'*Hemipneustes oculatus* de la Craie de Ciply et les autres espèces du genre *Hemipneustes*. *Annales de la Société Malacologique de Belgique* **25**, 1-10, pl. 1.

Cotteau, G. 1892b. Échinides nouveaux ou peu connus; 2nd series, 11th article. *Mémoires de la Société Zoologique de France* **5**, 731-742, pls 10-11.

Cotteau, G. & Gauthier, V. 1895. *Mission scientifique en Perse par J. de Morgan, tome 3. Etudes géologiques, partie 2 - paléontologie: échinides fossiles.* Leroux, Paris, 142 pp.

Cotteau, G., Peron, P.A. & Gauthier, V. 1881. *Échinides fossiles de l'Algérie: Fascicule 7: Étage Sénonien.* Masson, Paris, 1-197, pls 1-20.

Cotteau, G. & Triger, J. 1855-69. *Échinides du Département de la Sarthe, considérés au point de vue zoologique et stratigraphique.* Baillière et fils, Paris, 455 pp., 66 pls.

Cottreau, J. 1908a. Échinides du Soudan. *Bulletin de la Société Géologique de France; 4th Series* **8**, 551-553.

Cottreau, J. 1908b. Paléontologie de Madagascar 6; Les échinides. *Annales de Paléontologie* **3**, 145-188, pls 13-17.

Cottreau, J. 1922. Paléontologie de Madagascar 10; Fossiles crétacés de la cote orientale. *Annales de Paléontologie* **11**, 111-188, pls 9-19.

Cottreau, J. 1935. Quelques échinides fossiles de Madagascar. *Archives du Muséum d'Histoire*

Naturelle, Paris. 6th Series **12**, 259-264, pl. 1.

Courtillot, V., Jaeger, J.-J., Yang, Z., Féraud, G. & Hofmann, C. 1996. The influence of continental flood basalts on mass extinctions: Where do we stand? *In* Ryder, G., Fastovsky, D. & Gartner, S. (eds), *The Cretaceous-Tertiary Event and Other Catastrophes in Earth History. Geological Society of America Special Paper* **307**, 513-525.

Crutzen, P.J. 1987. Acid rain at the K/T boundary. *Nature* **330**, 108-109.

Currie, E.D. 1925. Jurassic and Eocene Echinoidea. *Monograph of the Geological Department of the Hunterian Museum, Glasgow University* **1**, 46-76, pls 8-10.

Currie, E.D. 1927. Jurassic and Eocene Echinoidea from Somaliland. *Transactions of the Royal Society of Edinburgh* **55**, 411-441, pl. 55.

Currie, E.D. 1943. Palaeontology of Harrar Province, Ethiopia. Part 2: Echinoidea. *Bulletin of the American Museum of Natural History* **82**, 14-29.

Cuvier, G.L.C.F.D. 1822. *Description Géologique des environs de Paris.* Paris, 428 pp., 16 pls.

Cys, J.M. 1967. The inability of dinosaurs to hibernate as a possible key factor in their extinction. *Journal of Paleontology* **41**, 266-267.

Dalloni, M. 1924. Note préléminaire sur les terrains crétacés des Monts de la Mina et du Massif des Beni Chougrane (Tell Oranais). *Bulletin du Service de la Carte Géologique de l'Algérie; Travaux Récents* **1**, 93-119.

David, B. 1987. Dynamics of plate growth in the deep-sea echinoid *Pourtalesia miranda* Agassiz: a new architectural interpretation. *Bulletin of Marine Science* **40**, 29-47.

David, B. 1988. Origins of the deep-sea holasteroid fauna. *In* Paul, C.R.C. & Smith, A.B. (eds), *Echinoderm phylogeny and evolutionary biology.* Clarendon Press, Oxford, 331-346.

Davies, L.M. 1943. Tertiary Echinoidea of the Kohat-Potwar Basin. *Quarterly Journal of the Geological Society of London* **99**, 63-79.

Desor, E. 1853. Notice sur les échinides du terrain nummulitique des Alpes avec les dignoses et plusiers espèces et genres nouveaux. *Actes de la Société Helvétique des Sciences Naturelles* **38**, 270-279.

Desor, E. 1855-58. *Synopsis des Échinides fossiles.* Reinwald, Paris and Kreidel & Niedner, Weisbaden, 490 pp., 44 pls.

Devriès, A. 1954. A propos de la symétries des échinides. *Bulletin de la Service Carte Geologique de l'Algérie* **1**, 91-128.

Devriès, A. 1967. Études sur des échinides fossiles de Turquie. *Travaux de l'Institut de Géologie et*

d'Anthropologie Préhistorique de la Faculté des Sciences de Poitiers **8**, 161-200, pls 1-6.

D'Hondt, S. & Lindinger, M. 1994. A stable isotopic record of the Maastrichtian ocean-climate system: South Atlantic DSDP site 528. *Palaeogeography, Palaeoclimatology, Palaeoecology* **112**, 363-378.

D'Hondt, S., Pilson, M.E.Q., Sigurdsson, H., Hanson, A.K. Jr & Carey, S. 1994. Surface water acidification and extinction at the Cretaceous-Tertiary boundary. *Geology* **22**, 983-986.

Ditchfield, P.W., Marshall, J.D. & Pirrie, D. 1994. High latitude palaeotemperature variation: New data from the Tithonian to Eocene of James Ross Island, Antarctica. *Palaeogeography, Palaeoclimatology, Palaeoecology* **107**, 79-101.

Doncieux, L. 1905. Catalogue descriptif des fossiles nummulitiques de l'Aube et de l'Héraut. *Annales de l'Université de Lyon; Nouvelle Série* **17**, 1-184.

Donovan, S.K. 1993. Jamaican Cretaceous Echinoidea. *Geological Society of America Memoir* **182**, 93-103.

Donovan, S.K. & Lewis, D.N. 1993. The H.L. Hawkins collection of Caribbean fossil echinoids: Annotated catalog of rediscovered specimens from the University of Reading, England. *Caribbean Journal of Science* **29**, 186-201.

Dru, L. 1884. Note sur la Géologie et l'Hydrologie de la région du Bechtaon (Russie-Causase). *Bulletin de la Société Géologique de France, 3rd Series* **12**, 474-515.

Düben, M.W. & Koren, J. 1844. Öfversigt af Skandinaviens Echinodermer. *Konglige Vetenskaps Akademiens Handlingar* **1844**, 227-328.

Duncan, P.M. 1889. A revision of the genera and great groups of the Echinoidea. *Journal of the Linnean Society of London; Zoology* **23**, 1-311.

Duncan, P.M. & Sladen, W.P. 1882a. The fossil Echinoidea from the strata beneath the trap (*Cardita beaumonti* beds). *Palaeontologia Indica; 14th Series* **1** (3), 1-20, pls 1-4.

Duncan, P.M. & Sladen, W.P. 1882b. The fossil Echinoidea from the Ranikot Series of nummulitic strata in western Sind. *Palaeontologia Indica; 14th Series* **1** (3), 21-100, pls 5-20.

Durham, J.W. & Melville, R.V. 1957. A classification of echinoids. *Journal of Paleontology* **31**, 242-272.

Dzhalilov, M.R. & Egorov, E.V. 1969. [Late Senonian sea urchins and some new data on stratigraphy of the Upper Senonian in the southwestern spurs of the Gissar Ridge.] *Izvestiya Akademiia Nauk Tadzhik SSR* **34**, 105-114. [In Russian].

Elliot, D.H., Askin, R.A., Kyte, F.T. & Zinsmeister, W.J. 1994. Iridium and dinocysts at the Cretaceous-Tertiary boundary on Seymour Island, Antartica: Implications for the K-T event. *Geology* **22**, 675-678.

Emlet, R.B. 1985. Crystal axes in Recent and fossil echinoids indicate trophic mode in larval development. *Science* **230**, 937-940.

Emlet, R.B. 1988. Crystallographic axes of echinoid genital plates reflect larval form: some phylogenetic implications. *In* Paul, C.R.C. & Smith, A.B. (eds), *Echinoderm phylogeny and evolutionary biology*. Clarendon Press, Oxford, 299-310.

Emlet, R.B. 1989. Apical skeletons of sea urchins (Echinodermata: Echinoidea): Two methods for inferring mode of larval development. *Paleobiology* **15**, 223-254.

Emlet, R.B. 1990. World patterns of developmental mode in echinoid echinoderms. *In* Hosht, M. & Yamashita, O. (eds), *Advances in invertebrate reproduction 5*. Elsevier, Amsterdam, 329-335.

Emlet, R.B. 1995. Developmental mode and species geographic range in regular sea urchins (Echinodermata: Echinoidea). *Evolution* **49**, 476-489.

Emlet, R.B., McEdward, L.R. & Strathmann, R.R. 1987. Echinoderm larval ecology viewed from the egg. *Echinoderm Studies* **2**, 55-136.

Ernst, G. 1972. Grundfragen der Stammesgeschichte bei irregulären Echiniden der nordwesteuropäischen Oberkreide. *Geologisches Jahrbuch; Series A* **4**, 63-175.

Erwin, D.H. 1989a. Regional paleoecology of Permian gastropod genera, southwestern United States, and the end-Permian mass extinction. *Palaios* **4**, 424-438.

Erwin, D.H. 1989b. The end-Permian mass extinction: What really happened and did it matter? *Trends in Ecology and Evolution* **4**, 225-229.

Erwin, D.H. 1990. The end-Permian mass extinction. *Annual Reviews in Ecology and Systematics* **21**, 69-91.

Erwin, D.H. 1996. The mother of mass extinctions. *Scientific American* **275**(1), 56-62.

Farris, J.S. 1988. *Hennig86, Version 1.5.* [MSDOS computer program].

Felsenstein, J. 1985. Confidence limits on phylogenies: An aproach using the bootstrap. *Evolution* **39**, 783-791.

Fischer, A.G. 1963. Essay review: Descriptive palaeoclimatology, Nairn, A.E.M. (ed.). *American Journal of Science* **261**, 282-293.

Fischer, G.A. 1966. Spatangoids. *In* Moore, R.C. (ed.), *Treatise of Invertebrate Paleontology, Echinodermata* **3** (2). Geological Society of America, Inc. & University of Kansas Press, Kansas,

U543-U628.

Fisher, D.C. & Bodenbender, B.E. 1993. CALCAXES: A program for computation of calcite crystallographic axis orientations. *Contributions from the Museum of Paleontology, University of Michigan* **28**, 327-363.

Flessa, K.W. 1990. The "facts" of mass extinctions. *In* Sharpton, V.L. & Ward, P.D. (eds), *Global Catastrophes in Earth History; An interdisciplinary conference on impact, volcanism and mass mortality. Geological Society of America Special Paper* **247**, 1-7.

Forbes, E. 1848. Report on the Fossil Invertebrata from Southern India, collected by Mr Kaye and Mr Cuncliffe. *Transactions of the Geological Society of London; 2nd Series* **7**, 97-174, pls 7-19.

Forbes, E. 1850. On *Cardiaster*, a new genus of Cretaceous Echinidae allied to *Holaster*. *Annals and Magazine of Natural History; 2nd Series* **6**, 442-444.

Forbes, E. 1852. Figures and descriptions illustrative of British organic remains. *Memoirs of the Geological Survey of the United Kingdom; Decade* **4**, 1-4, 10 pls.

Foster, R.J. 1974. Eocene echinoids and the Drake Passage. *Nature* **249**, 751.

Foster, R.J. & Philip, G.M. 1978. Tertiary holasteroid echinoids from Australia and New Zealand. *Palaeontology* **21**, 791-822.

Fourtau, R. 1913. *Catalogue des invertébrés fossiles de l'Égypte représentés dans les collections du Geological Museum au Caire: Terrains Tertaires 1: Échinides Éocènes.* Imprimerie Nationale, Cairo, 93 pp.

Fourtau, R. 1914. Catalogue des invertébrés fossiles de l'Égypte représentés dans les collections du Musée de Géologie au Caire: Terrains Crétacé 1: Échinodermes. *Geological Survey of Egypt Palaeontological Series* **2**, 109 pp, 8 pls.

Furon, R. 1941. Géologie du Plateau Iranien (Perse - Afghanistan - Béloutchistan). *Mémoires du Muséum National d'Histoire Naturelle; Nouvelle Série* **7**, 177-414.

Gale, A.S. The Cretaceous World. *In* Culver, S.J. & Rawson, P.F. (eds), *Biotic Response to Global Change: The Last 145 Million Years*, in press.

Gale, A.S. & Smith, A.B. 1982. The palaeobiology of the Cretaceous irregular echinoids *Infulaster* and *Hagenowia. Palaeontology* **25**, 11-42.

Gallagher, W.B. 1991. Selective extinction and survival across the Cretaceous/Tertiary boundary in the northern Atlantic Coastal Plain. *Geology* **19**, 967-970.

Gallemí, J. 1992. *Los Yacimientos con Equinidos del Cretacico Superior del prepirineo de la provincia de Lleida.* Unpublished PhD thesis. Universitat Autònoma de Barcelona, 429 pp.

Gallemí, J., López, G., Martínez, R, Muñoz, J. & Pons, J.M. 1995. Distribution of some Campanian and Maastrichtian macrofaunas in southeast Spain. *Cretaceous Research* **16**, 257-271.

Gauthier, H. 1957. Contribution à l'étude géologique des formations post-liasiques des bassins du Dadès et du Haut Todra. Notes et Mémoiires du Service Géologique (Maroc) 119, 212 pp, 14 pls.

Gauthier, V. 1887. Types nouveaux d'échinides crétacés. *Association Française pour l'Avancement des Sciences; 16th session (Toulouse)*, 527-534, pl. 16.

Gauthier, V. 1892. *Notes sur les échinides crétacés recueillis en Tunisie.* Annexe de la Carte Geologique de la Tunisie, Paris, 52 pp., 4 pls.

Gauthier, V. 1897. Contribution a l'étude des échinides fossiles. *Bulletin de la Société Géologique de France; 3rd Series* **25**, 831-841.

Gauthier, V. 1903. Contribution a l'étude des échinides fossiles. *Bulletin de la Société Géologique de France; 4th Series* **3**, 19-29.

Gill, C. & Martinell, J. 1994. Relationship between species longevity and larval ecology in nassariid gastropods. *Lethaia* **27**, 291-299.

Glen, W. 1994. What the impact/volcanism/mass-extinction debates are about. *In* Glen, W. (ed.), *The Mass-Extinction Debates: How Science Works in a Crisis.* Stanford University Press, California, 7-38.

Goldfuss, G.A. 1829-31. *Petrefacta Germaniae tam ea quae in Museo Universitatis Regiae Bourssicae Fridericiae Rhenanae servantur quam alia quaecumque in Museis Hoeninghusiano aliisque extant Iconibus et Descriptionibus illustrata.* **1**. Arnz & Co., Düsseldorf, 252 pp., 71 pls.

Gongadze, G.S. 1979. [*Late Cretaceous echinoids of the Georgian Republic and their stratigraphic significance.*] Tbilisi University Press, Tbilisi, 151 pp., 33 pls. [In Russian].

Grateloup. 1836. Mémoire de géo-zoologie sur les oursins fossiles (échinides), qui se rencontrent dans les terrains calcaires des environs de Dax (Département des Landes). *Actes de la Société Linnéenne de Bordeaux; 1st Series* **8**, 103-191, 2 pls.

Gravesen, P. 1979. Remarks on the regular echinoids in the Upper Maastrichtian and Lower Danian of Denmark. *In* Birkelund, T. & Bromley R.G. (eds), *Cretaceous-Tertiary Boundary Events Symposium I: The Maastrichtian and Danian of Denmark.* University of Copenhagen, 72-73.

Gray, J.E. 1855. *Catalogue of the Recent Echinida or sea eggs in the collection of the British Museum 1: Echinida Irregularia.* Woodfall & Kinder, London, 69 pp., 6 pls.

Gregory, J.W. 1892. The Maltese fossil Echinoidea and their evidence on the correlation of the Maltese

rocks. *Transactions of the Royal Society of Edinburgh* **55**, 585-639, pls 1-2.

Greyling, E.H. 1996. A new species of *Micraster* (Echinoidea: Spatangoida) and the first record of *Hemiaster (Bolbaster)* Pomel from the Upper Cretaceous (Maastrichtian/Campanian) of Zululand. *Durban Museum Novitates* **21**, 25-36.

Grossouvre, A. de 1901. Recherches sur la Craie supérieure: Stratigraphie générale. *Mémoires de la Service de la Carte Geologique de France*, 1013 pp.

Ham, R.W.J.M. van der. 1984. De zeeëgel *Hemiaster koninckanus* d'Orbigny, 1855 in het Maastrichtien van Zuid-Limburg en aangrenzende delen België en Duitsland. *Natuurhistorisch Maandblad* **73**, 169-176.

Ham, R.W.J.M. van der. 1985. De zeeëgel *Hemiaster aquisgranensis* Schlüter, 1899 in het Campaniën en het Maastrichtiën van Zuid-Limburg en aangrenzende delen van Belgiëen Duitland. *Natuurhistorisch Maandblad* **74**, 147-156.

Ham, R.W.J.M. van der. 1988. Echinoids from the early Palaeocene (Danian) of the Maastricht area (NE Belgium, SE Netherlands): preliminary results. *Mededelingen van de Werkgroep voor Tertiaire en Kwartaire Geologie* **25**, 127-161.

Ham, R.W.J.M. van der. 1995. *Hemiaster (Leymeriaster) eluvialis*, a new echinoid from the late Maastrichtian of NE Belgium and SE Netherlands. *Bulletin de l'Institut Royal des Sciences Naturelles de Belgique, Sciences de la Terre* **65**, 153-164.

Ham, R.W.J.M. van der & Birgelen, M. van. 1992. Zeeëgels uit het Maastrichtien van de Schneeberg en Omgeving (Aken, Duitsland). *Natuurhistorisch Maandblad* **81**, 139-153.

Ham, R.W.J.M. van der, Wit, W. de, Zuidema, G. & Birgelen, M. van. 1987. Zeeëgels uit het Krijt en Teriair van Maastricht, Luik en Aken. *Publicaties van het Natuurhistorisch Genootschap in Limburg* **36**, 1-91.

Hansen, T.A. 1978. Larval dispersal and species longevity in lower Tertiary gastropods. *Science* **199**, 885-887.

Hansen, T.A. 1980. Influence of larval dispersal and geographic distribution on species longevity in neogastropods. *Paleobiology* **6**, 193-207.

Hansen, T.A. 1982. Modes of larval development in early Tertiary neogastropods. *Paleobiology* **8**, 367-377.

Hansen, T.A. 1983. Modes of larval development and rates of speciation in early Tertiary neogastropods. *Science* **220**, 501-502.

Hansen, T.A. 1988. Early Tertiary radiation of marine molluscs and the long-term effects of the

Cretaceous-Tertiary extinction. *Paleobiology* **14**, 37-51.

Hansen, T.A., Upshaw, B. III, Kauffman, E.G. & Gose, W. 1993. Patterns of molluscan extinction and recovery across the Cretaceous-Tertiary boundary in east Texas; report on new outcrops. *Cretaceous Research* **14**, 685-706.

Haq, B. 1991. Sequence stratigraphy, sea-level change and significance for the deep sea. *International Association of Sedimentologists Special Publication* **12**, 3-39.

Hart, M.B. 1996. *Biotic Recovery from Mass Extinction Events.* The Geological Society, London, 392 pp.

Hassan, M.Y. 1969. Contribution to the echinoid fauna of the Maestrichtian-Paleocene strata of southwestern Egypt. *Proceedings of the Egyptian Academy of Sciences* **22**, 15-19, 1 pl.

Hawkins, H.L. 1923. Some Cretaceous Echinoidea from Jamaica. *Geological Magazine* **60**, 199-216, pl. 9.

Hawkins, H.L. 1924. Notes on a new collection of fossil Echinoidea from Jamaica. *Geological Magazine* **61**, 312-324.

Hawkins, H.L. 1935. Cretaceous Echinoidea. *Geology and Palaeontology of British Somaliland* **2**, 47-56, pls 6-7.

Hayami, I. 1997. Size changes of bivalves and a hypothesis about the cause of mass extinction. *Fossils* **62**, 24.

Hébert. 1875. Description de deux espèces d'*Hemipneustes* de la Craie supérieure des Pyrénées. *Bulletin de la Société Géologique de France; 3rd Series* **3**, 592-595.

Hennig, A. 1898. Faunan i Skånes Yngre Krita 1: Echiniderna. *Bihang till Kongliga Svenska Vetenskaps-Akademiens Handlingar* **24** (4) (2), 1-12, 1 pl.

Hildebrand, A.R. 1993. The Cretaceous/Tertiary Boundary impact (or the dinosaurs didn't have a chance). *Journal of the Royal Astronomical Society* **87**, 77-118.

Hildebrand, A.R., Penfield, G.T., Kring, D.A., Pilkington, M., Jacobsen, S. & Boynton, W.V. 1991. The Chicxulub crater: A possible Cretaceous-Tertiary boundary crater on the Yucatán Peninsula, Mexico. *Geology*, **19**, 867-871.

House, M.R. 1985. Correlation of mid-Palaeozoic ammonoid evolutionary events with global sedimentary perturbations. *Nature* **313**, 17-22.

Huber, B.T. 1996. Evidence for planktonic foraminifer reworking versus survivorship across the Cretaceous-Tertiary boundary at high latitudes. *In* Ryder, G., Fastovsky, D & Gartner, S. (eds), *The Cretaceous-Tertiary Event and Other Catastrophes in Earth History. Geological Society of*

America Special Paper **307**, 319-334.

Huber, B.T., Hodell, D.A. & Hamilton, C.P. 1995. Middle-Late Cretaceous climate of southern high latitudes: stable isotopic evidence for minimal equator-to-pole thermal gradients. *Geological Society of America Bulletin* **107**, 1164-1191.

Izett, G.A., Cobban, W.A., Obradovich, J.D. & Kunk, M.J. 1993. The Manson impact structure: $^{40}Ar/^{39}Ar$ age and its distal impact ejecta in the Pierre Shale in southeastern South Dakota. *Science* **262**, 729-732.

Jablonski, D. 1978. Transgressions, regressions, and endemism in Gulf Coast Cretaceous mollusks. *Geological Society of America Abstracts with Programs* **10**, 427-428.

Jablonski, D. 1982. Evolutionary rates and modes in late Cretaceous gastropods: Role of larval ecology. *In* Mamet, B.L. & Copeland, M.J. (eds), *Proceedings, Third North American Paleontological Convention 1.* University of Montreal, Montreal & Geological Survey of Canada, Ottowa, 257-262.

Jablonski, D. 1986a. Background and mass extinctions: The alternation of macroevolutionary regimes. *Science* **231**, 129-131.

Jablonski, D. 1986b. Larval ecology and macroevolution in marine invertebrates. *Bulletin of Marine Science* **39**, 565-587.

Jablonski, D. 1989. The biology of mass extinction: A paleontological view. *Philosophical Transactions of the Royal Society of London* **B325**, 357-368.

Jablonski, D. 1991. Extinctions: A palaeontological perspective. *Science* **253**, 754-757.

Jablonski, D. 1995. Extinctions in the fossil record. *In* Lawton, J.H. & May, R.M. (eds), *Extinction Rates.* Oxford University Press, Oxford, 25-44.

Jablonski, D. 1996. Mass extinctions: Persistent problems and new directions. *In* Ryder, G., Fastovsky, D. & Gartner, S. (eds), *The Cretaceous-Tertiary Event and Other Catastrophes in Earth History. Geological Society of America Special Paper* **307**, 1-9.

Jablonski, D. 1997. Progress at the K-T boundary. *Nature* **387**, 354-355.

Jablonski, D. & Raup, D.M. 1995. Selectivity of end-Cretaceous marine bivalve extinctions. *Science* **268**, 389-391.

Jackson, J.B.C. 1974. Biogeographic consequences of eurytopy and stenotopy among marine bivalves and their evolutionary significance. *American Naturalist* **108**, 541-560.

Jagt, J.W.M. & Michels, G.P.H. 1987. *Cyclaster platornatus* Kutscher, 1978: an addition to the echinoid fauna from the late Maastrichtian of NE Belgium. *Geologie en Mijnbouw* **66**, 57-63

Jagt, J.W.M. & Michels, G.P.H. 1990. Additional note on the echinoid genus *Cyclaster* from the Late Maastrichtian of northeastern Belgium. *Geologie en Mijnbouw* **69**, 179-185.

Jagt, J.W.M. & van der Ham, R. 1994. Early Palaeocene marsupiate regular echinoids from NE Belgium. *In* David, B., Guille, A., Feral, J.-P. & Roux, M. (eds), *Echinoderms through time*. Balkema, Rotterdam, 725-729.

Jeannet, A. 1928. Contribution à l'étude des échinides tertiaires de la Trinité et du Venezuela. *Mémoires de la Société Paléontologique Suisse* **48**, 1-49, pls 1-6.

Jeffery, C.H. 1997a. Revision of the echinoid *Enallopneustes* from the Upper Cretaceous of North Africa. *Cretaceous Research* **18**, 237-248.

Jeffery, C.H. 1997b. All change at the K-T boundary? Echinoids from the Maastrichtian and Danian of the Mangyshlak Peninsula, Kazakhstan. *Palaeontology* **40**, 659-712.

Jeffery, C.H. & Smith, A.B. Estimating extinction levels for echinoids across the Cretaceous-Tertiary boundary. *In* Mooi, R. & Telford, M. (eds), *Echinoderms: San Francisco*. Balkema, Rotterdam, in press.

Jeslonek-Szymanska, W. 1959. Remarks on the structure of the apical system of irregular echinoids *Acta Paleontologica Polonica* **4**, 339-351.

Johansen, M.B. 1989. Background extinction and mass extinction of the brachiopods from the chalk of northwest Europe. *Palaios* **4**, 243-250.

Joysey, K.A. 1954. The structure of the plastron of the echinoid *Somaliaster* Hawkins. *Geological Magazine* **91**, 45-48.

Kalho, K. 1994. Planktonic and benthic foraminiferal extinction events during the last 100 m.y *Palaeogeography, Palaeoclimatology, Palaeoecology* **111**, 45-71.

Kanazawa, K. 1992. Adaption of test shape for burrowing and locomotion in spatangoid echinoids *Palaeontology* **35**, 733-750.

Kauffman, E.G. 1978. Evolutionary rates and patterns among Cretaceous Bivalvia. *Philosophical Transactions of the Royal Society of London* **B284**, 277-304.

Keller, G. 1996. The Cretaceous-Tertiary mass extinction in planktonic foraminifera: Biotic constraints for catastrophe theories. *In* MacLeod, N. & Keller G. (eds), *Cretaceous-Tertiary Mass Extinctions* W.W. Norton & Company, New York, 49-84.

Keller, G.R., Barrera, E., Schmitz, B & Mattson, E. 1993. Gradual mass extinction, species survivorship, and long-term environmental changes across the Cretaceous-Tertiary boundary in high latitudes. *Bulletin of the Geological Society of America* **105**, 979-997

Kennedy, W.J. 1989. Thoughts on the evolution and extinction of Cretaceous ammonites. *Proceedings of the Geological Association* **100**, 251-279.

Kennedy, W.J. 1993. Ammonite faunas of the European Maastrichtian; diversity and extinction. *In* House, M.R. (ed.), *The Ammonoidea: environment, ecology and evolutionary change.* Systematics Association Special Volume 47, 285-326.

Kier, P.M. 1957. Tertiary Echinoidea from British Somaliland. *Journal of Paleontology* **31**, 839-902.

Kier, P.M. 1962. Revision of cassiduloid echinoids. *Smithsonian Miscellaneous Collections* **144** (3), 262 pp., 44 pls.

Kier, P.M. 1967. Sexual dimorphism in an Eocene echinoid. *Journal of Paleontology* **41**, 988-993.

Kier, P.M. 1969. Sexual dimorphism in fossil echinoids. *In* Westerman, G.E.G. (ed.), *Sexual dimorphism in fossil metazoa and taxonomic implications.* Schweizerbart'sche Verlagsbuchhandlung, Stuttgart, 215-222.

Kier, P.M. 1972. Tertiary and Mesozoic echinoids of Saudi Arabia. *Smithsonian Contributions to Paleobiology* **10**, 242 pp.

Kier, P.M. 1977. The poor fossil record of the regular echinoid. *Paleobiology* **3**, 168-174.

Kier, P.M. 1984. Fossil spatangoid echinoids of Cuba. *Smithsonian Contributions to Paleobiology* **55**, 336 pp.

Kier, P.M. & Lawson, M.H. 1978. Index of living and fossil echinoids 1924-1970. *Smithsonian Contributions to Paleobiology* **34**, 182 pp.

Kirchner, G. 1929. Über die Lage der optischen Achse in Skeletteilen von Seeigeln. *Zoologische Jahrbuecher* **51**, 299-312.

Koch, C.F. 1995. Sampling effects, species-sediment relationships, and observed geographic distribution: An uppermost Cretaceous bivalve example. *Geobios* **18**, 237-241.

Konglel, R. 1935. Contribution à l'étude du "siwak" dans les environs de Pulawy (plateau de Lublin). *Travaux de la Société des Sciences et des lettres de Wilno: Classe des Sciences mathématiques et naturelles* **9** (19), 59 pp., 8 pls.

Konglel, R. 1936. Sur quelques échinides nouveaux du Crétacé supérieur des environs de Pulawy. *Travaux de la Société des Sciences et des lettres de Wilno: Classe des Sciences mathématiques et naturelles* **10** (22), 10 pp.

Konglel, R. 1949. Les *Echinocorys* du Danien de Danemark de Suède et de Pologne. *Travaux du Service Géologique de Pologne* 5, 89 pp, 18 pls.

Konglel, R. 1950. Sur quelques échinides nouveaux du Maestrichtien supérieur des environs de Pulawy.

Kier, P.M. 1974. Evolutionary trends and their functional significance in the post-Palaeozoic echinoids. *Journal of Paleontology* **48** *(Supplement; Paleontological Society Memoir 5)*, 1-95.

Acta Geologica Polonica **1**, 311-329.

Konglel, R. & Matweljewówna, L. 1937. Matériaux fauniques de la Craie supérieure des environs de Pulawy. *Travaux de la Société des Sciences et des lettres de Wilno: Classe des Sciences mathématiques et naturelles* **11**, 115-148, pls 5-7.

Kossmat, F. 1897. The Cretaceous deposits of Pondicherri. *Records of the Geological Survey of India* **30**, 51-111.

Kugler, H.G. & Caudri, C.M.B. 1975. Geology and paleontology of Soldado Rock, Trinidad (West Indies). Part 1, Geology and biostratigraphy. *Eclogae Geologicae Helvetiae* **68**, 365-430, 2 pls.

Kutscher, M. 1978a. Neue Echiniden aus dem Unter-Maastricht der Insel Rügen: I. Holasteroidae Durham & Melville. *Zeitschrift für Geologische Wissenschaften*, **6**, 627-639.

Kutscher, M. 1978b. Neue Echiniden aus dem Unter-Maastricht der Insel Rügen: II. Spatangoida Claus, 1876. *Zeitschrift für Geologische Wissenschaften* **6**, 1025-1037.

Lamarck, J.B. 1816. *Histoire naturelle des animaux sans vertèbres 3.* 2nd edition. Paris, 586 pp.

Lambert, J. 1893. Études morphologiques sur le plastron des Spatangides. *Bulletin de la Société des Sciences Historiques et Naturelles de l'Yonne* **46**, 55-98.

Lambert, J. 1896. Note sur quelques échinides crétacés de Madagascar. *Bulletin de la Société Géologique de France; 3rd Series* **24**, 313-332, pls 10-13.

Lambert, J. 1898. Note sur les échinides de la Craie de Ciply. *Mémoires de la Société Belge de Géologie, de Paléontologie et d'Hydrologie* **11**, 141-190, pls 2-5.

Lambert, J. 1902. Sur un *Micraster* nouveau de la Craie de Maestricht. *Bulletin de la Société Belge de Géologie, de Paléontologie et d'Hydrologie* **16**, 121-128, pl. 6.

Lambert, J. 1903. Note sur quelques nouveaux échinides crétacés de Madagascar. *Bulletin de la Société Géologique de France; 4th Series* **3**, 75-88, pl. 3.

Lambert, J. 1907a. Note sur quelques échinides de la Haute-Garonne. *Bulletin de la Société Géologique de France; 4th Series* **6**, 695-723.

Lambert, J. 1907b. Descriptions des échinides fossiles des terrains miocéniques de la Sardaigne 1. *Mémoires de la Société Paléontologique Suisse* **34**, 1-74, pls 1-5.

Lambert, J. 1909. Liste critique des échinides du Calcaire à Baculites du Cotentin. *Bulletin de la Société Linnéenne de Normandie; 6th Series* **2**, 3-30, pl. 1.

Lambert, J. 1911. Description des échinides crétacés de la Belgique. II. Échinides de l'étage Sénonien. *Mémoires du Musée Royal d'Histoire Naturelle de Belgique* **4**, 1-81.

Lambert, J. 1917. Note sur quelques Holasteridae. *Bulletin de la Société des Sciences Historiques et*

Naturelles de l'Yonne **70**, 191-223.

Lambert, J. 1920a. Échinides fossiles des environs de Santander. *Annales de la Société Linnéenne de Lyon* **66**, 1-32, pls 1-3.

Lambert, J. 1920b. Sur quelques genres nouveaux d'échinides. *Mémoires de la Société Académique d'Agriculture, des Sciences, Arts et Belles-lettres du Département de l'Aube; 3rd Series* **55**, 145 174.

Lambert, J. 1927. Revision des échinides fossiles de la Catalogne. *Memorias del Museo de Ciencias Naturales de Barcelona. Serie Geologica*, **1** (1), 1-102, pls 1-4.

Lambert, J. 1931. Échinides Crétacés de la région d'Héraclée. *Annales de la Société Géologique de Belgique* **54** (Mémoires), M1-M12, pl. 1.

Lambert, J. 1932. Étude sur les échinides fossiles du nord de l'Afrique. *Mémoires de la Société Géologique de France; Nouvelle Série* **16**, 228 pp., 8 pls.

Lambert, J. 1933a. Échinides de Madagascar communiqués par M. H. Besairie. *Madagascar Annales Géologiques du Service des Mines* **3**, 1-49, pls 1-4.

Lambert, J. 1933b. Supplément à la révision des échinides fossiles de la Catalogne. *Butlletí de la Institució Catalana d'Història Natural* **33**, 183-195.

Lambert, J. 1935. Sur quelques échinides fossiles de Valence et d'Alicante communiqués par M. le Prof. Darder Pericás. *Boletín de la Sociedad Española de Historia Natural* **35**, 359-371, pls 41-42.

Lambert, J. 1936. Nouveaux échinides fossiles de Madagascar. *Madagascar Annales Géologiques du Service des Mines* **6**, 9-32, pls 1-4.

Lambert, J. 1937. Échinides fossiles du Maroc. *Service des Mines et de la Carte Géologique, Notes et Mémoires* **39**, 109 pp., 4 pls.

Lambert, J. & Charles, F. 1937. Échinides crétacés de la région de Djidde (Anatolie). *Bulletin de la Société Belge de Géologie, de Paléontologie et d'Hydrologie* **47**, 377-401, pls 8-9.

Lambert, J. & Pérébaskine, V. 1929. Notes sur quelques échinides du Soudan. *Bulletin de la Société Géologique de France; 4th Series* **29**, 471-477.

Lambert, J. & Thiéry, P. 1909-25. *Essai de nomenclature raisonnée des échinides.* Librairie Septime Ferrière, Chaumont, 607 pp., 15 pls.

Landman, N.H. 1984. Not to be or to be? *Natural History* **93** (8), 34-42.

Lawrence, J. 1987. *A Functional Biology of Echinoderms.* Croom Helm, London, 340 pp.

Lecuyer, C., Grandjean, P., O'Neil, J.R., Cappetta, H. & Martineau, F. 1993. Thermal excursions in the ocean at the Cretaceous-Tertiary boundary (northern Morocco): ^{18}O record of

phosphatic fish debris. *Palaeogeography, Palaeoclimatology, Palaeoecology* **105**, 235-243.

Leske, N.G. 1778. *Jacobi Theodori Klein Naturalis dispositio Echinodermatum. Additamenta ad I.T. Klein naturalem dispositionem Echinodermatum....* Officiana Gleditschiana, Lipsis, 175 pp.

Lessa, E.P. & Farlña, R.A. 1996. Reassessment of extinction patterns among the Late Pleistocene mammals of South America. *Palaeontology* **39**, 651-662.

Levinton, J.S. 1996. Trophic group and the end-Cretaceous extinction: did deposit feeders have it made in the shade? *Paleobiology* **22**, 104-112.

Leymerie, A. & Cotteau, G. 1856. Catalogue des échinides fossiles des Pyrénées. *Bulletin de la Société Géologique de France; 2nd Series* **13**, 319-355.

Loriol, P. de 1873. Échinologie Helvétique: Descriptions des oursins fossiles de Suisse 2: Échindes de la période crétacée. Geneva, 398 pp, 33 pls.

Loriol, P. de 1883. Eocaene Echinoideen aus Aegypten und der libyschen Wüste. *Palaeontographica* **30**, 1-59, pls 1-11.

Loriol, P. de 1888. Notes pour servir a l'étude des échinodermes. *Recueil Zoologique Suisse* **4**, 365-407, pls 15-18.

Lucas, G. 1953. Existence, dans l'appareil apical des oursins, de deux sortes de plaques génitales. *Comptes Rendus de l'Academie des Sciences, Paris* **237**, 405-407.

Maccagno, A.M. 1941. Osservazioni sul Genere *Somaliaster* Hawkins. *Bollettino della Società Geologica Italiana* **60**, 89-98, pl. 11.

MacLeod, K.G., Huber, B.T. & Ward, P.D. 1996. The biostratigraphy and paleobiogeography of Maastrichtian inoceramids. *In* Ryder, G., Fastovsky, D. & Gartner, S. (eds), *The Cretaceous-Tertiary Event and Other Catastrophes in Earth History. Geological Society of America Special Paper* **307**, 361-373.

MacLeod, N. 1996a. K/T redux. *Paleobiology* **22**, 311-317.

MacLeod, N. 1996b. Testing patterns of Cretaceous-Tertiary planktonic foraminiferal extinction at El Kef (Tunisia). *In* Ryder, G., Fastovsky, D. & Gartner, S. (eds), *The Cretaceous-Tertiary Event and Other Catastrophes in Earth History. Geological Society of America Special Paper* **307**, 287-302.

MacLeod, N. & Keller, G. 1991. How complete are Cretaceous/Tertiary boundary sections? A chronostratigraphic estimate based on graphic correlation. *Bulletin of the Geological Society of America* **103**, 1439-1457.

MacLeod, N. & Keller, G. 1992. Cretaceous planktic foraminifera in lowermost Tertiary sediments; reworked particles or the remains of living populations? *Geological Society of America Abstracts*

with Programs **24** (7), 332.

MacLeod, N. & Keller, G. 1994. Comparative biogeographic analysis of planktic foraminiferal survivorship across the Cretaceous/Tertiary (K/T) boundary. *Paleobiology* **20**, 143-177.

MacLeod, N., Rawson, P.F., Forey, P.L., Banner, F.T., Boudagher-Fadel, M.K., Bown, P.R., Burnett, J.A., Chambers, P., Culver, S., Evans, S.E., Jeffery, C., Kaminski, M.A., Lord, A.R., Milner, A.C., Milner, A.R., Morris, N., Owen, E, Rosen, B.R., Smith, A.B., Taylor, P.D., Urquhart, E. & Young, J.R. 1997. The Cretaceous-Tertiary biotic transition. *Journal of the Geological Society of London* **154**, 265-292.

Maczynska, S. 1989. Class Echinoidea Leske, 1778. *In* Malinowska, L. (ed.), *Geology of Poland, Volume 3: Atlas and Guide to Characteristic Fossils Part 2c, Mesozoic, Cretaceous.* Publishing House Wydawnictwa Geologiczne, Warsaw, 300-315.

Markov, A.V. 1994. [Morphology, systematics and phylogeny of schizasterid sea-urchins.] *Trudy Paleontologicheskogo Instituta Rossiiskaya Akademiya Nauk* **258**, 94 pp. [In Russian].

Marshall, C.R. 1995. Distinguishing between sudden and gradual extinctions in the fossil record: Predicting the position of the Cretaceous-Tertiary iridium anomaly using the ammonite fossil record on Seymour Island, Antarctica. *Geology* **23**, 731-734.

Marshall, C.R. & Ward, P.D. 1996. Sudden and gradual molluscan extinctions in the Latest Cretaceous of western European Tethys. *Science* **274**, 1360-1363.

McClure, M. & Bohonak, A.J. 1995. Non-selectivity in extinction of bivalves in the Late Cretaceous of the Atlantic and Gulf Coastal Plain of North America. *Journal of Evolutionary Biology* **8**, 779-794.

McGhee, G.R. 1996. *The Late Devonian Mass Extinction: The Frasnian/Famennian Crisis.* Columbia University Press, New York, 303 pp.

McKinney, M.L. 1985. Mass extinction patterns of marine invertebrate groups and some implications for a causal phenomenon. *Paleobiology* **11**, 227-233.

McKinney, M.L. 1987. Taxonomic selectivity and continuous variation in mass and background extinctions of marine taxa. *Nature* **325**, 143-145.

McKinney, M.L. 1995. Extinction selectivity among lower taxa: gradational patterns and rarefaction error in extinction estimates. *Paleobiology* **21**, 300-313.

McMamara, K.J. 1985. The spatangoid echinoid *Linthia* from the Late Eocene of southern Australia. *Transactions of the Royal Society of South Australia* **109**, 161-165.

McNamara, K.J. 1987. The holasteroid echinoid *Echinocorys* from the Maastrichtian of Western

Australia. *Records of the Western Australian Museum* **13**, 419-426.

McMamara, K.J. 1993. First record of a spatangoid echinoid from the Paleocene of the Perth Basin, Western Australia. *Records of the Western Australian Museum* **16**, 331-336.

McNamara, K.J. 1994. Diversity of Cenozoic marsupiate echinoids as an environmental indicator. *Lethaia* **27**, 257-268.

McNamara, K.J. & Barrie, D.J. 1993. A new genus of marsupiate spatangoid echinoid from the Miocene of South Australia. *South Australian Museum Records* **26**, 139-147.

McNamara, K.J. & Philip, G.M. 1980. Australian Tertiary schizasterid echinoids. *Alcheringa* **4**, 47-65.

Meek, F.B. & Hayden, F.V. 1858. Descriptions of new species and genera of fossils. *Proceedings of the Academy of Natural Sciences of Philadelphia* **9**, 117-148.

Mileva-Ilieva, T. 1994. Ontogenetic stages and sexual dimorphism in fossil irregular echinoids. *Review of the Bulgarian Geological Society* **55**, 65-68, pls 1-3.

Mileva-Ilieva, T. 1995. Echinoid zonation of the Upper Cretaceous rocks of North Bulgaria. *Proceedings of the 15th Congress of the Carpatho-Balcan Geological Association*, 237-242.

Mintz, L.W. 1968. Echinoids of the Mesozoic families Collyritidae d'Orbigny, 1853 and Disasteridae Gras, 1848. *Journal of Paleontology* **42**, 1272-1288.

Mool, R & David, B. 1996. Phylogenetic analysis of extreme morphologies: deep-sea holasteroid echinoids. *Journal of Natural History* **30**, 913-953.

Moore, R.C. 1966. *Treatise of Invertebrate Paleontology, Echinodermata* **3**. Geological Society of America, Inc. & University of Kansas Press, Kansas, 695 pp.

Morishita, A. 1962. Cretaceous echinoid *Hemiaster* from Shikoku, Japan. *Journal of Earth Science, Nargoya University* **10**, 113-116.

Mortensen, T. 1950. *A monograph of the Echinoidea: Volume 5, Part 1: Spatangoida 1.* Reitzel, Copenhagen, 432 pp., 25 pls.

Mortensen, T. 1951. *A monograph of the Echinoidea: Volume 5, Part 1: Spatangoida 2.* Reitzel, Copenhagen, 593 pp., 64 pls.

Morton, S.G. 1830. Synoposis of the organic remains of the ferruginous sand formation of the United States, with geological remarks. *American Journal of Science* **18**, 243-250.

Morton, S.G. 1833. Supplement to the synopsis of the organic remains of the ferruginous sand formation of the United States. *American Journal of Science* **23**, 288-294.

Morton, S.G. 1834. *Synopsis of the organic remains of the Cretaceous group.* Philadelphia, 88 pp, 19

pls.

Moskvin, M.M. 1964. [Echinoids of the genus Protobrissus from the Danian and Paleocene sediments of the USSR.] *Publication in honour of Academician Y.S. Yovchev.* Sofia, 185-202. [In Russian].

Moskvin, M.M. 1982. New Upper Cretaceous and Paleocene sea urchins of the family Palaeostomatidae. *Paleontological Journal* **16** (3), 100-107.

Moskvin, M.M. 1983. *Pseudogibbaster*: a new genus of Danian and Paleocene echinoids. *Paleontological Journal* **17** (3), 108-112.

Moskvin, M.M. & Poslavskaya, N.A. 1959. Echinodermata. *In* Moskvin, M.M. (ed.), [*Atlas of the Upper Cretaceous Fauna of the northern Caucasus and Crimea.*] Gas Industry of the U.S.S.R, Moscow, 237-304, pls 1-26. [In Russian].

Moskvin, M.M., Solovjev, A.N. & Endelman, L.G. 1980. Class Echinoidea. *In* Menner, V.V. *et al.* (eds), [*Evolution and change in invertebrates at the boundary of the Mesozoic and Cenozoic.*] Izdatel'stvo "Nauka", Moscow, 116-175. [In Russian].

Negi, J.G., Agrawal, P.K., Pandey, O.P. & Singh, A.P. 1993. A possible K-T boundary bolide impact site offshore near Bombay and triggering of rapid Deccan volcanism. *Physics of the Earth and Planetary Interiors* **76**, 189-197.

Néraudeau, D. 1993. Sexual dimorphism in mid-Cretaceous hemiasterid echinoids. *Palaeontology* **36**, 311-317.

Néraudeau, D. 1994. Hemiasterid echinoids (Echinodermata: Spatangoida) from the Cretaceous Tethys to the present-day Mediterranean. *Palaeogeography, Palaeoclimatology, Palaeoecology* **110**, 319-344.

Nestler, H. 1965. Die Rekonstruktion des Lebensraumes der Rügener Schreibkreide-Fauna (Unter-Maastricht) mit Hilfe der Paläoökologie und Paläobiologie. *Geologie* **49**, 1-147.

Nestler, H. 1982. *Die Fossilien der Rügener Schreibkreide.* 2nd edition. Ziemsen Verlag, Wittenberg Lutherstadt, 108 pp.

Nichols, D. 1959. Changes in the chalk heart-urchin *Micraster* interpreted in relation to living forms. *Philosophical Transactions of the Royal Society of London; Series B* **242**, 347-437.

Nicklès, R. 1892. Recherches géologiques sur les terrains Secondaires et Tertaires de la Province d'Alicante et du sud de la Province de Valence. *Annales Hébert* **1**, 219 pp.

Nietsch, H. 1921. Die irregulären Echiniden der pommerschen Kreide. *Abhandlungen aus dem geologisch-palaeontologischen Institut der Universität Griefswald* **2**, 1-47, pls 1-11.

Nisiyama, S. 1968. The echinoid fauna of Japan and adjacent regions, Part 2. *Palaeontological Society*

of Japan Special Papers **13**, 1-491.

Noetling, F. 1897. Fauna of Baluchistan 1 (part 3), Fauna of the Upper Cretaceous (Maëstrichtien) beds of the Mari Hills. *Palaeontologia Indica; 16th Series* **1** (3), 1-79, pls 1-23.

Oberhänsli, H. 1986. Latest Cretaceous-early Neogene oxygen and carbon isotopic record at DSDP sites in the Indian Ocean. *Marine Micropaleontology* **10**, 91-115.

Ødum, H. 1926. Studier over Daniet i Jylland og paa Fyn. *Danmarks geologiske Undersogelse; 2nd Series* **45**, 306 pp., 4 pls.

Officer, C.B. 1990. Extinctions, iridium, and shocked minerals associated with the Cretaceous/Tertiary transition. *Journal of Geological Education* **38**, 402-425.

Okazaki, K., Dillaman, R.M. & Wilbur, K.M. 1981. Crystalline axes of the spine and test of the sea urchin Strongylocentrotus purpuratus: Determination by crystal etching and decoration. *The Biological Bulletin* **161**, 402-415.

O'Keefe, J.D. & Ahrens, T.J. 1989. Impact production of CO_2 by the Cretaceous/Tertiary extinction bolide and the resultant heating of the Earth. *Nature* **338**, 247-249.

Orbigny, A. d'. 1854-60. Échinoïdes irréguliers. *Paléontologie Française. Description des Animaux Invertébrés. Terrain Crétacé 6.* Masson, Paris, 596 pp., pls 801-1006.

Paul, C.R.C. & Mitchell, S.F. 1994. Is famine a common factor in marine mass extinctions? *Geology* **22**, 679-682.

Peron, A. 1887. Histoire du terrain de craie dans le sud-est du bassin angloparisien; avec notes et descriptions des échinides par Gauthier et Lambert. *Bulletin de la Société des Sciences Historiques et Naturelles de l'Yonne* **41**, 114-424, pls 1-8.

Petitot, M.-L. 1959. Contribution à l'étude des échinides fossiles du Maroc (Jurassique et Crétacé). *Notes et Mémoires du Service Géologique (Maroc)* **146**, 183 pp., 17 pls.

Peucker-Ehrenbrink, B., Ravizza, G. & Hofmann, A.W. 1994. The marine $^{187}Os/^{186}Os$ record of the past 80 million years. *Earth and Planetary Science Letters* **130**, 155-167.

Phillip, G.M. & Foster, R.J. 1971. Marsupiate Tertiary echinoids from south-eastern Australia and their zoogeographic significance. *Palaeontology* **14**, 666-695.

Philippi, R.A. 1845. Beschreibung eineger neuer Echinodermen nebst kritischen Bemerkungen über einege weniger bekannte Arten. *Archiv für Naturgeschichte* **11**, 344-359, pl. 11.

Pictet, F.-J. 1857. *Traité elementaire de Paléontologie 4.* 2nd edition. Baillière et fils, Paris, 768 pp.

Plaziat, J.C., Toumarkine, M. & Villatte, J. 1975. L'âge des calcaires pélagiques et néritiques de la base du Tertaire (Danien, Paléocène), Bassin basco-cantabrique et béarnais (Espagne, France).

Mise au point sur leurs faunes d'échinides. *Eclogae Geologicae Helvetiae* **68**, 613-647, 2 pls.

Pohl, J., Stöffler, D., Gall, H. & Ernston, K. 1977. The Reis impact crater. *In* Roddy, D.J., Pepin, R.O. & Merrill, R.B. (eds), *Impact and explosion cratering*. Pergamon, New York, 343-404.

Pollack, J.B., Toon, O.B., Ackerman, T.P., McKay, C.P. & Turco, R.P. 1983. Environmental effects of an impact-generated dust cloud: Implications for the Cretaceous-Tertiary extinctions. *Science* **219**, 287-289.

Pomel, A. 1969. *Revue des echinodermes et leur classification pour servir d'introduction à l'étude des fossiles*. Deyrolle, Paris, 67 pp.

Pomel, A. 1883. *Classification méthodique et genera des échinides vivants et fossiles*. Aldolphe Jourdan, Alger, 131 pp.

Poslavskaya, N.A. & Moskvin, M.M. 1960. [Echinoids of the Order Spatangoida in Danian and adjacent deposits of Crimea, Caucasus and the Transcaspian Region.] *International Geological Congress 21st session: Reports of Soviet Geologists Problem 5: The Cretaceous-Tertiary Boundary*. Publishing House of the Academy of Sciences of the USSR, Moscow, 47-82. [In Russian].

Poslavskaya, N.A. & Solovjev, A.N. 1964. Class Echinoidea: Sea Urchins. Systematic Part (Order Spatangoida). *In Principles of Paleontology*. Nedra Press, Moscow, 174-189, pls 30-38. [In Russian].

Pospichal, J.J. 1996. Calcareous nannoplankton mass extinction at the Cretaceous/Tertiary boundary: An update. *In* Ryder, G., Fastovsky, D. & Gartner, S. (eds), *The Cretaceous-Tertiary Event and Other Catastrophes in Earth History. Geological Society of America Special Paper* **307**, 335-360.

Poulin, É. & Féral, J.-P. 1996. Why are there so many species of brooding Antarctic echinoids? *Evolution* **50**, 820-830.

Quaas, A. 1902. Die Fauna der Overwegiscichten und der Blatterhone in der libyschen Wuste. *Palaeontographica* **30**, 153-334, pls 20-33..

Quenstedt, F.A. 1874. *Petrefactenkunde Deutschlands 3: Echinodermen 1: Die Echiniden*. Tübingen & Leipzig, 720 pp, pls 62-89.

Radig, F. 1973. Beiträge zur Kenntnis der höheren Oberkreide der Baskischen Depression (Nordspanien) und ihrer Echinozoen-Fauna. *Erlanger Geologische Abhandlungen* **94**, 68 pp., 11 pls.

Rampino, M.R. & Haggerty, B.M. 1996. Impact crises and mass extinctions: A working hypothesis.

In Ryder, G., Fastovsky, D. & Gartner, S. (eds), *The Cretaceous-Tertiary Event and Other Catastrophes in Earth History. Geological Society of America Special Paper* **307**, 11-30.

Raup, D.M. 1962. The phylogeny of calcite crystallography in echinoids. *Journal of Paleontology* **36**, 793-810.

Raup, D.M. 1965. Crystal orientations in the echinoid apical system. *Journal of Paleontology* **39**, 934-951.

Raup, D.M. 1966. Crystallographic data for echinoid coronal plates. *Journal of Paleontology* **40**, 555-568.

Raup, D.M. 1986. Biological extinction in earth history. *Science* **231**, 1528-1533.

Raup, D.M. 1995. The role of extinction in evolution. *In* Fitch, W.M. & Ayala, F.J. (eds), *Tempo and Mode in Evolution.* National Academy Press, Washington, 109-124.

Raup, D.M. & Boyajian, G.E. 1988. Patterns of generic extinction in the fossil record. *Paleobiology* **14**, 109-125.

Raup, D.M. & Jablonski, D. 1993. Geography of end-Cretaceous marine bivalve extinctions. *Science* **260**, 971-973.

Raup, D.M. & Sepkoski, J.J. Jr. 1984. Periodicity of extinctions in the geologic past. *Proceedings of the National Academy of Sciences* **81**, 801-805.

Ravn, J.P.J. 1927. De irregulære echinider i Danmarks Kridtaflejringer. *Det Kongelige Danske Videnskabernes Selskabs Skrifter, Naturvidenskabelig og Mathematisk Afdeling; 8th Series* **11**, 309-354, pls 1-5.

Rhodes, M.C. & Thayer, C.W. 1991. Mass extinctions: Ecological selectivity and primary production. *Geology* **19**, 877-880.

Rigby, J., Landis, G. & Hengst, R. 1994. Can an extraterrestrial impact event explain the pattern of biotic crisis near the K/T boundary? *Lunar Planetary Institute Contributions* **825**, 93-94.

Robinson, N.D. 1995. Biogenic acid rain during the late Cretaceous as a possible cause of extinctions. *Journal of the Geological Society of London* **152**, 4-6.

Roman, J. 1970. Échindes crétacés et éocènes du Bas-Congo et de Cabinda (Côte occidentale d'Afrique). *Annales du Musée Royal de l'Afrique Centrale; Sciences Geologiques* **68**, 69-76.

Roman, J. 1983. Échinides "marsupiaux" (Fam. Temnopleuridae) dans le Néogène de l'Ouest Européen. *Annales de Paléontologie (Vert.-Invert.)* **69**, 13-42.

Roman, J. 1984. Les échinidés et la crise Crétacé-Tertaire. *Bulletin de la Section des Sciences* **6**, 133-147.

Roman, J. 1989. Echinoides Paléogènes du Bassin de Paris aperçus nouveaux. *Comptes Rendus du Congrès National des Sociétés Savantes; Section des Sciences* **114**, 293-304.

Roman, J. & Gorodiski, A. 1959. Échinides eocenes du Senegal. *Notes du Service de Géologie et de Prospection Minière* **3**, 1-91.

Rosen, B.R. & Turnsek, D. 1989. Extinction patterns and biogeography of scleractinian corals across the Cretaceous/Tertiary boundary. *Association of Australian Palaeontologists Memoir* **8**, 355-370.

Rouchadze, J. 1940. Les Échinides supracrétacés de la Géorgie. *Bulletin du Musée de Géorgie* **10**, 81-182, pls 1-3.

Rowe, F.W.E. & Vall, L.L. 1982. The distribution of Tasmanian echinoids in relation to southern Australian biogeographic provinces. *In* Lawrence, J.M. (ed.), *Echinoderms, Proceedings of the International Conference, Tampa Bay.* Balkema, Rotterdam, 219-225.

Sanchez Roig, M. 1926. Contribucion a la paleontologia Cubana: Los equinodermos fosiles de Cuba. *Boletin de Minas* **10**, 1-179.

Sanchez Roig, M. 1949. Los equinodermos fosiles de Cuba. *Paleontologia Cubana* **1**, 330 pp, 50 pls.

Sanchez Roig, M. 1953. Neuvos equinodos fosiles de Cuba. *Anales de la Academia de Ciencias Médicas, Fisicas y Naturales de la Habana* **91**, 135-176, pls 1-12.

Santos, M.E.C.M. & Cunha, F.L. de S. 1959. Sobre *Hemiaster jacksoni* Maury e outros Equinoides do Cretacico Brasileiro. *Divisao de Geologica e Mineralogica, Boletim* **186**, 1-18.

Savchinskaya, G.Y. 1974. [*Atlas of the Upper Cretaceous fauna of the Don Basin.*] Nedra Press, Moscow, 639 pp. [In Russian].

Savin, L. 1903. Catalogue raisonée des échinides fossiles de la Savoie. *Bulletin de la Société d'Histoire Naturelle de Savoie; 2nd Series* **8**, 59-249.

Scheltema, R.S. 1977. Dispersal of marine invertebrate organisms. Paleobiogeographic and biostratigraphic implications. *In* Kauffman, E.G. & Hazel, J.E. (eds), *Concepts and methods of biostratigraphy.* Dowden, Hutchinson & Ross, Pennsylvania, 73-108.

Schlüter, C. 1897. Ueber einige exocyclische Echiniden der baltischen Kreide und deren Bett. *Zeitschrift der Deutschen geologischen Gesselschaft* **49**, 18-50, pls 1-2.

Schlüter, C. 1899. Ueber einige von Goldfuss beschreibene Spatangiden. *Zeitschrift der Deutschen geologischen Gesselschaft* **51**, 104-124, pls 9-10.

Schlüter, C. 1900. Ueber einige Kreide-Echiniden. *Zeitschrift der Deutschen geologischen Gesselschaft* **52**, 360-379, pls 15-18.

Schmid, F. 1972. *Hagenowia elongata* (Nielsen), ein hochspezialisierter Echinide aus dem höheren Untermaastricht NW-Deutschlands. *Geologisches Jahrbuch; Series A* **4**, 177-195.

Schmidt, O.I. 1938. [Upper Cretaceous marine echinoids of Caucasus.] *Annals of the Russian Central Geological and Prospecting Scientific Research Museum* **1**, 75-83. [In Russian].

Schulz, M.-G. 1983. Die Echinodermen der Inoceramen-Mergel (Buntmergelserie, Ultrahelvetikum, Unter-Maastricht) des Moos-Grabens SE Siegsdorf (Oberbayern). *Zitteliana* **10**, 715-723.

Scotese, C.R., Gahagan, L.M. & Larson, R.L. 1988. Plate tectonic reconstructions of the Cretaceous and Cenozoic ocean basins. *Tectonophysics* **155**, 27-48.

Sepkoski, J.J. Jr. 1987. Environmental trends in extinction during the Phanerozoic. *Science* **235**, 64-66.

Sepkoski, J.J. Jr. 1993. Ten years in the library: New data confirm paleontological patterns. *Paleobiology* **19**, 43-51.

Seunes, J. 1888. Échinides crétacés des Pyrénées occidentales: Série I. *Bulletin de la Société Géologique de France; 3rd Series* **16**, 791-815, pls 28-31.

Seunes, J. 1889. Échinides crétacés des Pyrénées occidentales: Série II. *Bulletin de la Société Géologique de France; 3rd Series* **17**, 804-824.

Seunes, J. 1891. Échinides crétacés des Pyrénées occidentales: Série III. *Bulletin de la Société Géologique de France; 3rd Series* **19**, 23-32, pls 1-5.

Sheehan, P.M., Coorough, P.J. & Fastovsky, D.E. 1996. Biotic selectivity during the K/T and Late Ordovician extinction events. *In* Ryder, G., Fastovsky, D. & Gartner, S. (eds), *The Cretaceous-Tertiary Event and Other Catastrophes in Earth History. Geological Society of America Special Paper* **307**, 477-489.

Sheehan, P.M. & Hansen, T.A. 1986. Detritus feeding as a buffer to extinction at the end of the Cretaceous. *Geology* **14**, 868-870.

Shimanskii, V.N. & Solovjev, A.N. 1982. [*The Limit of the Mesozoic and Caenozoic in the Development of the Organic World.*] Nauka Publishing House, Moscow, 38 pp. [In Russian].

Shuto, T. 1974. Larval ecology of prosobranch gastropods and its bearing on biogeography and paleontology. *Lethaia* **7**, 239-256.

Sims, C. 1997. Determinig the extinction pattern at the Cretaceous-Tertiary boundary. *Geoscientist* **7**, 13-17.

Slocum, A.W. 1909. New echinoids from the Ripley Group of Mississippi. *Field Museum of Natural History Publication 134; Geological Series* **4**, 1-16, pls 1-3.

Smiser, J.S. 1935a. A revision of the echinoid genus *Echinocorys* in the Senonian of Belgium. *Mémoires du Musée Royal d'Histoire Naturelle de Belgique* **67**, 52 pp, 2 pls.

Smiser, J.S. 1935b. A monograph of the Belgian Cretaceous Echinoids. *Mémoires du Musée Royal d'Histoire Naturelle de Belgique* **68**, 1-98, pls 1-9.

Smit, J. 1990. Meteorite impact, extinctions and the Cretaceous-Tertiary boundary. *Geologie en Mijnbouw* **69**, 187-204.

Smith, A.B. 1980a. The structure and arrangement of echinoid tubercles. *Philosophical Transactions of the Royal Society of London* **B289**, 1-54.

Smith, A.B. 1980b. The structure, function and evolution of tube feet and ambulacral pores in irregular echinoids. *Palaeontology* **23**, 39-84.

Smith, A.B. 1984. *Echinoid Palaeobiology.* George Allen & Unwin, London, 190 pp.

Smith, A.B. 1994. *Systematics and the fossil record: Documenting evolutionary patterns.* Blackwell Scientific Publications, Oxford, 223 pp.

Smith, A.B. 1995. Late Campanian - Maastrichtian echinoids from the United Arab Emirates - Oman border region. *Bulletin of the Natural History Museum, London (Geology)* **51**, 121-240.

Smith, A.B. & Jeffery, C.H. Selectivity of extinction among sea-urchins at the end Cretaceous. *Nature*, in press.

Smith, A.B., Littlewood, D.T.J. & Wray, G. A. 1995. Comparing patterns of evolution: Larval and adult life history stages and ribosomal RNA of post-Palaeozoic echinoids. *Philosophical Transactions of the Royal Society of London* **B349**, 11-18.

Smith, A.B., Paul, C.R.C., Gale, A.S. & Donovan, S.K. 1988. Cenomanian and lower Turonian echinoderms from Wilmington, south-east Devon, England. *Bulletin of the British Museum (Natural History) Geology Series* **42**, 245 pp.

Sohl, N.F. 1987. Cretaceous gastropods: Contrasts between Tethys and the temperate provinces. *Journal of Paleontology* **61**, 1085-1111.

Sorauf, J.E. & Pedder, A.E.H. 1986. Late Devonian rugose corals and the Frasnian-Famennian crisis. *Canadian Journal of Earth Sciences* **23**, 1265-1287.

Stanley, S.M. 1986. Population size, extinction, and speciation: the fission effect in Neogene Bivalvia. *Paleobiology* **12**, 89-110.

Stefani, C. de. 1913. Fossili della Creta superiore raccolti da Michele Sforza in Tripolitania. *Palaeontographia Italica* **19**, 255-299, pls 23-27.

Stephenson, L.W. 1941. The larger invertebrate fossils of the Navarro Group of Texas. *University of*

Texas Publication **4101**, 1-641, pls 1-95.

Steuber, T. 1996. Stable isotope schlerochronology of rudist bivalves. Growth rates and late Cretaceous seasonality. *Geology* **24**, 315-318.

Stokes, R.B. 1975. Royaumes et provinces fauniques du Crétacé établis sur la base d'une étude systématique du genre *Micraster. Mémoires du Muséum National d'Histoire Naturelle. Nouvelle Série* **C31**, 1-94.

Stokes, R.B. 1979. An analysis of the ranges of spatangoid echinoid genera and their bearing on the Cretaceous/Tertiary boundary. *In* Christensen, W.K. & Birkelund, T. (eds), *Cretaceous-Tertiary Boundary Events Symposium II: Proceedings.* University of Copenhagen, 78-82.

Stokes, R.B. 1986. The echinoid *Isaster* from the Danian of Turkey. *Neues Jahrbuch für Geologie und Paläontogie Monatschefte* **1986**, 171-174.

Stoliczka, F. 1873. Cretaceous fauna of southern India, The Echinodermata. *Palaeontologia Indica; 8th Series* **4**, 69-127, pls 11-17.

Stolley, E. 1892. *Die Kreide Schleswig-Holsteins.* Verlag von Lipsius und Tischer, Kiel & Leipzig, 309 pp, 10 pls.

Strathmann, R.R. 1978. The evolution and loss of feeding larval stages of marine invertebrates. *Evolution* **32**, 894-906.

Strathmann, R.R. 1985. Feeding and nonfeeding larval development and life-history evolution in marine invertebrates. *Annual Review of Ecology and Systematics* **16**, 339-361.

Strathmann, R.R. 1990. Why life histories evolve differently in the sea. *American Zoologist* **30**, 197-207.

Sutherland, F.L. 1994. Volcanism around K/T boundary time; its role in an impact scenario for the K/T extinction events. *Earth Science Reviews* **36**, 1-26.

Swofford, D. L. 1993. *PAUP, Phylogenetic Analysis Using Parsimony, Version 3.1.* [Apple Macintosh compatible computer program].

Tanaka, K., Kanie, Y. & Obata, I. 1979. Maastrichtian and Danian echinoids from northwestern Madagascar. *Bulletin of the National Science Museum; Series C* **5**, 25-50, 3 pls.

Tessier, F. 1952. Contributions à la stratigraphie et à la paléontologie de la partie ouest du Sénégal (Crétacé et Tertaire) 3: Paléontologie. *Bulletin de la Direction des Mines* **14**, 283-477.

Tessier, F. & Roman, J. 1973. Études paléontologiques et géologiques sur les Falaises de Fresco (Côte d'Ivoire). 6, Échinides. *Annales de la Faculté des Sciences, Dakar* **26**, 139-171.

Thorson, G. 1950. Reproduction and larval ecology of marine bottom invertebrates. *Biological Reviews*

25, 1-45.

Traub, F. 1938. Geologische und Paläontologische bearbeitung der Kreide und des Tertiärs im Östlichen Rupertiwinkel, Nördlich von Salzburg. *Palaeontographica* **88**, 1-114, pls 1-8.

Troschel, F.H. 1851. Ueber die Gattung *Tripylus*. *Archiv für Naturgeschichte* **17**, 67-74, pl. 1.

Tzankov, V. 1934. Échinides fossiles de la Craie supérieure de Bulgarie de Nord. *Annuaire de l'Université de Sofia* **30**, 189-233.

Valentine, J.W. & Jablonski, D. 1986. Mass extinctions: Sensitivity of marine larval types. *Proceedings of the National Academy of Sciences* **83**, 6912-6914.

Wagner, C.D. & Durham, J.W. 1966. Holasteroids. *In* Moore, R.C. (ed.), *Treatise of Invertebrate Paleontology, Echinodermata* **3** (2). Geological Society of America, Inc. & University of Kansas Press, Kansas, U523-U543.

Wanner, J. 1902. Die Fauna der obersten weissen Kreide der libyschen Wüste. *Palaeontographica* **30** 91-152, pls 13-19.

Ward, P.D. 1995a. The K/T trial. *Paleobiology* **21**, 245-247.

Ward, P.D. 1995b. After the fall: Lessons and directions from the K/T debate. *Palaios* **10**, 530-538.

Ward, P.D., Kennedy, W.J. & MacLeod, K.G. 1991. Ammonite and inoceramid extinction patterns in Cretaceous/Tertiary boundary sections of the Biscay region (southwestern France, northern Spain). *Geology* **19**, 1181-1183.

Weber, G.F. 1949. [Class Echinoidea: sea urchins]. [*Atlas of the Leading Forms of the Fossil Fauna of the USSR*] **12**, 143-152. [In Russian].

Weil, A. 1994. K/T survivorship as a test of acid rain hypotheses. *Abstracts with Programs Geological Society of America* **26** (7), 335.

Welsbord, N.E. 1934. Some Cretaceous and Tertiary echinoids from Cuba. *Bulletins of American Paleontology* **20** (70C), 165-270.

Westrop, S.R. 1989. Macroevolutionary implications of mass extinction - evidence from an Upper Cambrian stage boundary. *Paleobiology* **15**, 46-52.

Westrop, S.R. 1991. Intercontinental variation in mass extinction patterns: Influence of biogeographic structure. *Paleobiology* **17**, 363-368.

Wilmsen, M., Wiese, F. & Ernst, G. 1996. Facies development, events and sedimentary sequences in the Albian to Maastrichtian of the Santander depositional area, northern Spain. *Mitteilungen aus dem Geologisch-Paläontologischen Institut der Universität Hamburg* **77**, 337-367.

Wingard, G.L. 1993. A detailed taxonomy of the Upper Cretaceous and Lower Tertiary Crassatellidae in

the eastern United States - an example of the nature of extinction at the boundary. *Professional Paper of the U. S. Geological Survey* **1535**, 131 pp., 22pls.

Wolbach, W.S., Lewis, R.S. & Anders, E. 1985. Cretaceous extinctions: Evidence for wildfires and search for meteoritic material. *Science* **230**, 167-170.

Wolbach, W.S., Gilmour, I. & Anders, E. 1990. Major wildfires at the Cretaceous/Tertiary boundary. *In* Sharpton, V.L. & Ward, P.D. (eds), *Global Catastrophes in Earth History; An interdisciplinary conference on impact, volcanism and mass mortality. Geological Society of America Special Paper* **247**, 391-400.

Wolfe, J.A. & Upchurch, G.R. Jr. 1987. North American non-marine climates and vegetation during the late Cretaceous. *Palaeogeography, Palaeoclimatology, Palaeoecology* **61**, 33-77.

Wray, G.A. 1995a. Punctuated evolution of embryos. *Science* **267**, 1115-1116.

Wray, G.A. 1995b. Evolution of larvae and developmental modes. *In* McEdward, L. (ed.), *Ecology of Marine Invertebrate Larvae.* CRC Press, Boca Raton, 413-447.

Wray, G.A. 1996. Parallel evolution of non-feeding larvae in echinoids. *Systematic Biology* **45**, 308-322.

Wright, C.W. & Wright, E.V. 1949. The Cretaceous echinoid genera *Infulaster* Desor and *Hagenowia* Duncan. *Annals and Magazine of Natural History; 12th Series* **2**, 454-474.

Wu, E.-Z. & Mu, Y.-R. 1976. [Cretaceous and Tertiary echinoids from the Mount Jolmo Lungma Region]. *In* [*A report of the scientific expedition in the Mount Jolmo Lungma Region (1966-1968)*]. Science Press, Beijing, 357-386. [In Chinese].

Zagbib-Turki, D. 1987. *Les échinides du Crétacé de Tunisie. Paléontologie generale: Systematique, Paleoecologie, Paleobiogeographie.* Unpublished PhD thesis. University of Tunis. 613 pp, 25 pls.

Zahnle, K.L. 1990. Atmospheric impact by large impacts. *In* Sharpton, V.L. & Ward, P.D. (eds), *Global Catastrophes in Earth History; An interdisciplinary conference on impact, volcanism and mass mortality. Geological Society of America Special Paper* **247**, 271-288.

Zittel, K.A. von. 1879. *Handbuch der Palaeontologie* **1**. Munich & Leipzig, 765 pp.

APPENDIX 1

MAASTRICHTIAN AND PALAEOCENE ATELOSTOMATE ECHINOID LOCALITIES

This appendix contains palaeolatitudes and palaeolongitudes for all Maastrichtian and Palaeocene localities yeilding identifiable atelostomate echinoids based on the palaeogeographic reconstructions of Scotese *et al.* (1988).

M = Maastrichtian locality; P = Palaeocene locality.

The Americas					
AM1	Alabama, USA	31 N	60 W	M	P
AM2	Arkansas, USA	32 N	67 W	M	P
AM3	Delaware, USA	36 N	48 W	M	
AM4	Georgia, USA	30 N	57 W		P
AM5	Mississippi, USA	31 N	63 W	M	
AM6	North Carolina, USA	33 N	49 W	M	
AM7	New Jersey, USA	37 N	46 W		P
AM8	Texas, USA	29 N	71 W	M	P
AM9	Wyoming, USA	47 N	78 W	M	
AM10	Cuba	18 N	63 W	M	
AM11	Jamaica	15 N	55 W	M	
AM12	Trinidad	4 N	42 W		P
AM13	NE Brazil	12 S	18 W	M	
Eurasia					
EU1	Denmark	48 N	9 E	M	P
EU2	S Sweden	49 N	14 E		P
EU3	E Greenland	58 N	19 W	M	P
EU4	Belgium	44 N	5 E	M	P
EU5	Maastricht area	45 N	5 E	M	P
EU6	Biarritz & Bidart, France	35 N	1 W	M	P
EU7	Normandy, France	42 N	1 W	M	
EU8	Paris region, France	42 N	3 E	M	P
EU9	SE France	36 N	9 E	M	
EU10	French Pyrenees	35 N	2 E	M	P
EU11	Alicante, Spain	31 N	1 E	M	P

EU12	Navarra, Spain	34 N	1 W	M	P
EU13	Santander, Spain	35 N	2 W	M	
EU14	Tremp, Spain	34 N	2 E	M	
EU15	Zumaya, Spain	35 N	1 W	M	
EU16	Bavaria	40 N	18 E	M	
EU17	Isle of Rügen	48 N	11 E	M	
EU18	NW Germany	47 N	8 E	M	
EU19	Austria	41 N	14 E		P
EU20	Bulgaria	38 N	18 E	M	
EU21	SE Poland	44 N	20 E	M	P
EU22	Azerbaijan	32 N	53 E	M	
EU23	Crimea	41 N	35 E	M	P
EU24	Dagestan	37 N	52 E	M	P
EU25	Don Basin	43 N	38 E	M	
EU26	Georgia	40 N	46 E	M	P
EU27	Kopet Dag	29 N	58 E	M	P
EU28	Mangyshlak, Kazakhstan	41 N	53 E	M	P
EU29	N Caucasus	41 N	46 E	M	P
EU30	Transcaspian Region	38 N	57 E	M	P
EU31	Turkmenistan	36 N	57 E	M	

Tethys (Africa & Middle East)

T1	Central Algeria	15 N	10 E	M	
T2	Constantine, Algeria	23 N	3 E	M	
T3	Oran, Algeria	23 N	1 W	M	
T4	Egypt	7 N	25 E		P
T5	Libya	18 N	12 E	M	P
T6	Morocco	22 N	3 W	M	P
T7	Tunisia	21 N	12 E	M	
T8	Angola	23 S	14 E		P
T9	Ivory Coast	4 S	8 W		P
T10	Nigeria	4 N	3 E		P
T11	Mozambique	27 S	40 E	M	
T12	Senegal	7 N	15 W	M	P
T13	Somalia	3 S	40 E	M	P
T14	Sudan	5 N	30 E		P
T15	Zululand	40 S	25 E	M	
T16	Central Turkey	32 N	48 E	M	
T17	NW Turkey	35 N	45 E	M	P
T18	Louristan, Iran	12 N	56 E	M	
T19	UAE/Oman	8 N	47 E	M	

Indo-Pacific (Madagascar, Far East & Austalasia)					
IP1	E Madagascar	35 S	53 E	M	P
IP2	NE Madagascar	25 S	53 E	M	
IP3	NW Madagascar	28 S	45 E	M	P
IP4	SW Madagascar	37 S	46 E	M	P
IP5	Baluchistan	8 S	68 E	M	
IP6	Pakistan	8 S	73 E		P
IP7	Assam, India	18 S	95 E	M	
IP8	S India	30 S	73 E	M	
IP9	Tadzhikistan	40 N	75 E	M	
IP10	foothills of Everest, China	10 S	95 E	M	
IP11	Japan	52 N	135 E	M	
IP12	Western Australia	50 S	101 E	M	P

Figure A1.1. Maastrichtian atelostomate echinoid localities plotted onto Maastrichtian palaeogeography.

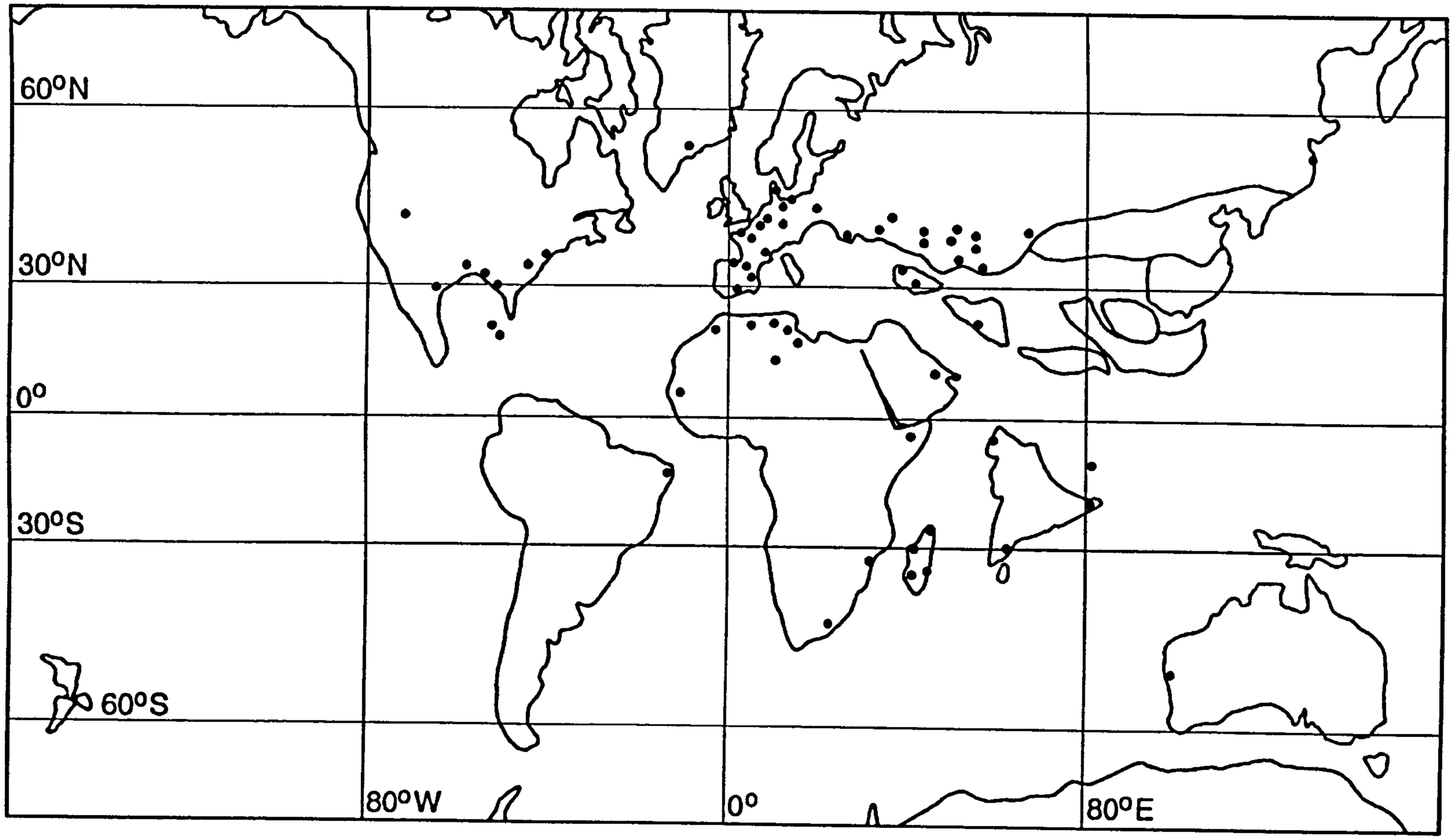
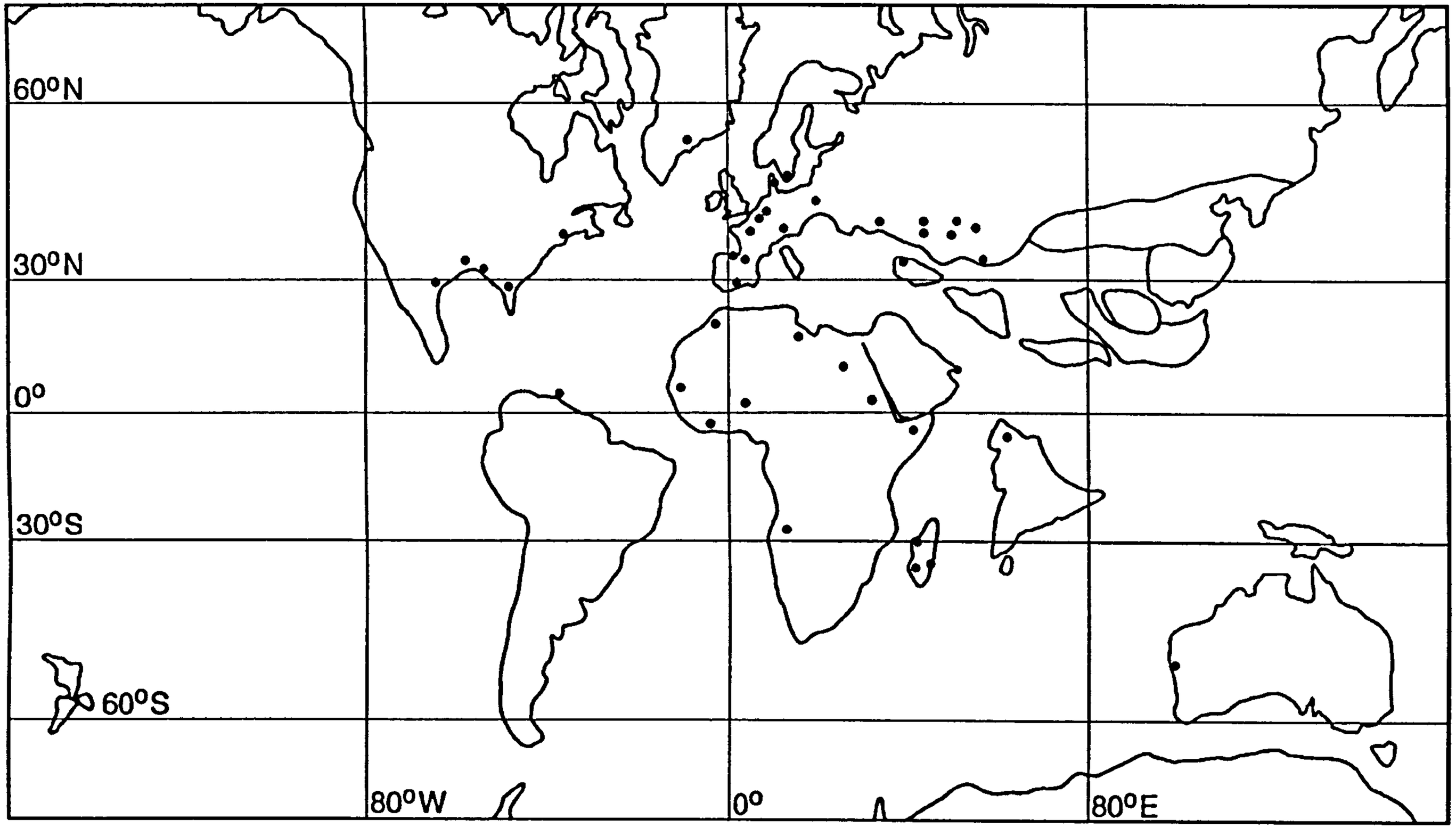

60°N
30°N
0°
30°S
60°S
80°W
0°
80°E

Figure A1.2. Palaeocene atelostomate echinoid localities plotted onto Maastrichtian palaeogeography.


60°N
30°N
0°
30°S
60°S
80°W
0°
80°E

APPENDIX 2

DETAILS OF MAASTRICHTIAN AND PALAEOCENE STRATIGRAPHIC UNITS YIELDING ATELOSTOMATE ECHINOIDS

This appendix comprises lithological and depositional details of all stratigraphic units from which identifiable Maastrichtian and Palaeocene atelostomate echinoids have been recorded. The following information is compiled from a computer database that is available on request.

Pd = planktic foraminifera zones P4-6

Pc = planktic foraminifera zone P3

Pb = nannoplankton zones NP3-4

Pa = nannoplankton zones NP1-2

Md = belemnite zone *Belemnitella casimirovensis*

Mc = belemnite zone *Belemnitella junior*

Mb = belemnite zone *Belemnitella occidentalis*

Ma = belemnite zone *Belemnitella lanceolata*

P = undifferentiated Palaeocene

T = undifferentiated Thanetian

D = undifferentiated Danian

M = undifferentiated Maastrichtian

upM = undifferentiated Upper Maastrichtian

lowM = undifferentiated Lower Maastrichtian

USA

Mount Laurel Sand	Ma	unconsolidated sand	shoreface - inner shelf	*Hemiaster wetherbyi*
Saratoga Chalk	Ma	chalk & calcareous sand	open shelf between fair and storm wave base, 25-50 m	*Cardiaster granulosus, Diplodetus americanus, Hemiaster wetherbyi*
Nacatoch Sand	Ma	sandstones & mudstones	delta & tidal flats	*Hemiaster parastatus, Hemiaster wetherbyi, Paraster variabilis*
Upper Pierre Shale	Mb	shales, silts & mudstones	restricted ocean, less than 20 m	*Hemiaster parastatus*
Ripley Fm	Mb-c	sands, silts & clays	fluviodeltaic, barrier & shoreface	*Diplodetus americanus, Hemiaster parastatus, Hemiaster wetherbyi*
Peedee Fm (Rocky Point Member)	Mc	sandy chalks	inner-mid shelf, 3-12 m	*Paraster variabilis*
Prairie Bluff Chalk	Mc-d	sandy chalk	offshore, mid-shelf	*Diplodetus americanus, Hemiaster wetherbyi, Paraster variabilis*
Corsicana Marl	Mc-d	clays and marls	deep water	*Cardiaster leonensis, Diplodetus americanus, Hemiaster wetherbyi, Paraster variabilis, Proraster atavus*
Clayton Fm	Pa	sand & fine-grained carbonates	nearshore, open shelf	*Linthia*? sp. indet., *Paraster sindensis*
Porters Creek Clay	Pa-b	montmorillonitic clays	offshore, stagnant basin	*Diplodetus*? sp. indet.
Wills Point Fm (Midway Gp)	Pb	sandy shales	shallow, open marine, 10-20 m	*Paraster sindensis*
Vincentown Sand	Pd	sands	nearshore bay	*Echinocorys scutata, Labrotaxis faxensis, Hemiaster stella, Hemiaster parastatus*

CUBA				
Cacarajicara Fm (Big Boulder Bed)	Mc	turbiditic clastic calcirudite & calcisiltite	shallow marine limestone clasts	*Linthia brodermanni*
"Late Cretaceous"	M?	?	?	*Cardiaster palmeri*, *Paraster canaliculatus*,*Proraster atavus*, *Proraster herrerae*
JAMAICA				
Guinea Corn Formation	Ma	rudist limestone with lignites	shallow; sometimes hyposaline	*Proraster atavus*, *Proraster herrerae*
TRINIDAD				
Soldado Fm (bed 2)	Pb	glauconitic limestone & calcareous sandstone	shallow marine	? *Paraster canaliculatus*
BRAZIL				
Gramame Fm	Md	calcarenite & calcareous sandstone	littoral; within wave base	*Mecaster fourneli*, *Paraster variabilis*
DENMARK & SOUTHERN SWEDEN				
white chalk	Mb-d	white chalk	deep water, 100-600 m	*Echinocorys scutata*, *Cardiaster granulosus*, *Cardiotaxis heberti*, *Hagenowia elongata*
Bryozoan Limestone	Pa	bryozoan rich limestone	150 m	*Galeaster bertrandi*, *Echinocorys scutata*, *Labrotaxis faxensis* , *Cyclaster suecicus*, *Cyclaster integer*
Cerithium Limestone	Pa	chalkstone with abundant gastropod moulds	below wave base 80-150 m	*Echinocorys scutata*, *Cyclaster integer*, *Cyclaster suecicus*
Faxe Limestone	Pa-b	coral limestone	shallow water	*Labrotaxis faxensis*, *Cyclaster suecicus*, *Hemiaster prunella*

Saltholm Limestone (=coccolith limestone)	Pb	bryozoan rich limestone	150 m	*Labrotaxis faxensis*, *Echinocorys scutata*, *Micraster* sp., *Cyclaster suecicus*, *Cyclaster integer*, *Hemiaster prunella*, *Mauritanaster kongieli*
Upper Danian	Pb	calcarenite	?	*Hemiaster stella*, *Paraster* sp. indet., *Proraster* sp., *Echinocorys scutata*
EAST GREENLAND				
reworked nodules in Kangilia Fm	bwM	laminated mud & sandstone	shelf	*Rispolia* sp. indet., *Trachyaster* sp. indet.
Kangilia Fm	D	mudstones & sandstones	marine shelf	*Hemiaster prunella*, *Paraster* sp. indet.,*Homoeaster tunetanus*
Agatdal Fm	P	sandstones & shales	shallow marine	*Hemiaster stella*, *Proraster* sp.
BELGIUM				
Ciply Phosphatic Chalk	Ma	phosphatic calcarenite	shallow marine	*Echinocorys scutata*, *Cardiaster granulosus*,*Cardiotaxis heberti*, *Micraster schroederi*
"Poudinge de la Malogne"	Mb	conglomerate		*Micraster schroederi*
Calcaire grossier de Mons	Pb-c	coarse calcarenite	warm, littoral	*Diplodetus coloniae*, *Linthia houzeaui*
MAASTRICHT AREA				
Beutenaken Chalk (Gulpen Fm)	Ma	grey marly chalk	deep water	*Micraster schroederi*
Vijlen Chalk (Gulpen Fm)	Ma-b	glauconitic fine grained chalk	below storm wave base	*Echinocorys scutata*, *Cardiaster granulosus*, *Diplodetus duponti*, *Diplodetus parvistella*, *Cyclaster platornatus*, *Hemiaster stella*
Lixhe Chalk (Gulpen Fm)	Mb	coccolithic wackestone	oceanic influence 80-150 m	*Echinocorys scutata*, *Cardiaster gransulosus*
Lanaye Chalk (Gulpen Fm)	Mb-c	coccolithic packstone	subtropical platform 40-80 m	*Cardiaster granulosus*, *Hemipneustes striatoradiatus*, *Diplodetus parvistella*, *Hemiaster prunella*, *Hemiaster koninckanus*, *Hemiaster stella*, *Leymeriaster eluvialis*

Kunrade Chalk (Maastricht Fm)	Mc	gravelly intrabio-microsparite	shallow subtropical platform, 20-40 m	*Cardiaster granulosus, Hemipneustes striatoradiatus, Diplodetus duponti, Diplodetus parvistella, Hemiaster prunella, Hemiaster koninckanus, Hemiaster stella, Leymeriaster maestrichtensis, Leymeriaster eluvialis*
Nekum Chalk (Maastricht Fm)	Mc	biocalcarenite & gravelly intrabiomicro-sparite	shallow platform, 20-40 m	*Cardiaster granulosus, Hemipneustes striatoradiatus, Hemipneustes oculatus, Hemiaster koninckanus, Leymeriaster maestrichtensis, Leymeriaster eluvialis*
Meerssen Chalk (Maastricht Fm)	Md	gravelly intrabiomicrosparite	very shallow, high energy, warm, 2-15 m carbonate platform	*Cardiaster granulosus, Hemipneustes striatoradiatus, Hemiaster prunella, Leymeriaster maestrichtensis*
Geulhem Chalk (Houthem Fm)	Pa	tuffaceous chalk	shallow, subtidal to intertidal	*Paraster sindensis*
BIDART, BIARRITZ & ZUMAYA				
Zumaya-Algorta Fm	Mb-d	limestone & marl alterations	continental shelf deep water	*Stegaster cotteaui, Stegaster altus, Stegaster bouillei, Tholaster munieri*
?	D	coccolith limestone	deep water	*Jeronia pyrenaica*
NORMANDY				
Calcaire à *Baculites*	Mc-d	tuffaceous bioclastic limestone	shallow marine	*Echinocorys scutata, Cardiaster granulosus, Hemiaster prunella, Hemiaster nucula*
PARIS BASIN				
Craie de Meudon	Ma	white chalk	deep water	*Cardiotaxis heberti*
Calcaire de Vigny	Pa-b	reefal limestone	nearshore	*Linthia houzeaui*

PYRENEES				
Upper Tercis Fm	Ma-b	micritic limestone with flints	deep water	*Stegaster altus*, *Stegaster bouillei*, *Stegaster cotteaui*, *Stegaster heberti*, *Tholaster munieri*, *Echinocorys scutata*, *Cardiaster* sp. nov., *Hemipneustes striatoradiatus*, *Hemipneustes pyrenaicus*, *Cyclaster integer*
?	D	marly chalks	bathyal	*Galeaster bertrandi*, *Echinocorys scutata*, *Jeronia pyrenaica*, *Cyclaster aturicus*, *Cyclaster gindrei*, *Cyclaster integer*, *Coraster vilanovae*, *Coraster beneharnicus*
?	Pc	sandy limestones	neritic-littoral platform	*Garumnaster michaleti*, *Echinocorys scutata*, *Eupatagus mortenseni*, *Diplodetus coloniae*, *Pseudogibbaster tercensis*, *Hemiaster stella*, *Paraster canaliculatus*
ALICANTE				
Upper Quipar-Jorquera Fm	M	marly limestones & slump episodes	transition from platform to trough	*Stegaster altus*, *Stegaster bouillei*, *Echinocorys scutata*, *Hemipneustes striatoradiatus*, *Hemipneustes pyrenaicus*, *Hemipneustes africanus*, *Micraster schroederi*, *Micraster aturicus*, *Diplodetus coloniae*, *Cyclaster heberti*, *Isaster aquitanicus*, *Coraster vilanovae*, *Homoeaster tunetanus*
Les Foies Blanques	D	marly limestone	debris flow	*Mokotibaster nicklesi*, *Pseudogibbaster akkajensis*,*Cyclaster vilanovae*, *Coraster vilanovae*, *Homoeaster tunetanus*
NAVARRA				
Olazaguthia Formation	bwM	sandy limestone & calcareous sandstone	outer platform, fairly shallow water	*Hemipneustes striatoradiatus*, *Hemipneustes pyrenaicus*, *Hemiaster prunella*, *Hemiaster koninckanus*
?	M	thick black shales with calcareous sands	basinal	*Stegaster altus*, *Stegaster bouillei*

Coraster beds	Pb	chalky limestones	basinal	*Jeronia pyrenaica*, *Coraster vilanovae*, *Coraster beneharnicus*, *Sphenaster larumensis*
Aristregui	Pb	marly limestones & marls	continental slope	*Echinocorys scutata*, *Jeronia pyrenaica*, *Rispolia*? sp. indet., *Coraster beneharnicus*
Casas di Oreyon	Pd	microconglomeritic calcareous sandstone	nearshore carbonate platform	*Echinocorys scutata*, *Labrotaxis* sp. indet., *Micraster tercensis*, *Isaster aquitanicus*
SANTANDER				
Cabo de Lata Fm	bwM	sandy limestones & calcarenites	inner platform within wave base	*Pseudoffaster caucasicus*, *Echinocorys scutata*, *Offaster dallonii*, *Hemipneustes pyrenaicus*, *Hemipneustes* sp., *Cyclaster gindrei*, *Isaster aquitanicus*, *Hemiaster prunella*
TREMP				
Areny Sandstone	bwM	sandy marls & calcarenites	sub-littoral	*Pseudoffaster caucasicus*, *Echinocorys scutata*, *Offaster pilula*, *Offaster dallonii*, *Cardiaster granulosus*, *Hemipneustes pyrenaicus*, *Hemipneustes* sp., *Cyclaster gindrei*, *Hemiaster prunella*, *Proraster atavus*
BAVARIA				
Inoceramus Marls	Mb	marls	deep water	*Guettaria fecunda*, *Homoeaster tunetanus*
ISLE OF RÜGEN				
Rügener Schreibkreide	Ma	white chalk	deep water	*Echinocorys scutata*, *Offaster pilula*, *Cardiaster granulosus*, *Cardiotaxis heberti*, *Hagenowia elongata*, *Cyclaster platornatus*, *Cyclaster ruegensis*, juvenile *Hemiaster*

NORTHWEST GERMANY				
Pommerschen Kreide	Md	white chalk	deep water	*Cardiaster granulosus, Micraster grimmensis*
white chalk	Ma	white chalk	deep water	*Hagenowia elongata*
AUSTRIA				
Kch11	T	chalky marl	deep water	*Echinocorys scutata*
BULGARIA				
Upper Chalk	lowM	white chalk	deep water	*Stegaster altus, Stegaster bouillei, Echinocorys scutata, Hemipneustes striatoradiatus, Hemiaster koninckanus, Coraster vilanovae, Homoeaster tunetanus*
Mezdra Fm	lowM	?	?	*Homoeaster tunetanus*
POLAND				
Maastrichtian	Ma-d	marl	deep water	*Echinocorys scutata*
Siwak	Pa	marly chalk	30-100m	*Echinocorys scutata, Pseudogibbaster depressus, Hemiaster* sp. indet.
AZERBAIJAN				
?	M	chalk	deep water	*Cyclaster integer*
CRIMEA				
?	Ma-Pb	white chalk	deep water	*Galeaster bertrandi, Stegaster bouillei, Echinocorys scutata, Cardiaster granulosus, Diplodetus coloniae, Homoeaster tunetanus*

?	Pa-d	calcarenite	shelf	*Garumnaster michaleti, Pseudogibbaster akkajensis, Pseudogibbaster depressus, Pseudogibbaster tercensis, Isaster aquitanicus*
DAGESTAN				
?	M-D	chalk	deep water	*Galeaster bertrandi, Basseaster rostratus, Coraster vilanovae, Homoeaster tunetanus*
?	T	chalk	deep water	*Garumnaster michaleti, Coraster vilanovae,Orthaster dagestanensis*
DON BASIN				
?	M	white chalk	deep water	*Echinocorys scutata, Cardiaster granulosus*
GEORGIA				
?	Ma-Pb	white chalk	deep water	*Galeaster bertrandi, Garumnaster michaleti, Stegaster altus, Stegaster bouillei, Stegaster* sp. indet., *Pseudoffaster caucasicus, Guettaria rocardi,* Echinocorys *scutata, Hemipneustes striatoradiatus, Micraster aturicus, Pseudogibbaster akkajensis,Pseudogibbaster depressus, Pseudogibbaster tercensis, Ovulaster zignoanus, Cyclaster gindrei, Cyclaster aturicus, Cyclaster integer, Coraster vilanovae, Orthaster dagestanensis, Homoeaster tunetanus*
KOPET DAG				
?	M-D	chalk	deep water	*Galeaster bertrandi, Stegaster bouillei, Pseudoffaster caucasicus, Guettaria rocardi, Orthaster alievi*

MANGYSHLAK, KAZAKHSTAN				
?	M	calcarenite	shelf	*Hemipneustes striatoradiatus, Proraster geayi*
?	Md-Pa	white chalk	deep water	*Galeaster bertrandi, Pseudoffaster caucasicus, Echinocorys scutata, Cardiotaxis heberti, Cyclaster integer, Cyclaster galei*
?	D+T	calcarenite	shelf	*Garumnaster michaleti, Garumnaster luppovi, Isaster aquitanicus, Linthia andrussovi, Paraster brevipetalus, ? Proraster geayi, Pseudolinthia triporata, Brisaster micropetalus, Kertaster termiri*
NORTHERN CAUCASUS				
?	Ma-Pb	chalk	deep water	*Galaester bertrandi, Stegaster altus, Stegaster bouillei, Pseudoffaster caucasicus, Echinocorys scutata, Guettaria rocardi, Micraster schroederi, Cyclaster aturicus, Cyclaster gindrei, Cyclaster integer, Hemiaster prunella, Coraster vilanovae, Orthaster dagestanensis, Orthaster alievi, Homoeaster tunetanus*
?	M	calcarenite	shelf	*Hemipneustes striatoradiatus*
?	Pa-c	calcarenite	shelf	*Pseudogibbaster akkajensis, Pseudogibbaster depressus, Pseudogibbaster tercensis*
TRANSCASPIAN				
?	Ma-Pb	chalk	deep water	*Galeaster bertrandi, Pseudogibbaster akkajensis, Cyclaster integer, Cyclaster aturicus, Cyclaster gindrei, Coraster vilanovae*
?	Pc-d	calcarenite	shelf	*Garumnaster michaleti, Paraster sindensis*
TURKMENISTAN				
?	upM	calcarenite	shelf	*Paraster sindensis*

TADEMAIT PLATEAU, ALGERIA				
c6a	bwM	intercalated marls & biomicrosparite	?	*Mecaster fourneli*, ? *Linthia payeni*
CONSTANTINE, ALGERIA				
?	M	chalky marls	deep water	*Rispolia subtrigonata*, *Ovulaster zignoanus*, *Ovulaster auberti*, *Leiostomaster bigoneti*, *Mecaster fourneli*, *Linthia payeni*, *Mauritanaster mirabilis*, *Homoeaster tunetanus*, *Homoeaster auberti*, *Homoeaster blayaci*
ORAN, ALGERIA				
?	M	marls	deep water	*Rispolia subtrigonata*, *Rispolia douvillei*, *Guettaria rocardi*, *Ovulaster zignoanus*, *Ovulaster auberti*, juvenile *Hemiaster*, *Leiostomaster gentili*, *Homoeaster tunetanus*, *Homoeaster auberti*
EGYPT				
Dakhla Fm	Pa-b	fine sand & siltstone with shales	inner shelf & deep marine alternations	*Paraster chargensis*, ? *Mauritanaster gentili*
Tarwan Chalk	Pd	marly/chalky limestone	outer shelf	*Echinocorys scutata*, *Linthia sudanensis*, *Paraster chargensis*, *Opissaster schweinfurthi*
LIBYA				
Al Gharbiyah Fm (Lower Tar Member)	Mc-d	calcarenites & marls	open littoral carbonate shelf, 50-200m	*Hemipneustes pyrenaicus*, *Hemiaster paronai*, *Mecaster foumeli*, *Linthia payeni*, *Paraster chargensis*, *Proraster geayi*
echinoid limestone, Sirte	Pa-b	bioclastic packstones & grainstones	high energy open marine, 15-30 m	*Linthia sudanensis*, *Opissaster schweinfurthi*

MOROCCO				
zone marno-schistose	M	schistose marls with limestone intercalations	deep water	*Rispolia douvillei*
?	Pd	sandy & marly limestones	neritic to littoral	*Eupatagus skourensis*, *Mauritanaster gentili*
TUNISIA				
?	upM	calcarenite	shallow shelf	*Mokotibaster amnicus*
white limestone	M	compact limestone	deep water	*Stegaster altus*, *Stegaster bouillei*
ANGOLA				
Landana bed 5	P3-4	limestone	?	*Eupatagus skourensis*
IVORY COAST				
Fresco lower beds 2- 5	Pd	glauconitic marl	tropical, littoral	*Paraster indicus*, *Holcopneustes cristatus*
MOZAMBIQUE				
?	M	?	?	*Homoeaster tunetanus*
SENEGAL				
?	upM	sandy limestone & chalky sandstone	shallow marine	*Stegaster cotteau*?, *Tessieria senegalensis*
?	P	oolitic & chalky limestone	carbonate platform	*Linthia brodermanni*, ? *Paraster indicus*
SOMALIA				
?	M	chalky limestone	?	*Iraniaster douvillei*
Lower Auradu Limestone	P	limestones & shales	shallow water	*Linthia sudanensis*, *Paraster chargensis*, *Opissaster schweinfurthi*, *Opissaster somaliensis*, *Leviechinus gregoryi*, *Brightonia macfadyeni*

NIGERIA & SUDAN				
Thanetian Limestone	T	limestone	restricted shelf-basin moderate depth	*Linthia sudanensis*
ZULULAND				
St Lucia Fm	bwM	decalcified siltstone	?	*Mokotibaster amnicus, Hemiaster stella, Gregoryaster jacobi*
CENTRAL TURKEY				
Ulupinar Fm	Ma-b	sandy limestone, marl & sandstone	shallow, within wave base	*Echinocorys scutata, Ovulaster zignoanus, Ovulaster auberti, Leymeriaster sexangulatus, Homoeaster blayaci*
Besni Fm	Mc-d	rudistic sandy bio-clastic carbonates	shallow water carbonate platform	*Hemipneustes pyrenaicus, Hemiaster paronai, Mecaster victoris*
NORTHWEST TURKEY				
Marnes de Bartine	M	marls	deep water	*Stegaster altus, Guettaria rocardi, Coraster vilanovae, Homoeaster auberti*
white chalk	M	white chalk	deep water	*Stegaster altus, Stegaster bouillei, ? Stegaster heberti*
?	D	marly chalk	deep water	*Echinocorys scutata, Mokotibaster? gregalis, Cyclaster vilanovae, Isaster aquitanicus, Corastervilanovae, Homoeaster tunetanus*
LOURISTAN, IRAN				
?	M?	marls & limestones	?	*Hemipneustes persicus, Proraster atavus, Proraster geayi, Iraniaster morgani, Iraniaster douvillei*

UAE/OMAN				
Simsima Fm	Mc	rudistic, foraminiferal packstone	carbonate platform	*Hemipneustes pyrenaicus, Hemipneustes persicus, Hemipneustes arabicus, Hemiaster paronai, Hemiaster hattaensis, Mecaster victoris, ?Linthia sudanensis, Proraster geayi, Pseudiraniaster omanensis*
EASTERN MADAGASCAR				
Maastrichtian - Danian	M-D	marl & fine chalky sandstone	open marine	*Basseaster rostratus, Diplodetus nutrix, Hemiaster stella, Hemiaster madagascariensis, Proraster geayi, ? Opissaster schweinfurthi*
NORTHERNMOST MADAGASCAR				
Diego Suarez	Ma	chalk	deep water	*Guettaria rocardi*
MAJUNGA BASIN, NORTHWEST MADAGASCAR				
Maastrichtian - Danian	Ma-Pb	chalky marl & marly limestone	lower neritic to bathyal	*Echinocorys scutata, Mokotibaster hourcqi, Mokotibaster nobilis, Diplodetus nutrix, Diplodetus gauthieri, Cyclaster integer, Cyclaster pfenderae, Hemiaster stella, Hemiaster madagascariensis, Gregoryaster jacobi, Paraster indicus, Paraster sindensis, Holcopneustes cristatus, Holcopneustes indicus, Abatus? pseudoviviparus*
MORONDAVA BASIN, SOUTHWEST MADAGASCAR				
Maastrichtian - Danian	Ma-Pb	marly limestone & chalky sandstone	open marine	*Basseaster rostratus, Hemipneustes pyrenaicus, Mokotibaster trangahyensis, Diplodetus gauthieri, Hemiaster stella, Hemiaster madagascariensis*

BALUCHISTAN				
Bed 4	M	sandy limestone	nearshore	*Hemipneustes pyrenaicus*, *Trachyaster oldhami*, *Holcopneustes indicus*
PAKISTAN				
Cardita beaumonti beds	Pa	dark shales with impure limestone	shallow, transgressive sea	*Paraster sindensis*
Khairabad Limestone (Ranikot Series)	Pd	nummulitic limestones & calcareous shales	nearshore & shallow shelf	*Paraster indicus*, *Proraster? alveolatus*, *Holcopneustes indicus*, *Prenaster oviformis*, *Opissaster elongatus*
ASSAM				
Mahadeo Fm	Mb	glauconitic sandstone	open marine, neritic - sub-littoral	*Hemiaster* sp. indet.
SOUTHERN INDIA				
Kallankurichchi Fm (Ariyalur Gp) = *Trigonoarca* beds levels D & E	Mc	bioclastic limestone	shallow shelf, medium energy	*Hemipneustes pyrenaicus*, *Hemiaster stella*, *Leymeriaster sexangulatus*, *Paraster expansus*, *Holcopneustes cristatus*, *Holcopneustes indicus*
Valudayar beds (Ariyalur Gp) level C	Mc	hard limestone	?	*Mokotibaster nobilis*
TADZHIKISTAN				
Maastrichtian	M	calcarenite	carbonate shelf	*Hemipneustes striatoradiatus*
CHINA				
JSG1; JSG17; JST3	upM	calcarenite with chalky matrix	nearshore, at or below wave base	*Hemipneustes pyrenaicus*, *Hemipneustes* sp. indet.

JAPAN				
Miyakura Fm	M	?	?	*Cardiaster* sp. indet., *Hemiaster* sp. indet., *Homoeaster* sp. indet.
WESTERN AUSTRALIA				
Miria Marl	Mc-d	marly clay	shelf sediments	*Echinocorys scutata*, *Giraliaster jubileensis*
Wadera Calcarenite (Cardabia Gp)	Pd	glauconitic calcarenite	open marine carbonate shelf	*Cardabia bullarensis*, *Echinocorys scutata*, *Giraliaster jubileensis*
Pirie Calcarenite (Cardabia Gp)	Pd	bryozoal calcarenite	open marine carbonate shelf	*Cardabia bullarensis*, *Giraliaster jubileensis*, ? *Paraster chargensis*
Cashin Calcarenite (Cardabia Gp)	Pd	fine grained bryozoal calcarenite	open marine carbonate shelf	*Cardabia bullarensis*, *Giraliaster jubileensis*, ? *Paraster chargensis*

APPENDIX 3

INFERRING ECHINOID LARVAL TYPE FROM APICAL DISC CRYSTALLOGRAPHY

The adult echinoid has a calcareous skeleton made up of many individual plates, each of which acts as a single crystal of calcite. In both organic and inorganic contexts, calcite is made up of a repeating array of calcium and carbonate ions. Axes are defined within the crystal lattice to form a consistent way of describing crystallography. In calcite there is one C-axis and three A-axes. Since there is a constant angular relationship between the crystallographic axes and the external faces of a crystal, the orientation of the C- and A- axes may be deduced from the orientations of face poles of the calcite crystal.

Methods and materials.

Until recently, studies of crystallographic patterns in echinoids (e.g. Raup 1962, 1965, 1966; Emlet 1985, 1988, 1989) have used polarized light microscopy of thin sections to determine C-axis orientations. However, a non-destructive technique is now available and was utilized for this study. Okazaki *et al.* (1981) described "crystal decoration" - a simple method of growing microscopic calcite crystals in optical continuity with the underlying calcite:

- 20 minutes in 0.05% acetic acid to clean surface and provide key for new crystal growth.
- 5 minutes in 0.1 *molar sodium* hydroxide to neutralize.
- Rinse in tap water and dry.
- 30 minutes to 1 hour in a 5:2 mixture of 0.1 molar sodium bicarbonate and calcium chloride.
- Rinse in 95% ethanol.

The form and orientation of these newly grown rhombs reveals information about the crystallographic axes of the underlying echinoid skeletal plates. Once decorated, each specimen was mounted on an optical goniometer and face pole orientations of apical disc plates were measured by rotating the specimen until a bright reflection was found. Crystallographic axes were calculated from this goniometer data by the computer program CALCAXES (Fischer & Bodenbender 1993), avoiding the problems of data degradation associated with manual plotting and manipulation of stereographic plots. The C-axes traces for each specimen were than plotted on a stereogram to create a "crystallographic signature". Finally, developmental strategy was inferred from these plots (see Figure 7.2) since Emlet (1985, 1988, 1989) has shown that calcite skeletal rods in echinoid larvae determine the orientation of optic axes in adult genital plates and thus developmental mode may be inferred from the orientations of crystallographic axes in the calcite of apical disc plates. In species with planktotrophic larvae, three of the five genital plates form from elements of the larval skeleton and retain the crystallographic orientation of the calcite rod present in the larva. In genital plates 3 and 5, the C-axis is almost tangential to plate surface whilst the remaining three genital plates have their C-axis more or less perpendicular to the plate surface. In irregular echinoids, where there is no fifth genital plate, crystallographic orientation of genital plate 3 is critical in inferring planktotrophy. For lecithotrophic larvae in which all adult skeletal plates are formed *de novo*, all genital plates have the C-axis perpendicular to plate surface.

Results are shown in Table A3.1.

Table A3.1. Larval development in Maastrichtian and Palaeocene echinoids, inferred from apical disc crystallography. P = inferred planktotroph; L = inferred lecithotroph.

REGULARS	*Cidaris falgeriensis*	Spain	353.07.33	L
	Goniopygus arabicus	UAE	EE3983	P
		UAE	EE4005	P
	Goniopygus durandi	Algeria	E4011	P
	Goniopygus heberti	Maastricht	E75820	L
	Goniopygus royanus	France	E81582	P
	Goniopygus supremus	Jamaica	EE2761	P
	Goniopygus persicus	Iran	Lambert	P
	Coenholectypus baluchistanensis	UAE	EE3389	P
	Salenia nutrix	UAE	EE3652	P
	Hattopsis sphericus	UAE	EE3661	P
		UAE	EE3708	P
	Orthopsis miliaris	UAE	EE3740	P
	Glyphopneustes hattaensis	UAE	EE3943	P
		UAE	EE4025	P
	Codiopsis lehmannae	UAE	EE5033	P
HOLECTYPOIDS	*Globator bleicheri*	UAE	EE4154	P
	Globator douvillei	UAE	EE4306	P
CASSIDULOIDS	*Petalobrissus subsetifensis*	Algeria	E3590	P
	Petalobrissus setifensis	Algeria	E3987	P
	Echinanthus pumilis	Arabia	E18343	P
	Pygopistes rudistarum	Jamaica	E83008	L?
	Vologesia rawdahensis	UAE	EE3385	P
	Petalobrissus linguiformis	UAE	EE4318	P
	Nucleopygus magnus	UAE	EE4339	P
HOLASTEROIDS	*Galeaster bertrandi*	Kazakhstan	EE5614	P
	Pseudoffaster caucasicus	Kazakhstan	EE5573	P
	Echinocorys scutata	Kazakhstan	EE5613	P
	Cardiotaxis heberti	Kazakhstan	EE5627	P
	Hemipneustes persicus	UAE	EE4098	P
SPATANGOIDS	*Diplodetus americanus*	USA	76285	P
	Cyclaster vilanovae	Spain	EE?	L
	Cyclaster integer	Kazachstan	EE5585	L
	Isaster aquitanicus	Spain	EE4524	P
	Hemiaster hawkinsi	Madagascar	E20098	P
	Hemiaster punctatus	France	E10384	P
	Hemiaster prunella	France	E4381	P
	Hemiaster hattaensis	UAE	EE4055	P
	Hemiaster paronai	UAE	EE5034	P
	Mecaster fourneli	Algeria	E4034	P
	Mauritanaster mirabilis	Algeria	E4052	L
	Linthia sudanensis	Niger	EE2262	P
	Opissaster somaliensis	Somalia	E582	P
	Coraster beneharnicus	Spain	EE4825	P
	Homoeaster tunetanus	Spain	EE4404	P
	Iraniaster douvillei	Iraq	E40574	P
		Somalia	E325	P

APPENDIX 4

EXTINCTION DATA AND POSSIBLE TAXONOMIC AND GEOGRAPHIC CORRELATES

This appendix comprises data on the fate of atelostomate clades at the end of the Cretaceous along with details of possible taxonomic and geographic correlates.

A Extinct / survive at Maastrichtian-Danian (. = not present in Maastrichtian strata; x = extinct; > = survive).

B Extinct / survive at Danian-Thanetian (. = not present in Danian strata; x = extinct; > = survive.

C Number of Maastrichtian species in clade (*Labrotaxis* has no Maastrichtian representative).

D Maastrichtian localities and regions clade known from (see Appendix 1).

E Number of Maastrichtian localities.

F Number of Maastrichtian regions.

G Absolute latitudinal range.

H Absolute longitudinal range.

I Size of latitudinal range with latitudinal tolerance (i.e. northern and southern latitudes combined) in parentheses.

J Size of longitudinal range.

Extinction levels in atelostomate echinoids.

Holasteroids	Maastrichtian	9/14 = 56%
	Danian	4/9 = 44%
Spatangoids	Maastrichtian	5/24 = 21%
	Danian	5/23 = 22%
Total	Maastrichtian	14/40 = 35%
	Danian	9/32 = 28%

	A	B	C	D	E	F	G	H	I	J
Cardabia	.	.	0							
Galeaster	>	x	1	EU23, EU24, EU26, EU27, EU28, EU29, EU30	7	1	29-41 N	35-58 E	12	23
Basseaster	>	x	1	IP1, IP4	2	1	35-37 S	46-53 E	2	7
Garumnaster	.	>	0							
Stegaster I	x		3	EU6, EU10, EU11, EU12, EU15, EU20, EU23, EU26, EU27, EU29, T7, T17	12	2	29-41 N	1W-58 E	12	59
Stegaster II (*Sanchezaster*)	>	>	1	EU6, EU10, EU15, T12	4	2	7-35 N	15 W-2 E	28	17
Tholaster	x		1	EU10, EU15	2	1	35 N	1 W-2 E	1	3
Pseudoffaster	x		1	EU13, EU14, EU26, EU27, EU28, EU29	6	1	29-41 N	2 W-58 E	12	60
Rispolia	>	x	2	EU3, T2, T3, T6	4	2	22-58 N	19 W-3 E	36	22
Guettaria	x		2	EU16, EU26, EU27, EU29, T3, T17, IP2	7	3	23-41 N 25 S	1 W-58 E	66 (18)	59
Echinocorys	>	>	1	EU1, EU4, EU5, EU7, EU10, EU11, EU13, EU14, EU17, EU20, EU21, EU23, EU25, EU26, EU28, EU29, T16, IP3, IP12	19	3	31-48 N 28-50 S	2 W-101 E	98 (22)	103
Offaster	x		2	EU13, EU14, EU17	3	1	34-48 N	2 W-11 E	14	13
Jeronia	.	x	0							
Cardiaster	x		4	AM2, AM8, AM10, EU1, EU4, EU5, EU7, EU10, EU14, EU17, EU18, EU23, EU25, IP11	14	3	18-52 N	71 W-135 E	34	206
Cardiotaxis	x		1	EU1, EU4, EU8, EU17, EU28	5	1	41-48 N	3-53 E	7	50

	A	B	C	D	E	F	G	H	I	J
Hagenowia	x		1	EU1, EU17, EU18	3	1	47-48 N	8-11E	1	3
Labrotaxis	>	>	0*							
Giraliaster	>	>	1	IP12	1	1	50 S	101 E	1	1
Hemipneustes	x		7	EU5, EU10, EU11, EU12, EU13, EU14, EU20, EU26, EU28, EU29, T5, T16, T18, T19, IP4, IP5, IP8, IP9, IP10	19	3	8-45 N 8-37 S	2 W-95 E	82 (37)	97
Micraster	>	x	3	EU4, EU5, EU11, EU18, EU26, EU29	6	1	31-47 N	1-46 E	16	45
Mokotibaster	>	x	4	T7, T15, IP3, IP4, IP8	5	2	21 N 28-40 S	12-73 E	61 (19)	61
Pseudogibbaster	.	>	0							
Diplodetus	>	>	6	AM2, AM5, AM8, EU5, EU11, IP1, IP3, IP4	8	3	29-45 N 28-37 S	71 W-53 E	82 (17)	124
Ovulaster (*Habanaster*)	>	>	2	EU26, T2, T3, T16	4	2	23-40 N	1 W-48 E	17	49
Cyclaster	>	>	7	EU5, EU10, EU11, EU13, EU14, EU17, EU22, EU26, EU28, EU29, EU30, IP3	12	2	31-48 N 28 S	2 W-57 E	76 (20)	59
Isaster	>	>	1	EU11, EU13	2	1	31-35 N	2 W-1 E	4	3
Eupatagus	.	.	0							
Hemiaster	>	>	9	AM1, AM2, AM3, AM5, AM8, AM9, EU5, EU7, EU12, EU13, EU14, EU20, T5, T15, T16, T19, IP1, IP3, IP4, IP7, IP8, IP11	22	4	8-52 N 18-40 S	78 W-135 E	92 (44)	213
Leiostomaster	x		2	T2, T3	2	1	23 N	1 W-3 E	1	4

	A	B	C	D	E	F	G	H	I	J
Leymeriaster	x		3	EU5, T16, IP8	3	3	32-45 N 30 S	5-73 E	75 (15)	68
Mecaster	x		2	AM13, T1, T2, T5, T16, T19	6	2	8-32 N 12 S	18 W-48 E	44 (24)	66
Gregoryaster	>	x	1	T15, IP3	2	2	28-40 S	25-45 E	12	20
Linthia	>	>	3	AM10, T1, T2, T4, T5, T19	6	2	7-23 N	63 W-47 E	16	110
Paraster	>	>	6	AM2, AM5, AM6, AM8, AM10, AM13, EU31, T5, IP3, IP8	10	4	18-36 N 12-30 S	71 W-73 E	66 (18)	144
Tessieria	x		1	T12	1	1	7 N	15 W	1	1
Proraster	>	>	3	AM8, AM10, AM11, EU9, EU14, EU28, T5, T18, T19, IP1	10	4	8-41 N 35 S	71 W-56 E	76 (33)	127
Trachyaster	>	>	1	EU3, IP5	2	2	58 N 8 S	19 W-68 E	66 (50)	87
Holcopneustes	>	>	2	IP3, IP5, IP8	3	1	8-30 S	45-73 E	22	28
Prenaster	.	.	0							
Mauritanaster	>	>	1	T2	1	1	23 N	3 E	1	1
Brisaster	.	>	0							
Pseudolinthia	.	x	0							
Abatus	>	>	1	IP3	1	1	28 S	45 E	1	1
Opissaster	.	.	0							
Kertaster	.	.	0							

	A	B	C	D	E	F	G	H	I	J
Coraster	>	>	1	EU11, EU20, EU24, EU26, EU29, EU30, T17	7	2	31-41 N	1-57 E	10	56
Orthaster	>	>	1	EU27, EU29	2	1	29-41 N	46-58 E	12	12
Homoeaster	>	x	3	EU11, EU16, EU20, EU24, EU26, EU29, T2, T3, T11, T12, T16, T17, IP11	13	3	7-52 N 27 S	15 W-135 E	79 (45)	150
Sphenaster	.	>	0							
Iraniaster	>	>	2	T13, T18	2	1	12 N 3 S	40-56 E	15 (9)	16
Pseudiraniaster	x		1	T19	1	1	8 N	47 E	1	1
Leviechinus	.	.	0							
Brightonia	.	.	0							

APPENDIX 5

EXTINCTION DATA AND POSSIBLE ENVIRONMENTAL AND BIOLOGICAL CORRELATES

This appendix comprises data on the fate of atelostomate clades at the end of the Cretaceous together with details of environmental and biological correlates.

A Extinct / survive at Maastrichtian-Danian (. = not present in Maastrichtian strata; x = extinct; > = survive).

B Extinct / survive at Danian-Thanetian (. = not present in Danian strata; x = extinct; > = survive.

C Maastrichtian water depth: littoral.

D Maastrichian water depth: onshore.

E Maastrichtian water depth: mid-offshore.

F Maastrichtian sediment type: chalk / marl.

G Maastrichtian sediment type: calcarenite / sandy limestone.

H Maastrichtian sediment type: sand / gravel.

I Maastrichtian sediment type: silt / mud.

J Life-position in sediment: i = fully infaunal; e = epifaunal to partially exposed. Life-position was inferred from test profile (Kanazawa 1992), tuberculation and presence of funnel and tunnel building tube feet.

K Larval strategy: p = planktrotrophic; l = lecithotrophic; b = brooded. Larval strategy was inferred using the methods outlined in Chapter 7 and Appendix 3.

L Feeding strategy: b = bulk detritivore; s = selective detritivore. Feeding strategy was inferred from the presence or absence of pores for pencillate tube feet around the mouth.

	A	B	C	D	E	F	G	H	I	J	K	L
Cardabia	.	.										
Galeaster	>	x			✔	✔				e	p	b
Basseaster	>	x			✔	✔	✔			e	p	s
Garumnaster	.	>										
Stegaster I	x				✔	✔				e	p	b
Stegaster II (*Sanchezaster*)	>	>			✔	✔	✔			e	p	b
Tholaster	x				✔	✔				e	p	b
Pseudoffaster	x			✔	✔	✔	✔			e	p	b
Rispolia	>	x			✔	✔	✔			e	p	b
Guettaria	x				✔	✔				e	p	b
Echinocorys	>	>		✔	✔	✔	✔			e	p	s
Offaster	x			✔	✔	✔	✔			e	p	s
Jeronia	.	x										
Cardiaster	x			✔	✔	✔	✔			i	p	s
Cardiotaxis	x				✔	✔	✔			i	p	b
Hagenowia	x				✔	✔				i	p	b
Labrotaxis	>	>		no Maastrichtian representative						e	p	s
Giraliaster	>	>			✔	✔				i	p	s
Hemipneustes	x		✔	✔	✔	✔	✔	✔		e	p	s
Micraster	>	x			✔	✔	✔			l	p	s

	A	B	C	D	E	F	G	H	I	J	K	L
Mokotibaster	>	x			✔	✔	✔			e	p	s
Pseudogibbaster	.	>										
Diplodetus	>	>	✔	✔	✔	✔	✔	✔	✔	i	l	s
Ovulaster (*Habanaster*)	>	>		✔	✔	✔				i	p	s
Cyclaster	>	>		✔	✔	✔	✔			i	l	s
Isaster	>	>			✔	✔	✔			e	p	s
Eupatagus	.	.										
Hemiaster	>	>	✔	✔	✔	✔	✔	✔	✔	i	p	s
Leiostomaster	x				✔	✔				i	p	s
Leymeriaster	x		✔	✔	✔	✔	✔			i	p	s
Mecaster	x		✔	✔	✔	✔	✔			i	p	s
Gregoryaster	>	x			✔	✔				i	p	s
Linthia	>	>		✔	✔	✔	✔			i	p	s
Paraster	>	>	✔	✔	✔	✔	✔	✔	✔	i	p	s
Tessieria	x			✔			✔			i	p	s
Proraster	>	>	✔	✔	✔	✔	✔			i	p	s
Trachyaster	>	>		✔	✔		✔			i	p	s
Holcopneustes	>	>		✔	✔	✔	✔			i	p	s
Prenaster	.	.										
Mauritanaster	>	>			✔	✔				e	l	s

	A	B	C	D	E	F	G	H	I	J	K	L
Brisaster	.	>										
Pseudolinthia	.	x										
Abatus	>	>			✔	✔				i	b	s
Opissaster	.	.										
Kertaster	.	.										
Coraster	>	>			✔	✔				i	p	s
Orthaster	>	>			✔	✔				i	p	s
Homoeaster	>	x		✔	✔	✔				i	p	s
Sphenaster	.	>										
Iraniaster	>	>			✔	✔				e	p	s
Pseudiraniaster	x				✔	✔				e	p	s
Leviechinus	.	.										
Brightonia	.	.										